KU LEUVEN

ARENBERG DOCTORAL SCHOOL
FACULTY OF ENGINEERING SCIENCE

IN-SERVICE BEHAVIOUR OF FLAX FIBRE REINFORCED COMPOSITES FOR HIGH PERFORMANCE APPLICATIONS

Farida Bensadoun

Members of the Examination Committee:

***em.* prof.dr.ir. Ignaas Verpoest**, promoter
prof. dr.ir. Aart W. Van Vuure, promoter
prof.dr.ir Jan Ivens
prof.dr.ir Karel Van Acker
prof.dr.ir Joris Van Acker
prof.dr.ir Larry Lessard
prof.dr.ir Wim Thielemans
prof.dr.ir Patrick Wollants, chairman

Dissertation presented in partial fulfilment of the requirements for the degree of Doctor in Engineering

July 2016

Uitgegeven in eigen beheer, Farida Bensadoun, Leuven.

Pictures were kindly provided by The European Confederation of Linen and Hemp
On top: Flax field. On the left side: selction of flax fibre semi-products. On the right side: Notox surfboard, Blackbird Ukulele, Phone flax case, Jean-Marie Massaud Flax arm chair, Delsey suitcase, Be.e scooter, Apollo bike helmet, URGE Mountain bike helmet, Focal flax speakers, Akonite skateboard, In'Bô bamboo-flax bike

Acknowledgements

Scientists dream about great things. Engineers do them
James A. Michener

Imagination is more important than knowledge
Albert Einstein

Today is the day that I write the last words of my thesis. If someone told me when I started my bachelor in mechanical engineering in 2005 that I will be doing a PhD, I would have said that they are crazy. 11 years later, here I am. This has been quite a journey and I enjoyed every moment of it.

A good support system is important to surviving and staying sane during your PhD. All those listed here have contributed in these four years of intense work, stress, laughs, cries and joys of scientific discoveries. These priceless moments are unforgettable and for that, I want to honor and show my recognition to everyone who contributed to the success of this thesis.

First and foremost, I would like to express my sincere gratitude to my supervisor, Ignaas Verpoest, for his continuous support, patience, motivation, and immense knowledge. I could not have imagined having a better advisor and mentor. His enthusiasm for flax fibre is contagious and inspiring. He believed in me and pushed me to give my 150%. He also trusted me with a very important job when he gave me the chance to be part of the European Confederation of Linen and Hemp. This gave me the chance to be behind the scene of the fascinating flax world and learn more that I could have ever imagine.

My very warm thanks to my co-promoter Aart W. van Vuure. It is because of him that I am here today. That decisive meeting in Korea he had with my master thesis promoter, Edu Ruiz, paved my way to Leuven. I would like to thank him for his help, hard work, dedication and great insight on natural fibres. Even though he was busy, he always found the time to answer my questions and spur my work in the right direction.

I wish to express my thanks to the members of my supervisory committee, Prof. Jan Ivens, Prof. Karel Van Acker and Prof. Joris Van Acker. Thank you for your continuous support throughout my PhD and for all the interesting discussions. Special thanks to Prof. Larry Lessard, Prof. Wim Thielemans and Prof. Patrick Wollants for accepting on being part of my jury and for the time you took in reading my thesis. Your precious feedback truly helped to improve this.

I would like to acknowledge the sponsors of this research which made this journey possible: The Fonds Du Québec–Recherche Nature et Technologies (FQRNT), the European Flax and Hemp Confederation (CELC) as well as the European Biobuild Project FP7 285689.

Many people participated in the completion and success of this research. I think it would be hard not to forget anyone, so please, I apologize in advance for those who are not listed here as it should.

This work would not have been possible without the technical support of Bart Pelgrims, Manuel Adams, Kris Van de Staey and Marc Peeters. Their valuable insight and advice on composite manufacturing and testing was the key of the success of this work. Warm thanks to all the technical and administrative staff of the Materials Department, especially Huberte, Jennifer, Nadine, Gert, Joop, Eddy, Louis, Johan, Dirk, Mieke, Mia, Danny W, Danny D.

To the CMG gang, you guys are the best! I came here all alone and you made me feel part of a nice and big family. A special thanks to my welcome committee when I arrived in Leuven 4 years ago. Dieter (aka Barney) thanks for being such a good friend, always laughing and making jokes. Yasmine M., you made me feel welcome and opened your home to me, I will never forget it and I hope I can repay your kindness one day. I can never forget all the special moments I had with Malika, Oskana, Nhan, Nghi, Anna, Ilya, Marina, Franziska, Katleen Q., Yentl, Mahoor, Joris, Marcin and Baris. A special mention to Stepan, Larissa, David and Frederick for your precious feedback throughout my PhD. I feel honoured to have been part of such a great research group!

I would like to make a very special thanks to Katleen Vallons. You have been not only my office mate but also friend, a counsellor and a motivator. I know that I could always ask you for advice and opinions on everything. I also would like to thank the other members of the exclusive "Girls office", Delphine, Man, and Anastasiia, for all the nice time we had babbling, drinking tea and eating chocolate.

To my dear Vale & Tanya *aka* the Chevakitos, thank you for being such good friends. You are always up to try new activities, new food and visit new places. We have shared so many memorable moments. Thank you for your sincere and honest talks. I am thrilled that you decided to call Montreal home as we will create so many more memories. To Yasmine A., Ali and Aram, Carlos and Mariangela, thank you for your friendship, your kindness. It's awesome to have friends like you!

I want to express my deep gratitude to Julie Pariset and all the CELC team, for believing in me and giving the chance to discover the flax world like never before. I learned so much working with you on the importance of good communication and networking. Special mention to the members of the European scientific committee of the CELC, Christophe Baley, Moussa Gomina, Peter Davis, Joris Van Acker, Jörg Mussig, Hans Lilholt, Mark Hughes and Gerhard Ziegmann. I also would like to thank Lineo, Hexcel, Safilin, B-Comp, Procotex, Ecotechnilin and Libeco for supplying the flax material and shared you knowledge with me and make this thesis a reality.

A special thanks to the theses students I had the chance to work with: Delphine Depuydt, Yao Zhao, Jan Vertommen, Bart Vanderfeesten, Elias Cloots, Bastien Grillet, Wouter de Saeger, Frederick Puttemans, Elias de Keyser and Kristof Vanden Bergh. Your enthusiasm, motivation and dedication to understand the flax composites was enlightening. You challenged me on being a better teacher and scientist, I will be forever grateful for that.

To the "running squad" Arturo, Ivonne, Robin, John, I cannot begin to express my gratitude and appreciation for your friendship. You have been my very own family here. In the last years, you also have been my motivation cheer squad and were always there when I needed a listening

ear. Our memorable BBQs and after-run drinks will always be some of the best memories of my life. Friends with hearts of gold are hard to find. Your kindness is truly unequalled. Thank you!

To Lina and Yadian, I shared so many laughs and good moments you. I had the privilege to see your beautiful family get together and grow. The arrival of the Pollos lindos, Irene and Santiago brought me a lot of joy and happiness. Being able to see them grow made me feel part of your family. Thank you for your kindness, especially during the times when I had the blues of being alone here. I will never forget your sweet gestures. Thank you for everything!

Je tiens également à remercier mes amis de Montréal. À Lamia, Chely, Dan, Joaquin, Marie-Eve, Xue-Meng, Nico, Aline, Laura et Amir. Malgré la distance, vous m'avez soutenue et motivée. Mes vacances à Montréal ont été inoubliables grâce à vous. Vous m'avez fait sentir comme si je n'étais jamais partie. Merci d'avoir partagé ces moments avec moi. I Miss you guys!

Cette thèse ne serait pas une réalité sans le soutien d'Edu Ruiz et François Trochu, mes directeurs de maîtrise. Vous m'avez donné la piqure des composites et ouvert de nouveaux horizons pour moi. Pour cela je vous remercie.

Je remercie toute ma famille en France, au Canada, aux Pays-Bas et en Algérie. Je remercie tout spécialement ma Tata alia aka Mamie Nova. Tu es la meilleure Tante dont une nièce peut rêver. Tu m'as encouragé à toujours donner le meilleur de moi-même depuis que je suis toute petite. À ma Tata, merci. Remerciements spéciales à Leila, Aicha, Chakib, Tarik, Ilies, Bdera, Samy, Badii, Isma et Kenza qui ont toujours gardé leur portes ouvertes lors des mes visites impromptues à Paris. *Wherever I will be, Paris will always be my home.*

Para el hombre que amo, mi mejor amigo y compañero, mi hormiga Eduardo. Te quiero agradecer por el apoyo, la ternura, la fortaleza, la alegría, el amor y la comprensión que siempre me has brindado. Tú eres la persona que siempre me ha alentado desde el primer día. Tu apoyo, paciencia y ayuda durante toda la tesis ha significado todo para mí. No puedo imaginar este logro sin ti a mi lado. Tu bondad es increíble. Me siento especial cuando estoy contigo. Gracias. Te amo.

Mes derniers remerciment vont à ma famille que j'aime pour leur amour, leur confiance, leur tendresse, leur soutien et leur encouragements qui me guident tous les jours. À mes parents, Yasmina et Said, que j'admire, parce que leur courage, leur humour et leur bonté me donnent le plus bel exemple qui soit. Vous avez cru en moi et avez toujours voulu le meilleur pour moi. Vous avez beaucoup de sacrifice pour Sarah et moi pour que nous puissions accomplir tous nos rêves et je vous en serai à jamais reconnaissante. Je voudrais faire une spiciale dedicace au *Maître de mon univers* ☺, ma soeur Sarah. Ta joie de vivre et tes rires sont contagieux. Un grand merci pour ton soutien et ta précieuse aide lors de la correction de cette thèse. C'est un peu grâce à toi que je suis là aujourd'hui. Tu m'as encouragé et tu m'as donnée le courage de foncer. Merci à vous trois. Nabrikoum.

Life is too short so be crazy, do crazy and let the world awesomeness take you
The only moment to be happy is life

Farida B.
4th of July 2016

Abstract

The use of flax fibres in the composites industry has been steadily growing, thanks to their good mechanical properties, manufacturing effectiveness, acoustic and thermal insulation, good vibration damping, low density and renewability. Flax fibres are a good alternative to less sustainable fibres, such as glass fibres, and they are good candidates to be used for high performance composite applications. The performance of flax fibre composites is believed to be controlled by the intrinsic properties of the flax fibres and the polymer matrix as well as the textile architecture features (e.g. twist). To achieve a good understanding of these effects on the flax composite properties, the following methodology was are undertaken:

1. Understanding the effect of textile architecture/matrix combinations on the quasi-static mechanical behaviour of flax composites;
2. Investigation of the internal geometry of the flax composite and their implementation in modelling tools to predict the quasi-static properties;
3. Evaluation of the effect of fibre architecture on the impact and fatigue behaviour of flax composites;
4. Environmental impact assessment of flax composites end-of-life technologies and a comparative life cycle assessment of the flax composites in comparison to standard materials for two automotive cases.

These studies were carried on using commercially available textile architectures (random mat, plain weave, twill 2x2, quasi-UD and UD) and two types of matrices, a thermoset epoxy and a thermoplastic maleic anhydride polypropylene (MAPP).

The internal geometry of textile reinforcements is known for having a significant influence on the mechanical properties of composites. The study of the quasi-static properties (tensile and flexural) showed that the matrix type intrinsic properties have an important effect of the stiffness and strength properties of the composite. No large difference between the different types of woven fabric was seen, although the effect of specific reinforcement geometry parameters (crimp, twist, weave style, wet or dry spun yarns) could be identified.

With the quasi-static properties known, the second step of this work aimed to predict these data through modelling. The combination of the textile features with the effective mechanical properties of the fibre/yarn and the matrix properties would make an easy tool to assess the potential of each textile architecture combination, while saving time on the trial-and-error methodology. The internal geometry was analysed via micro-CT imaging. The effective properties of the fibre/yarn used in the textile were assessed using the impregnated fibre bundle test method (IFBT). These parameters were then inputted into the Wisetex-Lamtex-Texcomp trio of software to reconstruct the textile 3D model and predict its quasi-static properties. The results showed that the predicted moduli were comparable to the experimental results with a maximal variation of 10%.

The investigation of the impact and fatigue properties of flax-based composites is key in order to understand which material parameters determine the safety and longevity of flax composite products. For impact, the matrix choice was found to greatly influence the absorbed energy as well as the damage area. The absorbed energy at perforation for the flax-MAPP composite was more than 50% higher than for the flax-epoxy one. Furthermore, the use of a MAPP instead of epoxy led to a decreased impact damage area by 38% to 59% with limited delaminations. The decrease of the flexural properties after impact of the flax-MAPP composite was marginal, which is related to the increased absorbed energy per area, while the flax-epoxy composites experienced a stronger decline in properties after impact. The hypothesis that the presence of

delaminations has an important influence on the impact performance of the flax composites has been proved wrong, since a limited amount of small delaminations was seen after a non-perforation impact. This was due to the high interlaminar fracture toughness properties of flax composites, which increases by at least 2-3 times over that of the unreinforced brittle epoxy polymer. The tensile toughness was found to be a good indicator of the capacity of a material to sustain perforation or non-perforation impact.

The characterization of the tension-tension fatigue properties of flax-epoxy composites showed that the fibre architecture has a strong effect on the fatigue behaviour, where higher quasi-static strength and modulus combinations present the best fatigue characteristics. They have a delayed damage initiation and increased fatigue life as well as a reduced damage propagation rate combined with higher energy dissipation in the early stages of fatigue loading. Furthermore, a comparison with a glass fibre benchmark showed that the behaviour of flax-epoxy composites is comparable to glass fibre reinforced composites, when expressed in terms of specific stress (stress/density) and thus, flax composites are suitable for many new or existing industrial applications.

To close the life cycle loop of the flax composite product, three end-of-life (EOL) options were investigated for the flax-MAPP composites: chemical recycling, mechanical recycling and incineration. It was found that the chemical recycling technique is feasible based on the mechanical properties of the recycled composite. However, its processing time, chemicals needed and equipment have negative effects on the environment. The second method, the mechanical recycling, resulted in a recycled, injection moulded composite with discontinuous fibres and hence somewhat lower mechanical properties compared to those of fresh random mat composites. The main advantage of the mechanical recycling technique is the speed of the process. Very large quantities of waste can be shredded and processed into new components while reducing the environmental burden of producing fresh MAPP and flax fibre. The last EOL method studied was incineration with energy recovery and it has been found to be a good alternative as well since all the material can be fully combusted and embodies a relatively high calorific value.

Finally, to justify the use of flax composites instead of standard materials, two cradle-to-grave comparative life cycle assessments (LCA) were carried on for two automotive cases, a car roof (flexural design) and a bumper (impact design). A mass factor methodology was used in order to fairly compare equivalent amounts of flax and glass fibre based on the mechanical performance that need to be achieved. For the impact design case, the results of the life cycle analysis showed that the replacement of glass composite by flax composite was beneficial in the 40% and 50% fibre volume fraction case. However, it was not the case for the 30% fibre volume fraction case since the mass factor was higher than 1. This means that, at 30% fibre volume fraction, a higher amount of flax (1.11 kg vs 1 kg of glass fibres) is needed to be used in a composite to fulfil the same impact resistance performance. For the flexural design case, it was found that the use of flax composite has lower environmental impact than their glass composites counterparts. Overall, the LCA results showed that flax fibre composites are an environmentally favourable choice in comparison to glass fibre composites. However, the trade-off between mechanical properties has to be evaluated for each design case specifically.

Samenvatting

Vlasvezels worden steeds meer gebruikt in de composietindustrie, omwille van hun goede mechanische eigenschappen, efficiënte productiemethoden, akoestische en thermische isolatie, goede trillingsdemping en laag gewicht, en tenslotte omdat zij een hernieuwbare grondstof zijn. Vlasvezels zijn een goed alternatief voor minder duurzame vezels zoals glasvezels, en zijn daarom uitstekend om gebruikt te worden in hoog-performante composiettoepassingen. De eigenschappen van vlasvezelcomposieten worden bepaald door de intrinsieke eigenschappen van de vlasvezels en de polymeermatrix, maar ook door de textielarchitectuur van de versterking (bijvoorbeeld de garentwist). Om deze laatste effecten beter te begrijpen, werd de volgende onderzoeksmethode toegepast:

1. Onderzoek naar het effect van verschillende combinaties van vezelarchitectuur en polymeermatrix op de quasi-statische mechanische eigenschappen van vlascomposieten;
2. Analyse van de interne geometrie van de vlascomposieten, en implementatie in modellen en software tools die de quasi-statische eigenschappen voorspellen;
3. Evaluatie van het effect van de vezelarchitectuur op de impact en vermoeiingseigenschappen van vlascomposieten;
4. Bepaling van de ecologische impact van verschillende einde-levensduur-technologiën, en een vergelijkende levenscyclusanalyse van vlascomposieten en ‘klassieke’ materialen voor twee automobieltoepassingen.

Deze studies werden uitgevoerd op commercieel beschikbare textiele versterkingen (matten, vlakke weefsels, weefsels met keperbinding, quasi-unidirectionele en unidirectionele preforms) en twee types matrices, een thermohardend epoxy en een thermoplastisch polymeer (maleïnezuur-anhydride gemodificeerd polypropyleen, MAPP).

Zoals bekend heeft de interne geometrie van de textiele versterkingen een belangrijke invloed op de mechanische eigenschappen van de composieten. De studie van de quasi-statische eigenschappen (in trek en buiging) toonde aan dat ook de intrinsieke eigenschappen van de matrix een rol spelen. Tussen de verschillende weefseltypes werd geen groot verschil waargenomen, maar er was wel een waarneembaar effect van enkele specifieke geometrische parameters (inweving, garentorsie, weefstijl, gebruik van natte of droog gesponnen garens).
Eens de quasi-statische eigenschappen gemeten zijn, kunnen deze vergeleken worden met de eigenschappen verkregen via modellering.De combinatie van de textielkarakteristieken met de effectieve mechanische eigenschappen van de vezels of garens laat immers toe om de potentiële eigenschappen van elke textielarchitectuur af te schatten en op die manier een behoorlijke tijdswinst te realiseren in vergelijking met de trial-and-error methode.

De interne geometrie werd opgemeten op micro-CT beelden. De effectieve mechanische eigenschappen van de vezels of garens werden gemeten met behulp van de ‘geïmpregneerde vezelbundel’-testmethode (IFBT). Beide data werden dan ingevoerd in het software-trio Wisetex-Lamtex-Texcomp, waarmee de textielarchitectuur kan gereconstrueerd worden en de quasi-statische mechanische eigenschappen kunnen voorspeld worden. De voorspelde Young’s moduli verschilden maximaal 10% van de experimenteel gemeten waarden.

Het onderzoek naar het impact- en vermoeiingsgedrag van vlascomposieten is belangrijk om goed te kunnen begrijpen welke materiaalparameters de duurzaamheid van vlascomposietproducten zullen bepalen. Voor de impacteigenschappen bleek de keuze van de matrix zeer belangrijk: de matrix heeft zowel op de geabsorbeerde energie als op het oppervlak van de beschadigde zone een grote invloed. De energie nodig voor perforatie van het laminaat

is meer dan 50% groter voor een vlas-MAPP-composiet dan voor een vlas-epoxy-composiet. Bovendien verkleint de beschadigde zone met 38 tot 59%, en zijn er slechts kleine delaminaties. De vermindering van de buigeigenschappen na impact was voor vlas-MAPP-composieten verwaarloosbaar, en is gerelateerd aan de hoge energie per eenheid beschadigd oppervlak, terwijl voor vlas-epoxy-composieten het verlies aan buigeigenschappen wel significant is. De hypothese dat delaminaties een belangrijke rol spelen bij de impacteigenschappen van vlascomposieten werd weerlegd, omdat slechts heel kleine delaminaties werden gevonden bij een niet-perforerende impact. De reden daarvoor is de zeer hoge interlaminaire breuktaaiheid van vlascomposieten, die 2 tot 3 keer hoger is dan de breuktaaiheid van een niet-versterkt epoxy. Daarentegen werd gevonden dat de taaiheid, gemeten als de energie tot breuk bij een trekproef, wel een goede indicator is voor de impacteigenschappen van vlascomposieten.

De resultaten van de trek-trek-vermoeiingstesten toonden aan dat de vezelarchitectuur een sterke invloed heeft op het vermoeiingsgedrag, en dat een hoge quasi-statische sterkte en stijfheid leiden tot de beste vermoeiingseigenschappen. Deze composieten vertonen een vertraagde schade initiatie, die gevolgd worden door een tragere schade ontwikkeling met hogere energiedissipatie, en een langere vermoeiingslevensduur. Een vergelijking met experimenten op glasvezelcomposieten toonde bovendien aan dat vlascomposieten even goed scoren als glasvezelcomposieten, wanneer de vergelijking gemaakt wordt op basis van naar densiteit genormaliseerde spanningen. Vlascomposieten zouden dus, voor vele bestaande of nieuwe industriële toepassingen, glasvezelcomposieten kunnen vervangen.

Om de volledige levenscyclus van een vlascomposiet te bestuderen, werden drie eindelevensduur-opties voor de vlas-MAPP-composieten bestudeerd: chemische recyclage, mechanische recyclage en verbranding. Er werd aangetoond dat chemische recyclage mogelijk is, en dat de mechanische eigenschappen van de composieten, vervaardigd met de gerecycleerde vezels, aanvaardbaar zijn. Echter, de lange procestijd en de gebruikte chemicaliën en apparatuur hebben een negatieve ecologische invloed. De tweede methode, mechanische recyclage door versnipperen en spuitgieten, resulteerde in composieten met eigenschappen die slechts iets lager zijn dan deze van de vlascomposieten versterkt met matten. Het grote voordeel van deze techniek is echter de snelheid van het proces: grote hoeveelheden materiaal kunnen op een korte tijd versnipperd worden en verwerkt tot nieuwe, spuitgegoten producten. Bovendien wordt de ecologische impact van het gebruik van nieuwe MAPP en vlasvezels dardoor vermeden. De derde methode, de verbranding met energie recuperatie, bleek eveneens een goed alternatief, omdat het gehele materiaal kan verbrand worden, terwijl het een hoge calorische waarde heeft.

Tenslotte, om de vervanging klassieke materialen door vlascomposieten kwantitatief te verantwoorden, werden twee ‘cradle-to-grave’ levenscyclusanalyse studies uitgevoerd, een op de binnenbekleding van het dak van een auto (design gericht op buigweerstand), een tweede op een bumper (impact design). De gewichtsfactor methodologie werd toegepast om correct de hoeveelheden vlas- en glasvezels te bepalen die nodig zijn om dezelfde mechanische performantie te realiseren. De resultaten voor de bumper toonden aan dat de vervanging van glas- door vlasvezel gunstig was voor vezelvolumegehaltes tussen 40 en 50%. Voor 30% was de gewichtsfactor echter hoger dan 1, wat betekent dat een hogere massa vlas (1.11kg) in plaats van glasvezels (1 kg) nodig is om dezelfde impactweerstand te realiseren. Voor de toepassing gericht op buigweerstand was het vlascomposiet steeds gunstiger dan het glasvezelcomposiet. Globaal toonde deze studie aan dat vlasvezelcomposieten een ecologisch verantwoorde keuze zijn, in vergelijking met glasvezelcomposieten, maar dat de vergelijking van de mechanische eigenschappen specifiek voor elke toepasssing moet uitgevoerd worden.

List of abbreviations

ANOVA	Analysis of variance
ASTM	American Society for Testing and Materials
BMC	Bulk Molding Compound
CAI	Compression After Impact
CM	Compression Moulding
DMA	Dynamic Mechanical Analyser
DMC	Dough Molding Compound
DCB	Double Beam Cantilever
ELV	End-of-Life Vehicles
ENF	End Notched Flexure Test
EOL	End-Of-Life
FAI	Flexure after impact
FBI	Flexure Before Impact
FRC	Fiber Reinforced Composite
FFRP	Flax Fibre Reinforced Composites
GFRP	Glass Fibre Reinforced Composites
IFBT	Impregnated Fibre Bundle Test
ISO	International Standards Organization
LCA	Life cycle assessment
LCM	Liquid Composite Molding
LVI	Low velocity impact
MFA	Microfibrillar angle
MAPP	Maleic Anhydride grafted Polypropylene
MTS	Mechanical Testing and Simulation machine
NFRP	Natural Fiber Reinforced Plastics
NL	Non-linearity
phr	parts per hundred
Quasi-UD	Quasi-unidirectional fabric
PP	Polypropylene
Prepreg	Pre-impregnated
RH	Relative humidity in %
ROM	Rule of mixtures
RT	Room temperature
RTM	Resin transfer moulding
SEM	Scanning electron microscope
SFT	Single Fibre Test
TGA	Thermogravimetric analysis
TEX	Unit of textile measurement (linear density)
TH	Thermoset
TP	Thermoplastic
TPM	Turns Per Meter
UD	Unidirectional
UTS	Ultimate Tensile Strength
VIS	Initiation of fracture obtained by visual observation during DCB test
XRD	X-Ray Diffraction
3PBT	Three-point bending test
4PBT	Four-point bending test

List of symbols

C_v	Heat capacity at constant volume
D1	Diameter of major axis an ellipse
D2	Diameter of minor axis of an ellipse
e	Thickness
E_1	Stiffness of the composite calculated between 0% and 0.1 % strain
E_2	Stiffness of the composite calculated between 0.3% and 0.5 % strain
$E_{f,1}$	Stiffness of the technical fibre calculated between 0% and 0.1 % strain
$E_{f,2}$	Stiffness of the fibre calculated between 0.3% and 0.5 % strain
E_m	Stiffness of the matrix
exp	Exponential function
dV	Infinitesimal change in volume
E	Modulus/stiffness
E_b	Flexural modulus
E_i	Absorbed energy upon impact
F	Load in Newtons
M_{Fc}	Critical mass factor
M_{Fo}	10% Overestimate of the mass factor
M_{Fu}	10 % Underestimate of the mass factor
N	Number of layers in a composite
P	Probability of failure
q	Heat added to the system
S_o	Initial static strength
T_g	Glass transition temperature
T_m	Melting temperature of a polymer
V_f	Fibre volume fraction
V_m	Matrix volume fraction
W_f	Weight fraction of fibres in %
w	Work done by the system
wt%	Percentage of weight
α	Level of confidence in a statistical analysis
Δ_m	Mass difference of the composite
Δ_{max}	Maximum deflection of a plate
ΔU	Change in internal energy
δ	Weight difference
ε	Strain at maximum stress
μ-CT	X-ray micro-tomography
μ_x	Mean value
ρ_{surf}	Fibre aeral density
ρ_{vol}	fiber density
$\boldsymbol{\rho_{subscript}}$	Density of the material indicated in the subscript
σ_f	Strength of the fibre
σ_c	Strength of the composite
$\boldsymbol{\sigma_x}$	Standard deviation
ν	Poisson coefficient

Table of contents

Chapter 1
Introduction

The historic agreement between 195 countries on the climate change at the Paris Conference on the climate (COP21) held in November 2015[1] is more than ever challenging our current lifestyle and new technological developments. All countries have agreed to new measures to limit the global world warming between 1.5°C and 2°C by 2100. Previous measures in October 2014 by European leaders agreed on a new package of measures to tackle climate change on top of the existing 2020 goals[2]. These include a 27% increase of energy efficiency, 27% of the energy will be generated with renewable sources and 40% reduction of greenhouse gases by 2030 in comparison to 1990 levels. The package stirred a debate between climate activists and politicians on whether these measures go sufficiently far to ensure emissions are cut to safe levels fast enough[3].

Another resolution from the European Union, the End of Life Vehicles Directive[4], involves stringent new rules for the re-use and recycling rate of automotive components which has increased up to 85% by weight. These new regulations make it clear that European countries as well as the rest of the world will have to continue de-carbonising their economies and in order to achieve these goals.

In recent years, the fibre reinforced polymer composite industry has grown exponentially in many areas such as automotive, aerospace as well as marine and construction. Various types of composites already exist, and their quality depends on the structural and chemical properties of the raw materials that are used, specifically the fibre reinforcement and polymer matrix, and how they interact with each other. Although the fibre-reinforced composites have good mechanical properties and long term performance (e.g. fatigue, impact and moisture resistance), most of the fibres are synthetic based (e.g. silica) while

[1] http://www.cop21paris.org/
[2] http://www.consilium.europa.eu/en/policies/climate-change/2030-climate-and-energy-framework/
[3] BBC News. EU leaders agree CO2 emissions cut, 26.10.2014. URL http://www.bbc.com/news/world-europe-29751064.
[4] http://ec.europa.eu/environment/waste/elv/

the resins are petroleum based. Unfortunately, oil resources are decreasing and alternative solutions must be proposed for the future in order to comply with increasing environmental awareness.

Lately, the use of natural fibres in replacement of less environmentally-friendly products, such as glass fibres, has become a strong interest in composite manufacturing in response to society's demand for using more renewable resources. The introduction of green materials is an interesting choice since their use will help reduce the world's dependence on petroleum products. Using natural fibres doesn't require major changes in the current methods for composite manufacture. The interest is growing thanks to their key functionalities such as acoustic and thermal insulation, vibration damping, and being renewable.

In terms of mechanical performance, flax fibres are known to be as tough as conventional glass fibres, and are the strongest of the natural fibre family. Also, the flax fibre modulus is comparable to that of glass but flax has a lower density. The excellent mechanical properties of flax, combined with the added functionalities bring some unique advantages that make them a very attractive potential material for fibre reinforced composites. However, in order to take advantage of all its benefits and achieve the envisioned improvements, a good understanding is required of the interaction between the natural fibres and the polymer matrix in composite materials.

In this thesis, the properties of flax composites will be thoroughly investigated by looking specifically at the influence of commercially available textile architectures on one hand, and of the matrix type on the other hand. The first step deals with the tensile and flexural properties characterization. This study is carried out in order to establish a reliable database for the materials selection process according to the desired application. This is followed by the characterization of the stiffness and strength properties of the fibres and yarns constituting the preforms. This information combined with the geometrical information of the yarn or fibre (twist, ends picks and counts, etc.) will allow the use of modelling tools to predict the mechanical performance of the fibres or yarns in composites.

It has long been recognised that fibre reinforced composites are sensitive to impact damage. Even very low impact energies could result in non-visible damage, with a sensible decrease of the residual properties. In order to penetrate with these materials into the high-end market, a full understanding of the impact behaviour will be established by looking closer at the influencing factors mentioned. One of the most common reasons of failure in any type of machine with moving components are when they are loaded with a cycling stress, called fatigue. Thus, a better understanding of the long term properties of flax fibres is essential to ensure the durability of a part.

The last part of this research closes the loop on the product life cycle. An investigation of end-of-life possibilities for the flax composites and their environmental impact is carried out. These data are later on implemented in a comparative life cycle study between flax and glass composites in two automotive cases. This last step is essential to ensure that the introduction of natural fibres instead of environmentally more harmful man-made fibre is beneficial for the environment and will participate in fulfilling the target of the COP 21 the other regulations in place.

Chapter 2
Flax fibres and their composites: A review

Lately, the use of natural fibres in the composites industry has been steadily growing thanks to their good mechanical properties, manufacturing effectiveness, acoustic and thermal insulation, good vibration absorption (damping), as well as their renewability [1, 2]. As of today, they have the potential to be used in many industries as high performance composite applications to replace less sustainable products such as glass fibre composites [3-6]. In 2012, more than 352 000 tons of wood and natural fibre biocomposites were produced in Europe, claiming an average 10-15% of the total composite market [7]. Their low density and high specific properties makes them interesting for this specific industry where lightness is synonymous with less fuel consumption [3, 8-10]. Table 2-1 summarizes all the advantages and drawbacks of using synthetic (e.g. glass) and natural fibre (e.g. flax) reinforcements.

	Glass fibres	**Flax fibres**
Advantages	Report mechanical properties / prices Specific resistance Good adhesion with all resins Temperature resistance Incombustibility Expansion and low thermal conductivity Good dielectric properties Good fire resistance	Very good mechanical properties Biodegradable and renewable Neutral CO_2 emissions Good thermal and acoustic insulation Non-toxic Good resistance in aggressive environments and UVs Low cost (short fibres)
Drawbacks	Not "environment-friendly" Premature aging in contact with water	Water sorption Poor dimensional stability Poor aging and thermal performance Relatively unknown long term properties: fatigue and impact behaviour unknown Sourcing

Table 2-1 : General advantages and drawbacks of glass (synthetic) and flax fibre (natural).

A selection of natural fibres is shown in Figure 2-1. The term "natural fibres" includes fibres of plants, animals or fibres of mineral origin. At the industrial level, the use of natural reinforcements may help to reduce the costs in addition to a lower environmental impact

and give better prospects for recycling. In the building sector, the interest is not only economic and aesthetic, but also technical by providing thermal insulation levels far superior to conventional materials such as rubber or glass wool [11, 12].

The "Synthetic by nature" exhibition at Gent Design museum in April 2015, prepared in collaboration with the KU Leuven and the LUCA School of Arts in April 2015, highlighted the newest and most innovative biocomposites designs. The exhibition showed about 50 products using flax or hemp fibre reinforced composites in a wide range of application domains, from cars to bikes and skis, fishing rods, chairs and tables. Some examples are presented in Figure 2-2 and Appendix A. In this chapter, a complete review of the state of the art on flax fibres and their composites is presented.

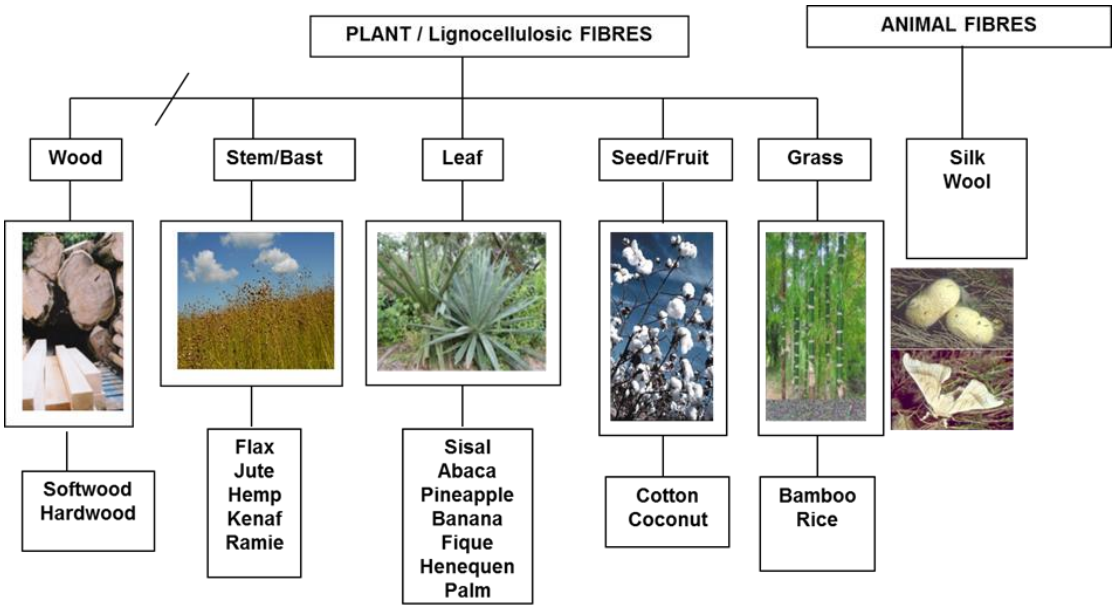

Figure 2-1: Overview of natural fibres types [12].

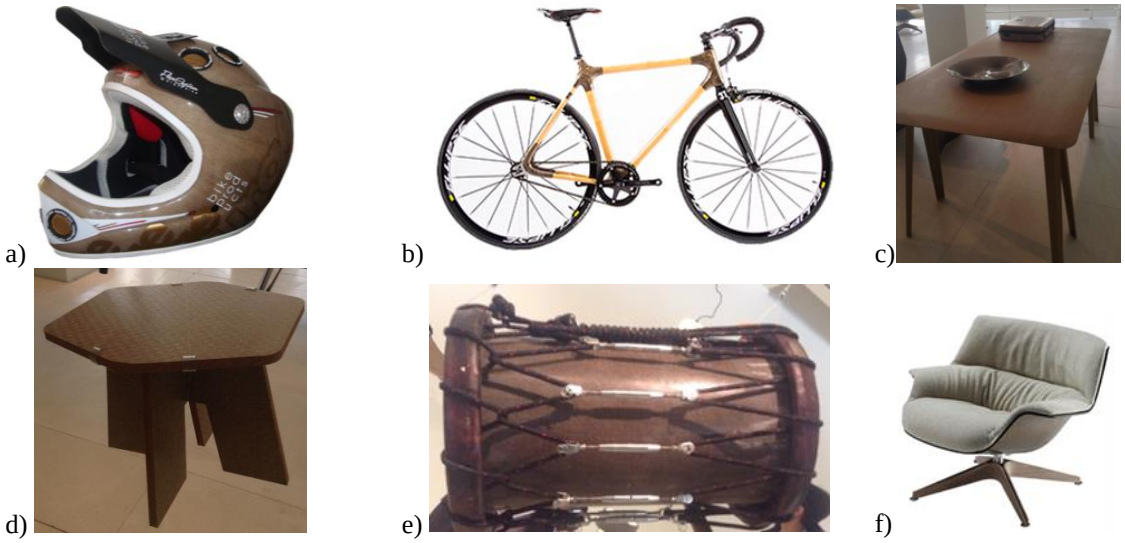

Figure 2-2: a) *Urge* mountain flax helmet, b) *Tiger Bamboo* bike with flax fibres joints from *Ozon Cyclery*, c) flax-Jute *Lightness table* from David Derksen with the *Flax Tray* from Bram Geenen, a) flax table from *Les M*, e) Chenda instrument from *McGill university* and f) flax composite chair with linen lining [13].

2.1 The flax fibre – Growing a composite

Flax, *Linum usitatissimum*, is part of the *Linaceae* family that includes a variety of 250 races such as Eden or Aramis[1]. It is potentially the first "domesticated" plant and amongst the oldest ones in the world. Flax was extensively cultivated in ancient Ethiopia and Egypt. Michael Balter [14], reported that spun, dyed, and knotted wild flax fibres were found in a Georgian prehistoric cave dating 30000 years, showing that flax was already used by humans at an early stage [14, 15]. The flax plant is an annual plant that can grow up to 1.2 m with slim stems. The cultivation of flax requires very few fertilizers or pesticides and 8 weeks after sowing, the plant can reach 10–15 cm in height, and will grow several centimetres per day under its optimal growth conditions, reaching 40–91 cm within 15-25 day period [16]. Flax fields are easily recognized thanks to their pure pale blue flowers as shown in Figure 2-3.

Throughout the world, flax is mainly grown for its seeds used in many food products to produce flax oil or as a food additive (e.g. bread), and is known as "seed flax". In Europe, the cultivated flax types called "fibre flax" is mainly destined to the production of flax yarns for linen fabric production. The flax fibre is extracted from the bast of the stem and has a soft, lustrous and flexible feel. The best quality fibres are used for the weaving of linen fabrics destined to the fashion industry, lace and sheeting and coarser grades are used for twine and rope. Flax can also be used for the manufacturing of high-quality paper or for printed banknotes.

Figure 2-3: A flax field in bloom in Normandy [17].

2.1.1 The extraction of the fibre

Before the flax fibre is ready for textile production, several steps are undertaken as seen in Figure 2-4. First, after approximately four months of growing (from April to June/July), the stem is pulled out of the soil and placed in the field for about 6 weeks. As seen in Figure 2-5 a. This process is called dew-retting and is used to loosen and separate the flax fibres bundles from the stem by degrading the pectin that surrounds the fibre bundles. During these weeks, the flax straws are rotated so that every side is in contact with the sun and the soil. It has been shown by several authors [18-20] that the degree of retting highly influences the fibre quality, the more pectins are dissolved the better quality. Retting is a

[1] http://www.saneco.com/spip.php?article5

rather simple and low cost step, however, this process is greatly dependent on weather conditions and therefore requires an extensive knowledge and experience in order to obtain the optimal flax properties.

Once this process is complete, the stem and the woody core are broken in several small parts (the latter named shives) and the loosened long fibres are extracted from the cortical tissue during a process called *scutchin*g. After this step, fibres (long and short) and shives are separated. After scutching, the fibres are still rough and thick and need a refining and purifying step named *hackling* which will result in fine and pure technical fibres. Two other by-product are created at this stage, the shives and tows. These produced short fibres can be later on transformed into slivers by carding or used in the production of flax mats or low-cost compounds for injection moulding. In the next step, the fibres can be spun into yarns or used as rovings to produce unidirectional structures. An overview of the flax processing step after dew-retting is presented in Figure 2-6.

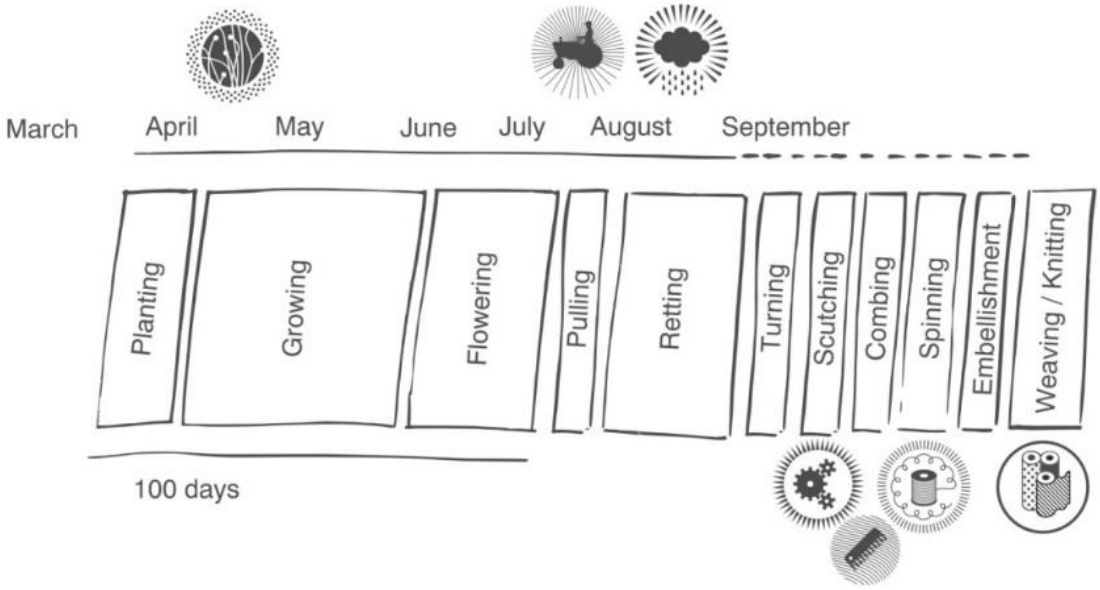

Figure 2-4: The traditional value-added chain from flax plant to textile products. From Chapter II in [2].

a)  b) 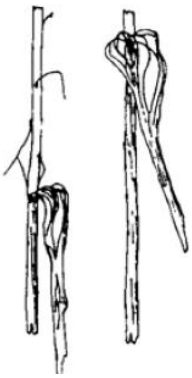

Figure 2-5: a) flax fibre in-field retting [21] b) Separating the fibres from the stem during retting [22].

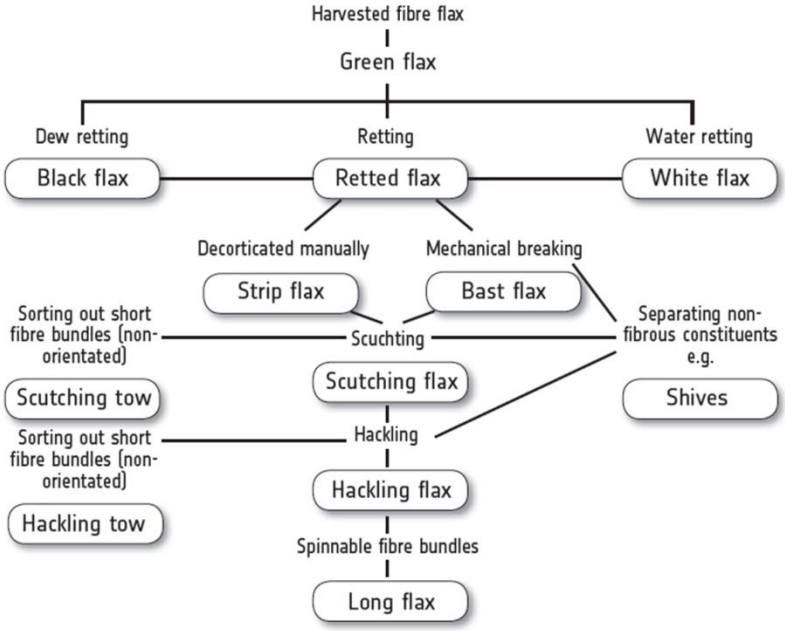

Figure 2-6: Overview of the flax processing. From Chapter II in [2].

2.1.2 Morphology and constituents

The flax stem is constituted of several fibre bundles and every bundle consists of technical fibres which are themselves composed of several elementary fibres as shown in Figure 2-7. The elementary fibres are the single plant cells with a thickness average between 20 µm and a length between 20 and 50 mm [23]. Their morphology consists of two cell walls arranged as concentric cylinders with a channel in the middle called the lumen (see Figure 2-8). The lumen can be as small as 1.5% of the cross section of the elementary fibre.

The primary cell wall is about 0.2 µm thick and is composed of the secondary cell walls S1 to S3. The S2 layer accounts for the highest proportion of the cell wall and is the one responsible for the structural performance of the plant (govern the strength and stiffness). This layer is constituted of highly crystalline cellulose microfibrils that are spirally wound oriented with a tilt angle of about 10° in a matrix of amorphous cellulose, hemicellulose and lignin.

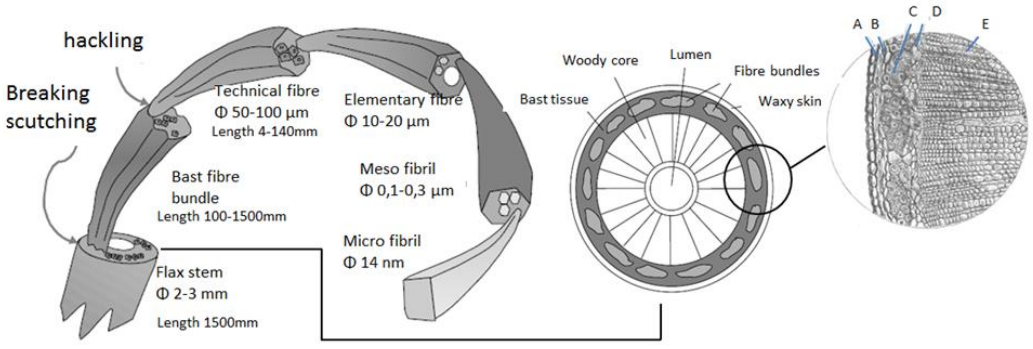

Figure 2-7: Flax plant structure of the flax fibre, a) the epidermis, b) the cortical parenchyma, c) the bast with fibre bundles, d) the cambium, and e) the wood core [24, 25].

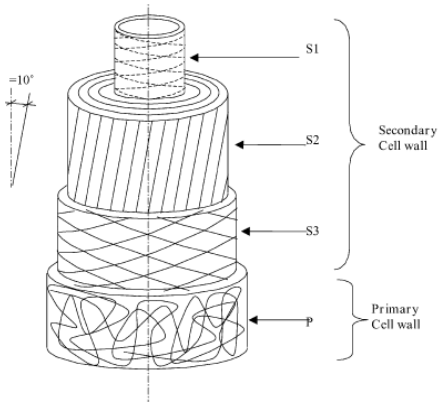

Flax constituents	
Cellulose (%)	65-85
Hemicellulose (%)	10-18
Lignin – Pectin (%)	2-7
Waxes and other components (%)	2

Figure 2-8: Internal structure of an elementary flax fibre [26] and the chemical composition of flax fibres [27, 28].

Flax fibres chemical composition is a mix of four main components: cellulose, hemicellulose, lignin and pectin [29, 30]. Their proportions are described in Figure 2-8. The pectin is primarily situated in the primary cell wall [31-33], which also contains some lignin, cellulose and hemicellulose [32]. A technical fibre is defined as the composition of several highly cellulosic elementary fibres glued together by weak pectin, lignin and hemicellulose materials. Secondary constituents like fats, waxes, lipids and ash are also present, but at a very low percentage.

Cellulose is an organic compound that is chemically based on the polysaccharides $(C_6H_{10}O_5)_n$. It is the most abundant organic polymer on earth [34] and is the main structural component of the primary cell walls of most plants such as flax, hemp and wood. The fibres are composed of the linear molecules (‘polymers’) consisting of 3000 to 10000 un-branched glucose units (‘monomers’) linked together in long chains through inter-molecular bonds (e.g. hydrogen bonds creating the 3D-structures making the cellulose semi-crystalline) and intra-molecular bonds (C-C bonds creating long chains) into highly ordered cellulose microfibrils. In the main structure of the fibres, the cellulose microfibrils are the ones which govern the stiffness and strength of the plant, meaning the higher the amount of cellulose, the stronger and stiffer the fibre. The cellulose present in the fibres are partly crystalline (at least 60%) and partly amorphous[35].

Hemicellulose is the second constituent of the flax fibres and is composed of polysaccharide chains like cellulose, but those chains are shorter (500 to 3000 glucose units) and branched. They have an amorphous state and they possess a lower molecular weight, which explains their low resistance to chemical attack. The hemicellulose is highly hydrophilic and plays a large role in the water sorption behaviour of the fibres.

The lignin is a complex three-dimensional chemical compound, composed of a cross-linked polyphenolic network situated between the hemicellulose regions surrounding the microfibrils, which is commonly present in the secondary wall of plants. It is the second most common organic compound on earth after cellulose. Lignin’s main function consists of filling the space in the cell wall between cellulose, hemicellulose and pectin components. It has an amorphous structure with a high molecular weight. The lignin is highly hydrophobic compound and thus impermeable to water absorption [36].

Pectin which is present is the non-wood primary cell wall of plants has similar polysaccharide chains as hemicellulose. It can be commercially produced and is usually

used as a thickener or gelling agent. In plant fibres, it is regarded as the "glue" that keeps the cell walls and the structure together [23, 37].

The chemistry and physical structure of the flax fibres determines their intrinsic characteristics and properties. A higher cellulose content is an indication of a higher stiffness and strength [38]. Each layer of the elementary fibre has its own orientation of microfibrils. The orientation of the microfibrils of the thickest layer, S2, determines the mechanical properties. In this layer, the microfibrils are fixed in a helical structure with a 10^o angle called the microfibrillar angle (MFA). The lower the MFA (towards the unidirectional directions - 0^o), the higher the stiffness will be as seen in Figure 2-9. In Table 2-2 it can be seen that flax has one of the lowest MFA amongst the natural fibres, explaining its good mechanical performance.

	Flax	***Sisal***	***Coir***	***Cotton***	***Jute***	***E-Glass***
Diameter (µm)	11-20	50-200	100-460	12-20	30-150	5-25
Density (g/cm³)	1,4	1,45	1,1-1,3	1,51	1,45	2,55
MFA (°)	10	10-22	30-49	/	8,1	/
Cellulose/Lignin (%)	65-85/1-4	67/12	43/45	85-98/-	63/12	/

Table 2-2: Comparison of various natural fibres characteristics vs glass fibres [39].

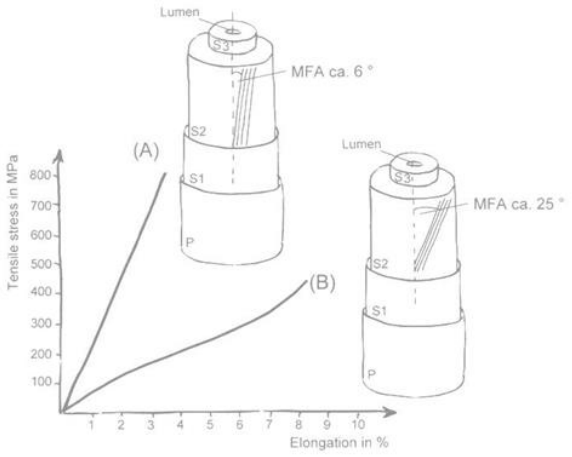

Figure 2-9: Influence of the cellulose microfibrillar angle (MFA) on the mechanical properties of plant fibres for a) hemp fibres and b) cotton fibres [40].

2.2 Flax fibres reinforced composites

2.2.1 Fibre properties

The mechanical properties of flax fibres (elementary and technical) are extensively reported in literature since these types of fibre have the potential to be used for composite reinforcements in replacement of synthetic fibres such as E-glass fibres. The main characteristics of the flax fibres are their low density of about 1.3-1.5 g/cm^3, their high aspect ratio (length/diameter: 700-2000) and excellent specific properties comparable to the E-glass ones [3, 23, 41-44]. When flax is compared to other natural fibres, it has consistently higher tensile properties. Their natural variability, such as origin, variety, quality of crop, maturity of the plant and harvesting, preconditioning and refinement method, may result in the spread of their properties which can be seen in Table 2-3 [8, 45]. However, it has to be emphasized that the larger variation in strength (800 to 1500 MPa) is mainly due to the fact that in these data both the strength of technical (lower values) and of elementary fibres (higher values) are combined, as will be discussed later. Other variations

may come from the location in the stem of the harvested fibre. In general, fibres located in the lower end of the stem have reduced properties and the higher the position in the stem, the higher the properties of the fibres will be [33, 46].

Technical fibre Property	E- GLASS	CARBON (T300-T700)	FLAX	HEMP	BAMBOO	JUTE
Density (g/cm^3)	2.55	1.8	1.45	1.48	1.4	1.46
Tensile Strength (MPa)	2000-2400	3530-4900	800-1500	550-900	750-950	400-800
Tensile Stiffness (GPa)	70-74	230	55-75	40-65	30-50	10-30
Specific Strength (MPa *cm^3 /g)	780-940	1900-2700	550-1030	370-600	535-680	275-550
Specific Stiffness (GPa *cm^3 /g)	27-29	128	38-52	27-44	21-36	7-21
ε (%)	3	1.5 - 2.1	1,5 - 2	1.6	1.9	1.8

Table 2-3: Mechanical properties of fibres [2, 47-50].

2.2.1.1 Elementary vs technical fibre

Flax fibres can be defined as either elementary or technical fibres. A distinction needs to be made as their properties will greatly differ. Technical fibres are defined as thin long fibres consisting of 10 to 40 elementary fibres (see Figure 2-10). There is a clear difference between the mechanical properties of an elementary and a technical fibre. The measured strength and initial modulus of the elementary fibres were found to be about 1500-1800 MPa and 60-80 GPa [51, 52], respectively, whereas the calculated strength and initial modulus of technical fibres were estimated to range between 800-1500 MPa for the strength and 55 and 75 GPa for the modulus. As the fibre cells bond by weak pectin, lignin and hemicellulose, this leads to a decrease of more than 40% in properties observed for technical fibres compared to elementary fibres. That is due to a weak inter-fibrillar bonding [37]. Lamy et al. [53] and Baley et al. [26] shown that a larger fibre diameter will give a lower stiffness compared to finer fibres. They observed that the tensile modulus of the elementary fibre, caused by the variation in lumen size between fibres, can vary from 39 to 78 GPa for a diameter of 35µm and 5µm respectively.

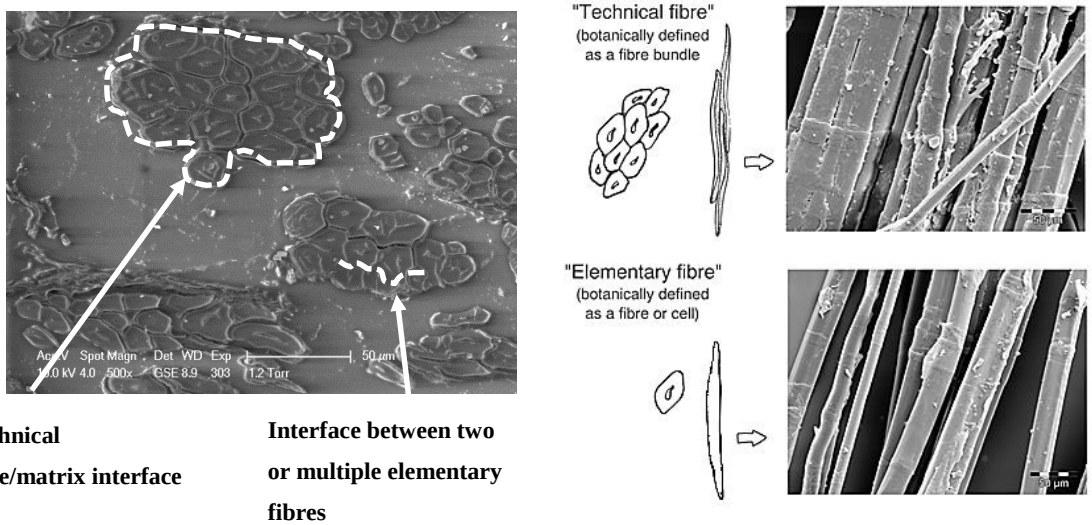

Figure 2-10: a) ESEM Image of a "technical fibre" and its constituting elementary fibres [35] and b) schematic and SEM images of "technical fibre" (upper part) and elementary fibres (lower part) adapted from [2, 54].

2.2.1.2 Stress-strain curves

Coroller et al [55] found a difference of tensile curves between glass and flax fibre as seen in Figure 2-11 a. Comparing to glass fibres whose tensile curve is quasi-linear, the one of flax has three parts:

1. The first part is a linear part;
2. The second is a non-linear part where an internal reorganization of the components related to the variation of the angle of cellulose microfibrils in the S2 layer;
3. The third section of the curve is again linear part.

Other types of curves were also observed during elementary and technical single fibre testing of flax fibres and are similar to the one observed for hemp (Figure 2-11b) [56]. This non-linear behaviour is also seen in the flax composites structure and further details are given in Chapter 5.

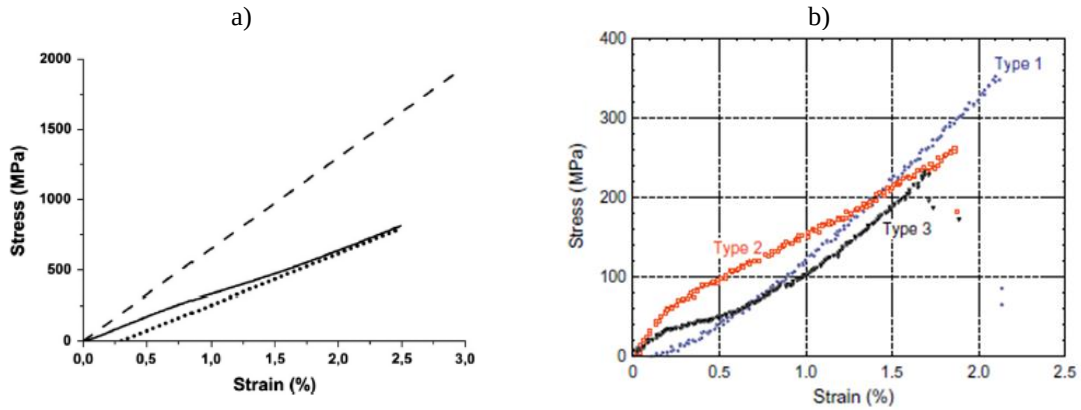

Figure 2-11: a) Tensile curves of glass fibre (dash line) and flax fibre (solid line) [55] and b) typical tensile stress-strain curve shapes for elementary hemp fibres [56].

2.2.1.3 Fibre properties through the impregnated fibre bundle test

The mechanical properties of fibres used in composite reinforcements are currently measured in three distinct ways: single fibre tensile tests (SFT) [57], dry fibre bundle tests [58] or the properties of the fibres are back-calculated from the results of the impregnated fibre bundle test (IFBT) [59]. In the IFBT case, a UD composite is loaded in tension in the fibre direction. From the end results, the fibre stiffness and strength can be back-calculated using micromechanical equations such as the law of mixture (see section 2.3.1). The back-calculated properties depend on the validity of the micromechanical equations used. This is not a problem for stiffness where the influence of matrix and interface are negligible. However, the influence of the matrix, the possible (local) fibre misorientation, the fibre volume fraction and the fibre-matrix adhesion have to be considered for the measured strength [60, 61]. The IFBT is well established for carbon and glass fibres, thanks to its intrinsic advantages [49]:

- A large number of fibres are tested simultaneously, resulting in a rather direct measurement of the average "effective" back-calculated fibre stiffness and strength;
- The test is much less complicated than a single fibre test where a delicate preparation of the tested fibre is required. Moreover, a very large number of individual fibres have to be tested, in order to provide statistically reliable results [57, 62];
- Easy manufacturing and testing of the specimens as they are common practice in the composite world;
- It's a well-established and reliable standard in the industry.

As of today, the IFBT techniques are not well known in the natural fibre community and the question arises whether it could be used to provide fibre data in technical data sheets [63]. Natural fibres, because of their complex morphology and microstructure, distinguish themselves from glass and carbon fibres which have continuous filaments with a stable constant cross section.

The heterogeneity of the glass and carbon fibre microstructure happens at the nanoscale (e.g. the orientation of graphitic layers in carbon fibres), which means the stiffness can be considered as homogeneous on the micro- or fibre scale. However, for natural fibres, and flax in particular, various types of in-homogeneities are present (varying number of elementary fibres over the length of the technical fibre, varying properties of the middle lamellae between the elementary fibre, etc…) which will create a scatter in the stiffness values. Together with these homogeneities, some defects (like kink bands, weak end spots in the middle lamellae due to the retting process etc…) will result in a similar (but not worse) stochastic nature of the strength as found for carbon and glass fibres.

2.2.2 Matrix Materials

The polymer matrix is the second constituent of a composite and used as a "binder" to keep the fibre together. It exists of two major polymer categories: thermosets and thermoplastics. The chemistry of these two categories is very different which will not only vary the composite properties but also determines the manufacturing process that will be used.

Matrix materials present a variety of characteristics as seen in Figure 2-12. Thermosets crosslink in a 3-D network upon curing and cannot be molten or reshaped after processing, whereas thermoplastics solidify after cooling and can be remolten at any stage and many times. Most thermosets have a brittle behaviour with low strain to failure (typically $\varepsilon < 5\%$). On the other hand, thermoplastics display a ductile behaviour, although brittle thermoplastics also exists (e.g. POM). Below the glass transition temperature (T_g), the moduli of thermosets and thermoplastics range from 1 to several GPa [64].

Table 2-5 presents the advantages and drawbacks on the properties and processing characteristics of thermoplastic polymers as compared to thermoset polymers. Furthermore, examples of some polymers, frequently used as matrix in composites, and their properties are given in Table 2-4. It has to be noted that a large variety of polymers exists and the data provided are only indicative. As of today, many polymers are developed for specific properties such as UV resistance or to increase fibre-matrix adhesion.

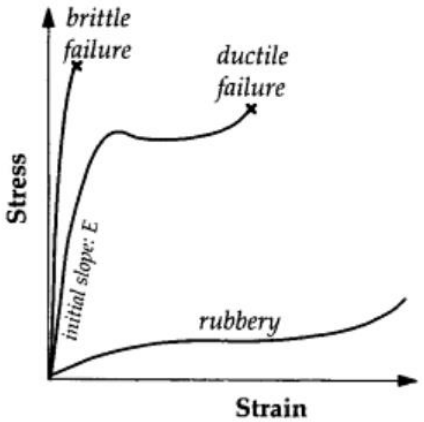

Figure 2-12: Typical stress-strain behaviour of polymers depending on the polymer type [64].

Properties	Thermoset				Thermoplastic		
	Epoxy	Polyester	Vinyl ester	Phenolic	PP	PA	PC
Density (g/cm³)	1.1-1.4	1.1-1.5	1.1-1.3	1.3	0.9	1.1	1.1-1.2
E-modulus (GPa)	2.5-6	1.3-4.5	2-5	4.5	0.1-2	2	2
Tensile strength (MPa)	35-90	50-85	70-80	60-80	25-40	60-70	45-70
Max strain at failure (%)	1-8.5	1-6.5	3-8	1.5	100-600	30-300	100

Table 2-4: Properties of various thermoset and thermoplastic matrix materials [65, 66].

Thermoplastic	Thermoset
Advantages	
✓ Short processing times	✓ Low viscosity
✓ Post-shaping	✓ Low pressure and temperatures needed
✓ Complex geometries possible	✓ Shrinkage limited
✓ High toughness	✓ Good creep resistance
✓ Impact resistance	✓ Good stiffness and strength
✓ Temperature resistance	✓ Good thermal resistance
✓ Easily recyclable	✓ Chemical resistance
✓ Post-formability	✓ Fire retardant
	✓ Creep resistant
Drawbacks	
× High melt viscosity	× In situ reaction requires good control
× Complex flow behaviour	× No reshaping possible after cure
× Shrinkage	× Toxicity of products
× Low thermal stability	× Rather brittle
× Low chemical resistance	× Recycling difficult
× Poor fibre-matrix interface	× Limited shelf-life

Table 2-5: Advantages and drawbacks of thermoset and thermoplastic matrices.

2.2.2.1 Thermoset resins

A thermoset polymer forms a 3-D network as a result of chemical interactions between linear polymer chains with strong covalent bonds, as in Figure 2-13. To obtain this 3D network, a polymerisation and crosslinking needs to take place and is achieved by mixing the polymer with a hardener (and/or catalyst). Thanks to the small molecular mass of the thermoset polymers, the viscosity is low and this allows an easier penetration of the matrix between the fibres at low pressures. If the temperature of the polymer is raised, the cross-linking process will speed-up and the viscosity will rise rapidly. This step is called curing and allows the polymer to form stronger bonds. To obtain suitable properties, a certain degree of cure is required within the polymer. The degree of cure is greatly dependant on time and temperature which are important process parameters.

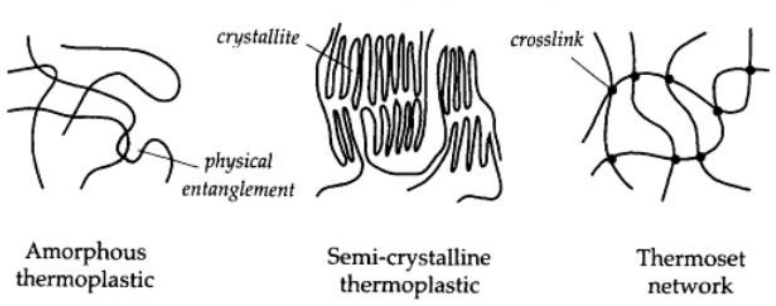

Figure 2-13: Schematic of the polymer structure for thermoset and thermoplastic [64].

The formation of the 3-D structure is a non-reversible process and no post-forming is possible [67]. The crosslinking makes thermosets very strong but brittle, expressed by a low strain to failure. The use of thermosets is also gaining interest in the area of natural fibre composites because of their better mechanical properties and improved fibre/matrix adhesion. Thermoset matrices can fit in many well-established manufacturing techniques such as hand lay-up, spray-up vacuum infusion, pultrusion, autoclave and resin transfer moulding (RTM). However, resins such as epoxies and vinyl ester are relatively more expensive which could be incompatible with high production volume applications. On the other hand, the polyester resins are cheap and can be bought "off the shelf", but their mechanical performances are lower than epoxy.

2.2.2.2 Thermoplastic resins

Most thermoplastic polymers have a crystalline structure, but can also have an amorphous phase like the thermosets as seen in Figure 2-13. In these crystalline areas, the polymer chains show alignment and order. Figure 2-14 shows the shear modulus measured as a function of temperature and the three main regions are shown: brittle, tough-leathery and melt. Below T_g, the polymer is brittle and above T_g, the thermal energy is high enough to break the weak Van der Waals and hydrogen bonds of the amorphous regions. Above the melting temperature of the crystalline part (T_m) the thermoplastic will start melting. When the polymer is cooled down again the material will solidify again. This reversible behaviour of the polymer under the influence of temperature is characteristic for a thermoplastic polymer. It has to be noted that the cross-linked thermosets will not melt and when a sufficiently high temperature is attained, the polymer starts to degrade.

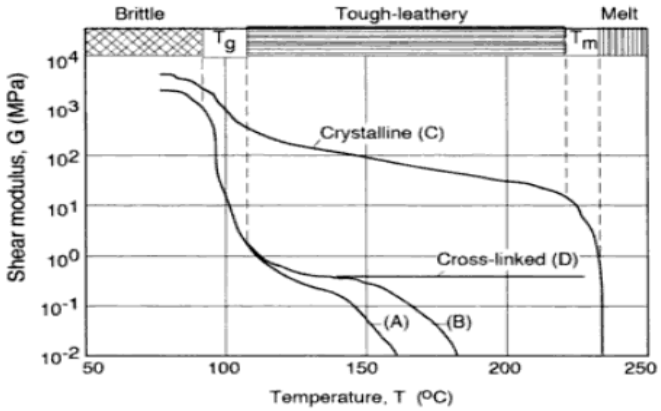

Figure 2-14: The shear modulus for different polymer: a) low molecular weight thermoplastic, b) high molecular weight thermoplastic, c) (semi)-crystalline thermoplastic, d) thermoset matrix [68].

The reversible phase transformation from solid to liquid in thermoplastic polymers opens a wide range of processing techniques. The polymer comes in the form of pellets to be directly used in injection moulding. Semi-finished products, i.e. films, are also popular alternatives for thermoforming or compression moulding processes. However, the viscosity of the molten thermoplastic is much higher than the not yet cross-linked thermosets. Therefore, higher pressures are required to obtain an adequate impregnation of the fibres by the molten thermoplastic matrix. The major benefit of the usage of thermoplastic matrices is the lack of a cross-linking step, which can drastically reduce the production time. The use of thermoplastic matrices is then very interesting and is already extensively used in high volume applications such as in sporting goods and the automotive industry. Figure 2-15 presents the two types of thermoplastic matrices and their characteristics.

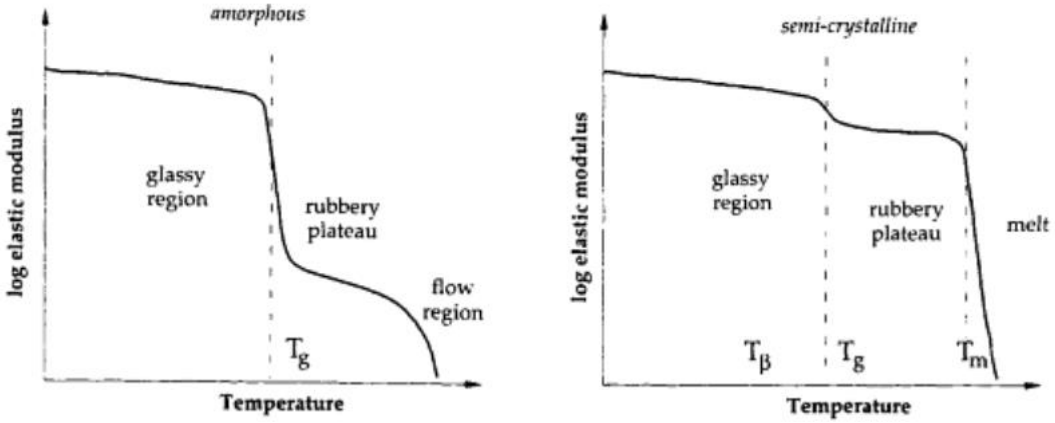

- No accurate melting point and gradually soften;
- Have a random orientation of molecules with polymer chains lying random orientation;
- Don't easily flow in-mould as crystalline polymer;
- Shrink less than Crystalline Polymers.
- Generally yield transparent, water-clear parts.

- Sharp melting point but require higher temperatures to flow;
- Ordered arrangement of molecule chains;
- High shrinkage causing a greater tendency for warpage of the pure polymer;
- Increase of the load-bearing capacity and decrease of warpage by the addition of reinforcements;
- Usually produce opaque due to their dense molecular structure.

Figure 2-15: Thermal transition for amorphous vs semi-crystalline thermoplastic and their characteristic properties [64].

2.2.2.3 Bio-resins

Lately, the increased environmental concerns related to climate change and limited fossil fuel resources are major drivers for companies to find alternatives to petroleum-based products. To solve this issue, bio-based resins have been introduced as new alternatives to petroleum-based resins such as epoxy and polypropylene. These new polymers are usually based on renewable feedstocks such as sugar-cane bagasse (furan), soy bean oil (polyester or PA11) and cashew nut shells (CSNL). Some examples are shown and compared to synthetic matrices in Figure 2-16.

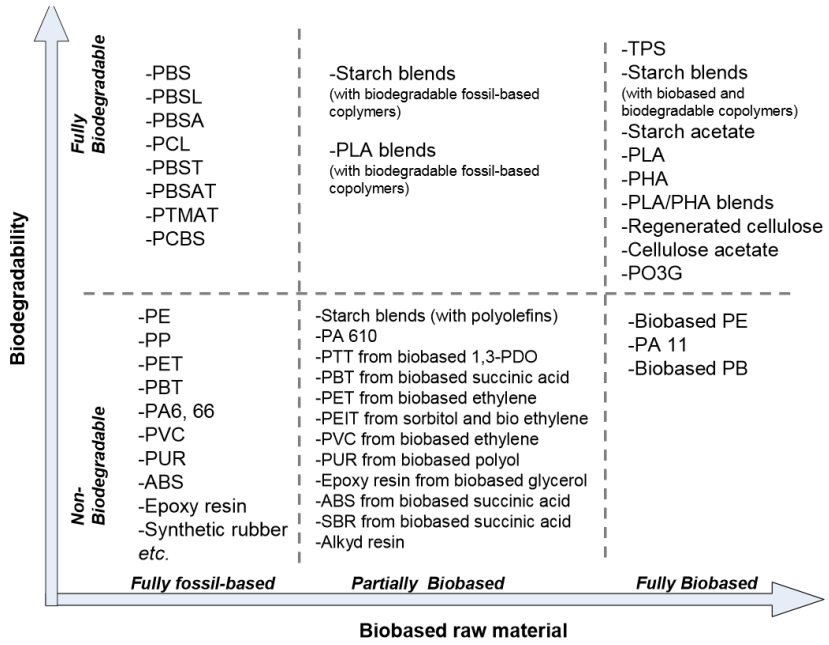

Figure 2-16: Current and new plastics and their biodegradability [69].

2.3 Flax fibre composite properties

Many studies [29, 70-73] have been carried out on flax technical and elementary fibres. The properties and overall quality of flax fibres are dependent on numerous factors such as growing conditions [74], fibre processing and their refinement [75-77]. These characteristics are intrinsically related to their internal structure and chemical composition [8]. Nevertheless, broader studies on the composite level are essential to evaluate the mechanical performance of flax fibre reinforced composites. The performance of the composite can be affected by several variables, such as the yarn twist and crimp, the fibre volume fraction, the manufacturing technique, the reinforcement type (UD, woven, etc.), the applied fibre treatment, the matrix material as well as the compatibility between the flax fibre and the matrix [5, 78, 79]. It has to be taken into account that all the refining process that the flax fibre will undergo (wet/dry spinning, weaving, drying and fibre treatment) will increase their environmental burden.

2.3.1 Influence of fibre volume fraction

The fibre volume fraction (V_f) is an important parameter to take into account as the mechanical properties increase with increasing V_f [1]. However, there is a maximum V_f that can be achieved and above that level, the properties decrease due to a lack of resin to fill all the inter- and intra-yarn spaces, leading to an increase of the void content [80, 81]. The maximum V_f is directly related to the packing arrangement and the fibre orientation and these two factors are directly connected to the manufacturing process and fabric nesting [81]. Madsen et al. [82] have found that for flax and hemp composites, the maximum fibre volume fraction for random mat is 40% and 60% for unidirectional fabrics. Using the fibre volume fraction data, the theoretical elastic properties of a composite can be calculated through the 'rule of mixture' for both modulus and strength as shown in Eq. 2.2 and Eq. 2.2:

$$E_c = E_f V_f + E_m(1 - V_f) \quad \text{(Eq. 2.1)}$$

$$\sigma_c = \sigma_f V_f + \sigma'_m(1 - V_f) \quad \text{(Eq. 2.2)}$$

Where, E_m and σ'_m are respectively the modulus and strength of the matrix and E_f and σ_f the properties of the fibres. It has to be noted that σ'_m the stress in the matrix at the failure strain of the composite calculated assuming elastic deformation of the matrix: $\sigma'_m = E_m * \varepsilon_{u,c}$ (moduli are given in GPa, strengths in MPa).

2.3.2 Influence of the textile architecture

At first, flax fibres were mostly available in short fibres and random mats intended for the thermoplastic composites industry. They were, and still are, processed by injection moulding with thermoplastic matrices or used to produce random mat fabrics [83, 84]. However, these architectures result in a composite with poor properties as the majority of the load is carried by the matrix and not by the fibres due to their random distribution and lower aspect ratio.

To address this issue, researchers have looked into the replacement of the random mats by textiles commonly used for synthetic fibres such as glass and carbon. Research went first towards the development of unidirectional fibre composites (UD) which have a high stiffness in the longitudinal direction (e.g. E=26 GPa and σ=250–300 MPa for flax/PP composites) [85, 86]. This type of configuration allows the building of preforms with various angle combinations from pure UD [0^o], cross-plies [0^o, 90^o]$_s$ to quasi-isotropic lay-ups. When designing a composite laminate, it is important to consider the stacking sequence

of plies as laminates have preferentially should be balanced and symmetric as seen in Figure 2-17. This is necessary in order to eliminate its tendency to bend or warp after demoulding, and it also reduces shear coupling.

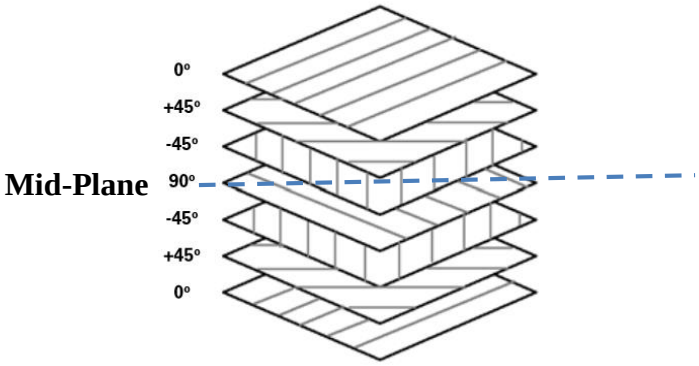

Figure 2-17: Quasi-isotropic configurations made from UD reinforcements [87].

Unidirectional layers are usually the most attractive type of configuration to be used in composites due to their high strength and stiffness. However, they are not easy to drape on a complex geometry mould. In this case, the possibility to use different types of reinforcement architectures, such as textiles, arises for easier composite processing. Textiles can be produced in various architectures defined by the pattern of interlacing of fibres. Several two-dimensional fabric configurations are listed in literature such as plain, satin and twill weaves, quasi-unidirectional, unidirectional (UD) and multidirectional non-crimp fabrics and braided textile configurations. Textile-based composites allow the industry to "tailor" the fibre reinforcement to specific applications in order to obtain the desired performance [88]. Furthermore, their use has significant advantages over unidirectional preforms since they are easy to handle, they have a good dimensional stability and they are easy to drape on complex mould geometries. Examples of textile architecture are shown in Figure 2-18.

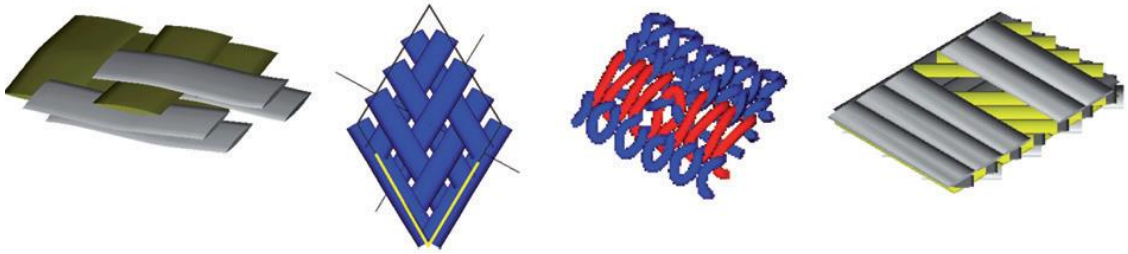

a) b) c) d)

Figure 2-18: Some textile architectures used as composite reinforcement: a)woven, b) braided, c) knitted and c) non-crimp fabrics (from Chapter I in [2]).

Though oriented textile reinforcements, also called fabrics, are out-performing random mat configurations, they still have some drawbacks. This includes a higher manufacturing cost due to the addition of the yarn spinning process. The latter introduces a twist in order to obtain a compact yarn with sufficiently high tensile strength, which allows further processing into a textile [43]. Four types of flax fibre bundles exist for the production of flax textile. They are listed below and shown in Figure 2-19 [78]:

- Hackled flax: which is delivered in a ribbon, without twist;
- Doubled flax: ribbon without twist, mixture of different hackled ribbon and therefore more homogeneous ;

- Roving: a bundle of fibres, with (very) low twist. It is a continuous bundle of different non-twisted or low-twisted technical fibres. It is also called sliver or bundle of technical fibres, and;
- Yarn: bundle of fibres with high amount of twist.

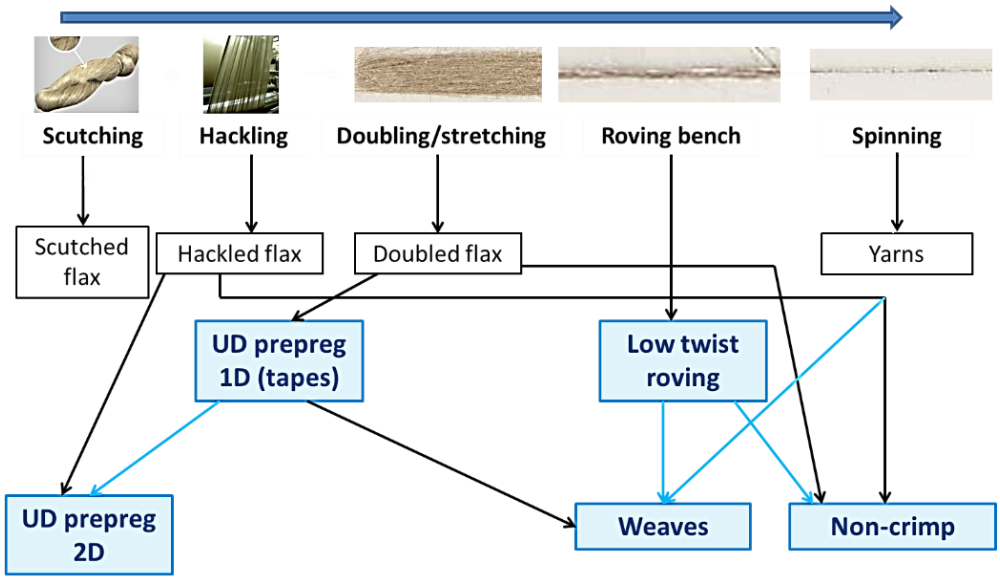

Figure 2-19: Selection of flax textiles for composite – from yarn to textile.

During the extraction process that the flax fibre encounters before refining, tows (containing short fibres of less than 30cm) and shives are also produced. The tows are mainly to be used in the production of flax fibre random mats or low quality yarns. Although the spinning process gives increased strength to the flax fibre yarn to be used for textile production, the more it is refined, the more expensive the yarn will be. Furthermore, by using rovings instead of yarns (at dry state), an increase in composite stiffness and strength of 20% can be achieved. A reduction of the cost is also possible as the fibre is used earlier in the value chain. The dry strength of rovings is lower than that of yarns, but can be high enough to make an easy production of composites possible. An additional advantage of using rovings is the fact that they enable a more homogeneous distribution (allow better nesting when several layers are compacted) of the fibres in the composite.

Once processed into a composite, it is important to keep the fixed orientation of the preform and avoid decrease of properties due to misalignment. It is important to know how the architecture can affect the composites' mechanical properties and in which applications they will provide their best properties. The optimisation of fibre orientation and choice of textile can lead to increased performance of the material [79]. As seen in Table 2-6, the mechanical properties found in the literature do not only depend on the choice of textile architecture but also on the type of matrix that is used. For instance, various UD configurations have different properties for different matrices when corrected for fibre volume fraction. The reported data is indicative and depend on the authors manufacturing techniques which are not further developed. Goutianos et al. [43] have, over the years, studied a wide of range flax textiles which are based on twisted yarns. They have found that replacing random mats by woven fabrics has increased by 3-4 times the mechanical properties as well as improved the toughness [43, 89]. However, adding extra process to the hackled flax will directly affect the embodied energy needed to produce a part due to additional electricity usage for spinning the fibre and weaving the yarns into a textile.

Matrix	Fabric type*		Vf (%)	E** (GPa)	σ** (MPa)	Reference
Polypropylene	Flax	UD	40-55	26	250-300	[86]
		UD warp knitted	28	15	160	[43]
		UD	28	14	140	[43]
	Glass	UD	35	26.5	700	[90]
Epoxy	Flax	PW	34.3	8	109	[91]
		UD	50	40	280	[92]
		UD	42	35	280	[93]
	Glass	UD	48	31	817	[92]
Unsaturated polyester	Flax	UD	58	29.9	304	[93]
	Glass	UD	42	30,6	695	
Low-melting Polyethylene Terephthalate	Flax	UD	38	27,6	292	[94]
Tannin	Flax	UD (0)8	50	9,6	140	[95]
		$[0, +45°, 90°, -45°]_2$		3,5	55	
		$[0, 90°]_4$		4,8	70	
		Non-woven		6,4	55	
		Quasi-UD		13,8	137,5	
Unmodified Acrylated Epoxidized Soy bean oil resin (AESO)	Flax	PW	60	32	280	[96]
		Twill 2x2		11	87	

*UD= Unidirectional, PW= Plain weave, **All values in longitudinal direction.

Table 2-6: Mechanical properties of various flax-textile based composites and reference glass fibre composites. Data taken from various literature references.

2.3.3 Effect of twist and crimp

The performance of the composite can be affected by several variables such as the yarn twist and crimp as well as the compatibility between the flax fibre and the matrix [5, 78, 79]. One of the main issues is the optimisation of the flax yarn, since flax fibres are not continuous by nature and their length can vary from 2-5 cm for elementary fibres to < 30 cm for scutched/ hackled tow (short fibres) and maximum of 1 meter for long technical fibres [97]. Therefore, flax fibres are twisted in order to be held together and create a long and continuous filament as seen in Figure 2-20.

By definition, the twist is the relative rotation of the two ends of a fibre bundle, and is introduced during the spinning process. A certain amount of twist is needed to bind the fibres together into a continuous yarn and to give the yarn sufficient strength and cohesion in order to sustain the high tensile loads during the textile process (weaving, braiding, knitting…) (see Figure 1a) [25, 26]. Depending on the value of turns per meter (TPM) that is introduced during spinning, the final product will be defined as a roving (low twist yarn) or as a yarn (high twist yarn) [78]. It has to be noted that normally a roving is a bundle of fibres with 0^o twist, but in the natural fibre world, also a low twist yarn is called a roving.

The spinning process increases the friction between the technical fibres but also creates an off-axis misalignment with the principal axis of the yarn. In a dry state, a roving has a lower strength than a yarn as found by Goutianos et al. [5]. This makes them unusable for certain processes such as textile manufacturing, as high pulling strengths are required for these processes. In terms of composite properties, a high degree of twist ($\approx 20^o$) in a yarn leads to a decrease in longitudinal strength and modulus of a UD composite by 20% compared to composites made of zero twist rovings [43]. Baets et al. [98] have found that the stiffness

of the fibres/rovings, back-calculated from the composite properties, decreases from 63 GPa to 43 GPa with the introduction of 19° twisted yarns compared to the twistless rovings. Moreover, a higher twist will reduce the permeability of the yarn which may lead to higher void content and lower composite properties [5, 99].

In order to optimize the use of flax fibres in composite parts, it is essential to enhance and optimize the yarn quality, e.g. a twist angle which needs to be suitably high to sustain the pulling force for weaving, knitting or drum-winding machines, but low enough to limit the negative effect of misalignment on the mechanical properties [5, 43].

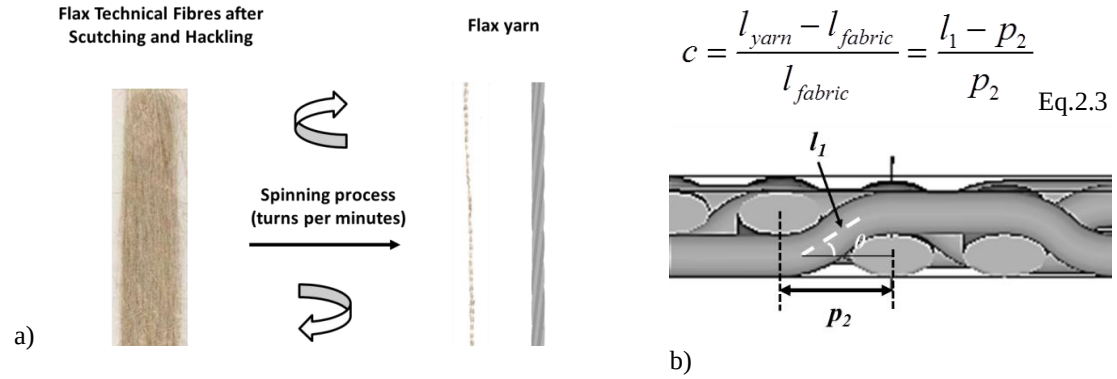

Figure 2-20: a) Definition of twist through yarn processing, b) Definition and calculation of the crimp angle.

During the textile weaving production, a waviness is introduced where yarns are interlaced, which causes an out-of-plane misorientation [100, 101]. This phenomenon, shown in Figure 2-20b, is referred as the "crimp". It can be calculated using the Eq. l, where l_1 is defined as the length of the yarn in the woven fabric and p2 as the straight, in-plane distance between two adjacent yarns. This inclination of the fibres combined with the anisotropy of the impregnated yarn causes a stiffness reduction of the composite, in both warp and weft directions. An average of 20% reduction in tensile strength and stiffness of carbon fibre reinforced composites has been found by Curtis et al. [102] for woven textile compared to several configurations of cross-ply laminates (with UD, non-crimp layers). The localised stress perturbations due to the crimp may also result in premature damage initiation in the composite [103]. Furthermore, a study from Duc et al. [104] on flax twill composites has also shown a decrease in tensile properties with increasing crimp, and hence out-of-plane, angle.

2.3.3 Effect of the interface of fibre and matrix

To ensure an effective stress transfer between the fibre and the matrix a good adhesion between the two is essential [65, 105]. A good fibre-matrix adhesion improves the strength properties. Because of the hydrophilic nature of the flax fibres and the hydrophobic nature of some matrices, this adhesion may not be perfect [106]. Three main types of adhesion exist: physical (deposition on the surface of the fibre), chemical (changes chemical composition of the fibres) and mechanical.

2.3.3.1 The physical adhesion

Physical adhesion is dependent on the surface energies of the matrix and the fibre. A good interaction is obtained when the matrix and fibre have a low wetting angle. This is the case if the surface energies of fibre and matrix are high. The wetting is described by Eq. 2.4 and Eq. 2.5 where γ_{SV} is the force tending to spread the liquid and γ_{SL} is the force tending to

pull it into a drop. Good wetting is obtained when θ approaches zero (equal to a high cosθ) which is achieved when there is chemical similarity between matrix and fibre. Thus, γ_{SV} and γ_{LV} are high and γ_{SL} is low. The work of adhesion, representing the wetting of a solid by a liquid, is described in Eq. 2.6.

$$\gamma_{SV} = \gamma_{SL} + \gamma_{LV} \cos\theta \quad \text{(Eq 2.4)}$$

$$\cos\theta = \left(\frac{\gamma_{SV} - \gamma_{SL}}{\gamma_{LV}}\right) \quad \text{(Eq 2.5)}$$

$$W = \gamma_{SV} + \gamma_{LV} - \gamma_{SL} \quad \text{(Eq 2.6)}$$

Several types of physical treatments exist, the most used for fibres being the cold plasma and the corona treatments. In the cold plasma treatment, fibres are exposed to plasma (partially ionized gas), which makes their surface more reactive without affecting their bulk properties. Depending on the gas employed, the plasma treatment can make the surface hydrophilic or hydrophobic. By exposing the fibres to a plasma, the hydrophilic properties of the fibres are enhanced by introducing polar functional groups such as –CO-, C=O- and –COOH-. These bonds are induced by the bombardment of the surface by the ions in the plasma [107]. However, to achieve a hydrophobic surface, plasma treatments containing fluorine are needed [108]. The corona treatment is based on the discharge that occurs when there is a localized electric field gradient on the surface, which in return causes the ionization and electrical breakdown of the air near the fibre surface. The polarity of the surface is increased during treatment by introducing polar functional groups. Excessive treatment of the fibres may however lead to fibre surface damage [109].

2.3.3.2 The chemical adhesion

Chemical adhesion is obtained by chemically bonding the fibre and the matrix. It can be done by introducing a coupling agent as a ternary reactant to form bonds between the hydrophilic fibre and the hydrophobic matrix. The chemical treatment can be performed on either the fibre or the matrix material. A commonly used treatment in flax-polypropylene (PP) composites is the addition of maleic anhydride (MA) to the PP to increase wetting and adhesion. The MA forms a covalent bond between the anhydride group of the MAPP (hydrophobic PP) and the OH group of the cellulose (hydrophilic flax) [110].

A series of chemical treatments are also applied to flax fibres, such as acetylation, mercerization or silanisation. The acetylation treatment involves the formation of acetyl groups (CH_3CO-) on the fibre surface to make the surface more hydrophobic and to improve the fibre-matrix bonding. However, the high non-uniformity of the acetylation of the fibres may cause important variation in properties [111]. With the alkali treatment, also known as the mercerization process [112], cellulosic fibres are treated with sodium hydroxide (NaOH) which aim at removing the hydrogen bonds. The addition of NaOH to flax fibre helps the ionization of the hydroxyl group to the alkoxide [113]. The mercerization process directly influences the cellulose, the degree of polymerization and the dissolution of lignin and hemicellulosic compounds. Indeed, the alkaline treatment not only makes the natural fibre less hydrophilic and thus, more moisture resistant, but it also "cleans" the fibre by removing impurities and a certain amount of hemicellulose, lignin, pectin and waxes. As a consequence the fibre surface becomes more uniform while the surface roughness increases resulting in increased mechanical interlocking and fibre-matrix adhesion [112].

In a silane treatment, silanol ($CH_2CHSi\ [OC_2H_5]_3$) reacts with the hydroxyl groups of the fibre. Originally the treatment is applied to modify the surface of glass fibres. Compared to the alkali treatment where some components are removed through dissolution, the silane is said to be a coating method [114]. Together with the change in the surface chemistry, this leads to an increase in adhesion and composite tensile strength properties [115]. Other chemical fibre treatments are more specific to the chosen matrix system. For example, a benzoylation treatment is often used to improve the adhesion with a polystyrene (PS) matrix. There is a variety of other chemical treatments, such as acrylation, permanganate peroxide or, isocyanate treatment, that could be used to chemically enhance the fibre-matrix bonds [112].

2.3.3.3 The mechanical adhesion

The mechanical adhesion is obtained when the matrix is mechanically locked into the fibres, if the fibres have a sufficiently rough surface. Treatments, such as the alkali treatment, can be designed to enhance the mechanical interlocking by roughening the fibres, without extensively damaging the fibres or decreasing its properties [112, 116]. This process can also be used as a pre-treatment to clean the fibre surface from impurities, while this improves the fibre matrix bonding, or to increase the efficiency of a physical or a chemical treatment [117].

2.3.4 Effect of moisture

Flax fibres and natural fibres in general are more sensitive to moisture than synthetic fibres. Grillet [118] has studied the effect of moisture absorption at different relative humidity levels RH (50%, 75% and 90%) on untreated and chemically treated (to make them more hydrophobic) UD flax-biopolyester composites (V_f=40%). For the untreated composite, the saturation level at 50% RH is around 2wt%, while it increase to 5wt% at RH 75% and 8wt% at RH 90%. If the glyoxal chemical treatment is applied, moisture uptake decreases to 1.5wt% at RH 50%, 3%wt at RH 75% and RH 90%. Other treatment, alkali and DMDHEU, lead to similar moisture uptake than the untreated flax below RH 75%. Above RH 75%, alkali and DMDHEU lead to 7wt% and 9wt% respectively.

Arbelaiz et al. [110]studied the effect of moisture on flax-PP composites. Since the PP matrix is hydrophobic, the water uptake of the composites was related to the presence of the flax fibres. They observed an increasing water uptake with increasing fibre volume fraction going from of 1wt% at V_f =20% to 15%wt at V_f =60% when the composite is fully immersed in water.

Chen et al. [119] studied the moisture absorption of bamboo/vinyl ester composites. They have found that the moisture content increase from 5wt% at RH 40% to 15% at RH 80%. This results was related to the internal structure of the bamboo fibre which have an open "honeycomb" type of structure where the water is held. Furthermore, bamboo fibre are known to have high lignin content (≈32%) which are hydrophilic and thus sensitive to moisture. Symington et al. [120] compared the modulus and failure strain of cellulose-based composite at different environmental RH: 50%, 65%, 90% and immersed in water (100%). He has found that flax fibre weight increases by a 120% when immersed into water while coir has a 70% and abaca 164% weight gain. They also observed that the moisture had negative effect on tensile strength and modulus. However, no clear influence was seen for the strain to failure. It has to be noted that full immersion (water ingression within the lumen) is considered as the "worst case scenario" is not likely to occur in real life application.

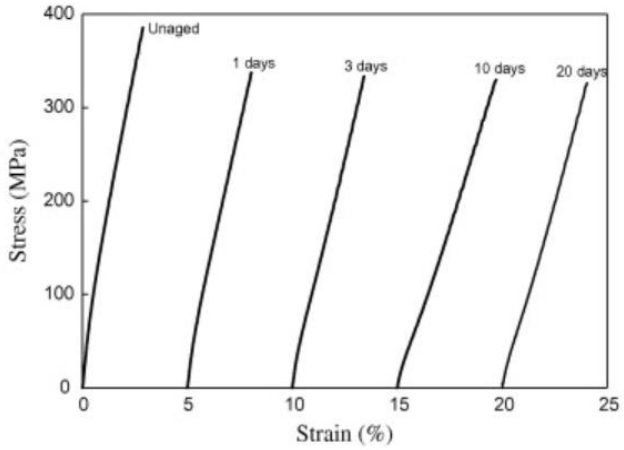

Figure 2-21: Stress-strain curve of flax fibre reinforced composites for different immersion times. Each graph has a 5 % strain offset [121].

Figure 2-21 shows the stress-strain curves of a UD flax-epoxy composite composed of 11 layers, and immersed in water for different times. A 13% drop in strength was found after one day of water immersion and then stabilized. On the contrary to the strength, the maximum strain to failure and the modulus remain immersion time dependent [121]. At saturation (after 20 days), the modulus decreased by 39% and the strain increased by 63%. The moisture uptake will increase faster if the system is heated without changing the damage mechanisms which allows researchers to simulate the long term water gain without lengthy tests [122].

2.3.5 Effect of fibre drying

The presence of the hydroxyl group in the main component of flax, namely cellulose, leads to poor adhesion with a hydrophobic matrix (like PP). Hence, before composite manufacturing, the fibre has to undergo a drying step to reduce its moisture content. The drying rate depends on the amount of free and bound water removal from the free surface and the movement of moisture from the interior to the surface. The temperature-time combination for the drying has to be optimal to avoid early degradation of the fibres [123].

Two main techniques used for fibres drying are conventional drying and microwave drying. In conventional drying, the fibres are placed in an environment where the humidity and temperature is controlled, such as an oven or a climate chamber. In this case, the heat enters the fibres from the surface. Microwave drying heats the fibres from within causing a volumetric heating [124]. When the microwaves hit with the water molecules in the fibres, they cause oscillations of the polar groups molecules leading to frictional heating. To reduce the drying time, microwave heating can be combined to conventional heating. Mixing these two techniques, creates a uniform drying and may lead to a better composite performance.

Different drying procedures were studied for nettle leaves. The first conclusion was that the drying time and energy consumption for microwave drying was significantly lower than for conventional drying[125]. As the drying of the fibres is a critical step before manufacturing, it will have an effect on the energy consumption and ultimately the environmental performance of the final product. Similar experiments conducted on flax fibres found that the drying rate increased with 48,5% when conventional hot air drying was combined with microwave drying as seen in Figure 2-22 [124].

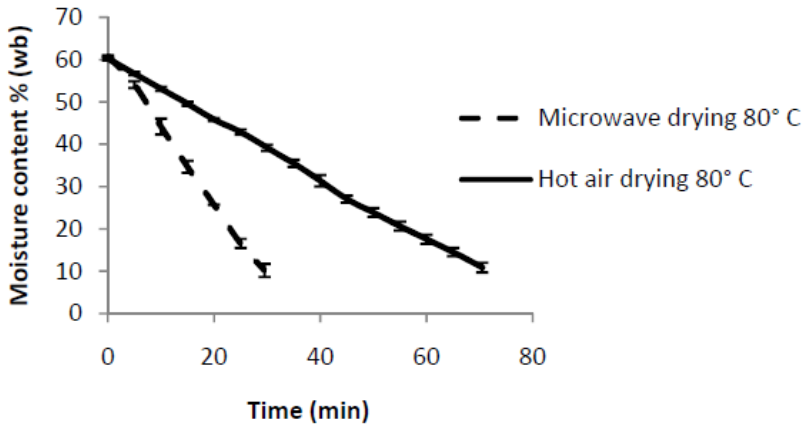

Figure 2-22: Comparison of drying rate of flax fibres for microwave drying and conventional hot air drying. Microwave drying can increase the drying rate up to 48,5% [124].

Baley et al. [126] compared the mechanical properties of flax fibre composites made with dried (7.1wt% of water was removed from the fibres) and undried fibres and the results are presented in Table 2-7. They have found that the maximum stress and strain are lower if dried fibres are used while the stiffness remains unchanged. As the water is removed from the fibre, this leads to a reduction in interaction between the different molecules that keep the elementary fibre together. Dehydration caused the space between microfibrils to shrink from 7.7 to 5.8 nm. At the technical fibre scale, drying causes mechanical stresses in the fibres resulting in a reduction of mechanical properties. However, minimal drying the fibre remain essential to avoid water inclusions in the plate that can vaporize during post-cure and may cause the delamination of the plate.

Material	V_f (%)	$E_{UD\,L}$ (GPa)	$\sigma_{UD\,L}$ (MPa)	$\varepsilon_{UD\,L}$ (MPa)
Flax/Epoxy	40.4 ± 1.2	22.50 ± 1.51	328 ± 18	1.6 ± 0.2
Dried flax/epoxy	40.0 ± 0.9	22.94 ± 2.65	210 ± 25	1.2 ± 0.1

Table 2-7: Mechanical properties of a dried compared to an undried UD flax-epoxy composite [126].

2.4 Manufacturing of flax fibre composites

A large variety of manufacturing techniques are available for composite manufacturing. The choice of one method will first be based on the targeted mechanical performance. This will determine the choice of matrix (thermoset or thermoplastic) and the fibre architecture used (weave, UD, etc…) and ultimately the manufacturing process. The Ashby-plot (Figure 2-23) shows the connections between all the cited parameters. The fibre reinforcement type and the manufacturing technique are linked, e.g. injection moulding resulting in parts with long flax fibres is not possible, and hence the properties of the injection moulded composites have lower mechanical properties. The plot only shows the tensile strength and the Young's modulus of the composite material, but charts for various combinations of material-properties exist as of today, based on the Ashby method [127].

Traditionally, biocomposites have been manufactured with techniques like injection moulding, compression moulding (CM), resin transfer moulding (RTM), vacuum assisted resin infusion (VARI) and pultrusion [128]. Pressurized methods are very popular, thanks to their high reproducibility, good surface finish, increased properties and low cycle times. It has to be noted that those techniques were previously developed for glass or carbon fibre reinforcements and can be "as is" used for natural fibres without changes. Table 2-8 lists the tensile modulus and tensile strength for some flax fibre composites manufactured using

various techniques. Different types of flax fabrics, such as plain weaves, UD or non-crimped, were developed for the composites industry. Some examples of parts are shown in Figure 2-24 and in Appendix A.

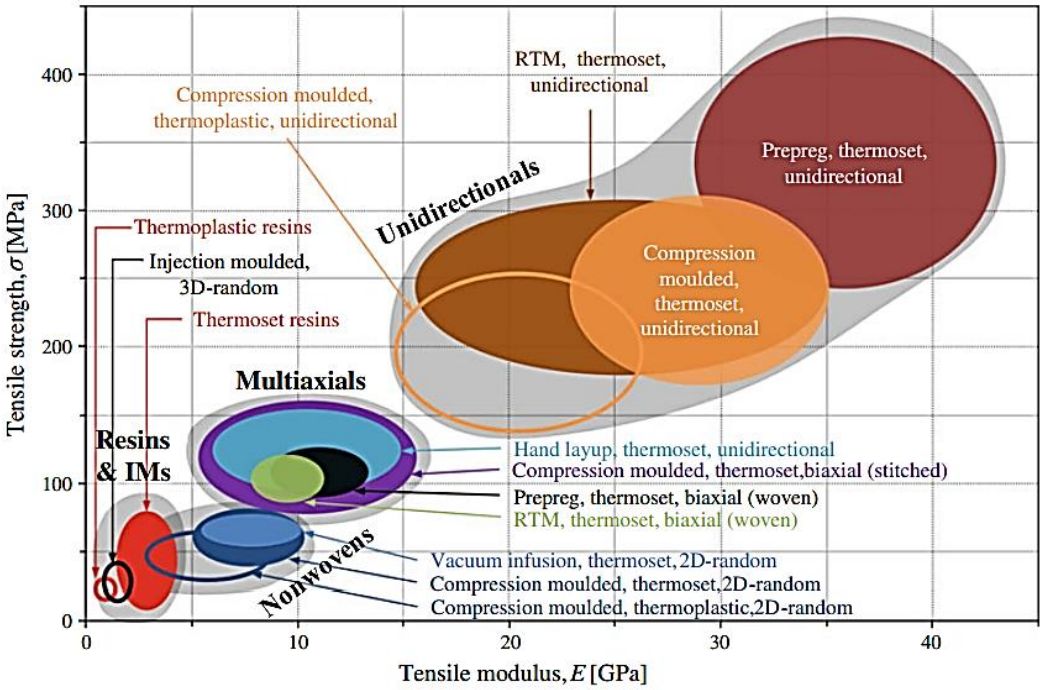

Figure 2-23: Ashby plot of all manufacturing processes [127].

Manufacturing technique	Reinforcement type	Matrix material	V_f (%)	Tensile modulus (GPa)	Tensile strength (MPa)	Source
Injection moulding	Short fibre, 3D random	PP	22	1,7	27	[129]
	Short fibre, 3D random	PP+5wt%MA	22	2,1	38	[129]
Compression moulding	Short fibre, 2D random	PP	40	8,8	57	[130]
	Short fibre, 2D random	PP+3,5%MA	40	8,6	68	[130]
RTM	Long fibre, UD	PP	43	26,9	251	[82]
	Long fibre, UD	Epoxy	42	35,0	280	[92]

Table 2-8: Effect of the manufacturing types on the properties of composites.

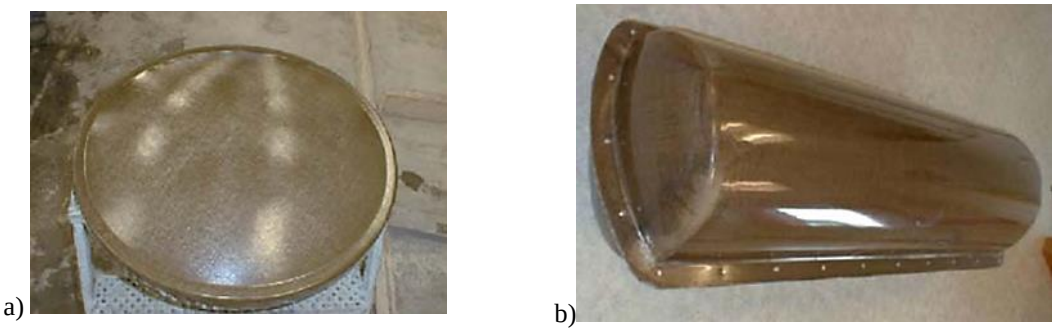

Figure 2-24: (a) Cover lid for siphon type solar panel accumulator tank made with flax biaxial fabric and (b) water accumulator tank [43].

2.5 In-service behaviour of Flax Fibre Reinforced Composites

2.5.1 Fatigue behaviour

In terms of mechanical performance, flax is one of the strongest of the natural fibre family and is known to be as stiff as glass fibre. As of today, a major lack of data on durability properties of flax fibre composites, such as its fatigue behaviour, has been limiting the use of these fibres in high performance applications like wind turbine blades and sporting goods.

In material science, the fatigue concept is based on the fact that the material becomes "tired" and fails at a stress level below the ultimate strength of the material (UTS). It is characterized as the progressive and localised structural damage that occurs when a material is subjected to cyclic loading. Since the original design strengths are not exceeded, the only warning sign of an imminent fracture is often just a micro-crack, at least in metals. In composite materials, multiple micro-cracks of different nature are preceding the final failure. The ASTM standard [131] defines the fatigue life, N_f, as the number of stress cycles that a specimen can sustain before failure occurs. For most materials, there is a value of stress amplitude at which the material will not fail for any number of cycles. This value is called the fatigue limit or endurance limit.

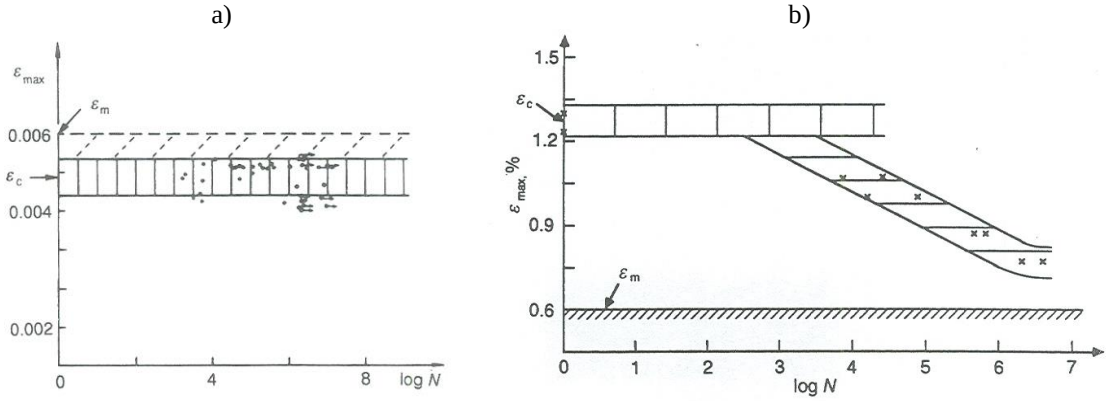

Figure 2-25: a) Ultra-high modulus fibre and b) intermediate modulus fibre.

Three methods to quantify the fatigue life of a material exists: the stress-life or strain-life method and the linear-elastic fracture mechanics method. The most commonly used method is the stress-life method characterized by an S-N curve, also known as a Wöhler curve, where S_o is the maximum stress, S is the applied stress and N is the logarithmic scale of cycles to failure. The load level is defined as the S/S_o and is expressed in MPa. The stress ratio (R-ratio) is another parameter of the test that must be defined. It is the ratio of the minimum stress applied during a cycle to the maximum stress applied during a cycle ($R=\sigma_{min}/\sigma_{max}$).

For materials with very high modulus like carbon fibres (Figure 2-25a), the quasi-static strength and endurance limit are coinciding, and only one region in the fatigue curve is obtained ; the reason is that the fibre stiffness is too high, and hence the applied strains too low, to induce fatigue damage in the matrix. However, for intermediate modulus fibres (Figure 2-25b), such as high strength carbon fibres, glass or natural fibres, the damage progressively grows until failure at stress levels below the quasi-static strength, but also a fatigue limit often can be observed. These particular types of S-N curve can be influenced by many factors such as the fibre type and textile architecture.

2.5.1.1 Effect of fibre type

The use of a particular fibre in a composite has a direct effect on its fatigue performance as it intrinsically depends on the fibre properties. Shah et al. [132] compared the fatigue behaviour of unidirectional flax, hemp and jute fibres, combined with polyester resin (Figure 2-26a). Although the natural fibre composites UTS properties are widespread (140 to 240 MPa), their fatigue strength coefficients *b* (which defines the slope of the S–N power law curve) are comparable, ranging from −0.0739 to −0.0623.

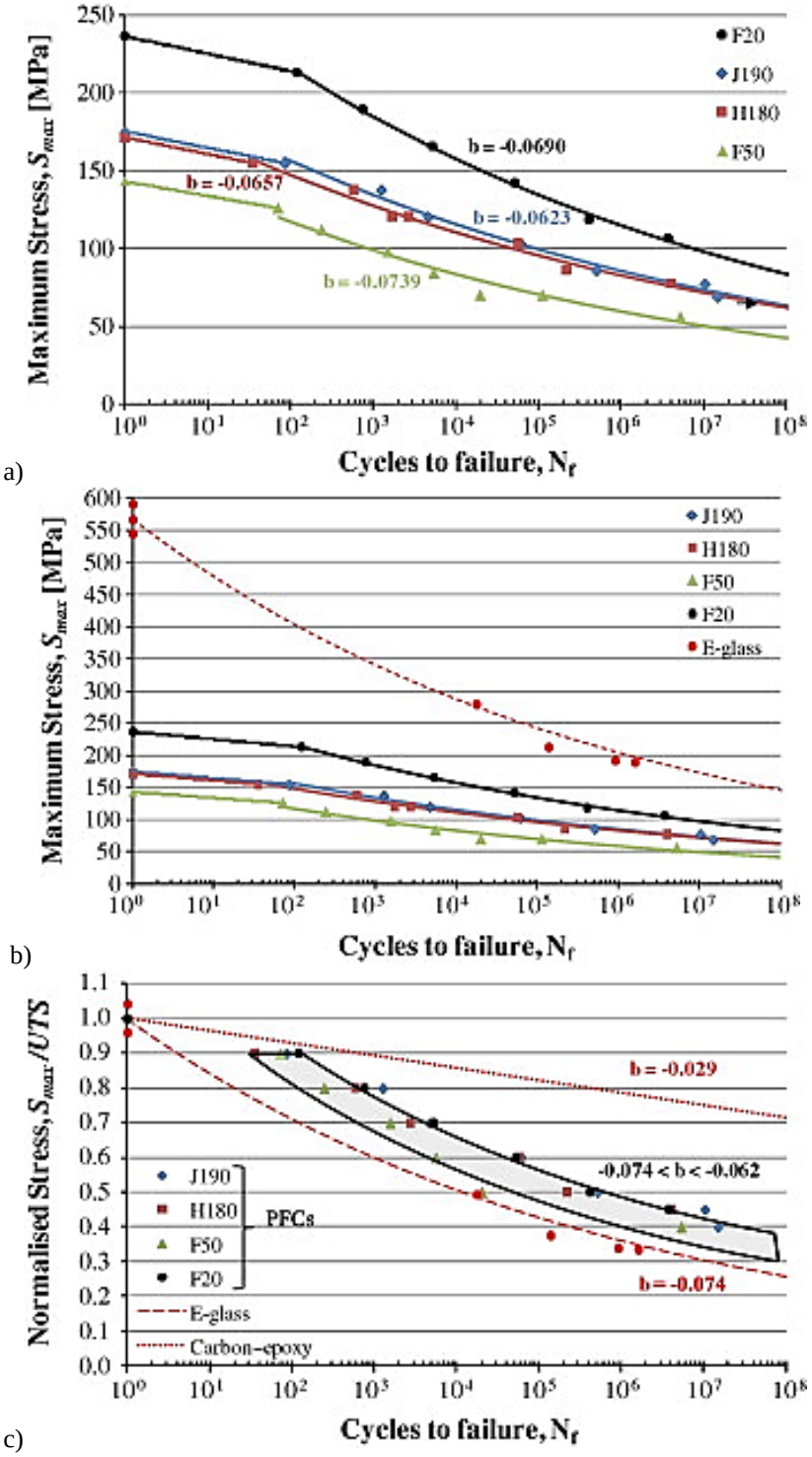

Figure 2-26: S-N curve comparison of flax (F), hemp (H), jute (J), glass and carbon polyester-based composites a) power–law regression curves, b) natural fibres composites vs glass composites and c) normalised *S–N* curves [132].

The authors concluded that the fatigue failure mechanisms in natural fibre composite and the resulting gradual strength degradation are independent of the fibre type. A potential cause of these similarities is that the jute, hemp and flax fibres are structurally similar. They have moreover a comparable interface bonding with the resin used, leading to similar failure mechanisms such as micro-crack growth rates at the fibre/matrix interface in the composite and the cellulose/hemicellulose-lignin interface in the fibre [133, 134]. While comparing the natural fibres composites to (synthetic) glass fibre composites, the authors have also found that the latter exhibit a higher resistance to fatigue loading, caused by their higher static strength as seen in Figure 2-26b. However, a steeper S–N curve is observed for glass fibres which indicates a more significant decrease in fatigue strength with increasing number of cycles.

All the natural fibres tested have a better performance (in terms of degradation rate) than E-glass, but worse than carbon fibres, at normalized stress as seen in Figure 2-26c. The normalisation of the data to the UTS allow a better comparison of all the material as they are compared based on the % of the maximum stress they are subjected. However, at the same stress level, the glass and carbon will experience higher stress than the natural fibres ones.

Yuanjian et al. [135] compared the S–N fatigue lifetime curves of random mat hemp fibre reinforced polyester composites (V_f = 44%) to the ±45° glass fibre polyester reinforced composites (V_f = 42%), as seen in Figure 2-27. The results show longer lifetimes for the hemp based composite at equivalent fatigue stress levels as well as superior static strength and fatigue strength at low numbers of cycles. However, the hemp composite displays a steeper slope of its S–N curve indicating a faster degradation of the fatigue strength compared with the glass fibre composites.

It has to be noted that the authors compared two composite which didn't have fibres in the loading direction (off-axis direction of the majority of the fibres in the hemp random mat), leading to very weak composites. The authors should have compared the hemp random mat to an equivalent one in glass fibres. Another study from Thwe and Liao [136] demonstrates that the hydrid bamboo–glass fibre reinforced polypropylene composites have a better fatigue resistance than the bamboo fibre reinforced polypropylene composites at all load levels.

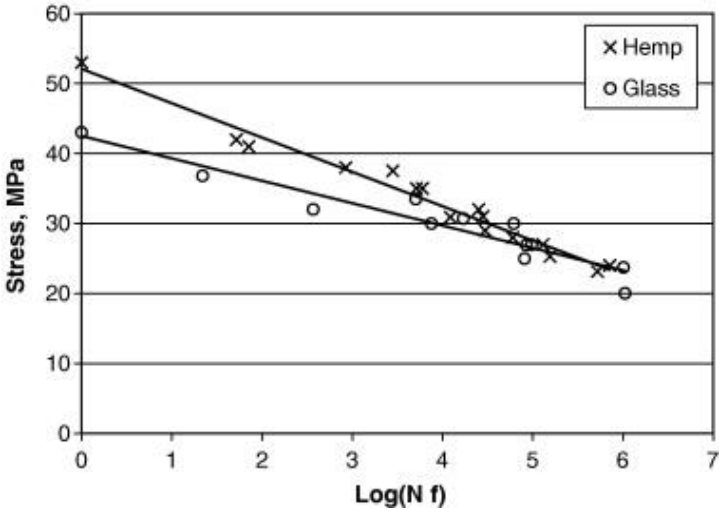

Figure 2-27: S–N fatigue lifetime data for hemp fibre mat reinforced polyester and ±45° glass fibre reinforced polyester [135].

2.5.1.2 Effect of fibre architecture

Liang et al. [137] have found out that non–crimp glass fibre/epoxy composites have an increased resistance to fatigue loading compared to non–crimp flax/epoxy composites which, both having a $[0,90]_{3s}$ lay-up, is due to their higher static strength (380 MPa vs 170 MPa). On the other hand, for the same lay-up, the glass composites have a larger reduction in fatigue life illustrated by a steeper specific S-N curve, in comparison to flax/epoxy, 56.2 MPa/decade vs 25.2 MPa/decade (which corresponds to a decrease of 15% of the fatigue strength (UTS) per decade for both of them) as seen in Figure 2-28. This demonstrates the steadier fatigue behaviour through time for the flax/epoxy composite. Silva et al. [138] have shown that for single technical sisal fibres, at fatigue stresses below 50% of the ultimate tensile strength UTS), all single fibre specimens resist more than 10^6 cycles. Furthermore, the authors have observed a slight increase in stiffness during the early cycles.

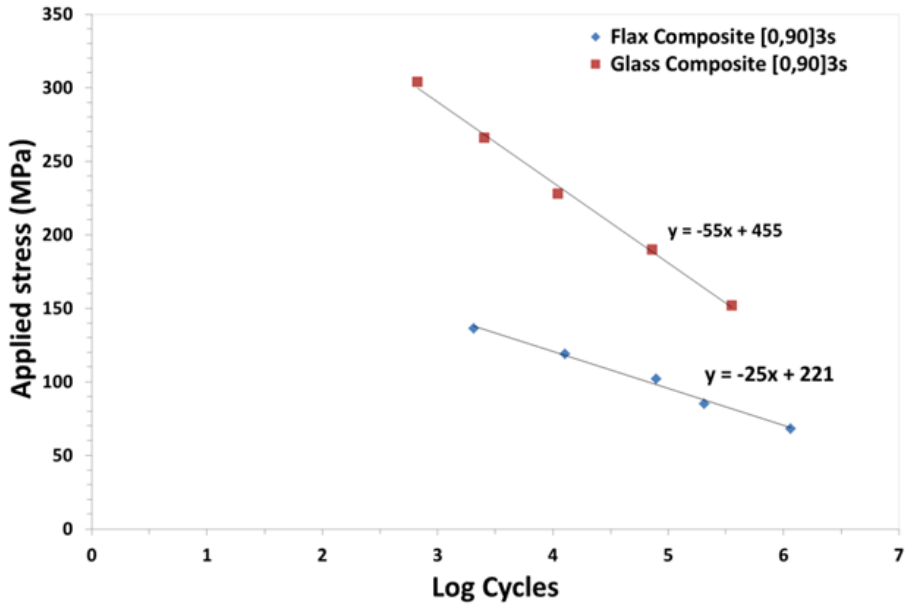

Figure 2-28: S-N curves of $[0,90]_{3s}$ cross ply flax/epoxy and glass/epoxy composites adapted from [137].

A study published in 2014 by Shahzad et al. [139] showed that short hemp fibre random mat composites were less fatigue sensitive than the glass fibre chopped strand mat counterpart in tension-tension fatigue, which could be related to the lower stiffness degradation at equal normalized stress levels (S/S_0). A steeper *S–N* curve (faster degradation) was observed for the $[\pm45]_4$ flax/-polyester laminate in comparison to unidirectional composite ($[0]_4$) laminate and the $[90]_4$. Tension–tension fatigue test results from the same author showed that the textile architectures with fibre orientations off-axis to the loading direction resulted in lower fatigue properties, which is in line with the significant drop in composite static strength in those off-axis directions.

As is the case for all property characterizations performed in these studies, the textile architecture, fibre and matrix types and fibre volume content were all found to have a strong effect on the fatigue life. It is expected that higher static properties are a sign of superior fatigue load-carrying capacities [132]. It was shown by Gassan et al. [140] that by using higher fibre strength and modulus unidirectional (UD) natural fibre-based composites, which have a better fibre–matrix adhesion, a delayed damage initiation and reduced damage propagation is observed. Furthermore, Shah et al. [132] found that the fatigue strength

degradation rates, obtained from the slope of the S-N curve of flax/polyester UD composites, are lower than for their glass counterparts.

Although fatigue loading does not instantly reduce the strength of the composite, it does have an effect on stiffness. During fatigue testing, early damage causes a fast and steep decrease of the stiffness, which is followed by a stabilisation and slow degradation of the composite properties. Close to failure, heavily damaged zones develop, leading to a strong decrease in stiffness, and this finally will cause the material to break [141, 142]. To monitor the damage, the cyclic hysteresis is used by many authors in order to evaluate the loss of stiffness, material energy dissipation and damage development [143, 144].

2.5.1.3 Residual properties after fatigue

During fatigue, a gradual build-up of residual strain in the samples is often noticed, especially in samples with none or only a limited amount of fibres in the testing direction [137, 145-147]. In tensile-tensile fatigue cases, if the strain at the minimally applied stress is plotted for each cycle versus the number of cycles, a steep increase is seen in the initial stages of the test, indicating a build-up of permanent or residual strain. After this, the increase of this strain becomes more moderate. The build-up of such residual strain during fatigue has been explained by the development of damage in the material, e.g. in [146, 147].

El Sawi et al. [147] have shown that there is a correlation between the residual strain increase and the matrix crack density in flax fibre reinforced epoxy manufactured with UD and ±45 cross ply laminates. Such permanent deformation has also been linked to creep phenomena occurring under the influence of a continuous tensile load for UD and cross-ply [0,90] laminates and this factor is even more pronounced in off-axis loading cases such as ±45 lay-ups [145].

The build-up of residual strain is accompanied by a decrease of the dynamic modulus (as measured during the fatigue cycling). De Vasconcellos et al. [148] have found that for the hemp-epoxy [0,90] laminate, the dynamic modulus decreases between the first and the last cycles by an average 22%, as seen in Figure 2-29a. On the other hand, the [±45] laminate shows a higher loss of the dynamic modulus of about 60% from the initial state (Figure 2-29b). The strain value at minimum stress in the [0,90] layup increases between 0.3–0.9% depending on the applied σ_{max}, while for [±45] laminate the residual strain varies more significantly, between 1.8% and 3%, during fatigue life as seen in Figure 2-29 c and d. These significant differences of dynamic parameter evolutions between both laminates are linked to the more "ductile" behaviour of [±45] composites.

Figure 2-30 shows the modulus degradation of random mat hemp and the [±45] glass fibre polyester composite samples during fatigue loading as found by Yuanjian et al. [135]. A steady decrease in modulus was observed for the glass composite with increased numbers of fatigue cycles until final failure. Meanwhile, the hemp fibre composites modulus remained relatively stable throughout fatigue cycling until the sudden brittle fracture of the specimens. A probable cause of the dissimilar damage development and difference in modulus decrease is the difference in architecture as the hemp laminate is made of randomly oriented preforms with some fibres along the testing axis which leads to a more distributed and reduced stress in the matrix compared with the glass reinforced composite, in which all fibres were at 45° to the stress axis. The lack of visible damage is an important characteristic for natural fibre composite. Though it ensures the dimensional stability and stable properties during its service life, it fails without warning.

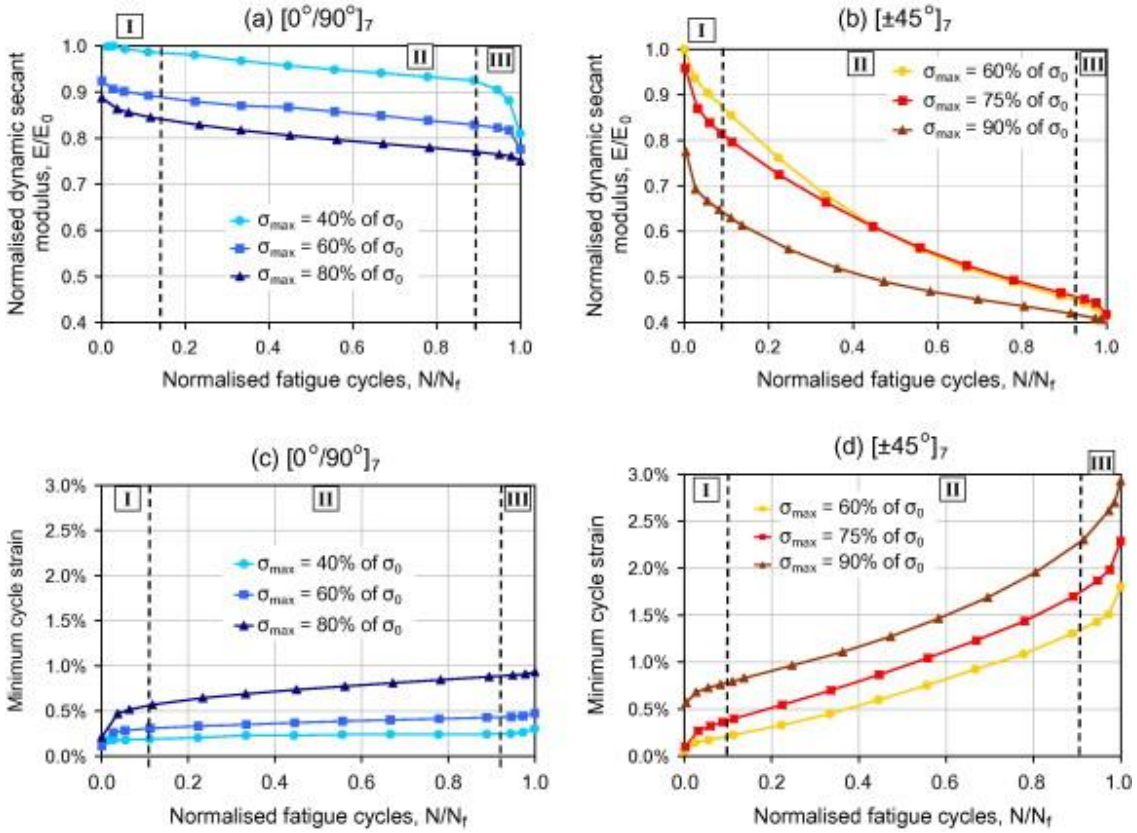

Figure 2-29: Dynamic modulus versus fatigue life for a) [0,90] and b) [±45] hemp/epoxy laminates. Minimum cycle strain versus fatigue life for c) [0,90] and d) [±45] hemp/epoxy laminates[148].

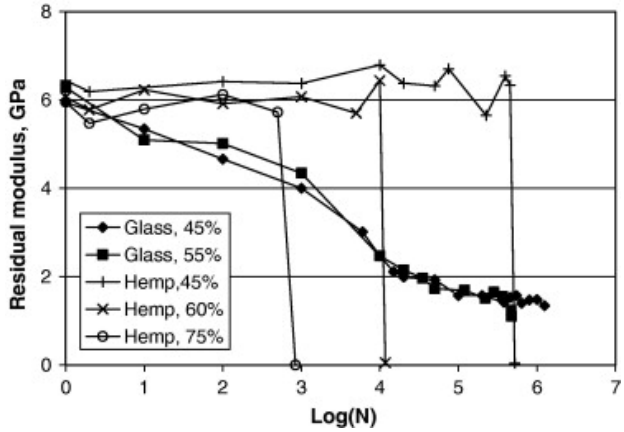

Figure 2-30: Modulus changes in random mat hemp and [±45°] glass fibre composites during fatigue cycling at different fatigue stress levels (the percentage figures represent the percentage of the UTS applied during testing) [135].

If fatigue testing is stopped before final failure has occurred, the residual quasi-static properties can be measured and compared to the pre-fatigue behaviour. Vallons et al. [146] have done this for cross-ply carbon-epoxy composites. They found no influence of the fatigue loading on the post-fatigue quasi-static behaviour when the loading was applied in the fibre direction. In the bias direction, however, small decreases in strength and stiffness were found and a significant decrease in failure strain. In another study on a carbon ±45 biaxial non-crimp fabric composites, fatigue stress levels that caused no visible damage in bias direction samples were found to have no effect on the post-fatigue tensile strength [149].

2.5.2 Impact behaviour

Impact damage, especially at low velocity, is commonly recognised as one of the most severe threats to composite structures. Therefore, a good understanding of the impact behaviour of composite structures is crucial for the design process. Impact properties cover three aspects, and can be measured in three ways: energy absorption through perforation tests, damage resistance (damage area after non-perforation impact) and damage tolerance by finding residual properties after impact [150]. Impact properties are influenced by many factors such as: matrix type, fibre type, fibre architecture, fibre orientations, laminate thickness and stacking sequence as well as matrix ductility and the interlaminar fracture toughness of the composite structure. Physical factors such as the panel geometry and its dimensions, constraint conditions and the impactor geometry should also be considered [151].

Several tests can be used to assess the impact resistance of a composite. An initial classification is made between low, intermediate and high velocity impact tests. In low velocity impact the whole structure will respond and there will be more elastic absorption. In intermediate and high impact velocity testing, the behaviour will be more localised and the incident kinetic energy will be dissipated over a small area giving rise to through thickness stress waves [152, 153]. These three impact responses are illustrated in Figure 2-31.

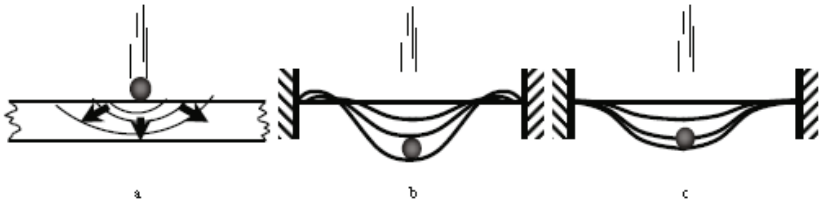

Figure 2-31: Impact testing classification: a) ballistic impact, very short impact times with dilatational wave dominated response, b) intermediate velocity impact, short impact times with flexural and shear wave dominated response and c) low velocity impact, long impact times with quasi-static response [154].

Low velocity impact typically occurs at velocities below 10 m/s [154, 155]. In low velocity impact the response is quasi static and the absorbed energy can be compared with the area beneath the stress-strain curve of a tensile test. This area is called tensile toughness. The most common test set-ups are the Charpy pendulum test, the Izod test and the drop-weight impact tests. When developing a new product with the objective of enhancing impact resistance, one should determine if it is designed for energy absorption, damage resistance or damage tolerance [150]. For example, if a design is optimised for energy absorption up to perforation, the perforation energy should be maximized.

The tests described up till now try to simulate an impact event on a structure. As the structure still has to fulfil its function, the investigation of the residual properties after impact is essential and can be carried out by looking at the residual tensile or compressive strength, flexural strength and fatigue life [153]. The residual tensile strength is influenced by the amount of fibre fracture while the compressive strength is mainly influenced by the amount of delamination in the structure [150, 153, 156].

Impacted composites are highly sensitive to compressive loading, due to the presence of delaminations which reduce the stability of the load bearing plies. The delamination divides the laminate into sub-laminates which have a lower bending stiffness than the original and are more sensitive to buckling [154, 155]. To quantify this phenomenon, the compression

after impact (CAI) test is carried out. The CAI test combines the effect of two phenomena, namely damage resistance and damage tolerance [157].

2.5.2.1 The effect of the matrix

The matrix is the binder that keeps the fibres together, protects the fibres from damage and allows alignment and stabilization of the entire composite structure. It has a large influence on the failure mechanisms, and its load bearing capacity will depend on the chemical structure, i.e. thermoset (brittle) or thermoplastic (ductile) [158]. When subjected to impact loads, laminates made with a brittle matrix (e.g. epoxy) will tend to fail through extensive delamination due to their low interlaminar crack growth resistance while tougher laminates made with ductile matrices will fail by transverse shear [150, 155]. Vallons et al. [159] have found that, for the same impact energy, the damaged area of non-penetrated woven glass epoxy-based composites was greater than for (more ductile) polybutylene terephthalate based composites with the same woven glass reinforcement, showing that the matrix ductility has an influence on the propagation of the damage.

Peijs et al. [150], with the help of a C-scan, found similar results comparing the brittle unsaturated polyester and a ductile vinyl ester resin. However, for the perforation tests, no clear correlation between the matrix ductility and the absorbed energy (up to perforation) could be made. As in this case the absorbed energy is mainly fibre dominated, there is only a small contribution from matrix cracking and delamination [150, 155]. This was also pointed out by Richardson et al. [153] who have found that the fibre shear out contributed to 50% of the energy absorption capacity.

2.5.2.2 Effect of fibre type

The ability to store elastic energy depends on the type of fibre used and corresponds to the area under the stress-strain curve. Figure 2-32 compares the stress-strain curves for various natural fibres with epoxy and polypropylene. It can be seen that the silk fibres have a larger area beneath the curve while flax and coir fibres are comparable, although flax fibres have a higher stiffness and strength [140]. Moreover, polypropylene fibres can absorb a large amount of energy before failure but show low stiffness and poor compressive properties due to low fibre stiffness.

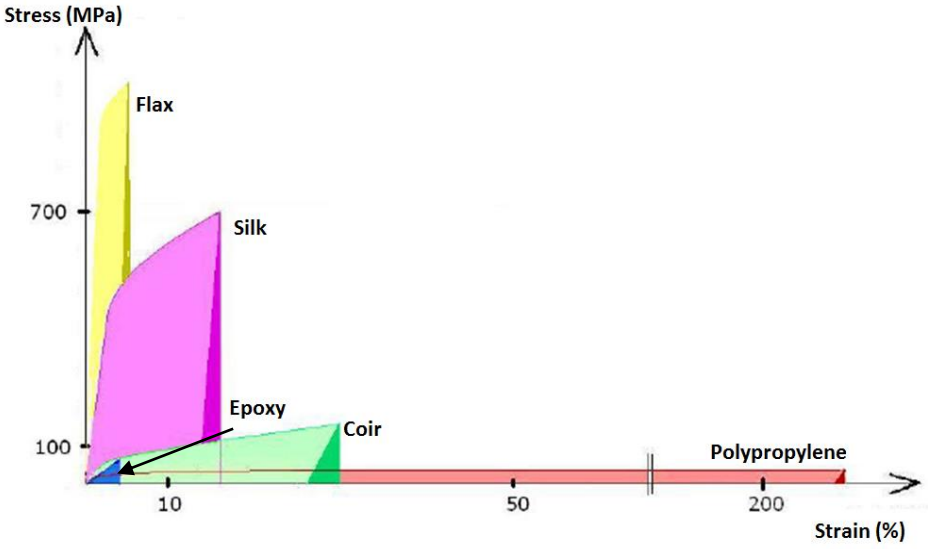

Figure 2-32: Comparison stress-strain curve natural fibres and polypropylene. Fibres listed from top to bottom: flax, silk, coir, epoxy, polypropylene [39].

Nowadays, a lot of work is dedicated to hybrid composites to improve the absorbed energy capacity of the composite [136, 160]. Combining the energy absorbing capability of low modulus fibres (e.g. coir fibre) with stiffer fibres (e.g. flax) would help improve the resistance to compressive loads [82]. However, both fibre and matrix should be altered to meet the desired requirements of impact, strength and stiffness.

2.5.2.3 The effect of fibre architecture, fibre orientation and laminate stacking

There is a wide range of fibre architectures that can be used for composite production. As mentioned in the previous section, the fibre content and/or structure will have a sizeable effect on the impact properties as well as on the toughness of the material. For high performance, unidirectional prepregs can offer flexibility in stacking sequence and optimisation of the properties. Other possibilities include the transformation of yarns into a textile to produce woven, braided and knitted fabrics. Beside woven textiles, there is also a range of nonwoven textiles that can be considered. If the fibres are randomly oriented, the fibre length has to be considered as the impact resistance increases with increasing fibre length [161].

Schrauwen et al. [150] compared a UD cross ply with stitched multiaxial non-crimp layers with a [0,90] lay-up and a 2x2 plain weave, all made of glass fibres and combined to a toughened vinyl ester or polyester resin. The results showed (Figure 2-33) that the absorbed energy at perforation was higher for the UD cross ply laminate than for the woven fabric. This was related to the higher strength properties of the UD laminate. Moreover, the UD multiaxial non-crimp composites displayed the best absorbed energy after perforation and the woven fabric displayed the best resistance to damage (low damage area following a non-perforation impact). However, the effect of fibre architecture on the perforation energy was marginal although a difference in damage shape was observed. In the woven fabrics based composite, the damaged area was smaller and circular and seemed to be restricted by the coarse fibre bundles that acted as crack stoppers.

Bibo et al. [79] investigated three glass fibre architectures: quasi-isotropic asymmetric stitched non-crimp ($[-45,90,45,0]_2$ $[0,-45,90,45]_2$), UD tape and satin weave combined to epoxy resin with an isotropic lay-up. The eight harness satin weave composite exhibited the best damage resistance (i.e. less delamination) and the UD exhibited the biggest delamination area due to less resistance to interlaminar crack initiation and propagation. The non-crimp fabric, which had a through the thickness stitching (low-tex polyester stitching yarn), showed an improvement of the damage resistance by a smaller delamination area. This is caused by the nesting of tows which forces the propagating crack to follow a tortuous path as it has to deviate due to the presence of crimp and the stitching yarn. The authors have also shown that the higher the angle mismatch between the layers, the bigger the delamination area was for the UD-based laminates. Thus, having a quasi-isotropic stacking has positive influence on the damage tolerance [79].

Vadori et al. [162] investigated woven fabrics versus UD glass-epoxy composites with different stacking sequences, $[0,+90]_s$, $[0,+45,-45]_s$, $[0,+60,-60]_s$. The highest perforation energy, was found for UD laminates with $[0/+90]_s$ stacking. It can be argued whether these results are contradictory with literature since it was stated earlier that the perforation energy is primarily dependent on the fibre volume fraction and only secondary on effects like fibre laminate stacking.

For penetration tests, the fibre volume fraction was found to be the dominant factor. The fibre architecture was only a second-order effect and the resin did not contribute any noticeable effects. Santulli et al. [163] have found that hemp/epoxy random mat (V_f=43%) composites have an increased resistance to perforation compared to plain woven jute/epoxy composites (V_f=46% with $[0,0,45,45]_s$ lay-up). This was explained by the possibility of redirecting the absorbed energy in two or more directions as an effect of the random orientation. However, one has to remark that hemp fibres (E_f= 40-65 GPa, σ_f = 550-900 MPa) are much stronger than jute fibres (E_f = 10-30 GPa, σ_f = 400-800 MPa) which are twisted and crimped, explaining the lower properties of the jute weaves [2]. Dhakal et al. [164] have found, for the plain weave jute/methacrylate soybean oil composites, that the weave architecture with the most cross-over points (higher picks and ends counts) as well as the type of weave (e.g. plain vs satin), leads to the highest resistance to impact damage and toughness properties.

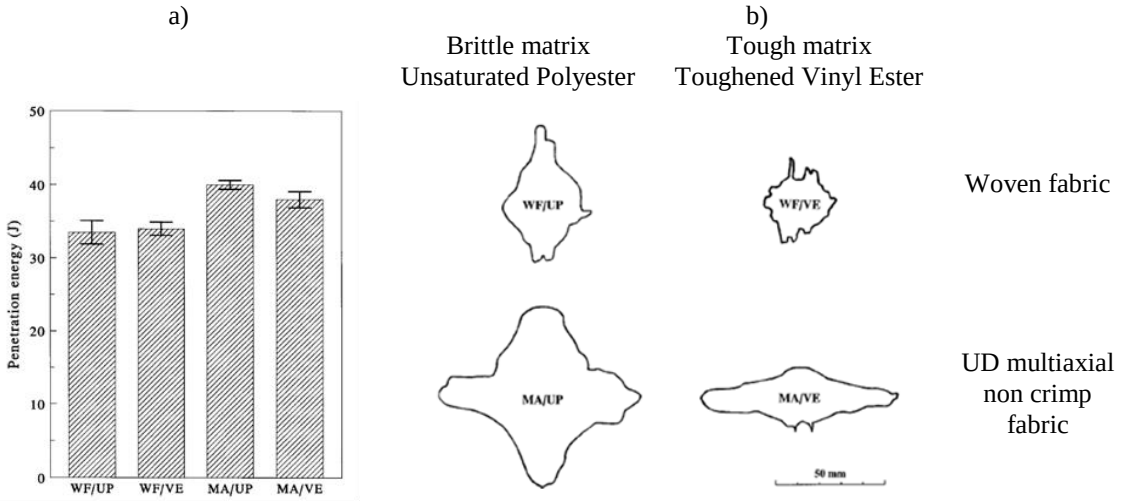

Figure 2-33: a) Penetration energy for the different laminate configurations as measured using full penetration falling weight impact tests. b) Size and shape of glass delaminated area after penetration.

2.5.2.4 Effect of fibre-matrix interface

The interface has an important effect on the failure mechanisms in composites, as previously mentioned for fatigue loading (see 2.5.1.1). Poor adhesion results in interface failure at low stresses, leaving clean fibres while a stronger adhesion results in failure in the matrix. An intermediate bond strength optimises the fibre pull-out but results in average mechanical performance since the load transfer between matrix and fibre is less effective [39]. In terms of impact, a better fibre-matrix interface leads to an increase in damage initiation loads, but the perforation threshold is lower [155]. Thus, a stronger interface enhances the stress transfer from matrix to fibre, but once a crack is present it does not grow through delamination at the fibre interface but breaks the entire specimen.

2.5.2.5 Effect of the interlaminar fracture toughness on the impact properties

The possibility of delamination is one of the concerns while designing composite structures. Therefore, it is essential to understand how a composite material resists to interlaminar fracture following an impact. By definition, the resistance against unstable interlaminar crack growth (delamination) is called interlaminar fracture toughness and is measured as the critical strain energy release rate G_c needed for interlaminar crack growth. This resistance can be determined for three loading modes: tension (mode I, G_{Ic}) in-plane shear (mode II, G_{IIC}) and out-of-plane shear (mode III) as presented in Figure 2-34.

For composite laminates, the loading in Mode I is usually obtained with the double cantilever beam (DCB) test, the second mode with the end notched flexural (ENF) test and the third with a mixed-mode bending method for delamination testing (MMB) as presented in Figure 2-36 [165].

For neat polymers, different test methods are used for measuring their fracture toughness, as proposed by ISO 13586 and ASTM D5045-99[166]:

- Single-edge notched bending (SENB): ideal for plastic materials. Nonetheless it is challenging to initiate a sufficiently sharp crack for brittle thermoset resins testing;
- Compact tension (CT): widely used in fracture mechanics and corrosion testing for metals.

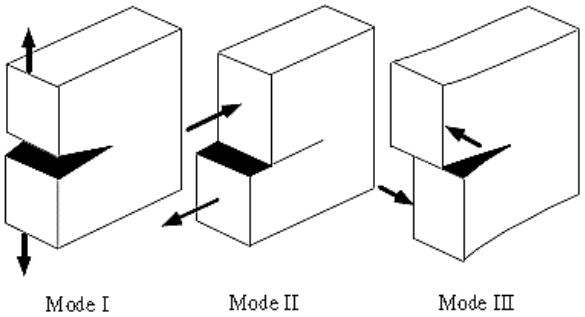

Figure 2-34: The fracture toughness loading modes: Mode I tension, Mode II-III shear [167].

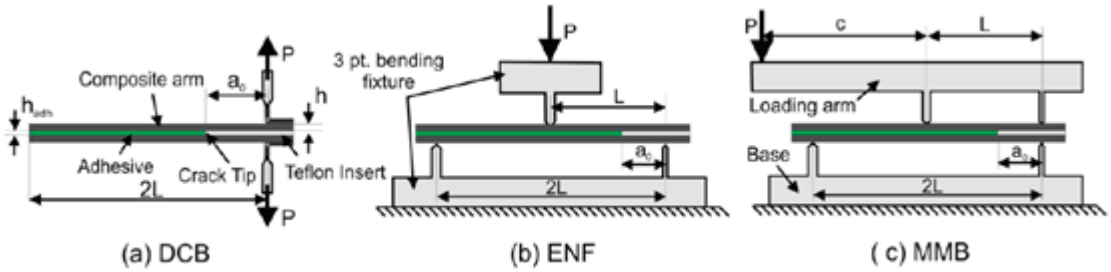

Figure 2-35: a) Double cantilever beam, Mode I test ; b) End notched flexural test, Mode II test and c) Mixed-mode bending test, Mode III [165].

Typically, the mode I interlaminar fracture toughness G_{IC} is used as a characteristic for the crack or damage resistance of a polymer matrix. For instance, for the unreinforced PES thermoplastic matrix G_{IC} is a factor of two or more greater than for toughened cyanate ester thermoset [168]. Sela et al. [169] have reported that thermoplastic matrices such as PEEK give an order of magnitude increase in interlaminar toughness of their composites, compared to epoxies. Ductile matrices help to reduce the spread of delaminations in composites by the creation of larger energy dissipating plastic zones around the crack tip, then in brittle thermoset matrices. However, these zones are limited by the presence of fibres in the composite, and hence, when they become too large, the energy dissipation is less effective. As a consequence, in brittle matrices the matrix toughness can be fully transferred to the composite whereas in ductile matrices it will be only partly transferred [155, 170, 171]. Thus, the polymer fracture toughness (G_{Ic}) is inherently connected to the composite interlaminar fracture toughness. A lot of research has been directed towards the improvement of the matrix toughness. One method consists of adding plasticizing modifiers, rubbers or thermoplastic particles [172, 173]. The other method is related to interleafing where discrete layers of a high shear strain resin are added between the layers

[150, 153, 174]. The composite is then able to support higher shear deformations without forming delaminations.

A matrix is considered brittle when the G_{IC} value is lower than 200 J/m^2. Once combined to a fibre reinforcement, the composite interlaminar fracture toughness in Mode I will typically be double or triple [170]. A linear relation was found between the Mode II interlaminar fracture toughness and the residual properties after impact (CAI) as the size of the damaged area is connected to G_{IIC} as found by Schrauwen et al. [150] and Cantwell et al. [155]. However, no correlation between the compression after impact properties and G_{Ic} was found. It is not yet understood why the residual compressive properties are mode II dominated as the mode I is also believed to play an important role because during the compression failure process, the delaminations are peeling off and hence definitely a mode I component must be present.

In natural fibres, the elementary fibres are grouped in technical fibres, which are spun to yarns. The density and the cross sectional shape of the yarn will determine the amount of crimp in the fabric. A higher linear density of the yarn leads to higher crimp in the composite. Hughes et al. [91] investigated the influence of higher linear density in weft direction, which leads to more crimp of the warp fibres, on the fracture toughness, by doing compact-tension (CT) tests, where the notch is running through the thickness and parallel to the weft direction. They have found an increased (through thickness) fracture toughness for composites with lower crimp on the warp yarn, thus higher linear density of the weft yarn. Composites with less crimp are more advantageous as they result in fewer resin-rich pockets and higher fibre volume fractions. Moreover, they have a smaller reduction in in-plane stiffness and strength, resulting in a higher toughness. Silva et al [89] compared the critical strain energy release rate of castor oil polyurethane matrix composites reinforced with woven sisal textiles or short sisal fibres. The found the former displayed "substantially higher plain strain fracture toughness values". By adding flax fibre mat to the pure HDPE polymer, a significant increase in toughness was reported by Singleton et al. [6]. Compared to other fibres, flax plays an important role in the toughening process. Table 2-10 and Table 2-11 present some toughness values for synthetic fibre-based composites from the literature.

Chamis et al. [175] carried out Izod impact tests (through-the-thickness test) in order to understand the controlling mechanisms of the energy absorption and dissipation in composite materials. They have found that flexure and interlaminar shear deformations are the main energy-absorbing mechanisms in impact resistance tests. Furthermore, they found that the area under the composite tensile stress-strain curve was a good approach for predicting the absorbed energy after a perforation impact. This area under the curve is defined as the tensile toughness. This tensile toughness is the quantity of energy (per unit volume) needed to completely fracture the material. Materials showing good impact resistance are generally those with high tensile toughness [176]. For a composite to be considered tough, it should withstand both high stresses and strains. Thus, composites with larger areas under the stress-strain curve are believed to have a better impact energy absorbing capacity up to penetration.

	G_{IC} (J/m^2)		References
Polymers			
Epoxy (thermoset)	69-150		[170]
Vinyl ester (thermoset)	410		[177]
PP/MAPP(thermoplastic)	1100-2100		[177, 178]
Fibre Reinforced Composites			
	Initiation	**Propagation**	
Thermosets			
Glass/epoxy	264		[170]
UD Glass/epoxy	243 - 268		[179]
UD Glass/ Polyester	282		
[±30] Glass/ Polyester	214	500	[180]
[±45] Glass/ Polyester	176	300	
UD Carbon/epoxy	115	203	[181]
UD Carbon/Epoxy	100-200	150-250	[182]
$[0]_{12}$ UD Carbon Epoxy	110-150		[183]
$[+2^{\circ}/0_{16},/-2^{\circ}/+2^{\circ}(0_{16}/-2]$ Carbon/toughened epoxy	145		[184]
UD Carbon/toughened cyanate	300	360	[168]
Cross-ply $[0_8/90/0_8]$ Carbon/ toughened cyanate	600	820	
Thermoplastics			
UD Carbon/PEEK	1406	1707	[181]
Carbon/PES	800	2000	[185]
UD Carbon/PES	1000	1500	[168]
Cross-ply $[0_8/90/0_8]$ Carbon/ PES	1000	2600	
UD Carbon/PEEK	2000		[186]
$[+2^{\circ}/0_{16},/-2^{\circ}/+2^{\circ}(0_{16}/-2]$ Carbon/PEEK	1318		[184]

Table 2-9: G_{IC} reference values for initiation and propagation.

Fibre Reinforced Composites	G_{IIC} (J/m^2)	References
Thermosets		
UD Glass/ Polyester	496	
[±30] Glass/ Polyester	976	[180]
[±45] Glass/ Polyester	1485	
UD Carbon/epoxy	550	[181]
UD Carbon/cyanate	1100	[168]
Cross-ply $[0_8/90/0_8]$ Carbon/ toughened cyanate	1350	
UD graphite/epoxy	1101	
[+15,+15] and [±15] graphite/epoxy	1210, 1081	[187]
[+30,+30] and [±30] graphite/epoxy	1042, 1041	
$[0]_{12}$ UD Carbon Epoxy	498-545	[183]
$[+2^{\circ}/0_{16},/-2^{\circ}/+2^{\circ}(0_{16}/-2]$ Carbon/toughened epoxy	455	[184]
Woven carbon /epoxy	560-920	[188]
UD Carbon/ toughened epoxy	930-991	
Thermoplastics		
$[+2^{\circ}/0_{16},/-2^{\circ}/+2^{\circ}(0_{16}/-2]$ Carbon/PEEK	1428	[184]
UD carbon/PEEK	1477-1530	[188]
Carbon/PES	1250	[185]
Cross-ply $[0_8/90/0_8]$ Carbon/ PES	1450	[168]
UD Carbon/PES	1250	

Table 2-10: G_{IIC} reference values (initiation only).

2.5.2.6 Low velocity impact damage

When a composite is subjected to low velocity impact leading to perforation of the specimen, matrix damage and fibre-matrix debonding will be the first form of damage to occur [158]. These matrix and interface cracks occur because of a to property mismatch

between the fibre and matrix as stated by Richardson et al. [158]; they are frequently oriented parallel to the fibres direction in UD layers. Joshi et al. [189] stated that the matrix cracks in the upper and middle layers of the composite start at the impactor area. The appearance of transverse shear stresses, leading to shear cracks, is linked to the striker contact force and area [190]. They also stated that the cracks appearing on the tensile side of the specimen are related to the high tensile forces at the tension side of the bent specimen.

How the matrix cracks will evolve throughout the structure is dependent on the thickness of the specimen and the fibre architecture [191]. When a certain threshold energy has been reached the present matrix damage can cause delaminations under influence of interlaminar stresses. Such delaminations run in the resin rich area between the plies; they occur normally between plies of different fibre orientation and not between lamina in the same ply group [158]. The delamination area becomes larger depending on the bending stiffness mismatch caused by the variation in stacking sequence. The greatest mismatch is established between the 0° and the 90° layers of UD layers, which show the largest delaminated area [158]. For long fibre-based composites, the absorbed energy at perforation and the damage resistance are influenced by the amount of pull-outs that occur after fracture, which is then directly related to the fibre-matrix adhesion.

Other factors influence the damaged area: constituent material properties (fibre, matrix, and interface) and laminate thickness. The delamination area is greater with an increased incident impact energy and laminate thickness [150, 152-154, 156]. Thick laminates with low interlaminar shear strength tend to delaminate more easily as they are stiffer. This implies an additional energy absorption by damage creation. On the other hand, the delamination area gets smaller when increasing matrix and fibre toughness and a small strain to failure.

When the fibres have a low strain to failure, part of the impact energy is absorbed through fibre breakage which leads to a decrease in the delamination development and growth [154]. A typical damage development in [0, 90, 0] laminates is shown in Figure 2-36. In this case, the delamination is preceded by matrix damage at the top (shear cracks under the impactor) and bottom (vertical bending crack) of the laminate. This is followed by the delamination in the consecutive plies [153].

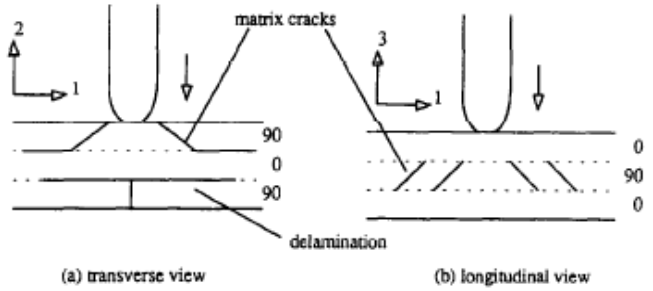

Figure 2-36: Initial damage in an impacted 0/90/0 composite plate [153].

The damage progression for thin and thick laminates is presented in Figure 2-37. Thin laminates develop a matrix crack at the bottom followed by progressive delamination in a form of a reverse pine tree. For thick laminates, matrix cracking appear at the top part of the laminate with delamination spreading in the pine tree shape [154].

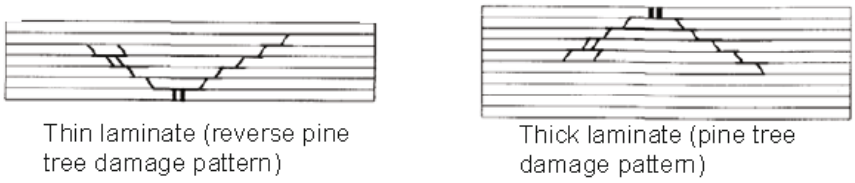

Figure 2-37: Low velocity impact response of thin versus thick laminates [154].

In composites with strong fibres, fibre failure occurs after matrix damage and delamination on the impactor side, and is caused by the high bending stresses. Fibre failure is a precursor to catastrophic penetration mode [153]. When the fibres can no longer deform, the impactor penetrates or indents the material. The major forms of energy absorption during penetration are fibre shear out, delamination and elastic flexure. Furthermore, Cantwell and Morton [192] have also mentioned that fibre shear out (i.e. removal of shear plug) contributed to 50-60% of the energy absorption capacity depending on the carbon fibre composite plate thickness. As the specimen becomes thicker, more energy is needed for penetration and consecutive perforation. For long fibre based composites, the damage resistance and the absorbed energy up to penetration are mainly influenced by the amount of pull-outs that occur after fracture, which is then directly related to the fibre-matrix adhesion.

2.6 End of Life possibilities for composites - EOL

Lately, the European Union's End of Life Vehicles Directive has stated that all vehicle constructors have to assure the re-usability and/or recyclability of the materials of new cars put on the market to a minimum of 85% of their total weight and the reusability and/or recoverability up to 95% of the total weight. Various materials can be used to construct a car such as steel, aluminium, plastics and composites. As for composites, mostly carbon and glass fibre reinforced composites are used, but a shift towards natural fibre based composites has been observed. This is thanks to their good mechanical properties, low density and lower environmental impact. Whereas the recycling of steel is well documented and researched, the recycling routes possible for composite materials and especially natural fibre composites, are much less investigated.

The European Union's End of Life Vehicles (ELV) Directive set's following target for the recycling and re-use of materials:

> *"No later than 1 January 2015, for all end-of-life vehicles, the reuse and recovery shall be increased to a minimum of 95% by an average weight per vehicle and year. Within the same time limit the reuse and recycling shall be increased to a minimum of 85% by an average weight per vehicle and year."* [193]

It is now of crucial importance, for the achievement of the target of the ELV directive, to look into possible recycling processes that can be used for composite materials and more specifically the recycling possibilities for natural fibre reinforced composites.

Recycling is not merely a single process but can be seen as a chain of processes, starting with the collection of sufficient materials that have reached their end-of-life (EOL). One of the reasons why composite materials have not been properly recycled is their heterogeneity. Since composite materials have to sustain a certain load during operation, separation of the materials is not wanted. In some recycling cases, the separation of the two (or more) materials is not complete: the mixture of materials is treated as a homogenous piece and will be recycled as such. The advantage of recycling is that the new material can be repurposed which will save energy and resources. However, recycling of composites could

lead to lower quality materials as the fibre length used are shortened during the shredding [194]. This concept is called down-cycling.

An important technological parameter affecting the EOL options for composites is the matrix material which could either be thermoset or thermoplastic. The important difference, from an EOL point of view, is the possibility to re-melt the thermoplastic polymers, whereas the thermoset polymers can be burned off in incinerators to produce energy or be digested to recuperate the reinforcing fibres. The use of thermoplastic composites is a rather recent and as such, their recycling is not yet a subject of a lot of research.

As of today, various technologies exist for the recycling of composite materials and they are separated in three main sections as seen in Figure 2-38: mechanical, thermal and chemical recycling. The landfill option could also be considered for bio-based composites as some of them may be degraded by either the environment and/or fungi.

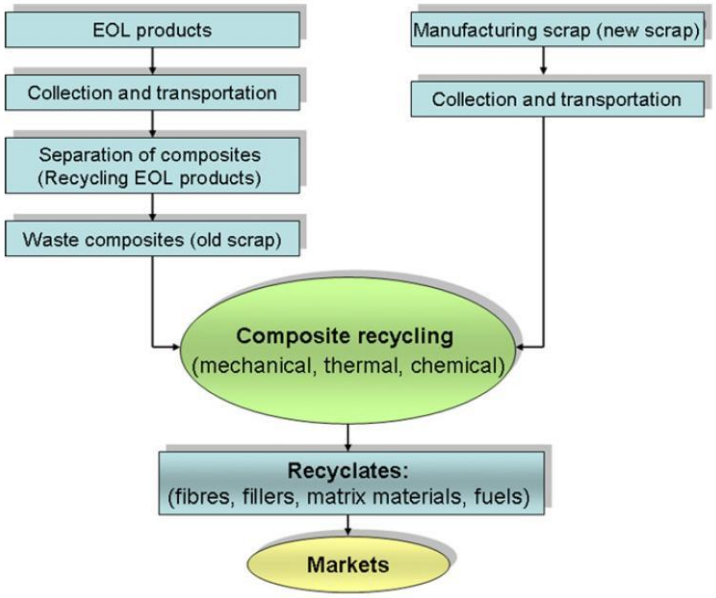

Figure 2-38: Process scheme for the entire recycling process. Starting from the EOL of the product or the manufacturing of scrap down to the recycling of the composite in the plant and ending with the recycled material that will be reused in the market [194, 195].

2.6.1 Mechanical recycling

Mechanical recycling is a promising technique to be used for natural fibre composites and it is currently being researched in some institutes [196]. However mechanical recycling will always yield short fibres as output material. Mechanical recycling of thermoset composites relies mainly on crushing, cutting and milling of the parts in order to reduce their size from 50-100mm to 50µm; the particles are later classified according to their particle size [195]. This classification is an important step as smaller particles will generally contain more matrix and the larger fractions contain more fibre material [195]. The ground material, such as glass fibre, is then used as filler material in bulk moulding compounds (BMC) and sheet moulding compounds (SMC). A study on the properties of a dough moulded compound (DMC) shows that by incorporating recycled material instead of the standard used fillers, such as calcium carbonate ($CaCO_3$), similar properties were achieved [197].

For natural fibre based thermoplastic composites, such as kenaf-polypropylene composites, mechanical recycling is a feasible technique and it is currently being researched in some

institutes [196]. However, by mechanically recycling, the output material will always consist of short fibres. The mechanical recycling consists of cutting and crushing the composite into small pellets. These pellets can later be used as feedstock for injection moulding processes. This is considered as a down-cycling of the material as the properties are decreased due to the reduced fibre length [198]. The recycled feed can also be mixed with virgin matrix material before being fed into an extruder in order to create different fibre content in the part.

A study on the mechanical recycling of boats made of glass-polypropylene composites showed that the recycled materials have good mechanical properties. However, these properties are still less than those of the virgin material [199]. Furthermore, it was found that when recycling short pine fibre reinforced PP composites, the Young's modulus and tensile strength decreases by only 13% and 17% respectively after eight recycling cycles as seen in Figure 2-39. The major influence in the decrease in properties is the breaking of the fibre into smaller pieces, and the damage introduced on the fibres [200]. In this study, the fibre breakage of natural fibres was evaluated. It was found that the fibres broke up into smaller fragments reducing their length but at the same time the fibre diameter was reduced, hence keeping the aspect ratio higher. Because of this effect, the aspect ratio only decreased by a factor of 6. The length reduction still remained higher than the diameter reduction [201]. Baley et al [202] have shown that hemp or sisal-PP composites do not fracture as easily as glass fibres during a mechanical recycling operation of hemp. In their case, this results in an almost constant aspect ratio for hemp-PP injection moulded composites with negligible loss in properties compared to glass-PP [202, 203].

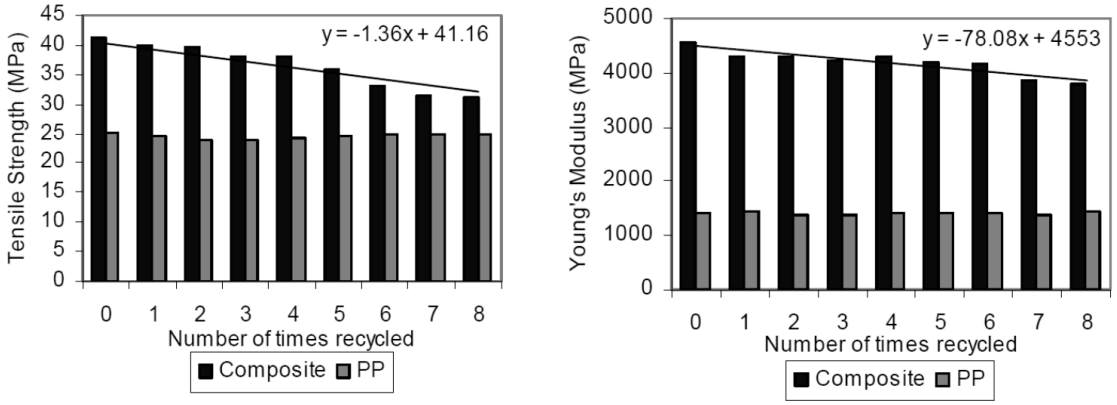

Figure 2-39: Evolution of the tensile strength and Young's modulus of a short pine fibre reinforced PP composite during eight recycling stages [200].

2.6.2 Thermal recycling

In a thermal recycling process, the glass and carbon fibre based composite undergoes a process at elevated temperatures which allows fibre recovery through combustion of the matrix material. This pyrolysis process uses temperatures ranging from 400-700°C in an oxygen free environment. Under these conditions the matrix material depolymerizes into lower molecular weight organic components. This technique allows the recovery of the fibres but also the usage of these lower molecular weight components in chemical processes [204]. The recovered glass fibres could be used in dough moulding compound (DMC) products. Testing of DMC composites with 20wt% recovered glass fibres showed that they still reached the manufacturers quality limits [205]. However, the mechanical strength of the recovered glass fibres decreased by 50% or more [195]. Nevertheless, new studies on the regeneration of the thermally recycled glass fibre thermoset composites showed

promising performance.Yang et al. [206] showed for chopped strand mat-epoxy composites a tensile strength decrease of 60% of the original properties (~220 MPa) after a thermal recycling was performed at 500°C for 30 min. However, a combination of chemical etching and post-silanization treatments on the recycled fibres helped recover 50% of the lost strength.

A fluidized-bed technology for the recycling of glass and carbon thermoset composites was developed at the University of Nottingham. In the reactor vessel, the temperature is set at 450°C. At this temperature, the polymer matrix is decomposed and the glass or carbon fibres are removed from the vessel [207]. The fibres obtained from the process do not show any loss in stiffness, however the strength of the fibres diminished in comparison to virgin fibres. For glass fibres, a reduction of 50% in strength was found [208]. In order to have a suitable process, the composite has to be cut into smaller fragments (squares of 10mm by 10 mm). Figure 2-40 shows a scheme of such a fluidized-bed process.

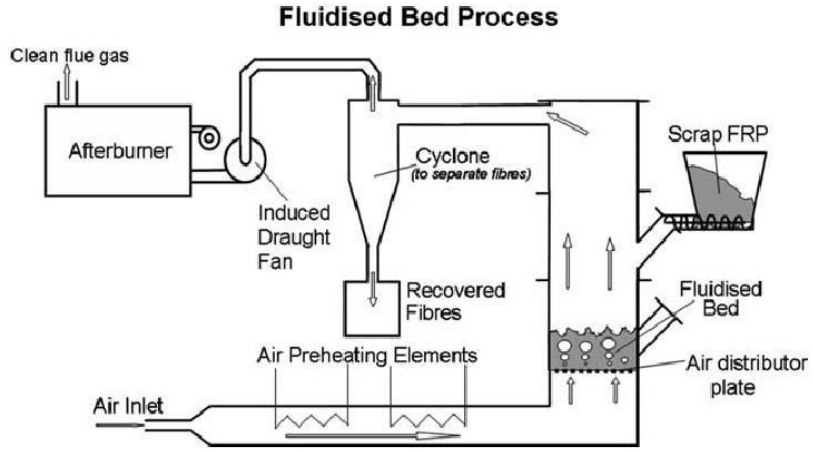

Figure 2-40: Fluidized bed process for the recycling of glass fibre reinforced composite [195].

One way of recycling the synthetic fibre reinforced thermoplastic composites is by direct reuse of the material. By heating above the melting point of the thermoplastic polymer matrix and re-moulding the structure, a new product can be obtained. This technic could be used for all types of composites, although the natural fibre based composite have a limited processing temperature of 200°C before the fibres start to degrade. Extra fibre layers can be added on top of the remoulded structure. The new product can then be reinforced to its needs. Another technique is "incineration with energy recovery" which involves the complete burning of the material to produce energy and/or heat [209]. The incineration of composite materials is not a recycling technique since no material is recovered. As of today, this is the most widespread disposal technique for composites after landfill [210-212]. However, due to the fast treatment and easiness of use, it is a commonly applied EOL technic for natural fibre based composites.

When the incinerator design maximizes the heat recovery after combustion of the material, 50% to 70% of the heat can be recuperated as energy [213]. Both the matrix and the fibres can be combusted in the case of natural fibre composites. In contrast, only the matrix material of glass fibre composites can be combusted while the glass fibres form a slag which sticks to the incinerator walls and requires an extra process to remove it. The non-combustible glass residue needs further treatments in order to dispose of, constituting one of the major disadvantages for the incineration of glass reinforced plastics [210]. For

natural fibres, incineration at high temperature will lead to complete combustion of the fibres and the matrix. Only ashes are found at the end of the process.

2.6.3 Chemical recycling

This method involves attacking the matrix with a solvent. Up to now, little work has been done on the chemical recycling of natural fibre composites with thermoplastic or thermoset matrix. However, if a chemical treatment would dissolve the matrix without damaging the fibres or reducing the properties of the fibres, this could be a possible recycling method. Three dissolution process can be used and they are classified into three major categories: hydrolysis [214, 215], glycolysis [216] and acid digestion [217]. These chemical recycling processes have already been used for the recycling of carbon and glass fibre composites. Figure 2-41 shows a SEM micrograph of carbon fibres after a glycolysis treatment on a carbon-epoxy composite. The fibres show a very clean and non-damaged surface.

Work has been done on the acid attack of sulphuric acid on Carbon/PEEK composites in order to degrade the matrix and recuperate the fibres [218]. The recycled material was then reprocessed into a carbon/PEEK composite, while adding a certain amount of fresh thermoplastic. Its properties where compared with those of the virgin composite and it was found that the flexural modulus of the recycled material only reached 20% of that of the virgin composite, the flexure strength decreased to a value of 10% of that of the virgin composite. The adhesion between the recycled carbon and the fresh PEEK matrix may not be optimum after recycling due to the change of the fibre surface chemistry which may lead to a strong decrease in properties. Furthermore, "physical" damage to the brittle fibres could have been induces during the recycling process.

Another important aspect in the chemical recycling processes is the role of temperature. In many processes a temperature of 250°C to 450°C is needed to successfully remove the matrix material [194]. For carbon fibres, the degradation of the material was limited and the fibres retained 85-99% of their original strength [216]. However, for glass fibres, this loss in mechanical properties was more severe due to the higher temperatures associated with the process. Up till now, these processes have only been tested on a lab scale and limited work has been done on the chemical recycling of natural fibre composites.

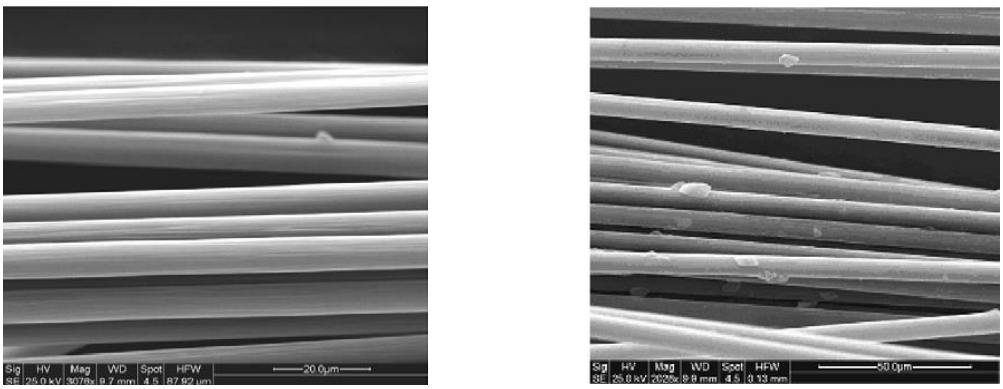

Figure 2-41: SEM micrographs of carbon fibres (bar left – 20µm, bar right – 50 µm). The picture on the left hand side shows a very clean fibre after dissolving the epoxy matrix (98wt% resin eliminated). The picture on the right hand side shows that there still is some epoxy left on the fibres (72 wt% resin eliminated)[216].

2.6.4 Landfill and composting

The landfill end-of life solution was once very popular, but landfilling occupies a very large area of land and does not allow any recovery of the embodied energy of the buried

materials. Additionally, the disposed waste has to be pre-treated to reduce the environmental impact of hazardous elements in the soil that could eventually end up in the water.

Natural fibre composites could also be composted, but the link between the intrinsic biodegradability of natural fibres and the compostability of their composites is not straightforward. So far, research is limited, but a study from Defoirdt et al. [219] showed that flax-epoxy composites have to be "attacked" by several types of fungi in order to be composted. Under the right moisture conditions, flax fibres act as a nutrient source for fungi, and it was shown that brown rot fungi are more effective than white rot fungi, because of the low lignin content of flax.

2.7 Life Cycle Assessment – LCA

The LCA is a multi-step procedure used to calculate the environmental impact of a product over its entire life cycle, from the production of the raw materials to its disposal. In between, the manufacturing of the products, its assembly, transport and use phase are taken into account. Figure 2-42 summarises the life cycle of a product. For the FFRP, the mining phase corresponds to the flax cultivation and polymer raw materials production. It also shows how the products, components or materials can be reintroduced in the life cycle and this hence reduces the amount of material that has to be recycled or disposed of.

An effective LCA allows analysts to quantify the environmental impact of a product. It also allows the identification of the positive or negative environmental impact and gives new avenues for improvement as well as enabling the comparison with other products. Moreover, the LCA allows experts to gather knowledge on the technological, economic, environmental and social aspects which are necessary to a complete product life cycle evaluation. Thus, with this quantitative data in hand, changes on a process can be justified with respect to the cost and environmental impacts.

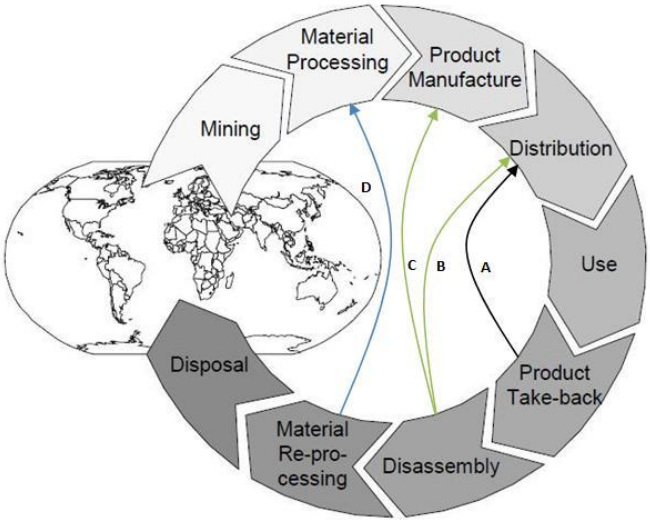

Figure 2-42: Cradle to grave life cycle with re-use possibilities: a) direct re-use of the product, b) direct re-use of components, c) remanufacturing of usable components, d) recycling of materials adapted from [220].

The environmental impact evaluation of a product is done according to the ISO 14040 and ISO 14044 standards. This an interactive and iterative process which contains four main steps as described in Figure 2-43.

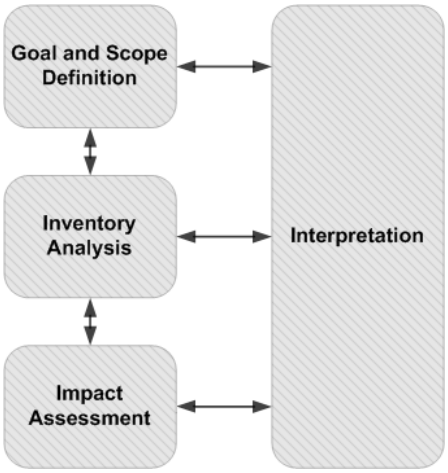

Figure 2-43 : Life cycle assessment framework[221].

- Step 1- Definition of the goal and scope determines the information needs, specificity, and the collection methods and data presentation.
  Assessment of the environmental performance of a certain product or material, it is important to define a certain unit of equivalence on which the environmental study is based. The functional unit defines qualitatively and quantitatively the functions of a product. Based on this functional unit, a comparison between alternatives can be made. Besides defining the goal of the life cycle assessment, the system boundaries, the assumptions and limitations, the allocation methods and the impact categories are chosen.
- Step 2 - The life cycle inventory (LCI) is the data collection portion of LCA, completed trough process diagrams, data collection and evaluation.
  This step is a straightforward accounting of everything involved in the studied system. It includes details and quantification of all in and out flows for the product. This includes raw materials, type of energy and the country mix, water and all the substances emitted to air, water and land.
- Step 3- The life cycle impact assessment (LCIA): this is when the inventory is analysed for environmental impact according to the impact categories and their weight.

After listing the different input and output parameters (inventory), these parameters are classified into various midpoint categories. This classification is based on the influence the component has on the environmental mechanisms operating, e.g. CO_2 has a known impact on the climate change. The LCIA considers the LCI data, but also gives a stronger basis for comparison. According to ISO 14042, impact category selection, classification, and characterization are required steps when performing an LCIA. Figure 2-44 gives an overview of how such classification is performed with the example of methane (CH_4).

Later on, the midpoint categories are further grouped into endpoint categories. The three endpoint categories are “Damage to human health”, “Damage to ecosystem diversity” and “Resource scarcity”. These categories are measured in a specific set of units. The damage to human health for example can be measured in disability adjusted life years (DALY), years of life lost (YLL) or the years of life disabled (YLD) [222]. When classifying the various emissions into midpoint categories, it is important to understand the underlying mechanisms that operate. However, when the effects are not fully known or understood, a high uncertainty arises. When looking at larger time scales, for instance effects after a

hundred or five hundred years, the uncertainty on the effects of different emitted sources will be even larger.

Two more optional steps can be performed: normalization and weighting. In the normalization step the impact can be placed into a certain reference system, for example the average European consumer. The weighting step allows the ranking of the different impact categories. This can be of interest if a comparison is made between multiple products and some impact categories have a higher interest to the producer of these components, for example because of governmental regulations on a certain impact category.

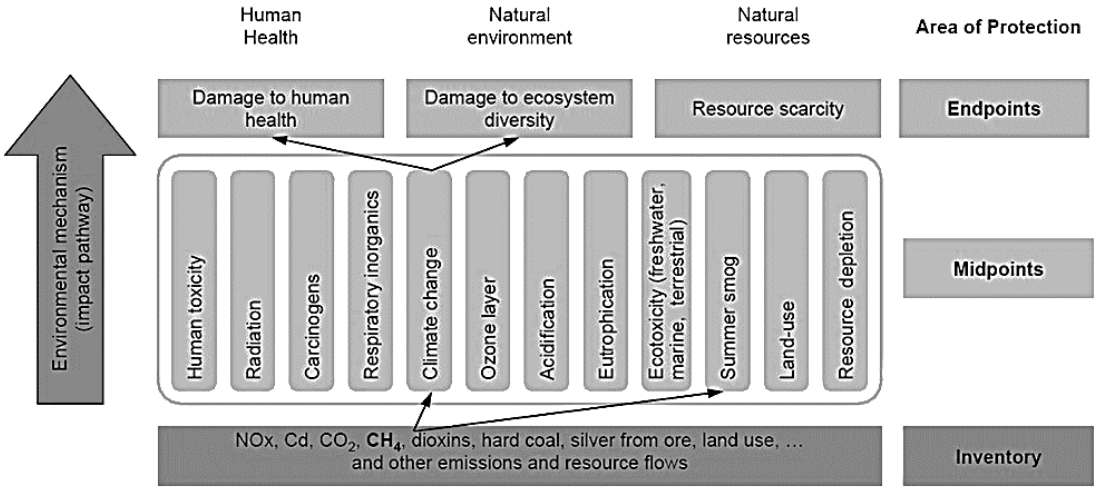

Figure 2-44: LCA assessment worksheet for methane [223].

- Step 4 – Interpretation is the final report which includes the significant data, the data evaluation and interpretation, the final conclusions and recommendations.

As a final step in the life cycle analysis, these results will have to be interpreted. In comparative studies this usually leads to the preference of product A over product B. However, it is also important to evaluate the various assumptions that are made in the study. In some cases a sensitivity analysis will have to be conducted in order to check the influence of a parameter on the global impact of the product.

2.7.1 Environmental impact of flax fibres

Flax is often compared to glass fibres as they both share similar specific properties as reported in many studies [2, 224, 225]. Thus, many comparative studies are made between glass and natural fibres in order to investigate whether the substitution of glass fibres by natural fibres is environmentally beneficial.

Life cycle studies [211, 226, 227] comparing flax and glass fibres have shown that flax fibres are undoubtedly beneficial for the environment compared to glass fibres as seen in Table 2-11, where the required energies are compared for different fibres and preforms. Furthermore, Le Duigou et Baley [228] have found that substituting glass fibres by flax fibres in a polypropylene composite with a similar material index reduces all the environmental impacts by 10% for abiotic depletion and global warming to 20% for acidification (Figure 2-45). Non-renewable energy used was also reduced by 12% passing from 109.8 MJ/kg for glass-PP composite to 96.5 MJ/kg for flax-PP composite. Deng et al. [210, 229, 230] using an equal stiffness criterion have shown that flax mat-PP with higher

volume fraction is environmentally more advantageous (impact category of climate change) when compared to glass mat-PP composite. Since flax fibres have a lower density than glass fibres (1.45 vs 2.55 kg/m^3), flax composites lead to lighter structure and contribute to a lower fuel consumption. However, if a higher quantity of flax is used to achieve the targeted properties, such as stiffness or strength, the environmental advantage of flax may reduce.

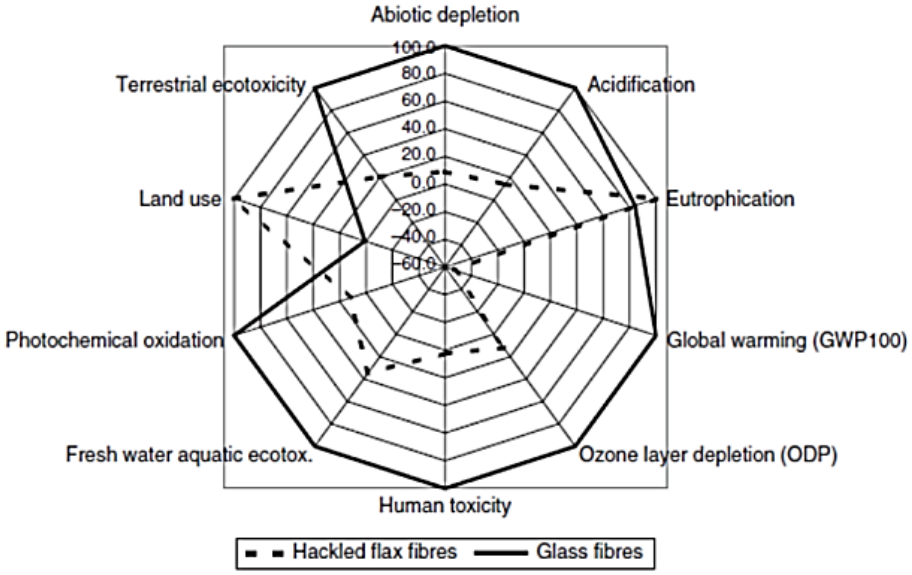

Figure 2-45: The environmental impact results of flax fibres vs. glass fibres [226].

Fibre production type	Non-renewable Energy Requirements	Source
Flax (Hackled)	11,7 GJ/ton fibres	[226]
Flax fibre mat	9,55 GJ/ton fibres	[211]
Flax fibres	12,4 GJ/ton fibres	[227]
Glass fibre mat	54,7 GJ/ton fibres	[211]
Glass fibres	45 GJ/ton fibres	[226]

Table 2-11: Non-renewable energy requirements of fibres [211, 226, 227].

Diverging observations were made by Dissanayake et al. [231] who found that the production of flax sliver in England and glass mat is comparable in terms of energy as seen in Table 2-12. This is caused by the fact that the entire environmental burden was assigned the flax fibre product alone, whereas the by-products, like scotched and hackled tows, were considered as waste. This is not realistic as all by-products (dust, shives, woody parts, etc…) are used in the industry to produce random mat, injection moulding compounds or flax boards. On the other hand, Le Duigou et al. [226, 232] allocated a significant part of the environmental burden to the by-products. Furthermore, the former authors [231] used wet spinning data of very fine linen yarns aimed for the fashion industry. The production of such yarn is more energy intensive since they need to be dried at the end of the production, and does not lead to a better composite, as has been stated earlier.

Another difference to take into account is geographical location of the flax production. Flax produced in England or in France uses the local energy production mixture, thus the impact associated to the energy production can vary substantially. Furthermore, the retting technique, the production yield of flax per hectare of land, the proportion of long flax fibres per stem of flax and the use of co-products in other industries all make a difference in the

data processing. The first set of studies [211, 226, 227, 229, 230, 233] was found to be more reliable because the inventory data is closer to the real production process of the flax fibres in continental Europe. This is especially in countries were flax fibres are produced in large quantities (like France and Belgium), and were the knowhow of the production process is high.

Fibre production type	Embodied Energy
Sliver (no till + warm water retting)	59 GJ/ton fibres
Yarn (no till + warm water retting)	86 GJ/ton fibres
Glass fibre mat	55 GJ/ton fibres
Continuous glass fibres	26 GJ/ton fibres

Table 2-12: Embodied energy per ton of fibres reported by [231].

Another option, which could be beneficial to reduce the impact of glass and carbon fibre, is to hybridize them with flax. This allows the optimization of the mechanical properties, reduces the weight (in the case of glass fibre) and increases vibration damping and acoustic performance. Figure 2-46 displays the energy needed to produce 1 litre of material (equal volume used as a normalising factor, in order to account for density differences) [234]. It can be seen that the sole use of flax fibre is beneficial for the environment in comparison to glass and carbon fibres. However, the carbon composite embodied energy can be drastically reduced by more than 50% if the carbon is hybridised with flax fibres.

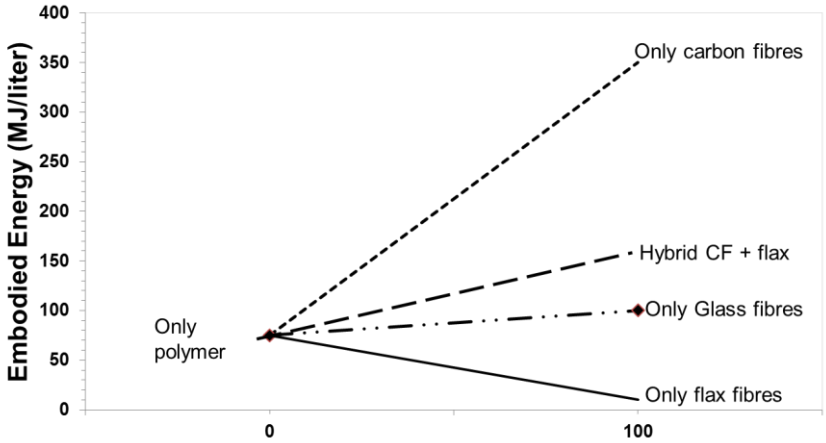

Figure 2-46: Required energy to produce of 1 litre of flax, glass and carbon fibre composites [234].

Finally, the type of load that a part sustains during its life cycle is also important as it affect the proportion of fibre and matrix. In an LCA, the critical load case is expressed as a mass flow of the used components. This is why the functional unit has to be clearly defined with the most relevant properties such as its mechanical function (tensile, impact or flexural), durability and minimum fibre content to fulfil the performance according to the applicable standards.

2.7.2 Life cycle analysis of EOL possibilities

The data on environmental impact of end of life techniques are as of today rather scarce or even non-existing as the studies on recycling of composites are themselves limited. Villanueva et al. [235] have looked at the paper and cardboard (cellulose based products similar to flax) waste recycling and have found an environmental benefit in recycling over incineration or landfill option.

Hedlund-Astrom [212] studied the disposal possibilities for polymer composites. The author found a lower environmental impact for the mechanical recycling compared to energy recovery by waste incineration for the same transport distance. However, the mechanical recycling induces higher operation costs. Furthermore, as the material properties are downgraded following a mechanical recycling, to achieve equal properties as the fresh material, more material is needed. Thus, there is an increase in environmental burden although it is still lower than incineration.

Yelin Deng [229] compared the environmental impacts of natural fibre reinforced polymer (NFRP) with glass fibre reinforced polymer (GFRP) for automotive applications, during the different life-cycle phases with the EOL scenario being incineration with energy recovery (see Figure 2-47). He has found that NFRPs provide fewer energy credits in the EOL phase if compared to GFRP. This is caused by the fact that less material is used for the NFRP products and thus, fewer materials to be incinerated. On the other hand, NFRP will require less energy during the production and use phases leading to a significantly reduced environmental impact for the total life cycle. The main environmental concerns for NFRPs, particularly bio-based polymers/natural fibres, are emission of nitrogen and phosphorus during cultivation, large arable-land requirements, and ecosystem quality. Currently, these impacts are too uncertain to be included in LCA studies and more data on the production-phase impacts of NFRPs are needed.

Products	NFRP	Replaced material	Production per piece	Use per piece	EoL per piece
[a]Transport pellet[67]	China reed/PP	GF/PP	-637MJ	-46~-1840MJ	+5.6MJ
[b]side panel of car[58]	Hemp/EP	ABS	-59MJ	-118MJ	+27MJ
[c]Car interior[83]	Bagasse/PP	Talc/PP	-222MJ	-19313MJ	+62.3MJ

Figure 2-47: Environmental impact comparison between natural fibre composites and the standard materials (fulfilling equivalent mechanical properties) for the total driven distance between 5000 and 200 000 km. [229].

2.8 Conclusions

The use of natural fibres as replacement of less environmentally-friendly products, such as glass fibres, sparks a strong interest in the composite industry, in response to society's demand for more renewable resources. In this context, the use of flax fibre is increasing, thanks to key functionalities, such as acoustic and thermal insulation, vibration damping, as well as renewability. In terms of mechanical performance, flax fibres are known to be as stiff as glass fibres, and even stiffer than glass when normalised to their low density. Furthermore, the flax fibre is the strongest of the natural fibre family. The growing use of flax fibres in composite materials in the past years has revealed a major lack of data on their in-service properties, such as moisture sensitivity and water sorption properties, durability (e.g. fatigue and impact) and LCA data. This has limited their introduction into high performance applications.

Knowledge of the basic tensile and flexural properties of a material provides important information for the material selection process. A material must have the required properties to work adequately for the expected product in-service lifetime. This the first step used for the classification and identification of the materials performance. As presented in this

review, there is an extended knowledge on these properties for different fibres architecture and matrix combinations.

As of today, very few researchers have attempted to study the fatigue and impact behaviour of flax fibres and their composites. Most studies were performed on glass fibre and carbon fibre composites, assessing the different influencing factors on the part design. The limited fatigue studies available showed the potential of flax composite in structural applications and have found that their performance is comparable to glass fibre composites at equivalent densities. However, no specific data on drop weight impact tests on flax fibre composites were found. A general study combining several different fibre architectures and different matrices, which aims to understand the different failure mechanisms, is still lacking.

LCA studies done on flax fibres and their composites show a large variability in the results, however they prove the environmental benefit when replacing glass fibres by flax fibres. These LCA studies only incorporate the production of the fibre material, but a complete environmental impact study should include the entire life phase of the component as the use phase has often the greatest share in the total environmental impact of a part. Furthermore, the recyclability of natural fibre composites is often claimed, but not many studies are available. In the future, a study which gives information on the properties of recycled natural fibre composites is necessary in order to have reliable results as in input for LCA analyses.

References

[1] Wambua P, Ivens J, Verpoest I. Natural fibres: can they replace glass in fibre reinforced plastics? Composites Science and Technology. 2003;63(9):1259-64.
[2] Verpoest I, Baets J, Van Acker J, Lilholt H, Mussig J, Hughes M, Baley C, et al. Flax and Hemp fibres: a natural solution for the composite industry. First Edition. In: Reux F, Verpoest I, editors. Paris, France. Prepared for JEC by the European Scientific Committee of CELC: JEC Group/CELC; 2012. ISBN 978-2-9526276-1-0.
[3] Kalia S, Kaith BS, Kaur I. Pretreatments of natural fibers and their application as reinforcing material in polymer composites—A review. Polymer Engineering & Science. 2009;49(7):1253-72.
[4] Berger C, Bledzki AK, Heim H-P, Bottcher A. Fiber-reinforced epoxy composites made from renewable resources. 2011 SAMPE Spring Technical Conference and Exhibition - State of the Industry: Advanced Materials, Applications, and Processing Technology, May 23, 2011 - May 26, 2011. Long Beach, CA, United states: Soc. for the Advancement of Material and Process Engineering; 2011. p. SAMPE Orange County Chapter.
[5] Goutianos S, Peijs T. The optimisation of flax fibre yarns for the development of high-performance natural fibre composites. Advanced Composites Letters. 2003;12(6):237-41.
[6] Singleton ACN, Baillie CA, Beaumont PWR, Peijs T. On the mechanical properties, deformation and fracture of a natural fibre/recycled polymer composite. Composites Part B: Engineering. 2003;34(6):519-26.
[7] Carus M, Eder A, Dammer L, Korte H, Scholz L, Essel R, Breitmayer E. Wood-plastic composites (WPC) and natural fibre composites (NFC): European and global markets 2012 and future trends. WPC/NFC market study. 2014;3:2014.
[8] Bledzki A, Gassan J. Composites reinforced with cellulose based fibres. Progress in polymer science. 1999;24(2):221-74.
[9] Miao M, Finn N. Conversion of Natural Fibres into Structural Composites. Journal of Textile Engineering. 2008;54(6):165-77.
[10] Ouagne P, Bizet L, Baley C, Breard J. Analysis of the film-stacking processing parameters for PLLA/flax fiber biocomposites. Journal of Composite Materials. 2010;44(10):1201-15.
[11] Baley C. Fibres naturelles de renfort pour matériaux composites. 2005. http://www.techniques-ingenieur.fr/base-documentaire/materiaux-th11/materiaux-fonctionnels-ti580/fibres-naturelles-de-renfort-pour-materiaux-composites-n2220/
[12] C.A.R.M.A. Glossaire des Matériaux Composites Renforcés des Fibres d'orgine Renouvelable. 2006.
[13] Gent DM. Synthetic by nature. 2015. http://www.designmuseumgent.be/ENG/exhibitions-2015/Synthetic-by-Nature.php
[14] Balter M. Clothes Make the (Hu) Man. Science. 2009;325(5946):1329.
[15] Kvavadze E, Bar-Yosef O, Belfer-Cohen A, Boaretto E, Jakeli N, Matskevich Z, Meshveliani T. 30,000-year-old wild flax fibers. Science. 2009;325(5946):1359-.
[16] Canada FCo, Commission SFD. Growing Flax. Canada2015.
[17] Abhervé M. Découvrir le lin par une véloroute. 2015.
http://alternatives-economiques.fr/blogs/abherve/2015/06/05/decouvrir-le-lin-par-une-veloroute/

[18] Pallesen BE. The quality of combine-harvested fibre flax for industrials purposes depends on the degree of retting. Industrial Crops and Products. 1996;5(1):65-78.
[19] Meijer WJM, Vertregt N, Rutgers B, van de Waart M. The pectin content as a measure of the retting and rettability of flax. Industrial Crops and Products. 1995;4(4):273-84.
[20] Kessler RW, Becker U, Kohler R, Goth B. Steam explosion of flax - A superior technique for upgrading fibre value. Biomass and Bioenergy. 1998;14(3):237-49.
[21] Mount B. Bring Our Flax Home. 2010. http://www.brahmsmount.com/blog/in-the-news/
[22] Brouwer W. Natural fibre composites in structural components: alternative applications for Sisal? 2000. http://www.fao.org/docrep/004/y1873e/y1873e0a.htm
[23] Bos HL. The potential of flax fibres as reinforcement for composite materials: Technische Universiteit Eindhoven; 2004.
[24] Bos HL. The potential of flax fibres as reinforcement for composite materials Eindhoven, Technische Universiteit Eindhoven; 2004.
[25] De Coster A. Telen en oogsten van vlas. Bereiding van de vlasvezel. In: Vlastechnologie TA, editor.: Centexbel; 2004.
[26] Baley C. Analysis of the flax fibres tensile behaviour and analysis of the tensile stiffnes increase. Composites Part A. 2002;33:943-8.
[27] Van de Weyenberg I. Flax fibres as reinforcement for epoxy composites,PhD, Leuven, Katholieke Universiteit Leuven; 2005.
[28] Müssig J. Untersuchung der Eignung heimischer Pflanzenfasern für die Herstellung von naturfaserverstärkten Duroplasten - vom Anbau zum Verbundwerkstoff Fortschritt-Bericht VDI; 2001.
[29] Baley C, Busnel F, Grohens Y, Sire O. Influence of chemical treatments on surface properties and adhesion of flax fibre-polyester resin. Composites Part A: Applied Science and Manufacturing. 2006;37(10):1626-37.
[30] Gorshkova TA, Wyatt SE, Salnikov VV, Gibeaut DM, Ibragimov MR, Lozovaya VV, Carpita NC. Cell-wall polysaccharides of developing flax plants. Plant Physiology. 1996;110(3):721-9.
[31] Mooney C, Stolle-Smits T, Schols H, de Jong E. Analysis of retted and non retted flax fibres by chemical and enzymatic means. Journal of biotechnology. 2001;89(2):205-16.
[32] Gorshkova TA, Sal'nikov VV, Chemikosova SB, Ageeva MV, Pavlencheva NV, van Dam JE. The snap point: a transition point in< i> Linum usitatissimum</i> bast fiber development. Industrial Crops and Products. 2003;18(3):213-21.
[33] Charlet K, Baley C, Morvan C, Jernot JP, Gomina M, Breard J. Characteristics of Hermes flax fibres as a function of their location in the stem and properties of the derived unidirectional composites. Composites Part a-Applied Science and Manufacturing. 2007;38(8):1912-21.
[34] Klemm D, Heublein B, Fink HP, Bohn A. Cellulose: fascinating biopolymer and sustainable raw material. Angewandte Chemie International Edition. 2005;44(22):3358-93.
[35] Lewin M, Pearce EM. Handbook of Fiber Chemistry, Revised and Expanded: Crc Press; 1998.
[36] Erdtman H. Lignins: Occurrence, formation, structure and reactions, K. V. Sarkanen and C. H. Ludwig, Eds., John Wiley & Sons, Inc., New York, 1971. 916 pp. $35.00. Journal of Polymer Science Part B: Polymer Letters. 1972;10(3):228-30.
[37] Bos HL, Van den Oever MJA, Peters O. Tensile and compressive properties of flax fibres for natural fibre reinforced composites. Journal of Materials Science. 2002;37(8):1683-92.
[38] Stamboulis A, Baillie CA, Peijs T. Effects of environmental conditions on mechanical and physical properties of flax fibers. Composites Part A: Applied Science and Manufacturing. 2001;32(8):1105-15.
[39] De Vriese L. Mechanische eigenschappen van unidirectionele kokosvezelcomposieten, MTM KULeuven; 2009-2010.
[40] CELC. Flax and Hemp fibres: a natural solution for the composite industry. Paris: JEC composites; 2012.
[41] Ivens J, Bos H, Verpoest I. The applicability of natural fibres as reinforcement for polymer composites. Proc Conference on Renewable Bioproducts-Industrial Outlets and Research for the 21st Century1997.
[42] Wang B, Panigrahi S, Tabil L, Crerar W, Sokansanj S, Braun L. Application of pre-treated flax fibres in composites. CSAE/SCGR Meeting2003.
[43] Goutianos S, Peijs T, Nystrom B, Skrifvars M. Development of flax fibre based textile reinforcements for composite applications. Applied Composite Materials. 2006;13(4):199-215.
[44] Hull D, Clyne T. An introduction to composite materials: Cambridge university press; 1996.
[45] Charlet K, Baley C, Morvan C, Jernot JP, Gomina M, Bréard J. Characteristics of Hermès flax fibres as a function of their location in the stem and properties of the derived unidirectional composites. Composites Part A: Applied Science and Manufacturing. 2007;38(8):1912-21.
[46] Charlet K, Jernot,J.P., Gomina, M., Bréard, J., Morvan, C., Baley, C. Flax fibre reinforced composites: influence of the fibre position in the stem on its mechanical , chemical and morphological properties. ECCM 12. Biarritz2006.
[47] Osorio L, Trujillo E, Van Vuure A, Verpoest I. Morphological aspects and mechanical properties of single bamboo fibres and flexural characterization of bamboo/epoxy composites. Journal of Reinforced Plastics and Composites. 2011:0731684410397683.
[48] Trujillo E, Moesen M, Osorio L, Van Vuure A, Ivens J, Verpoest I. Bamboo fibres for reinforcement in composite materials: Strength Weibull analysis. Composites Part A: Applied Science and Manufacturing. 2014;61:115-25.
[49] Toray Carbon Fibers. Technical data sheet - Torayca T700s. http://www.toraycfa.com/pdfs/T700SDataSheet.pdf
[50] Toray Carbon Fibers. Technical data sheet - Torayca T300. http://www.toraycfa.com/pdfs/T300DataSheet.pdf
[51] Yan L, Chouw N, Jayaraman K. Flax fibre and its composites – A review. Composites Part B: Engineering. 2014;56:296-317.

[52] Charlet K, Jernot J-P, Breard J, Gomina M. Scattering of morphological and mechanical properties of flax fibres. Industrial Crops and Products. 2010;32(3):220-4.
[53] Lamy B, Baley C. Stiffness prediction of flax fibers-epoxy composite materials. Journal of materials science letters. 2000;19(11):979-80.
[54] Müssig J, Haag K. 2 - The use of flax fibres as reinforcements in composites. In: Faruk O, Sain M, editors. Biofiber Reinforcements in Composite Materials: Woodhead Publishing; 2015. p. 35-85. ISBN 978-1-78242-122-1.
[55] Coroller G, Lefeuvre A, Le Duigou A, Bourmaud A, Ausias G, Gaudry T, Baley C. Effect of flax fibres individualisation on tensile failure of flax/epoxy unidirectional composite. Composites Part A: Applied Science and Manufacturing. 2013;51:62-70.
[56] Placet V, Cissé O, Lamine Boubakar M. Nonlinear tensile behaviour of elementary hemp fibres. Part I: Investigation of the possible origins using repeated progressive loading with in situ microscopic observations. Composites Part A: Applied Science and Manufacturing. 2014;56:319-27.
[57] Yao J, Yu W. Tensile strength and its variation for PAN-based carbon fibers. II. Calibration of the variation from testing. Journal of Applied Polymer Science. 2007;104(4):2625-32.
[58] Chi ZF, Chou TW, Shen GY. Determination of single fibre strength distribution from fibre bundle testing. Journal of Materials Science. 1984;19(10):3319-24.
[59] ISO 10618:2004 : Carbon fibre -- Determination of tensile properties of resin-impregnated yarn. 2004.
[60] Swolfs Y, Morton H, Scott AE, Gorbatikh L, Reed PAS, Sinclair I, Spearing SM, et al. Synchrotron radiation computed tomography for experimental validation of a tensile strength model for unidirectional fibre-reinforced composites. Accepted in Composites Part A: Applied Science and Manufacturing. 2015.
[61] Swolfs Y, McMeeking RM, Verpoest I, Gorbatikh L. Matrix cracks around fibre breaks and their effect on stress redistribution and failure development in unidirectional composites. Composites Science and Technology. 2015;108:16-22.
[62] Swolfs Y, Verpoest I, Gorbatikh L. Issues in strength models for unidirectional fibre-reinforced composites related to Weibull distributions, fibre packings and boundary effects. Composites Science and Technology. 2015;114:42-9.
[63] Bensadoun F, Verpoest I, Mussig J, Graupner N, Davies P, Gomina M, Kervoelen A, et al. Development and validation of an Impregnated Fibre Bundle Test for natural fibres, used as reinforcement in composites. Composite Part A. 2015.
[64] Lundquist L, Leterrier Y, Sunderland P, Månson J-AE. Life Cycle Engineering of Plastics: Technology, Economy and Environment: Technology, Economy and Environment: Elsevier; 2001.
[65] Verpoest I. Polymeercomposieten: cursustekst2009.
[66] Van Krevelen DW, Te Nijenhuis K. Properties of polymers: their correlation with chemical structure; their numerical estimation and prediction from additive group contributions: Elsevier; 2009.
[67] Goodman SW. Handbook of Thermoset Plastics, 2nd Edition1999.
[68] A.Osswald T. International Plastics Handbook: The eresource for Plastics Engineers2006.
[69] Shen L HJ, Patel MK. Product overview and market projection of emerging bio-based plastics. PRO-BIP; Final Report. Utrecht, The Netherlands, Utrecht University2009.
[70] Baley C. Analysis of the flax fibres tensile behaviour and analysis of the tensile stiffness increase. Composites Part A: Applied Science and Manufacturing. 2002;33(7):939-48.
[71] Bourmaud A, Morvan C, Baley C. Importance of fiber preparation to optimize the surface and mechanical properties of unitary flax fiber. Industrial Crops and Products. 2010;32(3):662-7.
[72] Defoirdt N, Biswas S, Vriese LD, Tran LQN, Acker JV, Ahsan Q, Gorbatikh L, et al. Assessment of the tensile properties of coir, bamboo and jute fibre. Composites Part A: Applied Science and Manufacturing. 2010;41(5):588-95.
[73] Huber T, Mussig J. Fibre matrix adhesion of natural fibres cotton, flax and hemp in polymeric matrices analyzed with the single fibre fragmentation test. Composite Interfaces. 2008;15(2-3):335-49.
[74] Biagiotti J, Puglia D, Kenny JM. A Review on Natural Fibre-Based Composites-Part I. Journal of Natural Fibers. 2004;1(2):37-68.
[75] Lomov SV, Bogdanovich AE, Ivanov DS, Mungalov D, Karahan M, Verpoest I. A comparative study of tensile properties of non-crimp 3D orthogonal weave and multi-layer plain weave E-glass composites. Part 1: Materials, methods and principal results. Composites Part A: Applied Science and Manufacturing. 2009;40(8):1134-43.
[76] Baley C. Influence of kink bands on the tensile strength of flax fibers. Journal of Materials Science. 2004;39(1):331-4.
[77] Symington M, Banks W, Thomason J, Pethrick R, David-West O. Kink Bands In Flax And Hemp Polyester Composites. The 18th International Conference on Composite Materials (ICCM 18). Jeju Island (Korea):2011.
[78] Baets J, Plastria D, Ivens J, Verpoest I. Determination of the optimal flax fibre preparation for use in UD flax-epoxy composites. The 18th International Conference on Composite Materials (ICCM 18). Jeju Island (Korea):2011.
[79] Bibo GA, Hogg PJ. Influence of reinforcement architecture on damage mechanisms and residual strength of glass-fibre/epoxy composite systems. Composites Science and Technology. 1998;58(6):803-13.
[80] Fu S-Y, Lauke B, Mai Y-W. Science and engineering of short fibre reinforced polymer composites: Elsevier; 2009.
[81] Ruzaimi M, Rejab M, Muhamad MN. An Investigation into the Effects of Fibre Volume Fraction on GFRP Plate. 2008.
[82] Madsen B, Lilholt H. Physical and mechanical properties of unidirectional plant fibre composites—an evaluation of the influence of porosity. Composites Science and Technology. 2003;63(9):1265-72.
[83] Garkhail S, Heijenrath R, Peijs T. Mechanical properties of natural-fibre-mat-reinforced thermoplastics based on flax fibres and polypropylene. Applied Composite Materials. 2000;7(5-6):351-72.
[84] Oksman K, Skrifvars M, Selin JF. Natural fibres as reinforcement in polylactic acid (PLA) composites. Composites Science and Technology. 2003;63(9):1317-24.

[85] Bledzki AK, Faruk O, Sperber VE. Cars from bio-fibres. Macromolecular Materials and Engineering. 2006;291(5):449-57.
[86] Madsen B, Lilholt H. Volumetric Interaction Model in Natural Fiber Composites A Concept to be Used in Design and Process Optimization of Composites. 16th International Conference on Composite Materials (ICCM16). Kyoto (Japan):2007.
[87] Gurit. Guide to Composite. http://www.gurit.com/files/documents/guide-to-compositesv5webpdf.pdf
[88] Mallick PK. Fiber-reinforced composites: materials, manufacturing, and design. 3 ed: CRC press; 1993.
[89] Silva R, Spinelli D, Bose Filho W, Claro Neto S, Chierice G, Tarpani J. Fracture toughness of natural fibers/castor oil polyurethane composites. Composites Science and Technology. 2006;66(10):1328-35.
[90] Garcia-Gil R. Forming and consolidation of textile composites,PhD, University of Nottingham; 2003.
[91] Liu Q, Hughes M. The fracture behaviour and toughness of woven flax fibre reinforced epoxy composites. Composites Part A: Applied Science and Manufacturing. 2008;39(10):1644-52.
[92] Oksman K. High quality flax fibre composites manufactured by the resin transfer moulding process. Journal of Reinforced Plastics and Composites. 2001;20(7):621-7.
[93] Hughes M, Carpenter J, Hill C. Deformation and fracture behaviour of flax fibre reinforced thermosetting polymer matrix composites. Journal of Materials Science. 2007;42(7):2499-511.
[94] Mehmood S, Madsen B. Properties and performance of flax yarn/thermoplastic polyester composites. Journal of Reinforced Plastics and Composites. 2012;31(24):1746-57.
[95] Zhu J, Njuguna J, Abhyankar H, Zhu H, Perreux D, Thiebaud F, Chapelle D, et al. Effect of fibre configurations on mechanical properties of flax/tannin composites. Industrial Crops and Products. 2013;50(0):68-76.
[96] Adekunle K, Cho S-W, Patzelt C, Blomfeldt T, Skrifvars M. Impact and flexural properties of flax fabrics and Lyocell fiber-reinforced bio-based thermoset. Journal of Reinforced Plastics and Composites. 2011;30(8):685-97.
[97] Bos HL, Müssig J, van den Oever MJ. Mechanical properties of short-flax-fibre reinforced compounds. Composites Part A: Applied Science and Manufacturing. 2006;37(10):1591-604.
[98] Baets J, Plastria D, Ivens J, Verpoest I. Determination of the optimal flax fibre preparation for use in unidirectional flax–epoxy composites. Journal of Reinforced Plastics and Composites. 2014;33(5):493-502.
[99] Shah DU, Schubel PJ, Clifford MJ. Modelling the effect of yarn twist on the tensile strength of unidirectional plant fibre yarn composites. Journal of Composite Materials. 2013;47(4):425-36.
[100] Rask M, Madsen B. Twisting of fibres in yarns for natural fibre composites. ICCM18 - 18th International Conference On Composite Materials. Jeju Island, Korea:2011.
[101] Baets J, Vanfleteren F, Verpoest I. UD-flax preforms for optimal natural fibre composites performance. Composites Week @ Leuven and Texcomp-11. Leuven, Belgium:2013.
[102] Curtis PT, Bishop SM. An assessment of the potential of woven carbon fibre-reinforced plastics for high performance applications. Composites. 1984;15(4):259-65.
[103] Kim J-K, Sham M-L. Impact and delamination failure of woven-fabric composites. Composites Science and Technology. 2000;60(5):745-61.
[104] Duc F, Bourban P-E, Månson J-AE. Dynamic mechanical properties of epoxy/flax fibre composites. Journal of Reinforced Plastics and Composites. 2014;33(17):1625-33.
[105] Gassan J. A study of fibre and interface parameters affecting the fatigue behaviour of natural fibre composites. Composites Part A: Applied Science and Manufacturing. 2002;33(3):369-74.
[106] Hargitai H, Rácz I. Influence of Water on Properties of Cellulosic Fibre Reinforced Polypropylene Composites. International Journal of Polymeric Materials and Polymeric Biomaterials. 2000;47(4):667-74.
[107] Wong KK, Tao XM, Yuen CWM, Yeung KW. Low Temperature Plasma Treatment of Linen. Textile Research Journal. 1999;69(11):846-55.
[108] Sparavigna A. Plasma treatment advantages for textiles. arXiv preprint arXiv:08013727. 2008.
[109] Mukhopadhyay S, Fangueiro R. Physical Modification of Natural Fibers and Thermoplastic Films for Composites — A Review. Journal of Thermoplastic Composite Materials. 2009;22(2):135-62.
[110] Arbelaiz A, Fernández B, Ramos JA, Retegi A, Llano-Ponte R, Mondragon I. Mechanical properties of short flax fibre bundle/polypropylene composites: Influence of matrix/fibre modification, fibre content, water uptake and recycling. Composites Science and Technology. 2005;65(10):1582-92.
[111] Zafeiropoulos NE, Williams DR, Baillie CA, Matthews FL. Engineering and characterisation of the interface in flax fibre/polypropylene composite materials. Part I. Development and investigation of surface treatments. Composites Part A: Applied Science and Manufacturing. 2002;33(8):1083-93.
[112] Li X, Tabil L, Panigrahi S. Chemical Treatments of Natural Fiber for Use in Natural Fiber-Reinforced Composites: A Review. Journal of Polymers and the Environment. 2007;15(1):25-33.
[113] Li X, Tabil LG, Panigrahi S. Chemical treatments of natural fiber for use in natural fiber-reinforced composites: a review. Journal of Polymers and the Environment. 2007;15(1):25-33.
[114] Van de Weyenberg I, Ivens J, De Coster A, Kino B, Baetens E, Verpoest I. Influence of processing and chemical treatment of flax fibres on their composites. Composites Science and Technology. 2003;63(9):1241-6.
[115] Kabir MM, Wang H, Lau KT, Cardona F. Chemical treatments on plant-based natural fibre reinforced polymer composites: An overview. Composites Part B: Engineering. 2012;43(7):2883-92.
[116] Van de Weyenberg I, Chi Truong T, Vangrimde B, Verpoest I. Improving the properties of UD flax fibre reinforced composites by applying an alkaline fibre treatment. Composites Part A: Applied Science and Manufacturing. 2006;37(9):1368-76.
[117] Wang B, Panigrahi S, Tabil L, Crerar W. Pre-treatment of flax fibers for use in rotationally molded biocomposites. Journal of Reinforced Plastics and Composites. 2007;26(5):447-63.

[118] Grillet B. Investigation on the influence of moisture on the mechanical properties of chemically treated flax fiber polyester composites,Master thesis, Leuven, KU Leuven; 2015.
[119] Chen H, Miao M, Ding X. Influence of moisture absorption on the interfacial strength of bamboo/vinyl ester composites. Composites Part A: Applied Science and Manufacturing. 2009;40(12):2013-9.
[120] Symington MC, Banks WM, West D, Pethrick R. Tensile testing of cellulose based natural fibers for structural composite applications. Journal of Composite Materials. 2009.
[121] Assarar M, Scida D, El Mahi A, Poilane C, Ayad R. Influence of water ageing on mechanical properties and damage events of two reinforced composite materials: Flax-fibres and glass-fibres. Materials and Design. 2011;32(2):788-95.
[122] Scida D, Assarar M, Poilâne C, Ayad R. Influence of hygrothermal ageing on the damage mechanisms of flax-fibre reinforced epoxy composite. Composites Part B: Engineering. 2013;48:51-8.
[123] Ghazanfari A, Emami S, Tabil LG, Panigrahi S. Thin-Layer Drying of Flax Fiber: II. Modeling Drying Process Using Semi-Theoretical and Empirical Models. Drying Technology. 2006;24(12):1637-42.
[124] Raveendran Nair G. Microwave Assisted Drying of Flax Straw and Fibre at Controlled Temperatures. XVIIth World Congress of the International Commission of Agricultural and Biosystems Engineering. Canada:2010.
[125] Alibas I. Energy Consumption and Colour Characteristics of Nettle Leaves during Microwave, Vacuum and Convective Drying. Biosystems Engineering. 2007;96(4):495-502.
[126] Baley C, Le Duigou A, Bourmaud A, Davies P. Influence of drying on the mechanical behaviour of flax fibres and their unidirectional composites. Composites Part A: Applied Science and Manufacturing. 2012;43(8):1226-33.
[127] Ashby M. The CES EduPack database of natural and man-made materials. Granta Material Inspiration-Bioengineering; 2008.
[128] EL HAJJ N. Manufacturing process of 100% vegetable composite plates: Effect of the flax-tow grading on mechanical and physical properties.
[129] Arbelaiz A, Fernández B, Cantero G, Llano-Ponte R, Valea A, Mondragon I. Mechanical properties of flax fibre/polypropylene composites. Influence of fibre/matrix modification and glass fibre hybridization. Composites Part A: Applied Science and Manufacturing. 2005;36(12):1637-44.
[130] van den Oever MJA, Bos HL, van Kemenade MJJM. Influence of the Physical Structure of Flax Fibres on the Mechanical Properties of Flax Fibre Reinforced Polypropylene Composites. Applied Composite Materials. 2000;7(5-6):387-402.
[131] D A. Standard Test Method for Tension-Tension Fatigue of Polymer Matrix Composite Materials. Am. Soc. Test. Mater. W. Conshohocken, PA; 2002.
[132] Shah DU, Schubel PJ, Clifford MJ, Licence P. Fatigue life evaluation of aligned plant fibre composites through S/N curves and constant-life diagrams. Composites Science and Technology. 2013;74:139-49.
[133] !!! INVALID CITATION !!!
[134] Hamad W. On the mechanisms of cumulative damage and fracture in native cellulose fibres. Journal of materials science letters. 1998;17(5):433-6.
[135] Yuanjian T, Isaac DH. Impact and fatigue behaviour of hemp fibre composites. Composites Science and Technology. 2007;67(15–16):3300-7.
[136] Thwe MM, Liao K. Durability of bamboo-glass fiber reinforced polymer matrix hybrid composites. Composites Science and Technology. 2003;63(3):375-87.
[137] Liang S, Gning PB, Guillaumat L. A comparative study of fatigue behaviour of flax/epoxy and glass/epoxy composites. Composites Science and Technology. 2012;72(5):535-43.
[138] Silva FdA, Chawla N, de Toledo Filho RD. An experimental investigation of the fatigue behavior of sisal fibers. Materials Science and Engineering: A. 2009;516(1–2):90-5.
[139] Shahzad A, Isaac D. Fatigue properties of hemp and glass fiber composites. Polymer Composites. 2014;35(10):1926-34.
[140] Gassan J. A study of fibre and interface parameters affecting the fatigue behaviour of natural fibre composites. Composites - Part A: Applied Science and Manufacturing. 2002;33(3):369-74.
[141] Van Paepegem W, Degrieck J. A new coupled approach of residual stiffness and strength for fatigue of fibre-reinforced composites. International Journal of Fatigue. 2002;24(7):747-62.
[142] Shokrieh MM, Lessard LB. Multiaxial fatigue behaviour of unidirectional plies based on uniaxial fatigue experiments—II. Experimental evaluation. International Journal of Fatigue. 1997;19(3):209-17.
[143] Hacker CL, Ansell MP. Fatigue damage and hysteresis in wood-epoxy laminates. Journal of Materials Science. 2001;36(3):609-21.
[144] Towo AN, Ansell MP. Fatigue of sisal fibre reinforced composites: constant-life diagrams and hysteresis loop capture. Composites Science and Technology. 2008;68(3):915-24.
[145] Liang S, Gning P-B, Guillaumat L. Properties evolution of flax/epoxy composites under fatigue loading. International Journal of Fatigue. 2014;63(0):36-45.
[146] Vallons K, Zong M, Lomov V, Verpoest I. Carbon composites based on multi-axial multi-ply stitched preforms - Part 6. Fatigue behaviour at low loads: Stiffness degradation and damage development. Composites Part a-Applied Science and Manufacturing. 2007;38(7):1633-45.
[147] El Sawi I, Fawaz Z, Zitoune R, Bougherara H. An investigation of the damage mechanisms and fatigue life diagrams of flax fiber-reinforced polymer laminates. Journal of Materials Science. 2014;49(5):2338-46.
[148] de Vasconcellos DS, Touchard F, Chocinski-Arnault L. Tension–tension fatigue behaviour of woven hemp fibre reinforced epoxy composite: A multi-instrumented damage analysis. International Journal of Fatigue. 2014;59:159-69.
[149] Vallons K, Lomov SV, Verpoest I. Fatigue and post-fatigue behaviour of carbon/epoxy non-crimp fabric composites. Composites Part a-Applied Science and Manufacturing. 2009;40(3):251-9.

[150] Schrauwen B, Peijs T. Influence of Matrix Ductility and Fibre Architecture on the Repeated Impact Response of Glass-Fibre-Reinforced Laminated Composites. Applied Composite Materials. 2002;9(6):331-52.
[151] Caprino G, Lopresto V. On the penetration energy for fibre-reinforced plastics under low-velocity impact conditions. Composites Science and Technology. 2001;61(1):65-73.
[152] Sutherland LS, Guedes Soares C. Impact tests on woven-roving E-glass/polyester laminates. Composites Science and Technology. 1999;59(10):1553-67.
[153] Richardson MOW, Wisheart MJ. Review of low-velocity impact properties of composite materials. Composites Part A: Applied Science and Manufacturing. 1996;27(12):1123-31.
[154] Abrate S. Impact engineering of composite structures. Carbondale: SpringerWienNewYork; 2011.
[155] Cantwell WJ, Morton J. The impact resistance of composite materials — a review. Composites. 1991;22(5):347-62.
[156] Vallons K. Invloed van de matrixtaaiheid op de impactweerstand van thermoplastische PBT composieten, MTM KULeuven; 2005.
[157] Zhang BY, Chen XB, Li P, Yi XS. Toughness and hot/wet properties of a novel modified BMI/carbon fiber composite. J Mater Sci Technol. 2001;17(1):17-8.
[158] Richardson M, Wisheart M. Review of low-velocity impact properties of composite materials. Composites Part A: Applied Science and Manufacturing. 1996;27(12):1123-31.
[159] Vallons K. Invloed van de matrixtaaiheid op de impactweerstand van thermoplastische PBT composieten,PhD KU Leuven; 2005.
[160] Mishra S, Mohanty A, Drzal L, Misra M, Parija S, Nayak S, Tripathy S. Studies on mechanical performance of biofibre/glass reinforced polyester hybrid composites. Composites Science and Technology. 2003;63(10):1377-85.
[161] Thomason JL. The influence of fibre length, diameter and concentration on the impact performance of long glass-fibre reinforced polyamide 6,6. Composites Part A: Applied Science and Manufacturing. 2009;40(2):114-24.
[162] Belingardi G, Vadori R. Low velocity impact tests of laminate glass-fiber-epoxy matrix composite material plates. International Journal of Impact Engineering. 2002;27(2):213-29.
[163] Santulli C, Caruso A. A comparative study on falling weight impact properties of jute/epoxy and hemp/epoxy laminates. Malaysian Polymer Journal. 2009;4(1):19-29.
[164] Dhakal HN, Skrifvars M, Adekunle K, Zhang ZY. Falling weight impact response of jute/methacrylated soybean oil bio-composites under low velocity impact loading. Composites Science and Technology. 2014;92(0):134-41.
[165] Girolamo D, Davila CG, Leone FA, Lin S-Y. Adhesive Characterization and Progressive Damage Analysis of Bonded Composite Joints.
[166] Ma J, Qi Q, Bayley J, Du X-S, Mo M-S, Zhang L-Q. Development of SENB toughness measurement for thermoset resins. Polymer Testing. 2007;26(4):445-50.
[167] Verpoest I. Course polymeercomposieten., MTM KULeuven; 2010-2011.
[168] Cowley KD, Beaumont PW. The interlaminar and intralaminar fracture toughness of carbon-fibre/polymer composites: the effect of temperature. Composites Science and Technology. 1997;57(11):1433-44.
[169] Sela N, Ishai O. Interlaminar fracture toughness and toughening of laminated composite materials: a review. Composites. 1989;20(5):423-35.
[170] Cheremisinoff N. Handbook of Ceramics and Composites - Volume 2: Mechanical Properties and Specialty Applications: CRC Press 1991.
[171] Hunston D, Moulton R, Johnson N, Bascom W. Toughened composites. American Society for Testing and Materials, Philadelphia, PA. 1987:74-94.
[172] Aravand M, Lomov SV, Gorbatikh L. Morphology and fracture behavior of POM modified epoxy matrices and their carbon fiber composites. Composites Science and Technology. 2015;110:8-16.
[173] Scott J, Phillips D. Carbon fibre composites with rubber toughened matrices. Journal of Materials Science. 1975;10(4):551-62.
[174] Mallick PK. Fiber-reinforced composites: materials, manufacturing and design: CRC; 2007.
[175] Chamis CC, Hanson MP, Serafini TT. Impact resistance of unidirectional fiber composites. Composite Materials: Testing and Design (Second Conference): ASTM International; 1972.
[176] Roylance D. Stress-strain curves. Massachusetts Institute of Technology study, Cambridge. 2001.
[177] Kim BH, Joe CR, Otterson DM. On the determination of fracture toughness in polymers. Polymer Testing. 1988;8(2):119-30.
[178] Arencón D, Velasco JI. Fracture toughness of polypropylene-based particulate composites. Materials. 2009;2(4):2046-94.
[179] Ducept F, Davies P, Gamby D. An experimental study to validate tests used to determine mixed mode failure criteria of glass/epoxy composites. Composites Part A: Applied Science and Manufacturing. 1997;28(8):719-29.
[180] Ozdil F, Carlsson L. Beam analysis of angle-ply laminate DCB specimens. Composites Science and Technology. 1999;59(2):305-15.
[181] Davies P, Kausch HH, Williams JG, Kinloch AJ, Charalambides MN, Pavan A, Moore DR, et al. Round-robin interlaminar fracture testing of carbon-fibre-reinforced epoxy and PEEK composites. Composites Science and Technology. 1992;43(2):129-36.
[182] Davies P, Moulin C, Kausch H, Fischer M. Measurement of G IC and G IIC in carbon/epoxy composites. Composites Science and Technology. 1990;39(3):193-205.
[183] Zhu Y. Characterization of interlaminar fracture toughness of a carbon/epoxy composite material, The Pennsylvania State University; 2009.
[184] Shedden J. Simplifying the Testing and Calculation of Fracture Toughness of Thermoplastic and Thermoset Matrix Composite Materials Bachelor, San Luis Obispo California Polytechnic State University; 2013.

[185] Hashemi S, Kinloch A, Williams J. The analysis of interlaminar fracture in uniaxial fibre-polymer composites. Proceedings of the Royal Society of London A: Mathematical, Physical and Engineering Sciences: The Royal Society; 1990. p. 173-99.
[186] Zahlan N. Mechanical properties of the carbon fiber/PEEK composite APC-2/AS-4 for structural applications. American Society for Testing and Materials Special Technical Publication. 1989(1044):199.
[187] Davidson BD, Altonen CS, Polaha JJ. Effect of stacking sequence on delamination toughness and delamination growth behavior in composite end-notched flexure specimens. ASTM special technical publication. 1996;1274:393-413.
[188] Tanaka K, Kageyama K, Hojo M. Prestandardization study on mode II interlaminar fracture toughness test for cfrp in japan. Composites. 1995;26(4):257-67.
[189] Joshi S, Sun C. Impact induced fracture in a laminated composite. Journal of Composite Materials. 1985;19(1):51-66.
[190] Choi HY, Wu H-YT, Chang F-K. A new approach toward understanding damage mechanisms and mechanics of laminated composites due to low-velocity impact: Part II—analysis. Journal of Composite Materials. 1991;25(8):1012-38.
[191] Abrate S. Impact on composite structures: Cambridge university press; 2005.
[192] Cantwell W, Morton J. Geometrical effects in the low velocity impact response of CFRP. Composite Structures. 1989;12(1):39-59.
[193] Schneider J. End of life vehicles: Legal aspects, national practices and recommendations for future successful approach. Environment, Public Health and Food Safety. 2010.
[194] Yang Y, Boom R, Irion B, van Heerden D-J, Kuiper P, de Wit H. Recycling of composite materials. Chemical Engineering and Processing: Process Intensification. 2012;51:53-68.
[195] Pickering SJ. Recycling technologies for thermoset composite materials—current status. Composites Part A: Applied Science and Manufacturing. 2006;37(8):1206-15.
[196] Srebrenkoska V, Gaceva GB, Avella M, Errico ME, Gentile G. Recycling of polypropylene-based eco-composites. Polymer International. 2008;57(11):1252-7.
[197] Palmer J, Ghita OR, Savage L, Evans KE. Successful closed-loop recycling of thermoset composites. Composites Part A: Applied Science and Manufacturing. 2009;40(4):490-8.
[198] Otheguy M, Gibson A, Findon E, Cripps R, Mendoza AO, Castro MA. Recycling of end-of-life thermoplastic composite boats. Plastics, Rubber and Composites. 2009;38(9-10):406-11.
[199] Otheguy ME, Gibson AG, Findon E, Cripps RM, Mendoza AO, Castro MTA. Recycling of end-of-life thermoplastic composite boats. Plast Rubber Compos. 2009;38(9-10):406-11.
[200] Beg MDH, Pickering KL. Recycling and its effects on the physical and mechanical properties of wood fibre reinforced polypropylene composites. Key Eng Mater. 2007;334-335:497-500.
[201] Morán J, Alvarez V, Petrucci R, Kenny J, Vazquez A. Mechanical properties of polypropylene composites based on natural fibers subjected to multiple extrusion cycles. Journal of Applied Polymer Science. 2007;103(1):228-37.
[202] Bourmaud A, Baley C. Rigidity analysis of polypropylene/vegetal fibre composites after recycling. Polymer Degradation and Stability. 2009;94(3):297-305.
[203] Bourmaud A, Baley C. Investigations on the recycling of hemp and sisal fibre reinforced polypropylene composites. Polymer Degradation and Stability. 2007;92(6):1034-45.
[204] Cunliffe AM, Jones N, Williams PT. Pyrolysis of composite plastic waste. Environmental Technology. 2003;24(5):653-63.
[205] Cunliffe AM, Williams PT. Characterisation of products from the recycling of glass fibre reinforced polyester waste by pyrolysis☆. Fuel. 2003;82(18):2223-30.
[206] Yang L, Sáez ER, Nagel U, Thomason JL. Can thermally degraded glass fibre be regenerated for closed-loop recycling of thermosetting composites? Composites Part A: Applied Science and Manufacturing. 2015;72:167-74.
[207] Pickering SJ, Kelly RM, Kennerley JR, Rudd CD, Fenwick NJ. A fluidised-bed process for the recovery of glass fibres from scrap thermoset composites. Composites Science and Technology. 2000;60(4):509-23.
[208] Kennerley JR, Kelly RM, Fenwick NJ, Pickering SJ, Rudd CD. The characterisation and reuse of glass fibres recycled from scrap composites by the action of a fluidised bed process. Composites Part A: Applied Science and Manufacturing. 1998;29(7):839-45.
[209] Villanueva A, Wenzel H. Paper waste–recycling, incineration or landfilling? A review of existing life cycle assessments. Waste Management. 2007;27(8):S29-S46.
[210] Duflou JR, Yelin D, Van Acker K, Dewulf W. Comparative impact assessment for flax fibre versus conventional glass fibre reinforced composites: Are bio-based reinforcement materials the way to go? CIRP Annals-Manufacturing Technology. 2014;63(1):45-8.
[211] Joshi SV, Drzal LT, Mohanty AK, Arora S. Are natural fiber composites environmentally superior to glass fiber reinforced composites? Composites Part A: Applied Science and Manufacturing. 2004;35(3):371-6.
[212] Hedlund-Åström A. Model for end of life treatment of polymer composite materials. 2005.
[213] Grosso M, Motta A, Rigamonti L. Efficiency of energy recovery from waste incineration, in the light of the new Waste Framework Directive. Waste Management. 2010;30(7):1238-43.
[214] Oliveux G, Bailleul J-L, Salle ELGL. Chemical recycling of glass fibre reinforced composites using subcritical water. Composites Part A: Applied Science and Manufacturing. 2012;43(11):1809-18.
[215] Morin C, Loppinet-Serani A, Cansell F, Aymonier C. Near- and supercritical solvolysis of carbon fibre reinforced polymers (CFRPs) for recycling carbon fibers as a valuable resource: State of the art. The Journal of Supercritical Fluids. 2012;66(0):232-40.

[216] Piñero-Hernanz R, García-Serna J, Dodds C, Hyde J, Poliakoff M, Cocero MJ, Kingman S, et al. Chemical recycling of carbon fibre composites using alcohols under subcritical and supercritical conditions. The Journal of Supercritical Fluids. 2008;46(1):83-92.
[217] Dang W, Kubouchi M, Sembokuya H, Tsuda K. Chemical recycling of glass fiber reinforced epoxy resin cured with amine using nitric acid. Polymer. 2005;46(6):1905-12.
[218] Ramakrishna S, Tan W, Teoh S, Lai M. Recycling of carbon fiber/PEEK composites. Key Engineering Materials. 1997;137:1-8.
[219] Defoirdt N, De Windt I, Van den Bulcke J, Van Acker J. Biological durability of natural fibre reinforced composites. 45th IRG Annual meeting: International Research Group on Wood Protection (IRG); 2014.
[220] Duflou J. DW. Course text: Ecodesign & Life cycle engineering 2013.
[221] Corporation SAI, Curran MA. Life-cycle assessment: principles and practice: National Risk Management Research Laboratory, Office of Research and Development, US Environmental Protection Agency; 2006.
[222] Sustainability EC-JRC-IfEa. International Reference Life Cycle Data System Handbook - Framework and Requirements for Life Cycle Impact Assessment Models and Indicators. Luxembourg2010.
[223] Sustainability EC-JRC-IfEa. International Reference Life Cycle Data System Handbook-General guide for Life Cycle Assessment. Luxembourg2010.
[224] Arbelaiz A, Fernandez B, Cantero G, Llano-Ponte R, Valea A, Mondragon I. Mechanical properties of flax fibre/polypropylene composites. Influence of fibre/matrix modification and glass fibre hybridization. Composites Part A: Applied Science and Manufacturing. 2005;36(12):1637-44.
[225] Bodros E, Pillin I, Montrelay N, Baley C. Could biopolymers reinforced by randomly scattered flax fibre be used in structural applications? Composites Science and Technology. 2007;67(3-4):462-70.
[226] Le Duigou A, Davies P, Baley C. Environmental impact analysis of the production of flax fibres to be used as composite material reinforcement. Journal of Biobased Materials and Bioenergy. 2011;5(1):153-65.
[227] González-García S, Hospido A, Feijoo G, Moreira MT. Life cycle assessment of raw materials for non-wood pulp mills: Hemp and flax. Resources, Conservation and Recycling. 2010;54(11):923-30.
[228] Le Duigou A, Baley C. Coupled micromechanical analysis and life cycle assessment as an integrated tool for natural fibre composites development. Journal of Cleaner Production. 2014;83:61-9.
[229] Deng Y. Life Cycle Assessment of Biobased Fibre-Reinforced Polymer Composites, University of Leuven; 2014.
[230] Duflou JR, Deng Y, Van Acker K, Dewulf W. Do fiber-reinforced polymer composites provide environmentally benign alternatives? A life-cycle-assessment-based study. Mrs Bulletin. 2012;37(04):374-82.
[231] Dissanayake NPJ, Summerscales J, Grove SM, Singh MM. Life Cycle Impact Assessment of flax fibre for the reinforcement of composites. Journal of Biobased Materials and Bioenergy. 2009;3(3):245-8.
[232] Duigou A, Deux J-M, Davies P, Baley C. PLLA/Flax Mat/Balsa Bio-Sandwich—Environmental Impact and Simplified Life Cycle Analysis. Applied Composite Materials. 2011;19(3):363-78.
[233] Duflou JR, Yelin D, Van Acker K, Dewulf W. Comparative impact assessment for flax fibre versus conventional glass fibre reinforced composites: Are bio-based reinforcement materials the way to go? CIRP Annals - Manufacturing Technology. 2014;63(1):45-8.
[234] Pil L, Bensadoun F, Pariset J, Verpoest I. Why are designers fascinated by flax and hemp fibre composites? Composites Part A: Applied Science and Manufacturing.
[235] Villanueva A, Wenzel H. Paper waste – Recycling, incineration or landfilling? A review of existing life cycle assessments. Waste Management. 2007;27(8):S29-S46.

Chapter 3
Problem statement

Flax has proven its good specific mechanical properties over the years in a wide variety of applications. Still, a knowledge gap is found concerning some key properties such as flexural and tensile properties, impact and fatigue which are critical in the design of a part and its use in a real working environment. The purpose of this PhD is to understand the effects of textile architectures on the mechanical properties as well as the impact and fatigue behaviour of flax-based biocomposites. Additionally, it is essential to ensure that these materials are mechanically efficient, environmentally-friendly and renewable in order to encourage industry to adopt these green materials.

The main objective of this study is to characterize the quasi-static mechanical properties, the impact and fatigue behaviour of the flax fibre composites. This is done by focusing specifically in the influence of the matrix and the fibre architecture. The main hypothesis suggests that the performance of flax fibres composites is controlled by the intrinsic properties of the flax fibres and matrices as well as the textile architecture features such as twist and crimp. A second objective is to assess its environmental impact of the flax composite materials from cradle to grave.

All of these aspects will allow to evaluate the potential of the flax fibre reinforced composite to replace less environment-friendly materials in some applications. Thus, some questions arise as:

1. Are these flax composite mechanically performant?
2. What is the effect of the flax textile architecture?
3. How well do flax composites perform on the long term?
4. Are they comparable to glass fibres composite and other natural fibre reinforced composites?
5. Can we achieve high performance flax biocomposites?
6. Are they environmentally beneficial in comparison to standard materials?

The answers to these questions will give a better understanding of the flax composite potential and enable us build a strong database to be used in the materials selection process by designers.

In order to achieve these objectives, several research activities need to be carried out and will be reported through the different chapters of this study, as is outlined in Figure 3-1.

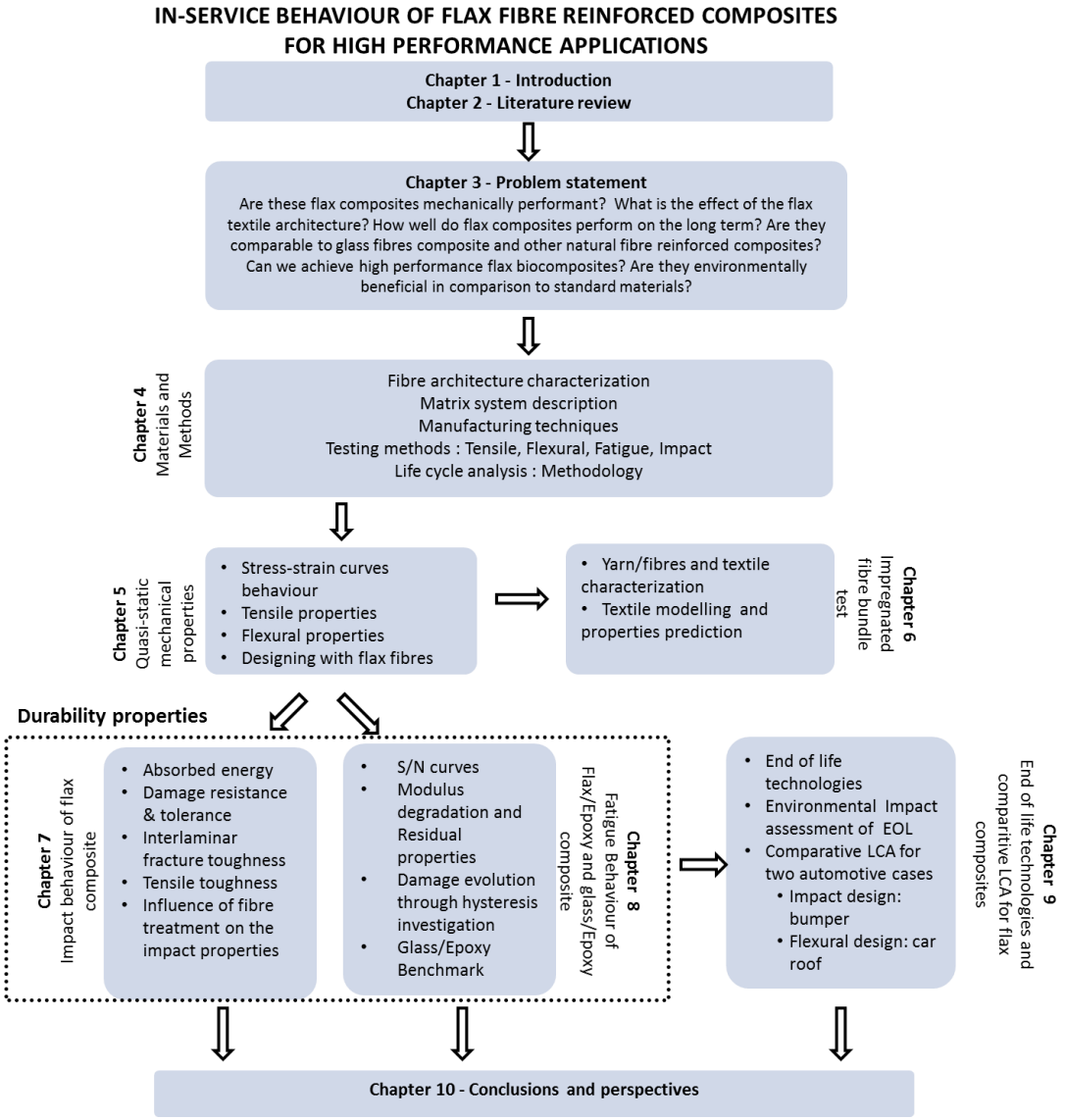

Figure 3-1. Schematic overview of all the research activities carried out in this thesis.

The first step of this study is to make a comprehensive literature review on the flax fibre composite technology, pointing out the key concepts from the plant growing until the end of life of a flax composite product. A thorough state of the art of natural fibres and natural fibre composites with emphasis on flax is presented in **Chapter 2**.

This is followed by the presentation of the materials and method used in this research in **Chapter 4**. The flax fibre architectures as well as the matrices are presented. Important specifications of the fabric that may influence the composite behaviour are measured: the crimp, twist, linear density, ends and picks counts, etc… as they are expected to play an important role. These features are measured using either optical microscopy or micro-tomography (µ-CT). The manufacturing processes, the testing methods as well as characterization techniques are also described in this section.
With all these information in hand, a complete characterization of the tensile and flexural properties based on a variety of textile configurations, such as unidirectional (UD), quasi-

unidirectional, woven and mat fabrics is carried out in **Chapter 5**. Gaining knowledge on the effect of fibre architecture and matrix choice on the strength, E-modulus and strain to failure will help to classify their performance. The relation between the stiffness and strength properties of flax fibre reinforced composites are expected to be dependent on the intrinsic properties of both the matrix and the architecture of the chosen fabrics. A thorough investigation of the stress-strain curves will try to uncover the particularities of flax-based composites and they will support the understanding of the composites properties. These data will be useful for design purposes in order to avoid the difficult and time-consuming material selection process, if based on trial and error.

As the quality of flax fibre is as an important asset, in **Chapter 6**, an exhaustive investigation of the yarn and fibre properties composing the studied performs is accomplished. The quality of the yarns can then be studied in relation to its degree of the twist, while eliminating the effect of the crimp. The samples are manufactured using the impregnated fibres bundle test techniques where the effective and average properties of the fibres or yarns are back-calculated from the unidirectional composite properties, using micromechanical equations such as the law of mixture. These data, combined to the textile geometry data as measured by µ-CT and microscopy, are then used in the modelling software Wisetex and TexComp to recreate the studied textile architectures and their composites, and to predict their mechanical performance (found in Chapter 5),. This will be a useful tool for the industry to predict the performance of the composites according to their textile architecture without having to manufacture and test it.

The investigation of the impact and the interlaminar fracture toughness performance of flax-based composites is the key in order to ensure the safety and longevity of the composite parts. In **Chapter 7**, the effect of fibre architectures and matrix types on the different aspects of impact was investigated. Their influence on the absorbed energy after perforation, on the damage resistance, as well as on the residual properties after impact (damage tolerance) were first quantified. Non-destructive analysis to characterise the overall quality, the damaged area and the failure mechanisms of the composite will be used. The interlaminar fracture toughness was also investigated in order to understand how the damage spreads once the samples are impacted, and to build a relation to the damage tolerance capacity of each composite system. However, in these flax composites, in contradiction to most glass and carbon fibre composites, almost no delaminations are found, and through-thickness cracks are predominant. Hence, also the tensile toughness, calculated from the tensile test data obtained in chapter 5, was studied and related to the absorbed energy at penetration during impact. Finally, the impact study is concluded by looking at the effect of chemical treatment of the flax fibres on the impact performance, as the quality of the interface has been found to be one of the predominant parameters to achieve a high energy absorption in synthetic fibre reinforced composites.

The characterization and evaluation of the fatigue behaviour of flax-epoxy composites will allow a better understanding of this behaviour and enable the prediction of fatigue properties, in order to assess the viability and long-term durability of these materials. The purpose of this work is to systematically compare the tension-tension fatigue behaviour of the flax fibre composites for the chosen textile architectures, embedded in an epoxy matrix, and is reported in **Chapter 8**. Firstly, the stress-life (S–N) diagrams are constructed from fatigue tests at stress ratios of R=0.1 and at various stress levels. The required ultimate tensile stress value, needed for determining the stress levels during the fatigue testing, was taken from the data in Chapter 5. Strain monitoring was used during fatigue testing in order to assess the stiffness degradation rates as well as the hysteresis loops. These data were also used to investigate the energy dissipation capability and the gradual build-up of the permanent strain of each material. The

post-fatigue properties are also evaluated in order to assess the degradation rate of the composite through time (or number of fatigue cycles). This investigation is crucial in order to understand the relation between the damage state, the post fatigue properties and the fatigue life. Lastly, a benchmarking with glass fibre composites was carried out in order to compare its performance to the flax fibres.

Flax fibre composites are now widely used in various industries, such as automotive, in replacement of less sustainable materials. One of the remaining challenges is to define the most environment-friendly end-of-life options for the flax fibre reinforced composites based on an environmental evaluation and comparison of the available techniques. In **Chapter 9**, an evaluation of three end-of-life (EOL) options for flax fibre reinforced composites is carried out. The chemical, mechanical and incineration strategies are investigated as well as their upscaling feasibility. A comparative life cycle analysis (LCA) on the various EOL options has been conducted in order to define which one will be the most suitable technique from an environmental perspective. These data is later on used in the comparative life cycle analysis of flax versus glass composites for 3 high volume applications: automotive (bumper and roof), building (roof system for slums). The comparative LCA is performed based on their mechanical equivalency in a certain application. In this case the Ashby methodology will be used as a basis to define equivalent amounts of material needed to fulfil a certain load case.

Finally, the links between the obtained results, tensile and flexural properties, impact and fatigue behaviour as well as the LCA are summarized in the general conclusions in **Chapter 10,** together with a presentation of future work.

Chapter 4
Materials and methods

The influence of the fibre architecture and the matrix on the quasi-static mechanical properties, the impact behaviour and the fatigue behaviour of flax fibre composites will be thoroughly investigated in this thesis. In the course of this work, different flax architectures and matrices are used, as well as composite manufacturing methods, testing procedures and analysis procedures.

4.1 Flax fibre reinforcements

In this study different flax textiles are used to reinforce the composite. The random mat is chosen as a reference fabric as it has isotropic in-plane material properties with fibres in "all" directions. Two type woven fabrics structures are considered: plain weave and twill 2x2. Four types of twill 2x2 are studied. They all possess varying yarn properties like the yarn's linear density and twist as well as a varying crimp angle and end picks and counts. One of these twills, the non-twist twill fabric, has a particularity to be made out of a non-twist fibres which are bound together with a polyester yarn wrapped around it creating a slight twist (3^o) and a side crimp (longitudinal misorientation) as shown in Figure 4-1.

Figure 4-1: Non-twist twill 2x2 yarn, non-twist flax fibres with a polyester yarn wrapped around it.

The Quasi-UD fabric has 90% of the fibre in warp direction and 10% are placed along the transverse direction and are used as binding yarns to keeps the UD fibres together. The unidirectional structure (UD) was also considered as it is supposed to give the highest properties if tested in longitudinal direction. The $[0,90]_{xs}$ cross-ply lay-ups these UD

architectures are also considered where *s* means that the laminate is symmetric and *x* is the number of times the layers are repeated.

The areal density used in the calculation in Section 4.4 was provided by the manufacturer. These values were also verified in-house by measuring the weight of several 30x30cm textile pieces and calculating the average weight per unit area. The values found were equivalent to the data provided by the textile suppliers. The other specifications, such as the areal density, yarn linear density, ends count, picks count and the twist angle and crimp, were measured directly on the fabrics and compared to the manufacturer's data sheet (see next sections for the characterization techniques). All the fibres used in this study are received untreated and without sizing except the unidirectional fabrics named UD1, which were received either pre-consolidated with MAPP or sized for epoxy for better compatibility with the resin. It has to be noted that the unidirectional fibres UD2 were water-treated during the processing of the fibres as presented by the patent [1].

It has to be noted that all architectures do not necessarily use the same quality of flax and there might be a difference in flax variety and refining process (degree of retting, hackling rate, wet-spun or dry-spun, etc...). These varying parameters may have a small effect on the mechanical properties, however, as all preforms were aimed for optimum reinforcement performance, it is assumed that optimum variety, growing conditions, refining (yarn's processing) and extraction parameters have been used by the suppliers.

For benchmarking flax purposes, four glass fibre reinforcements were chosen: random mat, twill 2x2, quasi-UD and UD. The characteristics of these fabrics were chosen in order to match the flax composite at equal areal density. The density of the glass fibres is considered to be 2.55 g/cm³, hence to use the same number of layers as the flax composites, the areal density of the glass fabrics will have to be higher than the flax fabric as seen in Table 4-1. For the chopped strand mat have a type E6 E-glass enhanced glass fibre with an E=82 GPa and σ=2387 MPa. The glass quasi-UD have a Polyethersulfone *(*PES) binding yarn of 110 dtex weaved around the glass yarn with tricot style.

These textile architectures and laminates were chosen because of their wide use in the industry for different applications. The choice was based on actual applications that are today made with glass or carbon fibres. For example, the random mat is widely used in automotive industry for low cost parts like bumpers and car door interior panels. The cross-ply laminates, UD and Quasi-UD (also called non-crimped fabrics) are also widely used in sporting goods, in the wind energy and aeronautics industries. The complete list of textiles architectures and their features is presented in Table 4-1.

4.1.1 The linear density

The linear density was calculated using yarn segments of 500 mm. Warp and weft yarns were extracted from the fabric and weighed. This weight was divided by the length to obtain the linear density in Tex (g/km). The density of the flax fibres is considered to be 1.45g/cm³ [2].

4.1.2 End picks and counts

The ends count and picks count represent the number of yarns per unit length (in cm) in respectively the warp and weft direction. To obtain the ends count a distance perpendicular to the warp direction is marked on the fabric and the yarns in between are counted; this

number is then divided by the distance over the yarns were counted. For the picks count a similar approach is used, for a distance perpendicular to the weft direction.

4.1.3 The crimp

The crimp of the fabric was measured according to the ASTM D3883 standard. A yarn is removed from a fabric and stretched with enough force to remove the waviness. The crimp is then calculated by Eq. 4.1, where l is the stretched length and l_0 the apparent length indicated on the fabric, 300 mm.

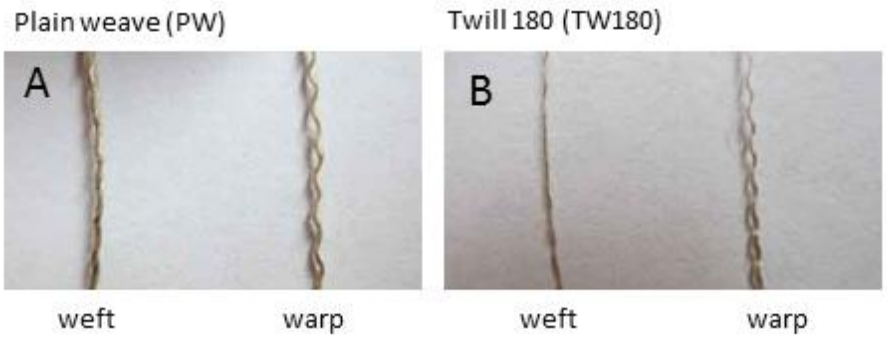

Figure 4-2: Waviness for waft and warp yarn of a) plain weave and b) twill medium-high twist.

The warp yarns show higher crimp than the weft yarns as seen in Figure 4-2. The high crimp found for Twill Medium-High Twist and the Twill High Twist was unexpected since this structure has less interweaving than the plain weave. However, these two fabrics taken into consideration do not have the same amount of ends or picks per count nor the same yarn linear density as the other studied weaves. The l_{yarn} measures the amount of waviness of the yarn, which depends on the weave style, the yarn thickness and the ends or picks counts. Hence, both a thickness of the yarn as well as a higher ends or picks per count will increase the l_{yarn} as seen in Figure 4-3. This shows how it is possible for the twill to have more crimp, even when it has less interweaving points than the plain weave fabric.

$$c = \frac{l_{yarn} - l_{fabric}}{l_{fabric}} \qquad \text{(Eq. 4.1)}$$

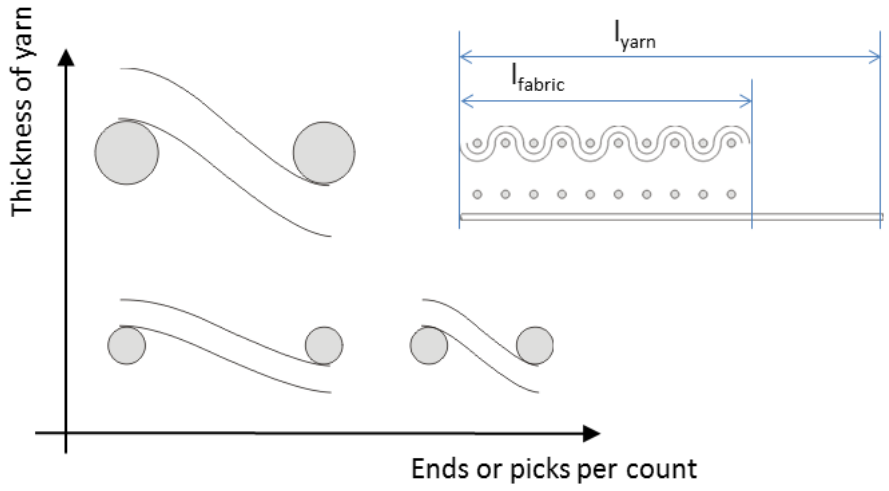

Figure 4-3: Influence on the thickness of the yarn and the ends or picks per count on the waviness of the yarn

	Areal density ρ_{sur} (g/m^2)	Twist angle warp/weft (º)*	Crimp warp/weft (%)	Fibre length (cm) or Linear density of yarn warp/weft (tex)	End picks (warp)/ end counts (weft) (cm^{-1})	Lay-up	Acronym		Suppliers
Flax fibre architectures									
Random Mat	300	-	-	8 cm	-	$[0]_3$	Random Mat		Ecotechnilin
Plain weave	285	High, 20/19	5.60/2.33	105/147	10.4/10	$[0]_4$	Plain weave	PW	Libeco
Twill 2x2	400	Low, 3/3	2.40/2	239/241	9/7	$[0]_4$	Twill Low Twist	NT	Composite Evolution
	200	Medium-Low, 9/9	1.0/1.0	68/68	14.7/14.7	$[0]_6$	Twill Medium-Low Twist	HF	Hexcel/Safilin
	180	Medium-High, 15/15	7.50/1.33	27/24	30/34	$[0]_7$	Twill Medium-High Twist	TW180	Libeco
	150	High, 21/17	8.1/1.6	31/27	24.5/25.5	$[0]_8$	Twill High Twist	TW150	Libeco
Quasi-UD	300	High, 20 (warp only)	0.4/0	97	13.6	$[0,90]_{2s}$ $[0]_4$,	Quasi-UD [0,90] Quasi-UD		B-Comp
UD/MAPP prepreg	122	-	0/0	-	-	$[0, 90]_2$ 0 $[90,0]_2$	UD1		Procotex
UD with epoxy sizing	122	-	0/0	-	-	$[0,90]_{3s}$ $[0]_{6s}$	UD1 [0,90] UD1		Procotex
UD	200	-	0/0	-	-	$[0,90]_{2s}$ $[0]_6$	UD2 [0,90] UD2		Lineo
Glass fibre architectures									
P20 Powder Chopped Strand Mat	450	-	-	5 cm	-	$[0]_3$	GMat		Jushi
HexForce 1113 Twill 2x2	390	-	0.9/1	68/68	5.9/6.6	$[0]_6$	GTwill		Hexcel
Quasi-UD	600	-	-	1200/68	-	$[0,90]_s$	GQUD		Saertex
UD	310	-	-		-	$[0,90]_{2s}$	GUD		Saertex

*low = 0º-3º, medium= 4º-15º, high= 16º+

Table 4-1: Description the flax and glass fibres used in this work.

4.1.4 Measurement of the twist angle

The measurements of the twist angle were done using optical microscopy on the surface of the fabric as shown in Figure 4-4. An average of 10% standard deviation was found for all measured textile. Straumit et al. [2] corroborated the data for the medium-low twist twill using micro-tomography images to extract the twist angle. They obtained an average value of 9.2° which is comparable to the optical microscopy data of 9°.

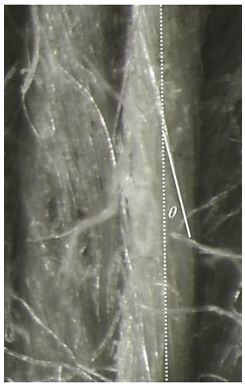

Figure 4-4: Example of the twist angle measurement for the Quasi-UD fabric defined by optical microscopy.

4.2 Matrices

4.2.1 Epoxy matrix

The thermoset resin (Th) used to produce the composites is the *Epikote 828 LVEL* from Resolution Performance Products. For the cross-linking, the epoxy resin was mixed with a 1.2-diaminocyclohexane *Dytek DCH-99* at a 15.2 phr ratio. This epoxy is a medium viscosity ($\eta \approx$ 10-12 Pa.s at 25°C) liquid epoxy resin produced from bisphenol-A and epichlorohydrin and does not contain any diluents. To establish the crosslinks, the material needs to be cured one hour at 70°C, and post-cured one hour at 150°C. Post-curing helps the epoxy to attain its maximal mechanical properties by reinforcing and completing the present crosslinks. During curing the size of the product does not change a lot because epoxies show very small cure shrinkage, which facilitates the production [32].

4.2.2 Maleic Anhydride Grafted Polypropylene matrix

The thermoplastic (Tp) matrix used in this study is Maleic Anhydride grafted Polypropylene (MAPP), *Bynel 50E725* from Du Pont. The matrix contains 0.11±0.02% of grafted maleic anhydride and was used in the form of film with 65 μm thickness. The melting point is 144°C. The maleic anhydride coupling agent is added to the polypropylene matrix in order to improve the interfacial bond between matrix and fibre. Natural fibres are typically hydrophilic because of their composition. The cellulose and hemicellulose have easy accessible hydroxyl groups which cause the strong hydrophilic character [3]. Polypropylene is hydrophobic, which leads to some interfacial problems when the fibre and matrix are combined. The maleic anhydride is added to form a bridge between both constituents. Covalent bonds can be established between the anhydride group of the MAPP and the OH group of the cellulose [4]. This leads to a strong interface with only a small addition of the maleic anhydride. The mechanical properties of the epoxy and MAPP matrices are presented in Table 4-2 below:

Matrix Type		Commercial Name	Density (g/cm^3)	Modulus (GPa)	Strength (MPa)	Strain to failure (%)
Thermoset	**Epoxy**	Epikote 828 LVEL	1.16	2.70	70	4.1
Thermoplastic	**MAPP**	Bynel 50E725	0.89	0.342	18	474

Table 4-2: Matrices description and mechanical properties.

4.3 Composite manufacturing

Different production methods for fibre reinforced composites exist. The form in which the fibres are supplied should be taken into account when choosing a production method. In this study all the fabrics, except the unidirectional comingled with MAPP or the one with epoxy sizing, were delivered as dry fabrics. For all flax fibre architectures and the MAPP sheets, an additional drying step, 24h at 60°C, was performed to remove moisture from the flax and to avoid defects in the composites. After drying, the fibres need to be impregnated with the matrix and consolidated rather quickly, in order to avoid moisture uptake from the environment.

For the thermoset based composites, the resin transfer moulding (RTM) process was chosen as it gives high quality and high mechanical properties which are well reproducible. For the thermoplastic composites manufacturing, the compression moulding process was chosen as it is a fast and cheap process. The processes are described in the following sections.

4.3.1 Resin Transfer Moulding

The thermoset composites were manufactured using the resin transfer moulding process (RTM) as seen in Figure 4-5a. The fabrics were placed between the two rigid steel mould parts, which were pressed together with a home-build hydraulic press with a pressure of 200 psi, equivalent to 14 bars (pressure needed to keep the mould closed). A spacer was added to adjust the depth of the cavity in order to obtain a thickness of 2mm ± 0.05mm. The resin is previously degassed to avoid injecting air into the plate.

The experimental parameters were: the inlet pressure P_{inlet}=1 bar and outlet or vacuum-connected pressure P_{vacuum}= -0.99bar, both values expressed relative to the ambient pressure (hence, $\Delta_{pressure}$= 1.99 bars). Once the injection is completed, a consolidation pressure of 3 bars is applied. The injection temperature was set at 40°C and the mould temperature was increased to 70°C for 1h to cure the part in-mould. Later on, the demoulded plates were post-cured at 150°C for 1h in a Nabertherm N60/A oven. The RTM equipment used has a peripheral resin inlet and a resin outlet at the middle of the upper mould as shown in Figure 4-5b. This results in short impregnation times but has as drawback, namely the presence of a weak spot in the centre of the plate. For the UD2 composite, the injection was done at 50ºC and the mould temperature was increased to 100°C for 1h to cure the part in-mould. This was done to avoid the evaporation of moisture during post-cure as the entrapped vapour will agglomerate and create bubbles on the surface of the composite. As the UD2 fabric consists of a thin layer of hackled fibres which leads to a greater contact of the fibres with the moisture in the air compared to more refine flax such as yarns.

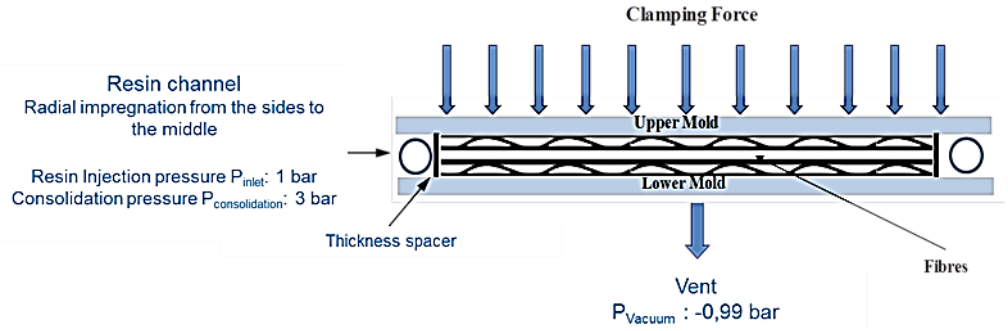

a)

b)

Figure 4-5: a) Schematic side view of the RTM manufacturing process [5] and b) picture of the RTM.

4.3.2 Compression Moulding

Thermoplastic composites were prepared by compression moulding (CM) using stacked flax preforms sandwiched between MAPP thermoplastic films as seen in Figure 4-6. This was done using the Pinette Zenith 2 press. To obtain good impregnation, the consolidation temperature and mould closing pressure used were 165°C and 40 bars for 15 minutes respectively (applied on spacer to ensure proper thickness would be reached, hence pressure on the composite is unknown). After the consolidation time, the pressed plates were cooled down, while under pressure, to 140°C. Afterwards, the composites were placed between the cooling plates and the same pressure is again applied for another 5 minutes. To remove any defects on the sides of the plate, a 2 cm margin on the sides is cut off using a "guillotine" plate cutter.

a) b)

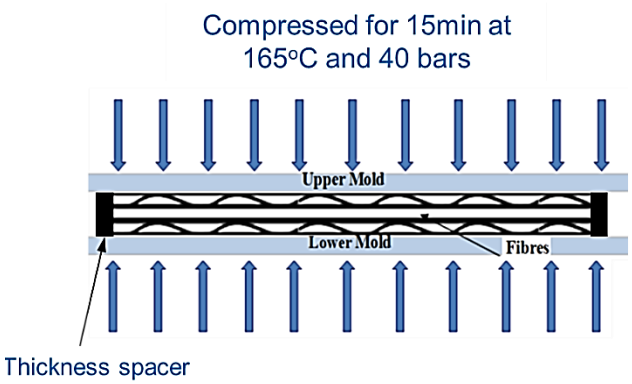

Figure 4-6: a) Schematic side view of CM manufacturing process and b) Pinette Zenith 2 press.

4.3.3 Impregnated fibre bundle test specimen preparation

The impregnated fibre bundle test has been performed according to a modified ISO 10618 standard. The fibres were pre-dried for 24 h at 60 °C, cut into a length of 25 cm and weighed in order to calculate the fibre volume fraction. Afterwards, the fibres were placed in the cavity of the mould according to Figure 4-7 a-b to create a unidirectional composite. This

set-up is a modified version of the one studied by Coroller et al. and Trujillo et al. [6, 7] and is comparable in geometry. The resin is then degassed and poured on top of the fibres. The counter-mould is placed on top of the impregnated fibres and the whole set-up is then positioned inside the press for consolidation. Once the curing is completed, the samples are demoulded and conditioned for testing.

The technique requires a wet impregnation followed by compression to consolidate the composite. It has to be noted that all samples should have a resin volume content of at least 35 %, a good orientation of the fibres in the unidirectional direction (0^o) and a limited porosity (< 2 %). Because the mass of the fibres, placed in the mould, is precisely controlled, the fibre volume fraction can be controlled by imposing a precise specimen thickness (the specimen width being determined by the mould width). This thickness control was achieved by using spacers (Figure 4-7 c). In this way unidirectional composite samples with small cross sections have been manufactured, with a limited number of defects, as well as a good control of the orientation of the fibres. They are moreover distributed evenly throughout the composite, as shown in the cross-section image obtained by micro-tomography (Micro-CT) in Figure 4-8.

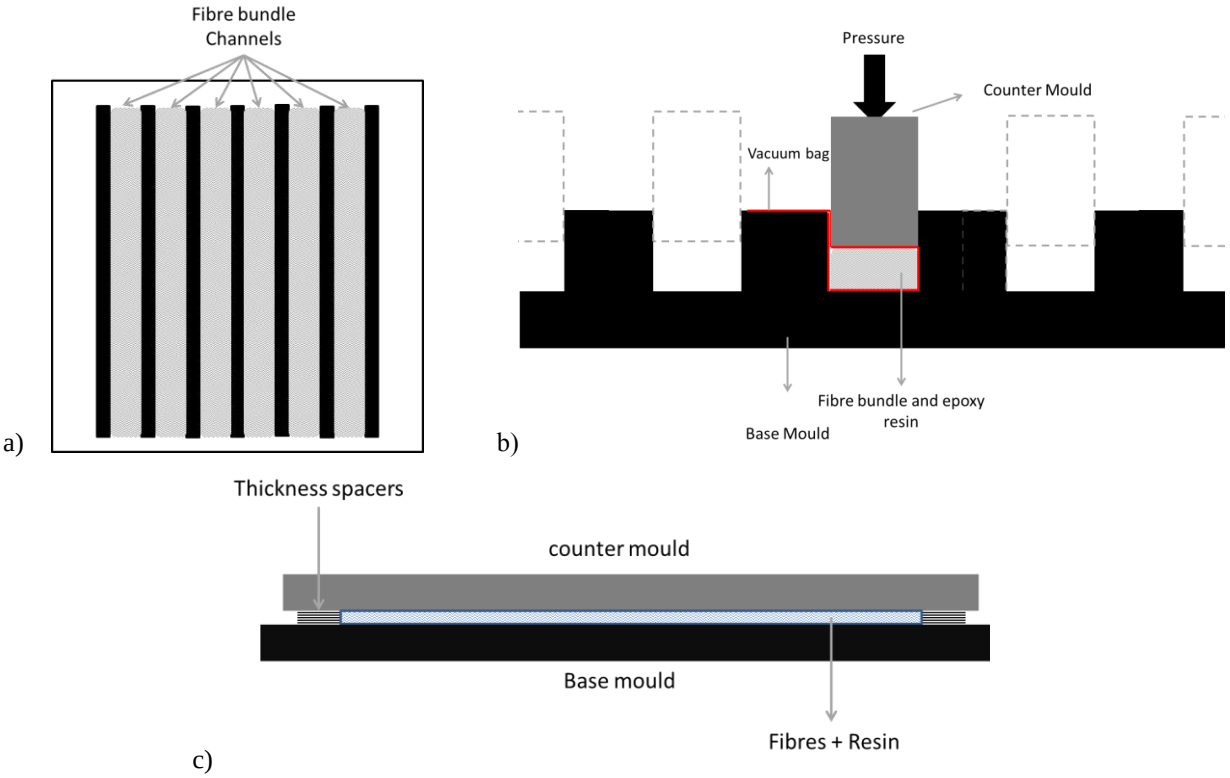

Figure 4-7: Impregnated fibre bundle test method I, a) top view of six mould cavities and b) Front view of one cavity of the mould (spacer not included) and c) cross section view of the counter-mould with the spacers.

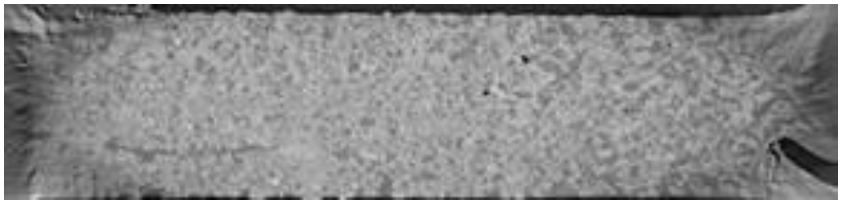

Figure 4-8: UD/Epoxy IFBT sample cross-section obtained by Micro-CT.

4.4 Fibre volume fraction calculation

The fibre volume fraction and lay-up of the fibres have an important influence on the mechanical properties of the composite. For that reason, in order to achieve easy to compare results from all samples, a V_f of 40% was aimed at, and hence this was the target volume fraction used to calculate the number of layers necessary to obtain a laminate thickness of 2 mm. Only the random mat preforms were consolidated at a V_f = 30% due to their bulky nature. The unidirectional [0,90] cross-ply composites have a thickness of 3mm in order to keep the laminate balanced and symmetric. A fibre density of 1.45g/cm³ (ρ_{flax}) is considered for the calculations of the amount of flax plies necessary to reach the desired V_f for a given composite thickness using the following Eq.4.2:

$$\boldsymbol{V_f = \frac{\rho_{surf} * N}{\rho_{flax} * h}} \quad \text{(Eq. 4.2)}$$

Where ρ_{surf} is the areal density (g/m^2 or gsm) and N is the number of layers used and h is the composite laminate thickness in meter. Whereas the produced composites fibre volume fraction was close to the target of 40%, it still presented a variation between 37% and 42%. Thus, the presented data are later on normalised to a 40% fibre volume fraction using the rule of mixture with E_f = 65GPa and σ_f = 650 MPa [8]. The porosity level was calculated using image analysis using the ImageJ program. The images were obtained through micro-tomography technique. The values found were all below 0.5% for all tested configurations.

The MAPP thermoplastic matrix comes in film of fixed thickness (65µm). Thus, to obtained the desired V_f, a certain number of matrix plies need to be added to the fabric. The amount of matrix layers can then be calculated using Eq. 4.3, given the thickness of a single matrix layer:

$$\#\text{resin layers} = \frac{t_{total} - N * \frac{\rho_{surface}}{\rho_{flax}}}{t_{resin}} \quad \text{(Eq. 4.3)}$$

Where t_{resin} is the thickness of one resin ply, $\rho_{surface}$ is the areal density of the fabric (g/m²), ρ_{flax} the density of flax, t_{tot} the aimed thickness of the sample (mm) and N the amount of layers. For the IFBT samples, the V_f calculation was performed according to the ISO 14127:2008 standard using the weight fraction of each components (fibre and matrix) as described by Eq. 4.4 [9]:

$$\boldsymbol{V_f(\%) = \frac{\frac{m_f}{\rho_f}}{\frac{m_f}{\rho_f} + \frac{m_c - m_f}{\rho_{res}}} x\ 100} \quad \text{(Eq. 4.4)}$$

Where, m_f is the mass of the fibres, m_c is the mass of the composites, ρ_{resin} is the density of the used resin and ρ_f the density of the fibres.

4.5 Back-calculation of the fibre properties

From the strength and stiffness of the impregnated fibre bundles, the properties of the flax fibres, as they are present and behave in a composite, can be determined, using the methodology developed for carbon fibres (ISO 10618:2004 [10]). From the measured composite properties on this "impregnated fibre bundle", the fibre properties can be back-calculated using the following Eq. 4.5 [11, 12]:

$$\boldsymbol{E_f = \frac{E_C - E_m * (1 - V_f)}{V_f}} \quad \text{(Eq. 4.5)}$$

$$\sigma_{u,f} = \frac{\sigma_C - \sigma'_m * (1 - V_f)}{V_f} \quad \text{(Eq. 4.6)}$$

Where, E_f is the modulus of the fibre, E_m is the modulus of the matrix and V_f is the fibre volume fraction, σ_f is the strength of the fibre and σ'_m the stress in the matrix at the failure strain of the fibres (if the V_f is high enough, it is also the failure strain of the composite). σ'_m can be calculated assuming elastic deformation of the matrix: $\sigma'_m = E_m * \varepsilon_{u,c}$ (moduli are given in GPa, strengths in MPa). Eq. 4.6 is valid only when the fibres fail first, meaning that they have a lower failure strain than the matrix. For this reason, the matrix needs to have a sufficiently high ductility.

4.6 Sample cutting & conditioning

Three techniques were used for the sample cutting of the flax fibre reinforced composite samples: a water-cooled diamond saw (thermoset only), waterjet cutting and a guillotine knife (thermoplastic only). For the sample subjected to the presence of water during cutting, there are dried afterwards for at least 24 hours at 60°C. All samples were then conditioned for at least 24h at a controlled temperature of 21°C ± 2°C and 50 ± 2 % relative humidity before testing. The moisture content in the composite at those conditions are around 2 wt%.

4.7 Quasi-static mechanical properties characterization

4.7.1 Tensile testing

Tensile tests were performed using an Instron #4505, # 5985 or #5567 testing machine. The tests were done according to the ASTM D3039 standard. Samples of 2x25x250 mm were tested using a strain rate of 4 min^{-1}, a load cell of 30 kN and a gauge length of 150mm. A 50 mm gauge length extensometer with a 10 mm travel was used to monitor the strain as seen in Figure 4-9. A minimum of 6 samples, were tested to ensure reproducibility and reliable standard deviations.

Figure 4-9: A flax-MAPP composite sample during a longitudinal tensile test on an Instron 5567.

A question was raised on whether to add end tabs to the specimens for tensile testing. Thus, a comparative analysis using several types of ends tabs was carried out. Glass-epoxy, tapered aluminium and flax-epoxy end tabs as well as sand paper were investigated and the results are shown in Figure 4-10. The variation in results was low although the flax-epoxy end tabs show a better performance in strength (↑20%). For practical reason, the choice was made to use the sand paper for all tensile testing, thus the strength values obtained in this thesis are considered as the lower bound.

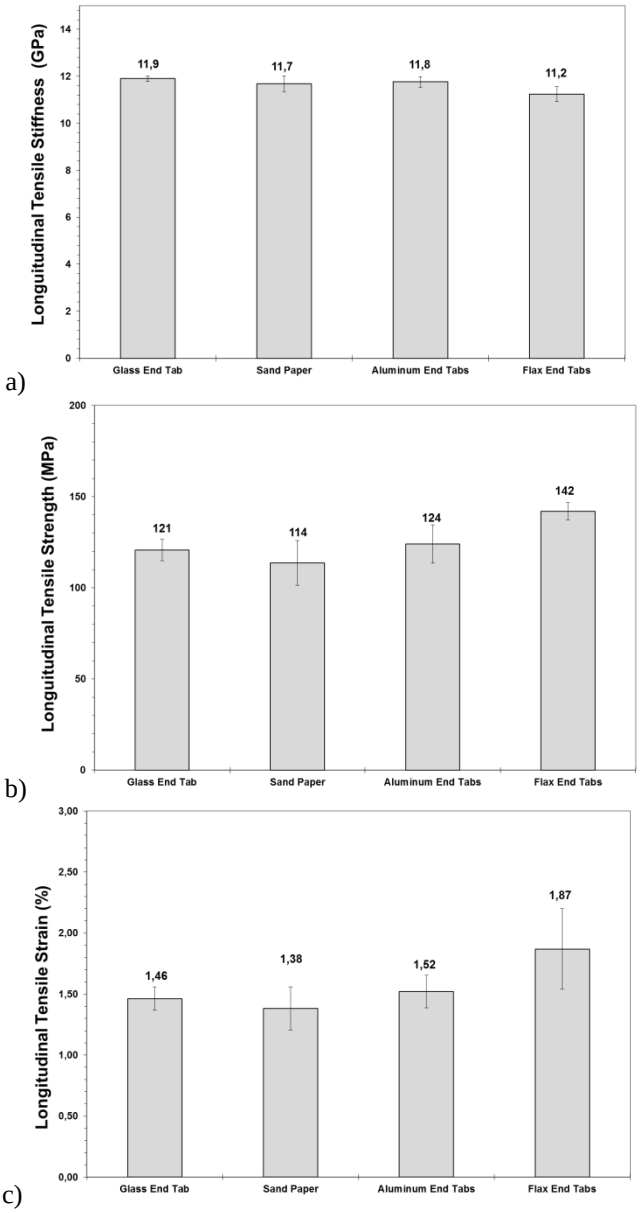

Figure 4-10: End tabs comparison in term of: a) tensile stiffness, b) tensile strength and tensile strain to failure for flax plain weave-epoxy composites.

4.7.2 Flexural testing

Flexural mechanical tests were performed using an Instron testing machine #4467 or #5567. Samples of 2x10x100 mm were tested using a strain rate of 4 min^{-1}, a load cell of 1 kN and a span length of 64 mm were used according to ASTM D790 standard. A minimum of 6 samples were tested to ensure reproducibility and reliable standard deviations.

4.8 Low velocity impact testing

The low velocity impact by the drop weight impact test method used in this research is displayed in Figure 4-11. It can be seen that a weight is dropped on a clamped specimen while force and displacement are registered. The energy absorption, the damage resistance and tolerance (as defined in Chapter 2 and 7) can be assessed by this test. The energy absorption is measured by penetration drop weight impact tests and the damage resistance and tolerance by non-penetrating drop weight impact tests followed by compression after

impact (CAI) tests. For both tests different criteria will be decisive in determining the suitability of the material. The test parameters are described in the next sections.

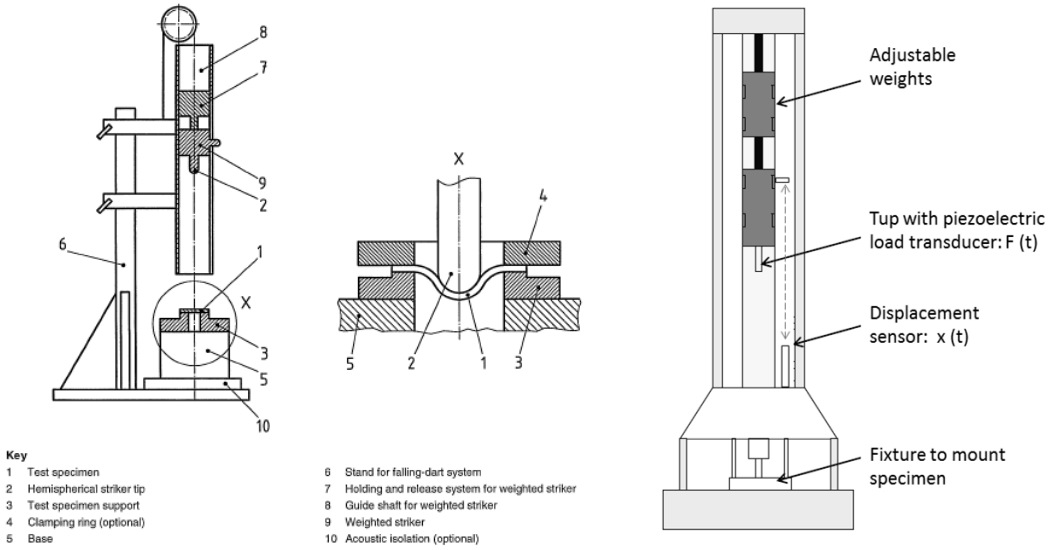

Figure 4-11: a) Low velocity instrumented drop weight impact test set up [13, 14].

4.8.1 Absorbed energy at perforation

Drop weight low velocity impact with perforation were performed according to the ISO 6603 standard on all studied fibre architectures. The samples were prepared with a [0,90] cross-ply stacking for the unidirectional and quasi-UD fabrics in order to be able to compare them with woven fabrics. The dimensions of the samples were 2x100x100mm. These tests were performed using a *Fractovis CEAST 6789*, seen in Figure 4-13. Samples of 100 mm x 100 mm were clamped with a pressurised clamping ring having an opening with a diameter of 40 mm, and impacted with a steel striker with hemispherical top and a diameter of 20 mm. The weight of the impactor was 3.170 kg, which was released from a height of 0.6 m for all thermoplastic samples and 0.4 m for all thermoset samples. This height was chosen to reach perforation for all samples. The impact energy for perforation of the thermoplastic and thermoset samples was respectively 6.2 J/mm and 9.33 J/mm. The absorbed energy increases with the incident energy, but reaches a maximum when perforation occurs [25]. For this reason, the impact energy for the thermoplastic and thermoset samples do not need to be the same to compare, as long as it is larger than the absorbed energy to perforation. Important formulas to calculate the velocity when the impactor arrives at the specimen and the impact energy are shown in Eq. 4.7 and Eq. 4.8.

$$v_0 = \sqrt{2gh_0} \quad \text{(Eq. 4.7)}$$

$$E_0 = mgh_0 \quad \text{(Eq. 4.8)}$$

During the impact event, the contact force, impactor displacement and time were recorded at a sampling rate of 200 kHz. The force and displacement are recorded during testing and the absorbed energy was quantified using the full integral method as displayed in Figure 4-13. More details on the calculation method will follow in Appendix E.

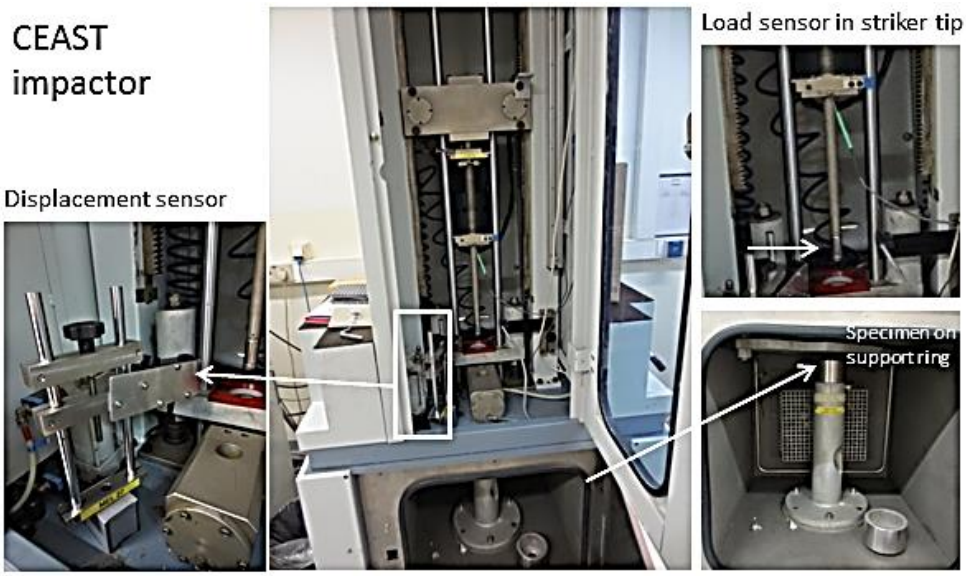

Figure 4-12: CEAST type 6789 impactor.

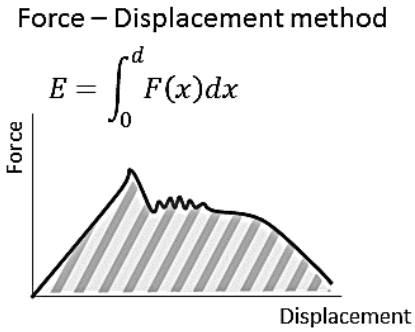

Figure 4-13: Graphical representation of the force-displacement method used to calculate the absorbed energy at perforation.

4.8.2 Damage resistance characterization

Non-perforation tests were carried out according to an adapted version of the ISO 6603 standard in which no perforation occurs. The specimen dimensions were of 100 mm x 100 mm x 2 mm. They were tested on the CEAST impactor with the same weight and striker diameter as used in the perforation tests. An anti-rebound mechanism was put in place to catch the stricker after the impact and ensure that there is only one hit on the sample. The clamping ring was enlarged to 80mm so that the spread of delaminations is not restricted by the clamping geometry. The sample were thus impacted with a drop height of only 0,1m, which is equivalent to 3.11J incident energy for both thermoplastic and thermoset 2mm thick samples. Visual inspection of the specimens was done and this drop height was found adequate for non-perforation impact tests.

4.8.3 Damage tolerance - Residual properties after impact

For the damage tolerance characterization, a quasi-isotropic, balanced and symmetric stacking sequence [+45,0,-45,90] was used to manufacture the composite. The produced composites specimens have a V_f between 40% and55% and dimensions of 150 x100 mm. This was done according to the ASTM D7137 standard for the investigation of the damage tolerance via compression after impact test. The standard prescribes another clamping mechanism, which is illustrated in Figure 4-14. Specimens are clamped with four rubber tipped clamps on the support fixture. This clamping setup is not compatible with the CEAST impactor, therefore an in-house built drop weight impactor was used. The set-up

is described in Figure 4-14. The support fixture was aligned in such a way that the striker hit the specimen in the centre. A hardened steel striker tip was chosen with a diameter of 16 mm and the sticker weight is 3.170 kg as well. All samples were impacted with an energy of 1.55 J/mm thickness of the specimen.

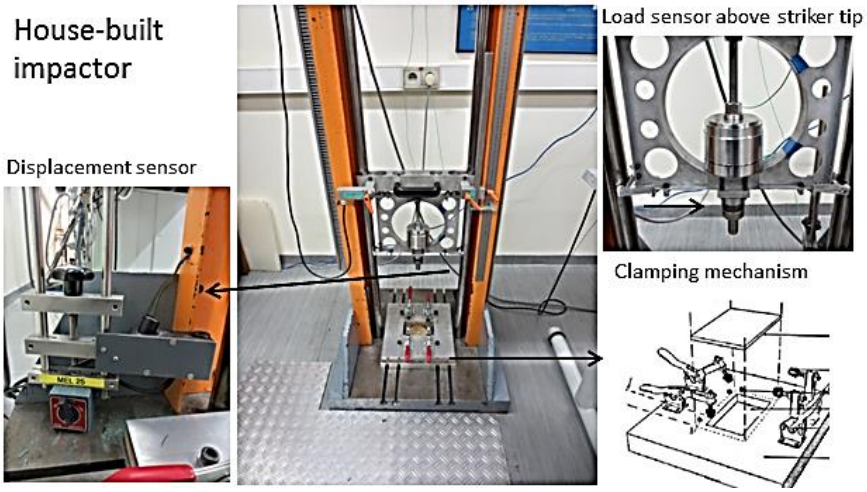

Figure 4-14: In-house built drop weight impactor used for non-perforation impact of quasi-isotropic specimens.

The drop height was calculated based on the specimen thickness, which varied between 3-5 mm, because of the symmetric layup constraint (for quasi UD layers this only leave the choice of 8 or 12 or 20 layers). The in-house built impactor is also equipped with a similar displacement measurement system and a piezoelectric load cell. Here the load cell is not incorporated into the tip of the striker (as in the CEAST equipment discussed previously) but is located directly above it, as can be seen in Figure 4-13.

Table 4-3 gives an overview of the test parameters used for the low velocity impact properties assessment. During the impact the contact force, displacement and time were measured with a sampling rate of 200 kHz.

	Absorbed energy	**Damage resistance**	**Damage resistance Damage tolerance**
Standard	ISO 6603	Modified ISO 6603	ASTM D7136
Machine	CEAST		In-house built
Clamping, support structure	pressurised, circular 40mm diameter	pressurised, circular 80mm diameter	rubber tipped clamps, rectangular 75mm x 125mm
Shape, diameter hardened steel striker	hemispherical, 20mm		hemispherical, 16mm
Drop height	Tp: 0,6m ; Th: 0,4m	Tp,Th: 0,1 m	Adjusted to thickness
Impact energy/mm	Tp: 6,2 J/mm ; Th: 9,33 J/mm	Tp, Th: 1,55 J/mm	Tp, Th: 1,55J/mm
Sample dimensions	100mm x 100mm		150mm x 100mm
Thickness specimens	2mm		3-5mm
Layup	[0,90] cross-ply		[+45,0,-45,90] quasi-isotropic
Amount of samples	8 x 7 architectures	4 x 7 architectures	4 x 4 architectures

Table 4-3: Overview of the test parameters for the drop weight impact tests.

4.8.4 Residual properties characterization

Following the 1.55J/mm impact, the residual properties of the composite are evaluated using the compression test. This was carried out according to the ASTM D7137 standard.

The compression tests were performed on an Instron 5985 testing machine, equipped with a 250 kN load cell and a strain rate of 2.5 min^{-1}. The test fixture, which has a design to avoid buckling of the specimen, is shown in Figure 4-15a. The buckling is not an accepted failure mode, instead failure needs to originate from the damaged area as seen in Figure 4-15b. However, due to the relatively low stiffness of the flax fibre reinforced composites, all compression after impact tests resulted in global buckling. Hence, a three point bending alternative was chosen which is called "Flexure After Impact" (FAI) test. From this test, failure could be attained for all specimens with a resulting flexural strength.

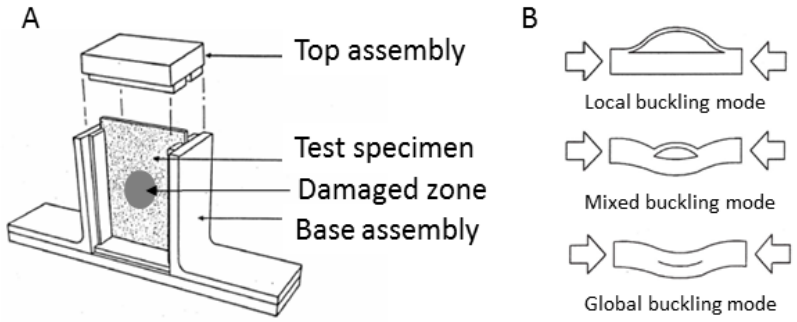

Figure 4-15: a) Support structure for compression after impact and b) different buckling modes [15].

Hence, the residual properties were then evaluated using a FAI test, following the three Point bending ASTM D790 standard, on an Instron 5985 testing machine. The span width was set to 128 mm with a strain rate of 13.6 min^{-1}. The residual flexural strength (FAI) was compared to the flexural strength measured on the same material before impact (FBI).

4.9 Interlaminar fracture toughness

Fracture toughness in mode I was measured following the Double Cantilever Beam (DCB) test procedure as defined in the ASTM D5528 standard [16] (see Figure 4-16a). The mode II fracture toughness was investigated using the End-Notched Flexure (ENF) test as described by Carlsson et al. [17] and the Japanese standard JIS K7086 [18] (see Figure 4-16b). Four to eight flax-epoxy samples were tested for both DCB and ENF. They have a thickness between 4-5 mm a width of 20 mm and a length of 170-200mm). The sample were reinforced at the outside with 4 layers of [0,90] quasi-UD glass fabric on each side (1 layer is 0.33mm with 90% of fibres in 0º direction and 10% in 90º direction) to avoid mixed-mode loading at the delamination tip due to heavy bending of the beams.

The pre-crack (a_0) was made using a high temperature polyimide film with a 12 μm thickness and a length between 50 and 55 mm. The DCB tests were carried out on an Instron 4505 tensile machine with a crosshead speed of 1 mm/min, to produce stable crack growth, and load cell of 1 kN. For the ENF, the tests were performed on an Instron 4467 with a 100mm span length and a crosshead speed of 1mm/min. All samples were delaminated up to 50mm from the tip of the pre-crack. During the test, the applied load and displacement were recorded as well as the crack length using a moving camera.

Mode I interlaminar fracture toughness calculation is based on the modified beam theory method was used to calculate the fracture toughness G_{IC} shown in Figure 4-16 a. The modified equation takes into account the relation between the compliance of the specimen and the detected crack length using Eq. 1. It corrects for the effects of transverse shear and deformation beyond the crack tip via the addition of a length correction, Δ, to the measured crack length [19]. The Δ correction factor accounts for the free movement of the beam on

the un-cracked end according to the compliance calibration value *C* defined in the modified compliance calibration method [16]. For the G_{IIC} strain energy release rate, the classical elastic beam theory (Eq. 2) was used and is presented in Figure 4-16 b.

In Mode I interlaminar fracture toughness, the initiation of fracture was defined using the three following methods [20]:

1. The non-linearity of the load-displacement curves (NL): the initiation fracture toughness is determined from the point where there is a deviation from linearity on the load-displacement curve. This point is supposed to be the closest to the real onset of delamination. The position is defined when stress level of the extrapolated linear elastic curves (drawn with data from the linear elastic part of the stress-strain curve) is 10% higher than the recorded stress strain curve.
2. The 5% offset: Obtained by drawing a straight line whose slope is 5% lower than the initial slope of load-displacement curve. The crack initiation point is defined as of the intersection of this straight line and load-displacement curve.
3. The visual observation (VIS): The point where crack onset is observed visually on the monitor, showing the video-image of the crack tip as seen in Figure 4-17.

The steady-state propagations value of G_{IC} is derived from the average propagation points when the G_{IC} value does not change with increasing crack length. Further description of the propagation value is found in Chapter 7.

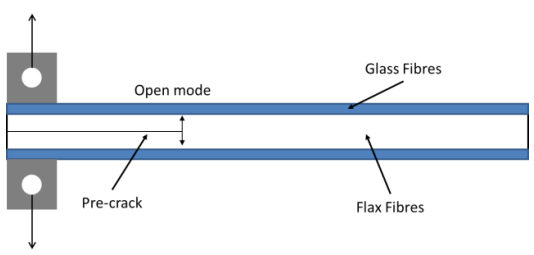

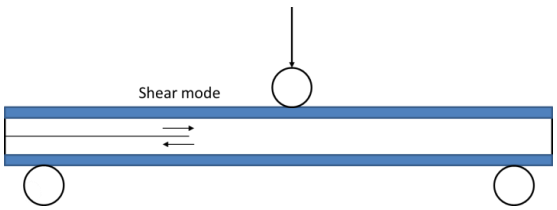

$$G_{IC} = \frac{3P\delta}{2b(a-\Delta)}\frac{F}{N} \qquad \text{(Eq. 4.7)}$$

$$G_{IIC} = \frac{9P\delta a^2}{2b(2L^3+3a^3)} \qquad \text{(Eq. 4.8)}$$

where P is the load (N), a is the delamination length (mm), b is specimen width, δ is the load point displacement (mm), L is the span length (mm), Δ value is calculated from a linear regression analysis of $(C/N)^{1/3}$ – delamination length curve (see [21] for graphical details), *C* is the compliance (δ/P), *F* and *N* are the correction factors for the large displacement and finite displacement of loading block

a) DCB Test b) ENF Test

Figure 4-16: Fracture toughness test definition: a) Mode I G_{Ic} definition obtained through DCB test and b) Mode II G_{IIc} using the ENF test (No correction was used for the calculation of the G_{IIC} value).

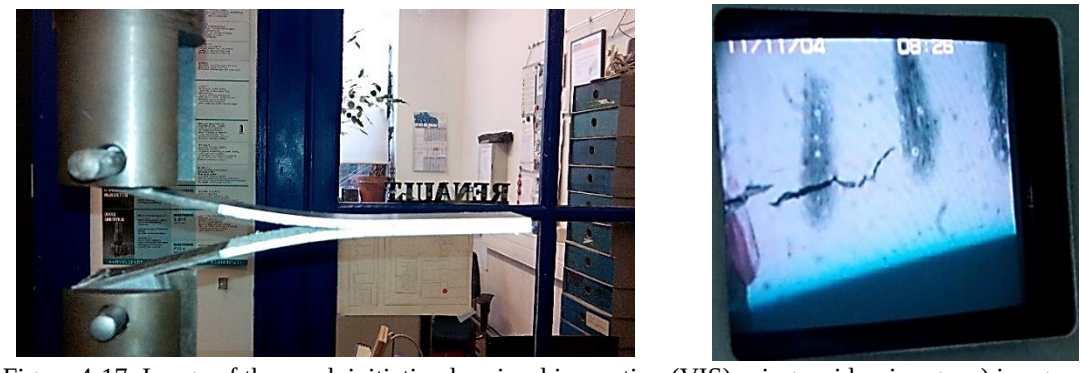

Figure 4-17: Image of the crack initiation by visual inspection (VIS) using a video-image: a) image of the set-up image and b) close-up of the crack initiation (circle zone).

4.10 Tensile toughness

The tensile toughness was found by integrating the area under the stress-strain curve, obtained during a tensile test. The obtained area under the σ-ε curve represents the energy per unit volume needed to break the sample is calculated using Eq.3. The tensile toughness will be compared to the results of the falling weight perforation impact test.

$$\text{Tensile Toughness } \left(\frac{J}{m^3}\right) = \int_0^{\varepsilon_f} \sigma \, d\varepsilon \qquad \text{(Eq. 4.9)}$$

Where σ is the stress (MPa), ε is the strain (%) and ε_f is the strain at failure (%).

4.11 Fatigue testing

Tension–tension fatigue tests were performed, following the ASTM D3479 standard, on an MTS hydraulic fatigue testing device with a 100kN load cell. The loading ratio was set to R= 0.1 with a loading frequency of 5 Hz and stress levels maximum applied stress normalised to the ultimate tensile strength (UTS), S/S_o, ranging from 0.3 to 0.9 of UTS. The fatigue tests were conducted in a temperature-controlled laboratory at 21°C using UTS data from the quasi-static tensile tests results presented in Chapter 5.

A tapered sine signal, as displayed in Figure 4-18 a, was applied to gradually build up the load amplitude and avoid an overshoot of the load during the early cycles. It took around 1000 cycles to reach the full stress amplitude. Samples were prepared with the same dimensions as for static tensile testing and end-tabbed with glass fibre-epoxy end-tabs. The test is set to stop if the samples do not fail after 10^6 cycles, referred to as N_{max}.

The hysteresis loops and stiffness degradation were captured continuously using a fatigue rated extensometer with a gauge length of 50 mm. The dynamic stiffness during cycling was measured in the first part of the loading curves of each hysteresis loop as shown in Figure 4-18 b. A minimum of 4 samples for each stress level was used.

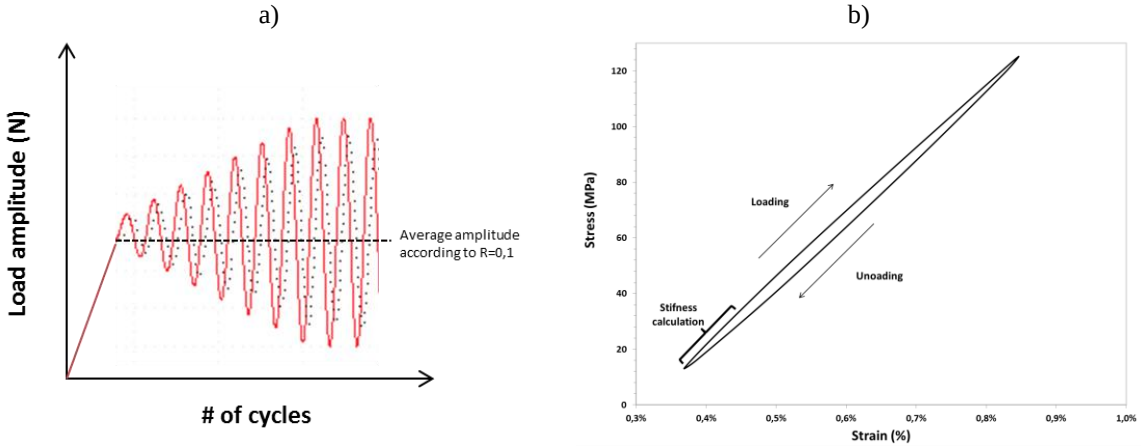

Figure 4-18: a) Tapered sine signal used for fatigue cycling and b) calculation of the dynamic stiffness from the loading curves of the hysteresis loop for monitoring of the stiffness degradation.

4.12 Image Analysis

4.12.1 Optical microscopy

Optical microscopy has been done using the stereo microscope *Leica MZ8*. The samples were cut and embedded in resin and the samples were polished for better observation of the composite surface.

4.12.2 SEM and ESEM

The scanning electron microscope (SEM) produces images of a sample by scanning it with an electron beam under vacuum condition. Typically, resolutions of 2 to 5 nm can be attained (under certain conditions) making SEM an ideal instrument to observe micro-level details which cannot be visualised by optical microscopy. Micrographs of the flax fibres and their composites were made using a Philips XL30 FEG electron microscope in secondary electrons mode. This mode has the smallest interaction volume thus revealing information about the surface which was of interest in this thesis. The microscope has a Schottky based gun design using a point-source cathode of tungsten which has a surface layer of zirconia (ZrO2). A CCD camera is mounted to allow the user to control the position of the sample inside the specimen chamber. The samples were sputter coated with gold-palladium (Au-Pd) for further observations using secondary electrons using a voltage between 10 and 15 kV.

An environmental scanning electron microscope (ESEM) Philips XL30 ESEM FEG was also used in order to avoid damage of the sample surface and fibres due to high vacuum of the SEM, which results in drying and shrinking of the fibres. The ESEM also allows easy handling of the samples without surface coating.

4.12.3 C-scan

The ultrasonic C-scan is a scanning acoustic microscopy (SAM) technique commonly used as a non-destructive technique to observe the damage in materials [14]. The A-scan, scans a point, the B-scan a line and the C-scan an entire surface. In this study, a through thickness C-scan was needed to detect damage over the entire composite sample surface and captured using the in-house built software.

The C-scans is used in pulse-echo mode which only requires one accessible side of the specimen. However, it gives an incomplete image of voids through the thickness. This is solved with the through-transmission system which requires a separate receiver and two accessible sides. However, in this study a pulse-echo set-up with the transmitter and receiver located at the same side of the sample is used. Figure 4-19 indicates the different parts of the c-scan apparatus, the transmitter, the receiver as well as the water tank and control system.

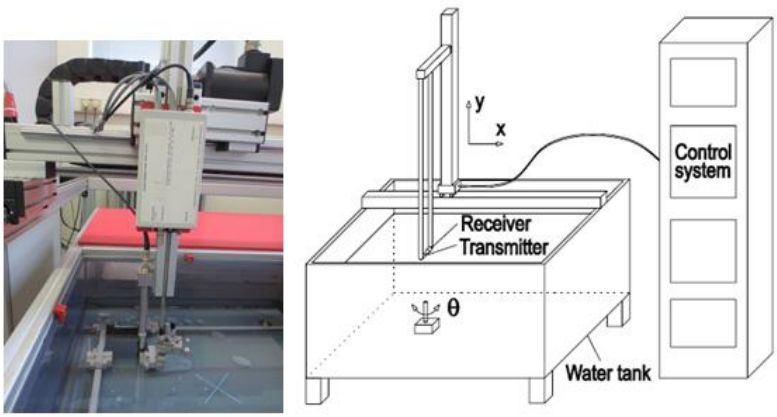

Figure 4-19: Configuration of the C-scan

The quantification of the damage area from the impact testing was done using a C-Scan with a 5MHz transducer from Panametrics (V309) and an Olympus pulser 5077PR. The frequency of the transducer is critical to establish the spatial resolution [14]. The voltage

of the pulser was adjusted according to the thickness of the specimen, either 100V or 200V. The step size determines the steps the transducer takes scanning the sample. For this research two step sizes were taken 1,011mm and 1,985mm.

The results of the scan are given as a pixelated grayscale image, where each pixel has a grayscale value with an intensity value between 0-225 (Figure 4-20 a-b). Afterwards, the image data are then extracted to obtain a map with iso-greyscale lines (Figure 4-20 c). A histogram, which records the number of points with that greyscale value, is also obtained as seen in Figure 4-20 d. Points with low intensity values are displayed black and indicate impact damage. A high and sharp peak at high greyscale values indicates a laminate free of defects or pores. Defects broaden the peak, thus giving an indication of the amount of damage.

This method has been chosen since different signal amplifications were used depending on the fibre architecture, thus making the absolute grayscale values incorrect. Samples were immersed in the C-scan water bath for approximately 15 minutes. The water uptake measured for the damaged specimens was between 0.2-0.3%, and for undamaged samples between 0.09% and 0.3%. As the values are low, its effect on the mechanical properties is assumed to be low as well. Nonetheless, the damage tolerance samples were re-dried for 24h at 60ºC before FAI testing.

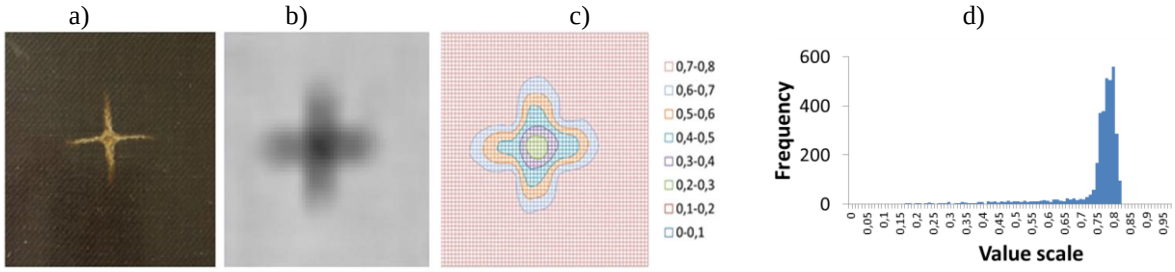

Figure 4-20: Determination of the damage area for the impact samples: a) visual image, b) C-scan image, c) extracted data with the iso-greyscale lines (the value 0-0.1 indicate a high damage area) example of C-Scan histogram of the medium-high twist twill-epoxy composite after impact.

4.12.4 Micro-tomography

X-ray computed micro-tomography (Micro-CT or μ-CT) allows the reconstruction of the 3D image of scanned object through a series of projections taken while the object is rotating around one axis. The resulting image is stored as a three-dimensional array of grey values and can be exported as a stack of images in in XY, XZ and YZ planes. By assigning appropriate threshold to the grey level, various components of the object can be distinguished. In this study, three different micro-CT systems were used according to the desired resolution level and are described in the following sections.

Using micro-CT in the study of natural fibre composite brings out many advantages such the evaluation of a successful manufacturing, establishing the fibre orientation, visualisation and quantification of the void content, delamination as well as the fibre volume fraction and the geometry of the internal structure. However, if the X-ray absorption coefficients of the natural fibres and the used matrix are close, then the differentiation between the fibre and the polymers cannot be entirely identified in the micro-tomography technique as also mentioned by Alemdar et al. [22].

Other filters and image processing software should be used in order to increase contrast between the different elements which will help determine the exact structure of the reinforced composite. In this study, several types of flax fibres reinforcements were studied using X-ray micro-tomography to determine their internal geometry.

The Phoenix Nanotom is an X-ray computed tomography system, developed by General Electric. It has a cone-beam setup, but with manually adjusted source-object and source-detector distances. The Nanotom has four tube modes, designated by the numbers from 0 to 3, which are characterised by more precise control of the focal spot. Higher tube modes impose lower limits on the maximum tube power, therefore reducing the focal spot size and penumbra blurring.

In addition, tube modes higher than 0 employ magnetic focusing system which further reduces the focal spot size. Nanotom can work in the fast-scan mode, when the object is rotated continuously while acquiring projections, which allows performing a scan in 10-20 min. This computed tomography system has been tailored to be used in many applications ranging from material science, biology to medicine and nano-electronics. Its high performance nanofocus X-ray tube can precisely scan an object with a maximum resolution of 400 nm. The scanning parameters are listed in Table 4-4.

Nanotom X-Ray Source Parameters		
Voltage	kV	42
Current	µA	325
Tube mode	-	0
Target	-	Molybdenum
Exposure time	ms	750
Averaging/skip	-	1/0
Voxel/pixel size	µm	3.25
Fod	mm	13
Fdd	mm	200
# Images	-	2400
Image size x	pixels	2304
Image size y	pixels	1800
Scan time	min	30

Table 4-4: X-Ray parameters for the flax composite.

4.12.5 Flax textile internal geometry and void content measurements

The void content, yarn diameter and composite crimp calculations were measured on micro-CT images using the public domain open source ImageJ software. The cross-sections were outlined by manually fitting an ellipse to a cross-section as seen in Figure 4-21.

The obtained value for aspect ratio shows that the yarn cross-sections have a non-round, elliptical shape. This is further discussed in Chapter 6. At least 30-40 measurements were done to ensure a reliable standard deviation. The distances are obtained in numbers of pixels which are later on converted to μm using the resolution data of the micro-CT images.

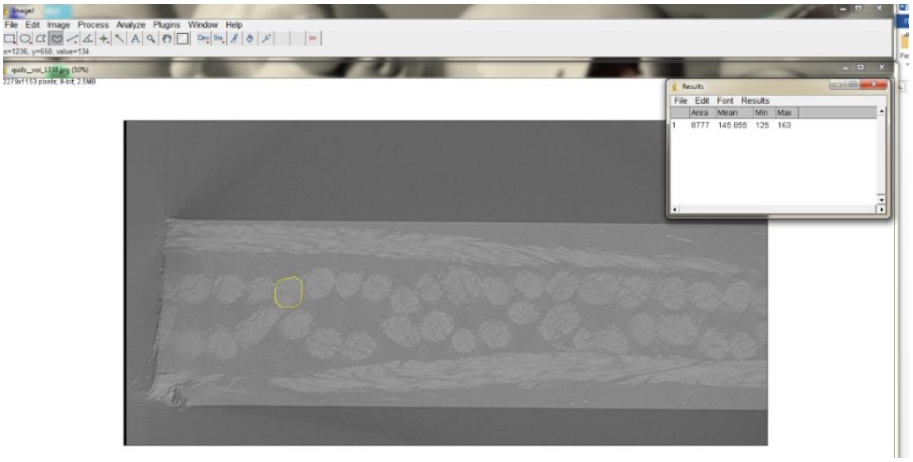

Figure 4-21: Yarn diameter measurement using the cross-section images obtained with micro-CT.

4.13 Statistical analysis- One way ANOVA

To compare the textile architectures, each test parameter [i.e. stiffness, strength and strain to failure) was statistically evaluated using a one-way analysis of variance statistical method, ANOVA. The confidential interval of 95% is used (α=5%). The post hoc single-step multiple comparisons (grouping) were done using the Tukey method. The calculations were using the Minitab 17 statistical software [23] or the JMP11 statistical discovery software from SAS software [24].

References

[1] Decorme J, Duval A, Vanfleteren E, Vanfleteren F. Method for producing a continuous web of fibers comprising long natural fibers, and associated apparatus and web. Google Patents; 2012.
[2] Straumit I, Vanaerschot A, Bensadoun F, Verpoest I, van Vuure AW, Vandepitte D, Wevers M, et al. Reconstruction and stochastic modelling of a twill flax/epoxy composite geometry from X-ray computed tomography data. submitted to Composite Part A. 2016.
[3] Van Vuure A. Course polymer composites II. Recent developments in composite materials science., MTM KULeuven; 2010-2011.
[4] Arbelaiz A, Fernández B, Ramos JA, Retegi A, Llano-Ponte R, Mondragon I. Mechanical properties of short flax fibre bundle/polypropylene composites: Influence of matrix/fibre modification, fibre content, water uptake and recycling. Composites Science and Technology. 2005;65(10):1582-92.
[5] Bensadoun F, Kchit N, Billotte C, Bickerton S, Trochu F, Ruiz. E. A Comparative Study of Dispersion Techniques for Nanocomposite Made with Nanoclays and an Unsaturated Polyester Resin. Journal of Nanomaterials. 2011;2011.
[6] Coroller G, Lefeuvre A, Le Duigou A, Bourmaud A, Ausias G, Gaudry T, Baley C. Effect of flax fibres individualisation on tensile failure of flax/epoxy unidirectional composite. Composites Part A: Applied Science and Manufacturing. 2013;51(0):62-70.
[7] Trujillo E, Moesen M, Osorio Serna L, Van Vuure WA, Ivens J, Verpoest I. Weibull statistics of bamboo fibre bundles: methodology for tensile testing of natural fibres. 15th European Conference on Composite Materials. Venice, Italy:2012.
[8] Madsen B, Lilholt H, Thygesen A, Arnold E, Weager B, Joffe R. Aligned flax fibre/polylactate composites - A materials model system to show the potential of biocomposites in engineering applications. Journal of Nanostructured Polymers and Nanocomposites. 2008;4(4):139-45.
[9] ISO 14127:2008 - Carbon-fibre-reinforced composites -- Determination of the resin, fibre and void contents. 2011.
[10] ISO 10618:2004 : Carbon fibre -- Determination of tensile properties of resin-impregnated yarn. 2004.
[11] Lamon J. A micromechanics-based approach to the mechanical behavior of brittle-matrix composites. Composites Science and Technology. 2001;61(15):2259-72.
[12] University of Cambridge. Strength of long fibre composites. 2014-2015. http://www.doitpoms.ac.uk/tlplib/fibre_composites/strength.php
[13] 6603-1 I. Plastics Determination of puncture impact behaviour of rigid plastics. 2000.
[14] Abrate S. Impact engineering of composite structures. Carbondale: SpringerWienNewYork; 2011.
[15] Hwang SF, Mao CP. Failure of delaminated carbon/epoxy composite plates under compression. J Compos Mater. 2001;35:1635-55.
[16] Standard A. D5528-94a. Standard test method for mode I interlaminar fracture toughness of unidirectional continuous fiber reinforced polymer matrix composites," Philadelphia, Pa, USA. 1994.
[17] Carlsson LA, Adams DF, Pipes RB. Experimental characterization of advanced composite materials: CRC press; 2014.
[18] Tanaka K, Kageyama K, Hojo M. Prestandardization study on mode II interlaminar fracture toughness test for cfrp in japan. Composites. 1995;26(4):257-67.

[19] Blackman B, Williams J, Benguediab M. 5722-CRACK LENGTH DETERMINATION DIFFICULTIES IN COMPOSITES-THEIR EFFECT ON TOUGHNESS EVALUATION. ICF11, Italy 20052013.
[20] Blackman BRK, Kinloch AJ, Paraschi M, Teo WS. Measuring the mode I adhesive fracture energy, GIC, of structural adhesive joints: the results of an international round-robin. International Journal of Adhesion and Adhesives. 2003;23(4):293-305.
[21] de Morais AB, de Moura MF, Marques AT, de Castro PT. Mode-I interlaminar fracture of carbon/epoxy cross-ply composites. Composites Science and Technology. 2002;62(5):679-86.
[22] Alemdar A, Zhang H, Sain M, Cescutti G, Müssig J. Determination of Fiber Size Distributions of Injection Moulded Polypropylene/Natural Fibers Using X-ray Microtomography. Advanced Engineering Materials. 2008;10(1-2):126-30.
[23] Software M. Using multiple comparisons to assess the practical and statistical significance of differences between means. 2015. http://support.minitab.com/en-us/minitab/17/topic-library/modeling-statistics/anova/multiple-comparisons/using-multiple-comparisons-to-assess-differences-in-means/
[24] JMP. Oneway Analysis- Compare Means. 2012. http://www.jmp.com/support/help/Compare_Means.shtml

Chapter 5
Quasi-static mechanical properties

Flax fibres have become excellent candidates to be used for high performance composites in new products or as a replacement of less sustainable products, such as glass fibre applications, due to their multiple advantages presented in Chapter 2. The flax fibres were found to have the best mechanical performance amongst other the natural fibres and have comparable stiffness with E-glass. Thanks to their low density, flax may even outperform the properties of E-glass in terms of specific stiffness.

The present chapter is devoted to the understanding of the effect of the textile architecture and matrix system on the mechanical properties of flax fibre composites. The tensile and flexural properties, based on unidirectional, quasi-unidirectional, woven and mat fabrics, are characterised. These preforms are combined to two matrix systems, a thermoset epoxy (Th) and a thermoplastic Maleic Anhydride Grafted Polypropylene - MAPP (Tp). The relations between the stiffness and strength properties of flax fibre reinforced composites are expected to depend on the intrinsic properties of both the matrix and the reinforcement architecture.

The consolidation of the composites is realized using the two most widely used processes in industry, resin transfer moulding (RTM) and compression moulding (CM). The fibre volume content was controlled and set to 40% in order to be able to compare the different reinforcements. Differences in properties between the fabric configurations (twills and plain woven) is expected and will depend on the yarn spinning process (wet or dry) and twist, as well as the crimp introduced during textile weaving. These will be compared to crimp-free structures, namely cross-ply [0,90] laminates, to extract then the influence of the twist and crimp on the properties. Detailed descriptions of the flax textiles, matrices, manufacturing processes and testing techniques is found in Chapter 4

In the first part of this chapter, the flax composites internal structure and manufacturing defects are investigated through optical microscopy and SEM. This is followed by a thorough investigation of the stress-strain curves to uncover the particularities of flax-based composites. Moreover, they will support the understanding of the composites properties. An overview of

the tensile and flexural properties obtained from the quasi-static tensile and bending tests highlights the influence of the matrix and the fibre architecture.

Tensile tests with loading, unloading and reloading cycles at gradually increasing strains are then performed in order to gain insight on the evolution of the plastic deformation of the flax fibre composites. Finally, the measured mechanical properties will be compared to the other composites materials through an Ashby plot. These data could then be used to establish a reliable database for part design where materials selection is key. This would avoid the difficult and time-consuming process of trial and error to find the right material for an application.

5.1 Qualitative assessment of the internal composite structure

Optical microscopy allows for the observation of small details and defects of a composite sample. In composites, this technique is mostly used for the initial examination and characterization of the internal microstructure and for the qualitative assessment of the impregnation. The flax fibre reinforced plate, shown in Figure 5-1a, has no apparent defects or presence of large porosities. At larger magnification only very small porosities are detected (Figure 5-1b). It has to be noted that these small spots may also be caused by a deficient wetting between fibres (exposed by grinding and polishing during sample preparation) and the matrix. All plates produced in this study were examined by optical microscopy and did not show obvious major defects and this was confirmed with the micro-tomography technique as displayed in Figure 5-1c. It has be noted that the average porosity level in all composites was below 0.5%.

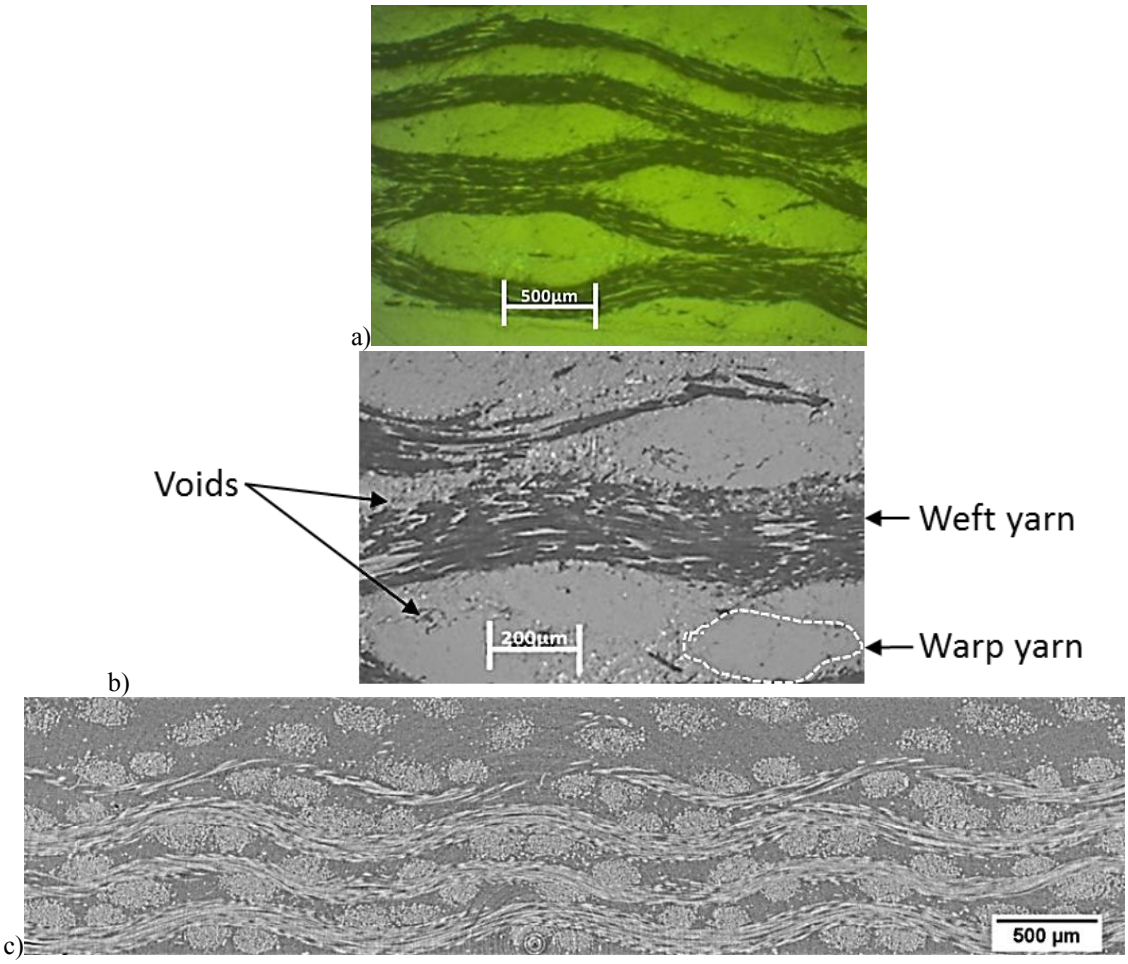

Figure 5-1: Medium-low twist twill/epoxy plate: a) optical microscopy at 500µm scale, b) optical microscopy at 200µm and c) cross-section obtained by micro-tomography.

At larger magnification, three types of micro-defects were observed using the SEM (Figure 5-2): non-impregnated zones (a), micro-cracks (b) and porosities (c). The first defect, the non-impregnated zones, seen in Figure 5-2a at the surface of the specimen, are directly related to the wetting capacity of the matrix and the permeability of the textile and yarn. The flax yarn itself is composed of several technical fibres of 50-100 microns in diameter [1], and it is difficult for the resin to permeate inside the yarns and to distribute around all of the fibres. Therefore, voids can be created in the composite.

The second observed defects, namely micro-cracks, were observed on the cross-sections of the composites (see in Figure 5-2b). These cracks could be related to the curing and post-curing process as residual stresses can be created during the composite cooling down due to the mismatch in the coefficient of thermal expansion (CTE) of the fibre and the matrix. Furthermore, the cutting saw used to prepare the small sample for the ESEM observation could have slightly contributed to the presence of micro-cracks as well. Hence, it is not clear whether these micro-cracks are artefacts (created during sample preparation) or real cracks, present in the specimen as such.

Third, porosities were also observed, but only for the composites with thermoplastic matrix and reinforced with woven fabrics (Figure 5-2c). This could be related to the dense packing of the yarns composing the weaves, and to the higher viscosity of the thermoplastic matrix compared to the thermoset epoxy. A weave composed of highly twisted yarns, thus having a higher packing density, is more difficult to impregnate. Additionally, the high viscosity of the TP matrix doesn't allow a good penetration of the matrix between the narrow gaps in-between the technical fibres and even more in-between the elementary fibres present in the technical fibres. It should be stated that the presence of these small defects is not expected to induce large deviations in the stiffness results. However, the strength can be affected by the presence of voids which can easily coalesce during testing.

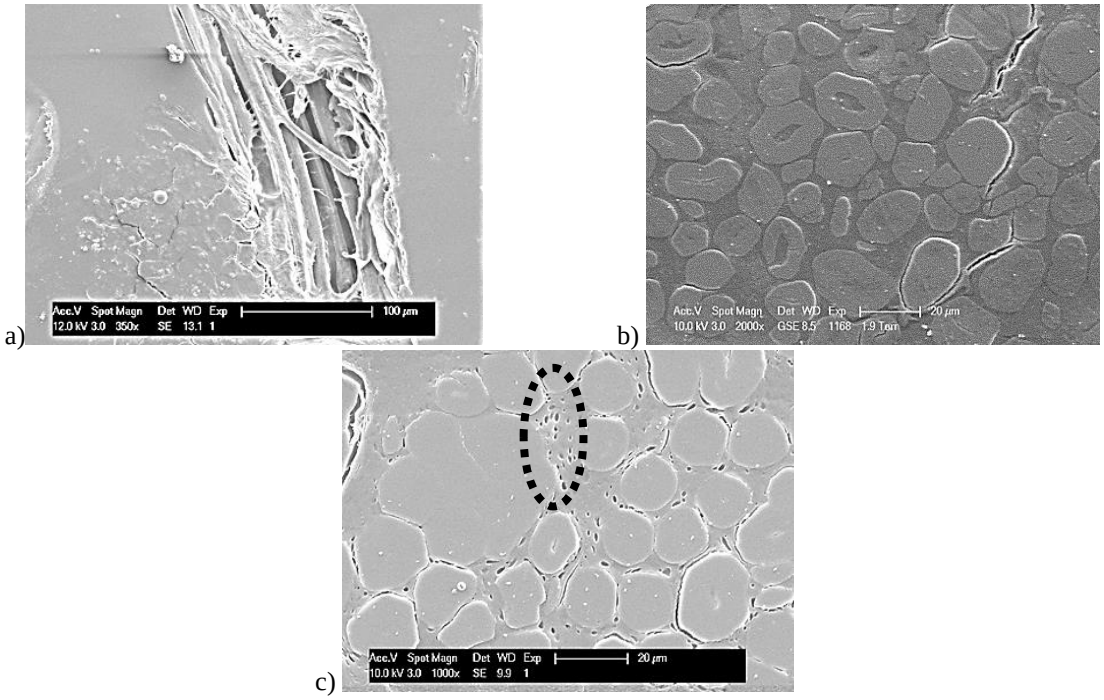

Figure 5-2: Micrographs of the micro-defects present in the flax composites a) surface view non-impregnated zones (SEM) for the high twist twill flax-MAPP composite, b) cross-section view of medium-low twist twill flax-epoxy composite micro-cracks at the fibre-matrix interface (ESEM) and c) micro-porosities in cross-section of low twist twill flax-MAPP sample (SEM).

5.2 The non-linear stress-strain curve of flax-epoxy composites

This section focuses on the non-linear behaviour of the flax fibre reinforced epoxy composites and its origins. The effect of the fibre architecture was also studied based on observations of the stress-strain curves obtained from the tensile test.

5.2.1 Non-linear behaviour of unidirectional composites

A non-linear stress strain curve is observed for the flax fibre reinforced epoxy composites. This phenomenon is different from the linear-elastic behaviour commonly observed in composites reinforced with synthetic fibres like glass or carbon fibres. The stress-strain curve is divided in three distinct regions (see Figure 5-3) [2-5]:

I. Linear-elastic region: the average tangent modulus is calculated between 0-0.1% strain. In this study, the tangent modulus value was calculated as a ratio of the stress increment to the strain increment for ten successive readings of the stress and strain, corresponding to an average strain increment of 0.004%.
II. Strain softening region: a knee in the curve (rapid change in tangent modulus E_t) is observed between $\varepsilon > 0.15$-0.3%. this could be due to:
    a. The visco-elastic or visco-plastic behaviour of the elementary fibres composing the technical fibres in the flax yarns;
    b. Idem for the middle lamella in-between the elementary fibres, which is a pectin rich region which has a low yield stress, σ_y;
    c. The gradual start of the reorientation of the microfibrils ($E_t \uparrow$) present in the S2 layer of the elementary fibres from 10^o to 0^o. This phenomenon happens independently of the fibre architecture and occurs also at the elementary fibre level [3]. This would however have a strain hardening effect, and hence counteract the two previous strain softening mechanisms;
III. Strain hardening: stop of the decrease of the tangent modulus E_t and then a gradual increase before failure. This could be caused by the different phenomena happening at the same time (IIa,b vs IIc), but additionally, other hardening mechanisms could occur such as the hardening of the pectin present between the elementary fibres or the gradual crystallization of the amorphous cellulose in the elementary fibre as hypothesized by Placet et al. [6].

Other authors have observed a similar behaviour, such as Alves et al [7] on sisal, coir and piassava single fibres and by Baley [3] on flax fibres. They also saw that the non-linear region started at low stress levels ($\sigma < 100$MPa).

From the stress-strain curve, the exact location of the yield point is not straightforward as seen in Figure 5-3. In elasto-plastic materials, the yield point σ_y, being the elastic limit, is defined as the deviation from linear-elastic behaviour, i.e. the point which coincides with the drop in the initially constant tangent modulus. In natural fibre based composites, where both fibre and matrix are visco-elastic/plastic, we propose to define the yield stress as the point when the stress level of the (extrapolated) linear elastic curves is 10% higher than the recorded stress strain curve (see Figure 5-3). It has to be emphasized that this yield stress hence is strain rate dependent, but in the framework of this study this dependence has not been studied further.

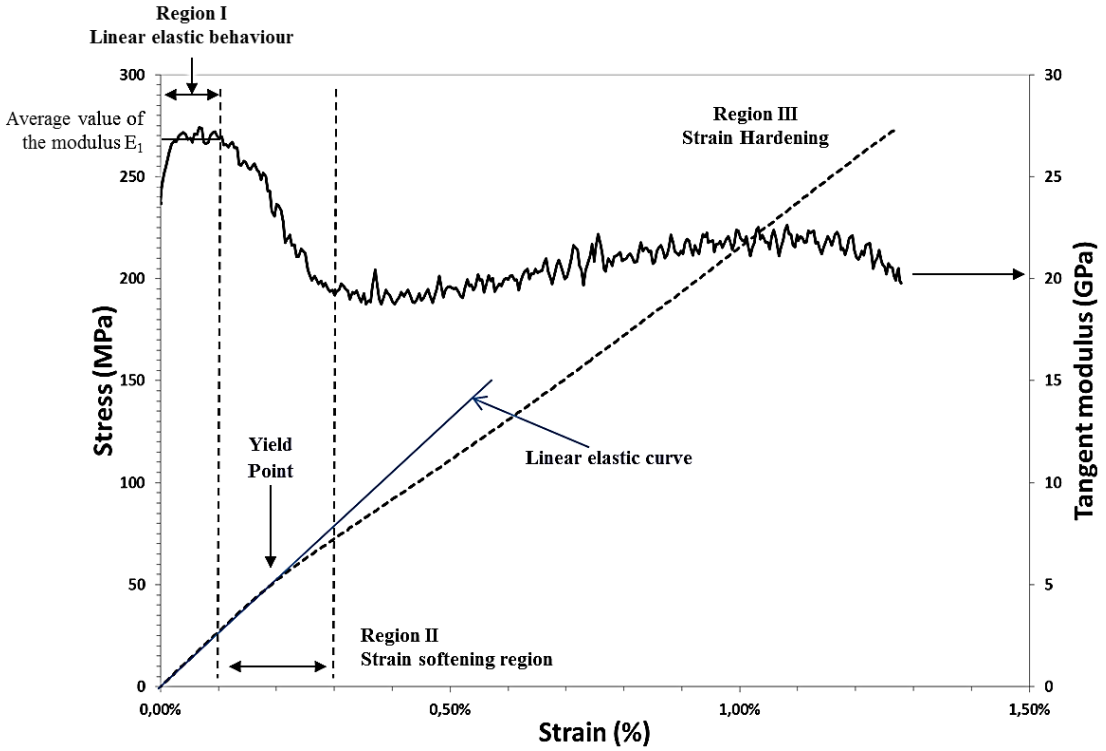

Figure 5-3: The non-linear behaviour divided in three regions, example using unidirectional flax composite UD2.

5.2.2 The non-linear behaviour in woven fabrics and laminates

The tensile stress-strain and modulus-strain curves for the flax-epoxy configurations are presented in Figure 5-4 and Figure 5-5, and the positions of the yield points were quantified and presented in Table 5-1. The curves show different stress-strain behaviour strongly dependent of the textile architecture, although all composites exhibited failure at low strain as it was also found in other studies [8]. This type of failure is usually referred to as a brittle fracture in literature even though a certain amount of plastic deformation is present in the tested sample.

The weave type as such (twill versus plain) does not have a systematic effect on the tensile properties, because at the same time also other geometric parameters are changing (degree of crimp and twist). This will be further discussed in section 5.3.2, along with an analysis of the differences between weaves and cross-ply laminates will be presented.

Table 5-1 shows that the yield point is, for all preform architectures, situated between 0.11 to 0.28% of strain. Hence, two stiffness values can be determined for flax fibre reinforced composites: one at very low strain values between 0 and 0.1% of strain in the elastic region and a second one after the yield zone between 0.3 and 0.5% of strain. These two moduli are identified as E_1 and E_2 respectively (see Figure 5-6) [9]. It is important to mention both values, as they are of interest for design purposes.

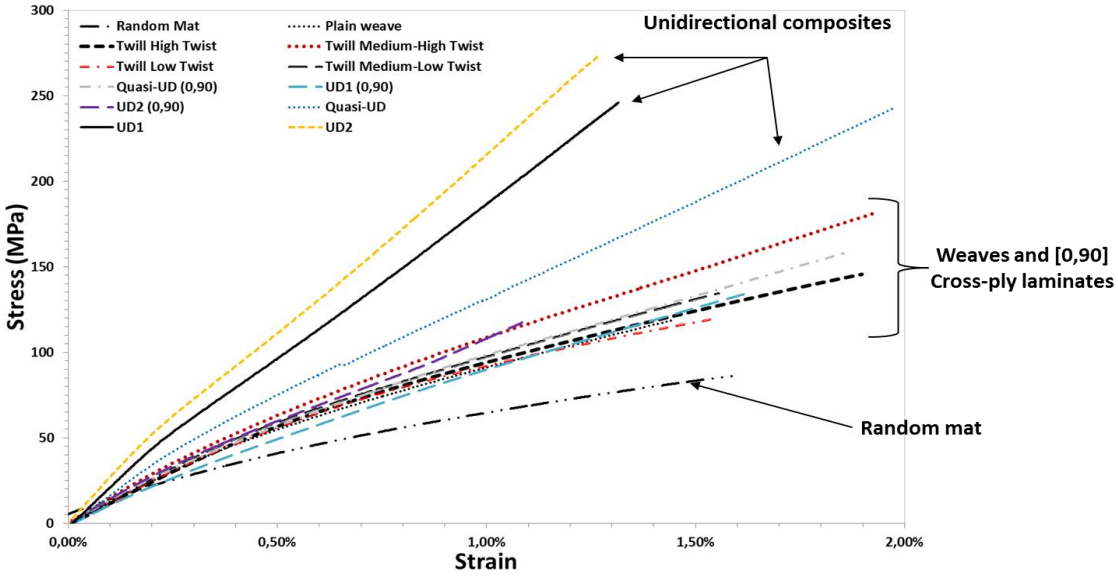

Figure 5-4: Typical stress-strain curves for flax-epoxy during quasi-static tensile testing for all studied architectures.

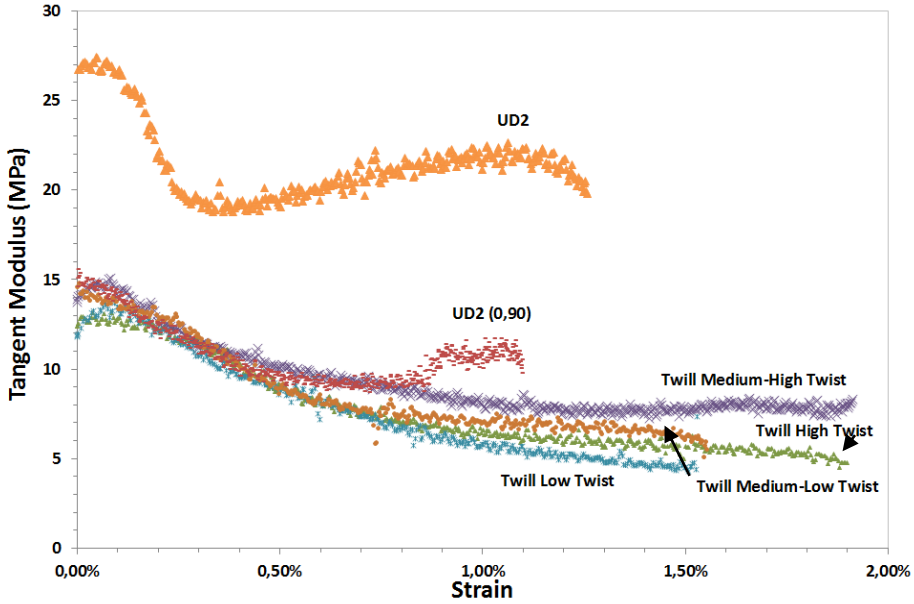

Figure 5-5: Woven fabrics vs UD [0,90] vs UD laminate modulus-strain curve for epoxy composites.

		Flax-epoxy		Flax-MAPP	
	Architecture	**σ_y(MPa)**	**ε_y (%)**	**σ_y(MPa)**	**ε_y (%)**
Random Mat	Random mat	15 ± 3	0.13 ± 0.05	13 ± 1	0.29 ± 0.08
Weaves	Plain weave	22 ± 5	0.19 ± 0.05	-	-
	Low Twist Twill	26 ± 1	0.22 ± 0.01	20 ± 1	0.21 ± 0.01
	Medium-Low Twist Twill	34 ± 6	0.28 ± 0.07	19 ± 2	0.20 ± 0.02
	Medium-high Twist Twill	31 ± 1	0.18 ± 0.01	20 ± 3	0.26 ± 0.04
	High Twist Twill	34 ± 2	0.28 ± 0.03	11 ± 2	0.13 ± 0.02
Cross-ply Laminates [0,90]	Quasi-UDS	24 ± 1	0.20 ± 0.02	22 ± 1	0.20 ± 0.01
	UD1S	22 ± 3	0.20 ± 0.03	25 ± 2	0.18 ± 0.00
	UD2S	19 ± 1	0.13 ± 0.02	18 ± 1	0.09 ± 0.02
Unidirectional	Quasi-UD	35 ± 6	0.17 ± 0.02	12 ± 4	0.09 ± 0.02
	UD1	31 ± 5	0.11 ± 0.03	-	-
	UD2	45 ± 3	0.17 ± 0.02	12 ± 3	0.07 ± 0.03

Table 5-1: Yield point values for flax-epoxy and flax-MAPP composites.

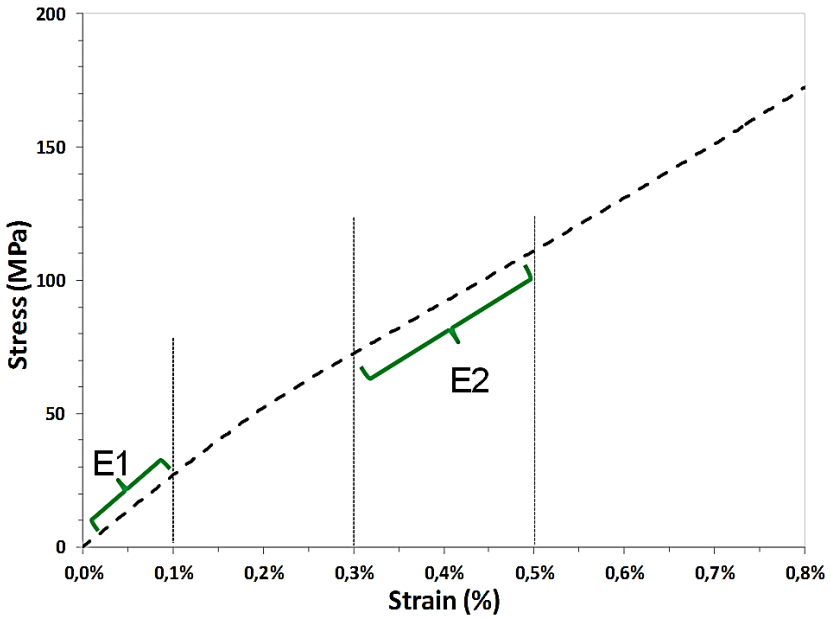

Figure 5-6: Zones where E1 and E2 are calculated.

5.3 Flexural and tensile properties: stiffness and strength

The effect of different textile architectures and matrices on the tensile and flexural properties is reported in Table B-1 to Table B-4 in Appendix B. The obtained results include the moduli E1 and E2, the ultimate stress or strength (σ_u) and deformation at maximum stress ε_{ult} (%) of flax-epoxy and flax-MAPP composites. All values are normalised to a fibre volume fraction of 40%. Due to difficulties related to a proper compaction, the fibre volume fraction of the random mat composites was limited to 30% in order to ensure good impregnation of the mat. Thus, it does not allow decent comparison with the other architectures, but only a comparison between an epoxy and a MAPP matrix

5.3.1 Effect of the matrix

From the obtained results, it was observed that all epoxy composites have a higher modulus in flexure and tension compared to MAPP ones, at equal fibre volume fractions. This behaviour was expected due to the higher intrinsic properties of the epoxy matrix (E= 2.7GPa) compared to MAPP (E= 0.34GPa). Moreover, the weak MAPP cannot give sufficient support, i.e. load bearing and load transfer capacities, to the fibres in case of a certain fibre curvature, which is always present in textile structures.

In Figure 5-7, the variation in non-linear behaviour (E_2 vs E_1) in the tensile and flexural tests is presented for both thermoset and thermoplastic composites. It can be seen that the % of modulus decrease is higher in tensile than in flexural loading in most cases. An exception is seen for the UD2 [0,90] and Quasi-UD [0,90], which will be explained in section 5.3.2.5.

Furthermore, epoxy composites under tensile stress show a stronger non-linear behaviour for medium-high to highly twisted yarn-based composites (except for the high twist twill which will be further discussed in section 5.3.2.3). The tensile E_1-E_2 variation for the plain weave, twill medium-high twist and quasi-UD [0,90] composites is in the 30% range, compared to the medium/low twist ones, which show E_1-E_2 differences of 21 to 25%. The average drop in tensile stiffness and flexural stiffness for the thermoset and thermoplastic composites is displayed in Table 5-2.

Average modulus decrease (E_1-E_2)/ E_1 (%)	Epoxy matrix	MAPP matrix
Tensile	24% ± 6%	30% ± 9%
Flexural	19% ± 6%	24% ± 9%

Table 5-2: Average drop in tensile stiffness and flexural stiffness for flax-epoxy and flax-MAPP composite.

For the MAPP composites, the observed E1-E2 modulus decrease is higher than in epoxy matrix in most cases except for the Quasi-UD under flexure load. Moreover, a less clear influence of the twist is observed. This could be due to the poor wetting of the fibre which leads to a reduced stress transfer across the fibre-matrix interface. This effect combined to the strong intrinsic non-linear behaviour of the MAPP matrix could mask the effect of twist in the woven fabrics. Further investigation is needed to determine the underlying causes.

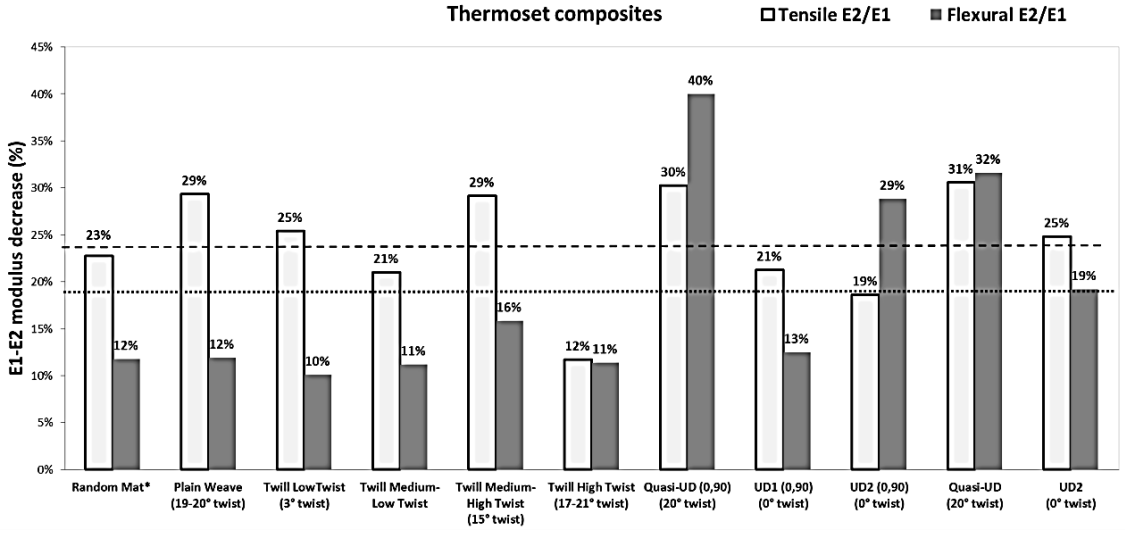

a)

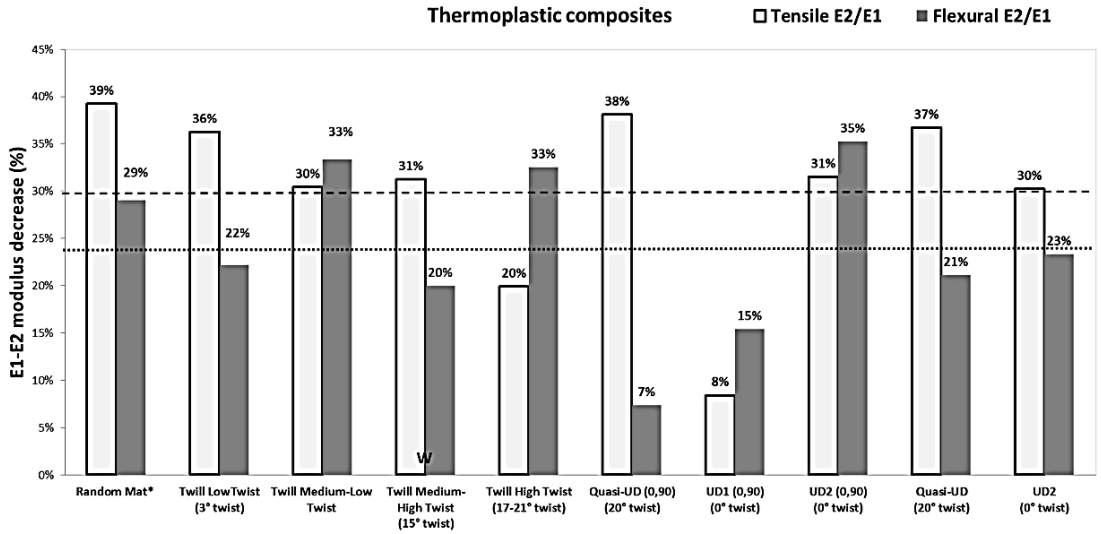

b)

Figure 5-7: a) Average modulus decrease in % between E1 and E2 for tensile and flexural properties a) for flax-epoxy composites and b) for flax-MAPP composites. The average values are indicated with dashed line: tensile properties (- - -) and flexural properties (····). The "w" indicates the wet spun yarn-based composites.

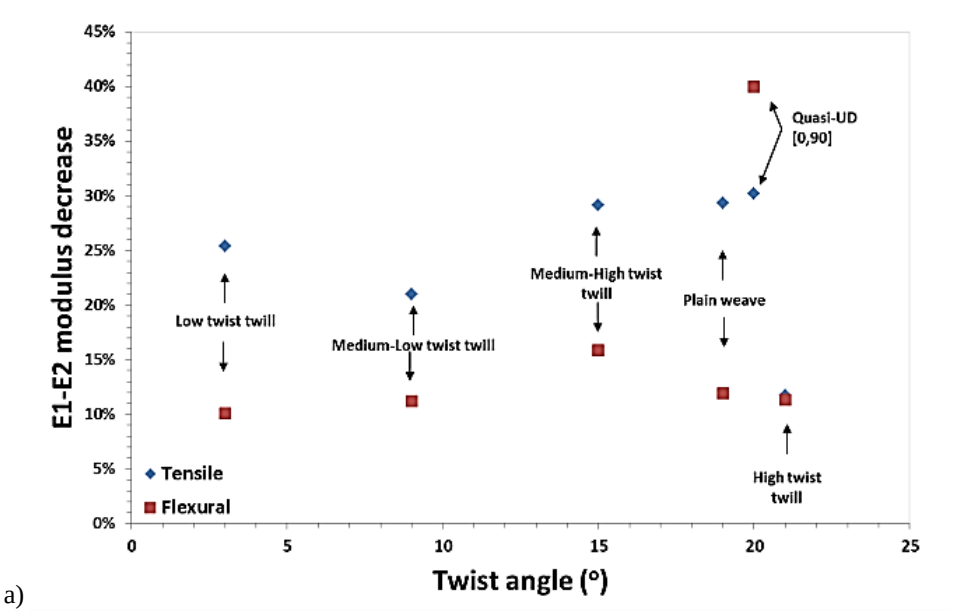

a)

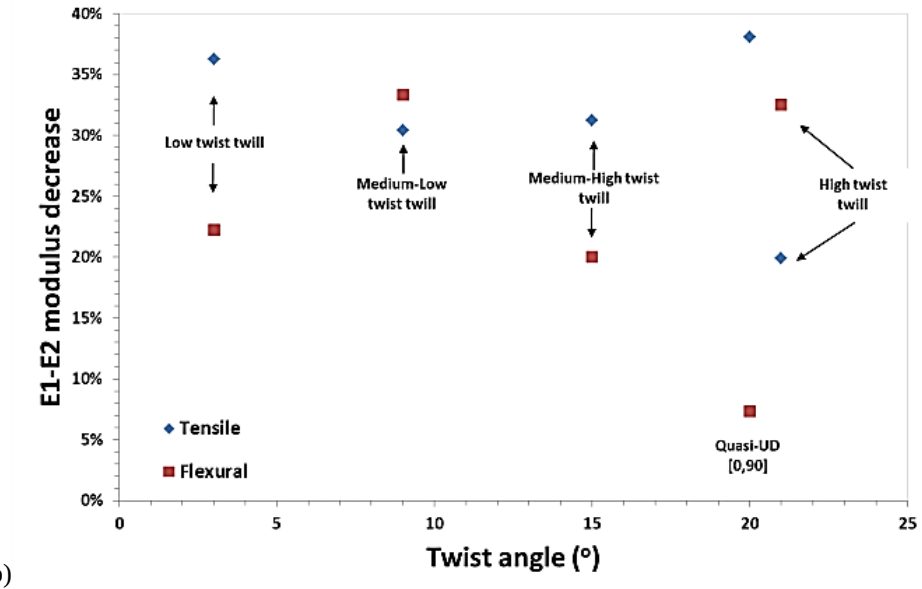

b)

Figure 5-8: E1-E2 modulus decrease according to twist angle: a) epoxy and b) MAPP composites.

For MAPP composites in comparison to the epoxy ones, a larger drop of the modulus for both tensile and flexural stiffness was observed (see Figure 5-8 and Table 5-2). Once again, in the majority of cases the drop is more important for tensile than flexural properties. As the MAPP matrix is 10 times weaker than the epoxy matrix in both modulus and strength, this causes the fibre to sustain most of the load with limited load transfer to the matrix. Hence, the softening mechanisms present in the fibre are being exploited to a maximum. Moreover, the weaker thermoplastic matrix creates less resistance to phenomena like the untwisting and de-crimping resulting in a further decrease of the tangent modulus E_2. The thermoplastic composites display a stronger non-linear behaviour with an average 30% drop in modulus in tension and 24% in flexure between E1 and E2. An example for the quasi-UD and UD composites is shown in Figure 5-9 where the increased non-linearity for the thermoplastic composite is displayed.

In the specific case of the plain weave fabric with highly twisted yarns ($\alpha \approx 20^o$), the composites with MAPP matrix had significantly lower properties in both strength and modulus than the other woven composites. This may be due to the difficulty of impregnation of the highly twisted

yarns by the viscous matrix, as the local permeability may be too low to allow an easy impregnation between and inside the technical fibres. It also has to be noted that both the plain woven and the high twist twill fabrics are woven with wet spun yarns. Because of the low tested properties, plain weave MAPP results were discarded in this study.

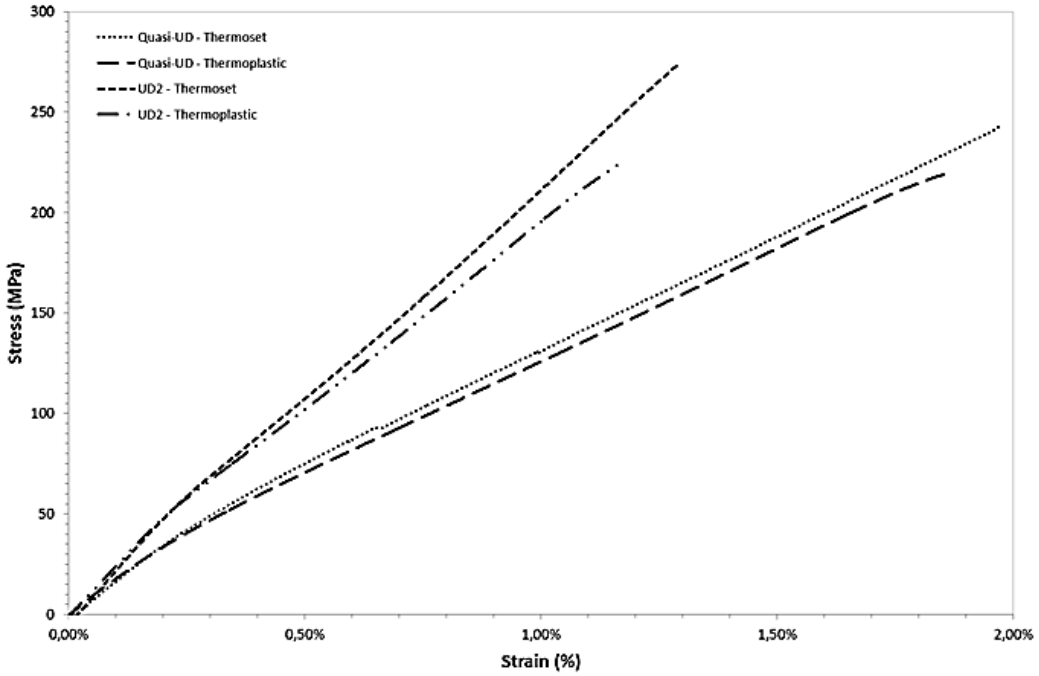

Figure 5-9: Display of stronger non-linear behaviour of the flax-MAPP composites vs the flax-epoxy composites.

5.3.2 Effect of the textile architecture

5.3.2.1 Woven textile based composites

From the results presented in Appendix B, the modulus and strength values for the random mat composite are lower than for all the other composites, which is consistent as the combination of lower fibre volume fraction and random orientation of the fibres will lead to lower properties. For the five configurations of woven fabrics, the four twills and the plain weave, it can be seen that the tensile properties for flax-epoxy composites (Figure 5-10) are rather close to each other, with an average E_1 of 12.9 ± 0.6 GPa and E_2 of 9.8 ± 0.7 GPa. For the MAPP combination (shown in Appendix B, Table B-3), an average E_1 of 8.9 ± 1 GPa and E_2 of 6.2 ± 0.5 GPa was measured. In this last case, the average includes only the four studied twills as manufacturing difficulties prevented the testing of the plain woven fabric (mentioned in section 5.3.1).

For the strength of the woven composites, all values fall in the same range with an average value at 141 ± 25 MPa for flax-epoxy composites and 112 ± 12 MPa for flax-MAPP composites (excluding the plain weave). Only the Twill Medium-High twist displays a higher resistance with a strength value of 184 ± 2 MPa for thermoset composite. This difference may be explained by the variation in yarn quality used in the textiles. Thus, single fibre and yarn testing, such as the impregnated fibre bundle test proposed by many authors [9-11], are needed to confirm these results.

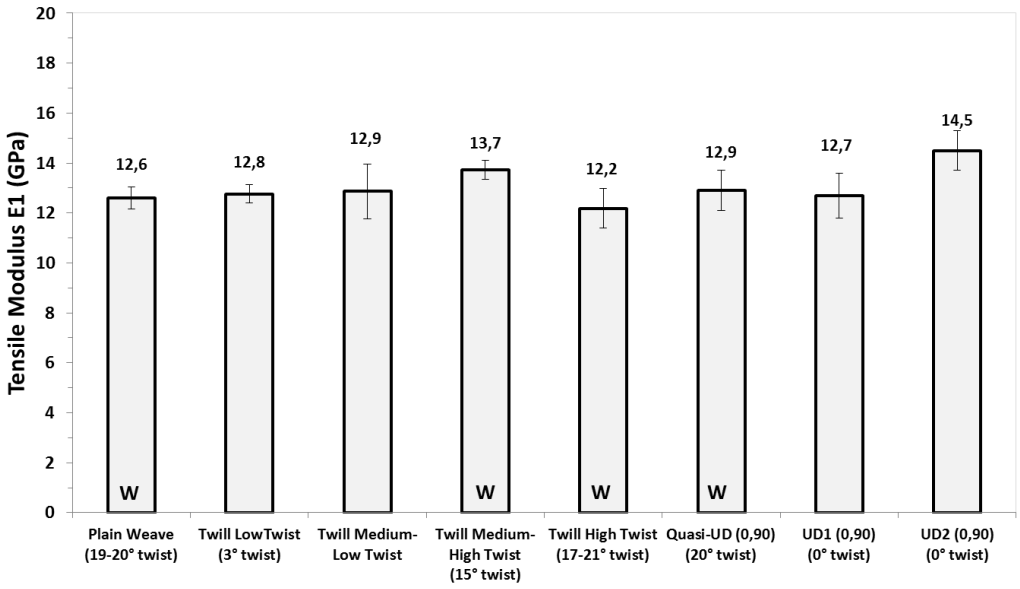
Tensile Modulus E1 (GPa)
20
18
16
14
12
10
8
6
4
2
0
12,6
12,8
12,9
13,7
12,2
12,9
12,7
14,5
W
W
W
W
Plain Weave (19-20° twist)
Twill LowTwist (3° twist)
Twill Medium-Low Twist
Twill Medium-High Twist (15° twist)
Twill High Twist (17-21° twist)
Quasi-UD (0,90) (20° twist)
UD1 (0,90) (0° twist)
UD2 (0,90) (0° twist)

a)

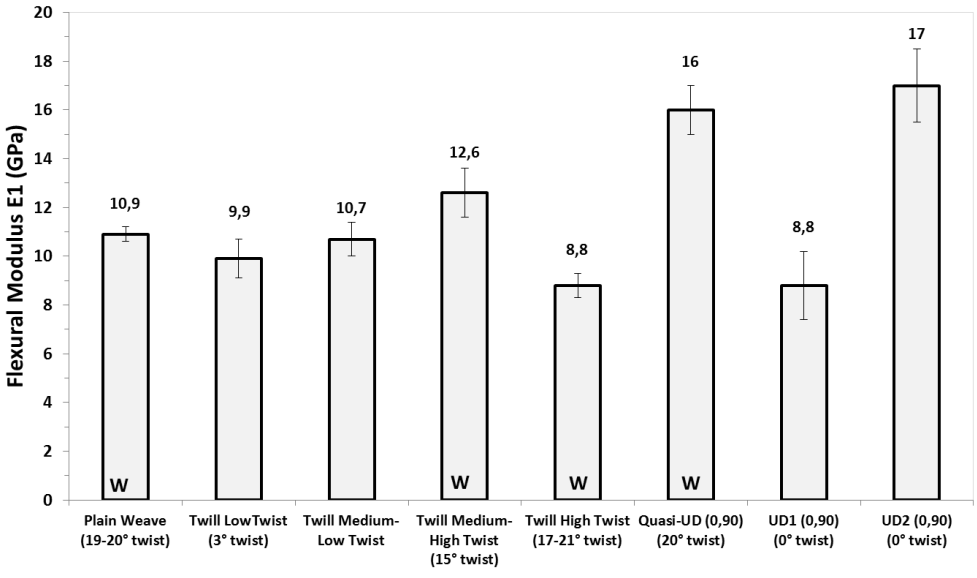
Flexural Modulus E1 (GPa)
20
18
16
14
12
10
8
6
4
2
0
10,9
9,9
10,7
12,6
8,8
16
8,8
17
W
W
W
W
Plain Weave (19-20° twist)
Twill LowTwist (3° twist)
Twill Medium-Low Twist
Twill Medium-High Twist (15° twist)
Twill High Twist (17-21° twist)
Quasi-UD (0,90) (20° twist)
UD1 (0,90) (0° twist)
UD2 (0,90) (0° twist)

b)

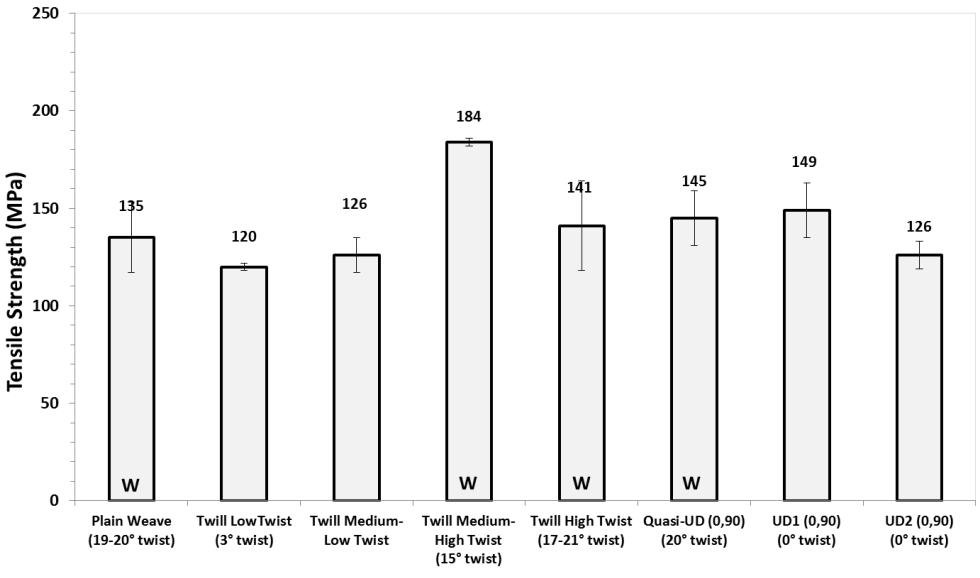
Tensile Strength (MPa)
250
200
150
100
50
0
135
120
126
184
141
145
149
126
W
W
W
W
Plain Weave (19-20° twist)
Twill LowTwist (3° twist)
Twill Medium-Low Twist
Twill Medium-High Twist (15° twist)
Twill High Twist (17-21° twist)
Quasi-UD (0,90) (20° twist)
UD1 (0,90) (0° twist)
UD2 (0,90) (0° twist)

c)

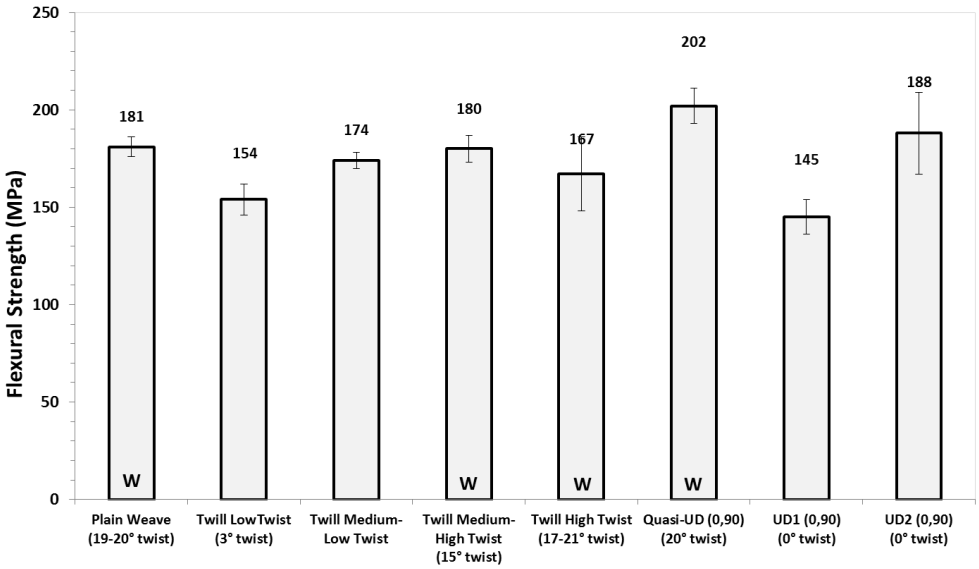

d)

Figure 5-10: Quasi-static mechanical properties of flax-epoxy woven fabrics and cross-ply laminates: a) Tensile E1 modulus, b) flexural E1 modulus, c) tensile strength and d) flexural strength. The "w" indicates the wet spun yarn-based composites.

5.3.2.2 The low twist twill composites

The Low Twist Twill weave composite is an exception, as it shows a lower strength under tensile and flexural loads compared to the other woven structures. This is due to the presence of a "side crimp". In the yarns used in this weave, a unidirectional bundle of fibres, with a low twist angle of only 3^o, is kept together by a spiralling binding yarn, as seen in Figure 5-11.

This binding yarn causes a crimp along the 0^o direction of the fibres, hence introducing a misalignment in the longitudinal direction causing a decrease in the composite properties. In this case, the limited yarn twist (3^o) does not give a strong and stiff composite even though it is expected that straighter fibres should lead to a higher strength [12-14]; the side crimp overrules this. The binding yarn also creates stress concentration points which increase the chance of damage. Coupled to the shear–induced damage between the fibres and the matrix, this induces an early yield point and a faster permanent deformation of the sample, and hence leads to a lower strength value compared to the other twill fabrics.

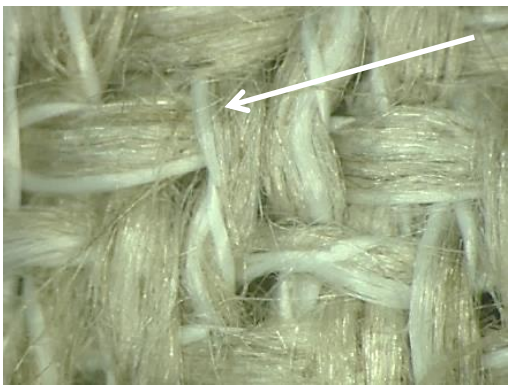

Figure 5-11: Flax yarn with binding polyester yarns from the low twist twill textile.

5.3.2.3 Weaves based on medium to high twist wet-spun yarns

The plain weave, the medium-high twist twill and the high twist twill architectures, all contain wet spun yarns, which are also highly twisted (15 to 21°). During the spinning of these yarns,

the fibres are wetted and the water (partially) dissolves the pectin which leads to partial or full separation of the elementary fibres called fibrillation. This fibrillation allows a better impregnation by matrix polymer within the technical fibres and around the elementary fibres present in the yarns [15], and hence may counteracts the two negative effects of twisting, namely reduction of the yarn permeability which hinders the impregnation on one hand, and the deviation of fibres from the yarn direction.

Overall, the wet spinning process seems to improve the fibre-matrix interaction and thus the load bearing efficiency, and leads to an increase of the strength properties. For the three mentioned architectures, their strength is at least 9% higher compared to dry spun yarn-based Medium-Low Twist Twill and comparable to the water-treated UD [0,90] and wet spun Quasi-UD [0,90] laminates strength values.

As mentioned in section 3.2.1, the high twist twill thermoset composite has the lowest drop in stiffness between E_1 and E_2 in both tensile (12%) and flexural testing (11%). Taking a closer look at the stress-strain curve of wet-spun based twill weaves shown in Figure 5-12, one can see that the High twist Twill has a delayed yield in comparison with the medium-high twist twill. This behaviour leads to a slower decrease in stiffness with increasing stress, explaining the low difference between E1 and E2.

In the case of woven fabrics and cross-plies, a slow and constant decrease in modulus is observed after the yield. This means that the E_2 modulus value is only an indicative value in those cases. Thus, a third modulus, E_3, could eventually be calculated at higher strain (around 1% strain) where the modulus stabilizes.

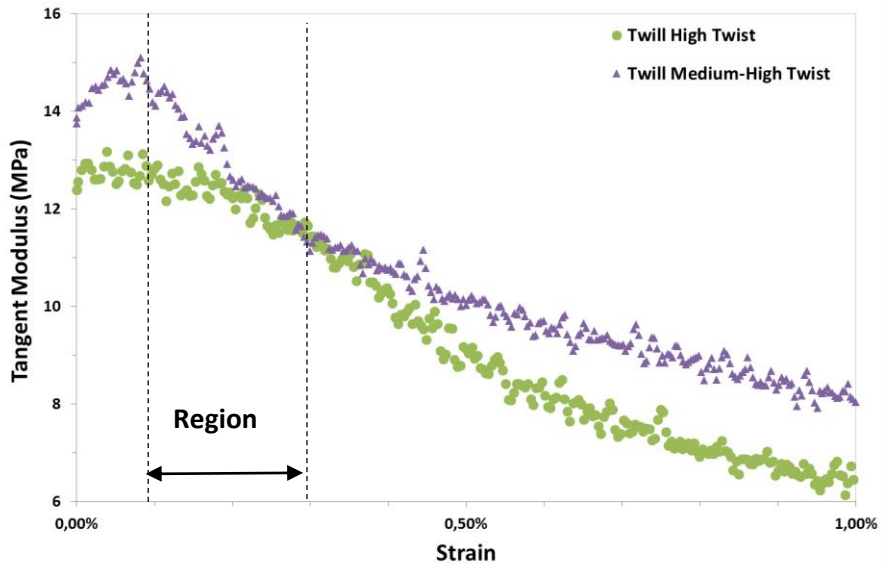

	E1	E2	σ_y(MPa)	ε_y (%)
Twill Medium-High Twist	13.7 ± 0.4	9.7 ± 0.3	31 ± 1	0.18 ± 0.01
Twill High Twist	12.2 ± 0.8	10.8 ± 0.8	34 ± 2	0.28 ± 0.03

Figure 5-12: Difference between the non-linear behaviour of the medium-high and high twist twill flax fibre-epoxy composites.

5.3.2.4 The [0,90] UD cross-ply laminates vs dry spun weaves

The [0,90] UD cross-ply laminates can be directly compared to the weaves with dry spun yarns (low twist twill and medium-low twist twill), because they both contain fibres which have not gone through a wet-spinning process.

The UD2 [0,90] cross-ply laminate has an increased E_1 and E_2 of 14.5 GPa and 11.8 GPa in epoxy respectively, but a comparable strength at failure (≈ 126 MPa) to the woven fabric with dry spun yarns. The same observation is made for the flexural properties. The crimp-free structure improves the stiffness as the fibres are all aligned along the axis while the fibres in the yarns are off-axis due to the twist. However, no improvement was seen for the strength, probably due to the fact the two weaves in question, low and medium-low twist twill, have a low crimp (1-2%), which is marginally higher than for the zero-crimp UD-based cross ply laminates. As the crimp value is low, the detrimental effect of crimp is not observed.

5.3.2.5 The sandwich-like effect

A thorough analysis of the Quasi-UD [0,90] and UD2 [0,90] laminates, shows that their flexural modulus E_1 is consistently higher than their tensile modulus E_1 for thermoset composites as shown in Figure 5-13. It is known that the lay-up sequence plays a more important role in the flexural properties than on tensile properties. Thus, if the stiffness of these laminates is controlled by the extreme 0^o layers of reinforcement, this leads to a sandwich-like effect leading to a high flexural stiffness [16, 17].

However, no difference is seen between the E_2 moduli which do not increase under flexural stress. In addition to plastic deformation and reorientation of the microfibrils, transverse compression damage may appear in the 90^o layer at higher strains (beyond the yield strain) [18]**.** This would cause a stronger non-linear behaviour during a bending test leading to a lower stiffness between 0.3-0.5% strain at the compression side.

Alternatively, Van Vuure et al. [19] have found that the longitudinal UD flax-epoxy composite compressive stiffness value is only 60% of the tensile one because of the micro-buckling of the technical fibres. This means that in bending a reduction in stiffness would be found due to fibres being loaded in compression. Furthermore, from the compression stress-strain curves reported in [19, 20], one can observe a strong non-linear behaviour of the compression beyond 0.3% strain where the E_2 in compression value decreases by 69% compared to E_1 (also in compression).

The sandwich-like phenomenon for E_1 is not observed for the UD1[0,90] laminate which has a lower flexural strength and modulus than the UD2 and Quasi-UD cross-ply laminates, but a similar tensile strength and modulus. It was previously mentioned that the UD1 flax had an epoxy sizing which may not be compatible with the epoxy used. The presence of this sizing may have led to weaker adhesion between the fibres and the matrix and thus the reduction in the stiffness and strength properties. Other factors could play a role in counteracting the sandwich and a deeper investigation is need to isolate all parameters.

The sandwich-like phenomenon was not observed at all for the flax-MAPP cross-ply composites. Most flax-MAPP composites tested in bending failed by global composite buckling on the compressive side of the sample. This effect may inhibit the sandwich-like phenomenon as the MAPP is not stiff enough to prevent fibre buckling.

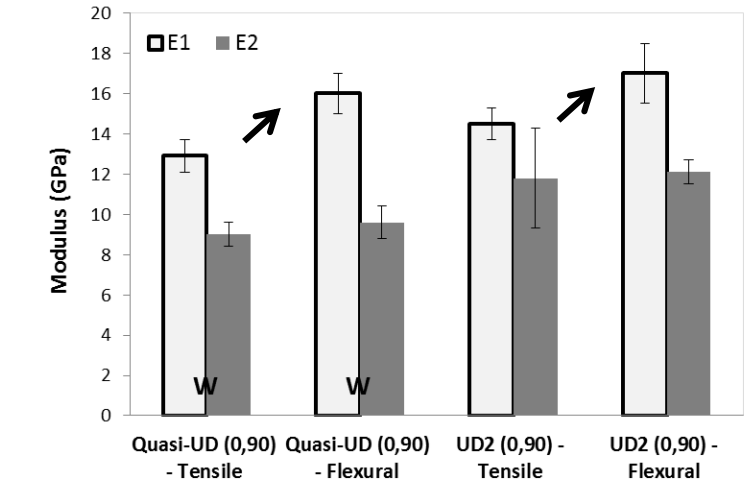

a)

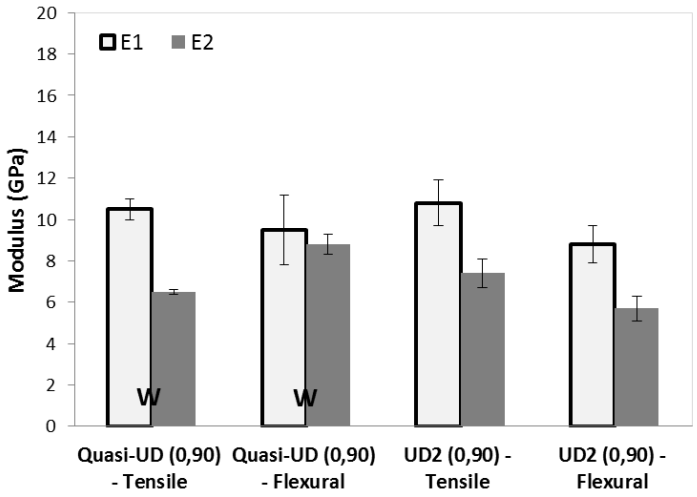

b)

Figure 5-13: Sandwich effect of the composites subjected to bending stress for a) epoxy and b) MAPP matrices**.** The "w" indicates the wet spun yarn-based composites.

5.3.2.6 The unidirectional laminates

The results obtained for the unidirectional composites made of the UD1 (epoxy sized or MAPP prepreg for UD1, UD2 was water-treated [21] and Quasi-UD (based on wet-spun yarns) reinforcement architectures outperform all the other configurations as expected. The first results on the yield point presented in section 3.2.2 showed that the onset of non-linearity starts earlier in UD composites. The parameters influencing this non-linearity, as presented in section 3.2.1, have the most direct influence on unidirectional laminates, because other possibly influencing parameters like twist and crimp are absent.

The fibres all being in the same direction for the UD1 and UD2 and with 90% of the fibre in 0^o direction for the Quasi-UD, it is possible to back-calculate the stiffness and strength of the constituting technical fibres using the rule of mixtures (ROM) equation below:

$$E_c = E_f V_f + E_m V_m \quad \text{(Eq. 5.3)}$$

$$\sigma_c = \sigma_f V_f + \sigma'_m V_m \quad \text{(Eq. 5.4)}$$

Where, E_f is the modulus of the fibre, E_m is the modulus of the matrix and V_f is the fibre volume fraction, σ_f is the strength of the fibre and σ'_m the stress in the matrix at the failure strain of the

composite which can be calculated assuming elastic deformation of the matrix: $\sigma'_m = E_m * \varepsilon_{u,c}$ (moduli are given in GPa, strengths in MPa). Eq. 4 is valid only when the fibres fail first, meaning that they have a lower failure strain than the matrix. For this reason, the matrix needs to have a sufficiently high ductility.

The results are reported in Table 5-3. The back-calculated "apparent" fibre stiffness E_{f1} were 55.2 GPa for UD1 and 62.5 GPa for UD2 for the epoxy matrix composites. For an assumed ('theoretical')stiffness of technical fibres of 65 GPa as reported in [1], this leads to an efficiency factor of 84% for UD1, 96% for UD2, where the efficiency factor is the ratio of measured value to theoretical value. For the MAPP combinations, an apparent E_{f1} of 53.4 GPa for UD2 was found. For the same reinforcement architectures, the composites with the MAPP matrix have a lower stiffness and an early yielding (see Table 5-3). This suggests that this MAPP matrix is too compliant to achieve an efficient stress transfer into the fibres. Thus, proper choice of matrix needs to be made in order to maximize the properties.

The Quasi-UD based composite is not composed of layers of straight flax fibres, but of highly twisted (20^o) yarns placed parallel to each other and connected by a small binding yarn; the high twist of the yarns explains the lower back-calculated "apparent" fibre stiffness . The theoretical models of Naik-Madhavan [22] and Rao-Farris [23] predict a back-calculated twisted yarn stiffness of 30 and 33 GPa respectively for a 20^o twist level and an assumed fibre stiffness of 65 GPa. If compared to the technical fibre properties, the composite performance reaches only 82% and 68% of the theoretical model for epoxy and MAPP composites respectively. This points out that the yarn twist has less effect in the epoxy-based than in the MAPP-based composites, which can be related to the matrix intrinsic properties as mentioned above.

		Quasi-UD	UD1	UD2
	Twist level in degrees ^{o}	20	0	0
Epoxy	Back-calculated fibre/yarn stiffness E1 (E_{f1}) in GPa	53.2	55.2	62.3
	Efficiency factor in %	82	84	96
	Back-calculated fibre/yarn strength in MPa	534	594	570
	Efficiency factor in %	67	74	71
MAPP	Back-calculated fibre/yarn stiffness E1 (E_{f1}) in GPa	43.8	-	53.4
	Efficiency factor in %	68		82
	Back-calculated fibre/yarn strength in MPa	498		446
	Efficiency factor in %	62		56

Table 5-3: The back-calculated tensile properties and efficiency factors of unidirectional composites.

5.3.3 Effect of crimp

When twisted yarns are used to produce woven textile reinforcements, during weaving, a strong crimp is created, because the yarns stay rounder than untwisted rovings during the further composite processing. This causes a second misalignment of the reinforcing (technical) fibres (the first being the twist) and thus increases stress concentrations in the composite under tension as well as local bending under compression loading. Even though there is a certain variation in crimp between the textiles, no clear observation of the crimp effect on the tensile properties of the woven fabrics was found.

On the other hand, the flexural properties show a clearer difference between the weaves and the UD non-crimped laminates. The crimp-free structure (Quasi-UD [0,90] and UD [0,90]

laminates) outperforms the woven laminate once combined into a thermoset or a thermoplastic composite. For example, when one compares between the plain woven fabric and the cross-ply configuration of the Quasi-UD (both with highly twisted wet spun yarn), an increase in strength and modulus is observed for the second. This may be attributed to the lower crimp of the Quasi-UD fabrics compared to the plain weave (0.4% vs 1.3% in weft -7.5 % in warp), which delays damage initiation by (micro-)buckling at the compressive side of the sample loaded in bending.

5.3.4 Strain at failure

The results presented in Appendix B show that the failure strain of the used matrices in this study decreased with the addition of the flax reinforcement, showcasing a brittle behaviour for flax-epoxy composites. For technical fibres (bundle of elementary fibres), the failure strain value reported in the literature is in the range of 1.5-2% [1]. Thus, the composite failure strain in this study intrinsically relates to the failure strain of the fibres. Furthermore, the fibre architecture was found to have an important effect on the strain to failure, which can be increased by 50-100% once the fibres are processed into woven fabrics as illustrated by the stress-strain curves in Figure 5-7.

The tensile strain to failure of the studied flax weave composites displays a higher elongation at break (≈1.8-2%) than the one usually found for glass fibre weaves (≈1.5%). The values found for unidirectional configurations (UD1, UD2) show an average tensile strain to failure of 1.19% for flax epoxy and 1.05% for flax-MAPP. The Quasi-UD fabric has higher strain values (1.51% and 1.91%) compared to UD due to the presence of the twisted yarns. This means that the fabric characteristics such as twist and crimp have a substantial positive effect on the strain at failure of the laminates, as supported by several studies [8, 12, 24]. In textiles, the twist is applied to a yarn to give it enough pulling strength for the weaving process. A highly twisted cord behaves like a coil spring; in contrast, a slightly twisted cord acts more like a rod [24]. During the final phase of a tensile test (at high strains near failure), the yarn will tend to untwist giving an extra elongation at the composite breaking point.

5.3.5 Statistical analysis

The observed variability in properties can be attributed to the variation in fibre characteristics such as the crop quality, extraction conditions, the refining steps (scutching, hackling, etc...). Other parameters on the composite level, such as variation in manufacturing and differences in fibre volume fraction can also be the cause of further variation. The quasi-static stiffness properties reported in this paper show that the flax composites are within the same range of variability (within one set of experiments) as the glass fibre based composites, showing a stiffness standard deviation of 0.5-2.5 GPa as reported by Zhou et al. [25].

To analyse if the woven and [0,90] laminated composites are statistically different in both tensile and flexural properties, a statistical ANOVA study was made using Tuckey's grouping method. The results of the analysis are reported in Table B-5 and Table B-6 in Appendix B. It has been found for most cases, the strength, failure strain and E-modulus for both epoxy and MAPP composites made of the UD2 [0,90] architecture are statistically different from the Quasi-UD [0,90] and woven fabrics within the 95% confidence level. The Quasi-UD[0,90], has a behaviour that is closer to the woven fabrics because of the crimp induced by the binding yarn and the high twist fibres in the spun yarns.

5.4 Evolution of the plastic deformation

In section 5.2, it was proposed to measure the E-modulus of flax composites in two zones, the first one in the linear elastic zone, E_1 between ε = 0-0.1%, and the second, after the yield, E_2

between ε = 0.3-0.5%. In order to visualize the moment were the elastic limit is reached and plastic deformation starts, a study of a gradual cyclic stress-strain behaviour of the material is carried on.

The elastic limit is defined as the highest stress a material can withstand without any quantifiable permanent strain and is determined using an incremental loading-unloading test procedure. The deformation in the elastic region is reversible and non-permanent, but once the limit is attained (at stress level higher than the yield stress), non-reversible permanent deformation occurs. If the sample is unloaded after this limit, the stress-strain curve follows its characteristic non-linear behaviour upon unloading and the curves shifts to the right compared to the original slope but never coming back to its initial position (ε = 0%). This kind of deformation is called residual strain (or cyclic creep when the loading/unloading cycle is repeated several times).

To determine the elastic limit of flax composites, five unidirectional flax-epoxy samples (UD2) were subjected to a load-controlled cyclic tensile stress. The strain was monitored with 50 mm extensometer with a maximum of 10% deformation. The samples had the same dimensions as the tensile tests and their average fibre volume fraction was 43 ± 0.5%. The loading-unloading strain rate was 4 s^{-1}.

Examples of the load-time increase as well as a representative stress-strain curve are shown in Figure 5-14. In order to avoid compressive stresses when the samples return to the zero position when unloading, the minimum load was set to be 100N. For the sake of clarity, only one typical curve is shown, but all samples behave similar. In the obtained curves, the modulus was calculated using the first 4 data points of the loading curve. The residual strains of each cycles were defined as the first point of the next loading curve. All results are shown in Table 5-4.

The appearance of a plastic deformation was observed after the third cycle, when the strain level goes above 0.16% and σ = 42 MPa as seen in Table 5-4. This validates the data found in section 5.2.2 where the yield point (elastic limit) for UD2 was defined as ε_y= 0.17 ± 0.02% once the σ_y= 45 ± 3 MPa stress is reached. In Figure 5-15, further increase of the residual failure strain is seen with increasing stress. This confirms the presence of plastic deformation in flax composites, showing the "irreversibility" of the deformation which is also observed for other natural fibre reinforced composite materials [26].

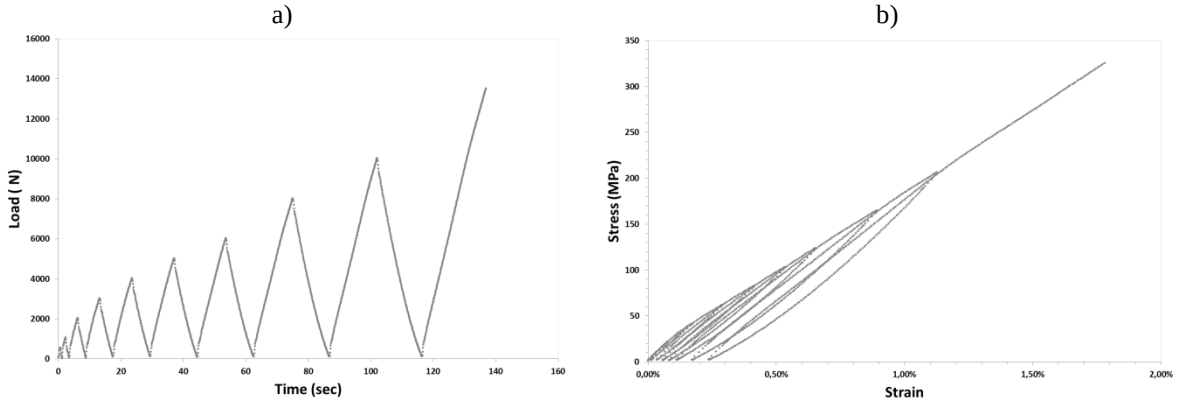

Figure 5-14: UD2 flax- epoxy composites subjected to a gradual increase in load (hysteresis): a) successive loading–unloading cycles with increasing load and b) the in-situ stress- strain response of the material showing an increase in plastic strain upon unloading in the early cycles.

Loading cycles	Average maximum applied stress σ (MPa)	Average maximum strain at maximum applied stress (%)	Average Modulus E (GPa)	Average residual strain after unloading (%)
0-500N	12 ± 1	0.04 ± 0.01	29.0 ± 0.2	0.00 ± 0
100N-1000N	22 ± 0	0.07 ± 0.02	29.0 ± 0.9	0.00 ± 0
100N-2000N	42 ± 1	0.16 ± 0.02	29.4 ± 0.5	0.01 ± 0
100N-3000N	62 ± 1	0.28 ± 0.03	29.1 ± 0.8	0.03 ± 0.01
100N-4000N	83 ± 1	0.40 ± 0.04	29.2 ± 1.1	0.06 ± 0.01
100N-5000N	103 ± 1	0.52 ± 0.05	29.6 ± 1.2	0.08 ± 0.01
100N-6000N	124 ± 2	0.64 ± 0.06	30.1 ± 1.1	0.11 ± 0.01
100N-8000N	165 ± 2	0.87 ± 0.07	30.3 ± 1.4	0.17 ± 0.01
100N-10000N	206 ± 3	1.10 ± 0.08	30.6 ± 1.4	0.23 ± 0.02
100N -Until failure	325 ± 41	-	31 ± 0.7	1.83 ± 0.10*

* Final failure strain

Table 5-4: Evolution of the modulus and residual strain after unloading for UD2 flax- epoxy composites subjected to the gradual load increase as described in Figure 5-14.

Shah et al. [26] proceeded to a similar study on UD flax-polyester composites. They have found that the plastic deformation starts at 0.17% tensile strain where a non-zero plastic strain of 0.016% was observed. A linear regression analysis between strain upon loading and plastic strain upon unloading showed that, in order to stay within the elastic limit, the tensile loading should remain below ε = 0.15%. Similarly to the previous authors, Hughes et al. [27] carried out a study on flax-polyester composites and found that the composite yielding occurred at ε =0.12%. It is a proof that the calculation of the elastic modulus E_1 between 0 and 0.1% strain and beyond the defined yield points for E_2 is appropriate.

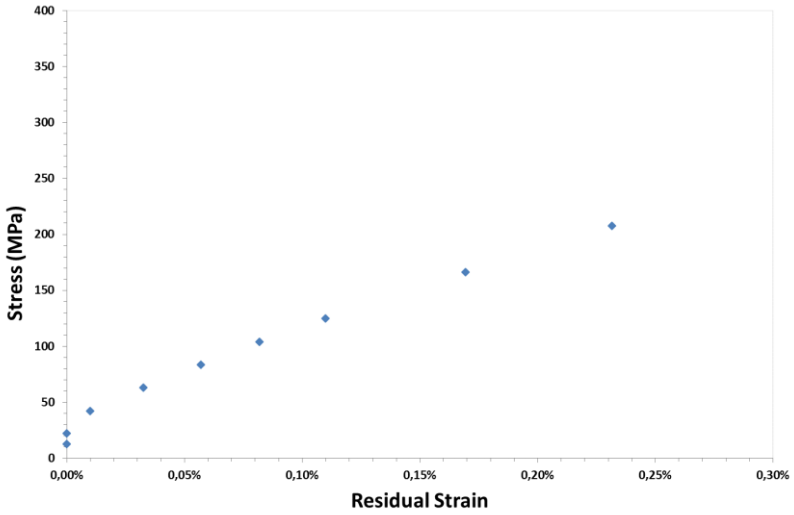

Figure 5-15: Residual strain increase with increasing stress. The last cycle is not included as it goes until failure of the specimen.

The stress-strain curve obtained after cyclic straining is different from that observed in monotonic straining as seen in Figure 5-16. Depending on the initial state of the material and the imposed testing conditions, the material can [28]:

- Cyclically harden/soften or;
- Be cyclically stable.

The mechanical properties of the studied flax samples under gradually increasing loading-unloading stress-strain curves vs a monotonic "one-shot" stress-strain curves, displayed some interesting results. First, it can be seen that the E-modulus seems to increase by 7% from 29.8 GPa in the first cycle to 31 GPa in the last cycle (see Table 5-4). This change is said to be related

to the microstructural changes and decrease of the microfibrillar angle. However, it is important to know if this small increase of the E-modulus depends upon the loading/unloading with a cyclic increase of the applied tensile stress or to the continued cycling during many cycles up to a constant stress level (low cycle fatigue, further explained in Appendix C). Although the modulus increase is low and statistically not significant, as seen in Figure 5-17 a, one can see that the gradual increase in stress has a positive effect of the strength and strain to failure properties.

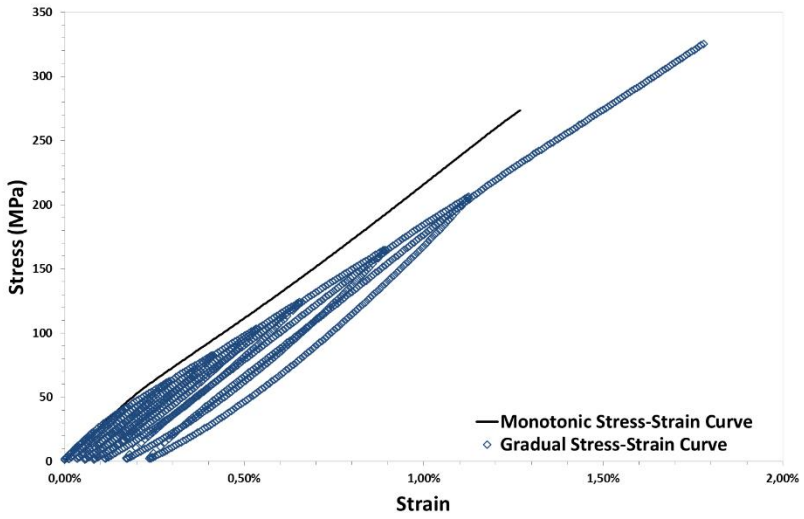

à

Figure 5-16: Typical curves for the monotonic and gradual stress-strain curves.

a) b)

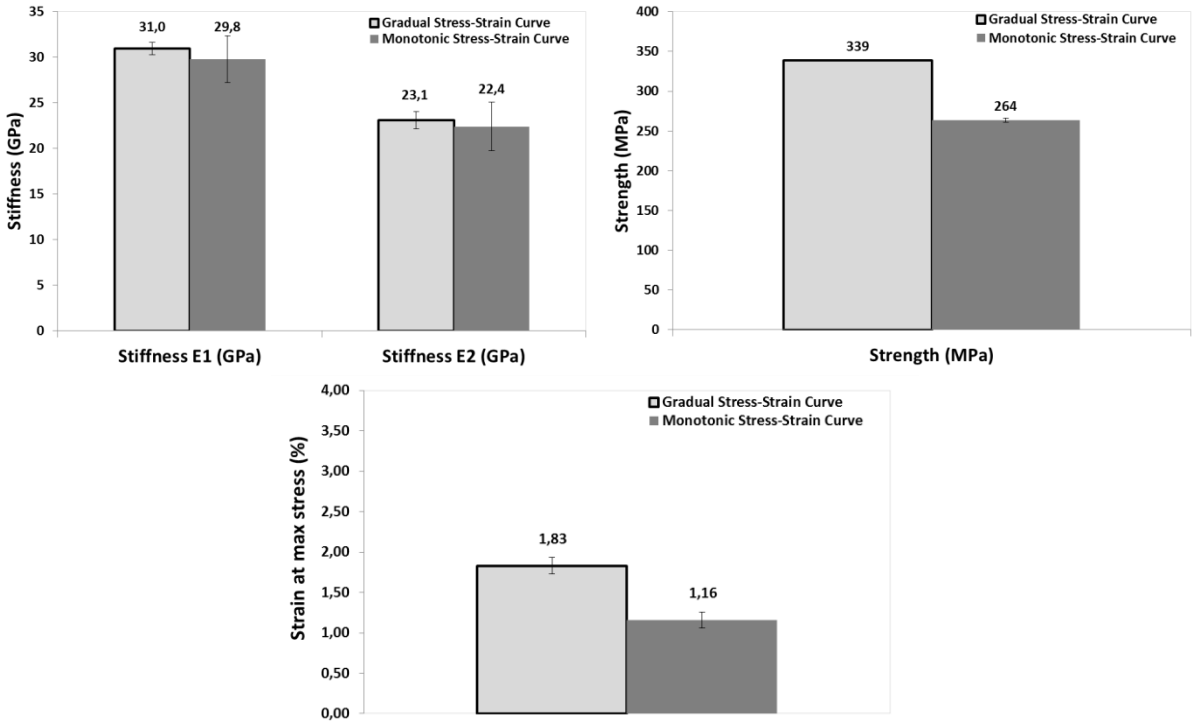

c)

Figure 5-17: Composite properties comparison between the gradual and monotonic stress-strain curve: a) stiffnesses E_1 and E_2 measured during the last cycle and b) the strength and c) strain at maximum stress.

For the strength, a 28% increase was observed in Figure 5-17 b. This could be linked to the increased orientation inside the elementary fibres as the microfibrils have time to fully orient in the loading direction. Since the test takes more time, this reorientation is more likely to happen under creep-like conditions than during the monotonic loading. Other strain hardening phenomenon (discussed in Section 5.2.1) may also be occurring and further investigation to unravel the underlying causes is needed.

A 64% increase in failure strain may be related to the gradual built-up, cycle-by-cycle, of plastic deformation as seen in Figure 5-17 c. This gradual plastic deformation is higher than the one obtained when the specimen is monotonically loaded because of the visco-plastic effect. Since the specimen is loaded during a longer time (125 sec vs 66 sec), a creep phenomenon occurs leading to higher failure strains.

5.5 Fractures profiles

The composite fracture surfaces presented in Figure 5-18 shows a brittle fracture behaviour, without major plastic deformation of the sample, for all the tested samples. The previous sections have confirmed the presence of some plastic deformation in the flax-epoxy composite. However, due to the low amount of permanent deformation occurring (< 0.5%, see Figure 5-15 in Section 5.4) compared to ductile composites it can be stated that the flax composite have a 'brittle' behaviour.

All the twill 2x2 fabrics showed a macroscopically brittle flat fracture surface due to the low strain to failure of the flax fibre, independently of the yarn type (wet or dry spun). For the random mat and woven fabrics, a similar brittle fracture was observed. For the UD and Quasi-UD, a fibre dominated failure can be seen with a "jagged" fracture surface, as well as longitudinal splitting extending to the full sample length. Overall, no signs of delamination were seen on the tested epoxy or MAPP samples. This may be related to the hypothetical high toughness of the flax fibres. This will be investigated and discussed in Chapter 7.

It has to be noted that for the flexural testing, all thermoset samples failed in tension (at the tensile side of the specimen) while the thermoplastic composites' main failure mode was buckling at the compressive side. This was due to the low load bearing capacity of the matrix and poor load transfer between the fibre and the matrix as mentioned previously in section 5.3.2.5.

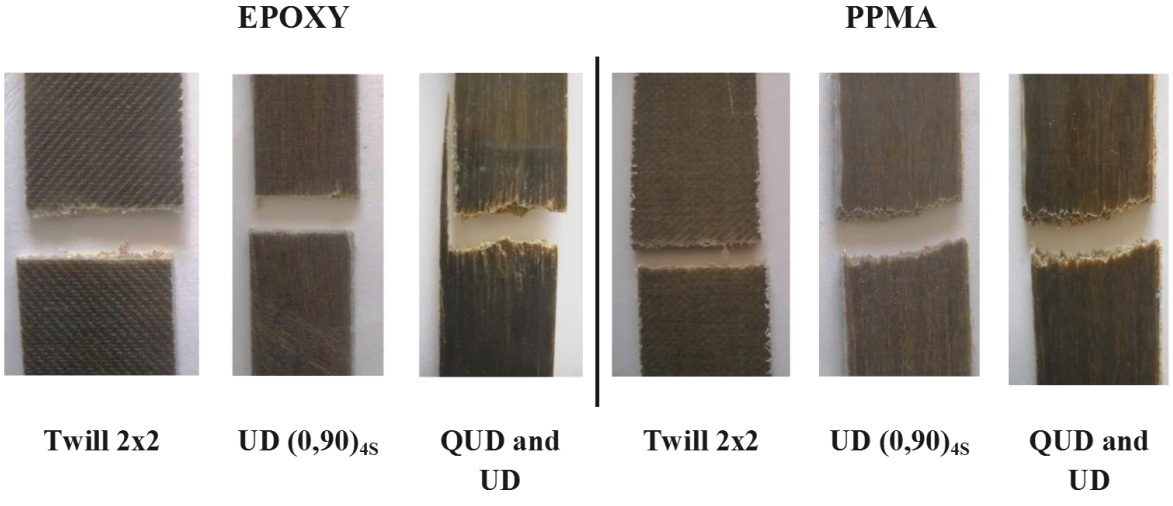

Figure 5-18: Tensile failure surface of selected flax-based composites.

5.6 Design with flax composites

The material properties are essential in the design process: starting from the basic concept and requirements of an application, where the designer looks at the widest possible selection of materials, it evolves into the detailed stage of the development where the selection of one or two materials is made [29]. In terms of design, lately a lot of attention has been given to sustainable and renewable materials. One of the main challenges though for natural fibres is to compete with synthetic fibres in terms of mechanical properties. Several tools for materials selection exist and one of the most used are the Ashby plots (see Figure 5-19). These allow a quick retrieval and comparison of the typical properties of a specific material during the product design stage and enable the substitution of a material for another with equivalent characteristics. The overall properties found in this study are added to the Ashby plot in Figure 5-19 in order to situate them in the engineering material spectrum. It can be seen that the flax-based composite may be able to compete with glass fibre reinforced composite (GFRP). Optimising the design of a composite part will, amongst others, aim at the best stiffness/strength ratio. The Ashby plot was created using the CES Edupack 2015 from Granta Design.

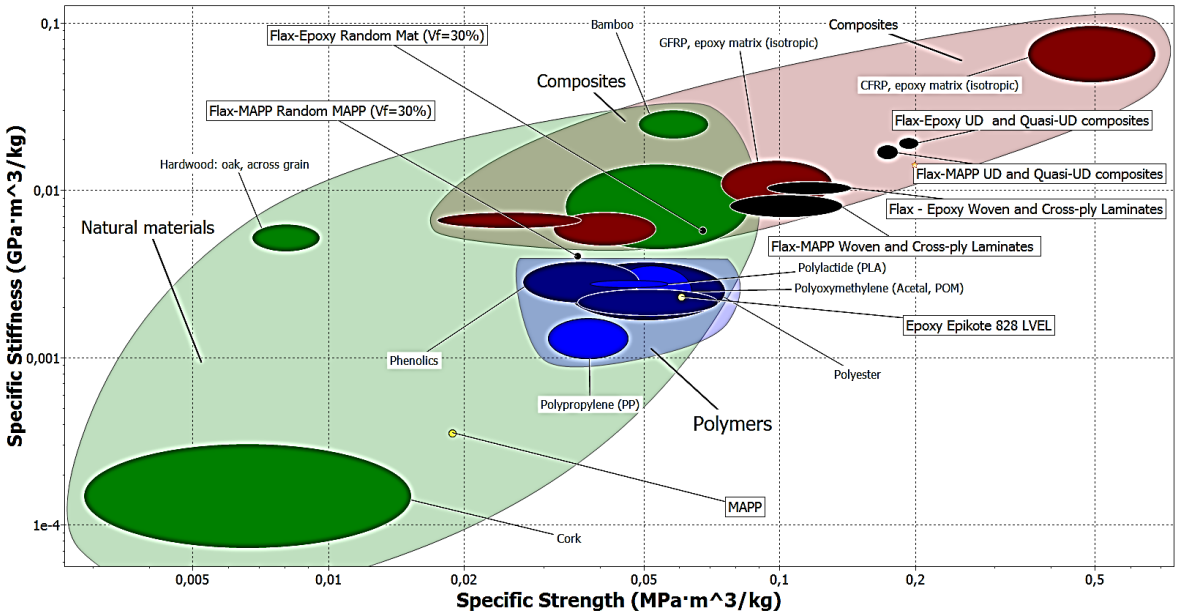

Figure 5-19: Ashby plot illustrating the specific stiffness vs the specific strength of various materials including the flax composites in this study (in black).

5.7 Conclusions

In this study, the effect of the textile geometry on the mechanical properties of flax-based composites was evaluated. The availability of such data in the literature is limited and sufficient information needs to be generated in order to establish correct guidelines to effectively control the textile geometry in order to optimize the composite properties for a specific application.

The flax composites have been found to have a characteristic non-linear behaviour. The stress-strain curves can be divided in three distinct regions, leading to the calculation of two stiffnesses, E_1 at low strains and E_2 at higher strains. The yield point, defined as the transition between the high and the lower tangent modulus domain, depends on the used reinforcement architecture: unidirectional composites and their cross-ply laminates will have an earlier yield than woven fabric reinforced composites. The mechanical properties of the unidirectional-based [0,90]s lay-ups are typically higher than for the weaves, which is expected because for the UD's the effect of crimp is practically non-existent.

The matrix type intrinsic properties have been found to have an important effect of the stiffness and strength properties of the final composite, with the epoxy matrix outperforming the MAPP. A larger drop in modulus for both tensile and flexural properties was also observed for MAPP composites. This is caused by the fact that the thermoplastic matrix is 10 time weaker than epoxy and creates less resistance to phenomena such as the untwisting and de-crimping occasioning in a further decrease of E_2. Furthermore, the random mat properties have been found to be the lowest due to the fact that the fibres are oriented in multiple directions and the fibre volume fraction was limited to 30%.

If wet spun yarns are used for the production of weaves, the increased fibrillation, caused by the dissolution of pectin in the water, allows a better impregnation by the polymer matrix inside the technical fibres. This may counteract the negative effects of twisting such as the reduction of the yarn permeability and the deviation of fibres from the yarn direction. The positive effect of low twist in one of the twill fabrics was not observed due to the fact that a binding yarn around the unidirectional flax fibres bundle induced a side crimp triggering a misalignment and decrease in mechanical properties in the longitudinal direction. The tensile and flexural properties of the woven fabric and the [0,90] cross-ply composites have exposed the effect of specific reinforcement geometry parameters such as crimp, twist, weave style.

The tensile samples displayed brittle fracture for both epoxy and MAPP, because the low failure strain of the fibres is predominant. In flexure, the flax-epoxy sample broke in tension while the flax-MAPP one failed through buckling on the compressive side, due to the low stiffness and yield strength of the MAPP.

Through the gradual stress-strain curve analysis of flax UD-epoxy composite, it was possible to identify the moment the plastic deformation starts, namely at a strain level 0.16%, corroborating the data obtained with the monotonic stress-strain curves. A small increase in stiffness (+7%) but a larger increase in strength (+28%) were observed following the gradual, cyclic build-up of stress. As the test is longer, the micro-fibrils have time to better orient in the load direction. A 65% increase was also observed for failure strain because of a more pronounced visco-plastic effect. Since the specimen is loaded during a longer time, the gradual build-up of plastic deformation will occur in the same way as in creep, leading to higher failure strains.

As of today, one of the major challenges for natural fibres is to compete with synthetic fibres, such as glass fibres, in terms of mechanical properties. By displaying the flexural and tensile results obtained in an Ashby plot, it was seen that flax composites have a comparable stiffness-strength combination as glass fibre composite. The stiffness-strength data obtained in this study highlight the potential of flax-based composites to be used in high performance applications.

References

[1] Verpoest I, Baets J, Van Acker J, Lilholt H, Mussig J, Hughes M, Baley C, et al. Flax and Hemp fibres: a natural solution for the composite industry. First Edition. In: Reux F, Verpoest I, editors. Paris, France. Prepared for JEC by the European Scientific Committee of CELC: JEC Group/CELC; 2012. ISBN 978-2-9526276-1-0.
[2] Charlet K, Baley C, Morvan C, Jernot JP, Gomina M, Bréard J. Characteristics of Hermès flax fibres as a function of their location in the stem and properties of the derived unidirectional composites. Composites Part A: Applied Science and Manufacturing. 2007;38(8):1912-21.
[3] Baley C. Analysis of the flax fibres tensile behaviour and analysis of the tensile stiffness increase. Composites Part A: Applied Science and Manufacturing. 2002;33(7):939-48.
[4] Silva FdA, Chawla N. Tensile behavior of high performance natural (sisal) fibers. Composites Science and Technology. 2008;68(15):3438-43.
[5] Thygesen LG. Quantification of dislocations in hemp fibers using acid hydrolysis and fiber segment length distributions. Journal of Materials Science. 2008;43(4):1311-7.

[6] Placet V, Cissé O, Boubakar ML. Nonlinear tensile behaviour of elementary hemp fibres. Part I: Investigation of the possible origins using repeated progressive loading with in situ microscopic observations. Composites Part A: Applied Science and Manufacturing. 2014;56:319-27.
[7] Alves Fidelis ME, Pereira TVC, Gomes OdFM, de Andrade Silva F, Toledo Filho RD. The effect of fiber morphology on the tensile strength of natural fibers. Journal of Materials Research and Technology. 2013;2(2):149-57.
[8] Liu Q, Hughes M. The fracture behaviour and toughness of woven flax fibre reinforced epoxy composites. Composites Part A: Applied Science and Manufacturing. 2008;39(10):1644-52.
[9] Bensadoun F, Verpoest I, Mussig J, Graupner N, Davies P, Gomina M, Kervoelen A, et al. Development and validation of an Impregnated Fibre Bundle Test for natural fibres, used as reinforcement in composites. Composite Part A. 2015.
[10] Coroller G, Lefeuvre A, Le Duigou A, Bourmaud A, Ausias G, Gaudry T, Baley C. Effect of flax fibres individualisation on tensile failure of flax/epoxy unidirectional composite. Composites Part A: Applied Science and Manufacturing. 2013;51(0):62-70.
[11] Trujillo E, Moesen M, Osorio Serna L, Van Vuure WA, Ivens J, Verpoest I. Weibull statistics of bamboo fibre bundles: methodology for tensile testing of natural fibres. 15th European Conference on Composite Materials. Venice, Italy:2012.
[12] Goutianos S, Peijs T, Nystrom B, Skrifvars M. Development of flax fibre based textile reinforcements for composite applications. Applied Composite Materials. 2006;13(4):199-215.
[13] Goutianos S, Peijs T. The optimisation of flax fibre yarns for the development of high-performance natural fibre composites. Advanced Composites Letters. 2003;12(6):237-41.
[14] Naik NK, Madhavan V. Twisted impregnated yarns: Elastic properties. The Journal of Strain Analysis for Engineering Design. 2000;35(2):83-91.
[15] Bensadoun F, Vallons KAM, Lessard LB, Verpoest I, Van Vuure AW. Fatigue behaviour assessment of flax-epoxy composites. Composites Part A: Applied Science and Manufacturing.
[16] Van Vuure A, Ivens J, Verpoest I. Mechanical properties of composite panels based on woven sandwich-fabric preforms. Composites Part A: Applied Science and Manufacturing. 2000;31(7):671-80.
[17] Munikenche Gowda T, Naidu A, Chhaya R. Some mechanical properties of untreated jute fabric-reinforced polyester composites. Composites Part A: Applied Science and Manufacturing. 1999;30(3):277-84.
[18] Yang B, Kozey V, Adanur S, Kumar S. Bending, compression, and shear behavior of woven glass fiber–epoxy composites. Composites Part B: Engineering. 2000;31(8):715-21.
[19] Van Vuure AW, Baets J, Wouters K, Hendrickx K. Compressive properties of natural fibre composites. Materials letters. 2015;149:138-40.
[20] Wouters K. Compressive properties of natural fibre reinforced composites,Master Thesis Leuven, KU Leuven; 2014.
[21] Decorme J, Duval A, Vanfleteren E, Vanfleteren F. Method for producing a continuous web of fibers comprising long natural fibers, and associated apparatus and web. Google Patents; 2012.
[22] Naik N, Madhavan V. Twisted impregnated yarns: elastic properties. The Journal of Strain Analysis for Engineering Design. 2000;35(2):83-91.
[23] Rao Y, Farris RJ. A modeling and experimental study of the influence of twist on the mechanical properties of high-performance fiber yarns. Journal of Applied Polymer Science. 2000;77(9):1938-49.
[24] Hockenberger A, Koral S. Effect of twist on the performance of tire cord yarns. Strain. 2004;2:3.
[25] Zhou G, Davies G. Characterization of thick glass woven roving/polyester laminates: 1. Tension, compression and shear. Composites. 1995;26(8):579-86.
[26] Shah DU, Schubel PJ, Clifford MJ, Licence P. The tensile behavior of off-axis loaded plant fiber composites: An insight on the nonlinear stress–strain response. Polymer Composites. 2012;33(9):1494-504.
[27] Hughes M, Carpenter J, Hill C. Deformation and fracture behaviour of flax fibre reinforced thermosetting polymer matrix composites. Journal of Materials Science. 2007;42(7):2499-511.
[28] Xiao X, Al-Hmouz I. Fatigue behavior of angle-ply AS4/PEEK Composites. Progress in durability analysis of composite systems Rotterdam. 1998:331-8.
[29] Ashby MF, Cebon D. Materials selection in mechanical design. Le Journal de Physique IV. 1993;3(C7):C7-1-C7-9.

Chapter 6
Modelling of the quasi-static mechanical properties

The internal geometry of textile reinforcements is known for having a significant influence on the mechanical properties of composites. Textile reinforcements in composites are usually anisotropic. Therefore, it is important to take into account all textile parameters (i.e. end picks and counts, crimp, linear density of yarns, twist angle, yarn mechanical properties, etc.), for an adequate description and further characterization of the mechanical properties of their composite materials.

This work aims to combine the textile features with the mechanical properties of the fibres and the matrix properties. This is done in order to predict the composite mechanical performance using several specialized modelling tools. The used methodology would be an easy tool for the industry to assess the potential of each combination while saving time and materials. The obtained data from micro-CT images and impregnated fibre bundle tests are used as input parameters into the Wisetex textile geometry modelling software to construct the 3D representation of the chosen fabric. The 3D model is implemented in the Lamtex software to produce the dry preform with the right amount of layers. The Lamtex preform is then combined with the matrix data in the Texcomp software to predict the stiffness performance of the flax-epoxy and flax-MAPP composites.

6.1 Determination of the yarn/fibre properties

Identification of the flax fibre mechanical properties has been receiving a lot of attention due to their growing use as reinforcement in composite materials in the sports and automotive industry [1-4]. The properties of the yarns used in textile production have a strong effect on the potential performance of the final textile and of the composite. The most commonly used methods to determine the mechanical properties of the fibres are the individual dry technical single fibre test (SFT) and the impregnated fibre bundle test (IFBT). In the latter, the properties of the technical fibres are back-calculated from the composite properties using micromechanical models, such as the rule of mixtures (ROM) [5-11].

According to the modified ISO 10618 test procedure used by Coroller et al.[12], Trujillo et al. [13], a set of impregnated unidirectional fibre bundles are manufactured and tested in tension along the fibre direction. After calculation of tensile moduli E_1 and E_2 of the unidirectional material, the fibre modulus and strength are back-calculated using the rule of mixtures, as previously mentioned in Chapter 4. Furthermore, in order to obtain reliable IFBT results, the fibres must be perfectly aligned with the longitudinal axis of the sample and the testing axis. A misalignment will introduce an error in the test results which leads to an underestimation of the properties if the ROM is used [14]. Even in glass or carbon fibre rovings, certain misalignment of fibres exist and may lead to lower properties [15-18].

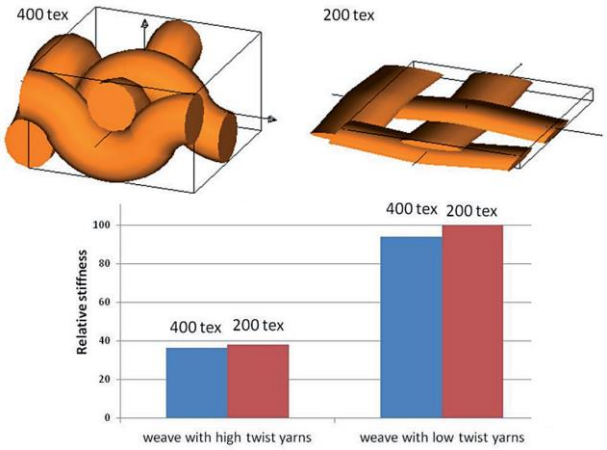

Figure 6-1: Influence of twist on the crimp angle and the relative stiffness of flax composites [19].

However, the IFBT can also be used to assess the 'effective' stiffness and strength of a reinforcement which is different from a non-twisted roving, like a twisted yarn (e.g. wet or dry spun flax) or a UD-roving which is strengthened by a wrapped-around fine yarn. This "effective" stiffness or strength is much more important for flax, than for glass or carbon fibres, as flax fibres are normally twisted into yarns for textile production. Highly twisted yarns have a negative effect on the composite properties (decrease in stiffness and strength), first because of a misorientation of the fibre inside the yarns, but also because highly twisted yarns are rounder and hence induce a higher crimp when used to produce woven fabrics (Figure 6-1).

6.1.1 Effect of twist on the effective modulus of the yarn

The impregnated fibre bundle test was used in this study to assess the "effective" properties of the flax yarns according to their degree of twist and its effect on the final composite. These data will serve as an input for the textile modelling in Wisetex. The samples were made with yarns manually withdrawn from four of the five studied woven architectures and of the quasi-UD and UD2 flax fabrics. It is has to be noted that the yarns are "uncrimped" with a flat iron while the twist is kept as is. In order to determine the back-calculated fibre or yarn properties, Eq. 4.5 and 4.6 have been applied separately to the data sets for each yarn or fibre bundle (UD). For the calculations, the fibre volume fractions of each specimen were individually measured. The results presented in Figure 6-2, clearly show the back-calculated fibre or yarn stiffnesses E_{f1} and E_{f2} , with as expected higher values for E_{f1} than for E_{f2}.

The E-modulus values, $E_{f,1}$ and $E_{f,2}$, have less scatter than the strength values. This was expected as the modulus is known to be less sensitive to imperfections at the fibre-matrix

interface, in the fibre or in the composite than the strength (if the defects are below a certain threshold [20, 21]). The first reason is because the stiffness is an average property (averaging out local defects and voids) measured at very low strain, whereas the strength is determined at much higher stress where the defects have more impact on the failure mechanisms.

The second reason is that the well-established linear rule of mixtures for continuous fibres, applies without considering the quality of the fibre–matrix adhesion. This is because interfacial stresses during longitudinal tensile tests of UD reinforced composites (with continuous fibres) do not occur. In practice, small misorientations or discontinuities in the UD composites could induce small interfacial shear stresses and shear stress in the matrix, leading to debonding. Moreover, as flax fibres are long (tens of centimetres) but not continuous, fibre ends might be present in an IFBT test sample, and debonds might also occur at their location. Hence, debonds at both the small misorientations and the fibre ends would have an impact on the stiffness and strength because the debonded fibres do not contribute anymore to the composite load bearing capacity. Thus, a minimum level of adhesion between fibre and matrix is required.

As expected from the composites results presented in Chapter 5, the average value for the stiffness E_{f2} at higher strains (0.3-0.5%), shown in Figure 6-2 a, is between 14-30% lower in comparison to the stiffness at very low strains (<0.1%) E_{f1}, which is in fact the real Young's modulus. The calculation of these two moduli was motivated by the presence of a non-linear region which starts between strains of 0.2 and 0.3% related to several possible phenomena exposed in Chapter 5 (section 5.2).

When the technical flax fibre contains a too large number of elementary fibres, the fibres in the core of the technical fibre are not in contact with the matrix which can lead to a decrease in the composite strength as not all fibres are loaded. In this case, the elementary fibres inside the technical fibre are bonded to their environment (= neighbouring elementary fibres) by only a weak pectin-rich layer, and shear deformation in these layers could occur. This reduces the contribution of these weakly bonded inner elementary fibres to the resistance of the total embedded technical fibre against deformation. Consequently, the measured and back-calculated stiffness of the embedded technical fibre decreases. This is not an "artefact", but an intrinsic behaviour of the technical fibre in a composite. The measured E_{f1} and $E_{f,2}$ are hence a correct representation of the behaviour of technical flax fibres in a composite. Therefore, it can be stated that the IFBT will provide a reliable, although average, fibre stiffness.

The variation in strength is higher than the stiffness variations, as seen in Figure 6-2b. This phenomenon was expected since the strength depends on the distribution of defect sizes and types. The results of the back-calculated "effective" yarn tensile strength in warp and weft directions reveal that the quality and twist angle of the yarns have an important effect on the composite properties. For example, the high twist plain weave compared to the medium-low twist twill yarn, display strengths of 309 MPa vs 443 MPa (warp yarns) and 343 MPa vs 451 MPa (weft yarns). Once these properties are translated into composites, it showcases that high quality yarns (e.g. Quasi-UD which has wet spun yarns and high quality fibres) help getting a higher quality composite. For the low twist twill, the lower properties of the composites are due to the lower yarn quality caused by an induced side crimp and small twist (3^o)along the length of the yarn (as exposed in section 5.3.2), creating a longitudinal misorientation in the testing direction.

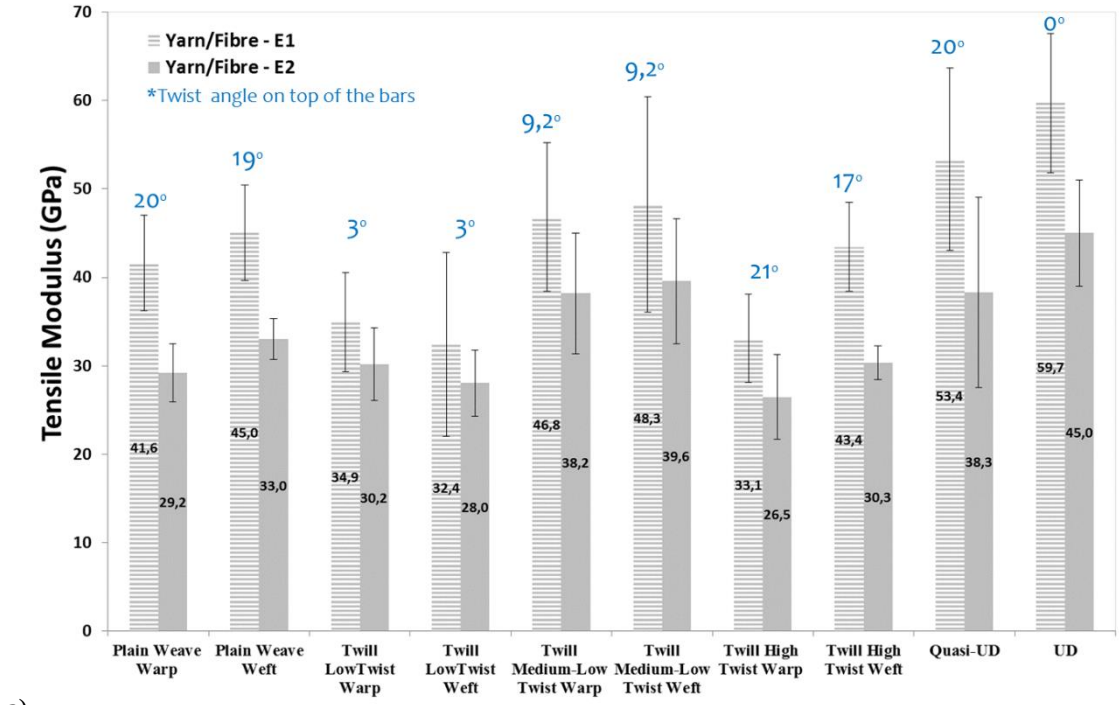

a)

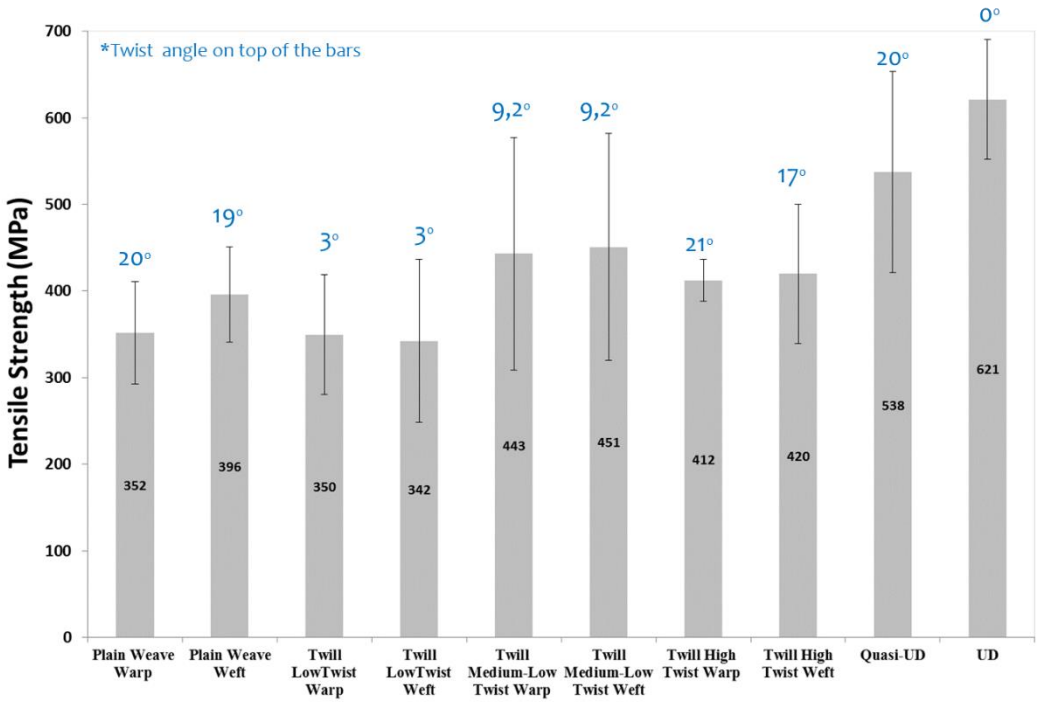

b)

Figure 6-2: Flax yarn's properties for a selection of three weaves, a quasi-UD and UD: a) E1 and E2 moduli and b) strength.

The large variation in flax yarn/fibre strength may also be attributed to the environmental conditions during growth, the crop quality, the flax fibre extracting conditions and the refining and the yarn production (wet or dry spinning, etc...). The yarns used to manufacture the IFBT samples were not identical since the textiles from which they were extracted came from different suppliers using different sourcing material. The yarns certainly had variation in retting and defects related to the hackling and further refining processes. As the same composite manufacturing method was used, the variation in strength observed cannot be related to a difference in composite production. However, a small misorientation of the

fibres or presence of voids could lead to a locally increased stress, and hence a decrease of the composite's longitudinal strength and its back-calculated fibre strength [22]. Finally, the fibres handling by the operator and the way the fibres are preserved before the composite manufacturing also play a role in the final properties of the composite. As the strength is a defect sensitive property, a big variation in strength suggests that even more attention should be paid to a fully randomised fibre selection and defect-free specimen preparation.

Goutianos et al. [23] have shown that very low twisted yarns, such as the low twist twill, exhibit a very low strength when tested in a dry state. This makes them unusable for certain processes such as textile manufacturing since high pulling strength is required during the process. Hence a minimum level of twist is required. On the other hand, when a twist is introduced, the strength properties of the composite can reduce drastically. There is a similar drop in strength for a twisted yarn and an off-axis composite, as both are caused by a loss of reinforcement orientation efficiency [23, 24]. Moreover, the presence of twist results in lower yarn permeability and an increase in the void content inside the yarns. Consequently, an optimum level of twist is needed for textile-based composites in order to ensure a good performance during textile processing and to limit the negative effect of fibre misalignment and low permeability, which is the case for the tested medium and low twist fabrics.

Highly twisted yarns may decrease permeability causing bad intra-yarn impregnation, leading to higher voids content and significant loss in orientation efficiency [23, 25]. At an average fibre volume fraction of 40%, it is believed that the impregnation of low and medium twist textiles would be more efficient and may help lowering the void content. The homogeneity of the fibre distribution will depend on the diameter of the yarn induced by the twist. The less twist, the better nesting and fibre distribution in the IFBT sample. A reduced permeability due to high yarn twist would lead to fast impregnation in-between the yarns and technical fibres, but to a slow infusion within the technical fibres (in-between the elementary fibres) which may produce micro-voids as seen in Figure 6-3 a. When the fibre volume fraction is high, the global permeability would be comparable to the yarn permeability [26, 27]. If the capillary pressure is larger within the yarn, it would allow a faster impregnation inside the yarn and technical fibres (see Figure 6-3 b) possibly creating macro-voids in between the yarns. Thus, the architecture type, as well as the yarn specifications, will have an effect on void content and location as well as the composite's mechanical performance. For example, the higher the twist, the less space in-between the yarn and the technical fibres inside the yarn.

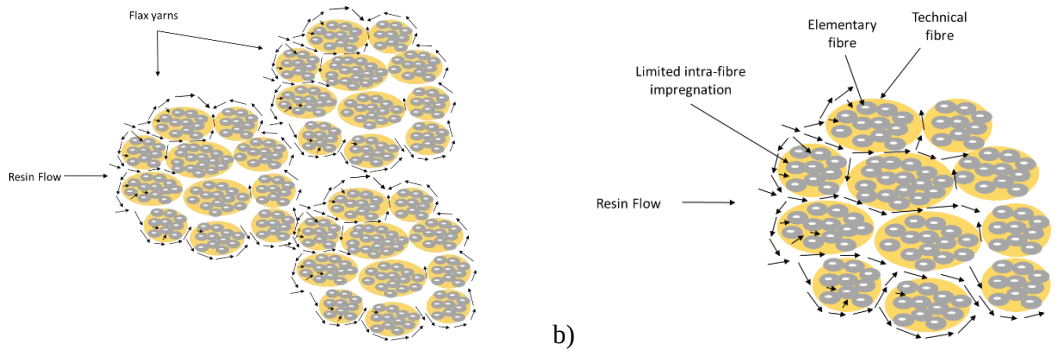

a) b)

Figure 6-3: a) Impregnation of the yarns in a flax composite with limited flow inside the yarns and technical fibres and b) resin flow inside of flax yarn.

6.1.2 Crimp vs un-crimped yarns

While making the IFBT samples, no special consideration was made to remove the crimp (undulation) of the yarns besides manual pulling when the fibres were inserted in the mould. Concerns were expressed regarding the potential small percentage of residual undulation of the yarns and its potential effect on the results. Thus, an additional IFBT test on fully un-crimped yarns was performed on plain weave warp and weft yarns where an iron was used to "flatten" the yarns and remove the crimp while keeping the twist. The results, shown in Table 6-1, clearly state that there is no difference in properties between the two used techniques and hence, it is possible to conclude that the results presented in Figure 6-2 are reliable even in the presence of low amount of crimp. A statistical analysis using the ANOVA method with the JMP software confirmed that the crimp vs non-crimped data are statistically equivalent with a 95% confidence level.

Yarns Type	Twist angle (º)	Crimp (%)	Tensile Modulus (GPa)		Tensile Strength σ (MPa)	Tensile Strain at max stress ε (%)
			E1	E2		
Plain Weave Warp	20	5,6	41.6 ± 5.4	29.2 ± 3.3	352 ± 59	1.20 ± 0.30
Plain Weave Weft	19	2,3	45 ± 5.4	33 ± 2.3	396 ± 55	1.10 ± 0.27
Plain Weave Warp - No Crimp	20	5,6	44.3 ± 5.1	31.8 ± 1.1	440 ± 106	1.30 ± 0.40
Plain Weave Weft - No Crimp	19	2,3	46.4 ± 4.4	32.8 ± 4.7	344 ± 46	1.00 ± 0.30

Table 6-1: Crimped versus un-crimped plain weave yarns; IFBT results.

6.1.3 Effect of twist angle – Comparison to theoretical models

The back calculated "effective" modulus and the strength were plotted as a function of the yarn twist and the results are presented in Figure 6-4 a-b. As expected and found by several authors [23, 25, 28, 29], a decrease in modulus was found with an increasing twist angle.

The evolution of the fibre bundle stiffnesses E_{f1} and E_{f2} were plotted against two models, predicting the stiffness of impregnated filament yarns as a function of the twist angle, by Rao-Farris [30] and Naik-Madhavan [31]. These models have been shown to predict accurately the longitudinal stiffness of UD composites reinforced with twisted yarns. Both models take into account the effect of fibre anisotropy, the fibre migration as well as micro-buckling. Nevertheless, both models require the input of several material constants, such as the Poisson's ratio and the shear moduli in all three directions. This makes them rather complex and to some extent less reliable as some values, i.e. the transverse modulus, are not yet experimentally determined on technical flax fibres. This issue does not arise for glass fibres since they are isotropic and the shear properties can be simply derived from the Young's modulus and Poisson's ratio.

Both models use the twist angle, defined as α, and the amount of twist is designated in turns per meters (TPM) in Eq. 6-1 below:

$$\tan \alpha = \frac{2\pi r}{h} \qquad \text{Eq. 6-1}$$

where r is the radius of the yarn and 1/h is the number of turns per meter [32].

The IFBT data from the tested yarns all are in line with both models as seen in Figure 6-4 a. As anticipated, the low twist twill lays below the prediction, due to the side crimp which lead to the similar performance as highly twisted yarn (which is not taken into account in these models). However, the quasi-UD yarn (high twist, 20º) overperformed according to the predictions. This could be due to the higher quality of fibre used in the wet spinning

process. This higher quality could be caused by the choice of a certain flax variety, a better crop and/or refining process. Glass fibre benchmark samples were produced in order to confirm the used technique is reliable. The E-modulus data obtained for glass fibres were 70.8 GPa and 71.3 GPa for E1 and E2 respectively and this corroborates data from literature (≈ 70 GPa) [19, 33, 34].

Baets et al. [28, 35] studied the effect of increasing twist, (obtained by ring-spinning) but originating from the same flax rovings, on the tensile modulus of flax-epoxy composites, and the experimental data matched the ones predicted by the models [30, 31]. On the other hand, Rask et al. [36] found no direct correlation between the amount of twist and the decreasing tensile properties. This might be due to the fact that the yarns were wrap-spun instead of ring-spun. Modelling the yarn's twist effect on stiffness is critical to visualise the reduction in properties when twisted yarns are used in woven reinforcements.

For the strength data in Figure 6-4 b, a linear correlation between the strength of the wet spun yarn and the twist was found. Two outlying data points were found for the quasi-UD (wet spun and high quality fibres) and the low twist twill (wrap spun, crimped yarns). They do not fit within the linear correlation because of their intrinsic specificities (high flax quality and side crimp in the warp yarn).

As of today, there are no existing models that accurately predict the effect of yarn twist on the strength. Studies from Ma et al. [37] and Shah et al. [25] have attempted to do so for sisal and flax fibres. However, the model of Ma et al.[37] did not account for the structure-property relationships in a twisted staple fibre yarn and its potential effect on composite tensile strength. The Shah et al. [25]' mathematical model, based on the rule of mixtures, the idealised twisted structure of a yarn and the Krenchel orientation efficiency factor was used to predict the influence of yarn twist on the composite strength. They have found that the model was in strong agreement with the experimental data taken from literature [23, 28].

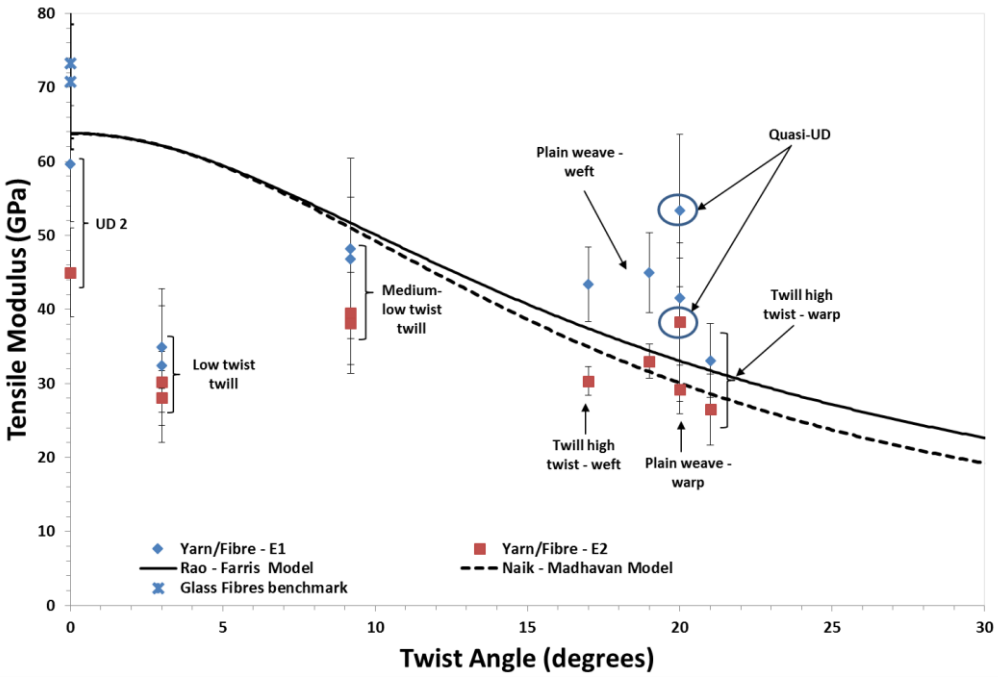

a)

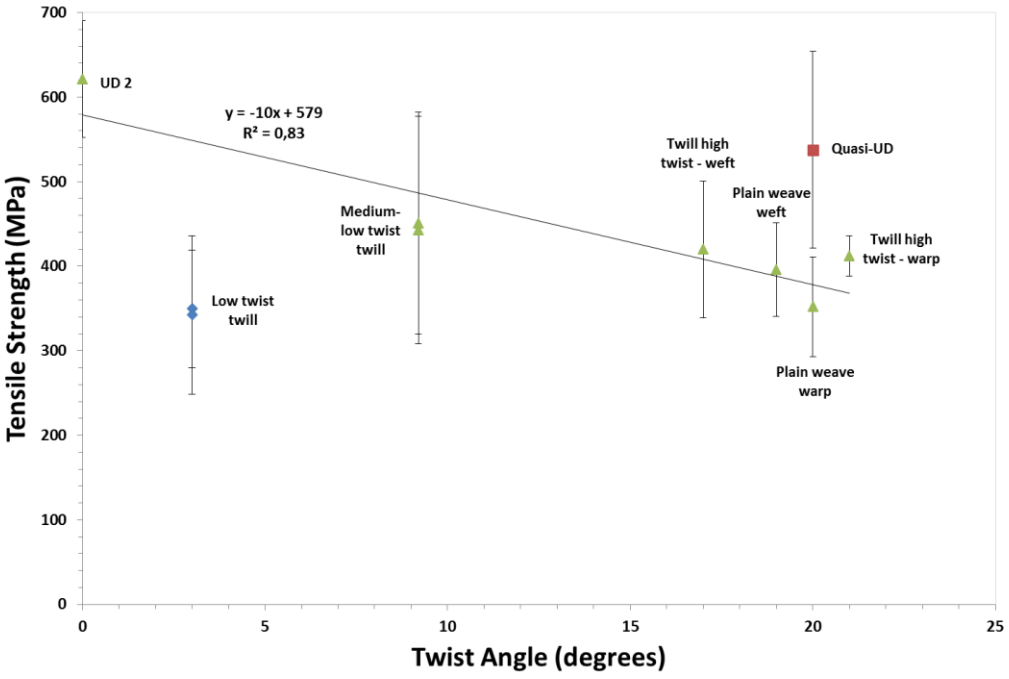

b)

Figure 6-4: a) Modelling of the stiffness degradation with increasing twist angle and b) linear correlation of the wet spun yarn strength properties according to the twist angle.

6.2 Composite properties prediction

Modelling tools such as Nastran, Abaqus and Texcomp are nowadays very often used to rapidly assess the potential performance of various material combinations. This also helps to avoid lengthy and costly trial and error experimental work. There are two different approaches to composite modelling. The first one consists of the construction of an ideal and virtual 3D geometrical model for the reinforcement, which does not yet exist, allowing its properties prediction before manufacturing [38]. In the second approach, the material is modelled on the basis of experimental geometrical data acquired after manufacturing. The observations on the internal geometry are usually carried out by using optical microscopy, C-scan, SEM or X-ray computed tomography. The latter techniques provide the most accurate data set that can be used for modelling. The X-ray computed tomography (or µ-CT) is used to scan the manufactured composites and to extract the internal textile structure after consolidation (see Chapter 4). The µ-CT is a non-destructive technique which uses attenuation of X-ray radiation in an object to reconstruct its internal three-dimensional structure.

Nowadays, industrial µ-CT is mainly used for quality control, such as the estimation of porosity and detection of defects. Resolution of µ-CT images can reach the value of 1 µm in terms of the image pixel size, which makes it a convenient alternative for microscopy in materials research. The data extraction process includes either a manual or semi-manual image processing to measure the various parameters of the reinforcement (yarn diameter, shape, end picks and counts, etc.). Using this information, a precise 3D model of the reinforcement can be made and can be used in modelling software to combine it to a specific matrix to calculate its performance.

In the next section, the properties prediction of some of the studied flax-epoxy and Flax-MAPP composites will be made with the help of the micro-CT images and Wisetex, Lamtex and Texcomp software developed by Lomov et al. [38-42] at the KU Leuven. The dataset used for the input parameters is extracted from the µ-CT images of the composites.

6.2.1 Extraction of the internal geometry data and modelling of the reinforcements

In order to run accurately and reproduce the textile structure in the Wisetex Software, data on the yarn cross-sectional shape, linear density, end picks and counts, twist, crimp and mechanical properties need to be defined using optical microscopy and μ-CT techniques.

The yarn elliptical cross-section diameters, D1 and D2, and the yarn crimp (see definition in Chapter 4 section 4.1.3) in the composite were quantified using ImageJ software since during the compression in manufacturing, the crimp of the dry textile changes. The results are presented in Table 6-2. The areal density, twist angles, yarn linear density, the preform lay-ups as well as the end picks and counts are presented in Table 4-1 in Chapter 4.

	D1 (mm)	D2 (mm)	Ellipticity D2/D1*	Yarn linear density (Tex)	Crimp (%)
Plain weave – Warp	0.43 ± 0.05	0.32 ± 0.05	0.74	105	13
Plain weave – Weft	0.65 ± 0.08	0.3 ± 0.04	0.46	147	1.9
Low Twist Twill – Warp and Weft	0.98 ± 0.09	0.31 ± 0.03	0.32	239/241	2-2.2
Medium Low Twist Twill - Warp and Weft	0.46 ± 0.04	0.21 ± 0.04	0.46	68	1
High Twist Twill -Warp	0.27 ± 0.02	0.19 ± 0.02	0.7	31	6,6
High Twist Twill - Weft	0.17 ± 0.03	0.13 ± 0.02	0.77	27	0.5

* A value of 1 is equivalent to a circle.

Table 6-2: Wisetex yarn input parameters for the textile modelling.

The use of a twisted yarn leads to an elliptical shape. The variation of the diameters D1 over D2 gives an idea of how close to a circle the ellipse is, where a ratio of 1 is equal to a circle. Furthermore, the higher the yarn's *Tex* and elliptical shape ratio (when D2 is measured in the thickness direction of the textile as done in this work), the higher the crimp will be and this will have a direct negative effect on the composite properties [35]. A higher crimp leads, of course, to a lower stiffness because of a higher out-of-plane misorientation of the yarns. Lastly, the "ellipticity" of a yarn also affects its ability to nest once compressed. This is opposite to the very flat glass and carbon rovings where the crimp is drastically reduced and the nesting is maximized.

The simulated thickness of the laminate and the fibre volume fraction were similar to the value obtained experimentally, with the thickness around 2 mm as seen in Table 6-3. As some variation of the V_f is expected, the modelled data was also normalized to a $V_{f=}$ 40% just like the experimental data in Chapter 5. The 2D and 3D representation of the textiles reproduced in Wisetex can be seen in Table 6-4 with the corresponding μ-CT images used for data extraction, as well as their visual aspect.

Experimental thickness	Flax-epoxy (mm)	Flax-MAPP (mm)
Plain weave	2.09 ± 0.01	1.87 ± 0.03
Low Twist Twill	2.09 ± 0.02	2.16 ± 0.01
Medium Low Twist Twill	2.02 ± 0.03	1.89 ± 0.04
High Twist Twill - Weft	1.97 ± 0.01	1.91 ± 0.02

Table 6-3: Experimental composite thickness for flax-epoxy and flax-MAPP composites.

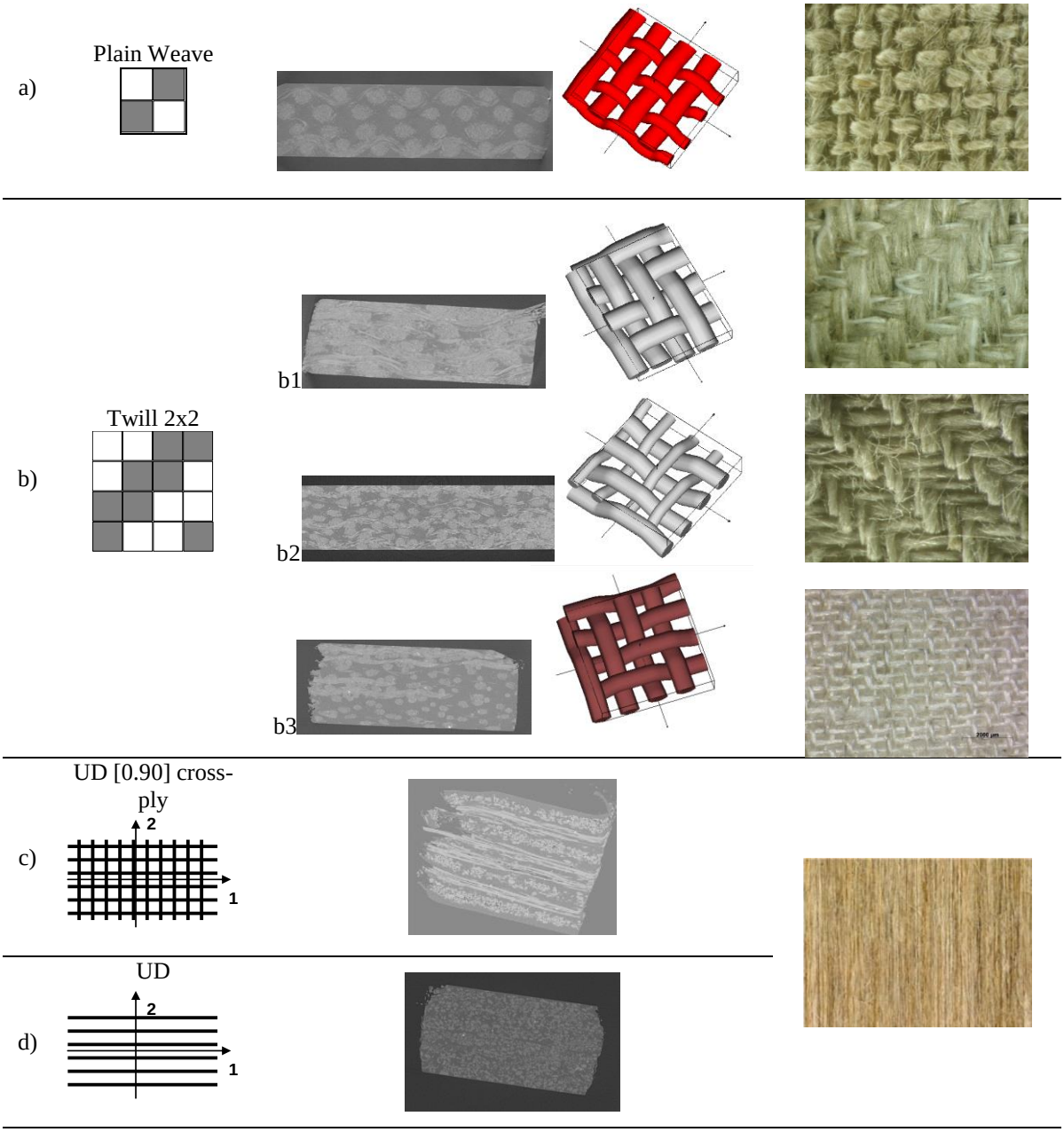

Table 6-4: 2D and 3D representations of the modelled architectures, their micro-CT image and their visual appearance of: a) plain weave, b) twill 2x2: b1: low twist twill, b2: medium-low twist twill and b3: high twist twill, c) UD2 [0,90] and d) UD2. The 2D representations are from Chapter 3 in [19].

6.2.2 Texcomp Modelling results

Once the textile model for one layer is constructed in Wisetex, the textile layer is transferred to the Lamtex software to create a dry preform with the right amount of layers and maximized nesting. The purpose is to reach the targeted thickness of 2mm and V_f of 40%. An example of such preform is shown in Figure 6-5.

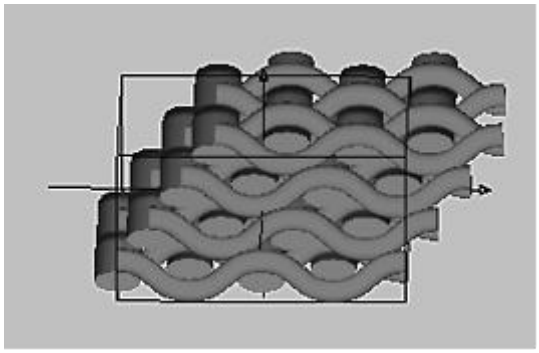

Figure 6-5: Example of nesting for the four layers plain weave preform.

This preform is then used in the Texcomp software to combine it with the epoxy or MAPP matrix in order to predict the properties of the composite. The simulation includes the textile geometry and the **"**effective" mechanical properties of the yarns (as discussed in section 6.1) and fibre volume fraction inside the reinforcement, which is obtained from Lamtex. These data, combined with the matrix properties, are then transformed into local properties of the impregnated yarns, using the Mori-Tanaka algorithm [38, 39, 43].

Texcomp models calculate the properties using the method of inclusions based on Eshelby's transformation concepts. It also uses the short fibre analogy to describe the mechanical behaviour of the curved yarn segments (see [42, 44] for more details). The calculations were made with the following fibre and matrix data assumptions:

- Flax fibre/yarns properties: longitudinal modulus of the yarns, $E_{f,L}$, is derived from IFBT testing (see section 6.1). The transverse modulus of the fibre, $E_{f,T}$, is back-calculated using the Chamis formula with the transverse tensile properties of a UD flax-epoxy of 4.1 ± 0.4 GPa. The back-calculated of $E_{f,T}$ is 6 GPa. The methodology is further explained in Appendix D;
- Flax yarn's Poisson coefficient ν = 0.25 in both longitudinal and transverse direction of the composite [14];
- Epoxy: E_m = 2.70 GPa, Poisson coefficient ν= 0.4;
- MAPP: E_m = 0.342 GPa, Poisson coefficient ν= 0.42;

The flax fibres' shear modulus, $G_{f,}$ was determined using data from the literature and back-calculated from the composite properties using the reverse Chamis equation (see Appendix D for calculation details). The value used in Wisetex is G_f = 4.6 GPa for the flax fibres and $G_{m,epoxy}$ = 1 GPa and $G_{m,MAPP}$ = 0.15 GPa.

Table 6-5 presents the results of the predicted stiffness of the four chosen flax textiles composites with epoxy or MAPP matrix. These values are theoretical and calculated using the above mentioned modelling method. These stiffness values of the four woven composites are further compared to the UD and [0,90] UD cross-ply composites (bottom row lines in Table 6-5), as these do not have any crimp. The properties of the UD and the UD-cross-ply were calculated using the *MicroMechanics* software using Chamis' micromechanical model (see Appendix D for more details).

It can be seen that the modelled composites stiffnesses are comparable to the experimental values, if the difference in the calculated fibre volume fraction is taken into account (for the experimental values, all are normalised to 40%). The UD composite with a V_f = 40 % of flax fibres in an epoxy matrix reaches the highest stiffness, with a predicted value of 26.8 GPa and an experimental value of 26.6 GPa in the fibre direction. The UD [0,90]

cross-ply has a higher experimental value for the flax/epoxy than predicted by the MicroMechanics software. This is because the rule of mixtures does not account for the additional stiffness provided in transverse direction, thus underestimating the experimental longitudinal properties.

For the flax-MAPP UD composites, the MicroMechanics software predicts higher properties, which is expected. The experimental data obtained for flax-MAPP is highly affected by the early yielding of the matrix which may lead to an underestimation of the modulus. It has to be noted that a cross-ply laminate composed of UD layers has zero crimp, thus the composite should have the same stiffness in both 0° and 90° directions for both flax/epoxy and flax-MAPP combinations.

Architectures	Wisetex/Lamtex/Texcomp Predicted values at V_f=4 0%		Experimental values at V_f=40%	
	Flax- epoxy	Flax-MAPP	Flax-epoxy	Flax-MAPP
Plain weave	11.9	9.4	12.6 ± 0.4	-
Low Twist Twill	11.2	8.7	12.8 ± 0.4	10.2 ± 0.3
Medium-Low Twist Twill	11.8	9.8	12.9 ± 0.9	9.2 ± 0.5
High Twist Twill	11.8	8.4	12.2 ± 0.8	8.1 ± 0.8
UD2 [0,90]*	13.4	12.6	14.5 ± 0.8	10.8 ± 1.1
UD2*	26.8	25.1	26.6 ± 2.3	21.5 ± 3.6

* Calculated with the Micromechanics software in longitudinal direction[1].

Table 6-5: Modelling of the experimental modulus results for flax-epoxy and flax-MAPP composites (GPa).

The effect of the crimp is well visible when the UD cross-ply laminate modulus is compared to the woven flax composites. Even with a low value of crimp, like the one for the Medium-Low Twist Twill (crimp ≈ 1%), the predicted stiffness decreases by ≈10% in comparison to the UD cross-ply. Similar effect of crimp is seen for the high twist twill (crimp is 6.6 and 0.5% in warp and weft direction) and the plain weave (crimp equals to 13.9 and 1.9% in warp and weft direction) fabrics, where the stiffness also decreases within the same range.

Overall, it can be said that the predicted modulus values are close to the experimental ones. At similar fibre volume fraction, the difference between the modelled and experimental properties is around than 10%. Combining these three modelling tools, Wisetex-Lamtex-Texcomp, will be useful for designers who would like to have an estimate of the potential performance of a fibre-matrix combination without experimentation.

6.3 Conclusions

This study aimed to theoretically predict the modulus of various flax architectures and matrix combinations investigated in Chapter 5. With this purpose, the "effective" properties of the yarns composing the textiles and the investigation of the internal geometry (i.e. yarn diameter, end picks and counts, percentage of crimp) were essential as input parameters.

First, the applicability and the reliability of the IFBT technique to determine the flax fibres/yarns properties back-calculated from the composite properties were investigated. Furthermore, the IFBT was used to assess the effect of twist on the stiffness. The results showed a strong correlation between the stiffness and the twist (stiffness ↓ with ↑ twist

[1] https://www.mtm.kuleuven.be/Onderzoek/Composites/software/micromechanical_software

angle). Furthermore, the quality of the yarn is an important feature to take into account. For example, the wet spun quasi-UD yarn performs better than expected by the proposed theoretical models because of its better fibre preparation and its wet spinning technique that leads to a higher flax quality has it helps fibrillating the fibres (thanks to the partial dissolution of the pectin) and potentially improve the fibre/yarn wetting.

On the other hand, the back-calculated strength data show higher differences in standard deviation than the stiffness values. The strength values are more sensitive to defects, fibre misorientation and distribution, as well as to the presence of voids within the composite, whereas the stiffness is an average property where small defects are averaged out and have much less impact. This highlights the importance of having a good and reliable sample preparation.

Furthermore, a linear relation between the twist angle and the strength properties is found. However, where the studied yarns had geometrical or fibre type specificities like the quasi-UD or low twist twill yarns, they did not correlate with the linear regression. The IFBT method was found suitable to assess the effective stiffness and strength of flax yarns, as they behave in a composite. These data could then be used to model the woven flax composites and predict their performance according to the yarn intrinsic properties.

The prediction of the flax composite properties, taking into account their yarn features and internal geometry once in the laminate, was carried out. Micro-CT, used to extract the yarn diameter and the crimp present in the laminates in warp and weft direction, was combined with Wisetex-Lamtex-Texcomp modelling tools. These data and the yarn properties were added within the Wisetex software to construct the 3D models of the four chosen textile composites. The textile model was then transferred to Lamtex to create the preform stacking, before proceeding to the calculation of the properties in Texcomp. The effective moduli obtained with the software calculations were found to be comparable to the experimental results with variations around 10%.

References

[1] Studio WD. Sustainable Design? http://www.waarmakers.nl/projects/be-e#sustainable-design
[2] Joseph S. Innovative and Green: Aparte Studio's Katra Chair. 2011. http://media.designerpages.com/3rings/2011/12/29/innovative-and-green-aparte-studios-katra-chair/
[3] Caperlan. CAPERLAN BLYSS DEEP TEAM 5" FLAX jig fishing rod. http://www.caperlan.co.uk/blyss-deep-team-5-flax-jig-fishing-rod-id_8164177-reviews
[4] Pil L, Bensadoun F, Pariset J, Verpoest I. Why are designers fascinated by flax and hemp fibre composites? Composites Part A: Applied Science and Manufacturing.
[5] Baley C, Le Duigou A, Bourmaud A, Davies P. Influence of drying on the mechanical behaviour of flax fibres and their unidirectional composites. Compos Part a-Appl S. 2012;43(8):1226-33.
[6] Baley C, Perrot Y, Busnel F, Guezenoc H, Davies P. Transverse tensile behaviour of unidirectional plies reinforced with flax fibres. Mater Lett. 2006;60(24):2984-7.
[7] Charlet K, Beakou A. Mechanical characterization and modeling of interfacial lamella within a flax bundle. Procedia Engineer. 2011;10.
[8] Charlet K, Eve S, Jernot JP, Gomina M, Breard J. Tensile deformation of a flax fiber. Mesomechanics 2009. 2009;1(1):233-6.
[9] Modniks J, Joffe R, Andersons J. Model of the mechanical response of short flax fiber reinforced polymer matrix composites. Procedia Engineer. 2011;10.
[10] Sparnins E, Modniks J, Andersons J. Experimental Study of the Mechanical Properties of Unidirectional Flax Fiber Composite. Icem15: 15th International Conference on Experimental Mechanics. 2012.
[11] Sparnins E, Nystrom B, Andersons J. Interfacial shear strength of flax fibers in thermoset resins evaluated via tensile tests of UD composites. Int J Adhes Adhes. 2012;36:39-43.
[12] Coroller G, Lefeuvre A, Le Duigou A, Bourmaud A, Ausias G, Gaudry T, Baley C. Effect of flax fibres individualisation on tensile failure of flax/epoxy unidirectional composite. Composites Part A: Applied Science and Manufacturing. 2013;51(0):62-70.

[13] Trujillo E, Moesen M, Osorio L, Van Vuure A, Ivens J, Verpoest I. Bamboo fibres for reinforcement in composite materials: Strength Weibull analysis. Composites Part A: Applied Science and Manufacturing. 2014;61:115-25.
[14] Lomov SV, Baets J. Architecture of textile reinforcements and properties of composites. status: published. 2012.
[15] Barwick SC, Papathanasiou TD. Identification of fiber misalignment in continuous fiber composites. Polym Composite. 2003;24(3):475-86.
[16] Kratmann KK, Sutcliffe MPF, Lilleheden LT, Pyrz R, Thomsen OT. A novel image analysis procedure for measuring fibre misalignment in unidirectional fibre composites. Compos Sci Technol. 2009;69(2):228-38.
[17] Pinho ST, Iannucci L, Robinson P. Physically based failure models and criteria for laminated fibre-reinforced composites with emphasis on fibre kinking. Part II: FE implementation. Compos Part a-Appl S. 2006;37(5):766-77.
[18] Pinho ST, Iannucci L, Robinson P. Physically-based failure models and criteria for laminated fibre-reinforced composites with emphasis on fibre kinking: Part I: Development. Compos Part a-Appl S. 2006;37(1):63-73.
[19] Verpoest I, Baets J, Van Acker J, Lilholt H, Mussig J, Hughes M, Baley C, et al. Flax and Hemp fibres: a natural solution for the composite industry. First Edition. In: Reux F, Verpoest I, editors. Paris, France. Prepared for JEC by the European Scientific Committee of CELC: JEC Group/CELC; 2012. ISBN 978-2-9526276-1-0.
[20] Summerscales J. Manufacturing defects in fibre-reinforced plastics composites. INSIGHT-WIGSTON THEN NORTHAMPTON-. 1994;36:936-.
[21] Huang H, Talreja R. Effects of void geometry on elastic properties of unidirectional fiber reinforced composites. Composites Science and Technology. 2005;65(13):1964-81.
[22] Berthelot JM. Effect of fibre misalignment on the elastic properties of oriented discontinuous fibre composites. Fibre Science and Technology. 1982;17(1):25-39.
[23] Goutianos S, Peijs T. The optimisation of flax fibre yarns for the development of high-performance natural fibre composites. Advanced Composites Letters. 2003;12(6):237-41.
[24] Baley C. Analysis of the flax fibres tensile behaviour and analysis of the tensile stiffness increase. Composites Part A: Applied Science and Manufacturing. 2002;33(7):939-48.
[25] Shah DU, Schubel PJ, Clifford MJ. Modelling the effect of yarn twist on the tensile strength of unidirectional plant fibre yarn composites. Journal of Composite Materials. 2013;47(4):425-36.
[26] Leclerc JSb, Ruiz E. Porosity reduction using optimized flow velocity in Resin Transfer Molding. Composites Part A: Applied Science and Manufacturing. 2008;39(12):1859-68.
[27] Shah DU, Schubel PJ, Licence P, Clifford MJ. Determining the minimum, critical and maximum fibre content for twisted yarn reinforced plant fibre composites. Composites Science and Technology. 2012;72(15):1909-17.
[28] Baets J, Plastria D, Ivens J, Verpoest I. Determination of the optimal flax fibre preparation for use in UD flax-epoxy composites. The 18th International Conference on Composite Materials (ICCM 18). Jeju Island (Korea):2011.
[29] Shah D, Schubel PJ, Clifford MJ, Licence P. Mechanical characterization of vacuum infused thermoset matrix composites reinforced with aligned hydroxyethylcellulose sized plant bast fibre yarns. 4th International Conference on Sustainable Materials, Polymers and Composites2011. p. 6-7.
[30] Rao Y, Farris RJ. A modeling and experimental study of the influence of twist on the mechanical properties of high-performance fiber yarns. Journal of Applied Polymer Science. 2000;77(9):1938-49.
[31] Naik N, Madhavan V. Twisted impregnated yarns: elastic properties. The Journal of Strain Analysis for Engineering Design. 2000;35(2):83-91.
[32] Bledzki AK, Faruk O, Sperber VE. Cars from bio-fibres. Macromolecular Materials and Engineering. 2006;291(5):449-57.
[33] Wambua P, Ivens J, Verpoest I. Natural fibres: can they replace glass in fibre reinforced plastics? Composites Science and Technology. 2003;63(9):1259-64.
[34] Joseph S, Sreekala MS, Oommen Z, Koshy P, Thomas S. A comparison of the mechanical properties of phenol formaldehyde composites reinforced with banana fibres and glass fibres. Composites Science and Technology. 2002;62(14):1857-68.
[35] Baets J, Vanfleteren F, Verpoest I. UD-flax preforms for optimal natural fibre composites performance. Composites Week @ Leuven and Texcomp-11. Leuven, Belgium:2013.
[36] Rask M, Madsen B. Twisting of fibres in yarns for natural fibre composites. ICCM18 - 18th International Conference On Composite Materials. Jeju Island, Korea:2011.
[37] Ma H, Li Y, Wang D. Investigations of fiber twist on the mechanical properties of sisal fiber yarns and their composites. Journal of Reinforced Plastics and Composites. 2014.
[38] Lomov SV, Gusakov A, Huysmans G, Prodromou A, Verpoest I. Textile geometry preprocessor for meso-mechanical models of woven composites. Composites Science and Technology. 2000;60(11):2083-95.
[39] Lomov SV, Huysmans G, Luo Y, Parnas R, Prodromou A, Verpoest I, Phelan F. Textile composites: modelling strategies. Composites Part A: Applied Science and Manufacturing. 2001;32(10):1379-94.
[40] Verpoest I, Lomov SV. Virtual textile composites software WiseTex: Integration with micro-mechanical, permeability and structural analysis. Composites Science and Technology. 2005;65(15–16):2563-74.
[41] Lomov S. WiseTex software suit. 2010.
[42] Lomov SV, Ivanov D, Verpoest I. Predictive models for textile composites. 7th Textile Science International Conference2010.
[43] Verpoest I, Lomov SV. Virtual textile composites software WiseTex: Integration with micro-mechanical, permeability and structural analysis. Composites Science and Technology. 2005;65(15):2563-74.
[44] Lomov SV, Bernal E, Ivanov DS, Kondratiev SV, Verpoest I. Homogenisation of a sheared unit cell of textile composites: FEA and approximate inclusion model. Revue Européenne des Éléments. 2005;14(6-7):709-28.

Chapter 7
Impact and fracture toughness properties of flax composites

The investigation of the impact properties and the interlaminar fracture toughness of flax-based composites is key in order to understand which material parameters determine the safety and longevity of flax composite products. In this study, the effect of fibre architectures and matrix types was investigated. Their influence on the absorbed energy after perforation, on the damage resistance as well as on the residual properties after impact (damage tolerance) were first quantified.

The interlaminar fracture toughness and the tensile toughness were later on analysed. It was found that while the matrix choice influences greatly the absorbed energy as well as the damage area, the type of architecture only has a limited effect. The fracture toughness investigation has revealed the potential of flax fibres as good reinforcement to produce tough composite materials. Flax fibre composites have higher G_{IC} initiation and propagation values compared to that of glass and carbon fibre composites. Additional improvements were observed when woven fabrics are used.

Limited amount of work on the drop weight impact and toughness properties of natural fibres, and flax in particular, is available as of today. This study aims to characterise the impact behaviour of flax reinforced composites. The originality of this work is that it seeks to understand the effect of the matrix and textile architecture combinations on the impact properties. The relation between the energy absorption capacity, the induced damage and the fracture toughness is investigated. It is hypothesized that the presence of delaminations will have an important impact on the impact performance of the flax composite.

The low velocity impact performance was investigated on various combinations of flax composites looking at the influence of the fibre architecture (random mat, plain weave, twill 2x2, quasi-UD and UD, see Table 7-1) and the matrix type (a brittle epoxy and a ductile maleic anhydride polypropylene (MAPP)). Three aspects of low velocity impact were investigated:

- Absorbed energy up to perforation using drop weight tests;
- Damage resistance with non-perforating drop weight tests;
- Damage tolerance investigation through three point bending tests after non-perforation impact.

Finally, the fracture toughness and tensile toughness were investigated in order to understand how the damage spreads in the impacted samples, and how the damage area relates to the damage tolerance capacity of the each composite system. All testing parameters and equipment as well as the properties calculation are presented in Chapter 4 and Appendix E.

Flax fibre preform architectures	**Lay-up**	**Acronyms**	
Random Mat	$[0]_3$	Random Mat	Mat
Plain weave	$[0]_4$	Plain weave	PW
Twill 2x2	$[0]_4$	Twill Low Twist	NT
	$[0]_6$	Twill Medium-Low Twist	TW180
	$[0]_7$	Twill Medium-High Twist	HF
	$[0]_8$	Twill High Twist	TW150
Quasi-UD	$[0,90]_s$	Quasi-UD [0,90]	QU
UD/MAPP prepreg	$[0, 90]_{3s}$	UD1[0,90]	UD1
UD with epoxy sizing	$[0, 90]_2$ 0 $[90,0]_2$	UD1 [0,90]	UD1
UD	$[0,90]_{2s}$	UD2[0,90]	UD2

Table 7-1: Description of the acronyms used flax preforms and matrices. The other features are described in Chapter 4 section 4.1.

7.1 Concept of low velocity impact

The set up for the drop weight impact test can be adjusted for non-perforation or perforation tests by adjusting the height or the weight of the impactor. Figure 7-1 displays the typical force-displacement curve for a perforation and a non-perforation experiment. Characteristic for a non-perforation experiment is that the impactor experiences a rebound after the maximum force P_m has been reached; this is seen as a loop in the force-displacement diagram (fig.7-1 a). For higher incident energies, higher forces are attained, till perforation instead of rebound occurs.

A closer look at the graph another threshold level can be distinguished. In Figure 7-1a, some researchers [1, 2] found that the start of oscillations indicates the transition between matrix damage and delamination, this is called the incipient damage point with force P_i. One can state that certain threshold energy is needed before delamination occurs.

The aim of a non-perforation test is to evaluate the residual properties of a structure after an impact event has occurred. It is accepted that the size of the damaged area is related to the compression after impact properties [2-4]. Thereby much attention is paid to the influencing factors of the damaged area. It is known that the damaged area gets larger with larger incident impact energy till perforation occurs [4-6]. While doing so the shape of the damaged area can also change [7]. Literature has shown that the damage resistance and tolerance depend on many material related factors: matrix type, fibre type, interface, fibre architecture, fibre orientations and laminate stacking and thickness [6].

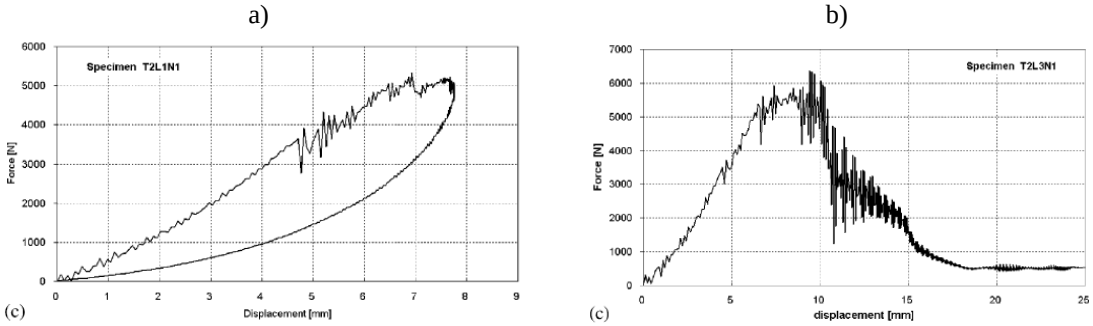

Figure 7-1: Typical low velocity impact graphs: a) perforation impact and b) non perforation impact [1].

By increasing the incident energy of the impactor, the absorbed energy increases till perforation is reached. A typical force-displacement curve where no rebound occurs and a perforation takes place, is shown in Figure 7-1b . In this force versus time graph, different thresholds can be distinguished. The first threshold is at P_i, with corresponding energy E_i seen in Figure 7-2. This point signifies, as in a non-perforation test, discernible matrix micro-cracking and the onset of delamination [8]. The second level is found where the load reaches its maximum value (P_m), with corresponding energy (E_m). This point signifies the maximum deflection of the sample.

For a perforation test, no rebound will occur, but the impactor fully penetrates the sample as can be seen in Figure 7-2. The end point of the curve, the total load point (P_t) and the total energy absorbed (E_t) already take a significant amount of friction between the impactor and the perforated sample into account. The point where this friction starts to be dominant is not always clear; usually it is accompanied with high oscillations and the force going up again. Here the failure load point (P_f) with corresponding failure energy (E_f) can be considered as this point.

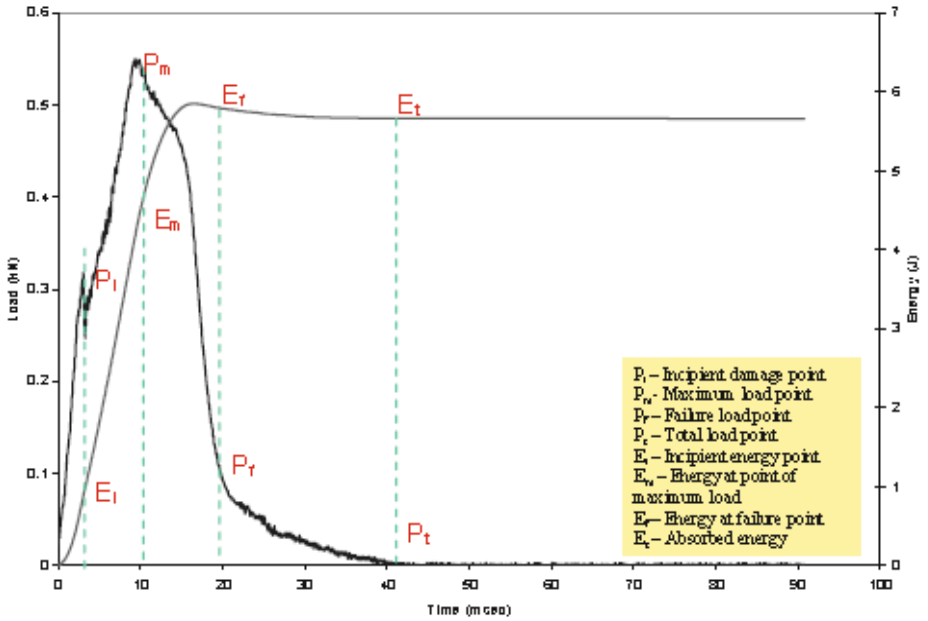

Figure 7-2: Typical load and energy versus time curve and characteristic points for post-impact analysis in a perforation test [8].

Literature has shown that the perforation characteristics of a material are influenced by other properties than for non-perforation tests. Here the matrix type, fibre type, interface,

fibre architecture, fibre orientations and laminate stacking and thickness only play a secondary role. The most decisive parameter is the fibre strength and the fibre volume fraction or the total fibre areal weight [5, 6]. It has been shown that for carbon and glass fibre composites the perforation energy varies linearly on logarithmic scale against the thickness of the plate multiplied by the fibre volume fraction ($t*V_f$), see Figure 7-3 a (for a given fibre, and hence a given fibre strength). Parallel lines can still be seen, this is due to the variation of the top diameter of the striker for the different impacted specimens that were tested. For larger top diameters higher penetration energy values are obtained.

Figure 7-3b takes the varying top diameter into account and it can be seen that the penetration energy follows a master curve for different kinds of matrix material, fibre architecture, lay-up, thickness and top diameter. Caprino et al. [6] were able to determine a power law for the carbon and glass fibre tested specimens to predict the perforation energy. Out of the failure mechanisms it was clear that perforation only occurs after matrix damage and delamination[6].

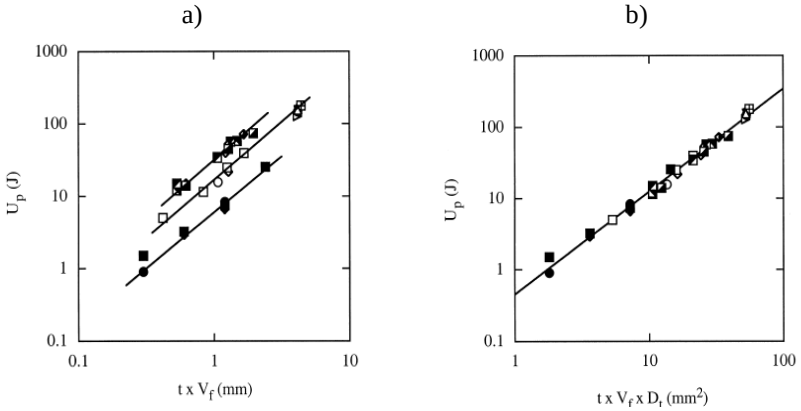

Figure 7-3: a) Penetration energy Up vs. total fibre thickness, t x V_f for different carbon fibre reinforced plastic laminates; b) Log-log plot of the penetration energy, Up, versus the quantity (t x V_f x D_t) for the CFRP laminates considered. t = thickness, V_f = fibre volume fraction, D_t = top diameter of the striker [6].

7.2 Impact properties of flax composite

In this study, the absorbed energy after impact, the impact resistance and damage tolerance are characterised via a drop weight impact test. This type of test was preferred to the Izod or Charpy tests, which are typically used methods to test polymers. Traditionally, the choice between drop weight and impact testing was determined by end-use application requirements of the material. However, many researchers find that Izod/Charpy tests have a lower accuracy and repeatability [9-11]. While they are still adequate for quality control, they do not provide reliable information on the failure mechanisms. On the other hand, drop weight impact is closer to a "real" impact scenario and has several key advantages over other methods.

The drop weight impact has an impact loading that is more realistic for fibre reinforced composites. It can be used for several types of materials from metals to polymers and fibre reinforced composites. The testing is unidirectional and does not have a preferential failure direction as the failure originates at the impact area and propagates from there [12]. Moreover, several types of failure (deformation, crack initiation, delamination or complete fracture) can be studied depending on the type of low velocity impact (perforation or no perforation). These factors make the drop weight testing a better simulation of real-life conditions.

7.2.1 The absorbed energy at perforation and its prediction

A power law method, presented by Caprino et al. [6] for carbon and glass fibre composites and used by other authors [13, 14], was used in this study to predict the absorbed energy at perforation, in brief the perforation energy. It has been found for carbon and glass fibre composites that the perforation energy varies linearly on a logarithmic scale against the thickness t of the plate multiplied by the fibre volume fraction V_f and the impactor top diameter D_t:

$$U_{perforation} = K(tV_fD_t)^{\alpha} \quad \text{(Eq. 7.1)}$$

Where K and α are two material parameters to be experimentally determined, *t* is the thickness in mm, V_f the fibre volume fraction and D_t the top diameter of the striker in mm. Since the striker used was the same for all the tests, the D_t can be left out of the formula. The value of α=1.3 was found to be the best fit for glass and carbon fibre composites and was also found to be the best fit for flax-based composites [6]. In Figure 7-4, the power law curve was plotted using the perforation energy versus the total fibre "thickness" (V_f x t). It has to be noted that the random mat was left out of the correlation because it showed an off trend behaviour (especially for the thermoset composite) potentially due to its random orientation.

The observation of two trends for each matrix type, thermoplastic (Δ) and thermoset (□), proves that the type of matrix used has a large influence on the perforation energy of natural fibre composites. The *K* values found for the flax-thermoplastic and flax-thermoset composites were respectively 12.52 and 9. Since the power law trend line represents quite accurately the relationship between the perforation energy and the total fibre thickness, one can predict the perforation energy when the total fibre thickness is known. No observable dependence on the fibre architecture could be observed.

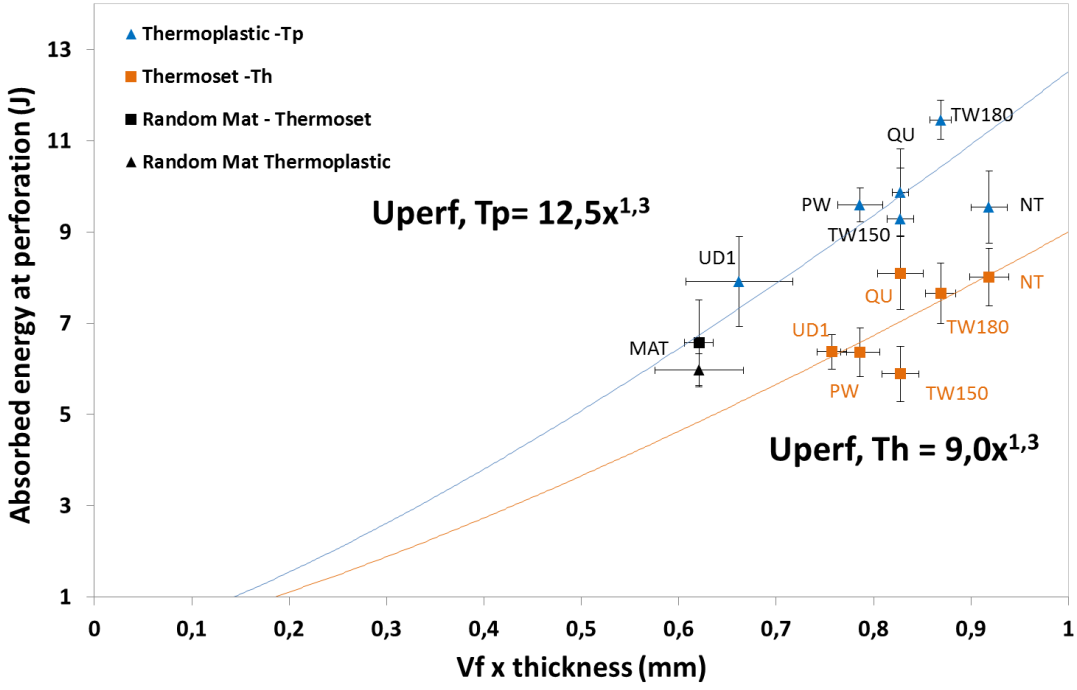

Figure 7-4: Relationship between perforation energy and 'total fibre thickness' V_f x t. MA = Random mat, PW = Plain weave, NT = Twill low twist, TW180 = Twill medium-high twist, TW150 = Twill high twist, QU = Quasi-UD [0,90], UD1 = UD1 [0,90].

The data of Figure 7-4 are presented in a more schematic way in Figure 7-5. Among the different combinations, the twill fabric (TW180, medium-high twist twill) shows the highest energy absorption. In literature, comparable results were seen for twill weave flax structures compared to plain weaves [15], but the fact that all preforms seem to follow the trend expressed by Eq. 2 suggests that this difference has to be attributed to a difference in 'total fibre thickness' V_f x t, and not to an intrinsic preform architecture effect. Further analysis will indeed show that impact performance of flax fibre composites (with good fibre-matrix adhesion) is fibre dominated and hence, dependent on the 'effective' amount of fibres and their orientation in the tested specimen.

A closer look at the data presented in Figure 7-5 shows that the matrix is found to play an important role. A general increase in perforation energy was detected for all flax-MAPP if compared to the thermosets values. Similar results were found by Cantwell et al. [16]. This high increase may be due to the fact that the ductile MAPP matrix allows more plastic energy absorption thanks to its high strain to failure ($\varepsilon_{MAPP} \approx 400\%$ vs $\varepsilon_{epoxy} \approx 4\%$). Excluding the random mat composites, the general increase in perforation energy is about 50% for the thermoplastic matrix.

This effect is less pronounced for the quasi-UD and the low twist twill, with a more modest increase of about 20%. Taking into account that one of the main fracture modes is fibre fracture, the perforation energy may be directly related to the yarn strength used in the textile. Impregnated fibre bundle tests performed in Chapter 6 have revealed that the Quasi-UD twisted yarn strength was significantly higher than in case of the other weaves, 538 MPa vs 412-451 MPa. A similar conclusion is made for the low twist twill which has a wrap yarn around the UD fibre which creates mis-orientations along the fibres and hinders its yarn properties and thus its perforation performance (see section 7.4 for further details).

For the tested flax composites, the polymer matrix has a significant influence on the absorbed energy. In perforation impact tests, the fibres have to be fractured in order to achieve perforation. Hence, the stronger the fibre, the more predominant is the contribution of the fibre fracture energy in the total perforation energy. Because the flax fibres are weaker than glass or carbon fibres, the relative contribution of the matrix ductility to the composite impact behaviour is more important.

Optical observations of the broken samples corroborated the results shown in Figure 7-5. In Figure 7-6, the thermoset composites present a sharper failure pattern characteristic of a brittle failure mechanism [17]. The measured load drop is also more abrupt. For the thermoset composites, parts of the samples broke away leaving a clean hole after impact. This phenomenon was not observed for the thermoplastic composites as they showed a more ductile perforation profile. The impactor encountered more resistance while penetrating the sample due to the higher strain to failure of the matrix. Therefore, the thermoplastic matrix delays the point of first damage because plastic deformation occurs prior to matrix failure. Both materials show very little fibre pull-out upon fracture, which is indicative of a good fibre-matrix adhesion in both cases.

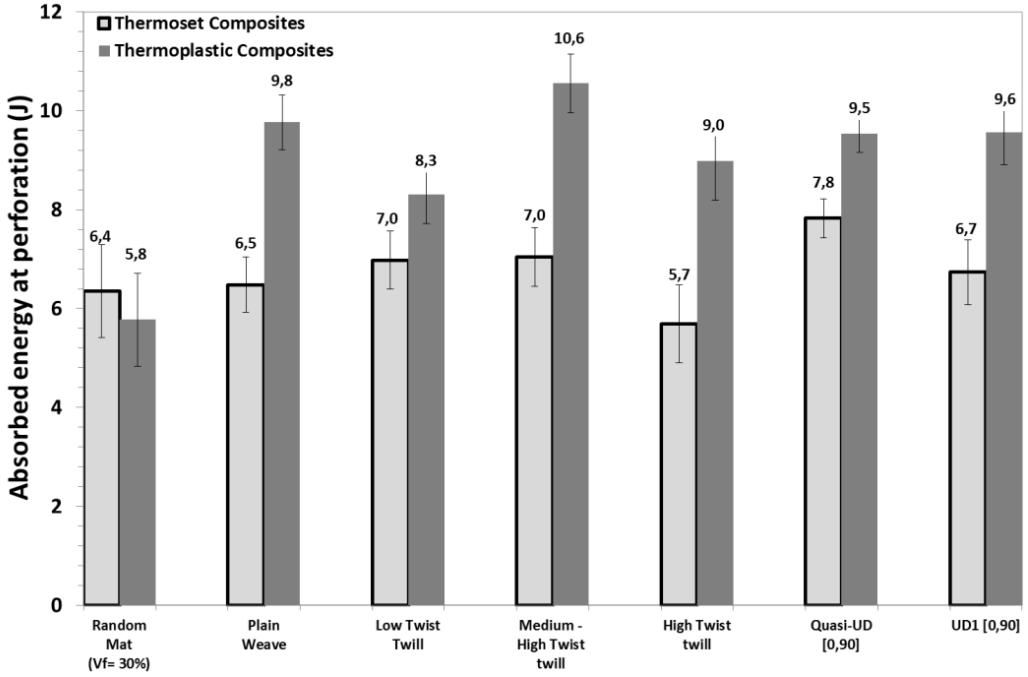

Figure 7-5: Total absorbed energy at perforation for a 2 mm perforated flax/epoxy and flax/MAPP plates. The data was normalized to same V_f x t of 30 or 40% x 2mm.

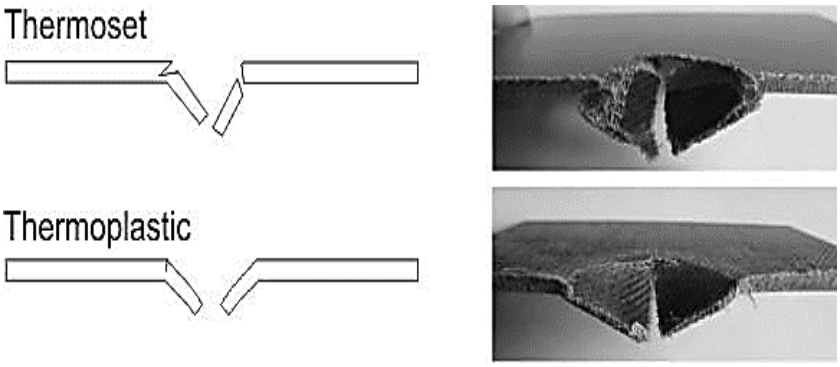

Figure 7-6: Fracture behaviour of flax/epoxy vs flax/MAPP composite after perforation.

The perforation energy variation between thermoset and thermoplastic composites can also be evaluated by splitting the energy absorbed before the peak (U_m) and the energy absorbed after the peak (U_p) from the force-displacement curve as displayed in Figure 7-7a. The quantification of the U_p and U_m are presented in Figure 7-7 b. It has to be noted that the energy was not normalised in order to quantify the absolute value of U_m and U_p. For thermosets the energy absorption before the peak is of equal magnitude as after the peak, but for the thermoplastic specimens, U_P is almost twice the energy as before the peak.

In the case of the flax-MAPP composites, the impactor encounters more resistance passing through a thermoplastic specimen. Due to the higher strain to failure (and hence fracture toughness, further explained in section 7.3), the sides stay longer attached to the specimen and give more resistance to the impactor when passing through the specimen. Furthermore, the U_m for thermosets was always slightly higher than for thermoplastics due to the intrinsically higher bending strength for the epoxy composites as the U_m value represents the maximum load a laminate can sustain before major damage [18]. This phenomenon is directly related to the bending stiffness of the composite. A stiffer materials will deform less under impact and sustains more load before its breached leading to an increase in energy absorption [19, 20].

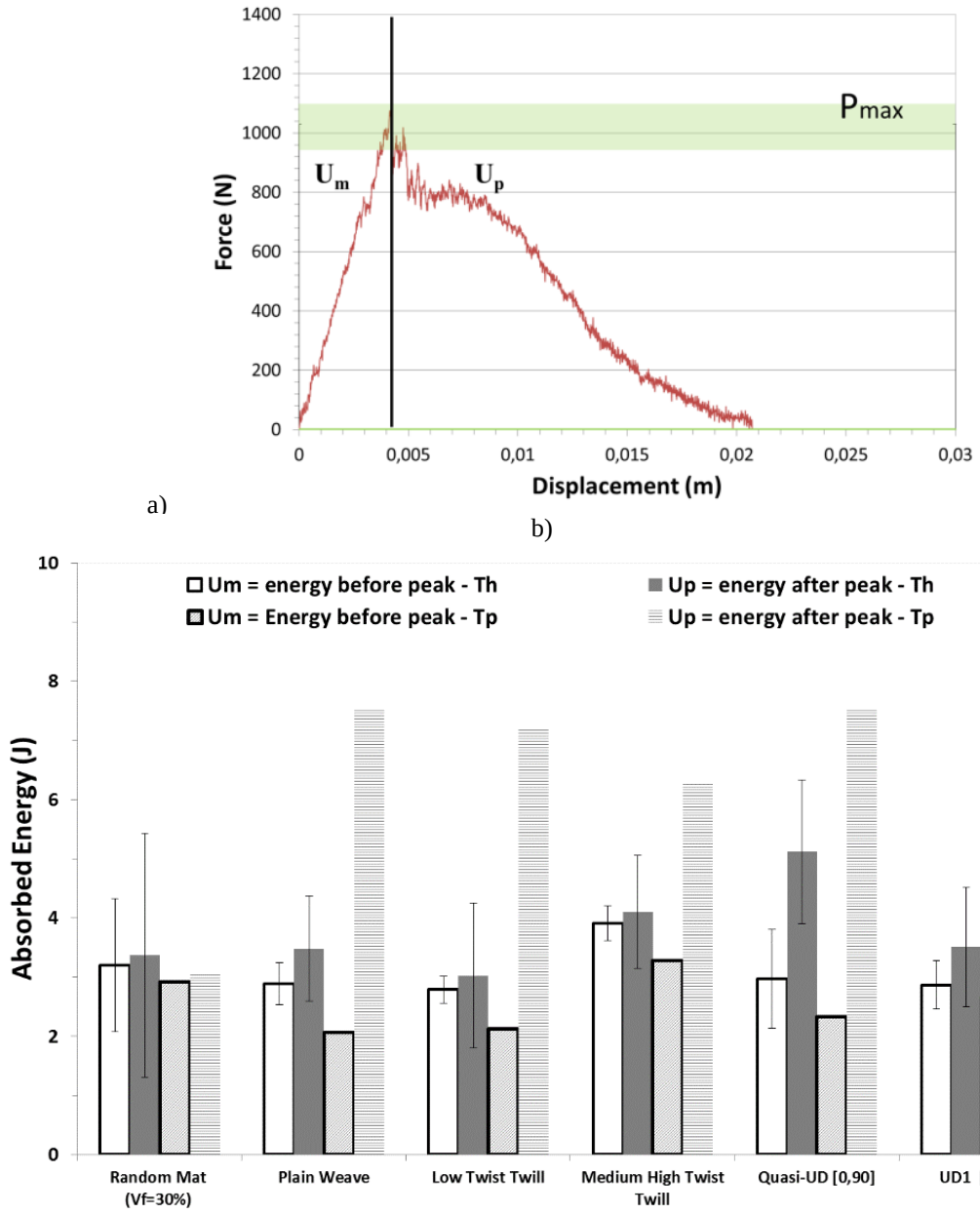

Figure 7-7: a) Force-displacement perforation graphs of the flax plain weave–MAPP composite with indication of the energy absorption before the peak (Um) and after the peak (Up) and b) Quantification of U_m and U_p for the different fibre architectures (the energy was not normalised).

7.2.2 Damage resistance characterization

7.2.2.1 Observation of damage

The damage resistance is defined as the damage area for a given impact force without full perforation of the sample. To define this damage area, surface and internal damage through the laminate thickness, optical microscopy and c-scanning techniques were used. Figure 7-8 and Figure 7-9 show the C-scan images of different flax/matrix combinations impacted with 3.11 J. The total damage area including delaminations and matrix cracks around a through the thickness crack, is displayed. It can be seen that the damaged area for all thermoset systems was higher than for the thermoplastic systems, as expected. It is worth noting that the fracture that can visually be observed after impact is not that much smaller than the fracture revealed by the C-scan.

For all woven fabrics and cross-ply laminates, the damage was represented by a star shape, following the warp and weft direction of the fabric or plies mainly caused by the matrix cracking in-between the textile yarns. Due to the relatively low (transverse) strength of the flax fibres, a through-the-thickness crack with fibre failure and limited delaminations around the main crack occur. The small delaminations are potentially due to the high fracture toughness (G_{IC}) of the flax composites. This is seen for all the thermoset and thermoplastic composites as seen in Figure 7-9 and previously in Figure 7-6. The matrix cracks are however more present than delaminations in thermoset composites due to the brittleness of the matrix. The non-woven mat either had three or four crack-lines not following any preferential direction. For the flax composites with a thermoplastic (MAPP) matrix, a concentrated impact is seen (round shape of the damage). In this case, the higher strain to failure of the matrix (higher deformation possible) allows higher energy absorption and limits the matrix cracks in the composite.

This is a very important difference in behaviour of flax fibre reinforced composites compared to glass and carbon fibre reinforced composites [21, 22]. The cracks perpendicular to the fibre direction start at the tensile side of the impacted specimen, and grow through the specimen thickness, creating only small delaminations, as seen in Figure 7-10. Furthermore, for the quasi-UD with epoxy, the crack follows the waviness of the fabric at the back side which limits the delaminations (see arrow in Figure 7-9 d). In glass fibre composites, the strong fibres do not break under non-perforating impact, and only matrix cracks (parallel to the glass fibres) are created, which then initiate large delaminations spreading between the plies [23].

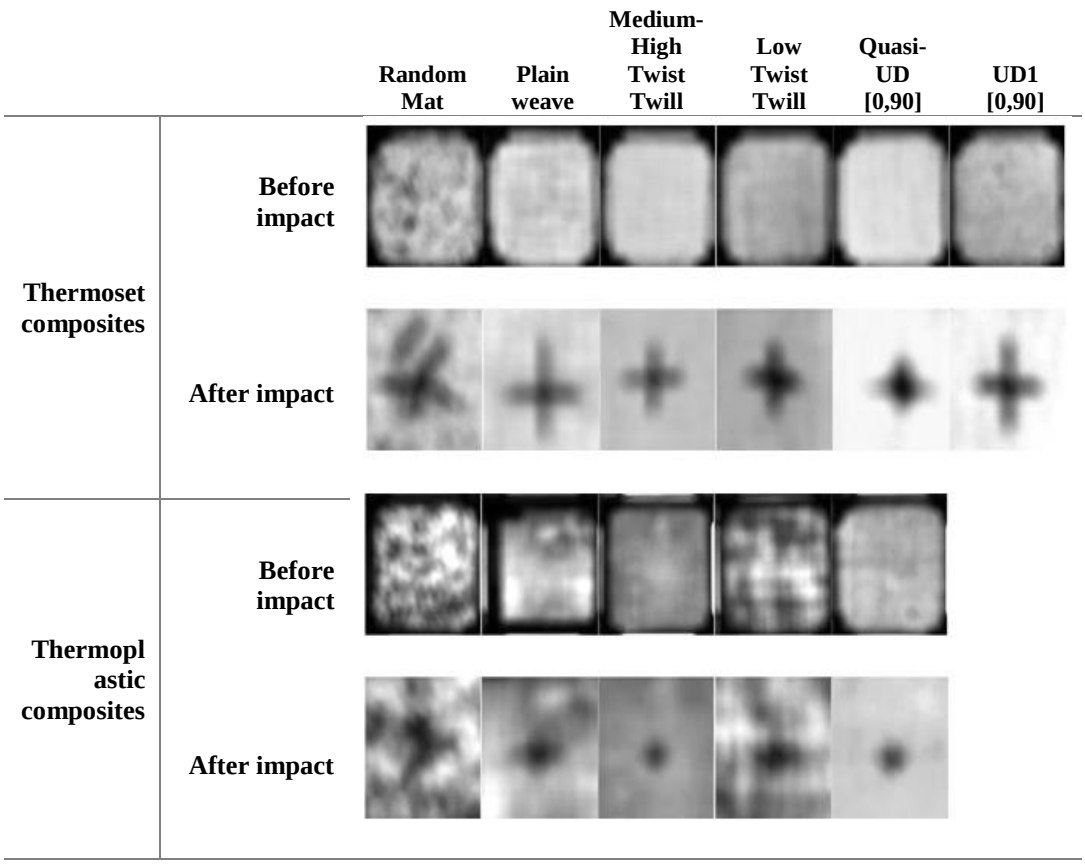

Figure 7-8: C-Scan results of the induced damage.

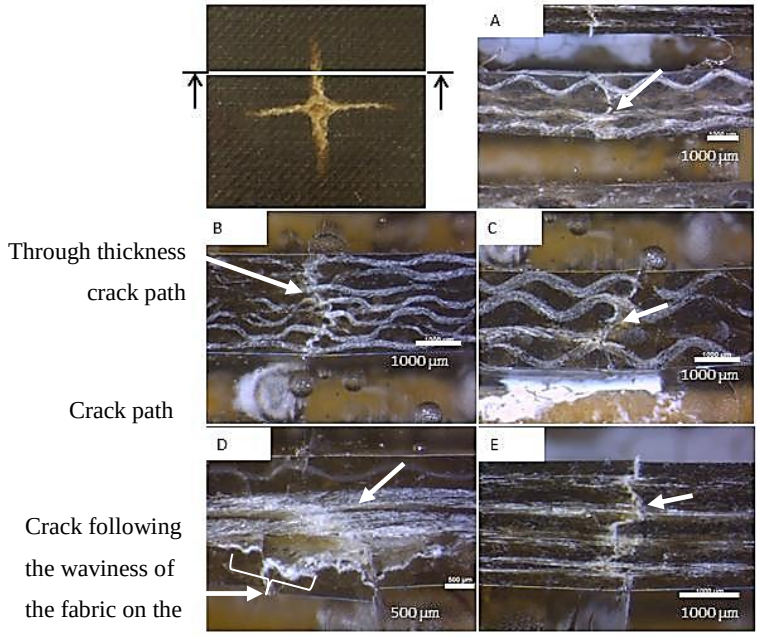

Figure 7-9: Through thickness observation on flax/epoxy and flax/MAPP composite after a 3.1 joules impact with a 10cm drop height on 2 mm thick samples: a) plain weave with MAPP; b) medium-high twist twill with epoxy; c) plain weave with epoxy; d) quasi-UD [0,90] with epoxy; e) UD [0,90] with epoxy.

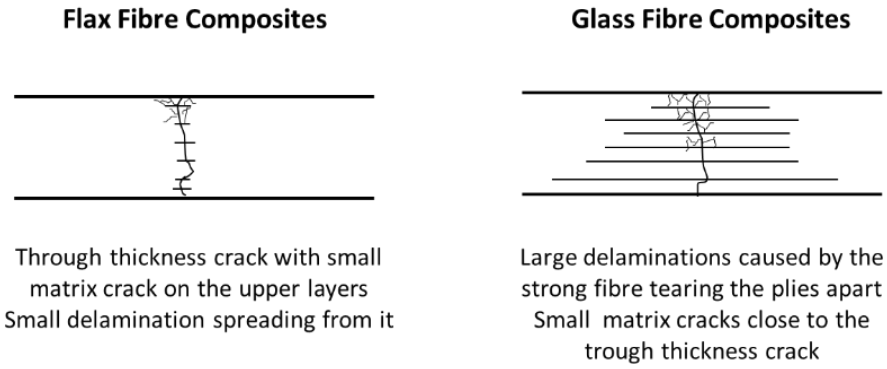

Figure 7-10: Damage spread for flax fibres vs glass fibres [0,90] cross-ply laminate following a low velocity impact.

7.2.2.2 Damage area per absorbed energy

Figure 7-11 summarizes the absolute absorbed energy, the induced damage and the absorbed energy normalised per damage area in order to compare the different architectures. The differences observed in absorbed energies per damaged area of non-perforated samples are a combination of differences in the absolute values and in the damage area presented in Figure 7-11 a and b. It has to be noted that in contrast with the total absorbed energy at perforation (Figure 7-5), the absorbed energies per damaged area of non-perforated samples are not normalised to the total fibre thickness, since no proof of dependency was found in the literature.

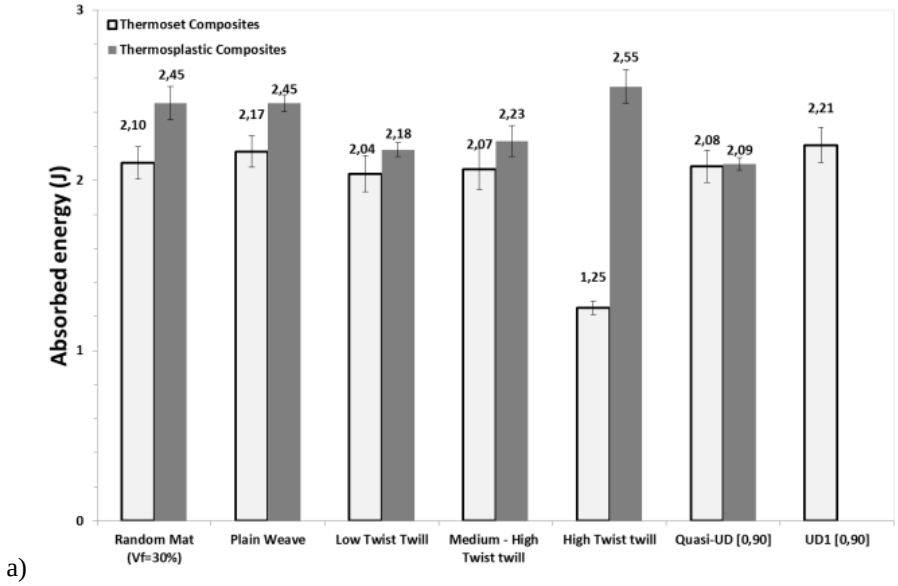

a)

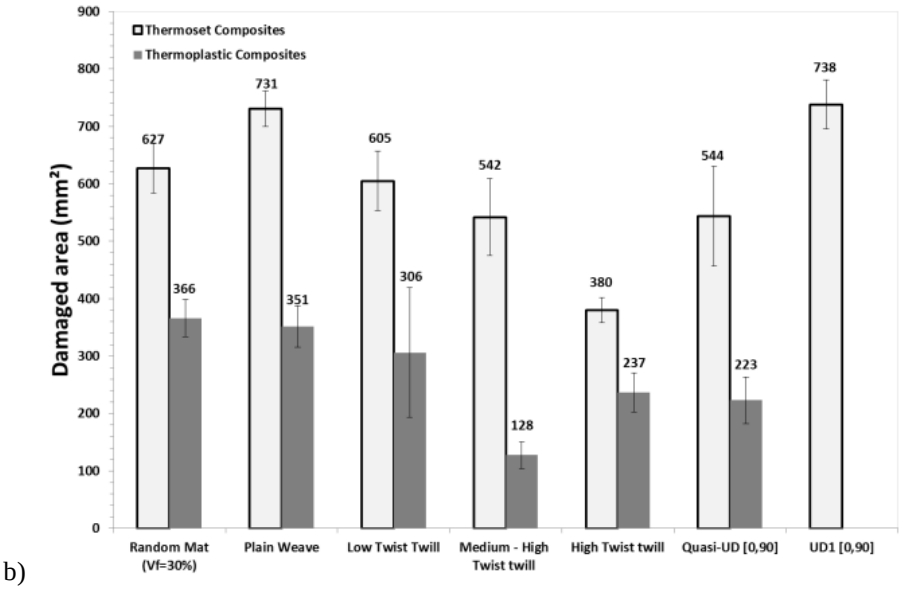

b)

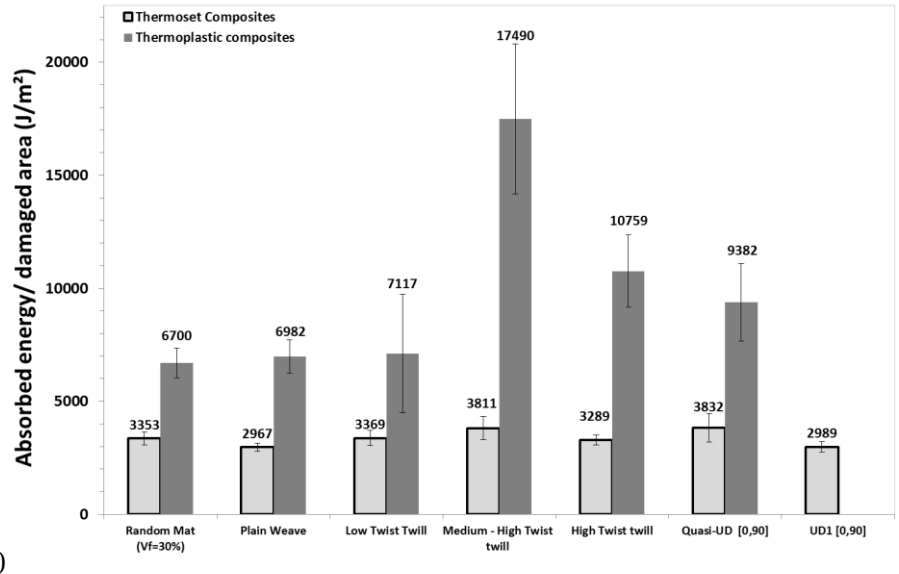

c)

Figure 7-11: a) absorbed energy, b) total damage area and c) absorbed impact energy per damaged area of non-perforated samples following an initial impact of 3.11J for thermoset and thermoplastic composites

In Figure 7-11 a, it is seen that most of the 3.11J impact energy (Th =65-70%, Tp =67-82%) is dissipated by the composite material. The rest of the energy is absorbed through matrix cracks, through thickness cracks and delaminations resulting in the damage area quantified in Figure 7-11b.

As expected, the thermoset composites have systematically a higher damage area than the thermoplastic ones due to their lower energy absorption. Thermoplastic composites showed, for the same impacted energy, a smaller damaged area as the ductile matrix was more effective in delaying matrix crack formation and delamination initiation and growth. The high twist twill thermoset composite only absorbed 40% of the impact energy. This could be caused by several factors as the lower fibre strength and low load transfer efficiency of the brittle matrix. Nevertheless, no clear causes were found. Further investigation should be undertaken focusing on this particular textile.

Combining Figure 7-11 and b, the absorbed energy per damaged area is obtained (Figure 7-11 c). It was observed that all thermoplastics outperformed the thermosets as they increase the absorbed energy per damage area by 2 to 5 times. For the thermoset composites, no large difference in absorbed energy per damaged area could be seen for the different fibre architectures. This could be caused by the brittle matrix, inducing mainly matrix cracking causing a higher damage area as previously explained.

For thermoplastic composite, the fibre architecture type seems to play a stronger role: the medium-high twist twill, the high twist twill and the quasi-UD [0,90] show an increased absorbed energy with low spreading of damage. Their common point is that they are all based on highly twisted wet spun yarns (15-20^{o} twist angle), which could be beneficial for the damage resistance. Furthermore, it was found that more ends and picks per count (reported in Table 7-1), due to a finer yarn, hinders the progressing damage (delaminations) and lowers the induced damaged area hence increases the absorbed energy per damaged area. This could be related to high fracture toughness of the specimens and will be further explored in section 7.3.

7.2.3 Damage tolerance - Flexure after impact (FAI)

Properties after impact are critical in order to predict the ability of a part to sustain the applied load after being impacted. Can the defects be sustained by the material until repair? How is the load bearing capacity affected? In the previous section, the quasi-UD and the high twist twill fabrics had the best performance for damage resistance and along with the plain woven fabric (as a reference), they have been chosen for the assessment of the properties after impact.

The impacted specimens with visible local damage are more sensitive to compression than to tensile loading, due to the buckling outwards of the delaminated parts. For this reason, the compression after impact (CAI) test is a good way to validate the residual properties, and hence the damage tolerance. Unfortunately, due to the relatively low stiffness of flax fibre composites, heavy buckling occurred during the CAI test, which is not allowed in the CAI-standard (ASTM D7136). As an alternative, a three point bending flexural strength after impact (FAI) test was used in order to quantitatively evaluate the material performance after impact. This might be justified, as the impact of flax fibre composites creates through-thickness cracks, which will certainly affect their flexural strength, and by extension the tensile strength. It has to be noted that all samples presented a through-the-thickness behaviour similar to the damage resistance samples presented in section 7.2.2.

The results in Figure 7-12 show that the decrease in flexural strength before and after impact was limited to 9% to 21% for thermoset composites while the flax-MAPP decrease in properties is very limited (0% to 6%). Furthermore, the residual flexural strength as well as the modulus was higher for thermoset samples than for thermoplastic samples which correlates very well with the results obtained from the flexural tests [24]. It can be said that the damage on the specimens does not lower the residual properties substantially besides for the High Twist Twill. When the flexural strength after impact (FAI) was plotted versus the damage area from an impact of 1.56J, a decreasing linear trend was observed, which means that the larger the damage is, the lower the properties will be. Thus, designing materials for damage resistance is designing for damage tolerance.

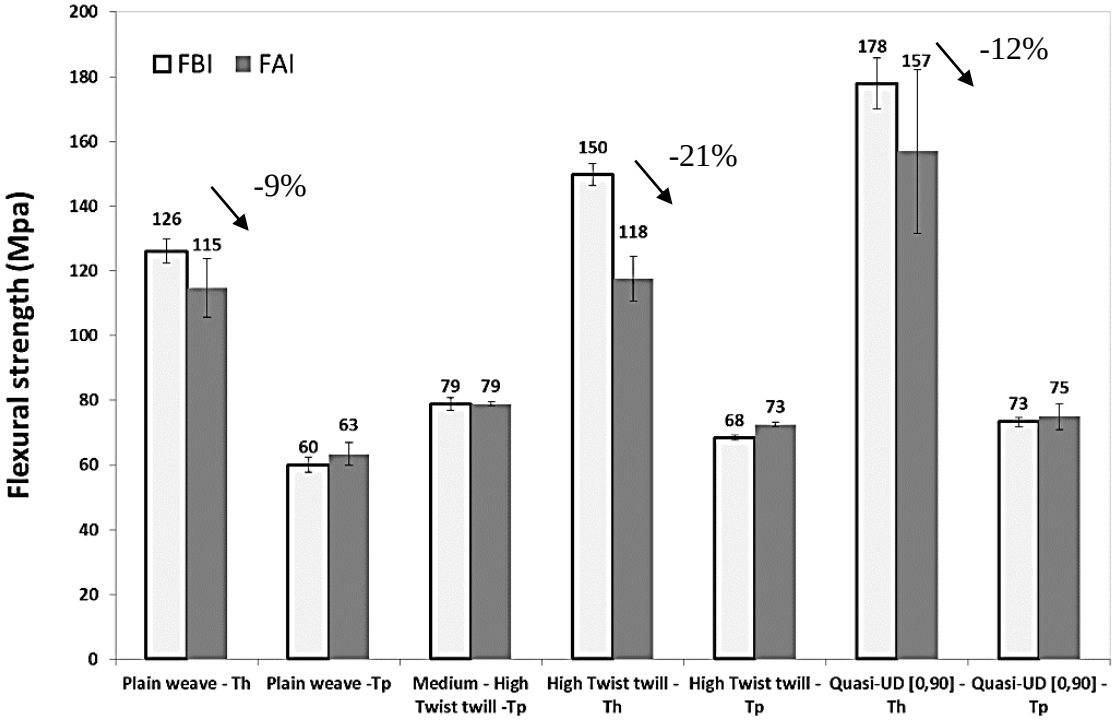

Figure 7-12: Flexural strength before and after impact.

In Figure 7-13a, it can be seen that the Quasi-UD-Tp combination has a lower performance than the other configurations. This sample did not display a growing crack from the impacted area which was visible for all the other specimens. Instead, it failed by local micro-buckling on the compression side probably related to very low matrix stiffness, combined with the absence of crimp. This phenomenon causes an underestimation of the failure strength and its overall residual properties (Figure 7-13b). The micro-buckling was also observed for the non-impacted specimen as seen in Figure 7-14 a, thus making it an intrinsic problem of this laminate.

As for the residual strength shown in Figure 7-13a, the percentage of decrease in properties seems to have a linear trend which is independent of the matrix and the architecture. The two exceptions are the quasi-UD-Tp (micro-buckling) and the plain weave-Th. As for the plain woven fabric, manufacturing difficulties lead to the presence of small surface defects detected as damage by the c-scan. These small defects may lead to an overestimation of the damage area after impact and ultimately lower residual properties.

In conclusion, it has been shown that damage tolerance is closely related to the damage resistance and that both the fibre architecture and the matrix ductility are important influencing parameters. To improve the damage tolerance, an optimization of the matrix choice, such as toughened epoxy, or the lay-up sequence must be considered and optimized. However, as the composite performance also depends on the presence of internal flaws such as interlaminar flaws and the propagation of damage, it is thus critical to understand how the damage propagates. As such, fracture toughness experiments are essential for further optimization.

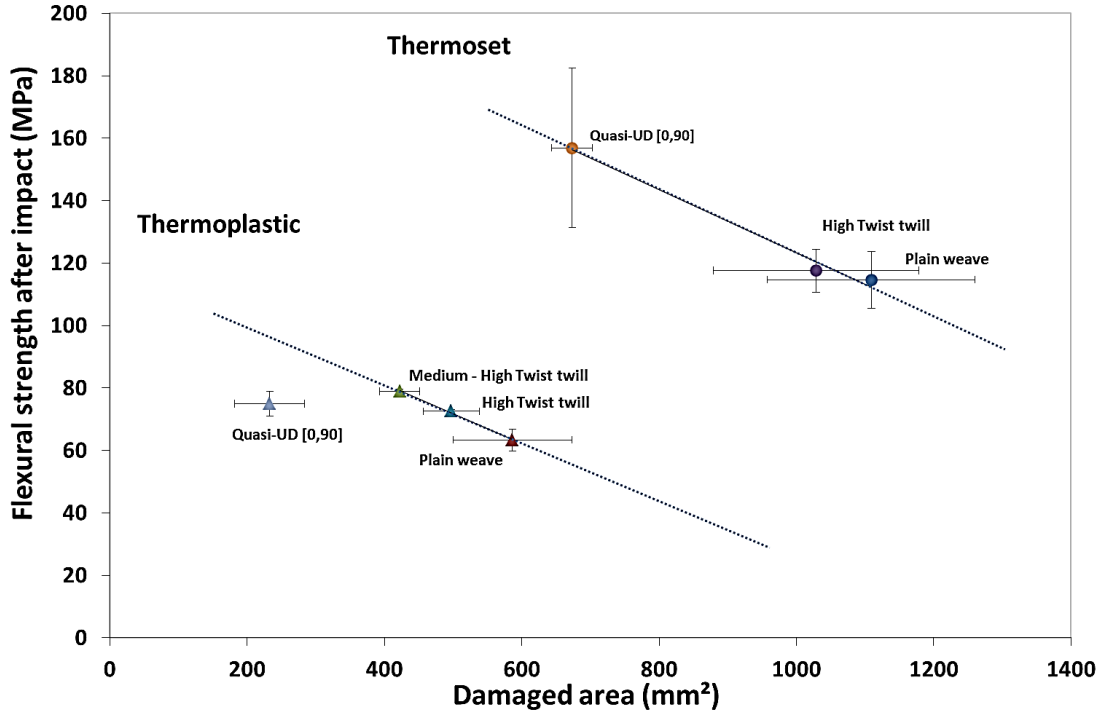

a)

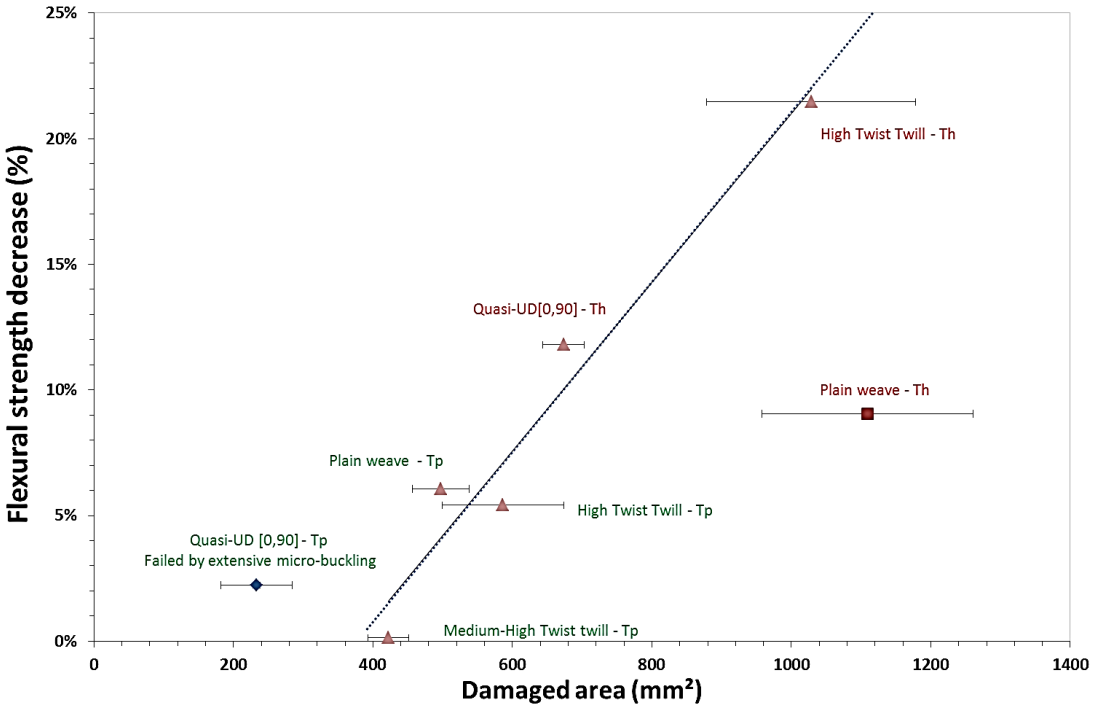

b)

Figure 7-13: Residual properties after impact according to the damage area a) residual flexural strength after impact and b) percentage of flexural strength decrease.

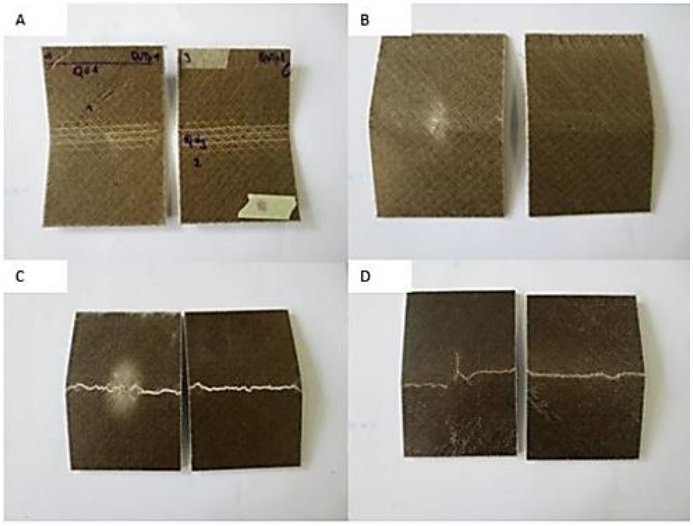

Figure 7-14: Failure modes after FAI test for both impacted *(left)* and non-impacted *(right)* samples (A) Quasi-UD–Tp showing with signs of buckling on the compression side, (B) tension side of the Quasi-UD-Tp, (C) Plain Weave–Tp and (D) Plain Weave–Th.

7.3 Interlaminar fracture toughness

In composite design, the fracture toughness helps to understand "how" the composite behaves once a crack propagates and a delamination spreads. The first transverse cracks are generated where a defect is present, e.g. a void, a matrix flaw or a weak interface. These defects will give rise to the initiation and further growth of delaminations, controlled by the initiation and propagation interlaminar fracture toughness of the composite [25]. The interlaminar fracture toughness was investigated for both Mode I (G_{IC}) and Mode II (G_{IIC}) for seven flax-epoxy architectures: three weaves, the quasi-UD and UD in both [0,90] and [90,0] lay-ups. The influence of the thermoplastic matrix was not investigated in this section.

7.3.1 Mode I Fracture toughness

Figure 7-15a presents the resistance of fracture curve (R-curve) for Mode I. The shape of the R-curve may be affected by the fibre bridging phenomenon as well as matrix cracking, tow cracking, multiple delamination, tow bridging and tow breaking in the case of woven fibre composites between others, as reported by Zhu [26]. For sake of clarity, the crack length starts at 0 which was the initial position of the crack tip (the whole crack length was taken into account in the calculations). The initiation fracture toughness value was determined using three methods as described in Chapter 4 section 4.9 (NL, 5% offset and VIS seen in Figure 7-15b).

It can be seen that visual determination of the initiation point (VIS) does not reliably represent the real value of the critical point for crack onset as it was closer to the propagation values in most cases, as seen in Figure 7-15b. This means that the crack already started to grow before one can visually observe it and therefore, the initiation value will be considered to coincide with the non-linearity of the load-displacement curve (NL), as it has been found to be the lowest value of all three methods.

The Quasi-UD [0,90] and UD [0,90] show an increase at the beginning of the crack development followed by a slow decrease and stabilization of the toughness value. The first increase is directly related to fibre bridging at the crack front displayed during the test. Similar results were found by Olave et al. [27] for twill 2x2 carbon-epoxy composites. The

following decrease and stabilization of the R-curve may be caused by a weak crack propagation resistance [28] or to the residual stress effects[29]. Although the potential mechanisms were identified for this phenomenon, further investigation is needed to corroborate them.

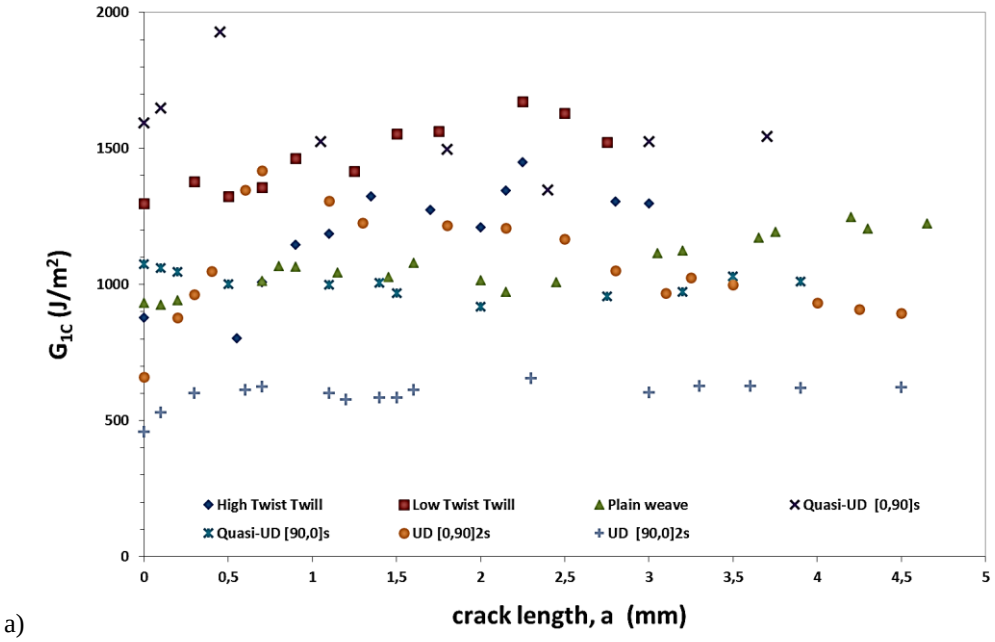

a)

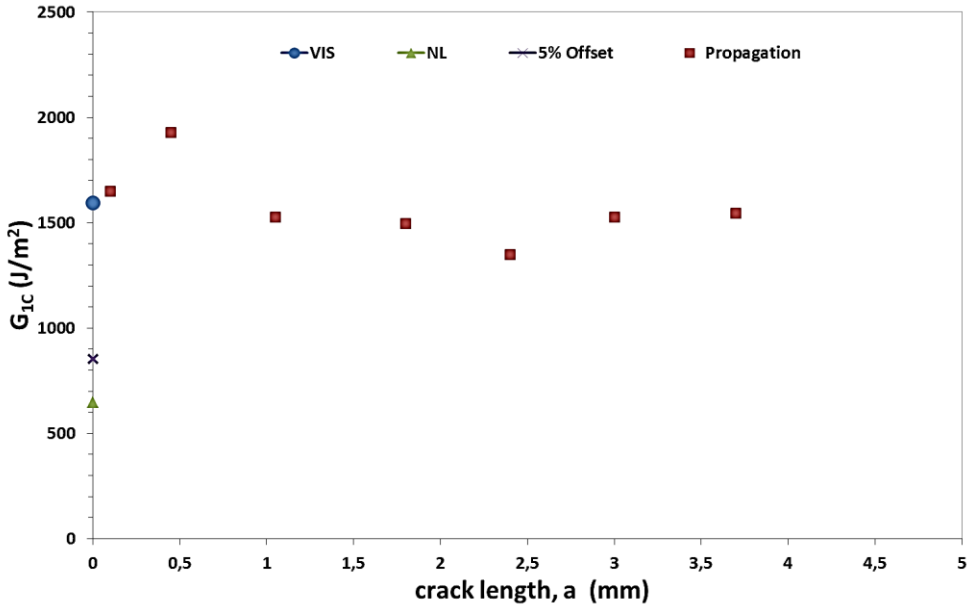

b)

Figure 7-15: a) Overview of the typical curves for all tested composites architecture R-curves from a DCB test and b) one R-curve curve of a flax quasi-UD [0,90] composite with the indication of the NL, 5% offset and VIS values.

The load-displacement (P-δ) curves of the Mode I DCB tests of the flax-epoxy composites are shown in Figure 7-16. An initial non-linearity in the curves is observed and commonly encountered in mode I fracture testing because of the "load take up effects" and the fact that it is the cross-head displacement that is initially recorded and not the actual beam opening [30]. The weave pattern and cross ply lay-up change; this leads to a different behaviour, indicated by the disparity of the curves in the plot. It has to be noted that for the

woven fabrics, the crack was running along the warp direction, whereas for the cross-ply laminates, the crack growth was between either the 0^o layers (in the [90,0] laminates) or the 90^o layers (in the [0,90] laminates). Small drops in load, before the maximum load was reached, were seen for all tested configurations.

The low twist twill fabric's P-δ curve, shown in Figure 7-16a, displays a non-linear increase in load with increasing displacement. After crack initiation, the load slowly rised with increasing displacement representing a steady crack growth and potential low fibre bridging [26, 31]. This phenomenon could be related to the textile geometry and textile nesting which is explored in the next section.

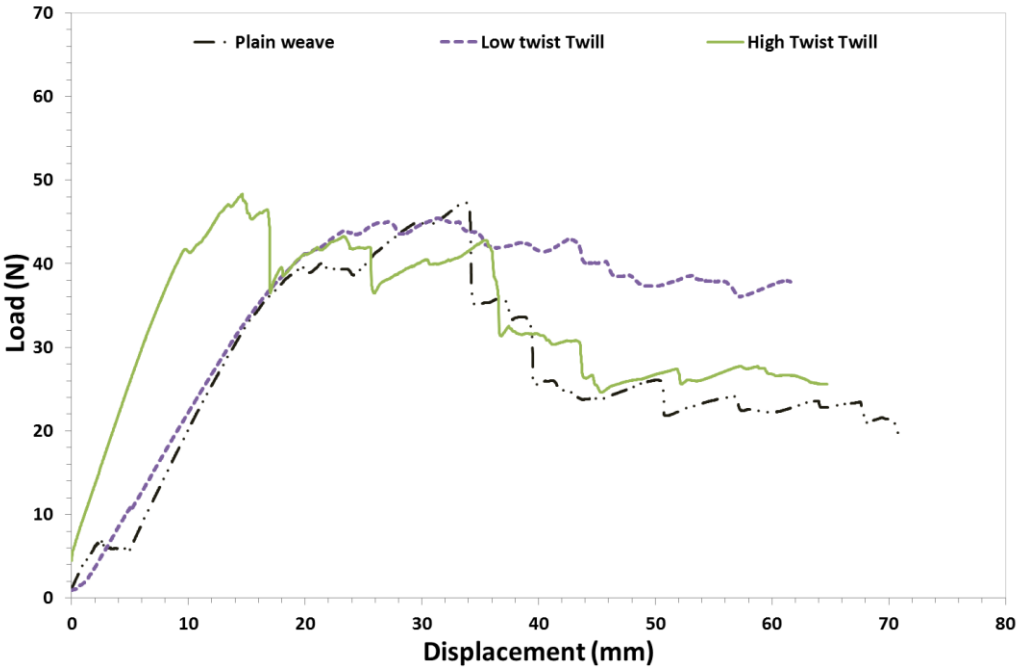

a)

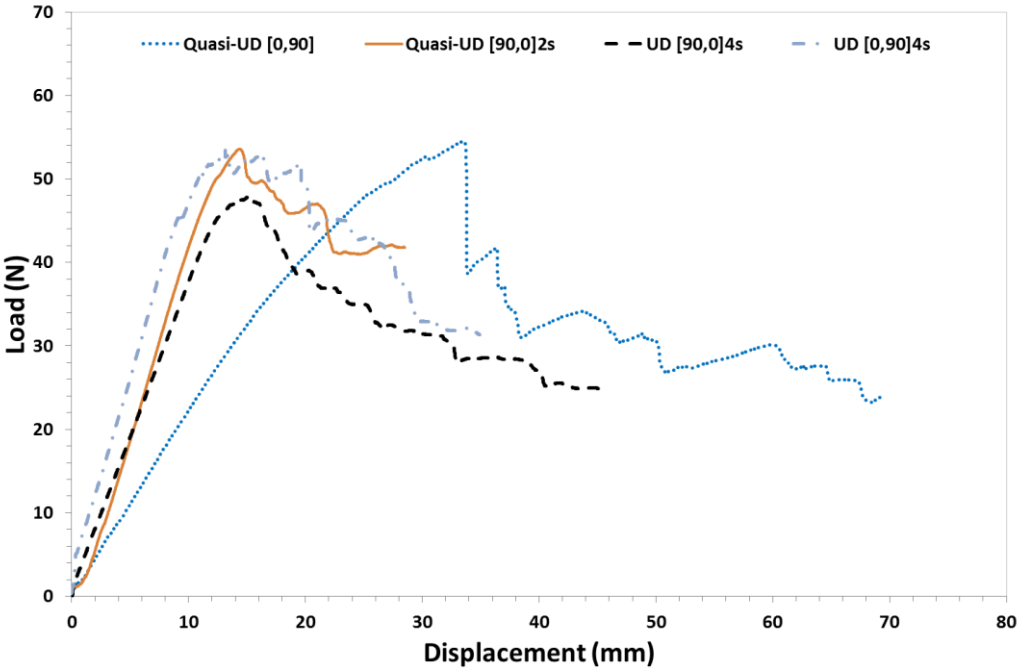

b)

Figure 7-16: Double Cantilever Beam test- Load/displacement curves for each tested architecture of the flax-epoxy matrix composites.

For the plain weave, the high twist twill and the Quasi-UD [0,90] presented in Figure 7-16a and b, the curves display a sharp decrease in load after the crack initiation point followed with a crack extension and a stable crack growth in the specimen. The sudden load drops observed correspond to an unstable crack growth at crack initiation point and depending on the amount of load drop (unstable crack growth), two types of P-δ can be seen [26, 30].

In the first case, when the displacement increases, only a small amount of load drop occurs immediately after the first crack onset. A small drop occurs with increasing displacement but overall a stable crack growth is observed. The second type features stick-slip behaviour (when the crack growth jumps and a load drop is seen) which occurs after the start of the crack propagation. In this case, a large amount of load drop may happen directly after crack onset with visually observable unstable crack growth. The unstable crack growth arrests after a certain amount of crack extension and may occur again as the load increases. These sudden drops could be caused by discontinuities in the composite structure such as geometry of the yarns and textile (high twist, crimp, etc...) which act as toughening mechanisms.

Both UD cross-ply composites and the Quasi-UD [90,0] (Figure 7-16 b) showed a similar P-δ pattern of crack propagation which started with non-linear increase in load with increasing crosshead displacement, followed by a constant decrease in load as the crack propagated. Furthermore, "mild stick-slip" phenomena were observed and are probably related to the periodical transverse cracking of the 90° mid-layer and crack jumping between two neighbouring 0°/90° interfaces where the Mode I fracture surfaces displayed a staircase-like morphology [32] as seen in Figure 7-18e for the UD [0,90]s. This will be further explained in the next sections.

In this study, an epoxy matrix has been used with an average fracture toughness of 300 J/m^2, as tested by Aravand et al. [33]. It is said that for brittle polymers such as epoxy, the interlaminar mode I-fracture toughness is 2-3 times higher than the matrix fracture toughness, due to the presence of the fibres [34-36], which was indeed the case in this study. In all cases, the addition of a fibre reinforcement results in an increase in fracture toughness over the unreinforced polymer as seen in Figure 7-17. The interlaminar fracture toughness for initiation varies from 457 J/m^2 for the plain woven composite to 777 J/m^2 for the Quasi-UD [90,0].

As the R-curves reach a plateau value for longer crack lengths (Figure 7-15b), a propagation value for the critical energy release rate could be defined. The propagation value varies from 663 J/m^2 for the UD [90,0] to 1597 J/m^2 for the Low twist. Compared to glass and carbon fibre UD and cross-ply composites with non-toughened epoxy matrix (G_{Ic}= 150-500J/m^2), as seen in Table 2-9, the mode I fracture toughness values of flax fibre composites are 3-5 times higher than for glass or carbon epoxy composites. It was also observed that the values are rather close to the carbon-PES and carbon-toughened epoxy values. Thus, if the fracture toughness of flax composites needs to be increased, a smart combination of flax with a tough and ductile thermoplastic would be optimum.

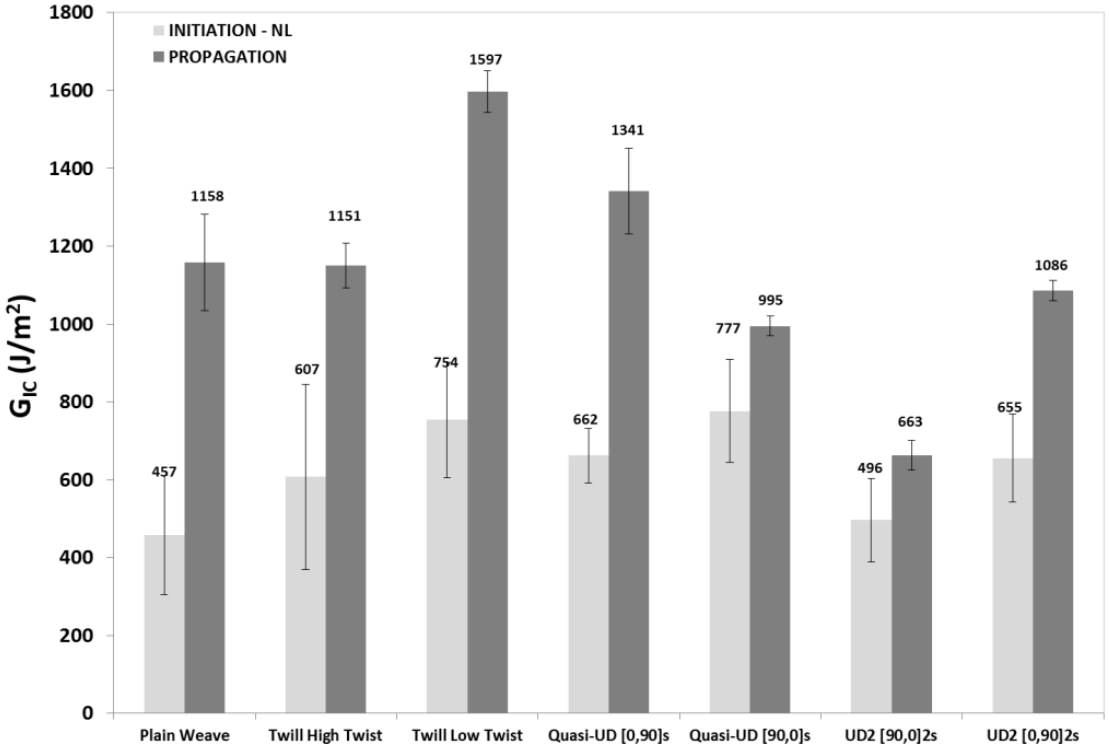

Figure 7-17: Double Cantilever Beam test - Fracture Toughness Mode I for flax-epoxy composites.

7.3.1.1 Toughening mechanisms

Several mechanisms contribute to the composites' interlaminar fracture toughness. The dominant toughening mechanism, crack deflection, occurs when the crack deviates to follow the yarn or fibre undulations as mentioned in the previous section [37]. This creates a new and/or larger crack area resulting in higher fracture energy. Kim et al. [38] have observed that since the fibres are stronger than the matrix, the presence of out-of-plane fibre bundles may hinder the crack propagation progress. This would then result in crack paths bypassing the unbroken out-of-plane fibre bundles which lead to extensive matrix deformation and fracture.

The second mechanism is the pull-out of the fibres from the matrix, dissipating the energy by friction. The third mechanism is related to fibre bridging: the fibres debond from the surface without breaking, and link both surfaces together. Hence, part of the applied stress is transferred to the bridging fibres delaying the crack progression (decrease of the driving force at the crack tip). Strong fibres will enhance the crack bridging effect, thus, when crack bridging occurs, the strength of the fibres plays an important role in toughness [21]. Additionally, the roughness of the fabric (hackled flax are less refined than yarn and there is direct contact between the resin and the technical fibres), may lead to an increase in crack bridging. This was observed for the UD [0,90] and the quasi-UD [0,90] which corroborate the increased toughness values that were found and the R-curves increase(see Figure 7-15). Finally, matrix and interface micro-cracking extends some way into the laminate from the crack tip.

7.3.1.2 UD vs woven

The woven fabrics and [0,90] laminates have an increased delamination resistance by a factor 1.5-2 compared to UD [90,0] reinforcements with propagation values varying from 1158 to 1597 J/m^2 compared to 663 J/m^2 as seen in Figure 7-17. This additional resistance may be due to the irregular path of the crack growth, caused by the yarns and crimp present.

In the case of cross-ply laminates, an increase in interlaminar toughness is observed when the crack propagates in-between the 90° layers instead of the 0° layers for both UD and quasi-UD.

When the crack propagates between the 90° layers, the plies are subjected to in-plane normal tension leading to an important transverse cracking inside the 90° layers [32, 39]. Furthermore, crack jumping between two neighbouring 0°/90° interfaces of UD [0,90] was observed in Figure 7-18e. This causes an increase in fracture toughness due to this deviation from the expected in plane crack path while for the UD [90,0] specimen, the crack propagated mid-plane. Similar observations were made by Marais et al. [32], Kalarikkal [40] and Rhee et al. [41].

7.3.1.3 Effect of weave and yarn geometry: twist, crimp, linear density, end picks and counts

During the preparation of the testing samples, the crack propagation direction was parallel to the warp direction. A closer look at the woven fabric structure shows that a decrease in the weft yarn linear density from 241 tex (low twist twill) to 27 tex (high twist twill) leads to a slight decrease in G_{IC} initiation and propagation values, because the thinner weft yarns will create less crimp and hence less crack deflections when the crack grows in the warp direction. However, no strong difference between the plain weave (147 tex) and the high twist twill propagation value was observed.

Next to the crimp created by weft yarns, the G_{IC} was strongly affected by the number of yarn crossovers (higher for low twist twill than for plain weave or high twill) factor of the woven composite preforms. Figure 7-17 shows that the G_{IC} for woven composites increases with decreasing end-pics and count (low tightness of the fabric leading to more open and more out-of-plane orientation of fibre bundles). As the layers are compacted during manufacturing, the merging of out-of-plane fibre bundles of the neighbouring layers increases as the end picks and counts factor decreases. This results in an increased nesting and the crack follows a more highly wavy path where side cracks and fibre bridging are expected and this results in higher G_{IC} [38].

7.3.1.4 Effect of nesting

The higher toughness of the low twist twill and the Quasi-UD [0,90] may also be due to the nesting phenomenon. When nesting occurs, the crack will follow a more tortuous path, hence increasing the energy needed to propagate the delamination and thus the interlaminar fracture toughness for propagation [27]. Images of the cross-sections of the investigated composites are presented in Figure 7-18. An increased nesting for the low twist twill (Figure 7-18b) and Quasi-UD [0,90] (Figure 7-18d) was observed compared to the other configurations. Although the plain woven fabric (Figure 7-18a) shows a certain degree of nesting, the presence of highly twisted yarns will tend to create large resin pockets where the crack easily propagates. For the highly twisted twill (Figure 7-18c), because of the low linear density of the yarn, the produced composite was made of very thin layers which will also create a "flat" surface where the crack can grow easily without having to get around the yarn. These observations were corroborated by Cheremisinoff [42].

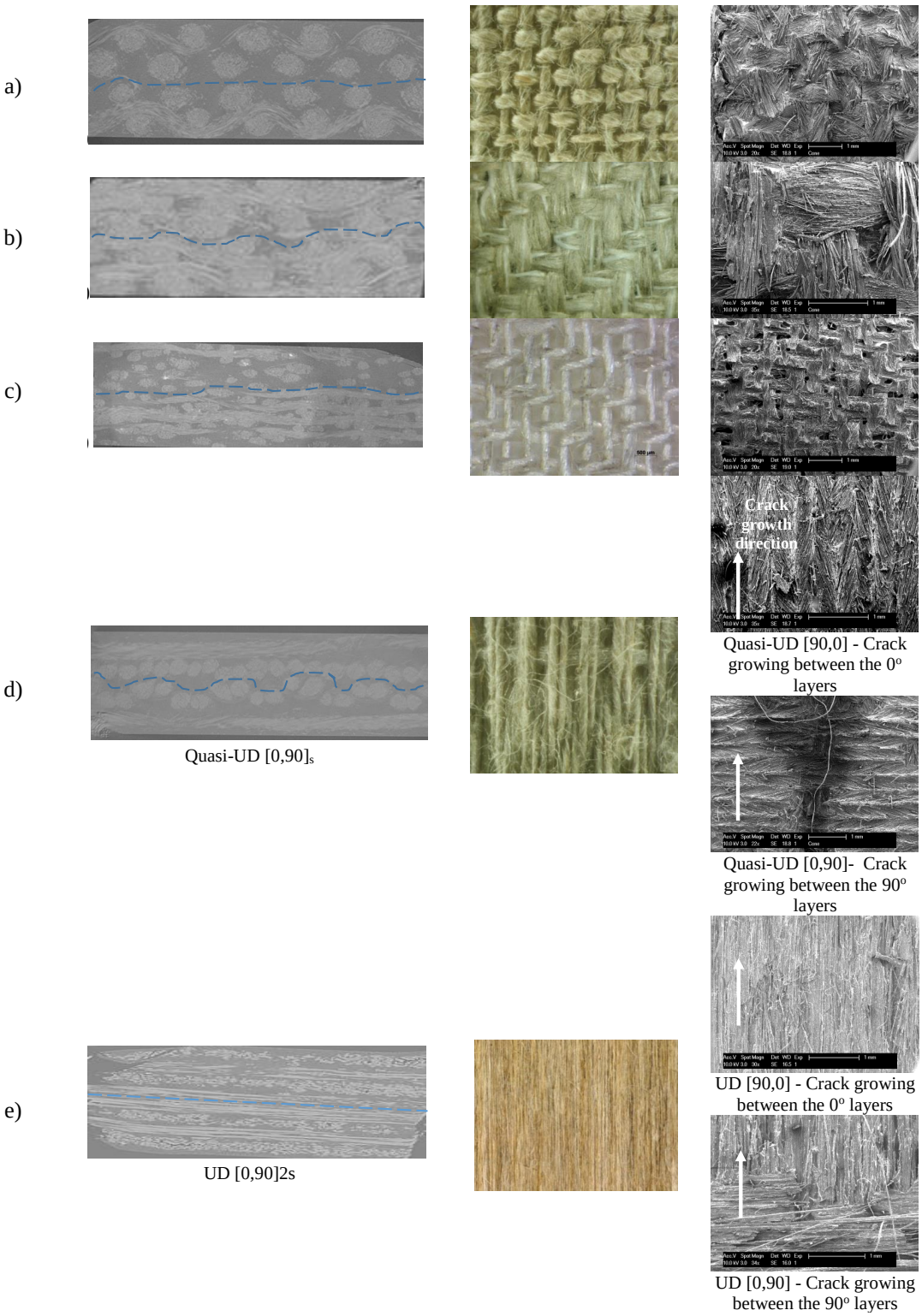

Figure 7-18: Micro-CT (cross-section), Optical microscopy (fabric surface) and SEM images of the composite to evaluate their nesting capabilities: a) plain weave, b) low twist twill, c) high twist twill, d) Quasi-UD and e) UD. The potential crack path is indicated on the micro-CT images with the dashed line).

7.3.2 Mode II interlaminar fracture toughness

Mode II of the fracture toughness was measured using the ENF test. The main difference between mode I and II is that the first is a tensile mode where the two half beams (vertical opening of the crack surfaces) move apart from each other. On the other hand, the mode II is an in-plane shear mode where the surfaces slide over each other perpendicularly. This

loading condition leads to an unstable crack growth allowing only the measurement of the crack initiation value presented in Figure 7-19. The crack does not move during the initial loading of the sample and will suddenly unstably propagate after a load drop. It has been mentioned in the literature [43-45], that the toughness of G_{IIc} always exceeds G_{Ic}. It has been mentioned that a brittle matrix with a low G_{Ic} value has a G_{IIc} value that is much higher, while the tougher matrix materials still have a higher G_{IIc} than G_{Ic} but their values are closer.

The energy absorbing mechanisms observed in mode II have similarities to the ones of the mode I such as matrix cracking, fibre breakage, the effect of internal structure of the composite (textile geometry) and crack path deflection previously discussed. However, fibre/matrix debonding, roller formation and shear cusp deformation (hackles due to matrix shear cracks) and coalescence. The plastic deformation on the fracture surface at the crack tip [46], shear friction [47] and transverse shear deformation [48], are also important energy absorbing mechanisms seen in Mode II [49].

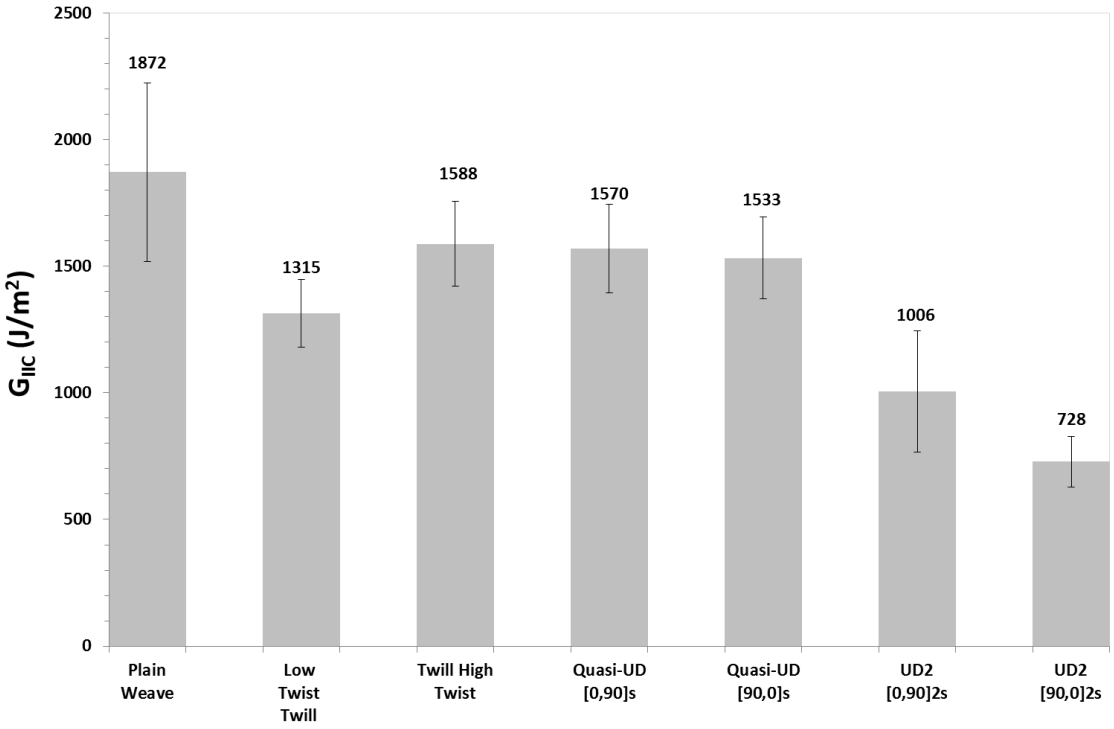

Figure 7-19: End Notched test – Fracture toughness Mode II.

The results for all configurations are presented in Figure 7-19 and show that the architecture type has an effect on the results. The high twist twill and the quasi-UD laminates have similar mode II fracture toughness values, which can be related to the fineness of the yarns used in these preforms, as discussed in previous sections. The UD [90,0] laminate displays lower properties as the crack easily travels in between the 0 degrees layers. As for the UD [0,90] laminate, more resistance to crack growth was seen as the crack grows perpendicular to the 90°-fibres, and hence it can deviate around the fibres and even "jump" to the neighbouring 0^o layers, in the same fashion as in mode I (see Figure 7-18e). The plain woven fabric seems to have the highest resistance to mode II crack growth, although it had an average performance for damage resistance. It can be said that the use of flax as a reinforcement increases the mode II toughness compared to synthetic fibres (see Table 2-10 in Chapter 2).

The only exception is the UD fabric which shows a similar value to unidirectional glass and carbon thermoset composites. This is probably caused by low fibre strength in the case of the UD [0,90] where the crack can "go through" the fibres. For UD [90,0], the crack has a clear and easy path along the fibres explaining the further decrease from the UD [0,90] value. Thus it can be said that the more complex the composite internal weave structure, the more the G_{IIc} increases as there is a higher resistance to crack growth in shear mode.

In woven composites, the presence of crimp (increased by the presence of high twist) will impede the sliding motion between the plies because of the possible mechanical interlocking of one ply upon the adjacent layer which becomes worse as the crack is progressing. On the other hand, UD composites have no crimp that could hinder the deformation and ultimately the crack progression. Zureick et al. [49] stated that the crimp "mechanical interference" has a behaviour that is equivalent to an exceptionally high "interfacial frication" between the plies which hinders the plies' sliding effect needed for crack growth.

7.3.3 The tensile toughness

The toughness of a material can be defined as the area under the stress-strain curve of a tensile test, and represents the strain energy per unit of volume, stored in the material up to the moment of fracture. Materials with high strength and high deformation to failure (ductility) have a high tensile toughness.

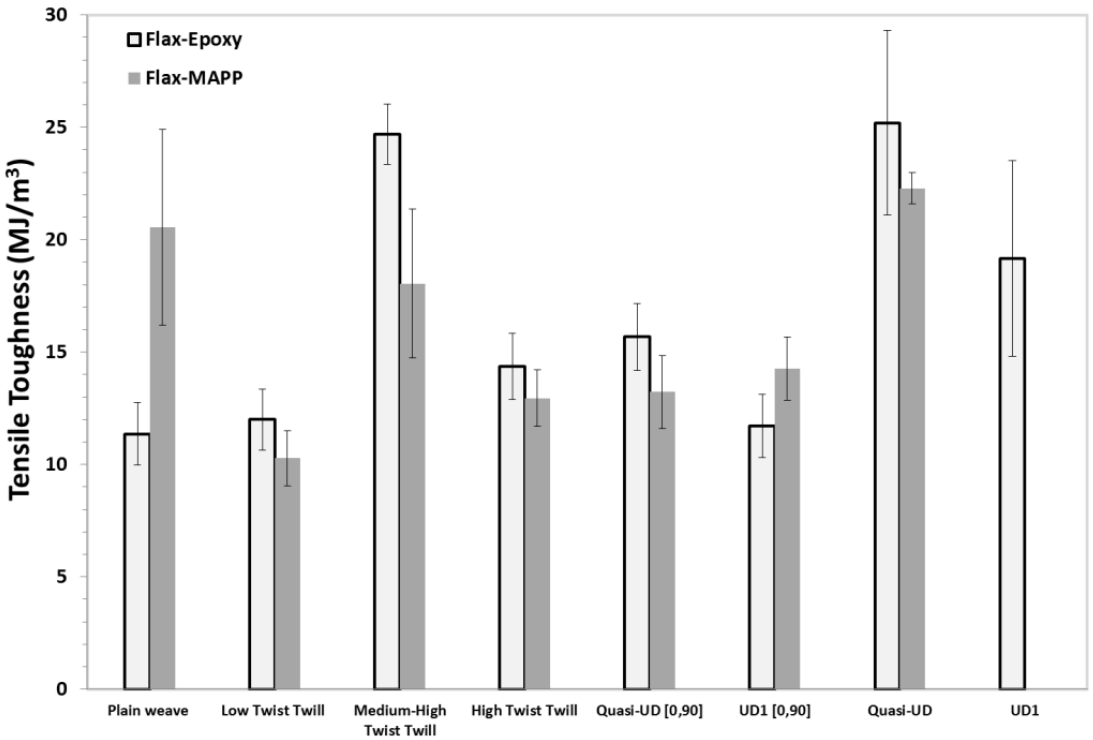

Figure 7-20: Tensile toughness of flax-epoxy and flax-MAPP composites.

Figure 7-20 presents the tensile toughness results for the studied thermoset and thermoplastic combinations. It can be seen that for most of the thermoset composites, the tensile toughness was higher than for the thermoplastic composites. The thermoset epoxy matrix was strong but not ductile, while MAPP thermoplastic matrix was ductile but 1/10 as strong. This leads to similarly shaped stress-strain curves, but significant variations in the strength and deformation values for the composite, and thus to a variation in area under

the curves. Indeed, the difference in strain to failure is apparent between thermoset (1.22-2.14%) and thermoplastic (1.6-2.65%) composites. Although the MAPP matrix is ductile, the composite failure strain is limited by the flax fibre failure strain which is in the range of 1.5-2% [50] thus giving a less stiff and strong composite.

The plain weave-MAPP composite was not taken into account because of the big differences in strength and stiffness (see Chapter 5 section 5.3.1). The obtained tensile toughness was much higher than for the plain weave-epoxy combination. The fabric was based on highly twisted yarns ($\alpha \approx 20^{o}$), which lead to impregnation difficulties as the local permeability may be too low to allow an easy impregnation between and inside the technical fibres present in the yarn as previously discussed in Chapter 5. The area under the curves is higher as the composite experiences higher strains as seen in Figure 7-21 [51]. Thus, the behaviour of the composite is fibre-dominated in tensile and dominated by the matrix ductility in impact and toughness properties.

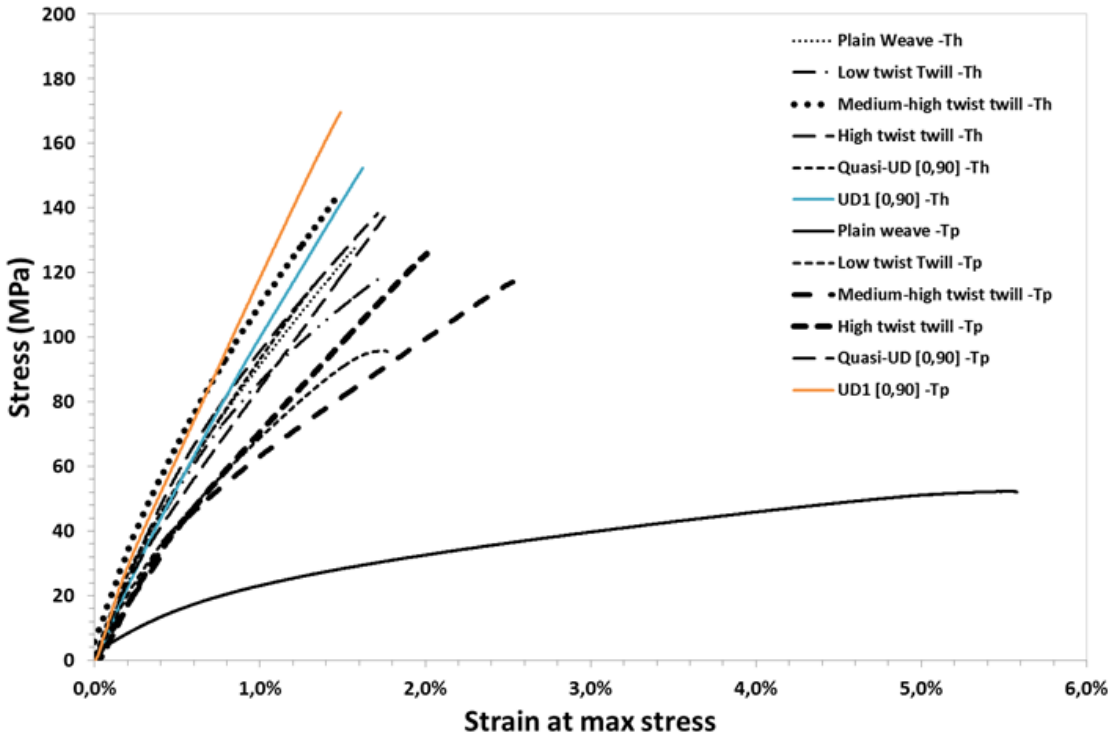

Figure 7-21: Examples of the stress-strain curves of the flax-epoxy and flax-MAPP composites used to calculate the tensile toughness.

7.4 On the correlation between toughness and impact properties

7.4.1 Fracture toughness vs damage resistance/tolerance

In literature, a good correlation was found between Mode I and II interlaminar toughness and the damage resistance/tolerance as the damaged area (propagation of delamination) is connected to these modes as mentioned by Cantwell et al. [16] and Schrauwen et al.[2]. It has to be taken into account that the G_{Ic} and G_{IIc} characterize the resistance to delamination growth, whereas the damage resistance includes a few main energy absorbing mechanisms: delaminations, fibre fracture, matrix cracking and interfacial debonding and pull-out.

In this study, the main impact damages observed were fibre fracture and matrix cracking. The delaminations were limited thanks to the high values of interlaminar fracture toughness obtained which lead to the composites failing due to a through thickness crack. Fibre debonding and pull-out was limited due to good fibre-matrix adhesion.

In the data obtained for the flax-epoxy, the above correlation was not straightforward with the damage tolerance data. The present work differs from that in [2] and [16] as they both use the compression after impact testing technique. However, in this study, a three-point bending test was done to characterise the failure after impact, leading to a mixed "bending-shear" phenomenon. The three point bending option was chosen in order to showcase the "worst case scenario", but a four point bending strategy (pure bending mode) for these materials would have been more suitable. Efstratiou [52] has hypothesized that the poor correlation to the FAI results may be due to**:**

- The fracture surface roughness which allows some shear transfer between the two half-beams;
- An inaccurate crack position due to the presence of secondary cracks branching out from the main crack;
- Large deformations that cause membrane forces on the beam.

Another reason may be related to the fact that the flexural strength after impact in flax composites is probably dominated by the through-thickness cracks and not by the (very small) delaminations observed.
This clearly brings the relation of damage resistance and damage tolerance to the front. Materials that perform well on damage resistance will perform well on damage tolerance.

7.4.2 Perforation energy vs tensile toughness

Generally, materials that show a good perforation energy performance are those with high tensile toughness [53]. The material tensile toughness comes in play when the impact force is applied over a short period of time and relates to the maximum force that a material can withstand upon sudden impact. The perforation energy is dependent of the material capability to deform upon impact. Thus, materials that show high deformation (strain) in a stress- strain curve have a better impact performance. Furthermore, composites with low modulus but high elongation (such as flax-MAPP composite in this study) would be tougher than those with high modulus and low elongation [54].

Many authors [16, 53, 55] have reported a direct correlation between the tensile toughness and the perforation energy under impact loading. It was observed that the higher the toughness, the better performance against perforation impact. Results presented in Figure 7-22 corroborate this assumption. The perforation energy of flax-MAPP composite correlates to the tensile toughness which displays an increased absorbed energy with increasing tensile toughness due to a matrix and architecture dominated failure mode.

However for flax-epoxy composites, the tensile toughness calculus using the composites' tensile stress-strain curve does not show a relationship with the perforation energy. As the main mode of failure in impact is fibre breakage (due to low transverse properties of the flax fibre), the perforation energy was evaluated against the flax yarn (from the tested textiles) tensile toughness calculated from the IFBT tests. A linear correlation was found in this case meaning that the failure mode of the thermoset materials is a fibre dominated phenomenon. The high twist twill composite tensile toughness data do not correlate due to its low perforation energy (5.7J), as previously discussed in section 7.2.1.

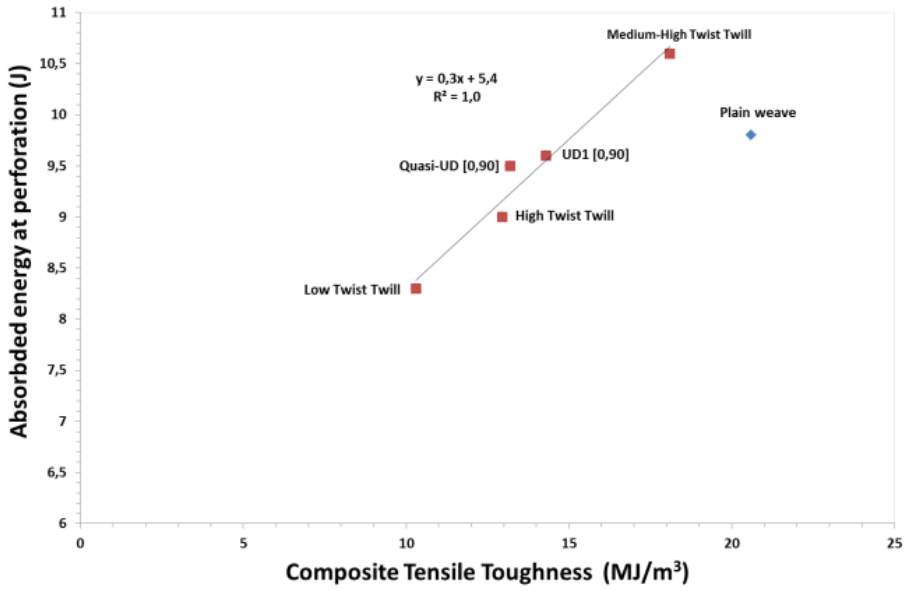

a)

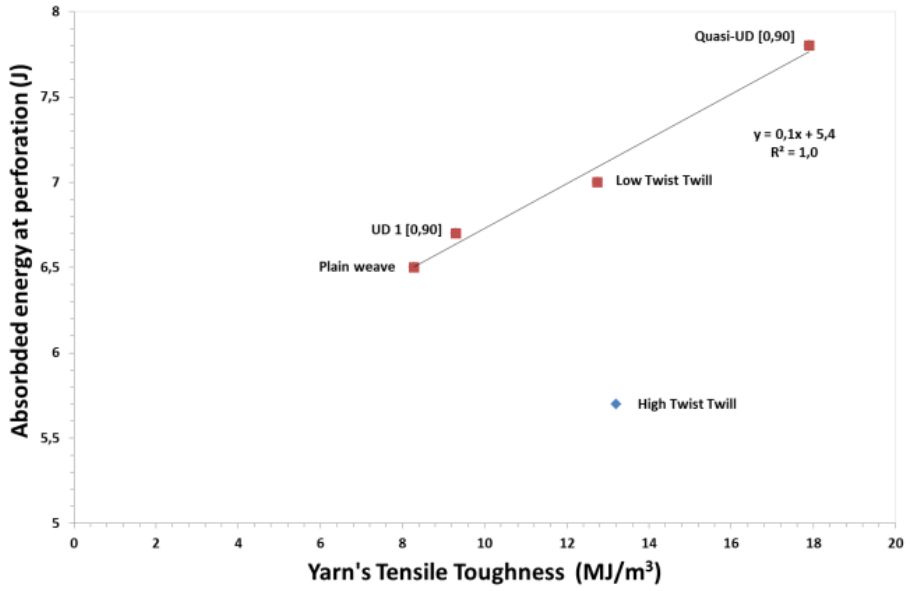

b)

Figure 7-22: Perforation energy vs tensile toughness: a) Flax-MAPP composite and b) Flax-epoxy composites.

7.5 Conclusions

The objective of this work was to determine the influence of fibre architectures and choice of matrix on the impact behaviour and the interlaminar fracture toughness of flax fibre composites. One of the major conclusions was that the matrix ductility has a large influence on the absorbed energy, damage resistance and damage tolerance while these are mostly fibre architecture independent. The absorbed energy at perforation for the flax fibres impregnated with MAPP was more than 50% higher compared to the epoxy based composites.

The total damage for non-perforated samples was constrained to the impact area with little delamination growth. This was the result of the high interlaminar fracture toughness, combined with the low transverse strength of the flax fibres, which concentrates the damage to cross-like macro-cracks with only small delaminations. Furthermore, low residual properties were observed for the thermoplastic composites. However, the decrease in

flexural properties after impact was marginal. The thermoset composites have higher flexural properties both before and after impact. Nevertheless, the decrease in properties after impact is higher due to the brittle nature of the matrix.

As in most composites, the damage area after impact is directly related to its capacity to resist delamination growth, it was essential to evaluate the interlaminar fracture toughness. This study showed promising results of the flax-epoxy composite performance in both mode I and mode II interlaminar fracture toughness. The hypothesis that the presence of delaminations has an important influence on the impact performance of the flax composites has been proved wrong as limited amount of delamination was seen thanks to high interlaminar fracture toughness properties. The addition of flax fibre increases both the G_{IC} and G_{IIc} of the materials over that of the unreinforced polymer and those of glass and carbon fibres. Further improvements are made with the use of woven textile compared to the [0, 90] cross ply lay-ups. Finally, the tensile toughness was found to be a good indicator of the capacity of a material to sustain perforation or non-perforation impact.

References

[1] Belingardi G, Vadori R. Low velocity impact tests of laminate glass-fiber-epoxy matrix composite material plates. International Journal of Impact Engineering. 2002;27(2):213-29.
[2] Schrauwen B, Peijs T. Influence of Matrix Ductility and Fibre Architecture on the Repeated Impact Response of Glass-Fibre-Reinforced Laminated Composites. Applied Composite Materials. 2002;9(6):331-52.
[3] Richardson MOW, Wisheart MJ. Review of low-velocity impact properties of composite materials. Composites Part A: Applied Science and Manufacturing. 1996;27(12):1123-31.
[4] Vallons K. Invloed van de matrixtaaiheid op de impactweerstand van thermoplastische PBT composieten, MTM KULeuven; 2005.
[5] Bibo GA, Hogg PJ. Influence of reinforcement architecture on damage mechanisms and residual strength of glass-fibre/epoxy composite systems. Composites Science and Technology. 1998;58(6):803-13.
[6] Caprino G, Lopresto V. On the penetration energy for fibre-reinforced plastics under low-velocity impact conditions. Composites Science and Technology. 2001;61(1):65-73.
[7] Sutherland LS, Guedes Soares C. Impact tests on woven-roving E-glass/polyester laminates. Composites Science and Technology. 1999;59(10):1553-67.
[8] Abrate S. Impact engineering of composite structures. Carbondale: SpringerWienNewYork; 2011.
[9] Duell JM. Impact Testing of Advanced Composites. Advanced Topics in Characterization of Composites. 2004;97.
[10] Cubberly WH. Tool and Manufacturing Engineers Handbook Desk Edition: Society of manufacturing engineers; 1989.
[11] François D, Pineau A. From Charpy to present impact testing: Elsevier; 2002.
[12] INSTRON. Instron Impact Test Types. 2016. http://www.instron.us/en-us/our-company/library/test-types/impact-testing/test-types
[13] Pagliarulo V, Rocco A, Langella A, Riccio A, Ferraro P, Antonucci V, Ricciardi MR, et al. Impact damage investigation on composite laminates: comparison among different NDT methods and numerical simulation. Measurement Science and Technology. 2015;26(8):085603.
[14] de Vasconcellos DS, D'Auria M, Iannace S, Sorrentino L, Sarasini F. POLY (ETHYLENE 2, 6-NAPHTHALATE)-PEN AS THERMOPLASTIC MATRIX FOR HIGH PERFORMANCE WOVEN COMPOSITES.
[15] Liu L-Y, Han Y-L, Zhang F. Experimental study on impact behavior of flax fiber reinforced PP laminates. 2011 International Conference on Textile Engineering and Materials, ICTEM 2011, September 23, 2011 - September 25, 2011. Tianjin, China: Trans Tech Publications; 2011. p. 735-8.
[16] Cantwell WJ, Morton J. The impact resistance of composite materials — a review. Composites. 1991;22(5):347-62.
[17] Zhao N, Rödel H, Herzberg C, Gao S-L, Krzywinski S. Stitched glass/PP composite. Part I: tensile and impact properties. Composites Part A: Applied Science and Manufacturing. 2009;40(5):635-43.
[18] Kim J-K, Sham M-L, Sohn M-S, Hamada H. Effect of hybrid layers with different silane coupling agents on impact response of glass fabric reinforced vinylester matrix composites. Polymer. 2001;42(17):7455-60.
[19] Sohn M, Hu X, Kim JK, Walker L. Impact damage characterisation of carbon fibre/epoxy composites with multi-layer reinforcement. Composites Part B: Engineering. 2000;31(8):681-91.
[20] ISA MT, AHMED AS, ADEREMI BO, TAIB RM, AKIL HM, MOHAMMED-DABO IA. Drop weight impact studies of woven fibers reinforced modified polyester composites. Leonardo Electronic Journal of Practices and Technologies. 2014(24):97-112.
[21] Liu Q, Hughes M. The fracture behaviour and toughness of woven flax fibre reinforced epoxy composites. Composites Part A: Applied Science and Manufacturing. 2008;39(10):1644-52.
[22] Baley C, Perrot Y, Busnel F, Guezenoc H, Davies P. Transverse tensile behaviour of unidirectional plies reinforced with flax fibres. Materials letters. 2006;60(24):2984-7.

[23] Shyr T-W, Pan Y-H. Impact resistance and damage characteristics of composite laminates. Composite Structures. 2003;62(2):193-203.
[24] Bensadoun F, Depuydt D, Baets J, Vuure V, Willem A, Verpoest I. Impact resistance, damage and absorbed energy Behaviour of Flax-Based composites. Composite week @ Leuven Leuven (Belgium):2013.
[25] Albertsen H, Ivens J, Peters P, Wevers M, Verpoest I. Interlaminar fracture toughness of CFRP influenced by fibre surface treatment: Part 1. Experimental results. Composites Science and Technology. 1995;54(2):133-45.
[26] Zhu Y. Characterization of interlaminar fracture toughness of a carbon/epoxy composite material, The Pennsylvania State University; 2009.
[27] Olave M, Vara I, Husabiaga H, Aretxabaleta L, Lomov SV, Vandepitte D. Nesting effect on the mode I fracture toughness of woven laminates. Composites Part A: Applied Science and Manufacturing. 2015;74:166-73.
[28] Laksimi A, Benzeggagh ML, Jing G, Hecini M, Roelandt JM. Mode I interlaminar fracture of symmetrical cross-ply composites. Composites Science and Technology. 1991;41(2):147-64.
[29] Melcher RJ, Johnson WS. Mode I fracture toughness of an adhesively bonded composite–composite joint in a cryogenic environment. Composites Science and Technology. 2007;67(3–4):501-6.
[30] Blackman B, Kinloch A. Protocol for the determination of the Mode I adhesive fracture energy, GIc, of structural adhesives using the double cantilever beam (DCB) and tapered double cantilever beam (TDCB) specimens. Version 00-08 European Structural Integrity Society Polymers, Adhesives and Composites TC4 Committee. 2000.
[31] De Moura M, Campilho R, Amaro A, Reis P. Interlaminar and intralaminar fracture characterization of composites under mode I loading. Composite Structures. 2010;92(1):144-9.
[32] de Morais AB, de Moura MF, Marques AT, de Castro PT. Mode-I interlaminar fracture of carbon/epoxy cross-ply composites. Composites Science and Technology. 2002;62(5):679-86.
[33] Aravand M, Lomov SV, Gorbatikh L. Morphology and fracture behavior of POM modified epoxy matrices and their carbon fiber composites. Composites Science and Technology. 2015;110:8-16.
[34] Parker DS, Sue H-J, Huang J, Yee AF. Toughening mechanisms in core-shell rubber modified polycarbonate. Polymer. 1990;31(12):2267-77.
[35] Bradley WL. Understanding the translation of neat resin toughness into delamination toughness in composites. Key Engineering Materials: Trans Tech Publ; 1991. p. 161-98.
[36] Hunston D, Moulton R, Johnson N, Bascom W. Toughened composites. American Society for Testing and Materials, Philadelphia, PA. 1987:74-94.
[37] Silva RV, Spinelli D, Bose Filho WW, Claro Neto S, Chierice GO, Tarpani JR. Fracture toughness of natural fibers/castor oil polyurethane composites. Composites Science and Technology. 2006;66(10):1328-35.
[38] Kim K-Y, Curiskis JI, Ye L, Fu S-Y. Mode-I interlaminar fracture behaviour of weft-knitted fabric reinforced composites. Composites Part A: Applied Science and Manufacturing. 2005;36(7):954-64.
[39] Allix O, Ladevéze P, Corigliano A. Damage analysis of interlaminar fracture specimens. Composite Structures. 1995;31(1):61-74.
[40] Kalarikkal SG. Fracture Toughness of Graphite/Epoxy Laminates at Cryogenic Conditions, University of Florida; 2004.
[41] Rhee KY, Koh SK, Lee JH. Mode I fracture resistance characteristics of graphite/epoxy laminated composites. Polymer Composites. 2000;21(2):155-64.
[42] Cheremisinoff N. Handbook of Ceramics and Composites - Volume 2: Mechanical Properties and Specialty Applications: CRC Press 1991.
[43] OBrien TK. Composite Interlaminar Shear Fracture Toughness, G (sub 2c): Shear Measurement of Sheer Myth? 1997.
[44] Lens LN, Bittencourt E, d'Avila VM. Mecánica Computacional, Volume XXVII. Number 17. Fracture, Fatigue and Damage Material Modeling (B). 2008.
[45] Dillard DA, Singh HK, Pohlit DJ, Starbuck JM. Observations of decreased fracture toughness for mixed mode fracture testing of adhesively bonded joints. Journal of Adhesion Science and Technology. 2009;23(10-11):1515-30.
[46] Roylance D. Introduction to fracture mechanics. Massachusetts Institute of Technology, Cambridge. 2001.
[47] Gillespie Jr JW, Carlsson LA, Pipes RB. Finite element analysis of the end notched flexure specimen for measuring mode II fracture toughness. Composites Science and Technology. 1986;27(3):177-97.
[48] Wang J, Qiao P. Novel beam analysis of end notched flexure specimen for mode-II fracture. Engineering Fracture Mechanics. 2004;71(2):219-31.
[49] Zureick A-H, Nettles AT. Composite Materials: Testing, Design, and Acceptance Criteria: ASTM International; 2002.
[50] Verpoest I, Baets J, Van Acker J, Lilholt H, Mussig J, Hughes M, Baley C, et al. Flax and Hemp fibres: a natural solution for the composite industry. First Edition. In: Reux F, Verpoest I, editors. Paris, France. Prepared for JEC by the European Scientific Committee of CELC: JEC Group/CELC; 2012. ISBN 978-2-9526276-1-0.
[51] Bensadoun F, Baets J, Verpoest I, Van Vuure A. Designing with Flax Fibre Reinforced Composites - Characterization of Textile Architectures. submitted to Composites Part A: Applied Science and Manufacturing. 2016.
[52] Efstratiou V. Investigation of the effect of the 2.5-D carbon fabric construction on fabric reinforced/polymer matrix composite toughness,PhD Thesis, Leuven (Belgium), KU Leuven; 1995.
[53] Roylance D. Stress-strain curves. Massachusetts Institute of Technology study, Cambridge. 2001.
[54] David DJ, Misra A. Relating Materials Properties to Structure with MATPROP Software: Handbook and Software for Polymer Calculations and Materials Properties: CRC Press; 2001.
[55] Tamin MN. Damage and fracture of composite materials and structures: Springer; 2012.

Chapter 8
Fatigue behaviour assessment of flax-epoxy composites

The investigation of the damage development will be performed through the assessment of modulus degradation and the cyclic creep phenomena, but also by observation of the hysteresis loops. The residual properties are later on evaluated and correlated to the observed modulus degradation and cyclic creep. Furthermore, the originality of this work is that it seeks to understand not only the fatigue behaviour of flax composites but also how the architecture such as woven, unidirectional and random orientation affects the properties.

The aim of this study is to investigate S–N diagrams constructed from fatigue data at stress ratios of $R = 0.1$ (tension–tension) at various stress levels for nine different flax textile architectures, described in Table 8-1, and combined with an epoxy matrix. The composites were manufactured via the resin transfer moulding process. The laminates are composed of several layers of fabrics in order to obtain a fibre volume fraction (V_f) of ≈ 40%, except for the random mat composite which has a $V_f \approx 30\%$.

Flax fibre preform architectures	Yarn type	Lay-up
Random Mat	dry fibres	$[0]_3$
Plain weave	wet spun	$[0]_4$
Twill Low Twist	dry roving with polyester binder yarn	$[0]_4$
Twill Medium-Low Twist	dry spun	$[0]_6$
Twill High Twist	wet spun	$[0]_8$
Quasi-UD [0,90]*	wet spun	$[0,90]_{2s}$
UD [0,90]**	water-treated	$[0,90]_{4s}$
Quasi-UD*	Wet spun	$[0]_4$
UD**	water-treated	$[0]_6$

* 90% of fibres in 0º direction and 10% in the 90º direction.**Flax UD2 from Lineo.

Table 8-1: Flax fibres and epoxy matrix characteristics.

The ultimate tensile strength (UTS) data necessary for the determination of the stress level for the tension-tension fatigue testing, is taken from the values reported in Chapter 5 and Appendix B. The tensile test sample dimensions and testing parameters are reported in Chapter 4. The tensile stiffness is calculated in two distinct regions, E_1 between 0 and 0.1% strain and E_2 between 0.3 and 0.5% strain as mentioned in Chapter 5.

The motivation for calculating two values for the stiffness is because of a typical decrease in stiffness for these materials around 0.2% strain in flax fibres, which is observed for all the studied configurations. The stiffness decrease rate (strain softening) will depend on the type of preform used in the composite. The more fibre-dominated behaviour, the more the softening will be visible which has to be taken into account while analysing Figure 8-1a. It is thus important to mention both values, as they both are relevant for design purposes. With these tensile tests, the stiffness, i.e. E_1 and E_2, and the ultimate tensile strength (UTS) were obtained (Figure 8-1b). The UTS is later used to determine the applied stress levels used during fatigue testing. These quasi-static properties are later on compared to the post-fatigue tensile properties obtained after the cyclic loading.

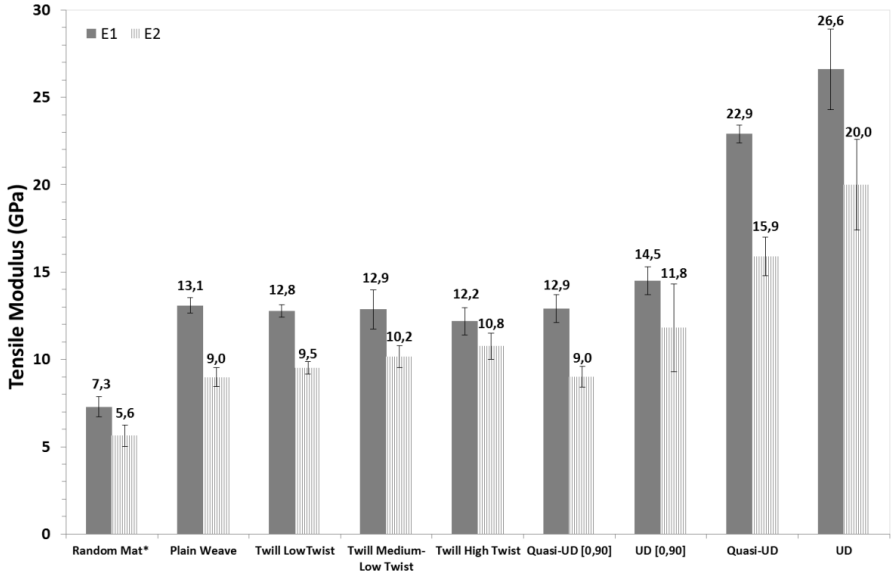

a)

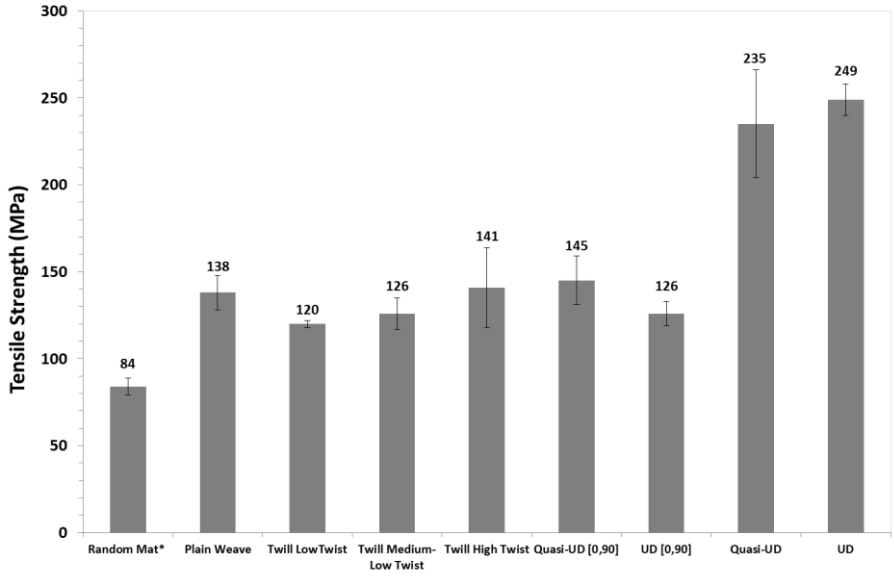

b)

Figure 8-1: a) the E_1 and E_2 moduli and b) the ultimate tensile strength of the flax/epoxy composites.

Strain monitoring was also used during fatigue testing in order to assess the stiffness degradation rates as well as the hysteresis loops. These data were also used to investigate the energy dissipation capability and the gradual build-up of the permanent strain of each material. The post-fatigue properties are also evaluated in order to assess the degradation rate of the composite through time. This investigation is crucial in order to understand the damage state, the post fatigue properties and fatigue life. This information will help to assess the durability of these types of composite materials, since these properties have a great influence on the service life, product safety and liability.

8.1 Fatigue life assessment

8.1.1 S-N curves

Tensile–tensile fatigue cycling was carried out at stress ratios of $R = 0.1$ and at maximum stress levels corresponding to various fractions of the UTS registered during quasi-static testing. This value of UTS is referred to as S_0, and it is later used to normalize the maximum stress levels that the samples are subjected to (S/S_o). Figure 8-2 presents a global, and hence rather crowded overview of the S-N curves, describing the fatigue life of the nine chosen flax/epoxy configurations.

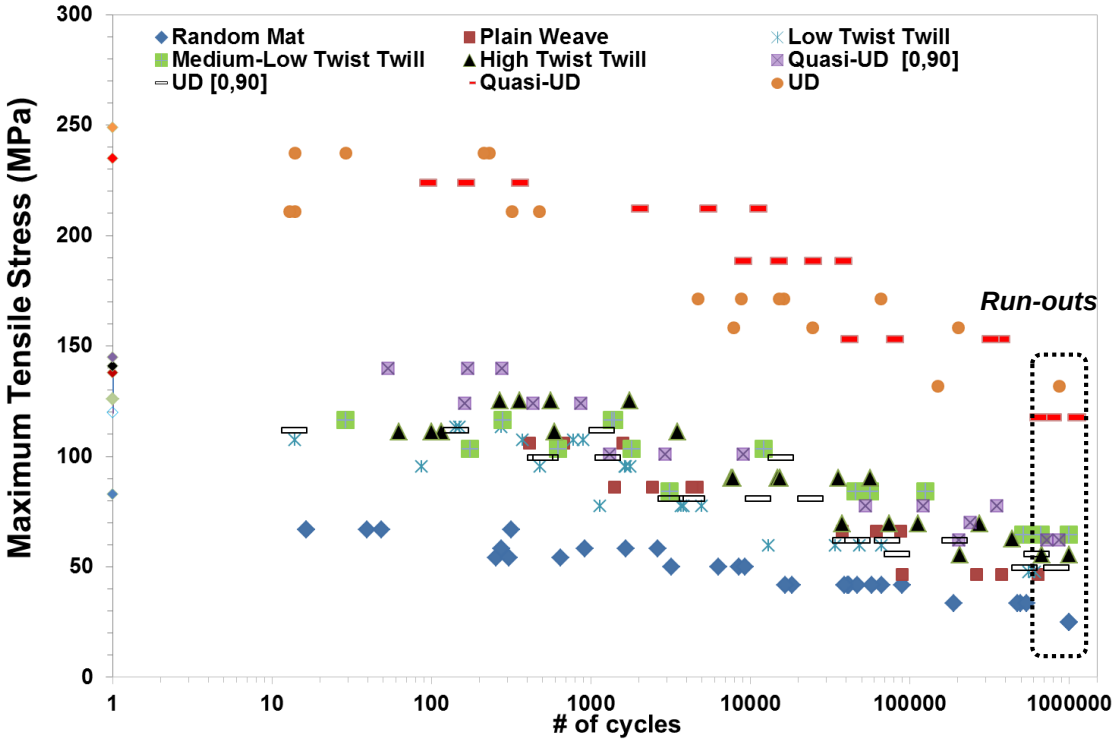

Figure 8-2: Stress-life data for untreated flax-epoxy composites at $R = 0.1$ (including quasi-static strengths values).

It can be observed that the random mat is the lowest performing laminate compared to textiles, cross-ply and UD laminates, as expected. Furthermore, the slopes of the S–N curves show a slightly steeper decrease for the Quasi-UD composite in comparison to the UD composite while all the textiles (plain weave, twills) and the cross-ply laminates display similar slopes for the S-N curves, as presented in Figure 8-2. This observation is consistent with the quasi-static test data, meaning that composites displaying high quasi-static strength have longer fatigue lifetimes when tested at the same maximum stress level. However, higher quasi-static strength becomes less important as the number of fatigue cycles imposed increases, just as Towo et al. [1] found for sisal fibre composites. Indeed, as the loading

level decreases, all textile and cross-ply laminates are achieving comparable lifetimes, which suggests that at lower stress levels (below UTS=30%), there is no need to use textile reinforcements with higher quasi-static strength. It is also observed that the degradation rate is faster for a UD-based cross-ply $[0,90)_{4s}$ than for the UD samples, as was also observed by Shah et al. [2] on polyester-flax composites.

The power–law regression curves, as presented in Table 8-2 (first column), are following the experimental data quite well (excluding the quasi-static strength values) with an $R^2 > 0.8$. As the S-N curves for the UD and the quasi-UD fabrics overlap, the quasi-static properties of both architectures were compared using the one-way analysis of variance statistical techniques, ANOVA, with a confidence interval of 95% (α=5%). This was combined to a post hoc single-step multiple comparisons (grouping) done using the Tukey´s method. The calculations were performed using the JMP11 statistical discovery software from SAS software [3].

	Fatigue life power law curves
Random Mat	$84x^{-0,08}$
Plain Weave	$226x^{-0,12}$
Low Twist Twill	$175x^{-0,10}$
Medium-Low Twist Twill	$158x^{-0,06}$
High Twist Twill	$193x^{-0,086}$
Quasi-UD [0,90]	$209x^{-0,088}$
UD [0,90]	$170x^{-0,086}$
Quasi-UD	$357x^{-0,074}$
UD	$271x^{-0,05}$

Table 8-2: Fatigue life power law curves for all configurations.

It has been found that for the quasi-static strength, the UD and the quasi-UD architectures are statistically equivalent within the 95% confidence level. As their quasi-static strengths are comparable and their fatigue curves overlap, it can be said that they present similar fatigue life and damage mechanisms. However, the fatigue life slope of the Quasi-UD composites slightly differs from the pure UD composite with a decrease of 28MPa/ decade vs 21 MPa/decade for the UD composite. As the Quasi-UD has 10% of fibre in the transverse direction and because the constituting yarns are twisted, this will create zones of stress concentration at the crossing of the yarns leading to early matrix cracking and thus early damage apparition, thus causing a steeper decrease of the S-N curve and a small decrease in the fatigue life of the Quasi-UD compared to the UD. Since UD2 has the lowest exponent b in absolute value, this is a sign of a slower and (maybe) gradual degradation of the composite.

As the cyclic loading decreases from 90% UTS to 40% UTS, the high initial strength is less dominant, i.e. it has less influence on the fatigue life, as observed in Figure 8-1 for Quasi-UD [0,90] versus the Low Twist Twill fabrics. For the UD versus the Quasi-UD, their performance almost coincides at 10^5 cycles. Since the fatigue testing takes a lot of time, modelling tools are handy when the prediction of the composite behaviour beyond the tested number of cycles is attempted. Talreja [4] has proposed a trilinear model to represent the S–N diagrams obtained from the fatigue experiments. The S-N curves are divided in three distinct regions (as seen in Figure 8-3a) [5, 6]:

- Region I: Non-progressive fibre damage - high stress amplitude are applied during cycling. In this region, the material behaviour is strongly influenced by its UTS and by the non-progressive fibre damage that takes place;

- Region II: Progressive matrix cracking – at an intermediate stress level, a progressive fibre-bridged matrix cracking occurs. This precedes fibre breakage and is described by linear dependency of maximum stress on the log (N) axis.
- Region III: limit region – at a high stress amplitude, the matrix cracks are stopped by the fibres. This region is defined when the fatigue life increases by several orders of magnitude in comparison to region II, and the S-N line is almost parallel to the log (N) axis.

In this study, when 1 million cycles is reached at a certain stress level, the fatigue limit (endurance limit) stress of the material is defined. The trilinear modelling of the flax composite fatigue life curves are displayed in Figure 8-3. In the region III, the line represents the 50% probability of failure of the specimens with a confidence level of 95%. It has to be noted that the UD2 composite presents a bilinear behaviour which is characteristic of the UD composites. Similar trends were found by Shah et al. [2] for UD flax-polyester composite and by Kawai et al.[7] for UD carbon-epoxy composites.

The endurance limit describes the cyclic stress amplitude at which stress can be applied without causing fatigue failure. As the test were stopped at S/S_o=30%, the endurance limit indicated in Figure 8-3 is an approximation of the 50% probability of failure at 30% UTS. Further investigation at higher cycling using the "staircase" method [8] .

a) Random mat

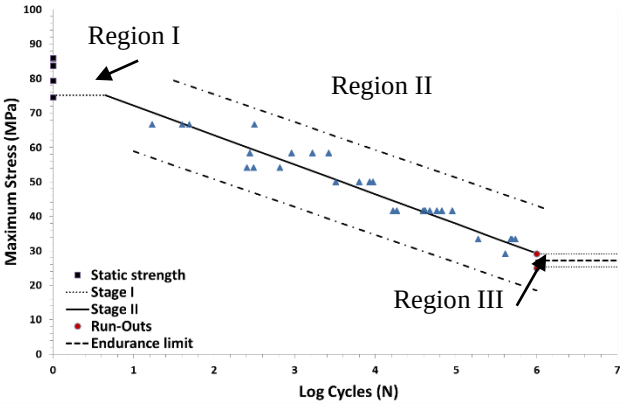

b) Plain weave

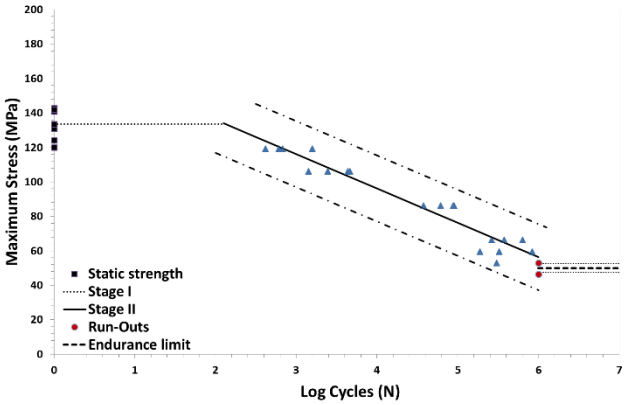

c) Low twist twill

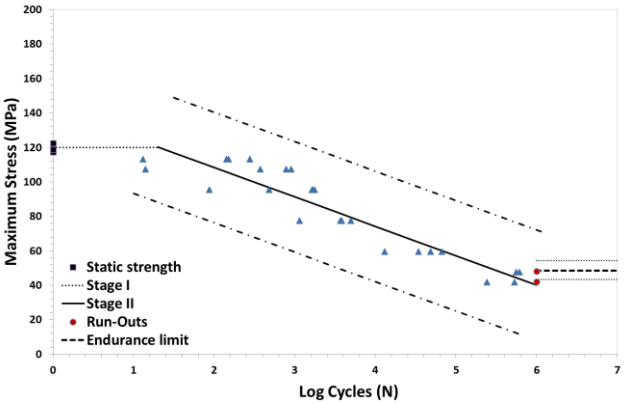

d) Medium-low twist twill

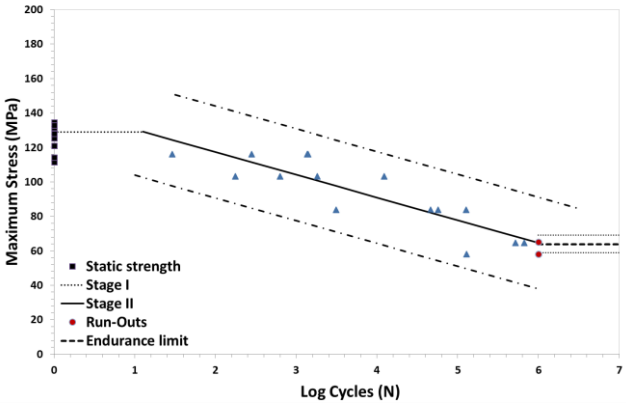

e) High twist twill

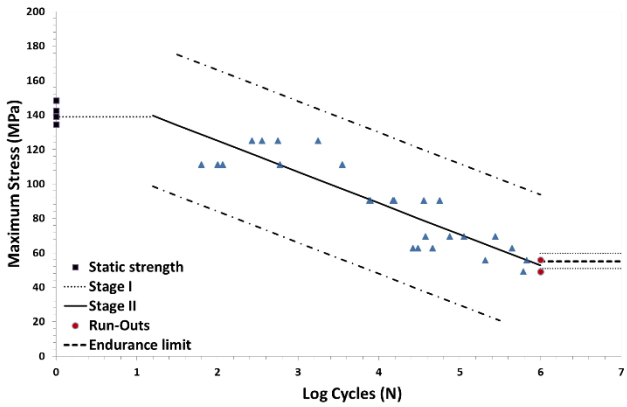

f) Quasi-UD [0,90]

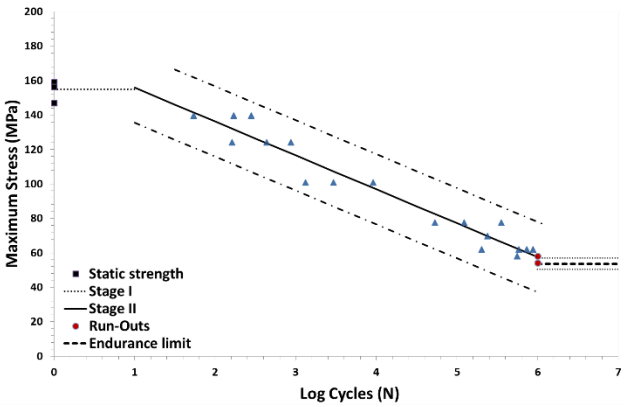

g) UD [0,90]

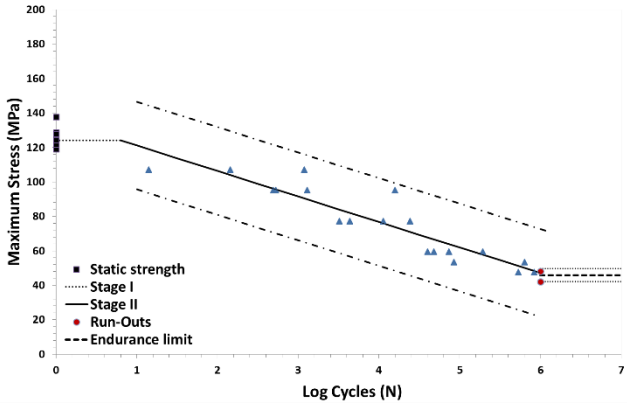

h) Quasi-UD

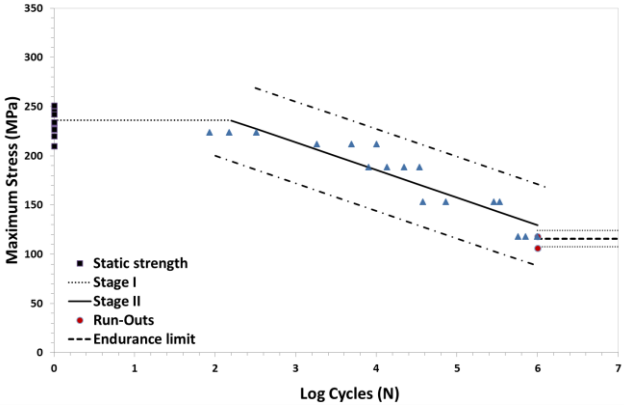

i) UD

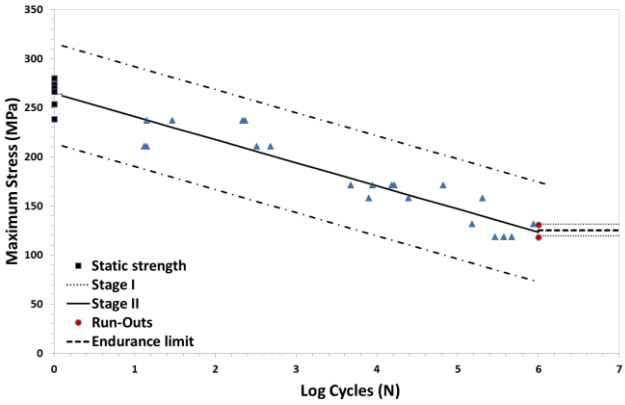

Figure 8-3: Trilinear modelling of the fatigue life diagrams for flax-epoxy composites.

8.1.2 Normalised fatigue results

To compare the fatigue sensitivity of the studied materials, the normalised stress (S/S_o) versus cycles to failure (N) curve method is used (see Figure 8-4). The normalized curves show that the fatigue strength of the different composites at high stress level (S/S_o=0.9 and 0.8) is rather scattered, and that the data points for the different reinforcement architectures overlap. At these higher stress levels, the fatigue strength steadily decreases by an average of 5-10% per decade of cycles of the quasi-static strength. A similar value of fatigue strength reduction was reported by Mandell [9] and Shazad [10] for UD E-glass fibre and randomly oriented hemp fibre reinforced composites respectively, which means that natural fibre composites demonstrate comparable fatigue sensitivity as unidirectional glass fibre composites [11].

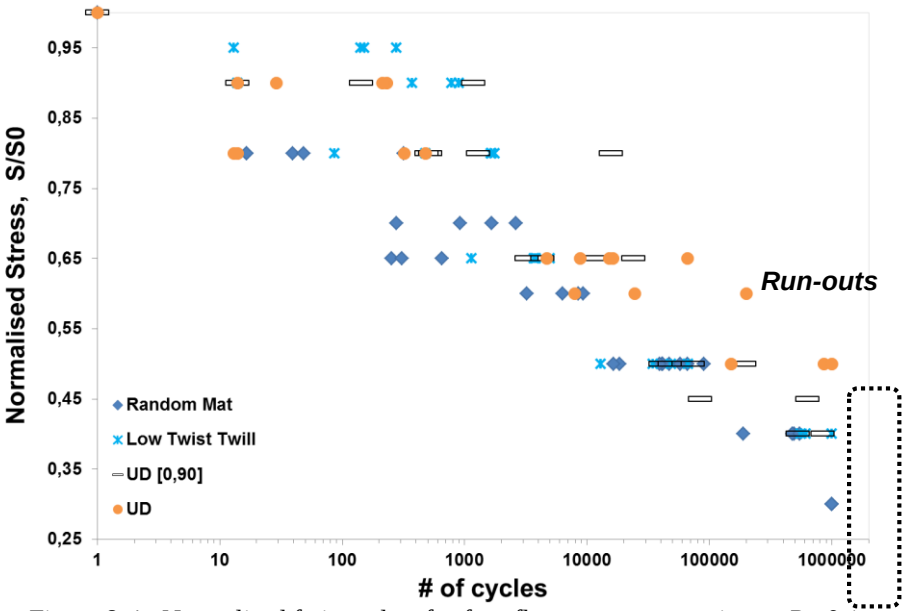

Figure 8-4 : Normalised fatigue data for four flax-epoxy composites at R= 0.1.

The scatter found in the flax fibre composite fatigue data is fairly common in fatigue lifetime data for composites. It has been previously reported that, for synthetic fibre-reinforced composites, the already existing scatter in quasi-static strength data is increased during the fatigue loading due to the appearance of damage [12]. In order to lower the scatter as much as possible, at least 3 to 4 samples were tested.

The trend lines, calculated from the data points of the normalized stresses S/S_o vs the number of cycles to failure, presented in Figure 8-4, are shown in Figure 8-5, and are clearly different. The endurance limit of the UD composite clearly exceeds the ones of the low twist twill, the cross-ply laminate as well as the random mat. Its endurance limit is 45% of the UTS, while for the UD [0,90] cross-ply laminate and for the Low Twist Twill it drops to 35% of the UTS and for the random mat even to 30%.

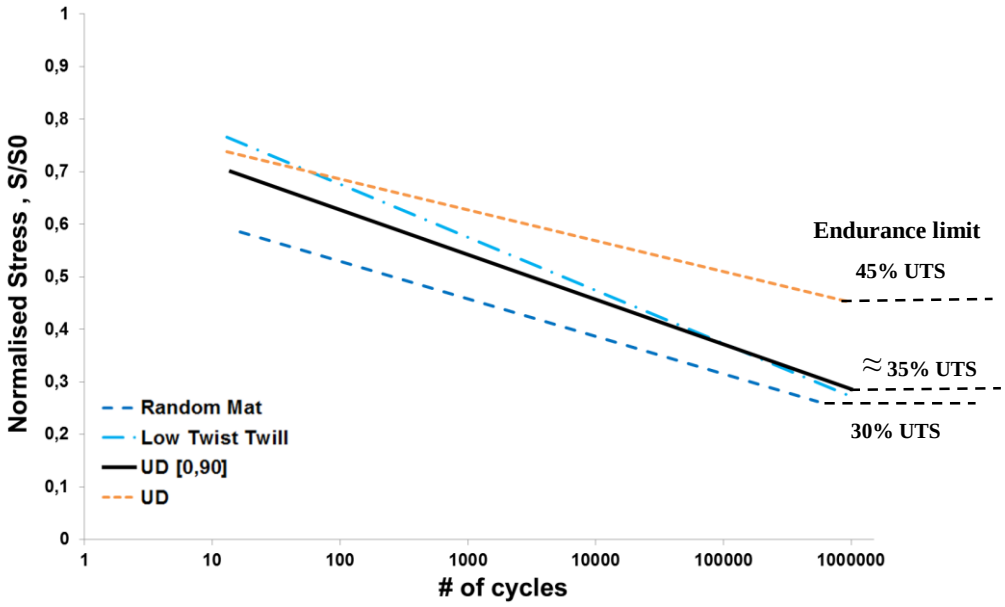

Figure 8-5 : Normalised fatigue data trend lines for four flax-epoxy composites at R = 0.1.

All the slopes show dissimilar trends, with the Low Twist Twill showing the highest degradation with time, due to its weaving pattern characteristics and yarn type (see section 8.2.3). The stacking sequence, the weave type and the fibre orientation also have an impact on the degradation rate obtained. It has been reported that a steeply decreasing slope reflects a strong influence of fatigue damage occurring at the fibre level (fibre breakage, fibre/bundle debonding, etc.), whereas a gradual slope reflects a matrix dominated damage mechanism [13].

8.2 Stiffness degradation, cyclic creep and post-fatigue properties

The influence of the textile architecture on the stiffness variation through time, the strain evolution and the post-fatigue properties were studied. To do so on a fair basis, all fatigue experiments were designed to survive the fatigue loading up to ½ million cycles and the samples were tested at the same stress level (S/S_o=0.3). After the fatigue cycling, all samples were subjected to post-fatigue tensile testing to find the residual properties. In the next section, the stiffness degradation, residual strain and post-fatigue properties are discussed.

8.2.1 Stiffness degradation

The influence of textile architecture on the stiffness variation through time was evaluated by determining the stiffness at each cycle through the initial slope of the stress–strain curve as shown in Figure 4-19.

In the early cycles, defined as Region I in Figure 8-6, an increase in stiffness is observed. This could be related to the reorientation of the microfibrils in the elementary fibre observed by several researchers. This could however be counteracted by some damage initiation as the microfibrils rotate toward the loading direction (0°) [10, 14]. Another phenomenon that may cause this stiffening is the strain-induced visco-plastic deformation of the amorphous cellulose in the elementary fibres which would increase the crystallinity of the fibres and thus the properties of the fibres and its composite [22].

It has to be noted that in region I, the applied stress was initially lower than in the region II due to the gradual increasing in stress (tapered sine signal). This was applied to gradually build up the stress in the sample and avoid an overshoot of the load during the early cycles (see section 4.11 in Chapter 4 for more details).

The stiffening phenomenon in Region I happens in different magnitude depending on the fabric structure, i.e either UD or woven. The stiffness values in cycle 5 and cycle 100 were compared to the initial quasi-static stiffness E1 presented previously in Figure 8-1a. The modulus of the first dynamic cycle was not used because the stiffness recorded during fatigue is affected by some starting artefacts, like the setting of the extensometer, and hence is not reliable.

For the Quasi-UD and UD and cross-ply laminate architectures, the stiffening effect is clearly visible as the modulus increases by 6 to 10% in the first 100 cycles. For the woven fabrics, the increase in modulus in the early cycles is possibly counteracted by other phenomena such as debonding, matrix cracking, and hence the stiffening is limited to values between 0 and 8%, as shown in Table 8-3. The limited stiffness increases for twill woven flax/epoxy composite by only 2-3% was also observed by Asgarinia et al. [15]. On the other hand, for the low twist twill, a strong decrease in properties was recorded as early as in the fifth cycle. This is hypothetically caused by the binding yarn wrapped around the

unidirectional fibre, which may have accelerated the appearance of damage. Further explanations are presented in section 8.2.3.

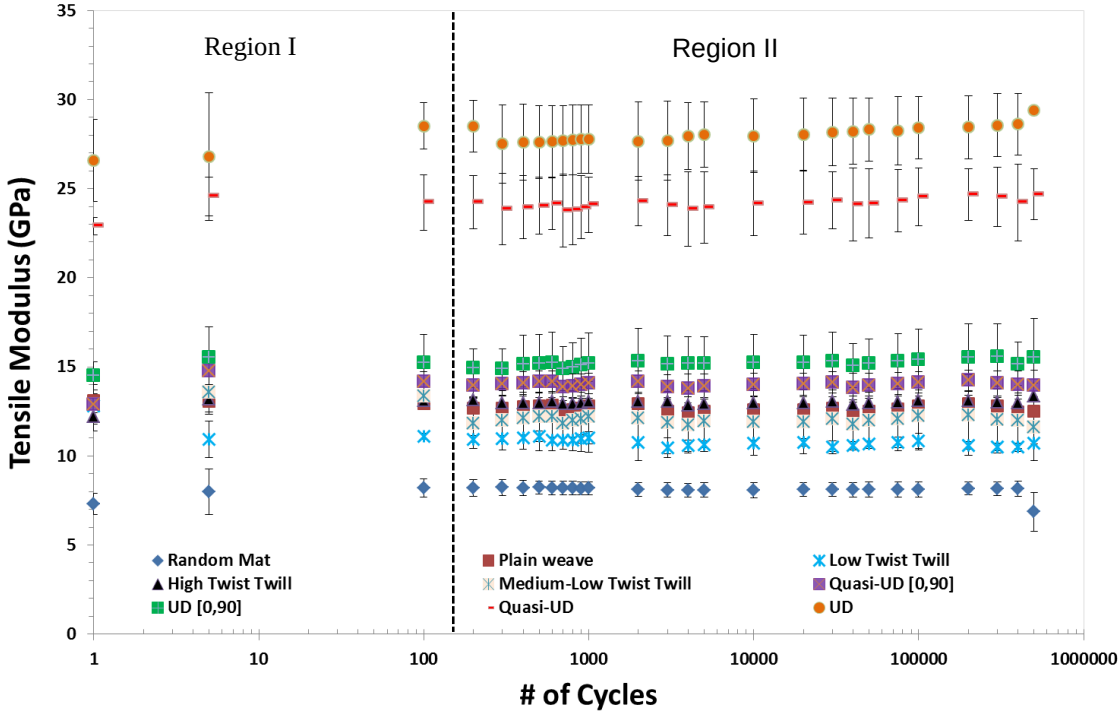

Figure 8-6 : Stiffness degradation curves at S/S0=0.3.

	Region I		Region II	
	$E_{cycle5}/E_{1\text{-quasi-static}}$	$E_{cycle100}/E_{1\text{-quasi-static}}$	$E_{cycle1000}/E_{cycle500}$	$E_{cycle400\,000}/E_{cycle500}$
Random Mat	1.09	1	0.99	0.99
Plain Weave	1	0.99	1	0.97
Low Twist Twill	0.85	0.87	0.99	0.95
Medium-Low Twist Twill	1.05	1.04	1	0.99
High Twist Twill	1.08	1.08	1.01	1
Quasi-UD [0,90]	1.14	1.10	0.99	0.99
UD [0,90]	1.07	1.05	1	1
Quasi-UD	1.07	1.06	1	1.01
UD	1.01	1.07	1.01	1.04

Table 8-3: Stiffness increase in Region I and stabilisation in the plateau region II.

The Region I is followed by a slight decrease and stabilisation of the modulus in a "plateau-region" (see also Figure 8-5 and Table 8-3, referred to as Region II). At low stress level, S/S_o=0.3, the stiffness degradation observed in region II is very small for all flax/epoxy combinations, from 1% to 3% showing a stable stiffness throughout the cycling. It has to be noted that, at this stress level, the samples did not fail after 500 000 cycles. Comparable results were found for carbon/epoxy composites reported by Vallons et al. [16]. Moreover, the absence of stiffness decrease was also observed in hemp random mat composites by Shahzad et al.[10]. However, the low twist twill shows a stronger decrease in stiffness properties which may be caused by its binding yarns around the flax fibre roving (see section 3.2.3 for more details).

If the flax composite samples were tested at higher stress level, they would have experienced a more severe stiffness drop. Indeed, Liang et al [17] found for flax/epoxy laminates, that the maximum stiffness decreases was 25% for the unidirectional and 38% for [0,90] cross-ply laminates at 80% of the UTS. The main damage mechanism reported by these authors is matrix micro-cracking at the fibre-matrix interface, which is intensified at higher stress level leading to a strong stiffness decrease.

The orientations of the fibres have been found to have a great influence on the initial stiffness properties and on how the damage develops through time. For example, the damage development pattern of the cross-ply, Quasi-UD [0,90] and UD [0,90] laminates, will be intrinsically different when crimp is introduced, as is the case in for instance the plain woven fabric. When loaded in one of the fibre directions, the 90° plies in a cross-ply laminate are exposed to in-plane tensile and, at the sample edges, interlaminar shear stresses, but when only one ply is analysed individually, this 90°-ply will act the same as a UD composite under transverse loading [4, 18].

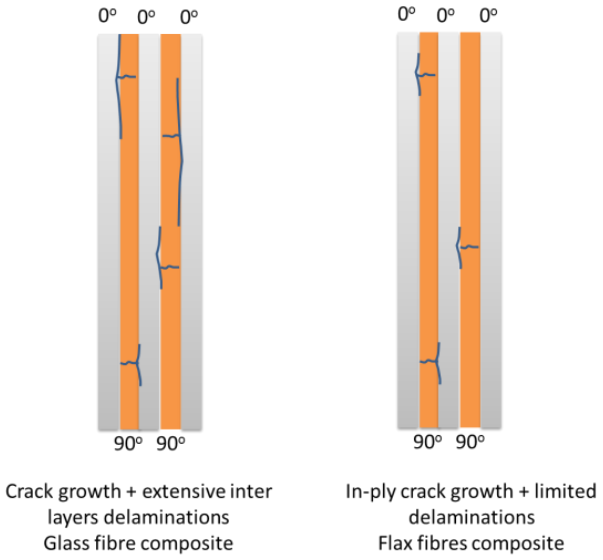

Figure 8-7: Crack propagation in a [0,90] cross ply laminate.

For the 90^{o} layer in a cross-ply laminate, the constraint of the 0^{o} ply is also present [18]. Thus, the laminate failure will not be caused by only a crack in the 90°-ply, but by shear-lag creating delaminations at the specimen edges in between the 0^{o} and 90^{o} plies causing a gradual stiffness decrease as illustrated in Figure 8-7. For flax composites, the interlaminar fracture toughness is higher compared to carbon or glass composites, which limits the propagation of delaminations, thus limiting the stiffness degradation [19]. On the other hand, no indication of imminent failure is given and the flax composites will tend to fail catastrophically due to the coalescence of cracks [10, 20].

It was expected that the behaviour of woven fabric composites in fatigue should be similar to cross-ply laminates, where the main failure mechanisms include matrix cracking in the off-axis fibre bundles [4]. Through cyclic loading, these cracks will grow and initiate local debonding between the fibre bundles (yarns) thus causing a faster decrease of the stiffness in comparison to a true cross-ply laminate [21]. In the case of natural fibre composites, where twist and crimp are present compared to the glass composite counterparts where only the crimp is present, extra matrix cracking will be initiated due to the more complex stress state in the twisted yarns oriented along the testing direction. This phenomenon could cause

the twisted yarns to try to "untwist" creating shear and normal stresses relative to the fibre orientation and resulting in additional micro-cracks at the fibre/matrix interface and at the yarns crossover area.

8.2.2 Post-fatigue residual properties

The samples exposed to fatigue cycling up to 500 000 cycles at a S/S_0= 30% load level were tested in quasi-static tension to determine their residual properties. The moduli E_1 and E_2, and the ultimate tensile strength were determined and are presented in Figure 8-8. The post-fatigue tensile tests show that the fatigue-tested samples exhibit similar properties to the pre-fatigue quasi-static-tested samples with no significant decrease in mechanical properties. The same behaviour was observed with hemp fibre based composites by Shahzad et al.[10]. Only the low twist twill displays a strong decrease of 20% for both E_1, E_2 and the tensile strength. For the remaining configurations, tensile values comparable to the pre-fatigue values were found. As discussed in the previous section, the damage that is formed during fatigue likely postpones the formation of new damage during the post-fatigue tensile tests as postulated by Vallons et al. [16, 18].

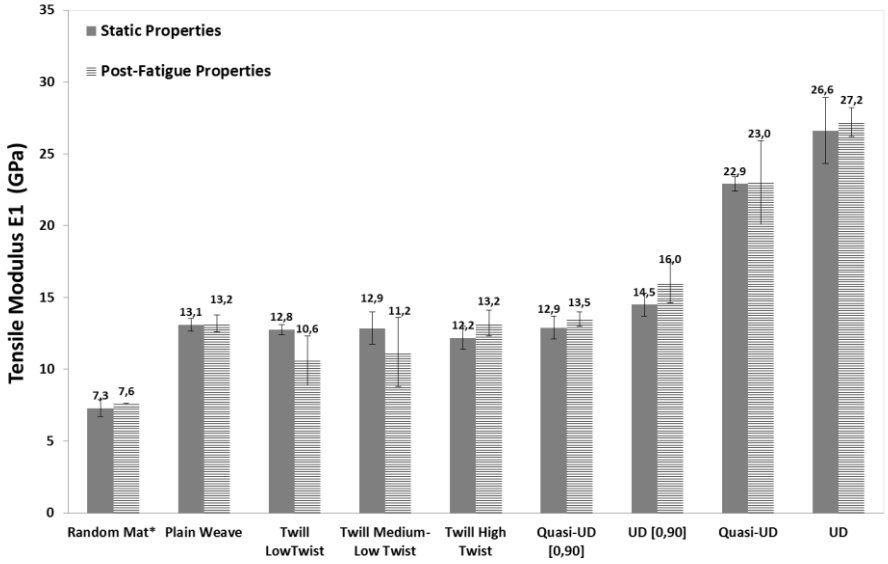

a)

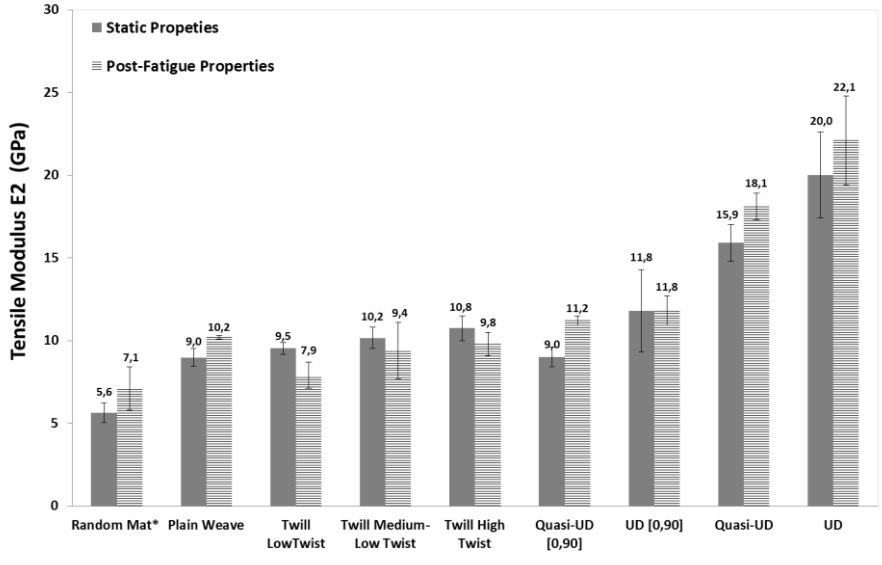

b)

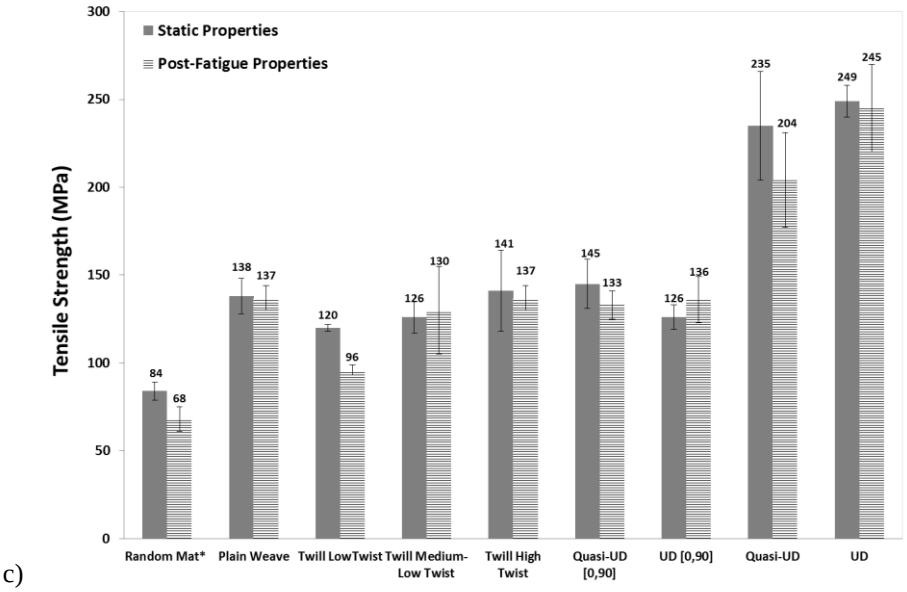

c)

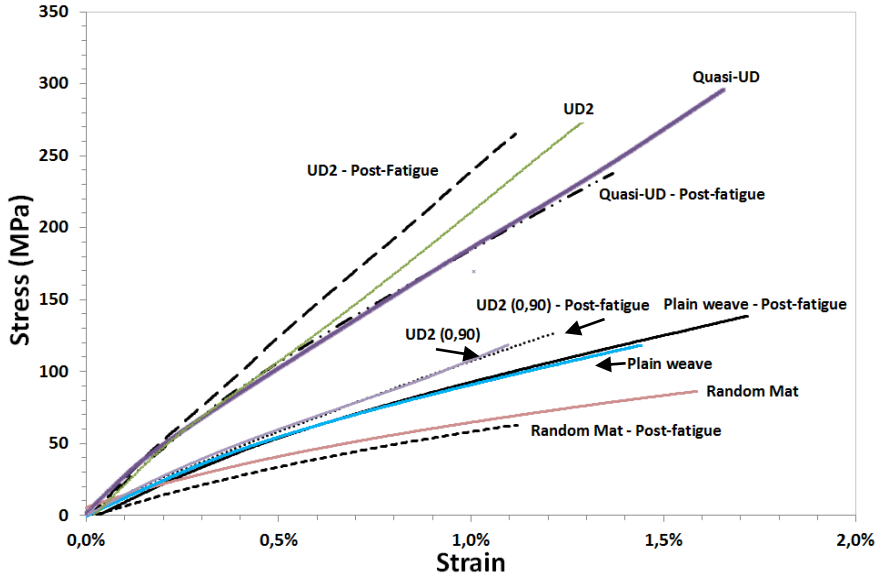

d)

Figure 8-8: Post-fatigue properties of flax-epoxy composite, a) tensile modulus E1, b) tensile modulus E2, c) the tensile strength and d) selection of stress-strain curves pre- and post-fatigue (residual) testing.

Taking a closer look at the results (presented in Figure 8-8), a moderate increase of the E1 moduli is observed for the Quasi-UD [0,90] by +5%, the UD [0,90] with 10%, whereas the E1-moduli for the quasi-UD (+ 0.5%) and UD composites (+ 2.5%) remain almost constant. A different behaviour is observed for their E2 modulus with stable behaviour (UD [0,90] or an increased modulus up to 25% for the Quasi-UD [0,90). For the previous laminates, all the strength values decrease compared to the quasi-static value, besides the UD [0,90] being the most stable composite configuration. By looking at the stress-strain curves before and after fatigue (seen in Figure 8-8d), a change in the non-linear behaviour was observed. The presence of the "kink" or" strain softening" region, occurring between 0.1% and 0.3 % strain, is less pronounced due to the fact that the cycling has occurred at stresses (S/S_o=0.3) above the yield stress (as defined in chapter 5) and hence into the visco-elasto-plastic region ($0.1 \geq \varepsilon \leq 0.3\%$). This has been observed for all configurations were they all display slightly straighter and steeper strain-curve curves after 500 000 fatigue cycles.

For the plain weave, the high twist twill and quasi-UD architectures, as the yarns are wet spun, the water dissolves the pectin which leads to partial or full separation of the elementary fibres (fibrillation) present in the yarns as seen in Figure 8-9. This fibrillation allows a better impregnation within the yarns and its technical fibres, increasing the fibre-matrix interface and its load bearing efficiency. In the case of the plain weave, the E1 remains stable while the E2 increases by 13% while for the high twist twill the E1 increase by 8%, but the E2 decrease by 10%. For the quasi-UD and its [0,90] cross-ply, the E1 values are stable while the E2 value increases by 12% and 20% respectively. Hence, for composites containing wet spun yarns, having an improved impregnation and fibre-matrix interaction compared to dry spun yarns, an enhanced fatigue performance is expected leading to lower degradation through time (see data on slope of fatigue curve, Figure 8-2 and Table 8-2) and an increased post-fatigue stiffness as reported in this study.

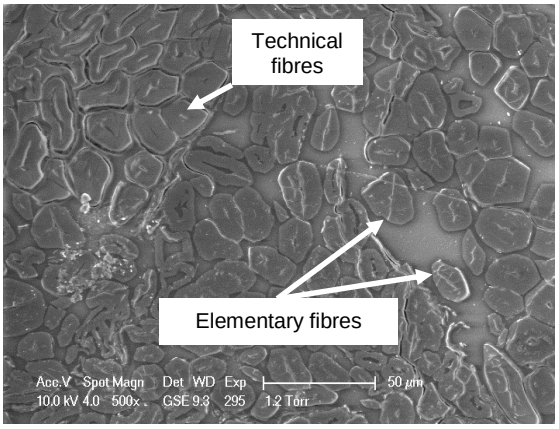

Figure 8-9: Micrograph of the plain weave/epoxy composite showing the fibrillation of the elementary fibres due to wet spinning.

8.2.3 Cyclic creep –Residual strain properties

For all investigated textile architectures, the hysteresis loops in each cycle are slightly shifted towards a higher strain, indicating a developing permanent elongation of the sample. It is seen that the hysteresis loops for the UD-composites show a smaller energy dissipation and a reduced shift to the right, compared to the random mat or the quasi-UD [0,90] composites. This indicates a lower permanent deformation and/or damage accumulation for the UD-composites.

As the applied stress is 30% of the UTS at R=0.1, the cycling goes from a minimum stress in the linear elastic region to a maximum stress in the transition zone (Figure 8-10a), as observed in a quasi-static tensile test (see Figure 8-1), and once more displayed by the dotted line in Figure 8-10b (■). Thus, the specimens are loaded into the "visco-elasto-plastic region". This lead to a permanent deformation, which can be related to plastic deformation but not necessarily to damage. This permanent deformation can be seen in Figure 8-11 showing an increase of the strain at the minimum stress as a function of the number of cycles.

The creep-like behaviour for a loading ratio of 0.1, observed in this study was also found by Monte et al. [22]. As the permanent strain increases with increasing number of cycles, the minimum strain and stress levels for damage initiation are both reached, leading to the shift of the hysteresis loops to higher strain for constant stress levels [18]. Hence the residual strain is a consequence of either plastic deformation or damage developing in the composite. When the permanent strain increased the chance of damage appearance and

growth, such as cracks, increases as well [23, 24].The permanent strain evolution of the flax/epoxy composites occurs in three stages as seen in Figure 8-11.

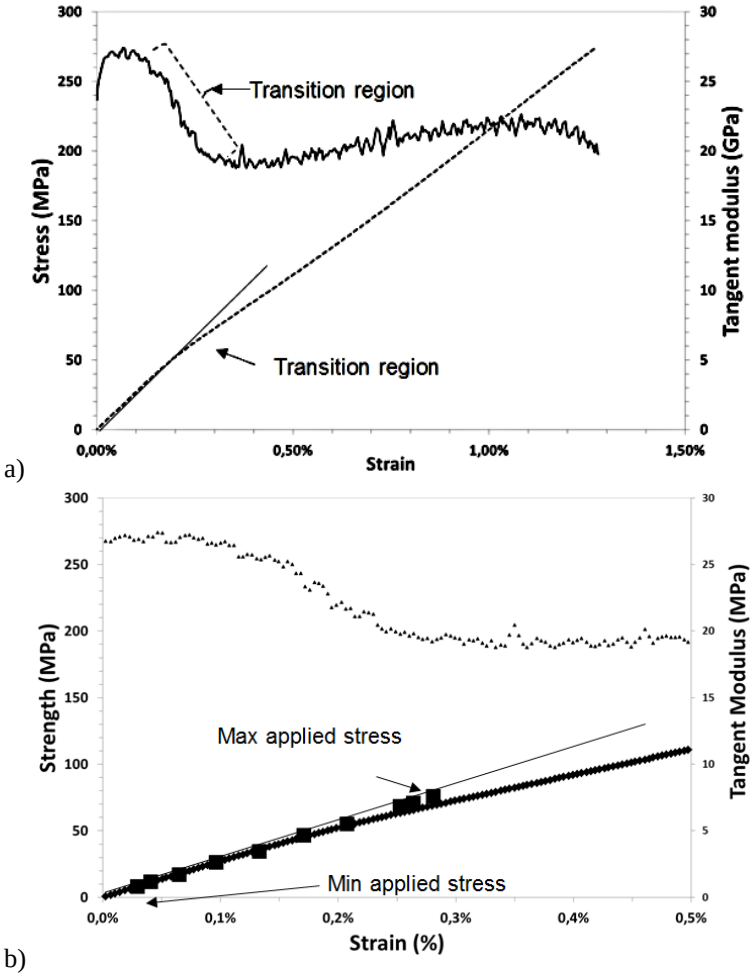

Figure 8-10: a) Position of the transition region in a quasi-static tensile test and the fatigue testing range at 30% of the UTS and b) zoom on the behaviour at low strains. Example for the UD configuration.

At first, a rapid strain change occurs due to plastic deformation and the apparition of damage (e.g. matrix cracking, fibre matrix debonding, etc…). It is then followed by a plateau region were the damage grows slowly, such as the spread of delamination in between the fibre layers and further debonding at the fibre-matrix interface. Then, in the end, there is a rapid and unstable increase of the permanent deformation before the complete failure of sample (not visualized in this study). Ellyin and Kujawski [25] have observed a comparable behaviour for glass-epoxy laminates and they stated that an initial rapid decay of the dynamic stiffness coincided with the first stages of the cyclic creep.

It is hypothesized that the initiation of the plastic deformation will start in the transition region towards the strain-softening region (where the tangent modulus will decrease) between 0.1% and 0.3% strain. In this region several phenomena may be happening such as the movement of the un-impregnated elementary fibres within a technical fibre and the visco-elastic or visco-plastic behaviour of the elementary fibre. Additionally, it should be considered that the middle lamellae which is a pectin rich region with very low σ capabilities, and the gradual start of the reorientation of the microfibrils (Et ↑). Beyond 0.3% strain, the plastic deformation will accelerate and there will be a stop in the decrease of E_t and a gradual increase of the tangent modulus occurs before failure (strain hardening)

which may be caused by various phenomena like the crystallization of the amorphous cellulose in the elementary fibre. The plastic deformation will not only occur in the matrix (matrix cracking isn't necessarily the first damage appearing) but also in the fibres through the various phenomena cited above. It has to be noted that most of the damage will happen in the early cycles as found by the following authors [1, 26, 27].

As the damage characterization was not carried out in this study, it is unfortunately not possible at this stage to state which phenomenon occurs first; hence, the hypotheses were based on literature findings. Kersani et al. [28] have found that the damage mechanisms in quasi-UD woven flax fibre laminates, tested in warp direction, are governed by damage processes happening in the technical flax fibres, which are then transferred to the yarn and ply level through fibre or yarn debonding. El Sawi et al [29] have found that the damage initiation in flax/epoxy laminates, with stacking sequences of $[0]_{16}$ and $[\pm 45]_{16}$, occurs within the interfaces in-between the elementary fibres. This suggests that the pectin layer, which bonds the elementary fibres together, is the "weakest" part in the composite. Thus, during fatigue, the cracks may start and propagate along the fibre-fibre interface.

	Applied Load S/S_o=0.3 @ R= 0.1		**Equivalent quasi-static strain**		**Power law trend**
	Min (MPa)	**Max (MPa)**	**at min load (%)**	**at max load (%)**	
Random Mat	2.5	25	0.07 ± 0.01	0.24 ± 0.02	$y = 0{,}0005x^{0{,}0636}$ $R^2 = 0.99$
Plain Weave	4	40	0.03 ± 0.002	0.34 ± 0.004	$y = 0{,}0002x^{0{,}0942}$ $R^2 = 0.79$
Low Twist Twill	3.6	36	0.03 ± 0.006	0.30 ± 0.01	$y= 0{,}0008x^{0{,}0691}$ $R^2 = 0.94$
Medium-Low Twist Twill	3.9	39	0.04 ± 0.007	0.32 ± 0.02	$y = 0{,}0006x^{0{,}0657}$ $R^2 = 0.90$
High Twist Twill	4.2	42	0.04 ± 0.006	0.34 ± 0.01	$y = 0{,}0006x^{0{,}0515}$ $R^2 = 0.95$
Quasi-UD [0,90]	4.7	47	0.03 ± 0.007	0.42 ± 0.03	$y = 0{,}0006x^{0{,}0597}$ $R^2 = 0.97$
UD [0,90]	3.7	37	0.03 ± 0.004	0.26 ± 0.04	$y = 0{,}0004x^{0{,}0609}$ $R^2 = 0.99$
Quasi-UD	7.1	71	0.05 ± 0.006	0.43 ± 0.06	$y = 0{,}0004x^{0{,}0682}$ $R^2 = 0.99$
UD	7.9	79	0.04 ± 0.006	0.31 ± 0.03	$y = 0{,}0007x^{0{,}0512}$ $R^2 = 0.99$

Table 8-4: Permanent strain trends according to the applied load and the equivalent quasi-static strain.

The results show that permanent deformation increases in a power law fashion with increasing number of cycles (see Figure 8-11). Upon a closer look at the results from the permanent strain, the fastest permanent strain increase is observed for the plain weave and the low twist twill with a variation of 38% and 32% between cycle 1000 and cycle 500 000, when fatigue loaded at 30% of UTS. This can be seen in Figure 8-11 and can be calculated using the power law equation to evaluate the residual strain at a specific cycle given in Table 8-4. It has to be noted that the fasted degradation is directly correlated by the value of the exponent (exponent ↑ = ↑ degradation).

Taking a closer look at the post fatigue properties, it is observed that the same configuration, i.e. the low twist twill, which shows the highest permanent strain, also encounters the strongest decrease in both stiffness and strength, as reported in the previous sections. This may be due to the physical shape of the yarns, in which a fine yarn is wrapped around a unidirectional bundle of fibres. This causes a misalignment of the fibres and thus a decrease in properties. These binding yarns (see Figure 8-12) create stress concentration points which increase the chance of damage coupled to the shear–induced damage between the fibres and the matrix, leading to an increase in the permanent deformation of the sample. As seen in the results obtained and presented in Figure 8-11 and Table 8-4, the introduction

of a misalignment has equivalent impact on the residual properties and permanent strain, as the presence of a combination of high twist and crimp. The quality of the fibre used by the supplier may also play a role in the weak behaviour of this composite.

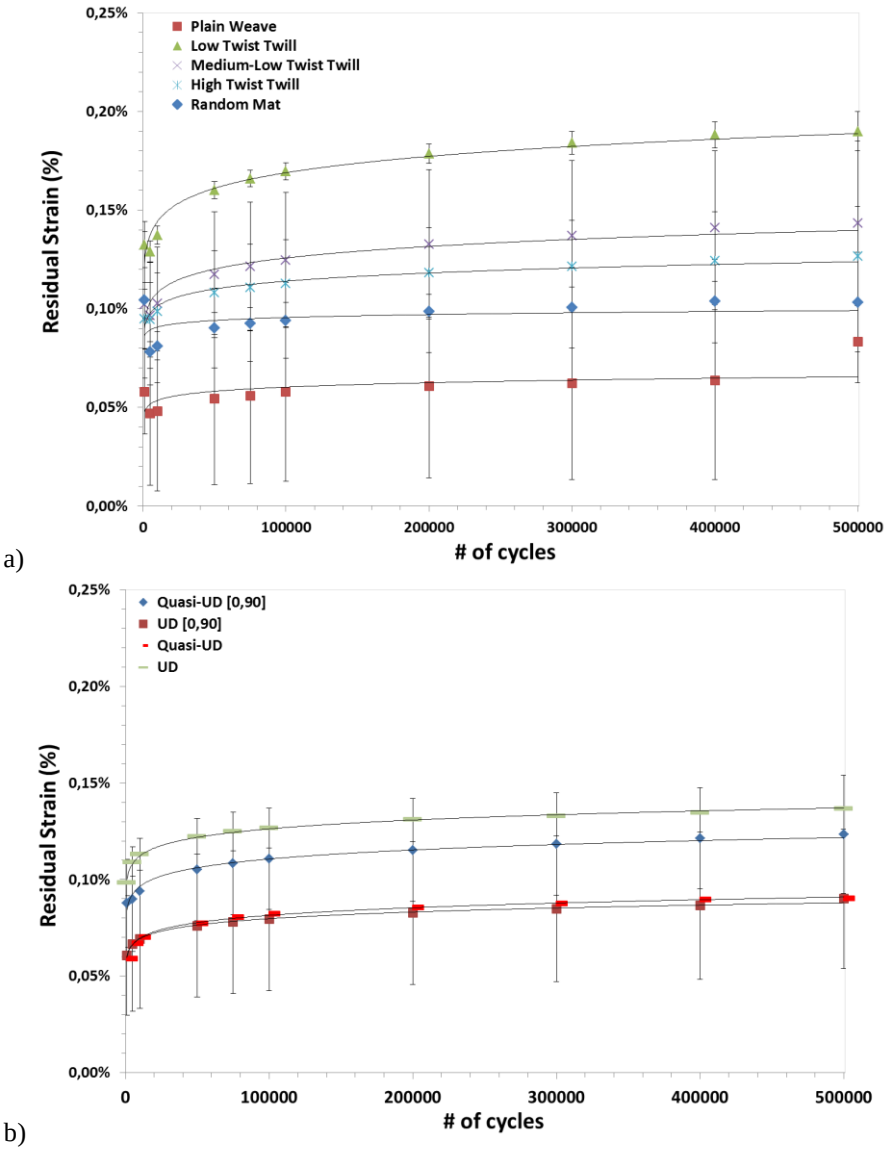

Figure 8-11: Permanent deformation through cycling. Display of the minimum strain level reached by the hysteresis during fatigue cycling at a stress level of S/S_0=0.3: a) random mat and woven composites and b) [0,90] cross-ply laminate and unidirectional composites.

Figure 8-12: Unidirectional flax roving with binding polyester yarn in the low twist twill textile.

8.3 Damage evaluation through hysteresis loop capture

During the fatigue testing, the (visco-elastic-plastic) deformation and creation of damage in flax/epoxy specimens will dissipate a certain amount of energy during the increasing

load phase, and only part of this energy is given back during unloading. This phenomenon will leave the specimen with a permanent strain that will accumulate through time and affect the overall mechanical properties of the composites (slight reduction of the stiffness in Region II of the fatigue experiment) as well as further defect propagation [20, 27].

The shift of the hysteresis loop as seen in Figure 8-13 towards increasing strain levels, is an indication of permanent deformation of the specimen [18]. A larger stress-strain (σ-ε) hysteresis loop area and a slight increase of the slope in the early cycles compared to cycles close to the failure of the sample was observed in the four architectures presented in Figure 8-14. It has to be noted that these samples were tested at 50% of UTS. When the loops get slimmer, this is a sign that no more damage or plasticity is created, i.e. the number of matrix cracks reaches a saturation state [18].

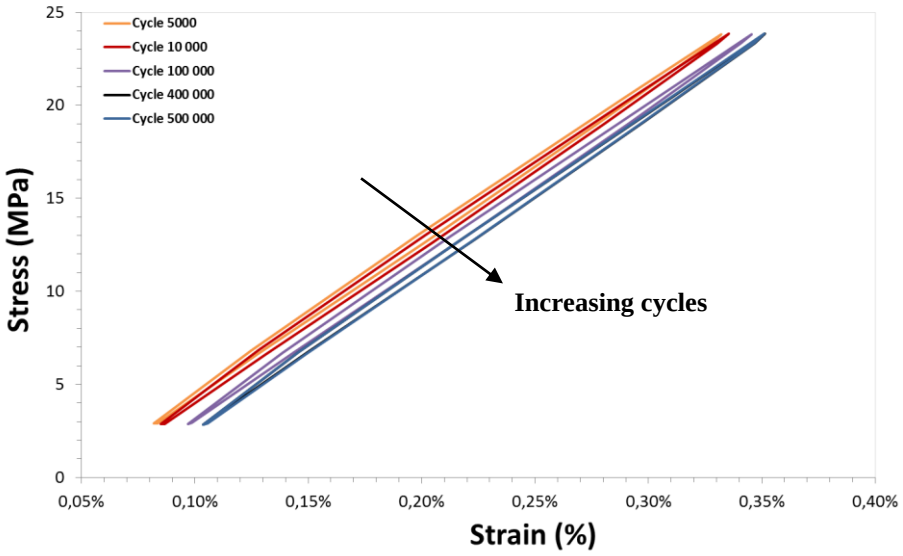

Figure 8-13: Stress-strain data from fatigue testing random mat – epoxy composite at S/S0=0.3.

For the random mat, a lot of energy is still being dissipated after 15000 cycles compared to UD- or the medium-low twist twill composites, where the loops are getting slimmer, which is a sign that no more damage is created, i.e. the number of matrix cracks reaches a saturation state [18]. For the random mat, since the fibres are in all directions, it is believed that their stiffening is gradual and limited by the orientation distribution of the fibres compared to the UD composite where all the fibres are oriented in the direction of the tensile testing. For this reason, in the random mat configuration the width of the hysteresis loops is significantly larger than in the other architectures.

The wide hysteresis loop during tension-tension fatigue of random mat composites may also be a sign of high damage activity during the initial phase of fatigue loading, possibly indicating greater energy dissipation at the fibre–matrix interface [30]. The evolution of hysteresis energy corresponds to the area enclosed within a hysteresis loop of the sample tested at 30% of the UTS. This area is calculated using the difference between the area under the loading and unloading curves of the same cycle (integration). A quantitative analysis of this energy dissipation in J/m^3 is presented in Figure 8-15 as a function of the number of cycles.

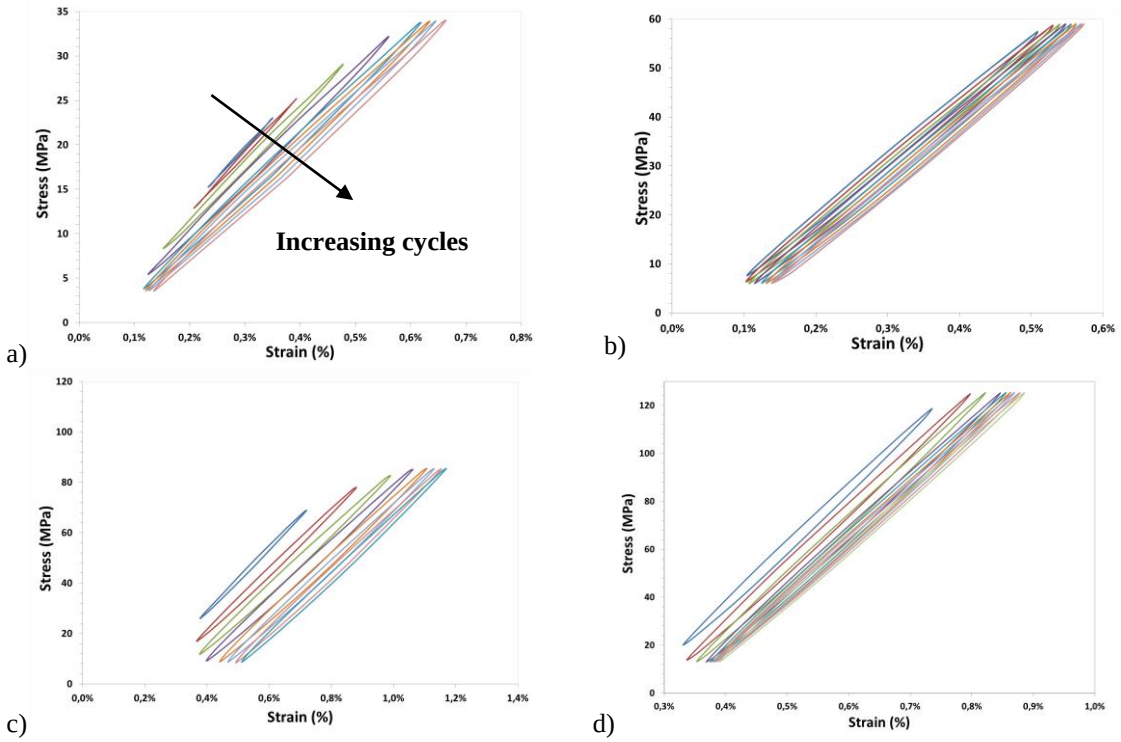

↑ energy dissipation = ↑ more damage = ↓ fatigue life

Figure 8-14: Stress-strain data from fatigue testing for the first 15000 cycles for a) random mat, b) medium-low twist twill, c) quasi-UD [0,90] and d) UD composites at S/So=0.5.

Similarly to cyclic creep, a two stage evolution is observed for all configurations, with a first rapid decrease in energy dissipation in the early cycles (below 100 cycles, see Figure 8-15a). This is related to the initial appearance of internal damage. The decrease slows down between cycle 5000 and cycle 10 000, and is then followed by a gradual decrease in energy dissipation when the damage saturation has occurred (see Figure 8-15b). The same behaviour is observed for all architectures. The UD composite has the highest energy dissipation in the early cycles (<1000 cycles) and shows a stable decrease from cycle 1000 on. Between cycle 1000 and cycle 5000, the energy dissipation of the random mat has the lowest drop with 40%, while the Quasi-UD encounters a drop of 60% and 62% respectively. The woven fabrics and [0,90] cross-plies decrease by 38% resp. 52% in the same range (see Figure 8-15).

Looking at the data between cycle 10 0000 and ½ million, the decrease in energy dissipation is limited to 11% for the random mat and 4% for the Quasi-UD. The weaves and cross-ply dissipated an average 20% less energy and the UD composite energy dissipation decreases by 33%. Matrix cracking and crack propagation are supposed to be the first damage mechanisms occurring in brittle composites. A reduction in energy dissipation may be the result of a lower amount of crack being created upon loading [31, 32]. A lower energy dissipation can also be caused by fibre/matrix debonding and interfacial friction as found by Gassan et al. [30]. Zhang et al. [33] stated that the creation and growth of micro-cracks in the epoxy matrix contributes to the energy dissipation under fatigue load, and that it may improve the fatigue behaviour of the material.

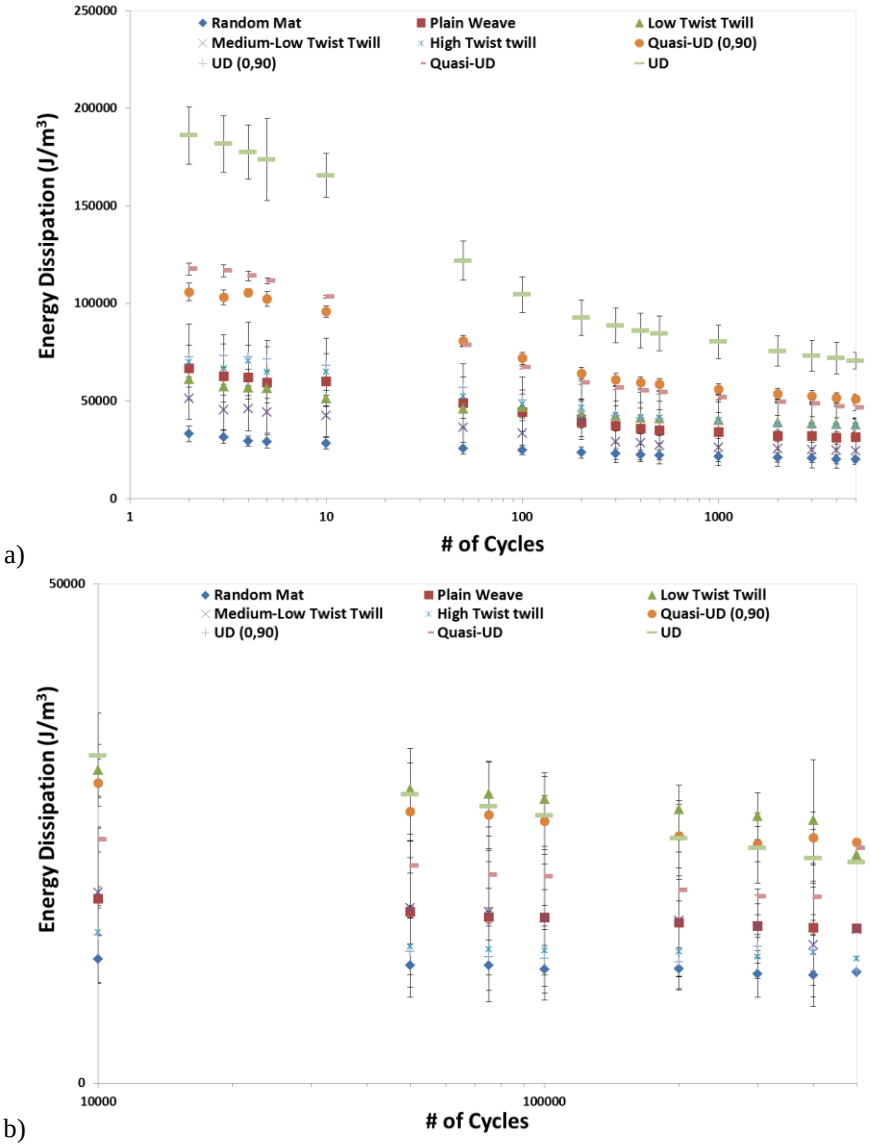

Figure 8-15: Evolution of energy dissipation for the studied flax-epoxy composites at 30%UTS: a) cycle 1 to 5000 and b) cycle 10 000 to 500 000 cycles.

8.4 Fatigue fracture surface characterization

Post-mortem microscopy on failed plain woven, random mat and unidirectional composites was made using a scanning electron microscope (SEM30 XL FEG). The samples were sputter coated with gold-palladium for further observations using secondary electrons using a voltage of 10kV. The images show that the main modes of failure were the matrix failure (brittle failure), fibre pull-out, fibre failure (transverse failure of the fibre) and yarn debonding.

For the plain woven-based composites, the cracks may have grown at the warp and weft yarns crossovers, as seen in Figure 8-16 a, and the inter-layer delamination was most probably caused by out-of-plane shear stress between the yarns and the edge effect. The crack propagation from the weft direction through matrix cracking was also found by Jacobsen et al. [34] for plain woven carbon composites. In Figure 8-16 b, the failure mainly happens at the yarn-matrix interface with extensive fibre pull-out where the crack runs around the yarns. It has been described that transverse cracks will appear first followed by longitudinal cracks and successive debonding at the yarn–matrix interface [35]. Similar

behaviour has been observed for synthetic cross-ply laminates and non-crimped fabrics [34, 36, 37]. The specific influence of crimp was not observed in this study, contrary to reports from Asgarinia et al. [15] who have found that crimp and fineness of the yarns play an important role in the woven fabric response to fatigue loading for flax/epoxy composites.

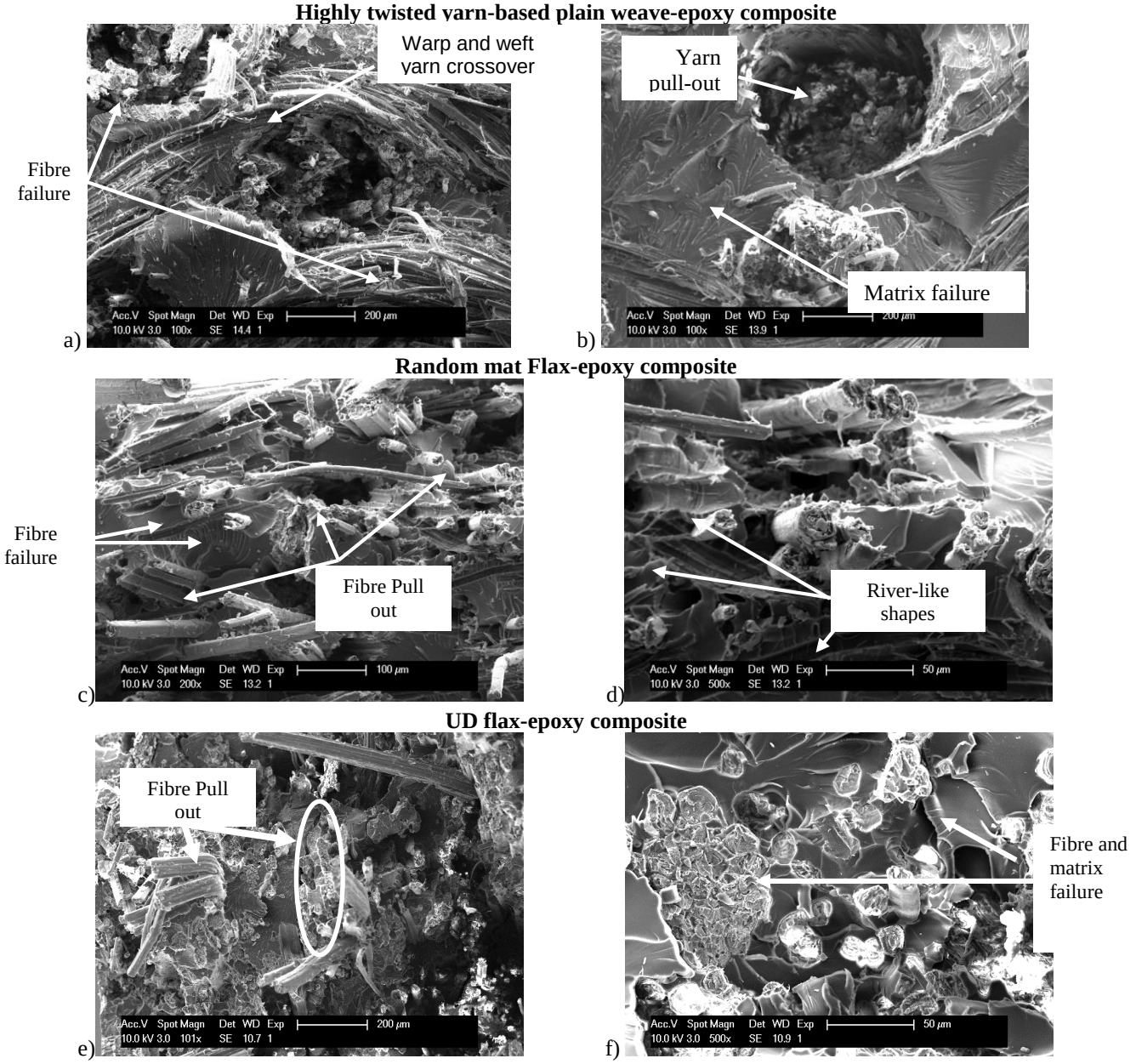

Figure 8-16: SEM images of flax-epoxy composites of highly twisted yarn-based plain weave composite after fatigue cycling: a) damage at the yarn warp and weft crossover and b) yarn pull out. SEM images of flax-epoxy random mat composite after fatigue cycling: c) pull-out and fibre failure and d) fibre-matrix debonding (arrows) and the SEM images of flax-epoxy UD composite after fatigue cycling: e) fibre matrix interface failure (arrows) and f) fibre and matrix failure.

For the random mat composite shown in Figure 8-16 c and d, fibre matrix debonding is the main failure mode combined with fibre pull out. Long river-like shape crack features can be seen in the SEM image, where at the fibre debonded from the matrix. Besides the extensive evidence of fibre pull-out, fibre failures were also observed. As the fibres are oriented in all directions, a mix of failure modes is observed.

For the unidirectional composites, Figure 8-16 e and f, displays a homogenous distribution of the fibres. With limited debonding and mainly fibre failures, the UD composites exhibit a fibre-dominated failure mode with extensive fibre splitting along the longitudinal direction, matrix failure and limited pull-out. As in glass fibres, the failure mechanism of a single flax technical fibre is connected to its brittle behaviour. This is mainly controlled by the defects present in the fibre as well as by the natural variability of the flax fibres, which include**s** the presence of irregular cell wall thickness, kink bands, nodes and dislocations [38-40]. All studied architectures presented variable degrees of fibre /matrix interface debonding.

8.5 Glass-epoxy composite benchmarking

8.5.1 Glass composite tensile properties

As flax is often compared to glass fibre in terms of performance, it is important to compare them fairly. Although glass fatigue studies are quite common, finding a comparable combination of fibre-architectures with epoxy, with similar parameters (V_f, thickness, testing frequency, etc.), is not easy. Therefore, to have reliable benchmark data, glass-epoxy composites were tested and produced using similar manufacturing parameters. Four glass fabrics were chosen: random mat, twill 2x2, quasi-UD [0,90] and UD [0,90]. Their areal weight has been chosen in order to match the flax composite, while using the same amount of layers, to obtain the targeted V_f (see section 4.1). All glass fibre had the basic silane treatment to make it compatible with epoxy (no other special treatment was applied).

The comparison of the resulting tensile properties of the flax and glass fibre epoxy composites is shown in the following Figure 8-17. It has to be noted that the density of the composite was theoretically calculated for the flax and glass composites in order to normalise the data. The results are presented in Table 8-5. This means that we can achieve the same performance with a potentially lighter product.

$\rho_c = V_f * \rho_f + V_c * \rho_c$	
Glass Fibre mat composite (Vf =30%) = 1.58	Flax Fibre mat composite (Vf =30%) = 1.25
Glass Fibre woven and laminates composites (Vf=40%) = 1.72	Glass Fibre woven and laminates composites (Vf=40%) = 1.28

Table 8-5: Calculation of the theoretical density of the flax and glass composite. Data to be used for the determination of the specific properties.

The quasi-quasi-static tensile moduli (Figure 8-17 a) of the glass composites are systematically higher than their flax composites counterparts due to their higher intrinsic mechanical properties. The glass quasi-UD modulus value is higher because a high quality of glass fibre has been used (Type E6 enhanced glass fibre, E= 82GPa and σ=2387 MPa), which has a higher modulus than the common E-Glass (72 GPa) used in the other fabrics. In the case of flax, the wet spun yarn is mechanically superior, since this process implies an increase in fibre fibrillation (as mentioned in section 8.2.2), and as a result leads to higher properties.

Higher stiffness properties were seen for the glass twill and quasi-UD [0,90] compared to the UD [0,90]. This could be caused by the fact that, in the UD [0,90], during manufacturing the fibre orientation may change from the preferential UD direction, thus leading to a stiffness reduction. In the case of the twill fabric and the quasi-UD, the tight weaving or stitching prevents the movement of the yarns in the textile. The tensile strengths of random mat and twill glass composites were at least double the value of the flax ones at similar fibre volume fractions. The same tendency is observed for the quasi-UD [0,90] and UD

[0,90] composites strength performance with the glass outperforming the flax. Also, this is related to the intrinsically higher strength of glass fibres compared to flax fibres. Finally, the use of flax fibres shows similar elongation at break as glass fibres for the random mat and the twill fabrics. However, the flax cross-ply composites have a limited strain to failure as they are intrinsically related to the maximum strain of the fibre as discussed in section 5.3.3.

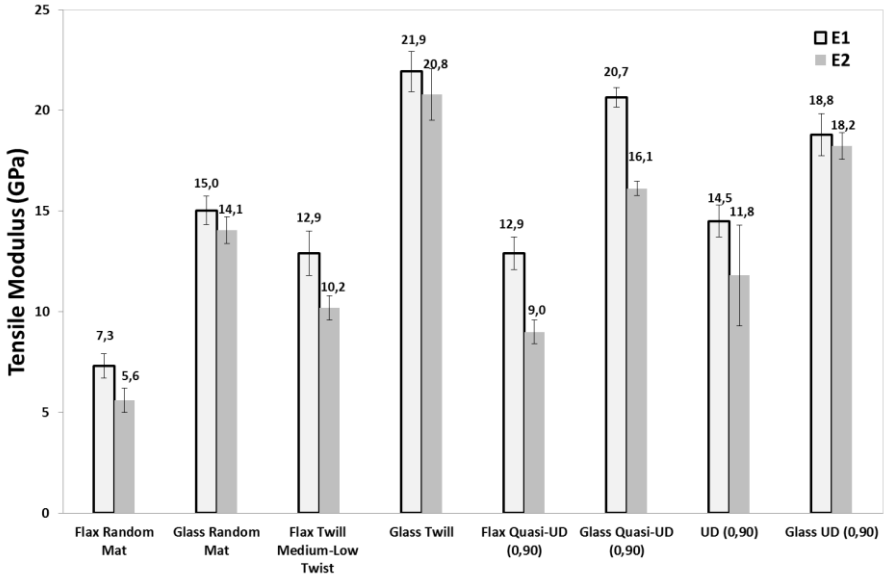

a)

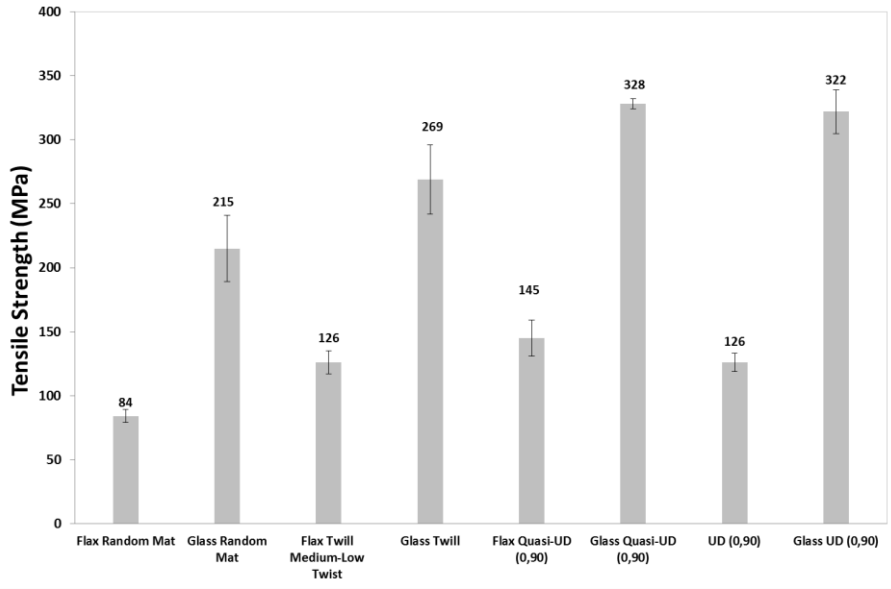

b)

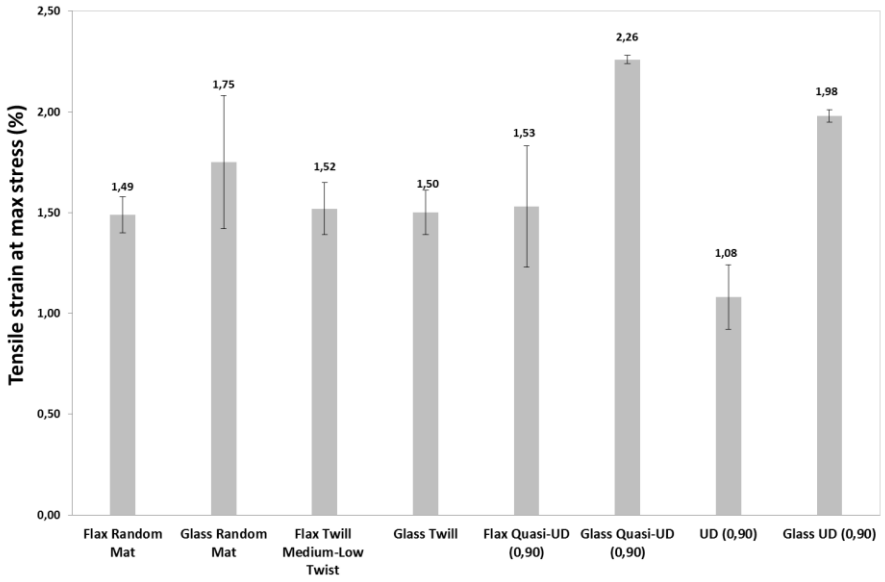

c)

Figure 8-17: Comparison of the quasi-quasi-static properties of flax and glass fibre composites normalized to Vf= 40%.

As for the properties-to-weight ratio (specific properties) presented in Figure 8-18, one observes that the specific stiffness values for the UD [0,90] composites are quite similar for glass and flax composites, but the specific strength is clearly higher for the glass composites. For the random mat, twill 2x2 and quasi-UD [0,90] architectures, the glass composite clearly outperforms the flax fibres, both in specific stiffness and strength. For the random mat, a better distribution (isotropic) of the short glass fibre compared to highly anisotropic flax fibres and the absence of impurities such as shives, may be the cause of higher properties. For the twill and the quasi-UD, the fact that the glass fibres can nest more efficiently, meaning that there is a better stress distribution in the specimen, leads to a stronger composite (↑ between 46-62%) than the natural reinforcement. For the flax, the presence of twist in the yarns of certain fabrics, making the yarns rounder, prevents an optimal fibre nesting which creates resin-rich zones more prone to damage initiation under testing.

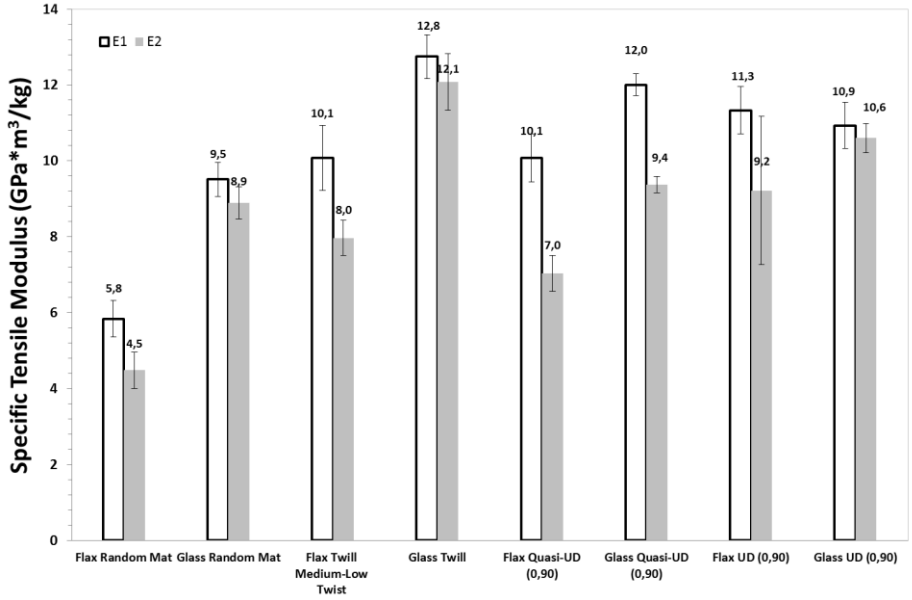

a)

b)

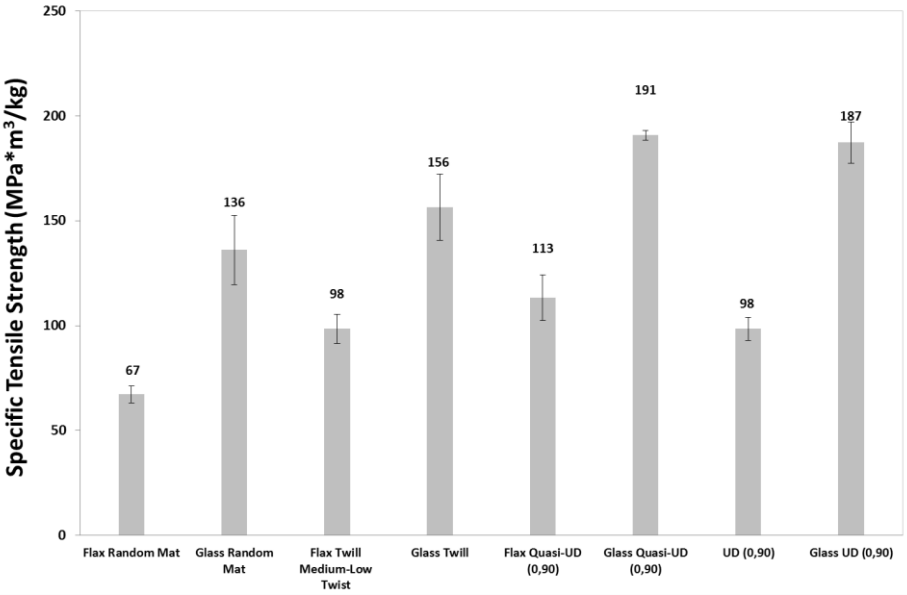

Figure 8-18: Specific tensile properties of glass and flax composites.

8.5.2 Comparative fatigue and post-fatigue performance

Based on quasi-static tensile test results presented in the previous section, the glass composites were subjected to tension–tension fatigue tests at R=0.1 and at different stress levels (% of UTS) to create their corresponding S-N curve. These data were then normalised to the density in order to be compare to the flax composites. The normalized stress/density-number of cycles to failure (S/ρ–N) curves are presented in Figure 8-19. The values were normalised according to theoretical densities calculated in Table 8-5. It has to be noted that although the data are normalised to the density, the material fatigue strength b exponent remains identical. This normalisation by density allows the comparison of the rate of fatigue strength degradation of the materials. The power–law models presented are a good fit to the experimental fatigue data. All regressions have an R^2 value > 0.90.

As expected, there is a gradual decrease in fatigue strength with increasing number of fatigue cycles and stress level. As mentioned by Shah et al. [2], this behaviour is generally common to composites whose fatigue life is dominated by matrix crack growth and inter-laminar cracking. Flax composites show a lower fatigue life than the glass composites, but the random mat and the Quasi-UD [0,90] flax composites have a slower degradation trough time having a lower *b* factor as seen in Table 8-6. The twill 2x2 and UD [0,90] composites flax and glass composite have comparable degradation speed (statistically equivalent).

Shah et al. [2] also found that the fatigue strength exponents of plant fibre (flax, hemp, jute) reinforced composites are higher than or comparable to GFRP, implying a slower damage development and strength degradation in plant fibre composites. Similarly, Liang et al. [14] also found a steeper fatigue life curve for GFRP in comparison to flax composites with similar textile architectures. Shahzad and Isaac [10] observed that hemp-polyester random mat and the chopped strand mat GFRP have a similar fatigue strength exponent *b* which is not the case in this study. The UD [0,90] trend observed for glass and flax are equivalent as was also observed by Gassan [30]. However, it doesn't mean that they possess the same degradation mechanisms. This is because the glass composite is more prone to matrix cracking and the presence of delaminations, since the stress concentrations around glass fibres are higher because the glass fibres are isotropic and hence their transverse stiffness is higher than in the case of flax fibres.

	Fatigue life power law curves	
	Flax composites	**Glass composite**
Random Mat	$84x^{-0,08}$	$200x^{-0,104}$
Medium-Low Twist Twill	$158x^{-0,06}$	$171x^{-0,065}$
Quasi-UD [0,90]	$209x^{-0,088}$	$255x^{-0,093}$
UD [0,90]	$170x^{-0,086}$	$313x^{-0,083}$

Table 8-6: Comparison of fatigue life power law curves for all configurations (on normalised to density data). The trendlines exclude the value at cycle 1.

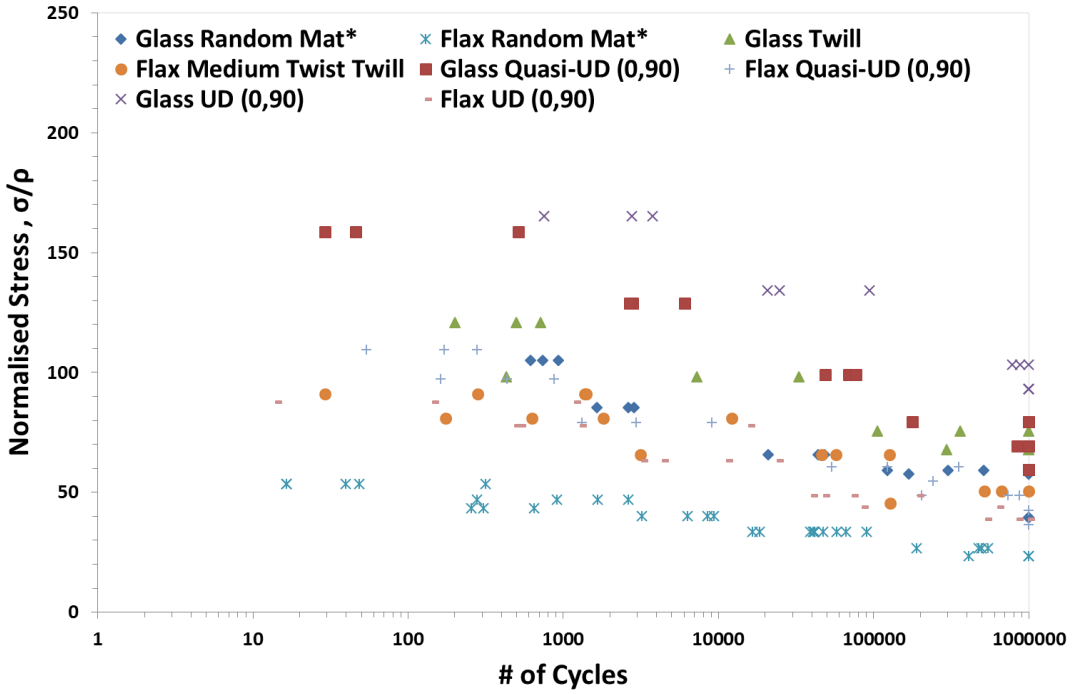

Figure 8-19 : Normalized S–N curves: comparison between flax and glass composites.

The observations on the glass composite show different failure mechanisms in quasi-static and in fatigue loading, which can be an explanation for the fact that the composite with the highest quasi-static UTS does not necessarily have the best fatigue performance. The Quasi-UD [0,90] had the highest quasi-static UTS followed by the UD [0,90], the twill and random mat respectively. In fatigue, the highest performance was registered for the cross-ply UD followed by the quasi-UD. The random mat and twill seem to have equivalent lifetimes. On the other hand, for flax composites, the higher the UTS, the better observed fatigue performance (lower strength degradation rate).

As the strength degradation for flax composites was found to be lower than the glass, a question arises as whether the same conclusions can be made for the stiffness degradation through time. From the results presented in Figure 8-20 and Table 8-7, it can be seen that the stiffness of all the glass composite architectures degrades faster than the flax ones in the early cycles (Region I), except for the glass UD [0,90]. A similar behaviour has been found for the strength (S-N curves). Although it is widely quoted in literature that flax composites have a lower strength than their glass counterpart, they still have a slower damage appearance and accumulation than glass fibre composites. This behaviour may be caused by the strain hardening phenomenon or to the progressive reorientation of cellulose microfibrils towards the loading direction as previously stated in section 8.2.3.

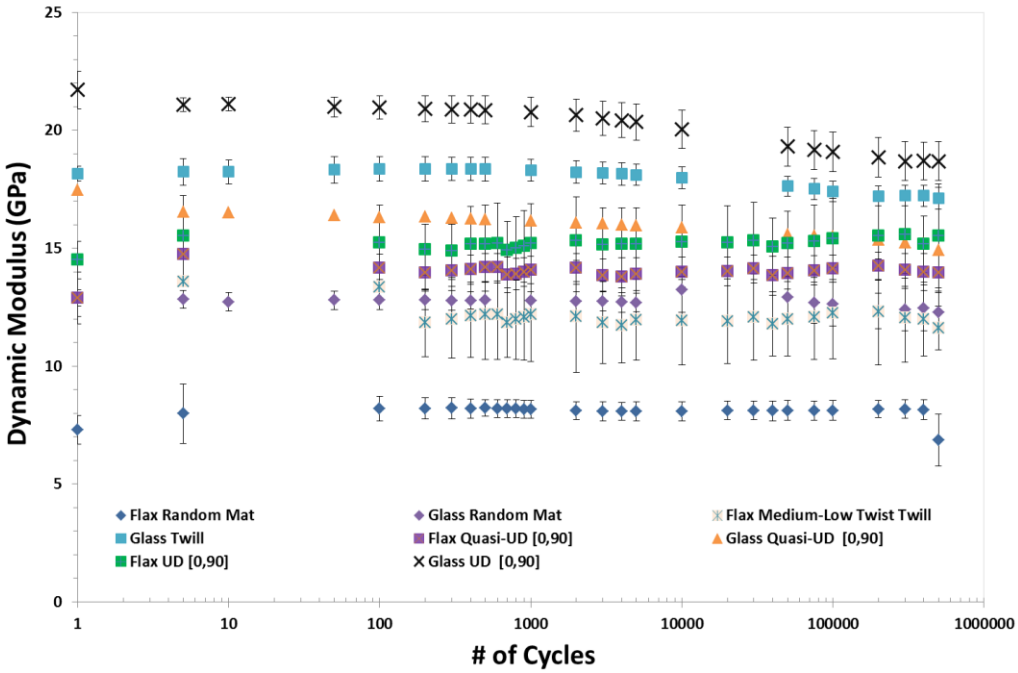

Figure 8-20: Stiffness degradation of glass versus flax fibre composites.

	$E_{cycle5}/E_{1\text{-}quasi\text{-}static}$	$E_{cycle100}/E_{1\text{-}quasi\text{-}static}$	$E_{cycle1000}/E_{cycle500}$	$E_{cycle500000}/E_{cycle500}$
Flax Random Mat	1.09	1	0.99	0.99
Glass Random Mat	*0.86*	*0.85*	*1.01*	*0.96*
Flax Medium-Low Twist Twill	1,05	1,04	1	0.99
Glass Twill	*0.83*	*0.84*	*1.01*	*0.93*
Flax Quasi-UD [0,90]	1,14	1,10	0.99	0.99
Glass Quasi-UD [0,90]	*0.8*	*0.7*	*1.01*	*0.92*
Flax UD [0,90]	1,07	1,05	1	1
Glass UD [0,90]	*1.12*	*1.11*	*1.02*	*0.90*

Table 8-7: Stiffness evolution of flax and glass composites

Another interesting observation is that the glass fibre stiffness degradation curves shown in Figure 8-20 have three distinctive regions instead of the two observed for the flax fibre; this can be best observed for the glass UD 0/90 (upper curve). Schulte et al. [21, 41, 42] have thoroughly studied the damage development of carbon/epoxy specimens with a $[0,90,0,90]_{2s}$ stacking sequence in tension–tension fatigue (R=0.1). They have distinguished three distinctive stages of stiffness degradation (see Figure 8-21):

- Stage I: a rapid stiffness reduction of 2–5% is observed. The development of transverse matrix cracks dominates the stiffness reduction;
- Stage II: stable phase where an additional 1–5% stiffness reduction occurs in an approximately linear fashion with respect to the number of cycles. The development of edge delaminations and additional longitudinal cracks along the 0° fibres are the observed damage mechanisms;
- Stage III: the stiffness reduction occurs in abrupt steps ending in specimen fracture. A transfer to local damage progression occurs, when the first initial fibre fractures lead to strand failures.

This thus explains the results found in Table 8-7 where two degradation regions, one in the first 100 cycles (Stage I) and the second one after 1000 cycles (Stage III). The stable phase II was identified between 100 and 1000 cycles. In that phase II stage, the stiffness decrease

for the glass composite is limited to 0.15% for the random mat, 0.36% for the twill, 1% for Quasi-UD [0,90] and 0.9% for the UD [0,90].

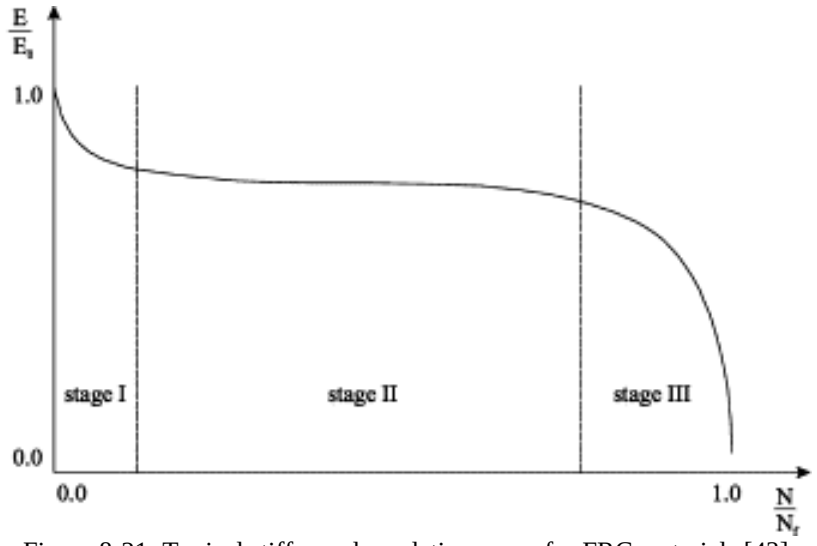

Figure 8-21: Typical stiffness degradation curve for FRC materials [43].

The gradual loss of modulus observed in Figure 8-20 could go hand in hand with an increase in the residual strain (Figure 8-22) and a faster damage accumulation. In the case of flax, it was mentioned that the specimens are loaded into the "visco-elasto-plastic" region which leads to a slow permanent deformation. This effect may be related to a plastic deformation but not necessary to damage growth, which explains why the stiffness remains rather stable throughout the experiment, even if the residual strain increases gradually.

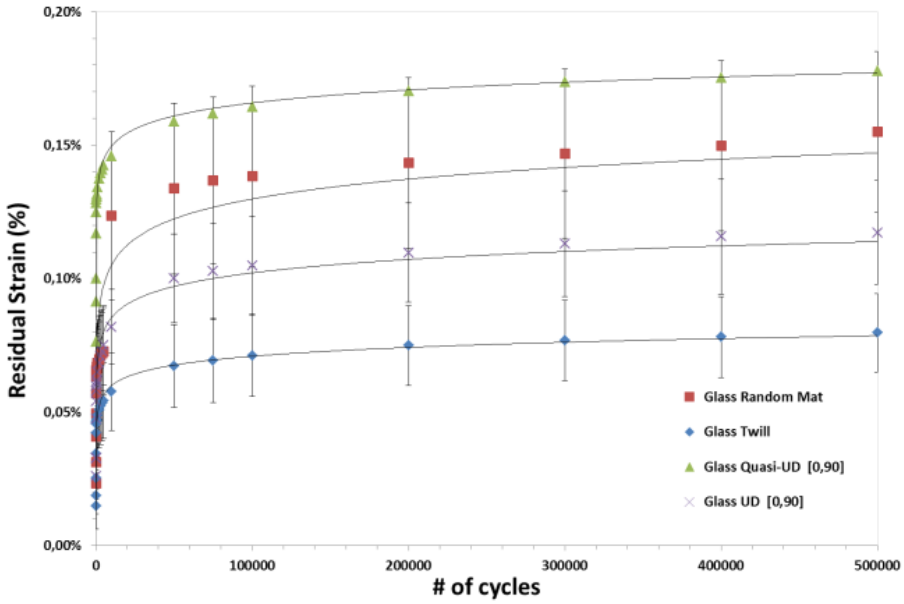

Figure 8-22: Cyclic creep of glass composites.

On the other hand, for glass fibres it can be seen that the residual strain rapidly grows in the early cycles as it is also observed for flax, which goes hand-in-hand with a loss in stiffness shown in Figure 8-20. After a thousand cycles and up to ½ million cycles, the flax composites stabilize and have only a slight increase of residual strain of 20% for random mat, 36% for the medium-low twist twill, 27% for Quasi-UD [0,90] and 10% for the UD [0,90]. The glass composites increase in residual strain for the same range by 44% for

random mat, 61% for the medium-low twist twill, 76% for Quasi-UD [0,90] and 55% for the UD [0,90]. During fatigue testing, the glass composite have a higher degree of damage growth and accumulation may be caused by a weak fibre-matrix bond [44]. As the glass fibre have a higher transverse stiffness, the matrix cracks appearing in the early cycle will lead to large debonded regions originating from flaws as previously shown in Figure 8-7 in section 8.2.1.

Combining these observations with the post-fatigue tensile properties of the glass-epoxy composite seen in Figure 8-23, it can be seen that the E1 and E2 moduli, both decrease in comparison to the initial quasi-static value in contrast to the flax composites, where there was virtually no decrease in stiffness (see also Figure 8-8). The rough surface of flax fibres, may lead to enhanced mechanical interlocking between the fibres, which in return, would increase the fibre-matrix stress and strain transfer unlike E-glass fibres, which have a smooth surface. Moreover, as has been mentioned earlier, the stress concentrations around flax fibres are lower than around glass fibres. Both effect will reduce the interface failures in the transversally loaded fibres.

For the quasi-UD [0,90], it can be seen that the E_2 value doesn't decrease after fatigue cycling. Non-crimp fabrics (NCF), such as the quasi-UD, in cross-ply directions are known for having a slight nonlinearity appearing quite early in the stress-strain curve, between 0.3% and 0.5% strain. This is an evidence that some type of initial damage is generated in this range of strain [6, 45], probably facilitated by the limited crimp in the fabric [45]. The E_2 modulus is located at the point of initiation and development of initial damage around 0.3-0.4% strain for epoxy composites. Thus, after fatigue cycling, the measured E_2 is the modulus of the composite with a 'saturation level' of transverse matrix cracks, and hence is similar to the pre-fatigue E_2 which also was measured in an already 'damaged' specimen (because E_2 is measured beyond the transition point). This explains why E_1 does go down as the damage is introduced in the post-fatigue sample, but the E_2 remains constant. No relevant literature work was found for the post-fatigue properties of glass fibre NCF reinforced composites to corroborate these results. Vallons et al. [46] have stated that although some work was done on carbon NCF, research on glass fibre NCF is very scarce, despite their importance in fatigue-sensitive applications.

As for the strength, all post-fatigue composites properties decreased, except for the UD [0,90]. This behaviour was expected for this cross-ply UD laminate as its composite systematically had the lowest residual strain accumulation, the lowest drop in moduli, as well as the slowest degradation in fatigue strength (observed form the S-N curve in Figure 8-19). The largest strength drop monitored was for the Quasi-UD [0,90] going from 330 MPa to 265MPa after ½ million cycles. The main reason for this it is the presence of heavy stitching used to keep the 0^o and 90^o layers together. Stitching is known to increase the presence of stress concentrators at the tip of these intra ply cracks, and thus increases the matrix damage which may cause a premature fibre fracture in the neighbouring layers and hence decreasing the quasi-static and dynamic properties. Similar results were found by Aymerich et al. [47] on stitched graphite/epoxy composite laminates and Khan et al. [48] on GFRP laminates. In both cases, the quasi-static properties were improved by the presence of stitching that had the capacity of bridging the delamination cracks, but the fatigue performance decreases due to the distortions induced during stitching.

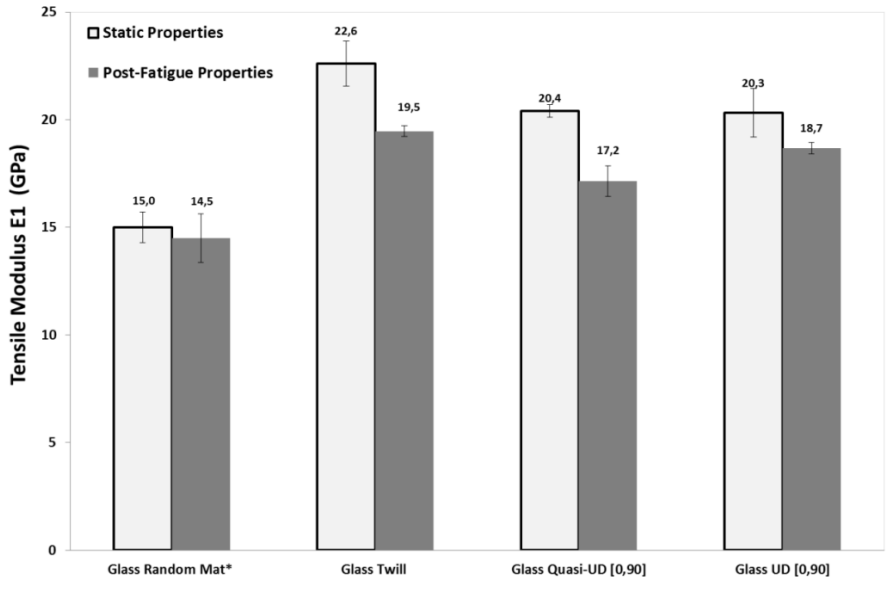
Static Properties
Post-Fatigue Properties
Tensile Modulus E1 (GPa)
25
20
15
10
5
0
15,0
14,5
22,6
19,5
20,4
17,2
20,3
18,7
Glass Random Mat*
Glass Twill
Glass Quasi-UD [0,90]
Glass UD [0,90]

a)

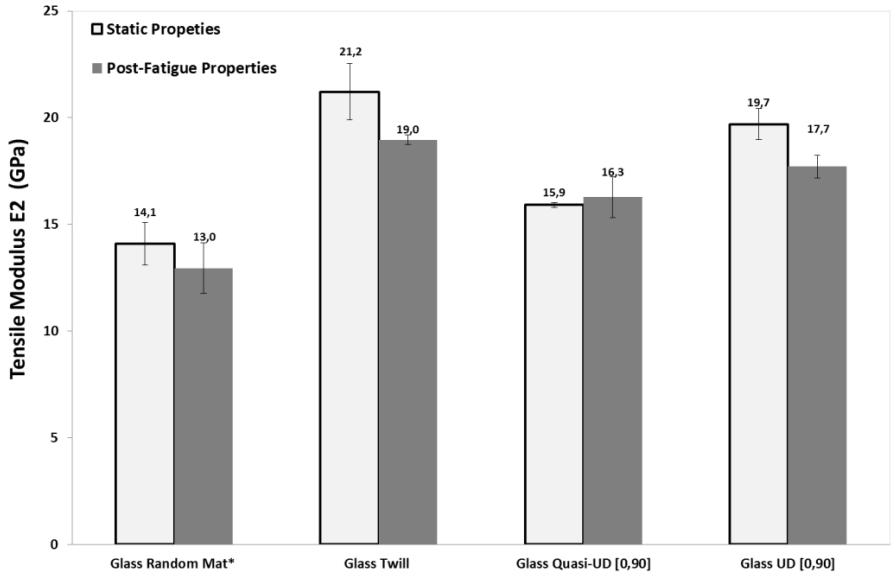
Static Propeties
Post-Fatigue Properties
Tensile Modulus E2 (GPa)
25
20
15
10
5
0
14,1
13,0
21,2
19,0
15,9
16,3
19,7
17,7
Glass Random Mat*
Glass Twill
Glass Quasi-UD [0,90]
Glass UD [0,90]

b)

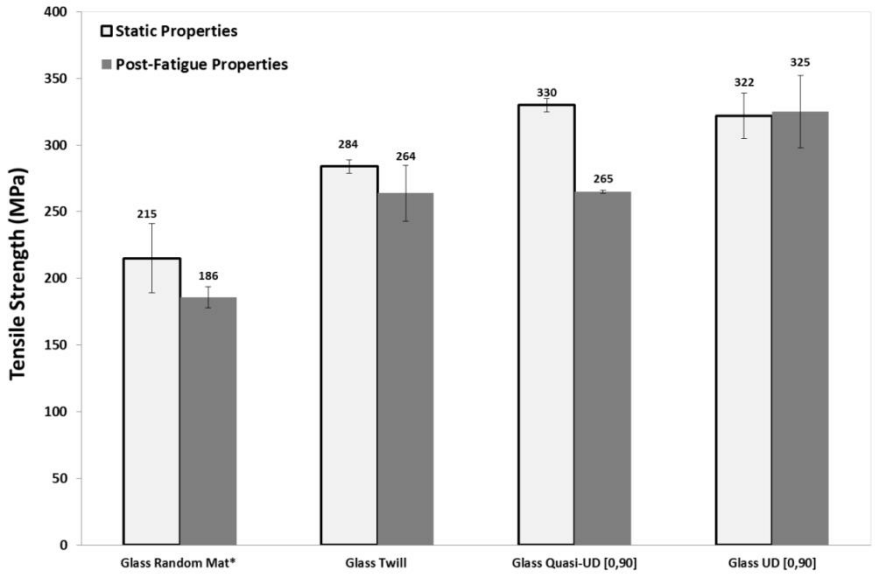
Static Properties
Post-Fatigue Properties
Tensile Strength (MPa)
400
350
300
250
200
150
100
50
0
215
186
284
264
330
265
322
325
Glass Random Mat*
Glass Twill
Glass Quasi-UD [0,90]
Glass UD [0,90]

c)

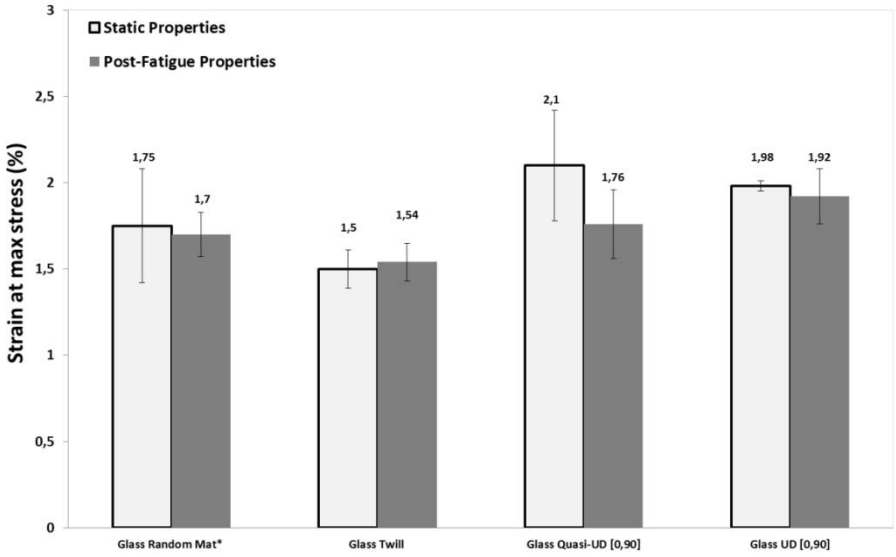

d)

Figure 8-23 : Glass composite residual properties after 500 000 cycles at 30% UTS.

8.6 Conclusions

Tension-Tension fatigue tests were carried out in order to assess the long-term behaviour of flax/epoxy composites. The main conclusions are:

- The results showed that the various textile architectures have different behaviour with random mat < weaves and UD cross-ply laminates < quasi-UD and UD.
- No clear influence of the fibre architecture between the woven fabric and cross-ply laminates nor between the UD and quasi-UD configurations on the fatigue life at lower stress levels.
- The stiffness degradation at low stress level (30% of the UTS) has been found to be stable after a small increase in the early cycles followed by a stiffness stabilisation. The slight increase in the early cycles is consistent with the hypothesis of the stiffening of the fibres (micro-fibrils alignment) in the fibre direction.
- The permanent strain has been found to be limited at low loading levels, and is affected by either plastic deformation of the composite and/or the appearance of damage. Most build-up of permanent strain happens in the early cycles.
- The post-fatigue properties were found to be comparable to the initial quasi-static tests results except for the low twist twill which had a stronger decrease in properties due to the presence of the binding yarns that act as stress concentrators. This was expected from the results of the S-N curves, the stiffness degradation results and permanent strain data.
- The flax composites with architectures that lead to higher quasi-static stiffness and strength (better fibre alignment, enhanced effect of the micro-fibril alignment not seen in weaves due to other artefacts e.g. crimp), show an increased fatigue life, delayed damage initiation and a reduced damage propagation rate. This was illustrated by the limited hysteresis (smaller loop area) and their low permanent strain, presenting low plastic deformation and/or damage accumulation.
- The fatigue properties of flax composites, normalised to the density, have been found to be comparable to glass. The strength degradation for flax fibre composites was found to be lower than the glass ones, and they had also a slower stiffness degradation and a smaller residual strain.

Overall, the behaviour of flax-epoxy composites is comparable to glass fibre reinforced composites and thus, suitable for many new or existing industrial applications.

References

[1] Towo AN, Ansell MP. Fatigue of sisal fibre reinforced composites: constant-life diagrams and hysteresis loop capture. Composites Science and Technology. 2008;68(3):915-24.
[2] Shah DU, Schubel PJ, Clifford MJ, Licence P. Fatigue life evaluation of aligned plant fibre composites through S/N curves and constant-life diagrams. Composites Science and Technology. 2013;74:139-49.
[3] JMP. Oneway Analysis- Compare Means. 2012. http://www.jmp.com/support/help/Compare_Means.shtml
[4] Talreja R. Fatigue of composite materials: Technomic; 1987.
[5] Karahan M, Lomov SV, Bogdanovich AE, Verpoest I. Fatigue tensile behavior of carbon/epoxy composite reinforced with non-crimp 3D orthogonal woven fabric. Composites Science and Technology. 2011;71(16):1961-72.
[6] Lomov SV, Bogdanovich AE, Ivanov DS, Mungalov D, Karahan M, Verpoest I. A comparative study of tensile properties of non-crimp 3D orthogonal weave and multi-layer plain weave E-glass composites. Part 1: Materials, methods and principal results. Composites Part A: Applied Science and Manufacturing. 2009;40(8):1134-43.
[7] Kawai M. Damage mechanics model for off-axis fatigue behavior of unidirectional carbon fiber-reinforced composites at room and high temperatures. Proc of 12th Int Conf on Composite Materials (ICCM-12) Paris, France: Citeseer; 1999. p. 5-9.
[8] Lin S-K, Lee Y-L, Lu M-W. Evaluation of the staircase and the accelerated test methods for fatigue limit distributions. International Journal of Fatigue. 2001;23(1):75-83.
[9] Mandell JF, Meier U. Effects of stress ratio, frequency, and loading time on the tensile fatigue of glass-reinforced epoxy. Long-term behavior of composites, ASTM STP. 1983;813:55-77.
[10] Shahzad A, Isaac D. Fatigue properties of hemp and glass fiber composites. Polymer Composites. 2014;35(10):1926-34.
[11] Shahzad A, Isaac D. Fatigue properties of hemp fibre composites. 17th International conference on composite materials (ICCM-17) Edinburgh, UK2009.
[12] Sendeckyj G. Fitting models to composite materials fatigue data. Test methods and design allowables for fibrous composites, ASTM STP. 1981;734:245-60.
[13] Munikenche Gowda T, Naidu A, Chhaya R. Some mechanical properties of untreated jute fabric-reinforced polyester composites. Composites Part A: Applied Science and Manufacturing. 1999;30(3):277-84.
[14] Liang S, Gning PB, Guillaumat L. A comparative study of fatigue behaviour of flax/epoxy and glass/epoxy composites. Composites Science and Technology. 2012;72(5):535-43.
[15] Asgarinia S, Viriyasuthee C, Phillips S, Dubé M, Baets J, Van Vuure A, Verpoest I, et al. Tension–tension fatigue behaviour of woven flax/epoxy composites. Journal of Reinforced Plastics and Composites. 2015;34(11):857-67.
[16] Vallons K, Lomov SV, Verpoest I. Fatigue and post-fatigue behaviour of carbon/epoxy non-crimp fabric composites. Composites Part a-Applied Science and Manufacturing. 2009;40(3):251-9.
[17] Liang S, Gning P-B, Guillaumat L. Properties evolution of flax/epoxy composites under fatigue loading. International Journal of Fatigue. 2014;63(0):36-45.
[18] Vallons K, Zong M, Lomov V, Verpoest I. Carbon composites based on multi-axial multi-ply stitched preforms - Part 6. Fatigue behaviour at low loads: Stiffness degradation and damage development. Composites Part a-Applied Science and Manufacturing. 2007;38(7):1633-45.
[19] Zhang Y, Li Y, Ma H, Yu T. Tensile and interfacial properties of unidirectional flax/glass fiber reinforced hybrid composites. Composites Science and Technology. 2013;88(0):172-7.
[20] Giancane S, Panella FW, Dattoma V. Characterization of fatigue damage in long fiber epoxy composite laminates. International Journal of Fatigue. 2010;32(1):46-53.
[21] Schulte K, Reese E, Chou T. Fatigue behaviour and damage development in woven fabric and hybrid fabric composites. Sixth International Conference on Composite Materials (ICCM-VI) & Second European Conference on Composite Materials (ECCM-II)1987. p. 4.89-4.99.
[22] De Monte M, Moosbrugger E, Quaresimin M. Influence of temperature and thickness on the off-axis behaviour of short glass fibre reinforced polyamide 6.6–cyclic loading. Composites Part A: Applied Science and Manufacturing. 2010;41(10):1368-79.
[23] Gao F, Boniface L, Ogin S, Smith P, Greaves R. Damage accumulation in woven-fabric CFRP laminates under tensile loading: Part 1. Observations of damage accumulation. Composites Science and Technology. 1999;59(1):123-36.
[24] Bassam F, Boniface L, Jones K, Ogin S. On the behaviour of the residual strain produced by matrix cracking in cross-ply laminates. Composites Part A: Applied Science and Manufacturing. 1998;29(11):1425-32.
[25] Ellyin F, Kujawski D. Tensile and fatigue behaviour of glassfibre/epoxy laminates. Construction and Building Materials. 1995;9(6):425-30.
[26] Fuwa M, Harris B, Bunsell A. Acoustic emission during cyclic loading of carbon-fibre-reinforced plastics. Journal of physics D: applied physics. 1975;8(13):1460.
[27] Dharan CKH, Tan TF. A hysteresis-based damage parameter for notched composite laminates subjected to cyclic loading. Journal of Materials Science. 2007;42(6):2204-7.
[28] Kersani M, Lomov SV, Van Vuure AW, Bouabdallah A, Verpoest I. Damage in flax/epoxy quasi-unidirectional woven laminates under quasi-static tension. Journal of Composite Materials. 2014.
[29] El Sawi I, Fawaz Z, Zitoune R, Bougherara H. An investigation of the damage mechanisms and fatigue life diagrams of flax fiber-reinforced polymer laminates. Journal of Materials Science. 2014;49(5):2338-46.

[30] Gassan J. A study of fibre and interface parameters affecting the fatigue behaviour of natural fibre composites. Composites - Part A: Applied Science and Manufacturing. 2002;33(3):369-74.
[31] van den Oever M, Peijs T. Continuous-glass-fibre-reinforced polypropylene composites II. Influence of maleic-anhydride modified polypropylene on fatigue behaviour. Composites Part A: Applied Science and Manufacturing. 1998;29(3):227-39.
[32] Gassan J. Fatigue behavior of cross-ply glass-fiber epoxy composites including the effect of fiber-matrix interphase. Composite Interfaces. 2000;7(4):287-99.
[33] Zhang Z, Hartwig G. Relation of damping and fatigue damage of unidirectional fibre composites. International Journal of Fatigue. 2002;24(7):713-8.
[34] Jacobsen TK, Brøndsted P. Mechanical properties of two plain-woven chemical vapor infiltrated silicon carbide-matrix composites. Journal of the American Ceramic Society. 2001;84(5):1043-51.
[35] John S, Herszberg I, Coman F. Longitudinal and transverse damage taxonomy in woven composite components. Composites Part B: Engineering. 2001;32(8):659-68.
[36] Mattsson D, Joffe R, Varna J. Damage in NCF composites under tension: effect of layer stacking sequence. Engineering Fracture Mechanics. 2008;75(9):2666-82.
[37] Lomov SV, Ivanov D, Truong T, Verpoest I, Baudry F, Bosche KV, Xie H. Experimental methodology of study of damage initiation and development in textile composites in uniaxial tensile test. Composites Science and Technology. 2008;68(12):2340-9.
[38] Hughes M, Carpenter J, Hill C. Deformation and fracture behaviour of flax fibre reinforced thermosetting polymer matrix composites. Journal of Materials Science. 2007;42(7):2499-511.
[39] Bos H, Molenveld K, Teunissen W, Van Wingerde A, Van Delft D. Compressive behaviour of unidirectional flax fibre reinforced composites. Journal of Materials Science. 2004;39(6):2159-68.
[40] Andersons J, Sparnins E, Porike E, Joffe R. Strength distribution of elementary flax fibres due to mechanical defects. International Inorganic-Bonded Fiber Composites Conference2008. p. 1-7.
[41] Schulte K, Baron C, Neubert N. Damage development in carbon fibre epoxy laminates: cyclic loading. Advanced Materials Research and Developments for Transport 1985 Composites. 1985:281-8.
[42] Schulte K. Stiffness reduction and development of longitudinal cracks during fatigue loading of composite laminates. Mechanical characterisation of load bearing fibre composite laminates. 1985:36-54.
[43] Van Paepegem W, Degrieck J. A new coupled approach of residual stiffness and strength for fatigue of fibre-reinforced composites. International Journal of Fatigue. 2002;24(7):747-62.
[44] Gamstedt EK, Berglund LA, Peijs T. Fatigue mechanisms in unidirectional glass-fibre-reinforced polypropylene. Composites Science and Technology. 1999;59(5):759-68.
[45] Lomov SV. Non-crimp fabric composites: manufacturing, properties and applications: Elsevier; 2011.
[46] Vallons K, Adolphs G, Lucas P, Lomov SV, Verpoest I. Quasi-UD glass fibre NCF composites for wind energy applications: a review of requirements and existing fatigue data for blade materials. Mechanics & Industry. 2013;14(03):175-89.
[47] Aymerich F, Priolo P, Sun C. Static and fatigue behaviour of stitched graphite/epoxy composite laminates. Composites Science and Technology. 2003;63(6):907-17.
[48] Khan MS, Mouritz A. Fatigue behaviour of stitched GRP laminates. Composites Science and Technology. 1996;56(6):695-701.

Chapter 9
Environmental impact assessment of flax composites

Thanks to their good mechanical properties and their lightness, the use of flax fibre composite materials has increased exponentially over the years in industries such as automotive, sporting goods and construction. Recent research is aiming at the use of environmentally-friendly composite materials as alternatives for the current and less sustainable ones. In order to replace those materials, flax composites would have to fulfil equivalent mechanical performance. Although flax has similar specific stiffness than glass (as presented in Chapter 8), they only have been incorporated in non-structural designs. With increasing knowledge on the flax composites, better processes and production methods, flax fibres have now the potential to be used in mechanically performant applications such as automotive. However, some problems still need to be tackled prior to the incorporation of flax composites as non- and semi-structural components in automotive applications.

With new directives such as the ELV and with the development of an EU framework for sustainable building, the development, re-use and recycling of natural fibres composites are crucial. Whereas the recycling of steel is well documented and researched, the possible recycling techniques for composite materials and especially natural fibre composites, are much less investigated.

A clear investigation of the end-of-life possibilities, and especially the recycling methods, has to be performed. It is necessary to prove that this directive is easy to achieve when incorporating composite materials in the automotive design. A second interesting remark is the question whether changing from manmade fibres to natural fibres, in (semi-)structural automotive applications, is environmentally beneficial or not. Previous studies show that the production of one kilogram of flax fibres is indeed environmentally less damaging than one kilogram of glass fibres. But, whereas in non-structural applications weight reduction is the main objective, in (semi-)structural applications the mechanical properties are of an even higher importance. The strength of glass fibres are better than flax fibres, at an almost equivalent stiffness, hence a trade-off between mechanical properties and weight gain exists. Therefore, it is necessary to analyse the entire life cycle of both composites in order

to decide which material is the most environmental friendly. In the next section, three End-of-Life (EOL) methods will be investigated for flax composites combined to an MAPP matrix. The chemical, mechanical and incineration strategies are investigated as well as their upscaling feasibility. A comparative Life Cycle Analysis (LCA) on the various EOL options has been conducted in order to define the most suitable technique, from an environmental perspective. This is followed by two cradle-to-grave comparative LCA's for two automotive cases (car roof and bumper). The flax composites will be compared to the current materials used such as glass fibres or steel.

The life cycle impact assessments are performed in accordance to ISO 14000 and ISO 14040. The PRé Consultants SimaPro 8 software was used to construct the LCA studies. The used LCA method was the ReCiPe Endpoint (H) method and the chosen normalization/weighting set was the Europe ReCiPe H/A set. The main impact categories that were identified and described in Table 9-1 and in Figure 9-1. Throughout the chapter, the environmental impact will be described using the two method described below:

- Characterization: quantification of the degree to which each polluting substance contributes to the different environmental impacts described in Table 9-1. Each mid-point relative contributions to the overall impact is expressed in % of the overall environmental impact. All impact scores are showed on a 100% scale, this means that maximum impact caused by the substitutions on each category is marked with ±100%. A positive value indicate a positive environmental burden and a negative value indicates savings of environmental burdens and means that the impact can be avoided by this approach;
- Single score: three endpoint categories (human health, ecosystems and natural resources) are normalized, weighted and combined into a single score. Figure 9-1 shows the relation between the 18 midpoint categories used for the characterization and the three endpoint categories included in the. The single score have the advantage of generating one, easy-to-communicate impact number and is expressed in millipoint (mPt) or point (Pt).

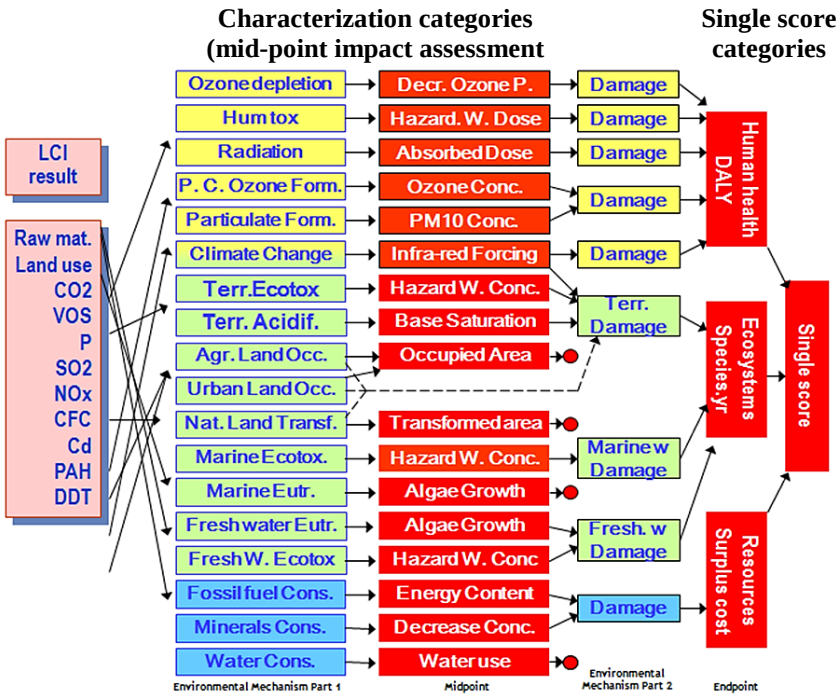

Figure 9-1: The relationship between LCI parameters, midpoint indicator used for the characterization analysis and endpoint indicator for single score assessment in ReCiPe 2008 method used in SimaPro.

Impact category group	Name of the midpoint impact category	Definition	Impact indicator	Damage categories (*Endpoint/single score categories)	Units
Acidification	Terrestrial acidification	Reduction of the pH due to the acidifying effects of anthropogenic emissions	Acidity increase in water and soil	Ecosystem quality and biodiversity decrease	$yr \cdot m^2$
Climate change	Climate change	Alteration of global temperature caused by greenhouse gases	Disturbances in global temperature and climatic phenomenon	Biodiversity decrease and abnormal climatic phenomenon	$W \cdot yr/m^2$
Depletion of abiotic resources	Metal depletion Fossil depletion	Decrease of the availability of non-biological resources as a result of their unsustainable use	Decrease of resources	Natural resources and possible ecosystem collapse	kg^{-1} MJ
Ecotoxicity	Freshwater ecotoxicity Marine ecotoxicity Terrestrial ecotoxicity	Toxic effects of chemicals on an ecosystem	Biodiversity loss and/or extinction of species	Ecosystem quality and species extinction	$yr \cdot m^2$
Eutrophication	Freshwater and Marine	Accumulation of nutrients in aquatic systems	Increase of nitrogen and phosphorus concentrations Formation of biomass	Ecosystem quality	$yr \cdot kg/m^3$
Human toxicity	Human toxicity	Toxic effects of chemicals on humans	Cancer/ respiratory diseases, other non-carcinogenic effects and effects to ionising radiation	Human health	-
Ionizing radiation	Ionizing radiation	Type of radiation composed of particles with enough energy to liberate an electron from an atom or molecule	Effects of radiations on health	Human health and ecosystem quality	$Man \cdot Sv$
Land use	Agricultural land occupation Urban land occupation Natural land transformation	Impact on the land due to agriculture, anthropogenic settlement and resource extractions	Species loss, soil loss, amount of organic dry matter content, etc...	Natural resource (non- and renewable) depletion	$yr \cdot m^2$
Ozone layer depletion	Ozone depletion	Diminution of the stratospheric ozone layer due to anthropogenic emissions of ozone depleting substances	Increase of ultraviolet UVB radiation and skin illnesses	Human health and ecosystem quality	ppt · yr *
Particulate matter	Particulate matter formation	Suspension in air of extremely small particles originated from anthropogenic processes such as combustion, resource extraction, etc.…	Increase of particles suspended on air	Human health	kg
Photochemical oxidation	Photochemical oxidant formation	Type of smog created from the effect of sunlight, heat, Non-methane volatile organic compound and nitrates	Increase in the seasonal smog	Human health and ecosystem quality	kg

Table 9-1: ReCiPe endpoint midpoint categories and their definition [1]. *The unit ppt refers to unit of equivalent chlorine

9.1 EOL techniques for flax-MAPP composites

In the following sections, a description is presented of the three selected EOL methods for flax-MAPP composites used in this study, being: chemical recycling, mechanical recycling and incineration with energy recuperation. For both chemical and mechanical recycling techniques, the starting material was a UD $[0, 90]_{3s}$ flax MAPP composite with a V_f=40%. The incineration with energy recovery method is not a recycling technique but a common EOL option for composites. In this work, the focus is not on the recycling of the matrix material, but on the recycling of the natural fibres. It has to be noted that the used plates all had an initial fibre volume fraction of 40%.

9.1.1 Chemical recycling

The goal of the chemical recycling process is to obtain a complete separation of the fibres and matrix material which would allow their re-use. In studies from the 80's and 90's, a recycling technique for polypropylene (PP) was proposed by Poulakis et al.[2]. The dissolution/re-precipitation process was suggested using para xylene (p-xylene) as a solvent. They have found that the recycled PP matrix had equivalent mechanical performance to the fresh PP. In this work, the focus is put on recuperating the fibre and not the matrix. The chemical recycling technique has to satisfy three criteria in order to be a feasible:

- The damage on the fibre surface should be minimal;
- The separation process should be technically feasible, and;
- The composite made of the recycled fibres should have good mechanical properties.

9.1.1.1 Chemical dissolution of the MAPP-matrix

The dissolution of the MAPP matrix was first done at small scale with pieces of composites of 1cm² and 4cm². The small scale test allows the determination of the dissolution parameters such as time and temperature. Each sample is weighed with an accuracy of 0,001 gram and plunged in a beaker containing the heated p-xylene solvent. Since the para-xylene (p-xylene) boils at 138ºC, the tests were done at a temperature of 120ºC. The solution is constantly stirred and an excess of solvent is used in order to keep a low viscosity. After the test, the sample is removed from the solution and rinsed with water to remove the remaining solvent. The samples are dried for 24h at 60°C. The dried samples are weighed and the weight loss for each sample is calculated.

The process is then scaled up to in order to recycle a 30x15 cm plate. A general schematic of the process is shown in Figure 9-2. The four litres solution is added in the glass container and placed on a heated sand bed and kept at 120ºC. The whole system was placed under a fume hood. When the solution reaches the required temperature, the composite plate is suspended by metal wires into the solution which allows the accessibility of the surface to the solvent. The plate remains in the solution for the required testing time and is then removed. The layers can be manually separated and rinsed with water. They were later on dried for 24h at 60°C.

For the production of the recycled composite plates, the compression moulding technique was used (see Chapter 4 for more details). Since not all of the MAPP dissolved, the calculation of the additional fresh MAPP was done based on the weight fraction calculations (Eq. 4.4 in Chapter 4) to obtain a fibre volume fraction of 40%. The amount of MAPP that has to be added can be calculated using the following formula:

$$\#\, resin\ plies = \frac{\Delta m_{composite}}{\rho_{resin} * Surface_{resin\ film} * t_{resin\ film}} \qquad \text{(Eq. 9.1)}$$

Where $\Delta m_{composite}$ is the weight loss of the composite plate, ρ_{resin} is the MAPP density (0.92 kg/m^3), surface $_{resin\ film}$ is the size of the composite plate and $t_{resin\ film}$ is the resin film thickness

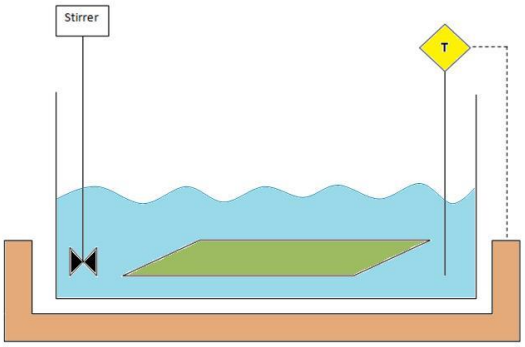

Figure 9-2: Schematic of the chemical recycling process. The temperature is controlled manually for the up scaled process.

9.1.1.2 Chemical recycling results

First, the potential surface damage induced by the p-xylene solvent on the fibres is discussed. Secondly, the ratio of polypropylene that can be chemically dissolved and finally, the mechanical properties of the composite containing chemically recycled fibres are investigated. The goal of the recycling technique is to dissolve the MAPP matrix and recover the continuous fibres with the same properties as fresh fibres without damaging the flax fibres. To evaluate the possible surface damage of the fibres, flax fibres are soaked in a p-xylene solution at 130°C for 5h. A microscopic inspection with SEM (Figure 9-3) shows no visible difference between the pure fibre and solvent-treated fibres. No damage on the fibre surface is visible. As the p-xylene is not expected to dissolve the flax fibre constituents (pectin, lignin and hemicellulose) no other type of damage is expected on the fibres.

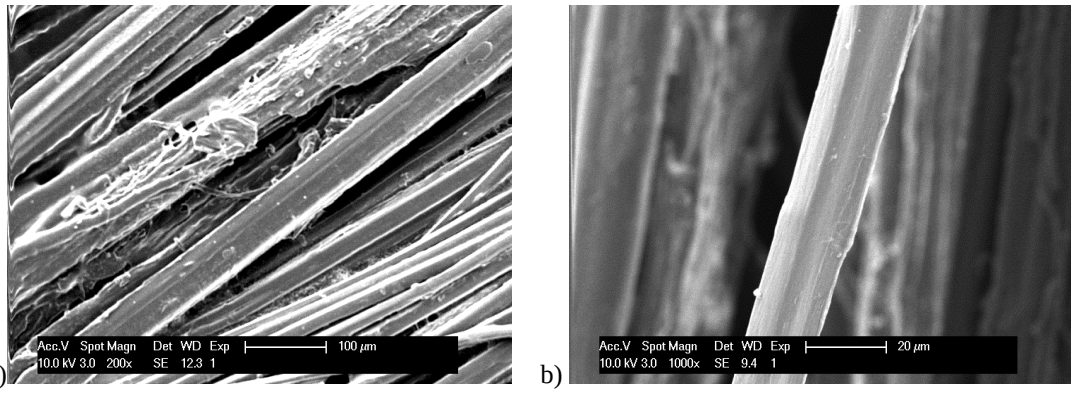

a) b)

Figure 9-3: SEM images of: a) non-treated fibres and b) fibres soaked in p-xylene at 130°C for 5h where no damage of the fibre surface is visible.

In order to determine the efficiency of the chemical recycling process, the polypropylene mass loss of the composite was measured over time. The temperature of the test was set at 120°C in order to have a slight margin with respect to the boiling point of the p-xylene which is located at 138°C. Figure 9-4 shows the mass loss of the composite over time. A rapid increase of mass loss can be observed in the first part of the test which is due to the rapid degradation of the MAPP layers on the outside of the composite which are in direct contact with the solvent. This is followed by a plateau after three hours when the mass loss stabilizes. As fresh p-xylene was introduced constantly, this effect is not due do to

saturation of the solvent. It is hypothesised that since the dissolution is made at temperatures lower than the polypropylene melting temperature, semi-crystalline polymers will not completely dissolve in organic solvents. The solvents will penetrate the non-crystalline regions to a certain level which results in the solvation of individual segments of polymer chains and overall swelling of the specimen [3-6].

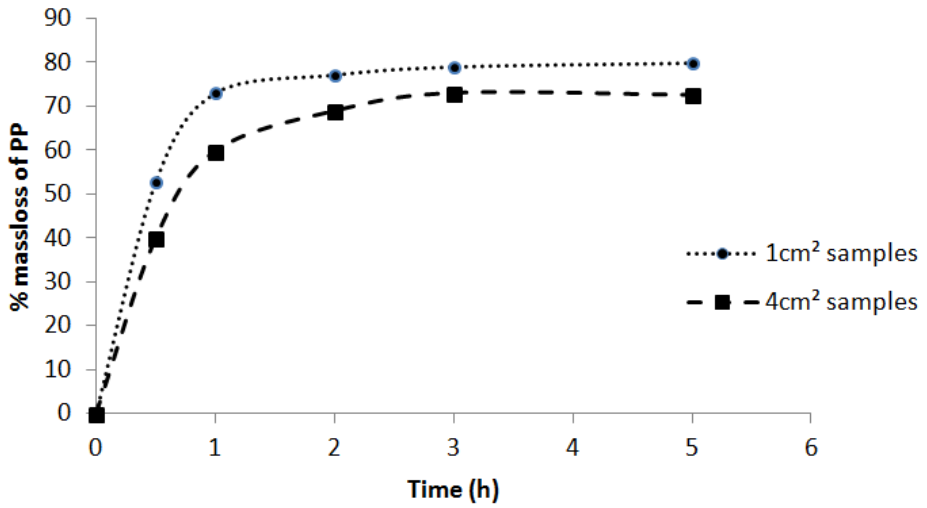

Figure 9-4: Mass loss of flax-MAPP composite soaked in p-xylene at 120°C for two different sample sizes.

Finally, at the end of the process, a slower mass loss for the larger sample is recorded which can be due to the longer diffusion times of the solvent from the outside to the centre of the composite. In comparison, the chemical recycling of synthetic fibres done through hydrolysis [7, 8], glycolysis [9] and acid digestion [10], achieve a higher degree of thermoplastic removal than the p-xylene. Furthermore, higher temperatures ranging from 250°C to 450°C can also be applied in combination to these chemicals to accelerate the dissolution rate. However, at higher temperatures, the glass fibres lose strength after the recycling process [10, 11]. This makes them less interesting as alternative to virgin glass fibres. For flax fibres, these higher temperatures can obviously not be used without causing severe damage of the fibre structure.

For the investigation of the mechanical properties of the chemically recycled composites, the plate size was increased from 1cm² and 4cm² plates to 450cm² plates. The increase in plate size was done in order to be able to cut tensile samples out of the plate and test the properties of a composite made with recycled fibres. The dissolution of the MAPP lasted for 1h30min and 56% of the MAPP was dissolved.

To make the recycled composite, the weight of lost MAPP was replaced by fresh MAPP in between each fibre layer and was remanufactured following the same compression moulding procedure. A reference plate was tested to compare the tensile test results of this reference plate with the recycled plate. When comparing the results of the tensile test shown in Table 9-2, it is clear that the reference composite and the recycled composite have similar properties. To verify this, a two sample statistical t-test was conducted. In order to verify whether the two samples have the same variance an F-test was performed too. It was found that the assumption that the strength, failure strain and E-modulus are the same is justified within the 95% confidence level.

	E-Modulus (GPa)	Strength (MPa)	Failure strain (%)
Reference flax-MAPP composite	14.8 ± 1.6	157 ± 13	1.23 ± 0.16
Recycled flax-MAPP composite	15.9 ± 0.9	156 ± 8	1.12 ± 0.04

Table 9-2: Quasi-static mechanical properties of the reference vs the recycled flax-MAPP composite at V_f = 40%.

9.1.2 Mechanical recycling

Mechanical recycling was investigated as a second recycling technique for flax fibres reinforced polypropylene (FFRP). The flax-MAPP composite is shredded into small pieces which reduced the fibre length and the properties of the recycled material. Two types of recycled products were then made: flakes and pellets as shown in Figure 9-5.

A part of the flakes is reprocessed "as is" while the rest is fed in a compounder to produce pellets for injection moulding. The use of pellets is more logical towards industrial injection processes since they are easier to stock and handle and they can be mixed with extra PP in the extruder. This extra compounding step makes the recycled material more homogeneous in its composition and size. However, as the fibre size is further reduced, the mechanical properties will also decrease. Due to technical limitations, such as sourcing of MAPP pellets, the plates were produced using compression moulding with MAPP films instead of injection moulding which required large amounts of polymer and flakes.

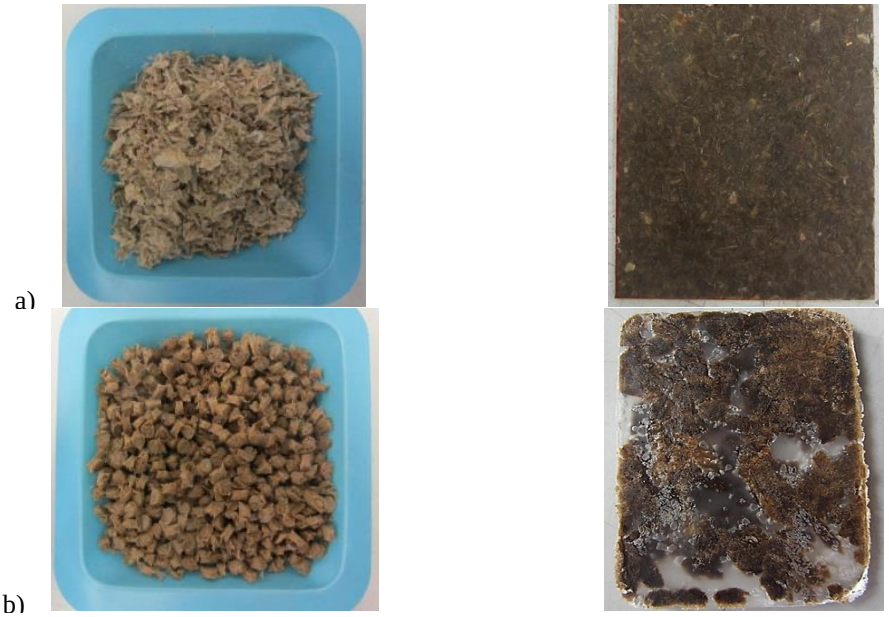

Figure 9-5: Image of: a) flakes and flakes composite and b) pellets and pellet composite.

In order to make new plates out of the recycled materials by compression moulding, two mixing procedures were proposed: a random mixture of compounded flax-MAPP pellets and a stacked structure by using fresh MAPP film. By altering the amounts of recycled material to fresh MAPP, composites with different volume fractions were made. A visual inspection of the recycled composite plates was performed and it was observed that with the flake composite, the orientation of the fibres does not change during the compression moulding step and the fibres remain oriented as in the original shredded flake. For the pellets, the fibres are randomly oriented because the extruder thoroughly mixes the fibres while melting the polymer matrix and it is not possible to distinguish the fibres from each other in the pellets composite. Due to bad fibre distribution of the pellets during

compression moulding, which lead to non-homogenized composites as seen in Figure 9-5b, only the plates made with flakes are tested.

9.1.2.1 Shredding and compounding

The flax-MAPP composites plates are shredded using a Piovan Plastics Tech shredder shown in Figure 9-6 a. The plates are first chopped by a plate cutter into 10cm x 10cm plates as larger pieces may block the device. The shredded material called flakes, has a mesh size of ≈6mm. Part of the material was kept to produce flake-based composite as it is and the rest was fed into the Leistritz ZSE 18 MAXX extruder with twin co-rotating screws, shown in Figure 9-6 b, to produce the compound. No additional polymer is added to the mixture. The shredded material is fed through the side entrance in order to reduce the retention time in the extruder. An increase in retention time would lead to the degradation of the flax and the matrix which detrimental properties for the final composite. The screws rotate at 180 rpm at a temperature of 190°C.

The extruded material is led through a round die with a diameter of 3.5mm and passes through a water bath to cool it down and a knife to cut then 8 mm long pellets. After extrusion, the pellets were dried for 24h at 60°C. Both, the pellets and the flakes, have a fibre volume fraction of 40%. Following the production of the pellets and flakes, they were reprocessed into plates with varying fibre volume fractions from 10 to 40%. Thus, besides the V_f =40% case, all the other plates have fresh MAPP added to them. Plates of 110mm x 100mm were produced using compression moulding.

In order to calculate the correct amount of matrix material, another procedure is used based on the mass fractions of fibre rather than the volume fraction. Since the wanted fibre volume fraction (V_f), the density of the fibres (ρ_f) and the density of the matrix material (ρ_m) are known, the fibre weight fraction (W_f) can be calculated using the following formula:

$$W_f = \frac{\rho_f * V_f}{\rho_f * V_f + \rho_m * (1 - V_f)} \quad \text{(Eq. 9.2)}$$

Based on the fibre mass fraction (W_f), the density of the fibres (ρ_f) and the density of the matrix material (ρ_m), the density of the composite (ρ_c) can be calculated by using the rule of mixture:

$$\rho_c = \rho_f * W_f + \rho_m * (1 - W_f) \quad \text{(Eq. 9.3)}$$

Since the plate size is known, the mass of each plate can be calculated using the density of the composite and the volume of the plate. The addition of polymer material can then be calculated according to the desired V_f using:

$$Weight\%_{recyled\ material} = \frac{W_{fibers\ in\ composite}}{W_{fibers\ in\ recyclate}} * 100 \quad \text{(Eq. 9.4)}$$

a) 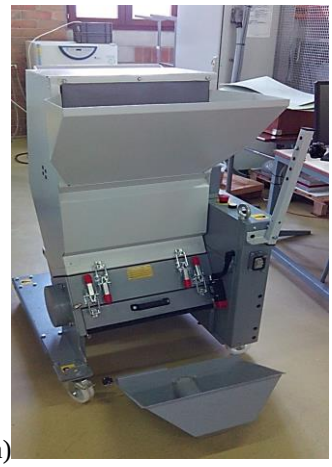 b) 

Figure 9-6: a) *Piovan Plastics Tech* shredder and b) *Leistritz ZSE 18 MAXX* extruder. These equipment are located in the Technology Cluster of KU Leuven in Oostende.

9.1.2.2 Mechanical recycling results

The properties of the recycled composites are compared with fresh random mat composites. Figure 5 compares the flexural modulus and strengths of the recycled flake composites vs the random mat composites and the pure MAPP (0%vol). It has to be noted that the intrinsic properties of the MAPP (E=0.342 GPa and σ=18 MPa), previously demonstrated in Chapter 5, are very low compared to pure PP which are E≈1-2 GPa and σ≈25-40 MPa. It can be observed that for V_f higher than 30%, no improvement in properties is seen for the mat material which might be due to the fact that the impregnation of the mat becomes more difficult at higher volume fractions of fibres. Even though the recycled materials do not reach the properties of the fresh composite, the observed difference is small except for the 30vol% case. This reduction in stiffness and strength is the result of the low fibre aspect ratio in the flake-based composite (fibre length ≈ 6 mm) compared to the random mat where the fibre length is 8 cm.

It is therefore feasible that the recycled materials can be used in non- or semi-structural applications. Especially since the 40vol% recycled composite reaches the same flexural modulus as a 30vol% random mat composite. It has to be noted that for the recycled composites tested in the three point bending test, the main failure mechanism was buckling at the compressive side of the 3P-bend specimen, instead of fibre breakage at the tension side, due to the weak matrix material.

Mechanical recycling is an established recycling technique for glass fibre composites (GFRP), but generally results ground up GFRP with a particle size around 0,1-1mm that are then used as filler in sheet moulding compounds or in cement. Furthermore, after multiple injection cycles (recycling), the fibre size further reduces leading to a continuous decrease in quasi-static properties. However, in the case of flax fibres, Baley et al. [12] have proven that successive injection (7 in total) of the flax-PP and hemp-PP do not affect the properties of the recycled composite unlike the glass-PP composite who suffered a decrease of ≈ 60% in stiffness and ≈ 50% in strength have stable stiffness and strength. They have related this stable behaviour to the fact that there is limited evolution of the aspect ratio over the number of cycles for flax and hemp fibre. A similar observation was made for the aspect ratio of flax-PLLA composite by Le Duigou et al. [13]. They have seen a large drop in aspect ratio (L/d) during the first injection, but no further reduction in subsequent recycling cycles on the contrary to glass fibres.

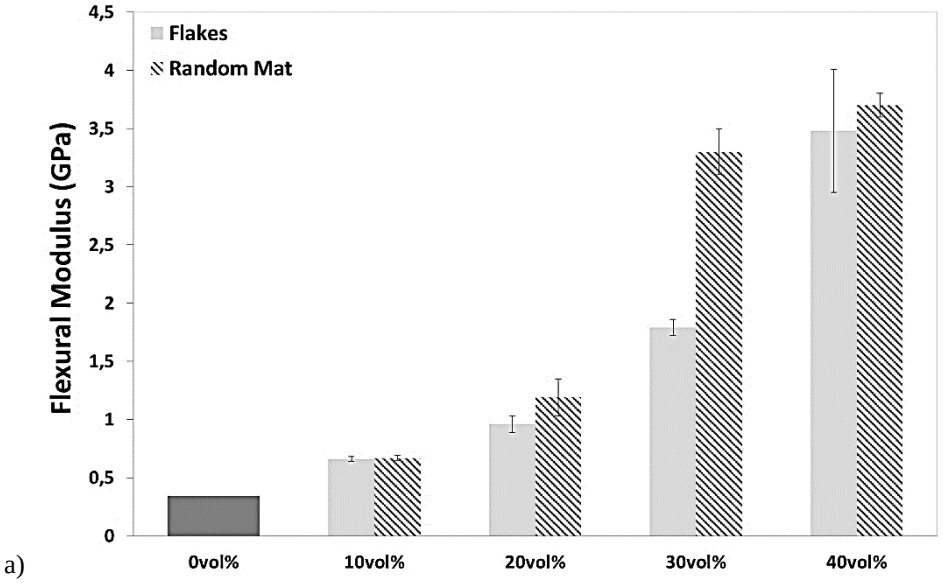

a)

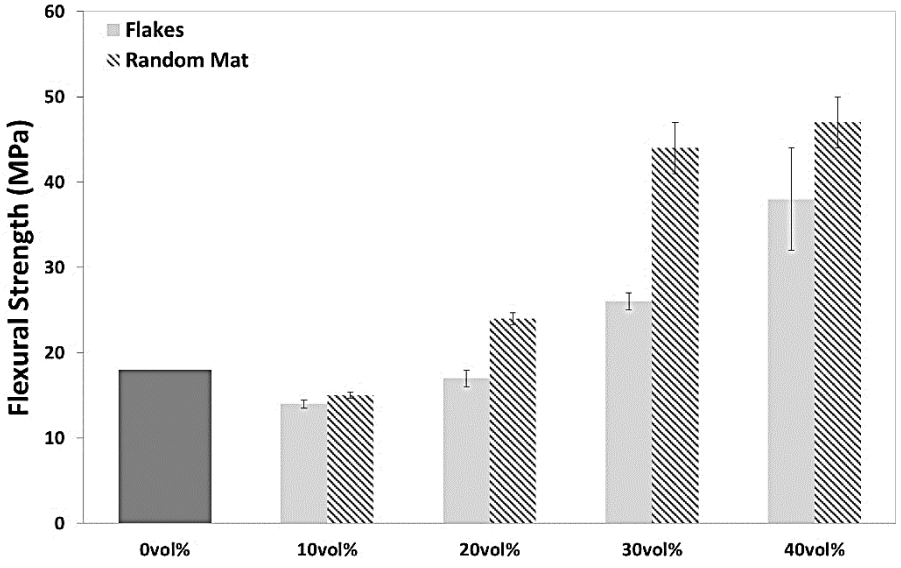

b)

Figure 9-7: a) flexural modulus and b) flexural strength of flake composites at different volume fractions of fibres as compared to random mat composite. The 0% data indicate the properties of the MAPP matrix.

9.1.3 Incineration with energy recovery

9.1.3.1 Calorimetric bomb experiments

To estimate the amount of energy that could be recuperated from the incineration of the flax/MAPP composites, the heat of combustion of the composite constituents was studied using a calorimetric bomb. The heat of combustion is released by the combustion of all carbon and hydrogen containing compounds with oxygen to form carbon dioxide and water. We noticed that oxidation of other elements (e.g. sulphur) can also occur. Oxygen bomb calorimeters are the standard instruments in measuring the calorific value of solid combustible materials. A Parr 1261 bomb calorimeter with a Parr 1108 oxygen combustion bomb, shown in Figure 9-8, was used in this study. The calorimeter calibration is made using a well-known material, benzoic acid, which has a calorific value of 6318 cal/gr.

Figure 9-8: Parr Instruments 1108 oxygen combustion bomb.

In the experiment, a sample is placed within an oxygen combustion bomb made out of stainless steel. A Pt-fuse wire is applied in such a way that only contact with the sample occurs. The fuse wire is then connected to an ignition source and the bomb calorimeter is sealed and filled with pure oxygen up to 420 psi (approximately 29 bars). The bomb is then placed in a bucket containing two litres of water (measured with an accuracy of 0,001 litre to reduce errors in the computation of the calorific value). The fuse is ignited and the sample is combusted. The water in the chamber around the bomb is continuously stirred while being heated by the sample's combustion heat. A thermometer records the temperature change in the water bucket. The calorific value is then computed using the data of the recorded temperature change.

After calculation of the calorific value of the reactants, a correction was made to correct calorific value of the tested samples taking into account the combustion of the fuse wire. By measuring the fuse length before and after combustion, the total heat of combustion caused by the fuse can be calculated. The fuse has a calorific value of 2,3 cal/cm.

9.1.3.1 Incineration results

The energy recuperation capacity during incineration of flax fibre vs glass fibre composites is estimated by measuring the calorific values in a bomb-calorimeter as described in the previous section. The calorific values for flax, MAPP, 40vol% glass fibre composites and 40vol% flax fibre composites were determined. Because glass fibres are non-combustible, their heat of combustion was considered as 0 MJ/kg. The results of the heat of combustion tests are presented in Table 9-3.

Material	Average heat of combustion [MJ/kg]	Standard deviation [MJ/kg]
Flax fibre	16,9	0,1
MAPP	46,1	0,1
Glass fibre	0	N/A
Flax-MAPP 40vol%	31,5	0,5
Glass-MAPP 40vol%	17,1	0,2

Table 9-3: Heat of combustion of glass and flax composites, flax fibres, glass fibres and MAPP.

As a composite material is a combination of two materials, the heat of combustion of the composite material is expected to be linearly dependent on weight fractions of both materials. Figure 9-9 shows how the calorific value changes when altering the weight fraction of fibres in the composite. The experimental value for the composites coincides very well with the calculated value, based on the simple weight averaging.

The residue that remained after the combustion of the bio-composite (flax-MAPP) was found to be less than 0.1% of the weight and it was a mixture of soot (carbon) and water. The waste gas from MAPP was not measured or analysed, however it can be expected that it is similar to the combustion gas of PP. The contribution of waste gasses from the combustion of flax will mainly be in the form of H_2O and CO_2 [14]. It was found that the larger contribution to the calorific value of the FFRP comes from the combustion of the MAPP rather than the fibre because the calorific value of hydrocarbons is superior (H/C ratio). The calorific value of flax is within the range of calorific values of other wood-like products.

The incineration of GFRP however leads to a molten glass residue that can stick to the incinerators wall. Because the glass fibres are non-combustible, the calorific value of these composites is lower as of the FFRP. The non-combustible glass residue will have to go through further treatments after incineration, which is their main disadvantage in the incineration process. As of today, these residues are used for road building and as a filler in concrete for the building industry [15, 16]. The incineration process for natural fibre composites has the advantage of being a fast technique and applicable for all fibre/matrix combinations.

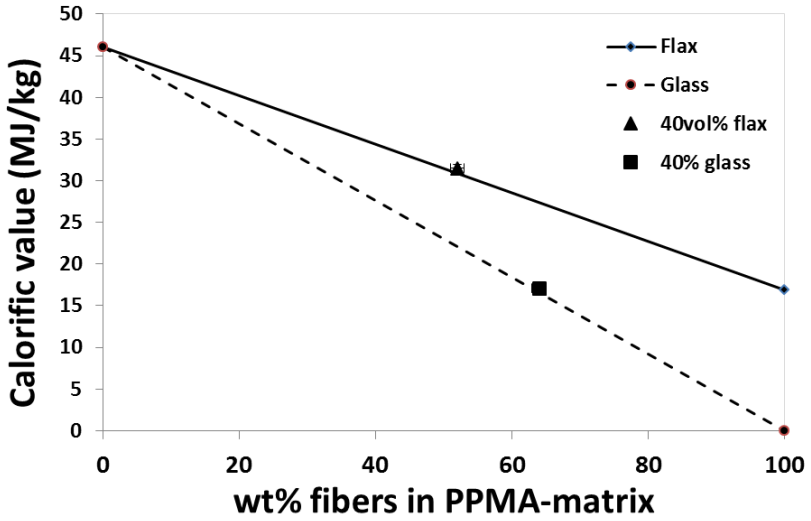

Figure 9-9: Calorific value of glass-MAPP and flax-MAPP composites as function of the wt% of fibres.

9.1.4 Life cycle Analysis of EOL techniques

In order to make a judicious choice in the end of life method, a comparative LCA study on FFRP was performed. The goal was to assess the environmental impact associated with the used techniques. The reference flow is defined as one kg of V_f = 40% long fibres FFRP waste. In the next sections, the LCA inventories of the flax and of each investigated end of life technique will be presented. This is followed by the assessment of their impact and their comparison.

9.1.4.1 Inventory for flax fibre composites

The inventory was partially constructed based on in-house measured data and partially with data from other sources. In this study, the inventory data of the production of flax fibres itself was taken from literature [17, 18]. Appendix G gives an overview of the inventory that was used as a basis for the production of long flax fibre composites, as well as all intermediate steps, like retting etc. In the current manufacturing practice, flax fibres are

usually dried before composite production. However, in many LCA studies this aspect is not taken into account. In theory, taking into account the specific heat of evaporation of water, 2257 kJ (latent heat of evaporation) are needed to evaporate 1 litre of water at atmospheric pressure. However, it has to be taken account that the oven will function for 24h at 60°C, thus the total energy used to evaporate the moisture will be far more superior.

A dataset for the oven drying of maize straw from the Ecoinvent 3.01 database was adapted for the drying process of flax fibres and is presented in Table 9-4. The energy consumption for drying was calculated based on a 2000W electrical convection dryer as the one available in the lab. It has to be noted, that this strategy was based on a lab-scale study while in industry, such drying operations are normally more efficient and often use "waste heat" from other processes in the factory. The moisture content of the flax fibres was assumed to be of about 15wt%. This value was based on a study of the moisture content of green flax at a relative humidity of 85% and 95%, being 14wt% and 17wt% respectively [19]. The average relative humidity in Belgium is slightly lower than 80%, however higher values of relative humidity do occur.

Resource category	Name	Value
Input	Electricity (BE)	4,52 MJ
Output	Drying of flax fibres	1E-3 m³

Table 9-4: Life cycle inventory for the drying of one litre of water out of flax fibres.

Once the fibres are dried, they are ready to be consolidated with the matrix through compression moulding process. Table 9-5 gives an overview of the life cycle inventory for the consolidation of a 40vol% flax composite corresponding to 52wt% of fibres. The Ecoinvent 3.01 database contains data for the thermoforming-calendering[1] of thermoplastics (process: Thermoforming, with calendering (RER)| production | Alloc Def, U) which is the closest to compression moulding. The type of thermoforming was not specified in the Ecoinvent database. Furthermore, as compression moulding require also pressure, using the thermoforming process lead to an underestimation of the final impact. Since the input material of the matrix consists of pellets, they have to be transformed into polymer sheets through calendering. By using the maximal energy consumption values, it was assumed that this process could also be applied to composites. All auxiliaries input such as the mould releasing agents etc., are also taken into account. The PP data for granules is also provided by the database. Over the entire process, a material loss of 3wt% was assumed. No post-consolidation processes were taken into account.

Resource category	Name	Value
Input	Polypropylene, granules	4,944E-1 kg
	Flax long fibres (dried)	5,356E-1 kg
	Thermoforming, with calendaring	1,03 kg
Output	Flax-PP V_f=40% composite	1 kg
Final waste streams	Flax-PP V_f= 40% composite waste	3E-2 kg

Table 9-5: Life cycle inventory for the consolidation of the flax composite.

9.1.4.2 Inventory for the EOL possibilities for FFRP

For the chemical recycling techniques two approaches were considered. In the first approach, there is only the recuperation of the flax fibres and the solvent, with PP handled as chemical waste. The second approach considered the recycling of both components. The

[1] Calendering is a finishing process that is used on plastic films to smooth, coat, or thin a material. For textiles, the fabric is pressed between rollers at high temperatures and pressures.

recuperation of the solvent and PP is done by a precipitation and distillation technique based on recycling studies of PP in the 1990's [2]. The uncertainties on the inventory for this second approach are higher because of the low availability of data on this process.

Table 9-6 gives the life cycle inventory for the both approaches. The data was taken from the experiments on the recycling of the flax composite. The chemical waste stream is a combination of PP and p-xylene. The major differences between the first and second approach is that the second allows the recuperation and avoids the new production of the p-xylene, the acetone and the PP, and furthermore yields a reduced final chemical waste stream. However, the complexity of the second case might lead to higher costs due to the need for a precipitation facility to precipitate the PP as powder and the need of a distillation tower to separate the p-xylene-acetone mixture.

Approach I: Chemical recycling, only recovery of flax
The recovery of fibres was estimated at 95%. Water was used to rinse the fibres of any remaining solvent prior to drying. The energy values were measured during the experiments.

Resource category	Name	Value
Input	P-xylene	2,35 kg
	Electricity	1,94 MJ
	Water, deionised	5E-1 kg
	Drying of flax	1,5E-4 m³
	Thermoforming, with calendering	1 kg
	Polypropylene, granules	4,944E-1 kg
Output	Flax-PP 40vol% composite	9,5E-1 kg
Final waste flows	Chemical waste, unspecified	2,856 kg

Approach II: Chemical recycling, recovery of flax, solvent and PP
Recovery of acetone and p-xylene were based on Poulakis study [2]. The energy usage for the recuperation of acetone and p-xylene estimated at 1kWh. The chemical plant usage was derived from other chemical processes in the Ecoinvent 3.01 database.

Resource category	Name	Value
Input	P-xylene	2,35E-2 kg*
	Acetone	1,395E-1 kg
	Chemical plant, organics	5E-9 p
	Electricity	5,54 MJ
	Water, deionised	5E-1 kg
	Drying of flax	1,5E-4 m³
	Thermoforming, with calendering	1 kg
Output	Flax-PP 40vol% composite	9,5E-1 kg
Final waste flows	Chemical waste, unspecified	1,63E-1 kg

Table 9-6: Life cycle inventory for the chemical recycling of 1kg of 40vol% long fibres flax composite waste. *only this small amount of p-xylene is used as the rest is recovered.

In mechanical recycling, as the fibres have been shortened through the shredding and pelletizing process, the most suitable manufacturing processes would be compression moulding (like for the random mat composites) or injection moulding. However, since the data for CM is not available, thermoforming with calendaring was applied as explained in the previous section. Both inventories are presented in Table 9-7. The injection moulding process requires an extra extrusion step to form the shredded material into pellets, those pellets can then be fed into an injection moulding device.

For the shredding, the electricity usage was derived from the power output of shredder used in this work, i.e. 5.7kW (calculated power used by the machine). The estimated throughput, based on the performance of the equipment in the laboratory, was of 15 kg/h. At an

industrial scale, it is believed that output will be more important and may reach tens of kilo per hour depending on the equipment used.

The second process uses a compounder to process the flakes into pellets after the shredding process. These pellets can then be used as feedstocks for an injection moulding machine the compounding process required 0.45 MJ/kg in energy (included in the inventory). Since the composite has to be shredded prior to compounding, the dataset for shredding had to be implemented in this dataset.

Mechanical recycling, thermoforming

Resource category	Name	Value
Input	Thermoforming, with calendering	1 kg
	Electricity	1,37 MJ
Output	Flax-PP 40vol% short fibres, thermoforming	9,5E-1 kg
Final waste flows	Flax-PP 40vol% composite	5E-2 kg
Mechanical recycling, injection moulding		
Resource category	**Name**	**Value**
Input	Injection moulding	1 kg
	Electricity	1,82 MJ
Output	Flax-PP 40vol% short fibres, injection moulding	9,5E-1 kg
Final waste flows	Flax-PP 40vol% composite	5E-2 kg

Table 9-7: Life cycle inventory for the mechanical recycling with thermoforming or with injection moulding (shredding and compounding included energy use).

The last EOL possibility is the incineration with energy recuperation. In this case the composite is combusted and the energy that is released upon combustion is used as heat or as electricity. According to the Confederation of European Waste-to-Energy-Plants [20], the recuperated energy efficiency upon combustion is 65% for all new installed plants. From this, 14.2% is recuperated as electricity and 50.8% is recuperated as heat. Table 9-8 lists the life cycle inventory for the incineration of 1 kg of a 40vol% flax composite. The disposal processes incorporate all the treatments and emissions related to the combustion of PP and flax which are assumed to be similar to that of wood. The impact associated with the production of the incinerator facility was incorporated into these waste treatment processes.

Incineration with energy recovery

Resource category	Name	Value
Output (avoided products)	Heat, natural gas, at industrial furnace	14,46 MJ
	Electricity	4,47 MJ
Waste to treatment	Disposal of PP to incinerator	4,8E-1 kg
	Disposal of wood to incinerator	5,2E-1 kg

Table 9-8: Life cycle inventory for the incineration with energy recovery for V_f = 40% flax-PP composites.

9.1.4.3 Impact assessment of recycling scenarios

Once the inventory is completed for each end of life technique, an impact assessment could be conducted. First, the different scenarios for chemical recycling and mechanical recycling are evaluated. Afterwards, the most suitable chemical and mechanical recycling techniques are selected and then compared with the third EOL technique, incineration. The electricity process used is the one covering the electricity generation in Belgium (*Electricity, medium voltage (BE)| market for | Alloc Def, U*). Only the impact of the recycling process (not the material production) is taken into account in the next sections.

Chemical recycling scenarios

As previously presented in section 9.1.1, two approaches of chemical recycling are proposed. Note that by recycling the PP and by re-using the chemicals, the environmental impact drastically decreases. In this case, the additional environmental costs needed to separate and re-use the chemicals and PP is relatively low compared with the potential gain. In the first scenario, fresh PP is needed to produce the recycled composite material. In the second scenario, the recycled PP can be used to produce the recycled composite as the properties of the PP did not degrade upon recycling. Furthermore, the amount of added PP is marginal due to the high recycling rate of PP [2]. Even though the available data was limited to construct a suitable inventory, it seems feasible to reduce the environmental burden by reducing the chemical products needed and by recycling the MAPP.

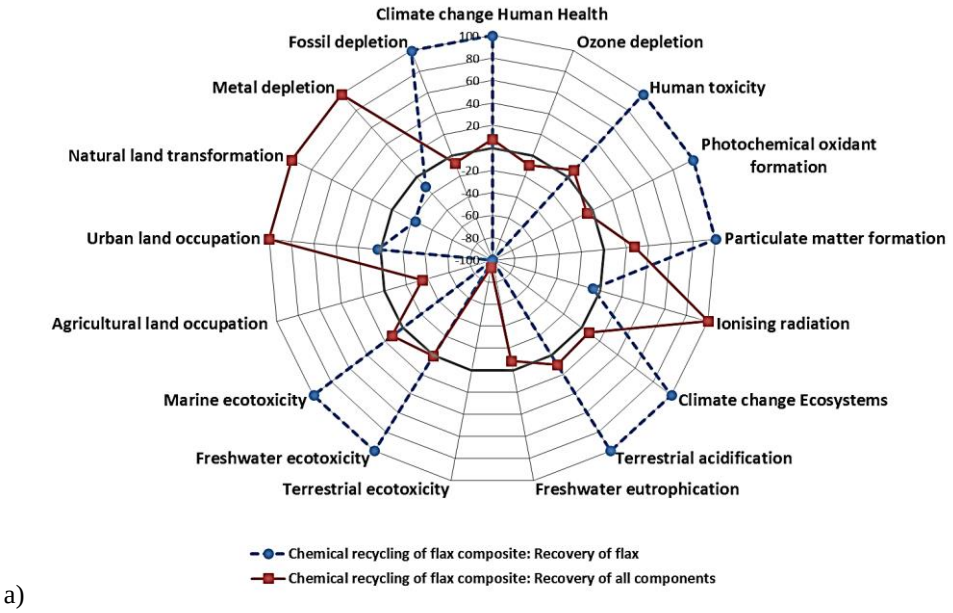

a)

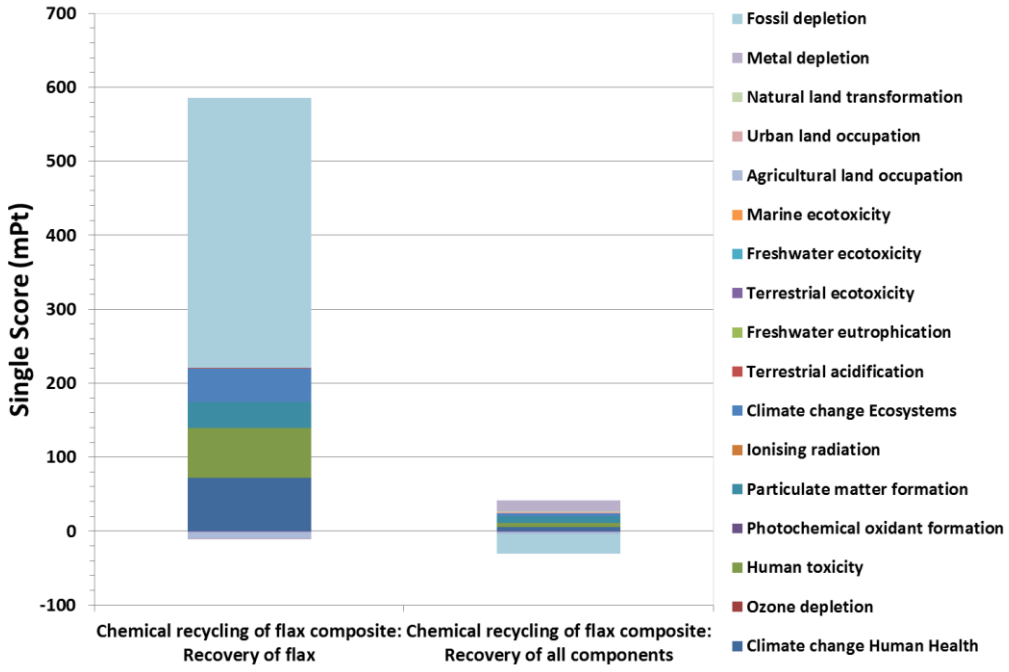

b)

Figure 9-10: a) Characterization and b) Single-score values for the two chemical recycling techniques. The single score value show a higher environmental burden if only the flax is recycled. The environmental burden decrease, but remain positive, if all components (flax, MAPP and p-xylene) are recycled.

The characterizations results in Figure 9-10 from the chemical process comparative study shows some noteworthy differences between the two chemical recycling processes. All impact scores are showed on a 100% scale, this means that maximum impact caused by the substitutions on each category is marked with ±100% as previously explained. The recycling of the three main components, the flax, the p-xylene and the MAPP, has a beneficial influence on the climate change, human health, photochemical oxidation, particulate matter formation, climate change ecosystems, terrestrial acidification and fossil depletion categories as compared to the recycling of solely the flax fibres. However, the extra energy, mainly electricity, needed to recycle the p-xylene and MAPP has a negative influence on the ozone depletion and ionizing radiation categories.

Moreover, if the p-xylene is not recycled, a negative influence on the human toxicity, marine ecotoxicity, urban land occupation, natural land transformation and metal depletion categories will be seen as it has to be treated as a waste. While the recycling of the flax fibres has a positive influence on the freshwater eutrophication category, the operation of the chemical plant has the opposite effect. For the terrestrial ecotoxicity and fresh water ecotoxicity categories, the absolute values are virtually the same for both recycling scenarios.

Overall, the benefit of recycling the PP and chemicals becomes clear if the two chemical recycling techniques are compared. However, both recycling technique result in a positive environmental burden as seen Figure 9-10 b. Other aspects, e.g. economic feasibility (expensive process), should also be taken into account. The chemical recycling process offers an interesting way of recycling long flax fibres but there is almost no environmental gain in recycling solely the fibres. When the MAPP and chemicals are recycled, the environmental burden is reduced, but a small positive burden still remains due to the waste flow (5% of the materials) that cannot be recycled.

Mechanical recycling scenarios

Two scenarios were proposed for the mechanical recycling. The first method is the shredding of the composite into flakes which are used as-is in the compression moulding process. The second method includes the addition of an extra compounding step with the production of pellets. These pellets have the advantage of facilitating storage and the material can be easily used as feedstock in injection moulding process. With the second method, it is possible to add fresh PP during the compounding to vary the fibre content, providing a good mixing between the fresh PP and the recycled one is achieved.

In the mechanical recycling scenario, both the fibres and the matrix are recovered which has a beneficial influence on the environmental impact. The overall environmental burden was found to be slightly lower for the shredding/thermoforming technique compared to the compounding/injection moulding technique as seen Figure 9-11. This is due to the environmental burden associated with the operation of the injection moulding machine which does not balance against the gain of the avoided injection moulded composite material. It can be concluded that both recycling techniques are suitable techniques from an environmental point of view. Other design parameters, e.g. economics, throughput speed, design of the component using the recycled material, etc., will determine which recycling technique is most suitable.

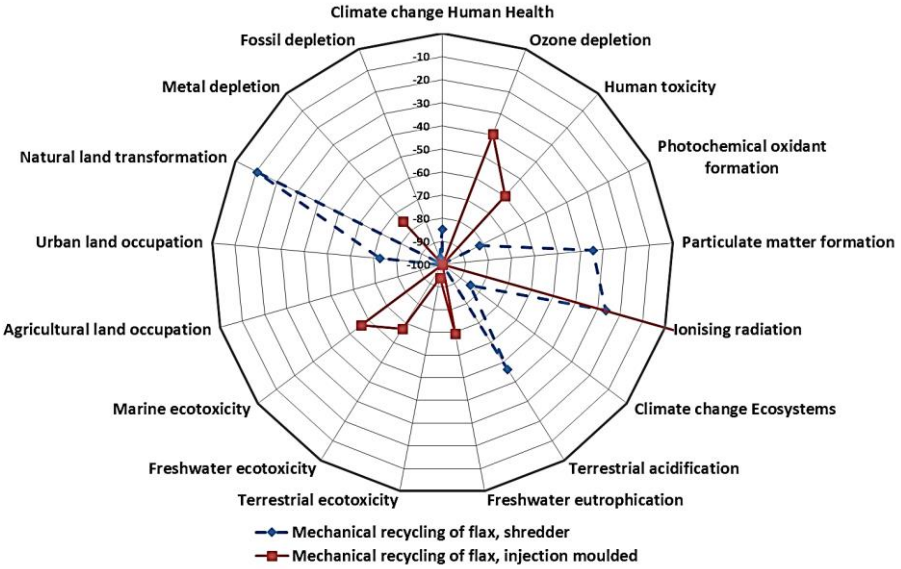

Figure 9-11: Characterization values for the comparison of the two mechanical recycling processes. The value from 0 (grey line) to -100 indicate that the process has a positive influence on the category.

Comparison of the three EOL techniques

The three EOL possibilities for flax-MAPP composites are compared in this section. For the chemical recycling technique, the scenario in which all the components, including the p-xylene, are recycled is chosen. For the mechanical recycling, the compounding/injection moulding scenario is chosen. The third EOL possibility, the incineration with energy recovery, the recuperation of energy reduces the resources necessary for the production of energy, as heat or as electricity. In this case the Belgian production mixture for electricity was used. Figure 9-12 shows the characterization values of the three different EOL possibilities for the flax-PP composites.

In the chemical recycling scenario human toxicity and metal depletion are also major categories. The results reveal that the chemical recycling technique yields an increased environmental burden, mainly associated with the use of chemicals and chemical equipment. This is due to a longer processing time and larger quantities of chemicals. The mechanical recycling technique shows the most promising result since the properties of the recycled composite are comparable to those of a fresh random mat composite. Figure 9-13 shows the single-score values of the three different EOL possibilities for the flax-PP composites.

Most of the environmental burden comes from four impact categories: climate change human health, particulate matter formation, climate change ecosystems and fossil depletion. In the chemical recycling scenario human toxicity and metal depletion are also major categories. This results confirms the potential (on a comparative basis) that the mechanical recycling scenario is a promising recycling technique for flax-MAPP composite. The key advantage of the mechanical recycling technique is the processing speed. Furthermore, it gives the highest environmental gain and recycling rate which would help industries meet the ELV directives.

Finally, the incineration method has been found to be environmentally beneficial due to energy recuperation. However, the incineration is not a recycling technique but it is an EOL possibility for natural fibre composites, as they can be fully combusted and give a relatively

high calorific value. The natural fibres are largely CO_2 neutral by carbon capture during growth, but the incineration does not allow recuperation of the materials and therefore is not the best option as to the waste hierarchy defined by the European waste directive.

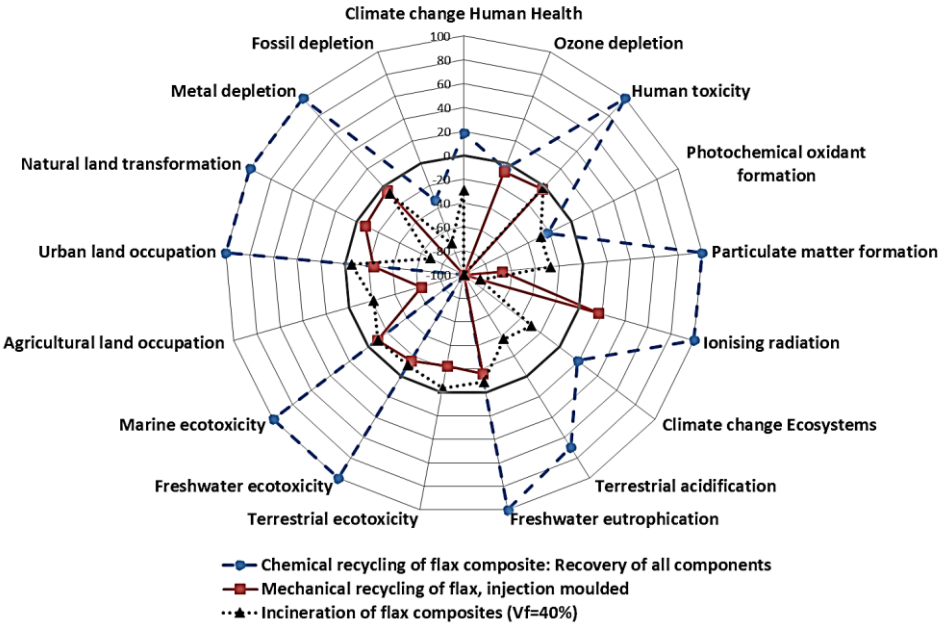

Figure 9-12: Comparative environmental of the three different EOL possibilities (characterization data).

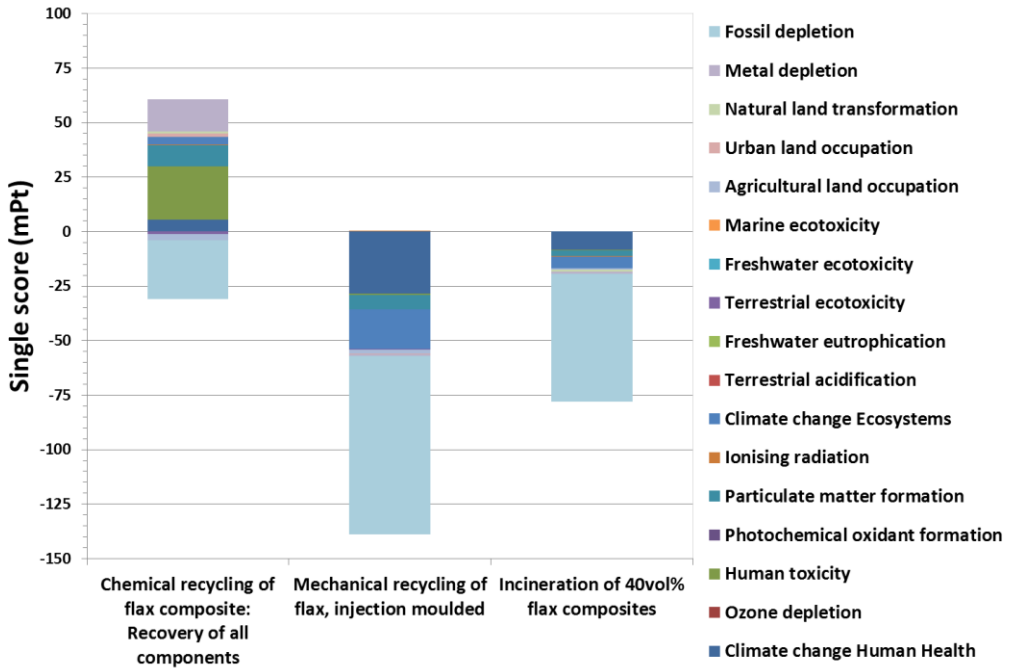

Figure 9-13: Single-score values for the three evaluated EOL possibilities for flax-PP composites.

9.2 Comparative LCA for automotive applications

As previously presented, flax fibre reinforced polymer composites (FFRP) are presented as a good alternative to glass fibre reinforced polymer composites (GFRP), thanks to their numerous advantages. However, until now, the usage of natural fibres concerned only non-structural applications, but a step forward would involve their usage in (semi-)structural components. Another point of interest is the potential reduction of environmental impact by using bio-reinforcement instead of glass fibre for example. It is well know that by

reducing the weight of a vehicle component, there is a positive impact during the use phase (less weight = less fuel usage).

The next sections discuss the comparative LCA performed to compare FFRP and GFRP for two automotive applications: a bumper and a car roof. One of the difficulties is the definition of a suitable basis of comparison in order to fairly compare them. First, the goal and scope definition is carried out to form a basis of comparison between the FFRP and GFRP. Then, the functional unit and the life cycle inventory will be carried out to identify the essential elements for an accurate LCA calculation. Another important aspect in the life cycle of car components is the use phase. A method was defined to calculate the avoided impact due to a weight difference by replacing GFRP by FFRP. This methodology is explained in the inventory analysis. Two load cases are discussed, being an impact design for a car bumper case and a flexural design for the car roof. For both cases, different replacement options are analysed and discussed.

9.2.1 Goal and scope definition

9.2.1.1 The concept of a mass factor

To properly compare the FFRP and GFRP, a mass factor methodology constructed based on the work of Ashby [21] was used. This gives the necessary mass of FFRP needed to fulfil the same mechanical function as 1 kg of GFRP. The mass factor (MF) depends on the load case that is being evaluated as well the composite material tested. For the calculations the laminate thickness is considered as a "free variable". In the next sections, the concept of a MF is elaborated for the two aforementioned load cases using flax-MAPP and glass-MAPP composites.

9.2.1.2 Mass factor calculations for impact design

From the impact studies carried on in Chapter 7, the impact properties of flax-MAPP were measured. The conclusion is that the absorbed energy upon impact depend on the type of matrix while the fibre architecture had less effect. The study measured the parameters of the empirical formula (Eq 7.1 in Chapter 7), as derived by Caprino et al. [22] for the impact properties of a plate. The mass of the plate can be calculated using the equation below:

$$m = \rho * a * b * t \qquad \text{(Eq. 9.5)}$$

With *m* being the mass of the plate, ρ the density of the composite, *a* and *b* are the length and width of the plate and t the thickness of the plate. Both equations are combined to derive the thickness of the plate:

$$t = \frac{1}{D * V_f} * \sqrt[\alpha]{\frac{U_i}{K}} \qquad \text{(Eq. 9.6)}$$

Where U_i is the perforation energy, K and α are two material parameters to be experimentally determined, t is the thickness in mm, V_f the fibre volume fraction and D_t the top diameter of the striker in mm. When comparing the GFRP and FFRP, the indenter factor is the same, since the object that hits the structure is the same. The length and width of the structures cannot change, but the thickness is not fixed and is defined as the free variable. In order to replace the GFRP, the FFRP should be designed to fulfil the same absorbed energy performance to be a viable replacement. The mass factor was defined taking 1 kg of GFRP as a reference and calculated by combining Eq. 9.5 and 9.6 into Eq. 9.7.

$$MF = \frac{\rho^{flax\ composite} * a * b * \frac{1}{D * V_f^{flax\ composite}} * \sqrt[\alpha]{\frac{U_i}{K^{flax\ composite}}}}{\rho^{glass\ composite} * a * b * \frac{1}{D * V_f^{glass\ composite}} * \sqrt[\alpha]{\frac{U_i}{K^{glass\ composite}}}} \quad \text{(Eq. 9.7)}$$

Simplified to:

$$MF = \frac{\rho^{flax\ composite} * V_f^{glass\ composite} * \sqrt[\alpha]{K^{glass\ composite}}}{\rho^{glass\ composite} * V_f^{flax\ composite} * \sqrt[\alpha]{K^{flax\ composite}}} \quad \text{(Eq. 9.8)}$$

It has to be noted that the composite densities in Eq. 9.8 are a function of the volume fraction of fibres. With the K and α factor independent of fibre architecture and volume fraction of fibres, the mass factor is only a function of the volume fraction of fibres. For the investigated flax-MAPP and glass-MAPP composites, various fibre volume fractions can be compared.

Table 9-9 gives an overview of the calculated MF for the impact design case. When the MF is lower than 1, the change from glass fibres to flax fibres would result in a lighter structure, which fulfils the same impact or flexural performance as glass fibre. A MF > 1 is not favourable as the structure would need to be heavier to achieve comparable performance. For example, a MF of 1.11 means that 1.11 kg of flax fibre composites is needed to fulfil the same the impact properties as 1kg of glass fibre composites.The use of the absorbed energy at perforation is a good and reliable parameter to characterise the behaviour of a bumper during a crash.

Mass factor for impact design			
***Glass*\Flax**	**30%**	**40%**	**50%**
20 %	0,84	0,66	0,56
30 %	**1,11**	0,87	0,73
40 %	1,32	**1,04**	0,88
50 %	1,49	1,18	**0,99**

Table 9-9: Mass factors for impact design. The percentage indicated are the V_f. In bold are the pairs that are compared. The MF calculation based on the composite V_f and is independent of the textile architecture.

9.2.1.3 Mass factor calculations for flexural design

The MF for the flexural design, to be used for the car roof, was calculated using the same methodology as the one developed for the impact design. Using continuum mechanics, the maximum deflection Δ_{max} of a plate (mm), described in Figure 9-14, under a constant distributed load P (N) can be calculated with Eq. 9.9.

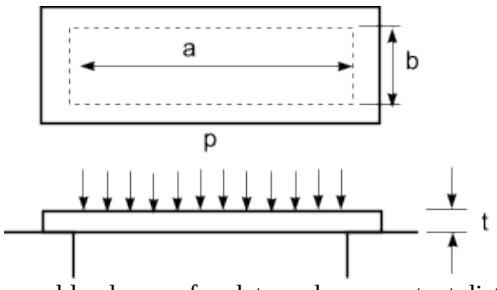

Figure 9-14: Flexural load case of a plate under a constant distributed load P.

$$\Delta_{max} = 0{,}142 * \frac{p * b^4}{E_b * t^3 * (2{,}21 * \left(\frac{b}{a}\right)^3 + 1)} \quad \text{(Eq. 9.9)}$$

Where E_b is the flexural modulus of the plate. Taking into account the plate mass (Eq. 9.5), the thickness of the plate is described as:

$$t = \sqrt[3]{\frac{0{,}142 * p * b^4}{E_b * \Delta_{max} * (2{,}21 * \left(\frac{b}{a}\right)^3 + 1)}} \quad \text{(Eq. 9.10)}$$

When comparing the GFRP and FFRP, the maximum applied load on the plate will be the same for a plate with similar dimensions. The deflection Δ_{max} is also limited to a maximum value allowing the calculation of the MF with Eq. 9.11 below:

$$MF = \frac{\rho_{Flax\ composite} \sqrt[3]{E_{Bending}^{Glass\ composite}}}{\rho_{Glass\ composite} \sqrt[3]{E_{Bending}^{Flax\ composite}}} \quad \text{(Eq. 9.11)}$$

Note that the flexural modulus is not only dependant on the V_f, but also on the fibre architecture and chosen lay-up. To calculate the MF for the flexural case, data from Chapter 5 and literature was used, as seen in Table 9-10, for various flax and glass reinforcements. These values were then used to calculate the mass factor for the flexural design case (see Table 9-11). The MF is only calculated when comparing similar fibre architectures.

An interesting fact seen in Table 9-11 is that almost all MF's are lower than 1 (but seldom below 0.8). This is a very important result and this means that the probability of achieving a more eco-friendly design is higher when using flax composites in the car roof that in the bumper. The most interesting and probably the most realistic substitution of the glass random mat composite with a V_f of 40% with a flax random mat composite with equivalent fibre volume fraction which gives a MF of 0.74.

Fibre type	Reinforcement type	Fibre volume fraction (%)	Flexural modulus (GPa)	Reference
Flax	UD cross ply [0,90]	40	5,3	
Flax	Plain weave	40	6,3	
Flax	Random mat	30	3,3	
Flax	Random mat	40	3,7	
Flax	UD	40	8,4	[23]
Flax	IM	25	3,5	[24]
Flax	IM	30	4,3	[24]
Glass	Plain weave	26	12,0	[25]
Glass	Random mat	20	4,8	[26]
Glass	Random mat	25	4,9	[26]
Glass	Random mat	30	5,3	[26]
Glass	Plain weave	50	16,2	[27]
Glass	UD/Twintex	35	24,0	[28]
Glass	UD	58	36,5	[29]
Glass	Random mat	40	9,1	[30]

Table 9-10: Flexural modulus of various flax-MAPP and glass-MAPP composites.

Glass\ Flax	UD 40%	Plain weave 40%	Random mat 30%	Random mat 40%	Injection moulding 25%	Injection moulding 30%
Pure UD 58 %	**0,98**	1,08				[31]
Plain weave 25,8%	0,95	**1,05**				
Plain weave 50%	0,81	**0,89**				
Pure UD/Twintex 35%	1,07	1,19				
Random mat 20%			0,98	0,99	0,94	0,90
Random mat 25%			0,92	0,93	**0,88**	0,85
Random mat 30%			**0,89**	0,90	0,85	**0,82**
Random mat 40%			0,97	**0,74**	0,91	0,87

Table 9-11: Mass factor for flexural design. The percentage indicated is the V_f . The indicated percentages (%) are the fibre volume fraction**.** The pairs that are in bold are the one that are compared because they have higher probability of achieving an eco-friendly design.

9.2.2 Definition of the functional unit

The MF is used to define which flax composite should be compared to the glass one in term of fibre volume fraction and/or architecture. In this work, this factor was calculated based on one specific and most important mechanical function (impact or bending). However, in practice, the structure will encounter multiple types of loads which need to be taken in account.

Based on the fatigue properties of both GFRP and FFRP presented in Chapter 8 and other studies [32, 33], it is reasonable to assume that the use phase of a glass and flax composite component are comparable. It is assumed in this work that the composite parts will not be replaced during the lifetime of the car. This means that the lifetime of the composite component is equal to the one of an average European car defined as 200.000 km. The functional unit is a composite component in an average European car fulfilling the defined load cases for a total driven distance of 200.000 km.

9.2.3 Life cycle inventory

For the inventory, the same data as in the EOL section and Appendix G were used. During the car use phase, if the car weight is decreased by choosing a lighter material, this will cause a reduction in fuel consumption and this decrease needs to be parameterized. A fuel consumption decrease of 0,03%/kg of weight reduction for cars using gasoline and 0,05%/kg of weight reduction for diesel cars was found by Tolouei et al.[34].

The environmental impact data associated with 1km travel for a passenger car with a gasoline/diesel (2/1 ratio) was available in the Ecoinvent 3.01 database. This ratio was used to measure the reduction factors and no further differentiation between petrol and diesel cars is made in this work. The reduced mileage due to a weight decrease was calculated as follows:

$$\text{Mileage reduction (km)} = \text{total driven distance} * \delta * 0{,}0367\% \quad \text{(Eq. 9.12)}$$

The replacement of GFRP by FFRP is studied based on the mass factor, which compares the mass of the flax composite to 1kg of glass composite, hence:

$$\delta = 1 - \text{mass factor} \quad \text{(Eq. 9.13)}$$

Where δ is the weight difference. The reduced or increased mileage and the attributed usage of fuel and the corresponding emissions are allocated to the flax composite. If the mass factor is smaller than one, this will result in a reduction of fuel consumption credited to the flax composite.

For the woven composite production, the bast fibre spinning/weaving process (Spinning and weaving, flax fibre (BEL)| processing | Alloc Def, U) in the Ecoinvent 3.01 database was used based on the study of Koç et al. [35] However, the energy usage was changed to the Belgian production mix for energy instead of the Indian energy used in the database. The random mat composites are assumed to be made out of long fibres. The incineration with the energy recovery EOL option was chosen for both the FFRP and GFRP.

9.2.4 Environmental impact of FFRP in automotive applications

The environmental impact assessment of the use of flax as a replacement for glass fibres is carried out. In Table 9-9 and Table 9-11, the pairs that will be compared are in bold. To verify if the replacement of the glass composite by the flax composite is suitable, a weight difference approach was applied as described above. In this approach, the environmental impact associated with the replacement of 1kg of glass-MAPP composite by an equivalent mass of flax-MAPP composite was calculated taking into account the use phase.

9.2.5 LCA of the Impact design – Car Bumper

For the impact design, three replacement scenarios are looked into (see Table 9-9, the replacement in independent of the flax textile architecture):

1. 30% glass fibres by 30% flax fibres (MF= 1.11);
2. 40% glass fibres by 40% flax fibres (MF= 1.04) and;
3. 50% glass fibres by 50% flax fibres (MF= 0.99).

For the first case, flax fibre composite with a V_f = 30% is used as a replacement for a V_f=30% glass fibres and the results are presented in Figure 9-15. As the MF is higher than 1 (MF=1.1, flax part heavier than the glass one), it led to an additional environmental burden associated with the extra use of fossil fuels during the use phase. Looking into the various impact categories, it can be seen that, in this first case, replacing glass by flax fibre leads to a significant decrease in human toxicity (-58%), ozone depletion (-40%), metal depletion (-49%) and ionizing radiation (-86%) categories.

It can also be mentioned that the large reduction in ionizing radiation is an effect of the chosen EOL technique, being incineration with energy recuperation which avoid the use of coal or nuclear energy power generation. In the terrestrial acidification, marine ecotoxicity, particulate matter formation and photochemical oxidant formation categories, a slight decrease (between 11 and 28%) in environmental impact was observed if flax is used instead of glass.

On the other hand, using flax instead of glass in this particular case increases the impact in the freshwater eutrophication, terrestrial ecotoxicity and agricultural land occupation categories. The freshwater ecotoxicity category and natural land transformation increase because of the need to use more land to grow flax leading to the presence of more fertilizer in the water. Overall, it is the use phase that holds an important share of the environmental impact. In this scenario, the MF determines whether the overall balance will become positive (extra environmental burden) or negative.

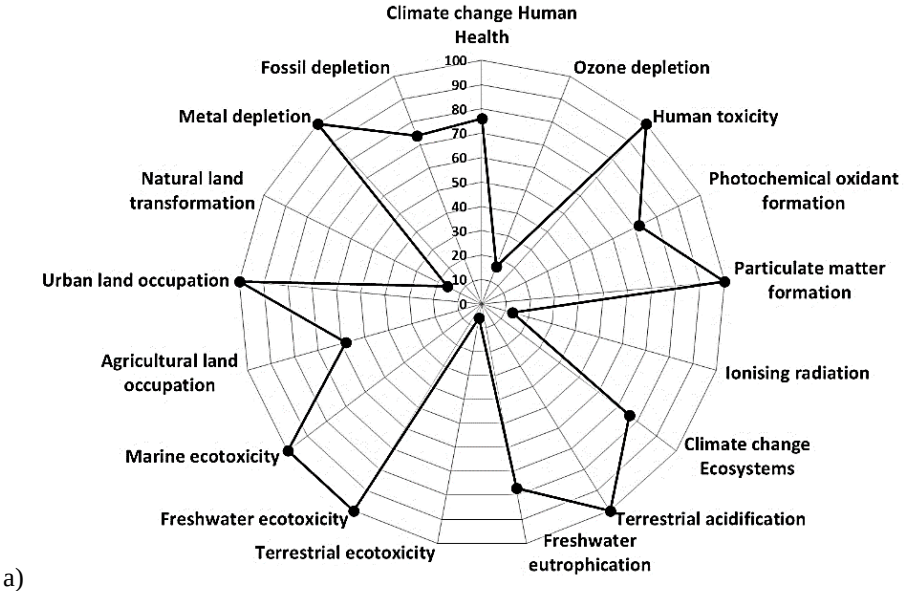

a)

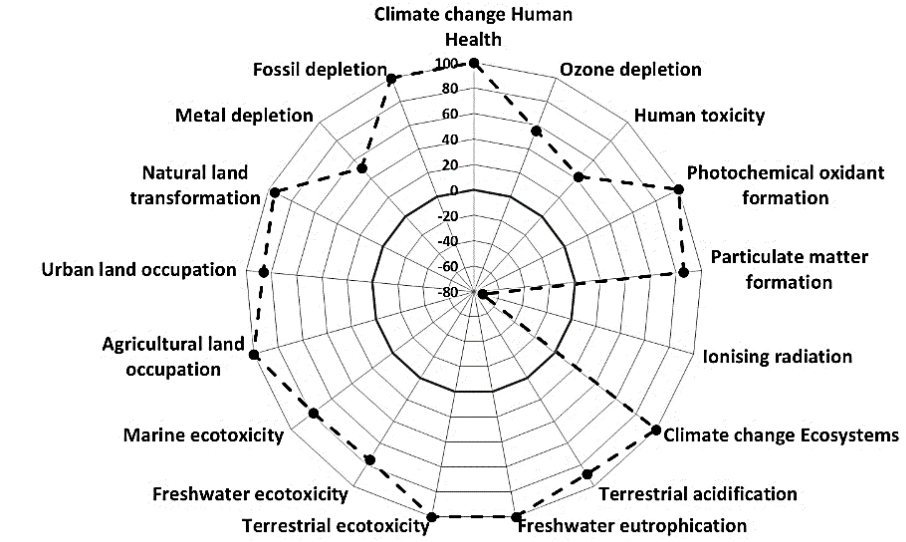

b)

Figure 9-15: Characterization of the first impact design case: environmental impact of a) glass composite with V_f=30% and b) flax composite V_f=30% (MF= 1.11) for a distance of 200 000 km.

By comparing the three replacement scenarios in Figure 9-16, the influence of the mass factor becomes clear. In the first and second scenario, the mass factor is larger than one (MF= 1.11 and MF = 1.04), in the third scenario the mass factor is smaller with a value of 0.99. Since all the impact categories are mainly influenced by the use phase, large differences can be seen. On the other hand, impact categories that are only dependant on the choice of fibres, small changes are visible as the volume fraction increases proportionally.

Figure 9-16 shows that the total score is positive for the first scenario and negative for the second and third scenario. This means that using flax instead of glass is harmful to the environment in the first case. In the other cases, woven, UD cross-plies and UD composites with higher V_f lead to a decrease in environmental impact. From these results, it can be concluded that it may be interesting from an environmental point of view to replace glass fibre composites by flax fibre composites for fibre volume fraction higher than 40%, when a design for impact is applied.

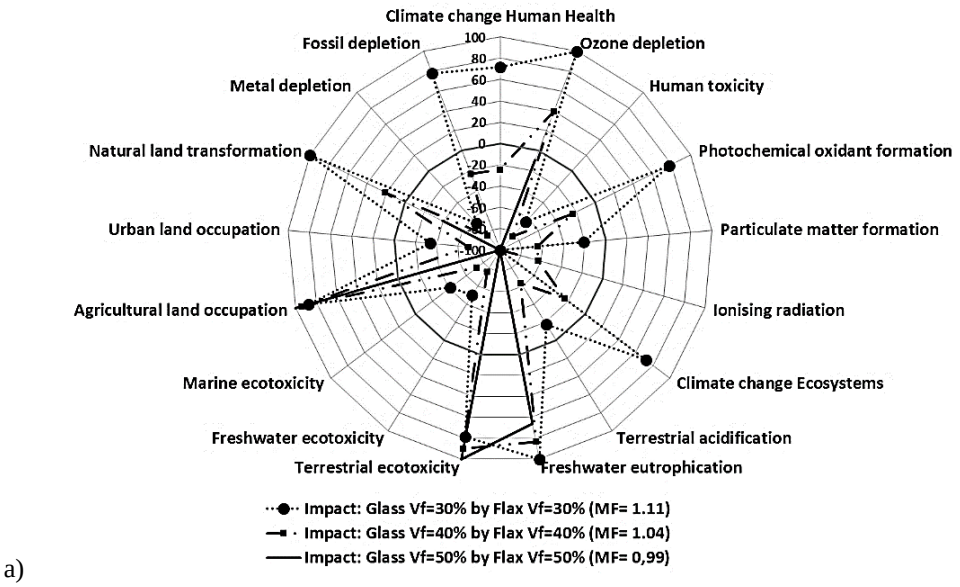

a)

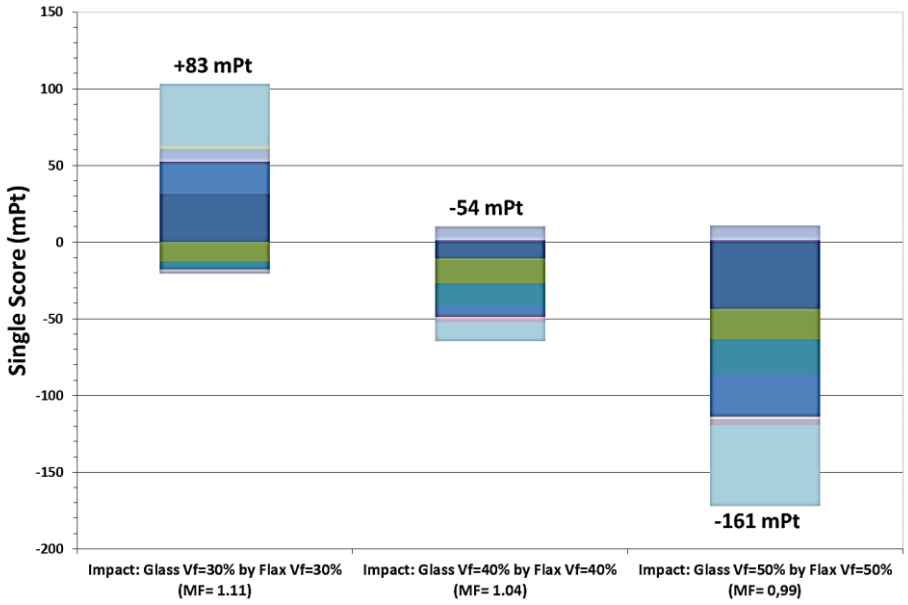

b)

Figure 9-16: a) Characterization and b) single-score values for the three impact design replacement cases (total driving distance = 200 000 km).

9.2.6 Flexural design

The second scenario that was looked into was the flexural design scenario. Four fibre architectures were studied: UD, woven, random mat and injection moulded. Only comparisons with the similar fibre architecture were investigated as seen in Table 9-11 bold).

9.2.6.1 UD composites

The potential substitution of glass by flax in the case pure UD composites is done for only one case where 58 % glass fibre-MAPP composite can be replaced by a pure UD 40% flax fibre-MAPP composite. A MF of 0.98 was calculated for this combination, thus the weight reduction is relatively small. It has to be noted that this case is theoretical as normally cross-ply composites are used to produce such a part. In Figure 9-17 a, the overall single-score value is negative, meaning that the replacement of glass fibres by flax fibres reduces the total environmental impact.

It is however interesting to look at the different stages in the life cycle of the replacement scenario presented in Figure 9-17 b. The single-score values for the different phases in the life cycle being the production of the flax composite (+297 mPt), the environmental impact in the use phase due to the replacement, the EOL option (incineration) for the flax composite and the avoided glass composite production (-362 mPt) are accounted for separately. It has to be noted that the EOL option for the glass composite is taken into account in the production of the glass composite. The little difference between the flax composite manufacturing is caused by the additional use of MAPP polymer due to lower fibre volume fraction. The glass composite has only a matrix volume fraction V_m of 42% compared to V_m=58% in the case of the flax-MAPP composite. Since the mass factor is close to one, the reduction in environmental impact associated with the weight decrease, is rather small. In this scenario the fibre production and EOL phases are dominant in the life cycle, but still, the replacement of the glass by the flax would be interesting for this specific case. It has to be mentioned that hackled flax fibres are used in this case. The limited processing of the flax, (no doubling or spinning process) help reduce the overall environmental burden of the composite.

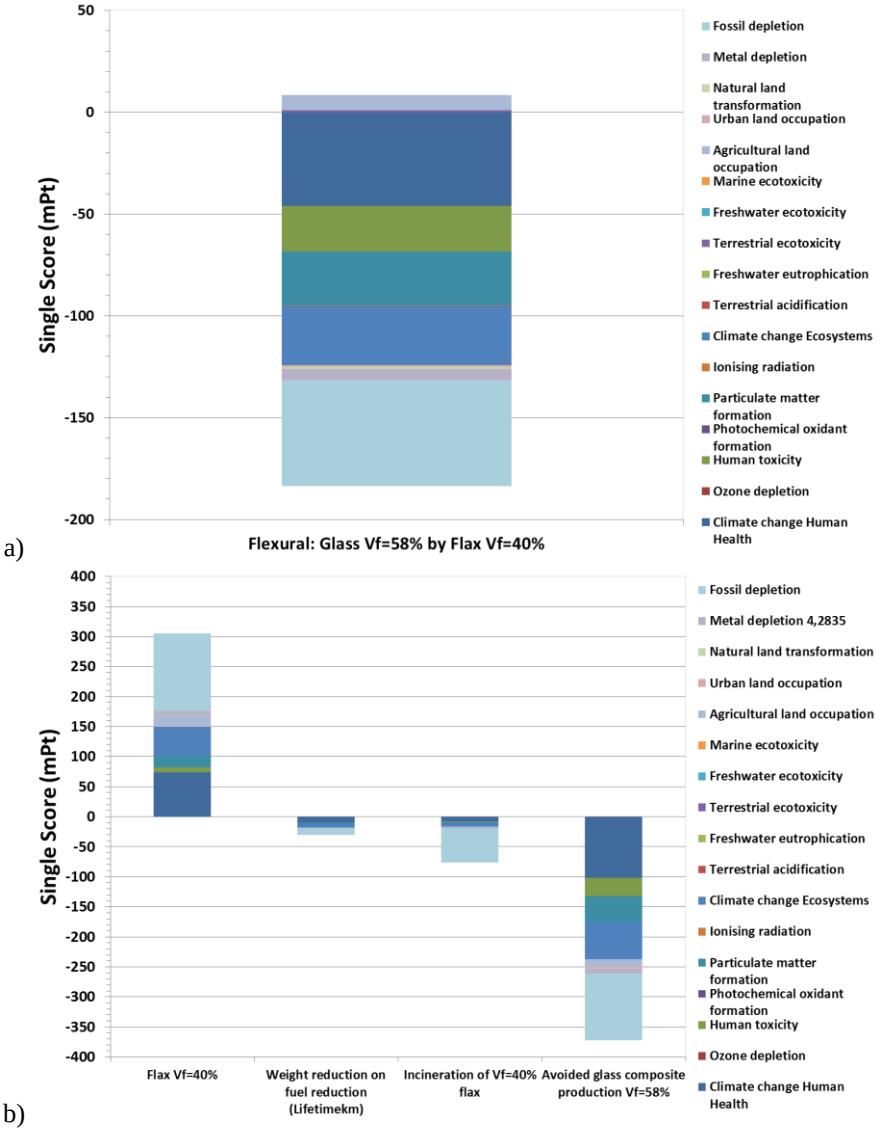

Figure 9-17: Replacement of UD glass composite with a V_f=58% by a UD flax composite with a V_f=40% a) overall single-score and b) single-score for different phases in the life cycle for the replacement for UD composites (total driving distance = 200 000 km).

9.2.6.2 Woven composites

The second architecture that has been looked into was the plain woven based composites. In Table 9-11, two pairs of woven composites were chosen for comparison as follows:

1. 25.8% glass composite by a 40% flax composite (MF =1.05) and;
2. 50% glass composite by a 40% flax composite (MF = 0.89).
3.

Figure 9-18 shows the characterization values for both replacement scenarios. The first scenario shows a higher environmental burden in all impact categories leading to an increase in the environmental impact. This may be caused by the energy-intensive yarn spinning process included in the weaving process from the Ecoinvent database. This is further discussed in section 9.3. For the second scenario, an MF of 0.89 leads to a much lighter structure which reduces the effect of the use phase and reduces the potential environmental impact, making the most viable scenario.

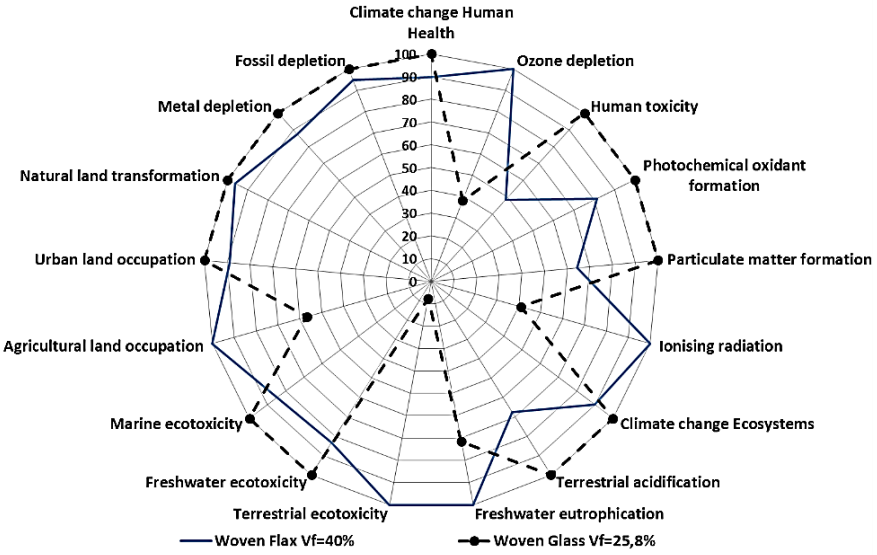

a)

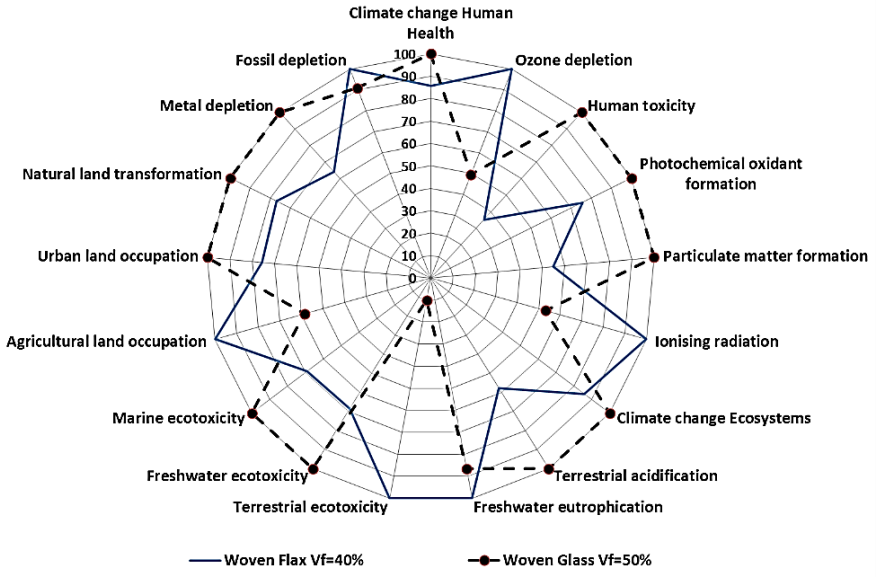

b)

Figure 9-18: Characterization values for the replacement of woven glass composites by woven flax composite: a) glass composite at V_f=25,8% vs flax composite at V_f= 40% and b) glass composite at V_f=50% by flax composite at V_f=40%. The total driven distance is 200 000 km.

9.2.6.3 Random mat composites and injection moulded composites

The third and last part discusses the replacement of glass fibre random mat by flax ones. The used flax fibres were assumed to be long fibres (8 cm) as delivered by the supplier. Figure 9-19 shows the characterization values for the two replacement cases. In both cases, the replacement of GFRP by FFRP reduces the total environmental impact. If the random mat composites are replaced by short fibre injection moulded parts, the overall environmental burden is once again reduced if flax composites are used instead of the glass ones as seen in Figure 9-20.

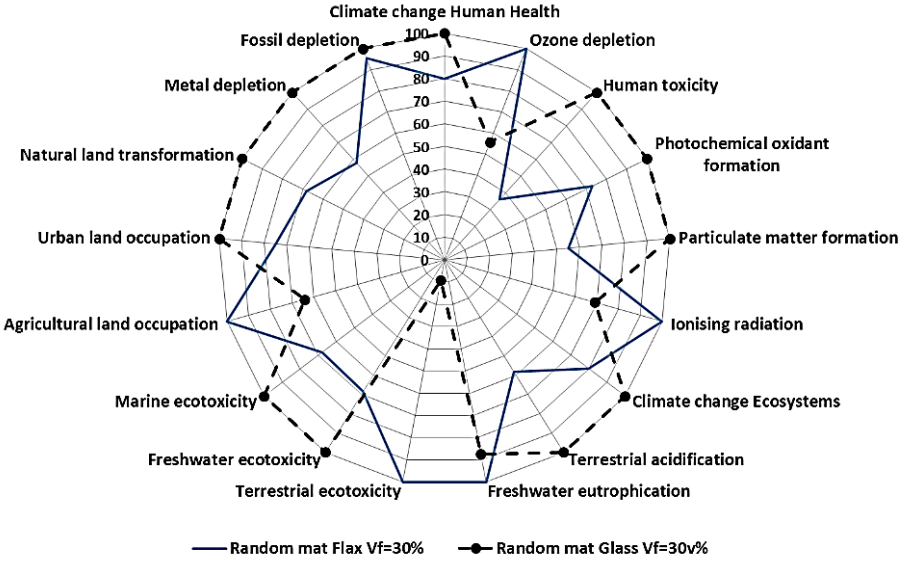

a)

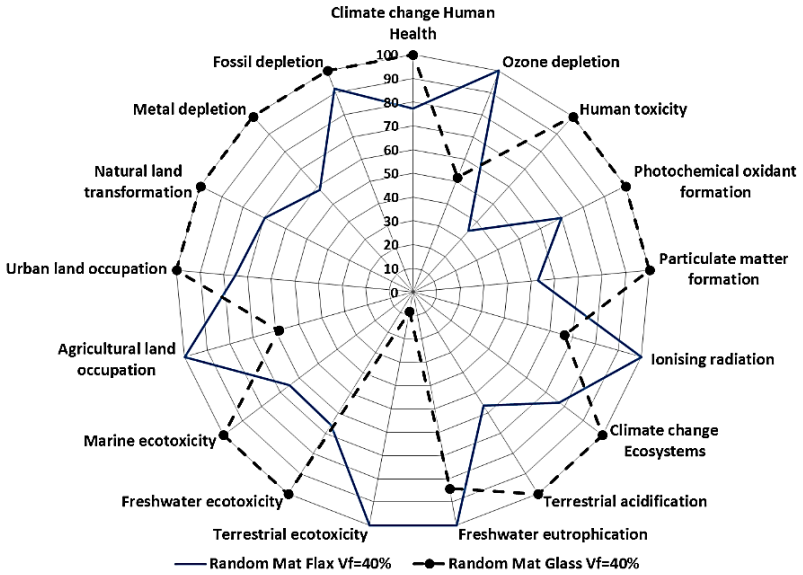

b)

Figure 9-19: Characterization values for the replacement of random mat glass composites by random mat flax composite: a) at V_f=30% and b) at V_f=40%. The total driven distance is 200 000 km.

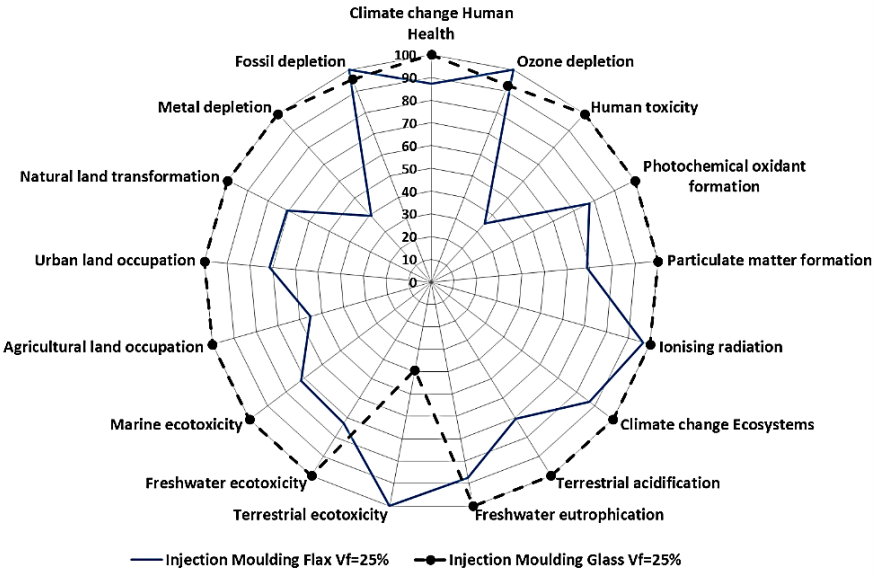

a)

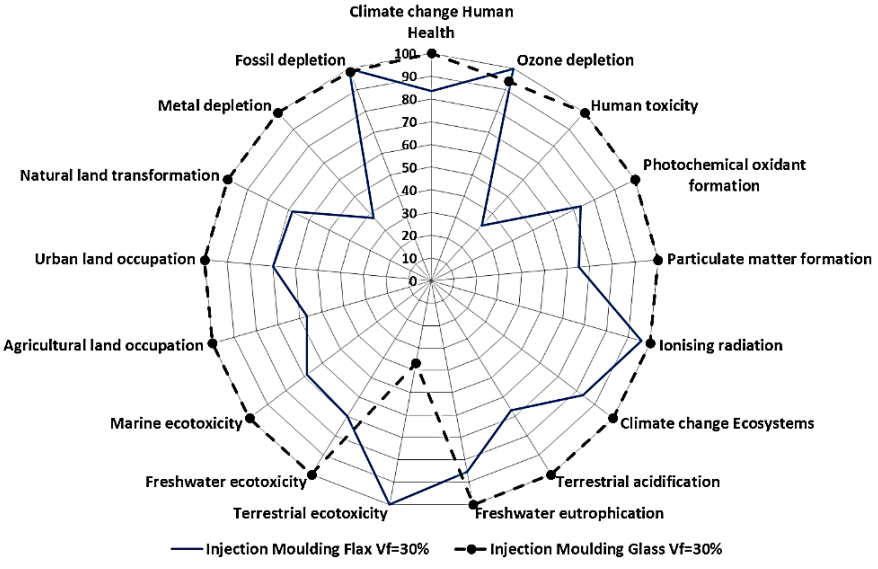

b)

Figure 9-20: Characterization values for the replacement of injection moulded glass composites by injection moulded flax composite: a) at V_f=25% and b) at V_f=30%. The total driven distance is 200 000 km.

9.2.7 Sensitivity on the results

A sensitivity analysis was carried on in order to observe the influence of varying parameters on the global impact of the product. For this analysis, the flax UD flexural case was chosen. The first parameter that may vary is the MF because of the inconsistency of the material properties which in turn could cause a slight variation in the inventory analysis used for the LCA study. The second vaiable parameter that was taken into account was the use phase. A total of 200.000km driven distance was assumed. However, high duty vehicles will have a larger driven distance which can go up to that can go up to 1 million km. This distance variation can influence the LCA results because they mark the time when the car components need to be changed.

The first step was to calculate the sensitivity of the single-score value (for the production of the flax composites) with varying MF values. The used inventory is sensitive to variations in production method such as the choice of machinery or the flax fibres types (scutched, hackled, etc.). Therefore, a 10% deviation interval was derived of the single-

score value. As an infinite set of mass factors can be calculated for each load case, it is important to define the critical mass factor (MF_C). The MF_C corresponds to the mass factor at which the environmental impact of the replacement is zero (replacement of glass by flax do not decrease the environmental burden). Figure 9-21 shows how the single-score value varies with changing mass factor. The solid line indicates the calculated single-value score for the UD-replacement case. The two dotted lines represent the assumed 10% deviation interval from the obtained results and their corresponding MF_C is indicated.

Four different regions were observed. The first region is the one were the actual mass factor is smaller than the underestimated mass factor, MF_U. This factor corresponds to the optimum MF to obtain a null environmental burden if the (material and component production related) single score results are underestimated. In this case, the choice of the flax composite over glass composite is environmentally beneficial. In the second region, the choice of the flax composite over the glass composite is verified between MF_U and MF_C. However, variability in the production methods may give an advantage to the glass composite. In the third region, the overestimated mass factor between MF_c and MF_o (10% Overestimate of the (production related) single score value), the choice of flax composite is not favoured. However, variations in the production method may give an advantage to the flax composites. In the last region, when the mass factors are larger than MF_O , the use of the flax composite is not recommended. Once again, any improvement of the production method, choice of manufacturing method or material performance requirements may cause variations in the critical MFs.

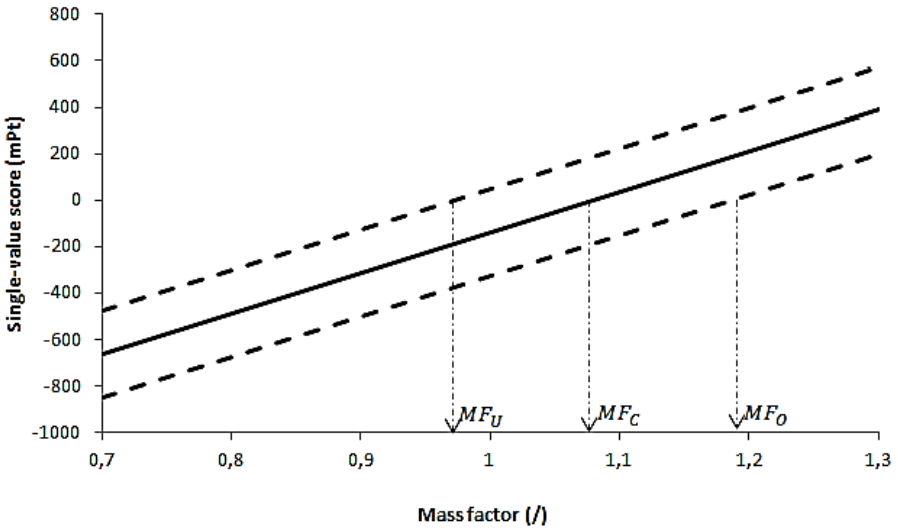

Figure 9-21: Variability of the single-value score when replacing glass by flax composites as a function of the mass factor and inventory analysis. The solid line indicates the calculated single-value score for the UD-replacement case. The dotted lines represent the plus and minus 10% interval.

In Figure 9-22, the different studies that were performed for the flexural design case are summarized. The results for these different fibre reinforcement types lay between the 10% deviation intervals of the UD case. The injection moulded cases slightly deviates the most from the UD curve. This was expected since short fibres are used and these reinforcements were only allocated[2] for 5% of the environmental impact in the production of long flax fibres. As short fibres are a co-products of the long flax fibre production (see Appendix G), part of the energy used to obtain the long fibre is dedicated to obtaining short fibres as it

[2] Allocation is the partitioning of the input/output of a process between the studied product (e.g. long flax fibres) and the by-product obtained during production.

represent 5% of the total weight of retted flax used to obtain long fibres. When a certain fibre reinforcement type is chosen for the composite, it does not have a great influence on the comparative study between glass and flax fibres in that composite, as long as the same reinforcement type is used.

For the second parameter, the use phase, a sensitivity analysis was carried out considering a driven distance of 200 000 km for passenger car and 1 000 000 before the component is replaced or the vehicle is taken out of the road. In Figure 9-23, the environmental impact of the total driven distance is displayed in function of the mass factor. The curves intersect at a MF of 1, because at a MF=1, the use phase is of no importance in the replacement of the glass composite by the flax composite, since the weight of both composites is equivalent. The slope of the curve gives an indication of the sensitivity of the environmental impact on the mass factor, for the two different driven distances. When we increase the driven distance, the influence of the use phase on the total environmental impact intensifies as clearly seen in Figure 9-23.

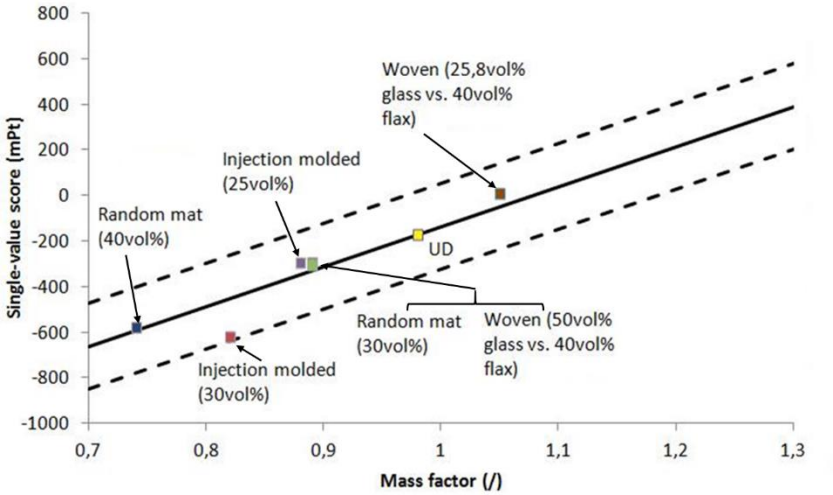

Figure 9-22: The different flexural design studies added in the variability plot of the UD flexural case. The MF factor mentioned in bold Table 9-11 are compared.

The critical mass factor also changes when the total driven distance increases. When increasing the total driven distance, the component weight becomes more critical and as such, the optimal MF for null environmental burden decreases. This is logical, since the higher the driven distance, the more critical the weight of the component becomes.

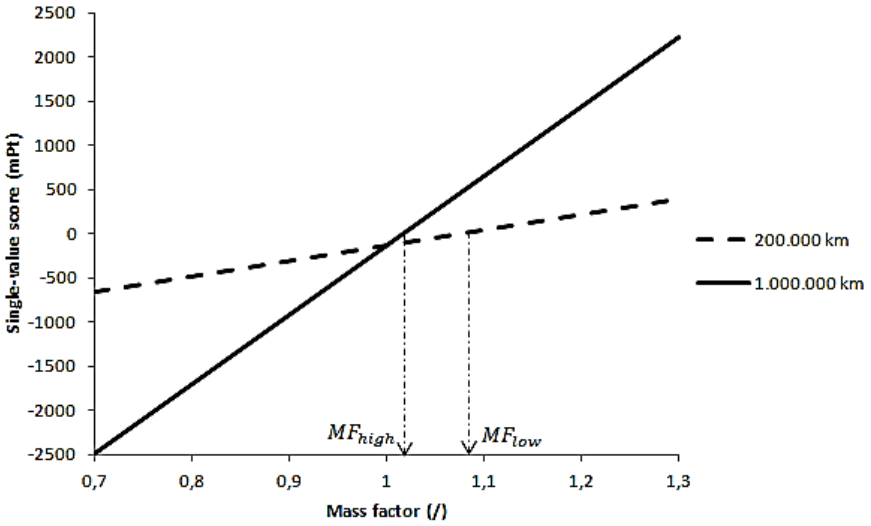

Figure 9-23: Variability on the total driven distance. Each curve has a different critical mass-factor.

9.3 Conclusions

In this study, three EOL-possibilities for flax fibre composites were investigated. It was found that the chemical recycling technique is feasible based on the mechanical properties of the recycled composite. However, its processing time, chemicals needed and equipment have negative effects on the environment. The second method, the mechanical recycling, has been found to result in a recycled composite with slightly lower mechanical properties compared to those of fresh random mat composites, but the recycled material still performs well enough to be used for non-structural applications. The main advantage of the mechanical recycling technique is the speed of the process as very large quantities of waste can be shredded and processed into new components. Table 9-12 summarizes the found advantages and disadvantages of the studied end of life techniques.

EOL technique	Advantages	Drawbacks
Chemical recycling	✓ Recovery of long fibres ✓ Recovery of PP	× Labor intensive × High capital and operation costs × Long processing time × Very specific to the matrix material
Mechanical recycling	✓ Fast process ✓ Recovery of PP ✓ Market in non-structural applications	× Downgrading of long fibre properties × Specific to matrix material
Incineration with energy recuperation	✓ Fast process ✓ Low labor intensive ✓ Not specific to matrix material	× No recycling of material × No improvement towards the recycling targets of the ELV directive in term of product re-use

Table 9-12: Technical advantages and disadvantages of the different EOL techniques for FFRP.

According to the LCA assessment of the mechanical recycling process, the environmental gain is the highest. It also contributes clearly to reaching the targets set by the end-of-life vehicles directive. The properties of the mechanically recycled materials should allow the material to be used in non-structural applications which give it an economic value. The last EOL method studied was incineration with energy recovery and it has been found to be a good alternative as well since all the material can be fully combusted and embodies a

relatively high calorific value. Furthermore, it was observed that this method is environmentally beneficial since energy is recuperated and replaced in case of the Belgian energy mix amongst other fossil fuel energy carriers. However, incineration does not allow recuperation of the materials and therefore no contribution to the recycling target of the end-of-life vehicles directive is made.

Three comparative life cycle analysis studies between glass and flax fibre reinforced plastics were performed, namely for two automotive cases, car roof and bumper. It was found that the replacement of glass fibre composites by flax fibre composites could be interesting from an environmental perspective. However, the mechanical properties of the fibres and composites made out of the fibres do not yet reach those of the glass composites. A trade-off between the weight and environmental benefit of the flax fibres and glass fibres exists. Therefore, a mass factor methodology was constructed which allowed to compare equivalent amounts of composite materials with each other, based on the mechanical performance for a certain design case. This methodology was partially based on the Ashby methodology for materials selection. By means of the mass factor, both the glass and flax composites could be compared with each other, which allowed the incorporation of the use phase as well. Pairs of flax and glass composites, with the same reinforcement type, were compared with each for two design cases: impact and flexural design.

In the impact design case, the results of the life cycle analysis showed that the replacement of GFRP by FFRP was beneficial in the 40% and 50% fibre volume fraction case, but not in the 30% case. Since the mass factor for the 30% case was higher than 1, this meant that the FFRP part needed to use 1,11 kg of flax fibre composite for 1 kg of glass composite to fulfil the same performance. That leads to an extra environmental burden associated with the use of more fossil fuels (more MAPP had to be used as well). For the flexural design case, it was found that the use of FFRP, with UD, random mat and injection moulded short fibre architectures, has lower environmental impact than their GFRP counterparts.

Since the data on the mechanical properties of flax-polypropylene composites was limited, a sensitivity study was further elaborated for the UD fabric of the flexural design. If new developments in the production of flax fibres or their composites occur, changes in mechanical properties and in the impact inventory may also take place leading to changes in the obtained LCA results. When evaluating these variations, the critical mass factor, or the flax weight needed to replace one kg of glass fibre composite and to still remain environmentally beneficial, was found to be 1.09. This means that the fibres and composites production have a large influence on the environmental impact while the use phase is of less importance. However for high duty vehicles, the use phase was more dominant and the critical mass factor decreases to 1.02. Based on the results of this environmental study, flax fibre composites prove to be an environmentally beneficial choice as compared to glass fibre composites. However, the trade-off between mechanical properties has to be evaluated for each design case specifically.

References

[1] Acero A, Rodríguez C, Ciroth A. LCIA methods–Impact assessment methods in Life Cycle Assessment and their impact categories. GreenDelta GmbH, Berlin, Germany. 2014:23.
[2] Poulakis JG, Papaspyrides CD. Recycling of polypropylene by the dissolution/reprecipitation technique: I. A model study. Resources, Conservation and Recycling. 1997;20(1):31-41.
[3] Blackadder DA, Le Poidevin GJ. Dissolution of polypropylene in organic solvents: 1. Partial dissolution. Polymer. 1976;17(5):387-94.
[4] Blackadder DA, Le Poidevin GJ. Dissolution of polypropylene in organic solvents: 2. The steady state dissolution process. Polymer. 1976;17(9):768-76.

[5] Blackadder DA, Le Poidevin GJ. Dissolution of polypropylene in organic solvents: 4. Nature of the solvent. Polymer. 1978;19(5):483-8.
[6] Drain KF, Murphy WR, Otterburn MS. Solvents for polypropylene: their selection for a recycling process. Conservation & Recycling. 1983;6(3):107-22.
[7] Oliveux G, Bailleul J-L, La Salle ELG. Chemical recycling of glass fibre reinforced composites using subcritical water. Composites Part A: Applied Science and Manufacturing. 2012;43(11):1809-18.
[8] Morin C, Loppinet-Serani A, Cansell F, Aymonier C. Near-and supercritical solvolysis of carbon fibre reinforced polymers (CFRPs) for recycling carbon fibers as a valuable resource: State of the art. The Journal of Supercritical Fluids. 2012;66:232-40.
[9] Piñero-Hernanz R, García-Serna J, Dodds C, Hyde J, Poliakoff M, Cocero MJ, Kingman S, et al. Chemical recycling of carbon fibre composites using alcohols under subcritical and supercritical conditions. The Journal of Supercritical Fluids. 2008;46(1):83-92.
[10] Dang W, Kubouchi M, Sembokuya H, Tsuda K. Chemical recycling of glass fiber reinforced epoxy resin cured with amine using nitric acid. Polymer. 2005;46(6):1905-12.
[11] Oliveux G, Bailleul J-L, Salle ELGL. Chemical recycling of glass fibre reinforced composites using subcritical water. Composites Part A: Applied Science and Manufacturing. 2012;43(11):1809-18.
[12] BALEY C, BOURMAUD A. Recycling composite materials reinforced with plant fibres. JEC composites. 2010(55):37-8.
[13] Le Duigou A, Pillin I, Bourmaud A, Davies P, Baley C. Effect of recycling on mechanical behaviour of biocompostable flax/poly(l-lactide) composites. Composites Part A: Applied Science and Manufacturing. 2008;39(9):1471-8.
[14] Beyler CL, Hirschler MM. Thermal decomposition of polymers. SFPE handbook of fire protection engineering. 2002;2:110-31.
[15] Ribeiro MCS, Meira-Castro AC, Silva FG, Santos J, Meixedo JP, Fiúza A, Dinis ML, et al. Re-use assessment of thermoset composite wastes as aggregate and filler replacement for concrete-polymer composite materials: A case study regarding GFRP pultrusion wastes. Resources, Conservation and Recycling. (0).
[16] Job S. Recycling glass fibre reinforced composites – history and progress. Reinforced Plastics. 2013;57(5):19-23.
[17] Le Duigou A, Davies P, Baley C. Environmental impact analysis of the production of flax fibres to be used as composite material reinforcement. Journal of Biobased Materials and Bioenergy. 2011;5(1):153-65.
[18] van der Werf HMG, Turunen L. The environmental impacts of the production of hemp and flax textile yarn. Industrial Crops and Products. 2008;27(1):1-10.
[19] Kymäläinen HR, Koivula M, Kuisma R, Sjöberg AM, Pehkonen A. Technologically indicative properties of straw fractions of flax, linseed (Linum usitatissimum L.) and fibre hemp (Cannabis sativa L.). Bioresource Technology. 2004;94(1):57-63.
[20] Reimann DO. CEWEP Energy Report III. In: Plants CoEW-t-E, editor.2013.
[21] Ashby MF, Cebon D. Materials selection in mechanical design. Le Journal de Physique IV. 1993;3(C7):C7-1-C7-9.
[22] Caprino G, Lopresto V. On the penetration energy for fibre-reinforced plastics under low-velocity impact conditions. Composites Science and Technology. 2001;61(1):65-73.
[23] Kannan TG, Wu CM, Cheng KB, Wang CY. Effect of reinforcement on the mechanical and thermal properties of flax/polypropylene interwoven fabric composites. Journal of Industrial Textiles. 2013;42(4):417-33.
[24] Cantero G, Arbelaiz A, Llano-Ponte R, Mondragon I. Effects of fibre treatment on wettability and mechanical behaviour of flax/polypropylene composites. Composites Science and Technology. 2003;63(9):1247-54.
[25] Khan RA, Khan MA, Zaman HU, Pervin S, Khan N, Sultana S, Saha M, et al. Comparative Studies of Mechanical and Interfacial Properties Between Jute and E-glass Fiber-reinforced Polypropylene Composites. Journal of Reinforced Plastics and Composites. 2010;29(7):1078-88.
[26] Lee N-J, Jang J. The effect of fibre content on the mechanical properties of glass fibre mat/polypropylene composites. Composites Part A: Applied Science and Manufacturing. 1999;30(6):815-22.
[27] Russo P, Acierno D, Simeoli G, Iannace S, Sorrentino L. Flexural and impact response of woven glass fiber fabric/polypropylene composites. Composites Part B: Engineering. 2013;54(0):415-21.
[28] Hagstrand PO, Bonjour F, Månson JAE. The influence of void content on the structural flexural performance of unidirectional glass fibre reinforced polypropylene composites. Composites Part A: Applied Science and Manufacturing. 2005;36(5):705-14.
[29] Rijsdijk HA, Contant M, Peijs AAJM. Continuous-glass-fibre-reinforced polypropylene composites: I. Influence of maleic-anhydride-modified polypropylene on mechanical properties. Composites Science and Technology. 1993;48(1–4):161-72.
[30] Lee N-J, Jang J. Performance optimisation of glass fibre mat reinforced polypropylene composites using statistical experimental design. Polymer Testing. 1997;16(5):497-506.
[31] Vanderfeesten B. Environmental impact of newly developed composites with thermoplastic matrix for high volume applications,Master, Leuven, KU Leuven; 2014.
[32] Shah DU, Schubel PJ, Clifford MJ, Licence P. Fatigue life evaluation of aligned plant fibre composites through S–N curves and constant-life diagrams. Composites Science and Technology. 2013;74(0):139-49.
[33] Bensadoun F, Vallons KAM, Lessard LB, Verpoest I, Van Vuure AW. Fatigue behaviour assessment of flax–epoxy composites. Composites Part A: Applied Science and Manufacturing. 2016;82:253-66.
[34] Tolouei R, Titheridge H. Vehicle mass as a determinant of fuel consumption and secondary safety performance. Transportation Research Part D: Transport and Environment. 2009;14(6):385-99.
[35] Koç E, Çinçik E. Analysis of energy consumption in woven fabric production. FIBRES & TEXTILES in Eastern Europe. 2010;18(2):79.

Chapter 10
General conclusions

In this thesis, the quasi-static, impact and fatigue properties of flax composites were thoroughly investigated. The focus was put on understanding the influence of the flax fibre architecture and the matrix type. A comparative LCA analysis between flax and glass fibre composites was carried out to evaluate the environmental benefit of bio-based composites. The study included data from the flax plant growing to its end-of-life. By understanding all these aspects, it was possible to show that flax-based composites have a real potential in replacing less environment-friendly materials in some applications. The following research questions were formulated in the beginning of this thesis:

> *Are these flax composite mechanically performant? What is the effect of the flax textile architecture? How well do flax composites perform on the long term? Are they comparable to glass fibres composite and other natural fibre reinforced composites? Can we achieve high performance flax biocomposites? Are they environmentally beneficial in comparison to standard materials?*

A summary of the most important conclusions is presented in the next sections.

10.1 Quasi-static mechanical properties

The first part of the thesis dealt with the characterization of quasi-static tensile and flexural properties. This study was also carried out in order to establish a reliable database for further impact and fatigue testing, as well as for the materials selection process. The effects of the textile geometry and matrix on the mechanical properties of flax-based composites were evaluated.

Looking at the obtained stress-strain curves, flax composites were found to have a non-linear behaviour with three distinct regions: the linear-elastic region (ε=0-0.1%), the strain softening region (ε=0.1-0.3%) and the strain hardening region (close to failure). This led to the calculation of two stiffnesses, E_1 between 0% and 0.1% strain and E_2 between 0.3% and 0.5% strain, to define the flax composite materials behaviour.

The intrinsic matrix properties have an important effect of the stiffness and strength of the final composite ($E_{epoxy} \approx 10 * E_{MAPP}$ and $\sigma_{epoxy} \approx 4 * \sigma_{MAPP}$), with the epoxy matrix outperforming the MAPP. This leads to a large drop in composite quasi-static mechanical properties. In terms of flax architecture effect, the random mat properties had the lowest tensile and flexural properties. This type of architecture is difficult to compress because fibres are randomly oriented, which leads to low nesting and limitation of the possible fibre volume fraction to a value of 30%.

The woven fabrics with wet spun yarns have an increased fibrillation (separation of the elementary fibres in the technical fibres) because of the dissolution of pectin, a direct effect of water during spinning. This type of yarn allowed a better impregnation by the polymer matrix inside the technical fibres and led to better quality composite with enhanced quasi-static properties. Furthermore, the side crimp, seen in the low twist twill fabric, caused by a binding yarn wrapped around the unidirectional flax fibres bundle, resulted in a decrease in mechanical properties in the longitudinal direction. Comparison of the woven fabrics to the [0,90] cross-ply composites has shown that the reinforcement geometry parameters, such as crimp, twist and weave style, are important factors influencing the tensile and flexural properties.

To pinpoint the moment the plastic deformation starts accumulating, an analysis was carried out of the "gradual" stress-strain curve (with stepwise increasing stresses, and intermediate unloading) of flax UD-epoxy composite. It was found to be similar to the one found with monotonic stress-strain curve analysis. However, from the last cycle data, an increase in stiffness (+7%), in strength (+28%) and failure strain (+65%) were observed following the cyclic stress build-up. As the test is longer, the micro-fibrils have time to better orient in the load direction. For the high strain increase obtained with the gradual build-up of plastic deformation, since the specimen is loaded during a longer time, a more pronounced visco-plastic effect was seen, which occurs in the same way as in creep.

Looking at the fracture profiles of the tensile and flexural samples, a brittle fracture for both epoxy and MAPP was found due to the predominant low failure strain of the fibres. However in flexure, the tensile failure was seen for the flax-epoxy samples while buckling of the specimens was the main mode of failure for the flax-MAPP samples, due to the low stiffness and yield strength of the MAPP.

10.2 Modelling of quasi-static properties

To understand the effect of yarn twist and quality (wet vs dry spun) and their effect on the quasi-static properties, an analysis of the stiffness and strength properties of the fibres and yarns constituting the preforms was carried out. The first step was to evaluate the "effective" properties of the yarns composing the textiles and to investigate the internal geometry, such as percentage of crimp, yarn diameter, etc., using micro-CT images. This was followed by the theoretical prediction the stiffness of composites with various flax architectures and matrix combinations investigated in this thesis.

To determine the "effective" properties of the yarns/fibres, the IFBT method was used. The properties were then back-calculated using the Chamis formula. The effect of twist on the stiffness and strength were investigated. Results showed a strong correlation between stiffness and twist, i.e. stiffness decrease with increasing twist angle as put forward by the models of Rao-Farris [1] and Naik-Madhavan [2]. The quality of the yarn and constituting fibres were also found to be important factor to considerate. A higher variation in back-calculated strength data was found compared to the stiffness ones. In this case, a linear relation between the twist angle and the strength properties was found. However, yarns/fibres with specific geometries,

such as low twist twill, did not correlate with the linear regression. This was related to the strength values that are more sensitive to defects, fibre misorientation and distribution in the specimens and voids. Thus, optimized sample preparation is needed to obtain reliable results. Overall, the IFBT method was found suitable for the characterisation of the effective stiffness and strength of flax yarns, as they would behave in a composite material.

These back-calculated yarn properties were then used as input parameters in the model for the woven flax composites to predict their performance. These data were combined to the geometrical features of the yarn/fibre obtained with micro-CT and optical microscopy (twist, ends picks and counts, etc.) to recreate the 3D model with the Wisetex software. The laminate with the correct number of layers was then created using Lamtex software and then transferred to Texcomp software for a prediction of the flax composite properties once combined to epoxy or MAPP. The effective moduli obtained with the software calculations were comparable to the experimental results found in Chapter 5 with variations lower than 10% at similar fibre volume fraction of 40%.

10.3 Impact properties of flax composites

The influence of the flax fibre architecture and matrix type was also assessed through low velocity impact. Like synthetic-based composites, flax fibre composites are also sensitive to impact damage. Even very low impact energies could result in damage such as delaminations and/or fibre breakage and matrix cracking. These would ultimately lead to a decrease of the material properties.

Three aspect of low velocity impact were studied: absorbed impact energy to perforation, damage resistance and damage tolerance. For all three aspects, it has been found that the matrix ductility has a large influence. The perforation energy data of flax-MAPP composite is 50% higher than the flax-epoxy ones. In terms of non-perforation, most of the impact-induced damage was constrained to fibre breakage and matrix cracking in cross shape with very limited delaminations. This was caused by the high interlaminar fracture toughness and low strength of the flax fibres. The flexural properties after impact showed that the decrease in flexural properties after impact was minimal for MAPP although the overall quasi-static properties are lower than the thermoset ones. The thermoset composites experienced a higher decrease in properties due to the brittle nature of the epoxy matrix. However, they showed higher flexural properties both before and after impact.

The capacity of the flax composites to resist to delamination growth after non-perforation impact is directly related to its interlaminar fracture toughness. Promising results were found in this thesis for flax-epoxy composites tested in mode I (G_{IC}) and mode II ($G_{II}C$) interlaminar fracture toughness. Unlike glass and carbon fibres, the presence of delaminations does not seem to influence the impact performance of the flax composite, since very low amount of delaminations were detected. The woven textile composites have been found to have superior G_{IC} and G_{IIC} values compared to the [0,90] and [90,0] cross ply lay-ups, thanks to features such as crimp and increased nesting.

The last part of the impact study involved the characterization of the tensile toughness calculated with by the integration of area under the tensile stress-strain curve of the quasi-static tensile tests. This tensile toughness was found to be a good indicator of the capacity of flax composites to sustain perforation or non-perforation impact. As such, a first probe into impact testing for new materials combination could already be done with the tensile test curves and make a smart selection of the sample that need further investigation.

10.4 Fatigue properties of flax-epoxy composites

Fatigue properties are one of the most important failure causes that are taken into account when designing new applications aimed for long term use. A better understanding of the long term properties of flax fibre composites is essential to warrant their durability.

S-N curves, obtained by the means of tension-tension fatigue tests, have shown no clear difference between the woven fabric and cross-ply laminates nor between the UD and quasi-UD configurations. The stiffness degradation at low stress level (30% of the UTS) has been found to be stable after a small increase in the early cycles followed by a stiffness stabilisation. The slight increase in the early cycles is consistent with the hypothesis of the stiffening of the fibres (microfibrillar alignment) in the fibre direction as previously found in the quasi-static properties characterization.

The residual strain (cyclic creep) observed with increasing cycles was limited at low loading levels (30% UTS) and could be caused by plastic deformation of the composite and/or the appearance of damage. The post-fatigue properties after ½ million cycles at 30% UTS were comparable to the initial quasi-static test results obtained in Chapter 5. One exception was noted for the low twist twill where the binding yarn acted as a stress concentrator and leads to a stronger decrease in properties. These results were predictable because of the S/N curves, stiffness degradation curves and cyclic creep results, where a stronger decrease was systematically observed for that specific low twist twill preform.

Overall, flax composites with high quasi-static stiffness and strength lead to an increased fatigue life, a delayed damage initiation and a reduced damage propagation rate. The small cycle loop area corroborates the hypothesis that low permanent strain and appearance of damage is occurring for flax composites.

Flax fibres are very often compared to glass fibres since they have similar stiffness properties. The fatigue performance of these two composites was found to be comparable, and once normalised to their respective composite densities, flax is superior to glass. Furthermore, lower stiffness and strength degradations as well as residual strains were found for flax fibre composites in comparison to the glass fibre composites.

10.5 Environmental impact assessment of flax composites

Flax composites have proven to be a good material for high performance applications. Their quasi-static properties and in-service properties, i.e. impact and fatigue behaviour, have shown that flax fibres can compete with glass fibres in some applications. In order to close the loop on the flax composite life cycle, an investigation of three end-of-life possibilities and their environmental impact was carried out. To narrow down the possibilities, the study focused on the EOL for flax-MAPP composites.

The first investigated EOL technique, chemical recycling, was found to be feasible as long fibres could be recuperated. If these long fibres are reprocessed into a composite, they result in equivalent mechanical properties, just like a fresh composite. However, this process is energy consuming and requires a large amount of chemicals which are harmful for the environment.

The second method, the mechanical recycling, leads to a recycled, compression moulded product with short fibres. Since the aspect ratio of the fibres decreases, this leads to a reduction of the recycled composite mechanical properties even if compared to fresh random mat composites. Although the performance is lower, they can still be used in non-structural

applications. The main advantage of this technique is the speed of the process as very large quantities of waste can be shredded and processed into new components. Regarding its LCA performance, the mechanical recycling process showed a reduced environmental burden which may help reaching the targets set by the ELV directives. Furthermore, it allows a direct re-use of the composite with or without the addition of additional polymer.

The third EOL technique, incineration with energy recovery, showed that more energy can be produced by combusting flax composites compared to glass composites. This method is environmentally friendly since part of the energy is recuperated to be used for the production of electricity.

The data obtained during the EOL investigation was then used in a comparative LCA which compares the use of flax composites against the market standard material. This was done for two automotive cases, a car bumper and a car roof. For both cases, the replacement of the standard material, glass fibres, by flax fibres was found to be environmentally beneficial. However, a trade-off between the composite weight, mechanical performance and environmental benefit exists. This is why the mass factor methodology was used in order to compare the flax and glass composites based on equivalent mechanical performance. The use phase and the incineration with energy recovery were also considered in this assessment.

For the automotive applications, two design load cases were considered: flexural load for the car roof and impact for the bumper. For the impact case, using FFRP instead of GFRP was beneficial for V_f higher than 40% and mass factor equal or lower than 1. A mass factor higher than 1 means that the weight of the FFRP part is higher than the glass in order to fulfil equivalent performance. That leads to an extra environmental burden associated with the use of more MAPP polymer which is derived from fossil fuels.

For the flexural design case, the use of injection moulded FFRP had lower environmental impact than their GFRP counterparts independently of the type of architecture used. A sensitivity analysis , carried on the UD flax-MAPP composites, showed that the fibre and composite production have a large influence on the environmental impact, while the use phase is of less importance if the bumper is made for a passenger car with a maximum mass factor of 1.09 (200 000 km). However, if the driven distance increases, the use phase becomes a more dominant factor and the part critical mass factor is limited to 1.02.

10.7 Recommendations for future work

Throughout the study, many topics were investigated and it became clear some subjects are worthy of further investigation. Several directions can be taken and some avenues are presented below. Proposals for complementary studies are also made for topics interconnected with the development of high performance flax composites.

In the present work, the textiles were chosen because of their market availability, which leads to fabrics using different fibre quality, yarns with different linear density, spinning type (dry or wet) and twist angle. In order to solely focus on the effect of weave type, it is proposed to use only one type of yarn to weave the different architectures to eliminate the other effects. Ultimately, the effect of crimp should be clearly visible.
To further investigate the effect of yarn twist on the stiffness and strength, rovings and yarns could be spun at various twist angles using the same batch of fibres using the IFBT method. These data can help strengthen the results obtained with the current models for stiffness

degradation with increasing twist, while developing a reliable model for strength which is yet to be established.

Three dimensional textile modelling was useful in order to predict the flax composite properties. A better understanding of the yarn features and weave pattern effect on the properties will help obtaining more accurate predictions. To make the models more accurate, a more systematic and automated process of measurement of the yarn geometrical characteristics needs to be featured through micro-CT images. Additional suggestions would be to adapt the modelling software to take into account automatically the distinctive geometry of natural fibres, such as twist.

In terms of impact behaviour, it would be interesting to investigate the potential use of more impact resistant fibre architectures such as knitted and 3-D-woven fabrics. These types of fabric were found to increase the perforation energy, damage resistance and interlaminar fracture toughness [3, 4]. This could also be done using flax fibres either in combination with a ductile matrix or by hybridising with a more ductile fibre. As the interface strength is one of the most important parameter as it determines which failure mode will occur, further investigation into weak interface to increase the energy absorption is need. A weak interface leads to extensive debonding and pull-out in the composite. Pull-out energy absorption is considered to be one of the most important contributors to impact energy absorption. C-scan has proven to be a good technique for the detection of the damage area in the specimen, however, the detection of small defect features is still a challenge.

To gain deeper insight of how the damage spreads following a low velocity impact, more accurate techniques such as X-ray tomography and infrared thermography (IR) are worth considering. These techniques could also be used to monitor the damage during fatigue cycling such as the appearance of matrix cracks, fibre fractures and delaminations as well as the global damage initiation and propagation. The advantage of the IR technique is that it allows an in-situ monitoring of the temperature build-up in the sample, which facilitates the visualisation of the energy dissipation stages and imminent failure. These two techniques would allow a better understanding of how the damage appears and progresses in flax composites since their behaviour has proven to be quite different from carbon and glass.

Another interesting avenue in fatigue testing would be to characterize more types of architecture in order to create a comprehensive database similar to the ones developed for glass and carbon fibres by the Montana State University [5] and the Delft University [6]. Looking at other stress ratios, such as tension-compression and compression-compression, to create a constant-life diagram is essential in order to simplify the choice of materials according to the design specification. Other studies such as fatigue in humid and high temperature environments can also be interesting.

In natural fibres, the influence of the fibre-matrix interface is one of hottest topics. However, having a good adhesion between the fibre and the matrix is not always wanted, depending on the load case of each application. In terms of stiffness, strength or fatigue design, a good interface is desired in order to maximise the load transfer from the matrix to the fibre. In impact, a poor adhesion is favoured to increase the properties. Thus it would be interesting to develop specific chemical treatments for each type of application, to ensure that the composites are performing as expected.
In this work, three end-of-life possibilities for flax fibre composites were studied. It was found that mechanical recycling and incineration with energy recovery are two viable solutions from an environmental point of view. The basic parameters were laid out but deeper research on large

scale quantities and injection moulding possibilities still need to be carried out. The re-use/recycling of natural fibre composites in general is very little researched and in order to reach the European environmental targets, more efforts should be made. More research towards applications in which the recycled materials can be used and towards the best operating conditions, could also be performed.

Other topics which are connected to the in-service behaviour of composites could also be looked into, such as:

- Creep of flax fibres and its composites;
- Flax fibre composite processing at high temperature in order to be used with higher property thermoplastic matrices;
- Flax composite manufacturing difficulties, such as permeability and wetting, as they are affected by the dense structure of twisted yarns;
- Combination with bio-matrices to develop mechanical and environment efficient biocomposites;
- Fundamental studies on the variation of the flax microfibrillar angle change and composition changes by using high-resolution X-ray tomography or XRD systems such as the synchrotron.

Flax fibres have been receiving a lot of attention in the last few years and their many advantages easily trumps their drawbacks. They are now been used in many applications from home furniture to tennis rackets, guitar, and car parts. Further optimization of their properties will put them on the forefront for use in new applications.

References

[1] Rao Y, Farris RJ. A modeling and experimental study of the influence of twist on the mechanical properties of high-performance fiber yarns. Journal of Applied Polymer Science. 2000;77(9):1938-49.
[2] Naik NK, Madhavan V. Twisted impregnated yarns: Elastic properties. The Journal of Strain Analysis for Engineering Design. 2000;35(2):83-91.
[3] Zhao N, Rödel H, Herzberg C, Gao S-L, Krzywinski S. Stitched glass/PP composite. Part I: tensile and impact properties. Composites Part A: Applied Science and Manufacturing. 2009;40(5):635-43.
[4] Zhang D, Sun Y, Chen L, Pan N. A comparative study on low-velocity impact response of fabric composite laminates. Materials & Design. 2013;50(0):750-6.
[5] Mandell JF, Samborsky DD. DOE/MSU composite material fatigue database: test methods, materials, and analysis. Sandia National Labs., Albuquerque, NM (United States); 1997.
[6] Nijssen R. OptiDAT-database reference document-The Knowledge Centre Wind turbine Materials and Constructions. Delft university of Technology. 2006.

Appendix A
Flax fibre reinforced composites applications

For consumer goods products, the non-technical characteristics of materials (e.g. material texture) can be equally or even more important than their technical properties (e.g. acoustic properties). The role of the designer in the product development process is to find the optimal combination between visual appeal and its technical function. It is not only related to the choice of material in a proper sense but also to processing, finishing of the product and societal and cultural impact. In the next sections, an exploration of the usage of flax in consumer good products is present.

A.1 Sporting goods

One of the first applications of flax fibres in sports good was the Artengo tennis racket in 2009 [1]. Thanks to the high damping capacity of flax fibres (15 wt.%), once combined to the stiff and strong carbon fibres (85wt%), an increase in damping factor by 22% was found. Hence, adding flax fibres effectively reduced vibrations and the risk of muscular injury such as tennis elbow. An increase in vibration damping allows a better control of the equipment by the athlete. As of today, the flax is also added to the skin or the core of skis to improve the precision of manoeuvring of skiers [2-4]. In this case, glass fibres or carbon fibres are combined to a bio-based balsa wood core, reinforced in the thickness direction with strips of +/- 45° flax allowing a further reduction of weight and an increase in damping capacity.

Vibration reduction is also beneficial for ski poles (using flax braids) [5], professional fishing rods [6], bow for competition archers [7] or for the frames of high-end race bicycles [8]. In other products, like in the surfboards [9] or the 'Le Ventoux' bike, the environmental impact was one of the main reasons for choosing natural fibres over synthetic fibres. For "Le Ventoux" bike, pre-impregnated flax tapes were used to join the bamboo culms into a traditional diamond-type obtained a 100% bio-based bicycle frame [10]. All mentioned applications are presented in Figure A-1.

Figure A-1: Various applications of flax composites in sporting goods: a) Artengo tennis racket, b) Notox surfboard, c) Caperlan fishing rod, d) ArcWin Archery bow, e) Kang flax ski poles and f) Le Ventoux bamboo-flax bike.

A.2 Music and sound

Flax composites have also been introduced in the music world thanks to their good mechanical properties and design flexibility. Hybrid flax/glass woofer cones as seen in Figure A-1a are used by FOCAL [11] in the production of automotive speakers. They provide better dynamics as well as a homogeneous sound in a richer range. The glass-fibre skins provide controlled stiffness and the flax core in-between provides vibration absorption giving the cone's sound neutrality [12]. Furthermore, flax fibres are increasingly used in concert instruments with the arrival of 100% flax-based *El Capitan* guitar and *Clara* ukulele from California instrument builder, Blackbird presented in Figure A-2 b and c [13].

Figure A-2: a) Aria column speaker 900 and flax cone from FOCAL [11], b) El Capitan Blackbird Guitar, c) Blackbird flax Ukulele and d) Flax electric Guitar from Depestele [11, 13].

The main advantage of using flax composite their comparable sound to the vintage wood along with exceptional acoustic quality and lightness. The guitar is made of cross-ply laminates based skins combined to UD flax fibre layers and a bio-based cashew-nut-based

resin. Since then, more musical instruments have been manufactured such as the electric guitar from Depestele and a ukulele and a chenda (indian percussion) from Mc Gill university [14, 15].

A.3 Transportation

The transportation industry is a high volume market which is constantly aiming at higher performing vehicles. With new and more stringent environmental regulations such as the ELV mentioned in the previous section, the pursuit of performance is key. Weight reduction seems one of the most important parameters to reduce the environmental impact of a vehicle [16]. If a vehicle is lightweight, it requires less propellant and thus, less emissions in the atmosphere. However, these materials should still be able to reach the yet established specifications which govern the safety of the passengers in the vehicle. Using natural fibres in transportation has many advantages such as:

- Unique aesthetics;
- Reduced weight and cost compared to glass fibre parts;
- High specific mechanical properties comparable to glass fibre;
- Superior damping of carbon fibre components, reducing noise, vibration and harshness;
- Lower environmental impact compared to glass and carbon fibres.

a) b) c)

Figure A-3: Flax composites transportation: a) the BioMobile [17], b) the Be.e electric scooter [18], c) the EGIDE bicycle helmet [19].

a)

b)

c)

Figure A-4: a) the i-car Racing [22], b) Faurecia Flaxpreg for multi-position trunk load floor[1] and c) FibriRock for aircraft galleys Ecotechnilin for aeronautics[2].

[1]http://www.faurecia.com/en/faurecia-flaxpregtm-wins-jec-europe-2015-innovation-award-semi-products-category
[2] http://www.agrobiobase.com/en/database/bioproducts/transport/fibrirock

As of today, there are many examples of flax fibre use in mobility applications. The aforementioned bicycles are a first example and several other applications are displayed in Figure A-3. A fully covered reclining bike *BioMobile* was developed at ETH Zürich which used flax fibres textiles and ribs in its structural elements, further reducing the weight without sacrificing on stiffness and durability [17]. The *Be.e*" electric scooter designed by Waarmakers [18] is a monocoque random mat flax structure. The design was motivated by the potential of avoiding multi-part frame and to produce a sustainable product. A similar approach was used for the EGIDE city bike helmet where the flax non-crimp fabric preform is visible through the transparent varnish, allowing the cyclist to make an ecological statement [19].

Lately, many researchers have focused on the incorporation of natural fibres into the automotive industry, especially in non-structural applications [20, 21]. For example, the flax fibre composite was used in the design of the i-Car Racing seen in Figure A-4a [22]. This electric three-wheeler car, capable of racing at 160 km/h, refers with its rounded, aerodynamic shape to organic forms in nature, and reinforces this by making the natural fibres visible, putting its unique aesthetic at the forefront of the design.

One of the latest innovations, namely the Flaxpreg, will be applied in the large scale production of a Peugeot passenger car trunk load floor, thanks to drastic weight reduction and excellent mechanical properties of the unidirectional long non–woven flax fibres used (Figure A-4b). This allowed a 35% weight reduction compared to glass mat - polyurethane sandwich. Other factors such as renewable resources, low production cycle times and reduced material costs were also key factors in trunk floor development.

The newest material innovations, such as the bio-sourced FibriRock composite seen in Figure A-4c, are now also going toward aircrafts parts such as galley carts. This product combines flax and basalt fibres to a sugar-based furan bio-resin and Nomex core. It is a rigid, fast-curing and lightweight composite which allows a 50% weight reduction from traditional aluminium galleys. Furthermore, it meets both the mechanical performance requirements and the fire performance (smoke, toxicity and heat release) compulsory to certify aeronautical parts.

A.4 Furniture and interior design

Furniture design with bio-based composites is at the moment, with sporting goods, the biggest market for flax fibre based composites. Designing with bio-based composites doesn't only focus on the material properties but also the material formability, texture, structure, random patterns, natural color shades and visual aspect as well as imperfection, diversity, irregularity, in analogy with what exists in nature and real life[12]. These properties create new avenues for designers to create contemporary state-of the art complex designs. The combination of innovative material and more traditional values is an essential feature of designing with bio-based composites. The use of flax composite materials provided a unique and creative option for new furniture in terms of the variety of shapes, textures, durability, innovative applications and local sourcing [12, 23, 24]. Some examples of chairs are displayed in Figure A-5. The Chair "Collection Lin 94" by François Azambourg (Figure A-5a) allies, from the aesthetics perspective, a minimalistic design with modern lines. Furthermore, the 'Flax Chair' by Christien Meindertsma (Figure A-5b), was a waste-free production process which used stacks of rectangular compression moulded flax-PLA random mat preforms. The chair is then cut from the composite to shape the seat and the legs. As the legs surround the seat to make the rectangular preform no

material is wasted. The third example, Studio Katra designers made the Katra chair (Figure A-5c) look like a sheet of paper folded as if its maker were origami masters to highlight the potential variety of shapes [23].

a) b) c)

Figure A-5: a) Chair "Collection Lin 94 " by François Azambourg [24], b) the Flax Chair by Christien Meindertsma [25] and c) Studio Katra Chair [26].

Another telling example is the product description of 'Flax Tray', shown in Figure A-6, which identifies as a bio-based composite and underlines the difference with traditional composites [27]. In this tray, the combination of the strength and lightness of the material and its formability are utilized. Other objects, where the technological aspect is less predominant are presented in Figure A-6. The flax weave-PLA "Cocoon" by Virgine Breton for *BBdor* allies lightness and strength to transport a baby with the openness needed for the baby to interact with the outside world [28]. The woven structure of "les Danseuses'"(2009) lampshade, from az&mut (Figure A-6b), give it an ethereal look [29] while the 3D printed desk lamp 'L1' from Drawn and the flax screen from Culture In (Figure A-6c and d), both made of flax fibre-PLA composites, highlights the textile texture and color versatility.

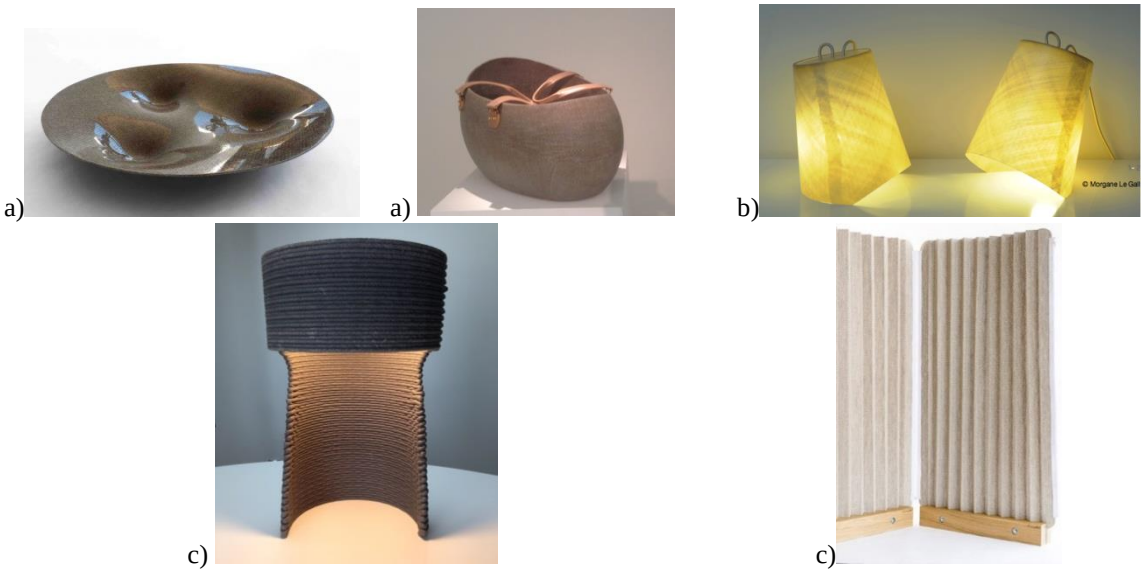

a) a) b)

c) c)

Figure A-6: a) Flax tray by Bram Geenen [27], b) B-Bdor cot from Virginie Breton [28], c) "Les Danseuses lamp" from az&mut [29], d) L1 lamp from DRAWN[30] and e) flax-PLA composite screen using VARIAN[3].

[3] http://varian.culturein.eu/realisations/le-paravent-varian/

References

[1] nature Llc. Une raquette de tennis légère et confortable - Du lin dans les raquettes de tennis. 2009. http://www.lelin-cotenature.fr/FR/Une-raquette-de-tennis-legere-et-confortable-46.html
[2] Bcomp. bCore - The lighest wood core. http://www.bcomp.ch/31-0-bCores.html
[3] Salomon. Q-BC LAB Skis. 2015. http://www.salomon.com/us/product/q-bc-lab.html
[4] Free D. Countdown All Mountain Freeride skis. 2015. http://www.downskis.com/skis#countdown
[5] Kang. Kang ski poles. 2015. http://en.kangpoles.com/
[6] Caperlan. CAPERLAN BLYSS DEEP TEAM 5" FLAX jig fishing rod. http://www.caperlan.co.uk/blyss-deep-team-5-flax-jig-fishing-rod-id_8164177-reviews
[7] Archery A. Wiawis series Bow. http://win-archery.com/products#inno-series
[8] Gordon J. Flaxen Beauties: Professional Racing Bikes Made of Flax Fiber. 2009. http://www.treehugger.com/sustainable-product-design/flaxen-beauties-professional-racing-bikes-made-of-flax-fiber.html
[9] Notox. 2010. http://www.notox.fr/en/
[10] IN'BÔ. Le Ventoux Bike http://inbo.fr/en/wood-and-bamboo-bikes/9-le-ventoux.html
[11] FOCAL - Flax Cone. http://www.focal.com/en/209-flax-cone-2-3-way-driverspeaker-kits
[12] Pil L, Bensadoun F, Pariset J, Verpoest I. Why are designers fascinated by flax and hemp fibre composites? Composites Part A: Applied Science and Manufacturing.
[13] Blackbird El Capitan Guitar. https://blackbirdguitar.com/content/blackbird-el-capitan
[14] Phillips S, Lessard L. Application of natural fiber composites to musical instrument top plates. Journal of Composite Materials. 2011:0021998311410497.
[15] Damodaran A, Mansour H, Lessard L, Scavone G, Babu AS. Application of composite materials to the chenda, an Indian percussion instrument. Applied Acoustics. 2015;88:1-5.
[16] Mildenberger U, Khare A. Planning for an environment-friendly car. Technovation. 2000;20(4):205-14.
[17] Biomobile. http://biomobile.ch/
[18] be.e - Electric bio-scooter. http://vaneko.com/be-e
[19] Egide Helmets - Apollo Lin. http://egide-paris.com/en/
[20] Hufenbach W, Böhm R, Thieme M, Winkler A, Mäder E, Rausch J, Schade M. Polypropylene/glass fibre 3D-textile reinforced composites for automotive applications. Materials & Design. 2011;32(3):1468-76.
[21] Corum JM, Battiste RL, Ruggles MB, Ren W. Durability-based design criteria for a chopped-glass-fiber automotive structural composite. Composites Science and Technology. 2001;61(8):1083-95.
[22] Lallemand P. i.Car 333 - urban electric vehicle http://www.pierrelallemand.com/main.html#/GALLERIES/Cars
[23] Joseph S. Innovative and Green: Aparte Studio's Katra Chair. 2011. http://media.designerpages.com/3rings/2011/12/29/innovative-and-green-aparte-studios-katra-chair/
[24] Azambourg F. Lin 94 chair http://www.azambourg.com/projet.php?no=collection_lin_94
[25] Meindertsma C. Flax Chair. http://www.labelbreed.nl/collections/collection-2015-1.00/christien-meindertsma-enkev/products/flax-chair/
[26] Katra S. http://www.studio-katra.com/en/
[27] Dauriac C. Flax tray by Bram Geenen. http://blog.europeanflax.com/flax-tray-by-bram-geenen/
[28] Breton V. B-Bdor Cot. http://inspiration-design.net/enfant/0-ans/
[29] Az&mut. Les Danseuses Lamp. http://www.az-et-mut.fr/def_gb/pots_lin.html
[30] Javelle S. Drawn L1 Lamp. http://www.lyoncitydesign.fr/drawn/

Appendix B
Mechanical properties and statistical analysis results for flax composites

	***E_1**:Tensile modulus (GPa) between 0 and 0,1% strain*	***E_2**:Tensile modulus (GPa) between 0,3 and 0,5% strain*	*E_2 vs E_1 difference* (%)	*Tensile strength σ (MPa)*	*Tensile failure strain @ max stress ε_{ult} (%)*
Random Mat*	7.3 ± 0.6	5,6 ± 0.6	23	84 ± 5	1.49 ±0.09
Plain Weave	12.6 ± 0.4	8,9 ± 0.2	29	135 ± 18	1.69 ±0.32
Twill Low Twist	12.8 ± 0.4	9.5 ± 0.4	25	120 ± 2	1.65 ± 0.14
Twill Medium-Low Twist	12.9 ± 1.1	10.2 ± 0.6	21	126 ± 9	1.52 ± 0.13
Twill Medium-High Twist	13.7 ± 0.4	9.7 ± 0.3	29	184 ± 2	2.14 ± 0.12
Twill High Twist	12.2 ± 0.8	10.8 ± 0.8	12	141 ± 23	1.78 ± 0.1
Quasi-UD [0,90]	12.9 ± 0.8	9 ± 0.6	30	145 ± 14	1.53 ± 0.3
UD1 [0,90]	12.7 ± 0.9	10 ± 0.6	21	149 ± 14	1.58 ± 0.06
UD2 [0,90]	14.5 ± 0.8	11.8 ± 2.5	19	126 ± 7	1.08 ± 0.16
Quasi-UD	22.9 ± 0.5	15.9 ± 1.1	31	235 ± 31	1.51 ± 0.4
UD1	23.7 ± 1.3	17.2 ± 1.1	27	259 ± 31	1.22 ± 0.07
UD2	26.6 ± 2.3	20 ± 2.6	25	249 ± 9	1.16 ± 0.1

*V_f=30%, all the other combination are at V_f=40%

Table B-1: Tensile properties of flax-epoxy composites with V_f =40%.

	***E_1**:Flexural modulus (GPa) between 0 and 0,1% strain*	***E_2**: Flexural modulus (GPa) between 0,3 and 0,5% strain*	*E_2 vs E_1 difference* (%)	*Flexural strength σ (MPa)*	*Flexural failure strain @ max stress ε_{ult} (%)*
Random Mat*	5.1 ± 0.5	4.5 ± 0.2	12	95± 5	3.13 ± 0.16
Plain Weave	10.9 ± 0.3	9.6 ± 0.4	12	181 ± 5	3.01 ± 0.09
Twill Low Twist	12.6 ± 1	10.6 ± 0.3	10	180 ± 7	3.16 ± 0.15
Twill Medium-Low Twist	8.8 ± 0.5	7.8 ± 0.3	11	167 ± 19	3.27 ± 0.16
Twill Medium-High Twist	9.9 ± 0.8	8.9 ± 0.4	16	154 ± 8	2.62 ± 0.17
Twill High Twist	10.7 ± 0.7	9.5 ± 0.3	11	174 ± 4	3.08 ± 0.15
Quasi-UD [0,90]	16 ± 1	9.6 ± 0.8	40	202 ± 14	3.8 ± 0.2
UD1 [0,90]	8.8 ± 1.4	7.7 ± 0.8	13	145 ± 9	2.81 ± 0.35
UD2 [0,90]	17 ± 1.5	12.1 ± 0.6	29	188 ± 21	1.8 ± 0.2
Quasi-UD	19.3 ± 0.7	13.2 ± 0.5	32	225 ± 6	3 ± 0.2
UD2	22.9 ± 0.5	18.5 ± 2	19	290 ± 25	2.51 ± 0.16

*V_f=30%, all the other combination are at V_f=40%

Table B-2: Flexural properties of flax-epoxy composites with V_f =40%.

	***E_1**:Tensile modulus (GPa) between 0 and 0,1% strain*	***E_2**:Tensile modulus (GPa) between 0,3 and 0,5% strain*	*E_2 vs E_1 difference* (%)	*Tensile strength σ (MPa)*	*Tensile failure strain @ max stress ε_{ult} (%)*
Random Mat*	4.5 ± 0.9	2.7 ± 0.4	39	56 ± 7	2.4 ± 0.07
Twill Low Twist	10.2 ± 0.3	6.5 ± 0.3	25	95 ± 4	1.76 ± 0.09
Twill Medium-Low Twist	9.2 ± 0.5	6.4 ± 0.4	36	123 ± 5	2.27 ± 0.06
Twill Medium-High Twist	8 ± 0.8	5.5 ± 0.9	30	115 ± 24	2.62 ± 0.12
Twill High Twist	8.1 ± 0.8	6.5 ± 0.3	31	113 ± 7	1.95 ± 0.1
Quasi-UD [0,90]	10.5 ± 0.5	6.5 ± 0.1	38	114 ± 9	2.11 ± 0.14
UD1 [0,90]	10.7 ± 1	9.8 ± 0.8	8	158 ± 1	1.60 ± 0.15
UD2 [0,90]	10.8 ± 1.1	7.4 ± 0.7	31	89 ± 12	1.09 ± 0.06
Quasi-UD	17.7 ± 1.1	11.2 ± 0.1	37	210 ± 1	1.92 ± 0.09
UD2	21.5 ± 3.6	15 ± 0.6	30	189 ± 17	1.05 ± 0.18

*V_f=30%, all the other combination are at V_f=40%

Table B-3: Tensile properties of flax-MAPP composites with V_f =40%.

	***E_1**: Flexural modulus (GPa) between 0 and 0,1% strain*	***E_2**: Flexural modulus (GPa) between 0,3 and 0,5% strain*	*E_2 vs E_1 difference (%)*	*Flexural strength σ (MPa)*	*Flexural failure strain @ max stress ε_{ult} (%)*
Random Mat*	3.1 ± 0.2	2.2 ± 0.2	29	46 ± 1	3.79 ± 0.15
Twill Low Twist	5.5 ± 0.3	4.4 ± 0.2	22	66 ± 5	3.64 ± 0.25
Twill Medium-Low Twist	8.3 ± 0.5	5.6 ± 0.4	33	78 ± 4	3.04 ± 0.04
Twill Medium-High Twist	8.1 ± 0.5	6.3 ± 0.4	20	93 ± 4	3.03 ± 0.26
Twill High Twist	8.1 ± 0.4	5.4 ± 0.3	33	77 ± 3	3.11 ± 0.52
Quasi-UD [0,90]	9.5 ± 1.7	8.8 ±0.5	7	70 ± 6	2.9 ± 0.39
UD1 [0,90]	7.8 ± 0	6.6 ±0	15	92 ± 0	2.55 ± 0.30
UD2 [0,90]	8.5 ± 0.9	5.7 ± 0.6	35	92 ± 12	2.58 ± 0.51
Quasi-UD	12.8 ± 0.4	10.1 ± 0.2	21	100 ± 3	1.88 ± 0.37
UD2	18 ± 1.3	13.8 ± 1.2	23	175 ± 16	2.01 ± 0.02

*V_f=30%, all the other combination are at V_f=40%

Table B-4 : Flexural properties of flax-MAPP composites with V_f =40%.

Tensile	Strain @ Max Stress	E1	E2	Strength
Plain weave	B	B C	C	B C
Twill Low Twist	B	B C	B C	C
Twill Medium-Low Twist	B	B C	B C	C
Twill Medium-High Twist	A	A B	B C	A
Twill High Twist	B	C	A B	B C
Quasi-UD [0,90]	A B	B C	C	B
UD2 [0,90]	C	A	A	B C

Flexural	Strain @ Max Stress	E1	E2	Strength
Plain weave	B	C	C	A
Twill Low Twist	C	C D	C	B
Twill Medium-Low Twist	B	C	C	A
Twill Medium-High Twist	B	B	B	A
Twill High Twist	B	D	D	A B
Quasi-UD [0,90]	A	A	B	A
UD2 [0,90]	D	A	A	A

*Means that do not share a letter are significantly different. **Grouping with Tukey method

Table B-5: Statistical analysis of tensile and flexural properties of flax-epoxy composites.

Tensile	Strain @ Max Stress	E1	E2	Strength
Twill Low Twist	B	B	B	B
Twill Medium-Low Twist	B	C	C	B
Twill Medium-High Twist	B	C	C	B
Twill High Twist	B	B C	B	B
Quasi-UD [0,90]	B	B	B	B
UD2 [0,90]	A	A	A	A

Flexural	Strain @ Max Stress	E1	E2	Strength
Twill Low Twist	A B C	A B	B C	A
Twill Medium-Low Twist	A B C	A B	D	B C
Twill Medium-High Twist	A B	C	E	C
Twill High Twist	A B C	A B	C D	B C
Quasi-UD [0,90]	B C	A	A	C
UD2 [0,90]	C	B	B	A B

*Means that do not share a letter are significantly different. **Grouping with Tukey method

Table B-6: Statistical analysis of tensile and flexural properties of flax-MAPP composites

Appendix C
Low-cycle fatigue

LCF testing is defined as the cyclic application of high loads to a material over a limited number of cycles. During LCF testing, loads may reach 90-95% of the ultimate tensile strength (UTS), hence the material behaviour of the composite's constituents may no longer be regarded as linear [1]. When strains beyond the yield point are reached, accumulation of plastic deformation is observed. Damage such as fibre fracture and matrix cracking and fibre-matrix interfacial debonding may occur within the composite. The effect of LCF conditions on the damage mechanisms needs to be examined, however they are believed to be similar to damage occurring in high cycle fatigue (as exposed in Chapter 8). LCF testing is carried out in order to understand the change in modulus, a stiffening of the flax composite happening early in stress-strain curves ($\varepsilon > 0.1\%$) was observed in Chapter 5, found in both the tensile, bending and fatigue tests.

UD2 flax-epoxy tensile samples were subjected to load controlled LCF loads. The strain was also monitored with a 50 mm gauge length extensometer. The testing frequency was 0,4Hz and the same cyclic stress was applied for a total of 60 cycles. The maximum stress in the successive loading-unloading cycles was determined as a percentage of the ultimate tensile stress (UTS) of 264 MPa. Several stress ratios (R-ratio from 0.015 to 0.03) were used and the load applied varied from 3 MPa (1% of the UTS) to 40, 50, 60, 70 and 75% of the UTS. A rapid increase in modulus was observed in the first five cycles for all the tested load levels. This was followed by a gradual increase and stabilisation of the modulus around 26 GPa. The variation on modulus value are caused by the variation in fibre volume fraction, which was determined to be between 41 and 44%. Another test where the stress was varied from 20 (8% of the UTS) to 200 MPa (75% of UTS) comparable to a stress R ratio of 0.1 was performed in order to assess the speed of the E-modulus increase. The LCF loading-unloading profiles are presented in Figure C-1a.

LCF tests were used to assess the effect of cycling at high stress levels on the modulus of flax-epoxy composites and to characterize the associated nonlinear behaviour and identify the expected damage and failure modes. In figure C-1b, typical loading curves of the cyclic hysteresis are displayed. It can be seen that with increasing number of cycles, the

stress-strain curves shift to the right showing signs of accumulation of residual strain (cyclic creep). As discussed in Chapter 8, this cyclic creep phenomenon may be an effect of either the appearance of plastic deformation and/or the appearance of damage.

Figure C-1c demonstrates the stiffness response during the first 60 cycles. Similar to high cycle fatigue testing, an increase in stiffness is observed between cycle 1 and cycle 5, after which the dynamic stiffness equilibrates, and the corresponding stress–strain curves become similar to each other. In Figure C-1d, the maximum stress is kept constant, and one can remark that with decreasing R-ratio, the stiffening phenomenon is less observable. When the cyclic stress is applied between 3-200 MPa (R-Ratio = 0.015), the stiffness increase by 27% compare to 11-17% for 20-200 MPa (R-Ratio = 0.01).. It can be concluded that the lower the stress ratio (at constant maximum stress), the stiffer the flax composite becomes in the early cycles.

From figure C-1c and d, it difficult to conclude which test parameter has the determining influence, the stress ratio R or the maximum applied stress. In the test data presented in Figure C-1c both parameters are varying at the same time (maximum stress increases, while the stress ratio decreases because the minimum stress is kept constant), but the variation of R (decreasing from 0.03 to 0.015) is much smaller than the increase of the maximum stress (increasing from 100 to 200 MPa). The data presented in figure C-1d however suggest that, at constant maximum stress, the stress ratio still has an influence.

Applied cyclic load (MPa)	**R-Ratio**	**% of stiffnesses increase Cycle 1 –Cycle 5**	**% of stiffnesses increase Cycle 1 –Cycle 60**
3-100	0.03	17	17
3-125	0.024	15	15
3-150	0.02	15	15
3-175	0.017	11	11
3-200	0.015	27	24

Table C-1: Percentage of stiffness increase between the cycle 1 and cycle 5 or 60.

Baley et al. [2] stated that this stiffening phenomenon could be related to the reorganisation of the cell structure by the movement of the microfibrillar angle in the elementary fibre as shown in Figure C-2. When a tensile test is done in the direction of the fibre axis, the cellulose fibrils present in the secondary wall will reorient towards the direction of load (0^o) and start sliding one with respect to the others. Hornsby et al. [3] has also put this in evidence for the strain-hardening of flax fibres and interpreted it as a progressive reorientation of microfibrils. Other causes of this stiffening behaviour could also be related to [2, 4, 5]:

- The lengthening of the fibrils and the non-crystalline regions in-between under tensile load;
- Extension of the elementary fibres like a spiral spring accompanied by bending, twisting of the fibrils and decrease in volume of the inter-fibrillar matrix of non-crystalline material. The latter can only happen when part of the non-crystalline (amorphous) materials shows a “strain-induced” crystallization as suggested by Placet et al. [6];
- Shearing of the non-crystalline region following the fibrillar restructuration, and hence strain hardening of these regions.

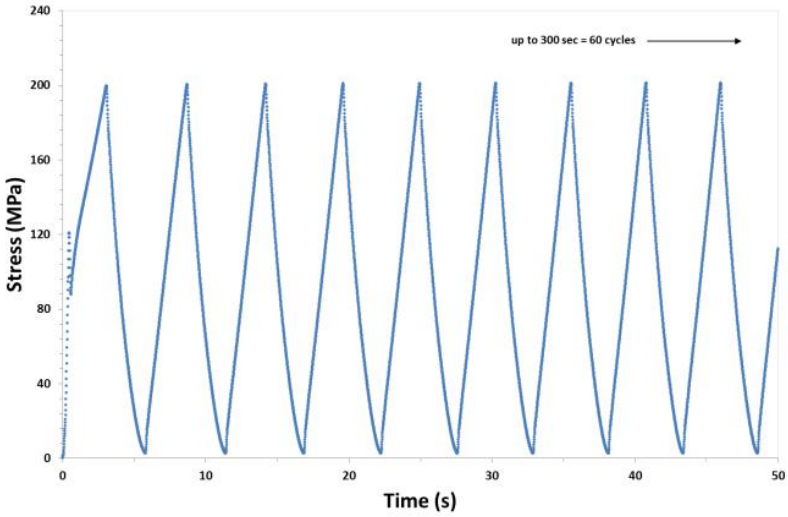
up to 300 sec = 60 cycles
Stress (MPa)
Time (s)
0
40
80
120
160
200
240
0
10
20
30
40
50

a)

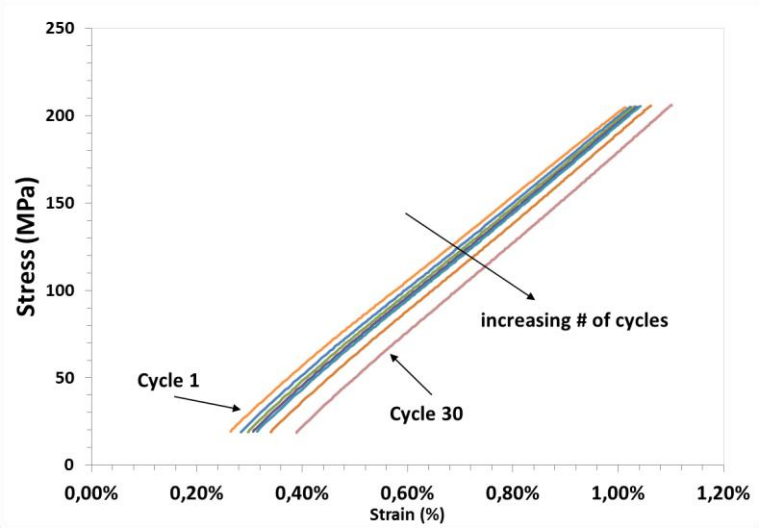
Stress (MPa)
Strain (%)
increasing # of cycles
Cycle 1
Cycle 30
0
50
100
150
200
250
0,00%
0,20%
0,40%
0,60%
0,80%
1,00%
1,20%

b)

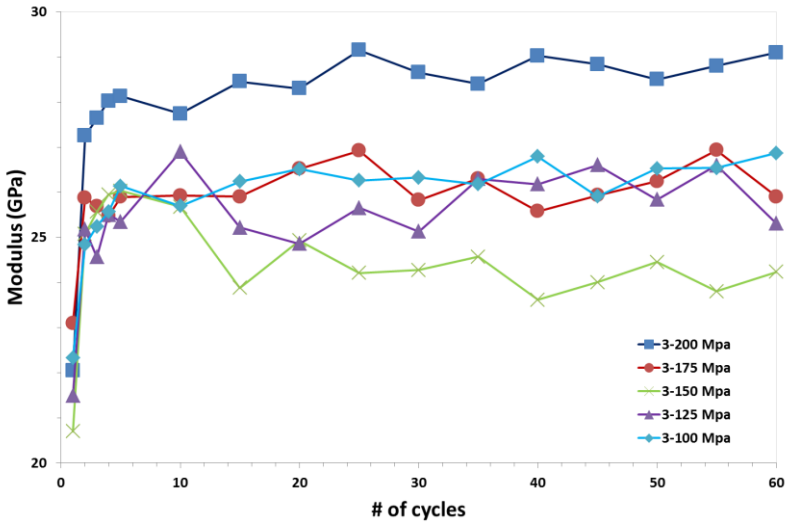
Modulus (GPa)
# of cycles
3-200 Mpa
3-175 Mpa
3-150 Mpa
3-125 Mpa
3-100 Mpa
20
25
30
0
10
20
30
40
50
60

c)

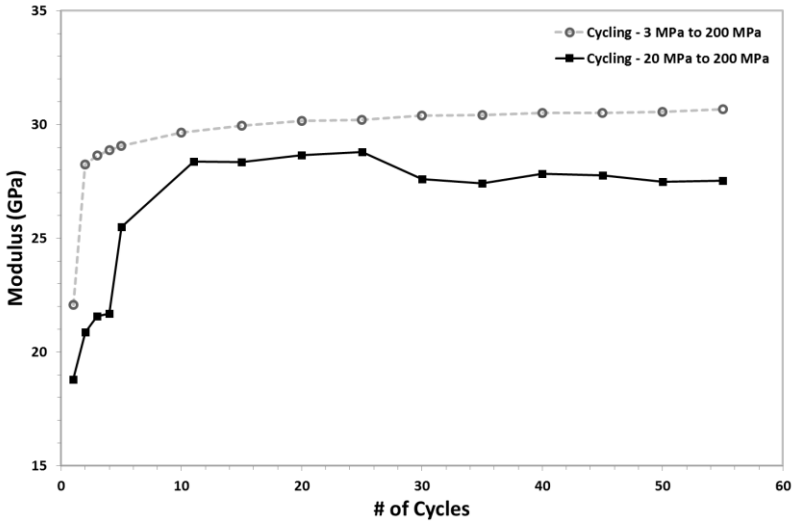

d)

Figure C-1 : a) Definition of low cycle loading profile: successive loading–unloading cycles 1-80% UTS, b) loading curves shifting with increasing cycles signs of plastic deformation, c) evolution of the E-modulus at various stress levels and d) modulus evolution for 1-75% UTS and 8-75%UTS load levels.

a) b)

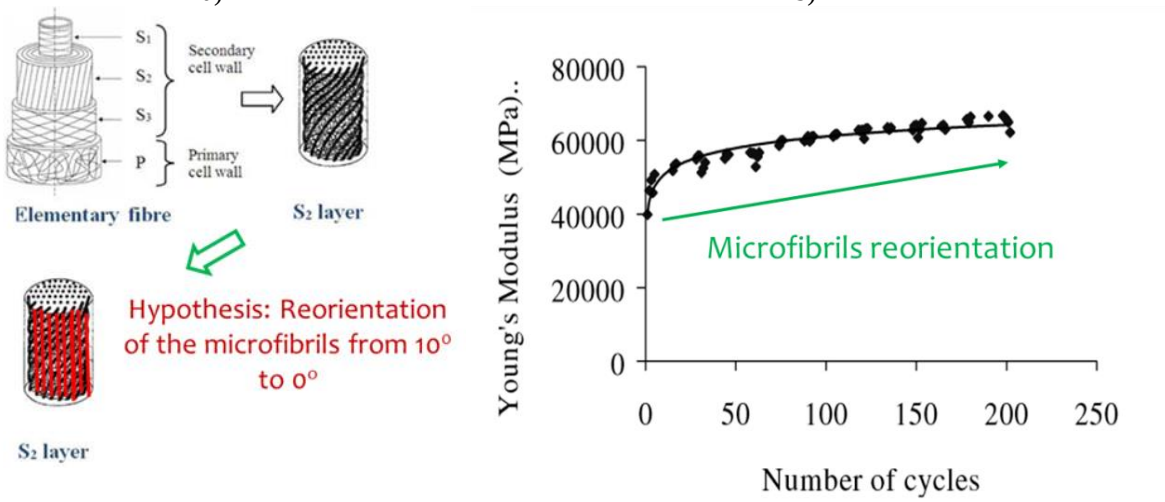

Figure C-2 : a) Multi-scale structure of the flax fibre and its microfibrillar reorientation process [7] b) Low cycling load cycling on elementary flax fibres observation of the tensile stiffness increase [2].

References

[1] Harik VM, Fink BK, Bogetti TA, Klinger JR, Gillespie Jr JW. Low Cycle Fatigue of Composite Materials in Army Structural Applications: A Review of Literature and Recommendations for Research. DTIC Document; 2000.

[2] Baley C. Analysis of the flax fibres tensile behaviour and analysis of the tensile stiffness increase. Composites Part A: Applied Science and Manufacturing. 2002;33(7):939-48.

[3] Hornsby PR, Hinrichsen E, Tarverdi K. Preparation and properties of polypropylene composites reinforced with wheat and flax straw fibres: Part I Fibre characterization. Journal of Materials Science. 1997;32(2):443-9.

[4] Hearle J. The fine structure of fibers and crystalline polymers. III. Interpretation of the mechanical properties of fibers. Journal of Applied Polymer Science. 1963;7(4):1207-23.

[5] Ueki Y, Lilholt H, Madsen B. Fatigue behaviour of uni-directional flax fibre/epoxy composites. 20th International Conference on Composite Materials2015.

[6] Placet V, Cissé O, Boubakar ML. Nonlinear tensile behaviour of elementary hemp fibres. Part I: Investigation of the possible origins using repeated progressive loading with in situ microscopic observations. Composites Part A: Applied Science and Manufacturing. 2014;56:319-27.

[7] Célino A, Fréour S, Jacquemin F, Casari P. The hygroscopic behavior of plant fibers: A review. Frontiers in chemistry. 2013;1.

Appendix D
Calculation of the flax fibre transverse properties and shear modulus

The fibre properties are an important input for the property modelling of a composite. As presented in Chapter 6, the IFBT data were used to determine the apparent longitudinal stiffness of a twisted yarn (composed of twisted technical fibres), which is a function of the degree of twist and of the longitudinal, transverse and shear stiffness of the technical fibres in the yarn.

The longitudinal modulus of a technical fibre, $E_{f,L,}$ can be measured by testing a single technical fibre in simple tension along the fibre length. However, it is much more challenging to test technical fibres at any other orientation. Consequently, the transverse modulus, $E_{f,T}$ and shear moduli of flax fibres have never been directly measured. The transverse fibre stiffness $E_{f,T}$ is very often approximated by a value between 5 and 8 GPa [1-4] or defined as 5-10 times lower than $E_{f,L}$ [5]. Furthermore, it is not clear how large an effect the amount of twist in the yarn would have on the apparent transverse properties of a twisted yarn.

The fibre shear modulus is another important input parameter for the modelling which should be defined. However, very little data are available in the literature. Charlet et al. [6] reported a 18.7 ± 10.1 kPa shear modulus for the layer in-between two elementary fibres; it could be assumed that this value would give a good estimate of the shear modulus of a technical fibre.

However, the shear modulus of a technical fibre heavily underestimates the shear modulus of the flax fibre within a composite, because the matrix can penetrate into the intra-yarn space between the technical fibres, and in fact ‘gluing’ them together, but probably also in-between the elementary fibre inside the technical fibres. Hence, the matrix type plays an important role on the shear behaviour, thus the shear modulus at composite level should be back-calculated from the composite properties.

C.1 Calculation of the flax fibre transverse properties

In this thesis, we propose to use the transverse properties of a unidirectional flax-epoxy composite, such as the UD2 data, and back-calculate the effective transverse stiffness using the Chamis equations (C-1 to C-3) presented in Figure C-1. The plies are assumed to be transversely isotropic under plane stress condition [7, 8].

Longitudinal modulus: $E_L = E_f V_f + E_m V_m$ (Eq. C-1)

Transverse modulus: $E_T = \frac{E_m}{1-\sqrt{Vf}(1-\frac{E_m}{E_{f,2}})}$ (Eq. C-2)

Shear modulus: $G_{12} = \frac{G_m}{1-\sqrt{Vf}(1-\frac{G_m}{G_{f,2}})}$ (Eq. C-3)

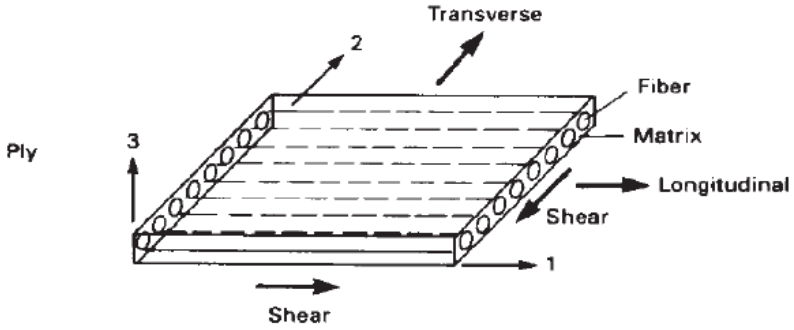

Figure C-1: Fiber Composite Geometry and properties calculation. (image from [9]).

Taking the experimental data for UD2 in the transverse direction and using reverse Chamis equation C-4, it is possible to extract the value of $E_{f,T}$. The matrix stiffness value is E_m = 2.7 GPa. The average $E_{f,T}$ value found was 5.8 ± 1.1 GPa was found.

Transverse fibre modulus: $E_{f,T} = \frac{E_m}{1-\frac{1}{\sqrt{Vf}}(1-\frac{E_m}{E_T})}$ Eq. C-4

This value was introduced in the *MicroMechanics* (which uses the Chamis' equations)[1] software to verify if the approximation of the composite properties using the calculated $E_{f,T}$ of 5.8 GPa and $E_{f,L}$ of 62.3 GPa (see section 5.3.2.5). Taking into account flax-epoxy UD2 composite experimental values of E_L = 26.6 ± 2.3 GPa and E_T = 4.10 ± 0.4 GPa, the back-calculation of the properties is reliable as seen in Figure C-2.

Since the longitudinal properties are affected by the changes in fibre twist, it is possible for the transverse properties to change according to the twist angle. An impregnated twisted yarn is a composite material in its own and is rather similar to an off-axis UD composite as seen in Figure C-3. Therefore, the properties of off-axis laminate with varying θ angle (connected to the twist angle) can be linked to the properties of twisted yarns. By predicting the stiffness of various off-axis plates, the transverse properties of the flax yarn can be predicted for each change of twist. To do so, the ESAComp software was used to create the flax-epoxy ply and the corresponding laminates with varying θ values from 0º to 45º.

[1] https://www.mtm.kuleuven.be/Onderzoek/Composites/software/micromechanical_software

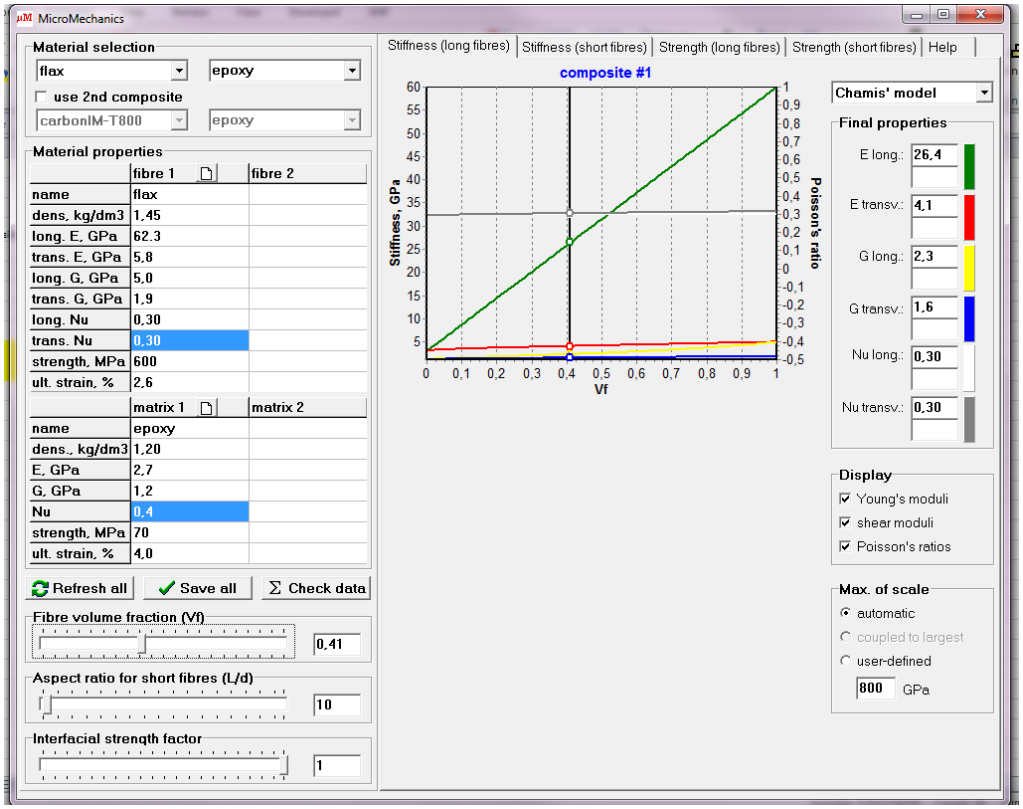

Figure C-2: Prediction of the composite properties using the back-calculated value obtained from experimentation.

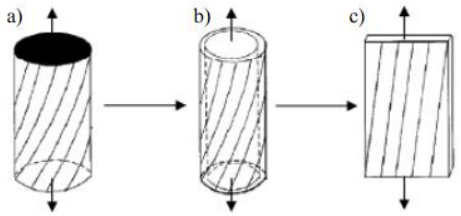

Figure C-3: Correlation between an impregnated yarn with surface twist angle α and its layer (a and b) and an open-up structure of the layer corresponding to a laminate with off-axis loading angle θ (c) [10].

The first step is to create a flax epoxy ply with the composite properties found above, E_L = 26.4 and E_T = 4.1, as seen in Figure C-4a. The longitudinal shear modulus G_{12} of the flax-epoxy composite ply value (1.9) was taken from literature[11]. By applying micromechanics principle, one could derive the properties of the ply at different θ angles. As seen in Figure C-4b, the longitudinal stiffness reduces with an increasing angle while the transverse stiffness increases as expected. A sharper increase in seen for the transverse stiffness for θ > 45°, so it is believed that once the ply placed in an off-axis laminate of ±θ angles, the properties below θ = 45° will not vary significantly.

The stiffness results, presented in Table C-1 and Figure C-5, show a slow increase in composite transverse stiffness with increasing θ as expected. This leads to a slight increase in $E_{f,T}$ (back-calculated using Chamis Eq. C-4). Thus, for yarns having a twist angle below 20°, the flax fibres transverse stiffness can be considered equal to 6 GPa. This value is used in the modelling of flax-epoxy composite presented in Chapter 6. Similar value, $E_{f,T}$ = 7 ± 2 GPa, was back-calculated using Halpin-Tsai model from the transverse properties of a dew-retted-hackled flax fibre-polyester resin by Baley et al. [3].

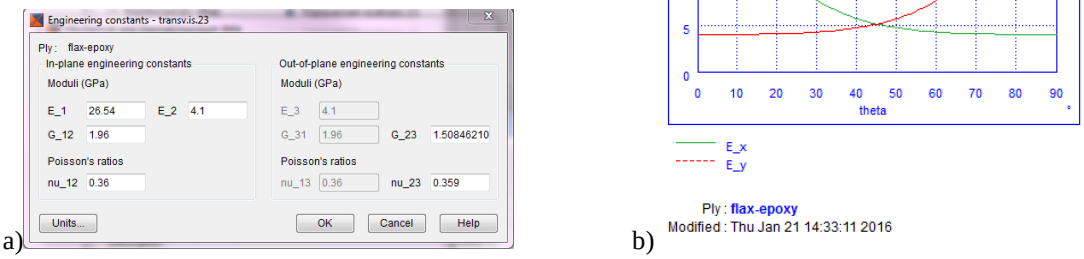

Figure C-4: Value of the $E_{L,\ composite}$ and $E_{T,\ composite}$ at different angles for 1 ply.

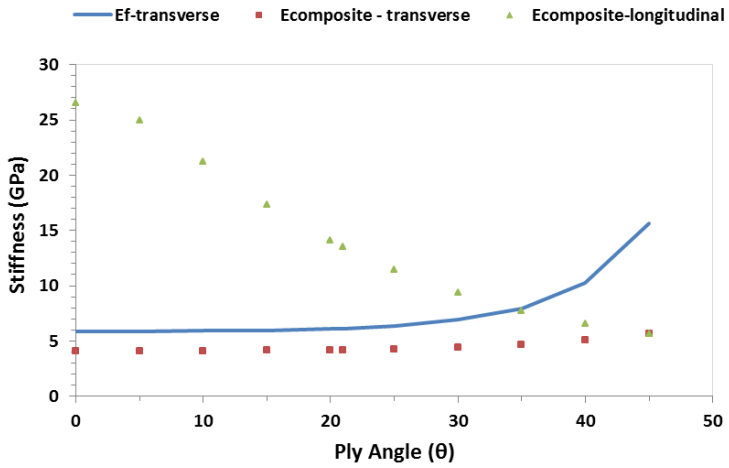

Figure C-5: Variation of the composite longitudinal and transverse stiffness and the back-calculated flax fibres transverse stiffness according to the off-axis angle.

θ	**$E_{L,composite}$**	**$E_{T,\ composite}$**	**Fibre volume fraction**	**Back-Calculated $E_{f,T*}$**
0	26,54	4,10		5,87
±5	24,92	4,10		5,87
±10	21,26	4,11		5,90
±15	17,37	4,12		5,93
±20	14,07	4,16		6,07
±21	13.48	4.17	40%	6,10
±25	11,43	4,24		6,34
±30	9,36	4,39		6,90
±35	7,75	4,64		7,97
±40	6,54	5,05		10,2
±45	5,66	5,66		15,6

Table C-1: Back-calculation results of the flax fibre transverse stiffness $E_{f,T}$.

C.2 Calculation of the flax fibre shear modulus

Flax fibres are often described has having a low shear modulus [4, 12]. However little to none quantitative data is available to corroborate or refute this statement. In order to properly predict the composite properties, the shear modulus needs to be defined using available literature.

In this study, the quantification of the shear modulus is carried out using the longitudinal stiffness data from an off-axis ±45° as during a tensile test the maximum shear planes are located at ±45◦ from the principal planes. The stiffness and shear modulus values can thus be used to back-calculate the flax fibres shear modulus [13] using the Chamis Eq. C-5 and C-6.

Fibre shear modulus: $G_f = \frac{G_m}{1-\frac{1}{\sqrt{Vf}}(1-\frac{G_m}{G_{composite}})}$ (Eq. C-5)

Matrix shear modulus: $G_m = \frac{E_m}{2(1+\nu_m)}$ where ν_m= 0.4 for epoxy (Eq. C-6)

Composite shear modulus for isotropic materials:

$$G_{composite} = \frac{E_{composite}}{2(1+\nu_{composite})}$$ (Eq. C-7)

However, the flax fibres are not isotropic materials, and another approach was implemented to calculate the fibre shear modulus $G_{12,f}$ using literature data.

Kersani et al. [2] have experimentally defined, stiffness properties of a pure UD $[0^o]_8$ and a UD $[-45^o,+45^o]_{2s}$ cross-ply flax-epoxy plates. The authors used a flax quasi-UD-epoxy prepreg provided by Lineo. The fabric has an areal density 170 g/m^2 with 95.5% flax fibres in the warp direction and 4.5% flax fibres in the weft direction. The composites has a fibre volume fraction of 47 ± 2 %.

Using the data of the pure UD composite (E_c=27.2 GPa, E_m=2.7GPa), the "apparent" flax fibre modulus was calculated using Eq. C.1 and a value of 54.8 GPa was found. Using the ESAComp software, a [±45°] laminate was created combining the properties of the matrix and fibre using the calculated "apparent" fibre modulus. Since the $G_{12,f}$ is unknown, an iterative approach is carried. Several shear modulus values were used in the program until the correct stiffness of the $[-45^o, +45^o]_{2s}$ composite ($E_{c,\pm45^o}$ = 5.7 ± 0.11 GPa) was found. Table C-2 present all the tested possibilities and the fibre shear modulus of flax was found to be 4.6 GPa.

Iteration	$G_{12,f}$ used in the model	Obtained $E_{c,\pm45^o}$
1	1.5	3.85
2	2	4.3
3	3	4.98
4	3.5	5.24
5	4	5.46
6	4.5	5.65
7	4.6	**5.68**

Table C-2: Determination of the flax fibre shear modulus, an iterative approach using ESAComp software.

References

[1] Lomov SV, Baets J. Architecture of textile reinforcements and properties of composites. status: published. 2012.
[2] Kersani M, Lomov SV, Van Vuure AW, Bouabdallah A, Verpoest I. Damage in flax/epoxy quasi-unidirectional woven laminates under quasi-static tension. Journal of Composite Materials. 2014.
[3] Baley C, Perrot Y, Busnel F, Guezenoc H, Davies P. Transverse tensile behaviour of unidirectional plies reinforced with flax fibres. Materials letters. 2006;60(24):2984-7.

[4] Cichocki Jr F, Thomason J. Thermoelastic anisotropy of a natural fiber. Composites Science and Technology. 2002;62(5):669-78.
[5] Sparnins E. Mechanical properties of flax fibers and their composites: Luleå tekniska universitet; 2009.
[6] Charlet K, Beakou A. Mechanical properties of interfaces within a flax bundle Part I: Experimental analysis. International Journal of Adhesion and Adhesives. 2011;31(8):875-81.
[7] Rao Y, Farris RJ. A modeling and experimental study of the influence of twist on the mechanical properties of high-performance fiber yarns. Journal of Applied Polymer Science. 2000;77(9):1938-49.
[8] Pan N. Development of a constitutive theory for short fiber yarns: Mechanics of staple yarn without slippage effect. Textile Research Journal. 1992;62(12):749-65.
[9] Miracle DB, Donaldson SL, Henry SD, Moosbrugger C, Anton GJ, Sanders BR, Hrivnak N, et al. ASM handbook: ASM International Materials Park, OH, USA; 2001.
[10] Shah DU, Schubel PJ, Clifford MJ. Modelling the effect of yarn twist on the tensile strength of unidirectional plant fibre yarn composites. Journal of Composite Materials. 2013;47(4):425-36.
[11] Liang S, Gning P, Guillaumat L. FATIGUE BEHAVIOR OF FLAX/EPOXY COMPOSITE.
[12] Thomason J. Why are natural fibres failing to deliver on composite performance? 17th international conference on composite materials, ICCM172009.
[13] Thomason J. Dependence of interfacial strength on the anisotropic fiber properties of jute reinforced composites. Polymer Composites. 2010;31(9):1525-34.

Appendix E
Drop weight impact test - Impact energy calculations

One of the output from an impact test contains a measure of energy, expressed in Joule. However different sensors are mounted on an impactor device seen in Figure E-1, which allow the use of several calculation methods of this energy. As presented in Chapter 4, the impactor tip is fitted with a piezoelectric load transducer, which registers the force and next to the impactor a displacement sensor registers the displacement.

With the time dependent registration of these two parameters, the absorbed energy in function of time can be calculated via two different methods: the velocity method and the force-displacement method, graphically represented in Figure E-2. The velocity method uses the speed before the impact event and directly after, by which the difference in kinetic energy is calculated and gives directly the absorbed energy. The velocity needed for this calculation is the tangent at the displacement-time curve, registered by the displacement sensor.

The force-displacement method calculates the energy as the integral of the force-displacement curve as shown in Figure E-2. The corresponding formulas of the velocity method and the force-displacement method are formula 4.4 and 4.5 in which ΔE is the energy expressed as the difference in kinetic energy, which can also be seen as the work calculated with the velocity method W_v [J] with v_0 the velocity at the moment right before the moment of impact and v_f [m/s] at time τ [s], m the mass of the drop weight [kg]. W_{fd} is the work done as calculated with the force-displacement method [J], F the force [N] and x the displacement [m]. The equations are displayed below.

$$W_v = \Delta E = E_0 - E_f = \frac{1}{2} m (v_0^2 - v_f^2) \quad \text{(Eq. E.1)}$$

$$W_{fd} = \int_0^d F\, dx \quad \text{(Eq. E.2)}$$

Where, v_0 the initial velocity, v_f at time τ.

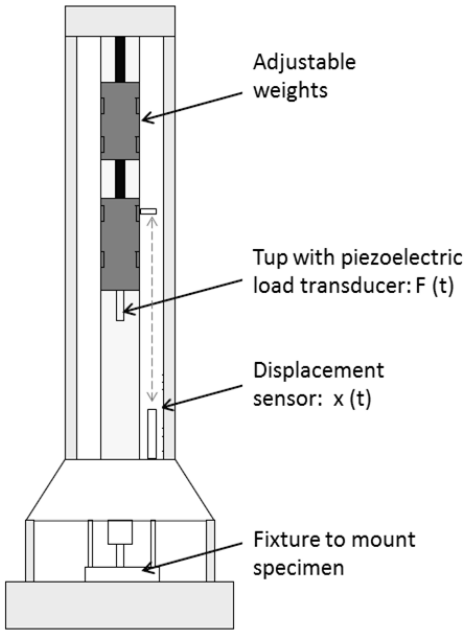

Figure E-1: Low velocity instrumented falling weight impact testing equipment; adapted from [1].

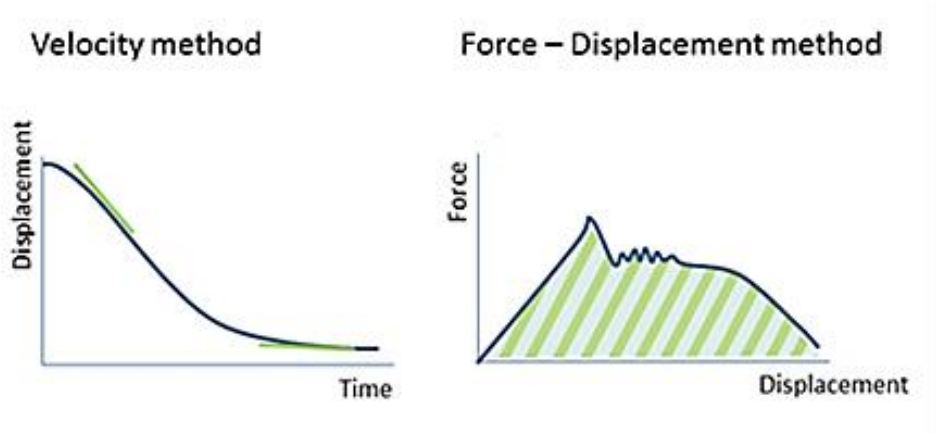

Figure E-2: Graphical representation of the velocity and force-displacement method used to calculate the absorbed energy during an impact event.

E.1 Theoretical proof of the difference between velocity and force-displacement method

The velocity and full integral methods are not completely equivalent. This is shown by the following derivation that starts from the simple second law of Newton:

$$m * a = \sum_i F_i \quad \text{(Eq. E.5)}$$

Where F_i are all forces that act on the impactor, m is the mass of the impactor and *a* is the acceleration during the drop weight. If one assumes the force to be measured in the tip of the drop-weight:

$$\sum_i F_i = F_z - F_{measured} \quad \text{(Eq. E.6)}$$

Where F_z is the gravitational force acting on the drop weight (F_z = m * 9.81 m/s²). This is depicted in Figure E-3. Because a = dv/dt and v = dx/dt where v is the velocity of the drop-weight and x is the position of the drop weight, the Newtonian equation can be rewritten as follows:

$$m * v * \frac{dv}{dt} = \left(F_z - F_{measured}(x)\right) * \frac{dx}{dt}$$
$$m * v * dv = (F_z - F_{measured}(x)) * dx \quad \text{(Eq. E.7)}$$

Integrating this equation between state 0 and state f yields:
$$m * \int_{v_0}^{v_f} v * dv = F_z \int_{x_0}^{x_f} dx - \int_{x_0}^{x_f} F_{measured}(x)\, dx \quad \text{(Eq. E.8)}$$
$$m * -\frac{(v_0^2 - v_f^2)}{2} = F_z\,(x_f - x_0) - \int_{x_0}^{x_f} F_{measured}(x)\, dx \quad \text{(Eq. E.9)}$$

This can be rewritten as
$$W_v = W_{fd} - F_z\,(x_f - x_0) \quad \text{(Eq. E.10)}$$

This result shows indeed that the two methods are not completely equivalent and that the velocity method (W_v) will yield lower values than the force displacement method (W_{fd}). Typical values for W_v or W_{fd} found in this study on flax fibres, are around the order of 4-10 J whereas F_z ($x_f - x_0$) typically is about 0,6 J, based on a displacement of 0,02 m and a drop weight of 3,170 kg. The difference between these methods is therefore not negligible. In fact, the velocity method calculates the resulting difference in energy of the impactor. This is the energy transferred to the sample minus the energy $F_z\,(x_f - x_0)$ received by the gravitational force. It is the energy transferred to (and therefore absorbed by) the sample that is calculated by the force-displacement method. The force-displacement method is therefore the theoretically correct method to use when determining the absorbed energy.

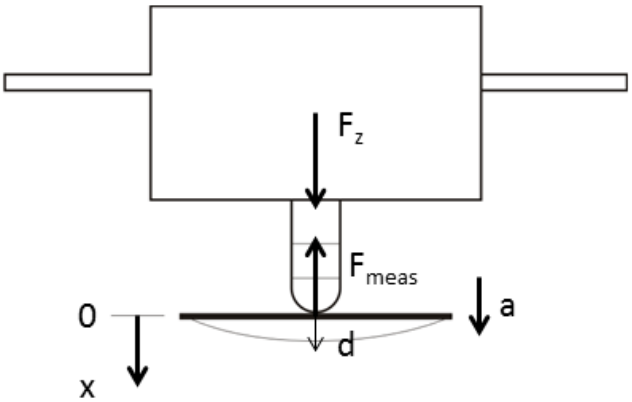

Figure E-3: Schematic of how the impactor registers an impact event. F_z the gravity force working on the drop weight, F_m the measured force, *a* the acceleration, d the displacement.

This result might be counterintuitive at first but a simple example can bring the influence of the gravitational term to the front. For example imagine a material that has such properties that the force exerted by it on the impactor ($F_{measured}$) during the perforation equals the gravitational force F_z acting on the drop weight (see Figure E-4). In that case the resulting force on the impactor and accordingly also its acceleration is zero during the perforation event. Since no acceleration is present, the speed remains constant throughout the whole perforation. Via the velocity method the calculated energy will therefore also be zero: $W_v = 0$. The force-displacement method however will have registered $F_{measured}$, in this case F_z, over a displacement d equal to the thickness of the sample ($= x_f - x_0$) and will correctly calculate the energy absorbed by the material as $W_{fd} = F_z * (x_f - x_0)$.

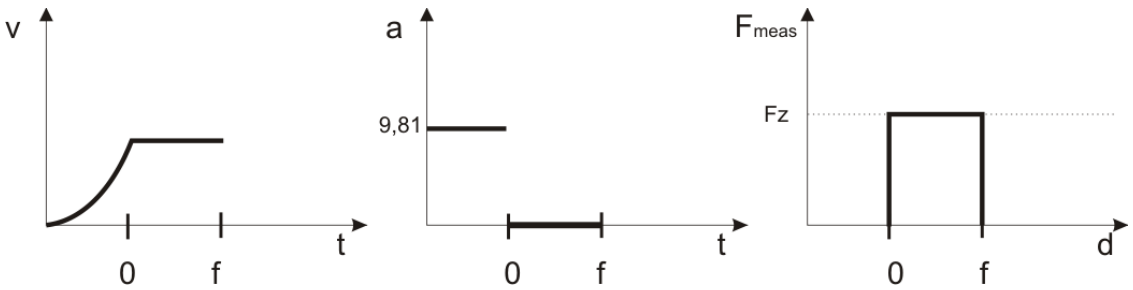

Figure E-4: Illustration of a fictive material to show the influence of the gravitational component.

Comparing the CEAST 6789 impactor with the in house built impactor, there is another structural difference between both machines: the weight in front of the impactor load sensor. A higher weight in front of the load sensor will result into a lower measured force, than the actual force that is exerted by the specimen. Consider Figure E-5 where the drop weight is divided into three components. The first is the weight above the load cell m_1, the second the load cell itself m_2, and the third the weight below the load cell m_3. The bodies are made free, and the forces are indicated. Note that F_3 is the force exerted by the specimen, and the one we would measure if the load cell was localised at the outer tip of the impactor. This is not the case, instead F_2 is measured. Considering the drop weight as a rigid assembly $a_1 = a_2 = a_3$. Next, considering m_2 as negligible state: $m_2 = 0$. Now looking at the second equation in the Figure E-5, it can be seen that F_{z2} and m_2a become zero. This leads to $F_1 = F_2$, which equals $F_{measured.}$ Considering the first and the last equation and the fact that $a_1 = a_3$ due to the rigid body assumption, leads to two equations with two unknowns: a_1 and F_3.

$$F_{z1} - F_1 = m_1 a_1 \quad \text{(Eq. E.11)}$$

$$F_{z3} - F_2 - F_3 = m_3 a_3 \quad \text{(Eq. E.12)}$$

Combining Eq. E.11 and Ez. E.12, the solution is the following:

$$a_1 = \frac{F_{z3} - F_{measured}}{m_1} = a_3 \quad \text{(Eq. E.13)}$$

$$F_3 = F_{z3} + F_{measured} - \frac{m_3}{m_1}(F_{z1} - F_{measured}) \quad \text{(Eq. E.14)}$$

Where $F_{z3} = m_3 g$ and $F_{z1} = m_1 g$.

$$F_3 = (1 + \frac{m_3}{m_1}) F_{measured} \quad \text{(Eq. E.15)}$$

From this solution it can be seen, that the higher m_3 in comparison with m_1 the bigger difference between the $F_{measured}$ and the force exerted by the specimen $F_{3.}$ In the dissertation of Philips [2], this effect was experimentally observed, now the theoretical explanation has been written down. However caution should be taken upon comparing the work of Philips [2] with the here described velocity method and force-displacement method. Although Philips also describes the use of a force sensor, he does not calculate the energy by the force-displacement method, but integrates it to find the velocity.

The results measured in this work on the in house built drop weight impactor showed lower values for the integral method than for the velocity method, which is in contradiction with the first part of the derivation. This was the motivation for the second part of the derivation, looking for a difference between both machines. However it is not believed that the larger mass in front of the load cell is the only effect contributing to the observed difference. Therefore it is strongly suggested, to take a closer look at both

machines and analyse them analytically and experimentally. The onset for the analytical analysis has been given here and a first experimental step has been performed by checking the calibration files for the displacement. This is done by placing a specimen of known thickness between the impactor head and the support, and registering the voltage, and then recalculating it to mm. Both displacement sensors seem to work correct, and no abnormalities in the displacement files were seen.

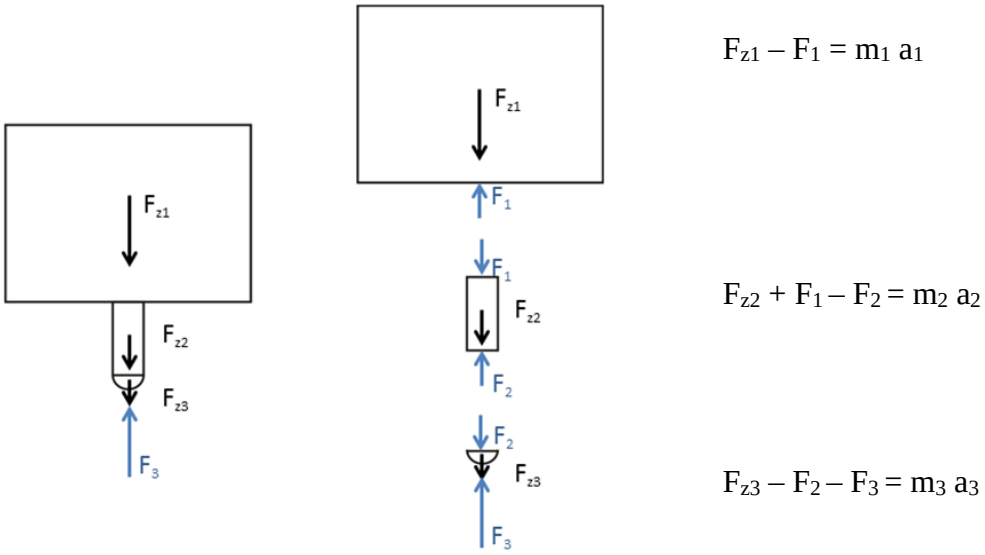

Figure E-5: Force equilibrium impactor devided in three components; m1 impactor weight above the load sensor; m2 load sensor; m3 impactor weight below the load sensor.

E.2 Comparison of the absorbed energy calculation methods

Looking at the two calculation methods applied to the test data from the sample presented in Chapter 7, it can be seen that the velocity method typically gives lower values than the force-displacement method. The reason is the gravity term, which is not taken into account in the velocity method, the theoretical proof as stated in the previous section. From that derivation, it is concluded that the force-displacement method is the theoretical correct way of determining the absorbed energy.

Also the variation on the velocity method's mean is higher than the force-displacement method. In the velocity method the time gate for calculation the velocity after impact needs to be selected by the operator, which is very arbitrary and explains the large scatter on the measurements. Very large scatter is seen for the mat with PPMA (random mat-MAPP, MATp) for which it was almost impossible to quantify the absorbed energy via the velocity method. The impact duration was very short, seen through the analysis of the impact time, and almost no velocity difference before and after could be measured. The failure was also very brittle in contrast with the other thermoplastic samples. Still via the force-displacement integral method it was possible to measure the absorbed energy.

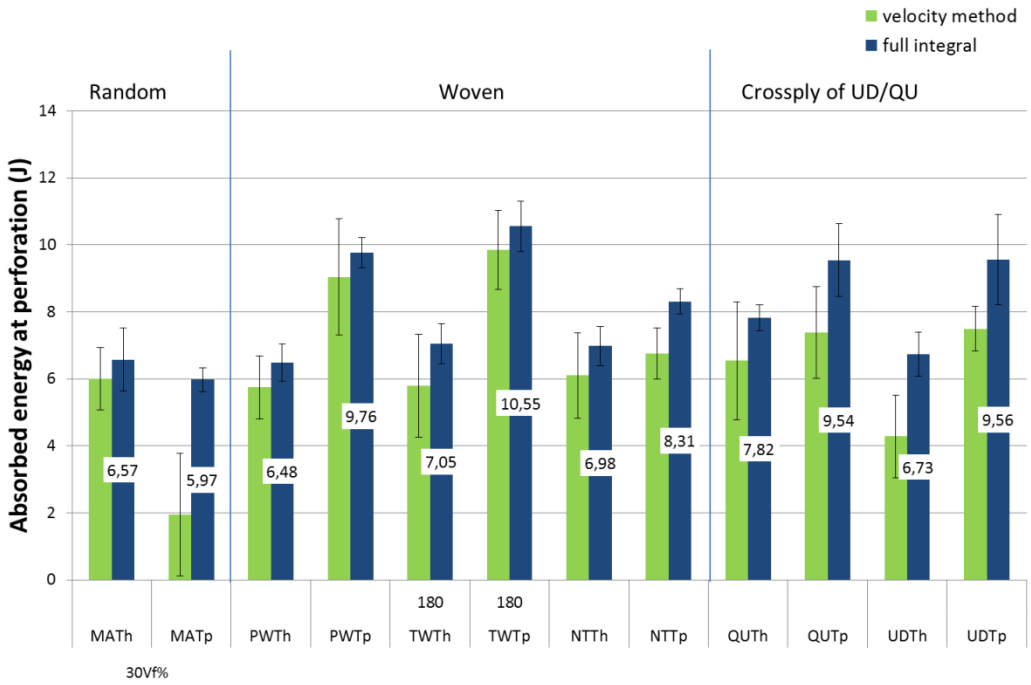

Figure E-6: Absorbed energy at perforation for the different fibre architectures. Normalised to the same Vf*thickness value of 40% and 2mm. Thermoset epoxy (Th), thermoplastic PPMA (Tp), MA = mat, PW = plain weave, TW180 = twill 180g/m², NT = non twist twill, QU = Quasi UD cross-ply, UD = Unidirectional cross-ply.

References

[1] S. Abrate, "Impact engineering of composite structures," ed. Carbondale: SpringerWienNewYork, 2011.
[2] D. Philips, Characterisation and development of 3D-knitted composites: KU Leuven, 1999.

Appendix F
Fatigue Data of flax-epoxy and glass-epoxy composites

In this appendix, the data of the fatigue cycling used to produce the S-N curves in Chapter 8 are reported. Tension–tension fatigue tests were performed, following the ASTM D3479 standard, on an MTS hydraulic fatigue testing device with a 100kN load cell. The loading ratio was set to R= 0.1 with a loading frequency of 5 Hz and stress levels maximum applied stress normalised to the ultimate tensile strength (UTS), S/S_o, ranging from 0.3 to 0.9 of UTS. The fatigue tests were conducted in temperature-controlled laboratory at 21°C.

S/S_0	Maximum Applied load (MPa)	Number of cycles (N)	log cycles
0,3	25	1000002	6,00
0,3	25	1000002	6,00
0,3	25	1000002	6,00
0,35	29	1000000	6,00
0,35	29	1000000	6,00
0,35	29	408900	5,61
0,4	33	495038	5,69
0,4	33	188986	5,28
0,4	33	475951	5,68
0,4	33	544574	5,74
0,5	42	40839	4,61
0,5	42	89791	4,95
0,5	42	66510	4,82
0,5	42	41371	4,62
0,5	42	41578	4,62
0,5	42	47077	4,67
0,5	42	38992	4,59
0,5	42	18401	4,26
0,5	42	16555	4,22
0,5	42	57795	4,76
0,6	50	3214	3,51
0,6	50	6302	3,80
0,6	50	8511	3,93
0,6	50	9312	3,97
0,65	54	650	2,81
0,65	54	254	2,40
0,65	54	307	2,49
0,7	58	277	2,44
0,7	58	915	2,96
0,7	58	1659	3,22
0,7	58	2626	3,42
0,8	67	17	1,22
0,8	67	40	1,60
0,8	67	17	1,22
0,8	67	49	1,69
0,8	67	317	2,50
1	83	1	0,00

Figure F-1: Flax random mat-epoxy composite with a Vf = 30% and a UTS = 83 MPa.

S/S0	Maximum Applied load (MPa)	Number of cycles (N)	log cycles
0,35	46	1000002	6,00
0,35	46	1000002	6,00
0,35	46	1000002	6,00
0,35	46	1000002	6,00
0,4	53	1000000	6,00
0,4	53	1000000	6,00
0,4	53	1000000	6,00
0,4	53	1000000	6,00
0,4	53	305219	5,48
0,45	60	324291	5,51
0,45	60	832576	5,92
0,45	60	189336	5,28
0,5	66	636230	5,80
0,5	66	376864	5,58
0,5	66	263818	5,42
0,65	86	90158	4,96
0,65	86	37660	4,58
0,65	86	87670	4,94
0,65	86	61711	4,79
0,8	106	1417	3,15
0,8	106	4635	3,67
0,8	106	2450	3,39
0,8	106	4326	3,64
0,9	119	413	2,62
0,9	119	609	2,78
0,9	119	678	2,83
0,9	119	1586	3,20
1	133	1	0,00

Figure F-2: Flax plain weave-epoxy composite with a Vf = 38% and a UTS = 133 MPa.

S/S0	Maximum Applied load (MPa)	Number of cycles (N)	log cycles
0,45	58	1000004	6,00
0,45	58	128057	5,11
0,45	58	1000002	6,00
0,5	65	517435	5,71
0,5	65	664414	5,82
0,5	65	1000000	6,00
0,65	84	46156	4,66
0,65	84	126429	5,10
0,65	84	3127	3,50
0,65	84	56932	4,76
0,8	103	12204	4,09
0,8	103	629	2,80
0,8	103	175	2,24
0,8	103	1817	3,26
0,9	116	1371	3,14
0,9	116	281	2,45
0,9	116	1408	3,15
0,9	116	29	1,46
1	129	1	0,00

Figure F-3: Flax medium-low twist twill-epoxy composite with a Vf = 41% and a UTS = 129 MPa.

S/S_0	Maximum Applied load (MPa)	Number of cycles (N)	log cycles
0,35	42	1000002	6,00
0,35	42	531553	5,73
0,35	42	243400	5,39
0,4	48	559158	5,75
0,4	48	1000002	6,00
0,4	48	613286	5,79
0,5	60	48600	4,69
0,5	60	67074	4,83
0,5	60	34399	4,54
0,5	60	12992	4,11
0,65	77	4969	3,70
0,65	77	3696	3,57
0,65	77	3812	3,58
0,65	77	1148	3,06
0,8	95	480	2,68
0,8	95	1766	3,25
0,8	95	1661	3,22
0,8	95	1641	3,22
0,8	95	87	1,94
0,9	107	901	2,95
0,9	107	373	2,57
0,9	107	781	2,89
0,9	107	14	1,15
0,95	113	276	2,44
0,95	113	142	2,15
0,95	113	151	2,18
0,95	113	13	1,11
1	119	1	0,00

Figure F-4: Flax low twist twill-epoxy composite with a Vf = 40% and a UTS = 133 MPa.

S/S_0	Maximum Applied load (MPa)	Number of cycles (N)	log cycles
0,35	49	1000000	6,00
0,35	49	611121	5,79
0,35	49	1000000	6,00
0,4	56	1000002	6,00
0,4	56	207789	5,32
0,4	56	677361	5,83
0,45	63	30462	4,48
0,45	63	46187	4,66
0,45	63	26179	4,42
0,45	63	442378	5,65
0,5	70	274662	5,44
0,5	70	74933	4,87
0,5	70	113439	5,05
0,5	70	37795	4,58
0,65	90	56613	4,75
0,65	90	7647	3,88
0,65	90	14918	4,17

0,65	90	15439	4,19
0,65	90	7782	3,89
0,65	90	35701	4,55
0,65	90	14918	4,17
0,65	90	15439	4,19
0,8	111	116	2,06
0,8	111	100	2,00
0,8	111	3507	3,54
0,8	111	593	2,77
0,8	111	63	1,80
0,9	125	560	2,75
0,9	125	268	2,43
0,9	125	1763	3,25
0,9	125	357	2,55
1	139	1	0,00

Figure F-5: Flax high twist twill-epoxy composite with a Vf = 40% and a UTS = 139 MPa.

S/S_0	**Maximum Applied load (MPa)**	**Number of cycles (N)**	**log cycles**
0,3	46,52	1000000	6,00
0,3	46,52	1000000	6,00
0,3	46,52	1000000	6,00
0,35	54,27	1000000	6,00
0,35	54,27	1000000	6,00
0,35	54,27	1000000	6,00
0,375	58,15	1000000	6,00
0,375	58,15	1000000	6,00
0,375	58,15	1000000	6,00
0,375	58,15	554710	5,74
0,4	62,03	584547	5,77
0,4	62,03	872634	5,94
0,4	62,03	203513	5,31
0,4	62,03	729681	5,86
0,45	69,78	240013	5,38
0,5	77,54	122679	5,09
0,5	77,54	354756	5,55
0,5	77,54	53364	4,73
0,65	100,80	2933	3,47
0,65	100,80	9096	3,96
0,65	100,80	1315	3,12
0,8	124,06	435	2,64
0,8	124,06	870	2,94
0,8	124,06	162	2,21
0,9	139,56	279	2,45
0,9	139,56	170	2,23
0,9	139,56	54	1,73
1	155,07	1	0,00

Figure F-6: Flax quasi-UD [0,90]-epoxy composite with a Vf = 42% and a UTS = 155 MPa.

S/S_0	Maximum Applied load (MPa)	Number of cycles (N)	log cycles
0,35	44	1000002	6,00
0,35	44	1000002	6,00
0,35	44	1000002	6,00
0,4	50	1000000	6,00
0,4	50	528635	5,72
0,4	50	838565	5,92
0,45	56	634211	5,80
0,45	56	84316	4,93
0,5	62	73142	4,86
0,5	62	193552	5,29
0,5	62	40021	4,60
0,5	62	47755	4,68
0,65	81	4356	3,64
0,65	81	24084	4,38
0,65	81	3214	3,51
0,65	81	11314	4,05
0,8	99	489	2,69
0,8	99	15671	4,20
0,8	99	527	2,72
0,8	99	1287	3,11
0,9	112	1181	3,07
0,9	112	144	2,16
0,9	112	14	1,15
1	124	1	0,00

Figure F-7: Flax UD2 [0,90]-epoxy composite with a Vf = 39% and a UTS = 124 MPa.

S/S_0	Maximum Applied load (MPa)	Number of cycles (N)	log cycles
0,45	106	1000000	6,00
0,45	106	1000000	6,00
0,45	106	1000000	6,00
0,5	118	1000002	6,00
0,5	118	706259	5,85
0,5	118	571062	5,76
0,5	118	991104	6,00
0,65	153	336631	5,53
0,65	153	72378	4,86
0,65	153	37537	4,57
0,65	153	286208	5,46
0,8	189	34329	4,54
0,8	189	13554	4,13
0,8	189	8021	3,90
0,8	189	22121	4,34
0,9	212	10003	4,00
0,9	212	1817	3,26
0,9	212	4892	3,69
0,95	224	148	2,17
0,95	224	322	2,51
0,95	224	85	1,93
1	236	1	0,00

Figure F-8: Flax quasi-UD-epoxy composite with a Vf = 43% and a UTS = 236 MPa.

S/S_0	Maximum Applied load (MPa)	Number of cycles (N)	log cycles
0,45	119	1000002	6,00
0,45	119	290370	5,46
0,45	119	463981	5,67
0,45	119	371618	5,57
0,5	132	865030	5,94
0,5	132	1000002	6,00
0,5	132	150470	5,18
0,6	158	201266	5,30
0,6	158	7896	3,90
0,6	158	24632	4,39
0,65	171	16299	4,21
0,65	171	8819	3,95
0,65	171	4708	3,67
0,65	171	15133	4,18
0,65	171	66045	4,82
0,8	211	478	2,68
0,8	211	321	2,51
0,8	211	14	1,15
0,8	211	13	1,11
0,9	237	230	2,36
0,9	237	14	1,15
0,9	237	214	2,33
0,9	237	29	1,46
1	264	1	0,00

Figure F-9: Flax UD2-epoxy composite with a Vf = 44% and a UTS =264 MPa.

S/S_0	Maximum Applied load (MPa)	Number of cycles (N)	log cycles
0,3	62	1000000	6,00
0,3	62	1000000	6,00
0,3	62	1000000	6,00
0,4	91	168128	5,23
0,4	91	1000000	6,00
0,4	91	1000000	6,00
0,45	93	511650	5,71
0,45	93	122194	5,09
0,45	93	301536	5,48
0,5	104	48120	4,68
0,5	104	20817	4,32
0,5	104	43911	4,64
0,65	135	2615	3,42
0,65	135	1650	3,22
0,65	135	2846	3,45
0,8	166	612	2,79
0,8	166	737	2,87
0,8	166	932	2,97
1	207	1	0,00

Figure F-10: Glass random mat-epoxy composite with a Vf = 29% and a UTS =207 MPa.

S/S_0	Maximum Applied load (MPa)	Number of cycles (N)	log cycles
0,45	107	294328	5,47
0,45	107	1000000	6,00
0,45	107	1000000	6,00
0,5	119	105353	5,02
0,5	119	1000000	6,00
0,5	119	361289	5,56
0,65	155	7227	3,86
0,65	155	431	2,63
0,65	155	32953	4,52
0,8	190	710	2,85
0,8	190	497	2,70
0,8	190	200	2,30
1	238	1	0,00

Figure F-11: Glass twill-epoxy composite with a Vf = 35% and a UTS =238 MPa.

S/S_0	Maximum Applied load (MPa)	Number of cycles (N)	log cycles
0,3	94	1000000	6,00
0,3	94	1000000	6,00
0,3	109	1000000	6,00
0,35	109	1000000	6,00
0,35	109	1000000	6,00
0,35	125	843923	5,93
0,4	125	1000000	6,00
0,4	125	178230	5,25
0,4	156	1000000	6,00
0,5	156	68984	4,84
0,5	156	76530	4,88
0,5	203	48888	4,69
0,65	203	2795	3,45
0,65	203	6085	3,78
0,65	250	2678	3,43
0,8	250	46	1,66
0,8	250	515	2,71
0,8	312	29	1,46
1	94	1	0,00

Figure F-12: Glass quasi-UD [0,90]-epoxy composite with a Vf = 38% and a UTS = 312 MPa.

S/S_0	Maximum Applied load (MPa)	Number of cycles (N)	log cycles
0,45	146	1000000	6,00
0,45	146	1000000	6,00
0,45	146	1000000	6,00
0,5	163	779655	5,89
0,5	163	876438	5,94
0,5	163	1000000	6,00
0,65	211	20750	4,32
0,65	211	94004	4,97
0,65	211	24823	4,39
0,8	260	2770	3,44
0,8	260	3771	3,58
0,8	260	749	2,87
1	325	1	0,00

Figure F-13: Glass UD [0,90]-epoxy composite with a Vf = 41% and a UTS = 325MPa.

Appendix G
Long flax fibre and EOL inventories

These inventories were derived from literature data [1-3]. These studies have been chosen because of their extensive and reliable database for mainland Europe flax cultivation. In this case, the allocation was not derived on mass or on economic value. To give the most conservative representation of flax cultivation, the environmental burden was allocated for 100% to the flax straw, and for 0% to the flax seed (6% of the total weight). The seeds don't have an environmental burden here are they are sold to the food industry for the production of oil and flour. Turunen et al. [1] study has reported the following production of 1 hectare of field yields:

- Green stems: 6000 kg/ha;
- Scutching step produces: 1550 kg of scutched fibres, 365 kg seeds, 2960 kg of shives, 850 kg of tows, 530 kg of flakes and 665 kg of waste.
- Hackling yields around 1000 kg of long fibres, 465 kg of tows and 80 kg of waste.

Flax straw

Resource category	Name	Value	Remarks
Input	Flax seed	75 kg	Modelled as 'rape seed'
	Ammonium nitrate	40 kg	
	Phosphorous fertilizer	32 kg	
	Potassium chloride	60 kg	
	Lime	666 kg	
	Pesticides	1,36 kg	
	Carbon dioxide in air	9211 kg	
	Land usage	1 ha*a	
	Ploughing	3 ha	Three times applied
	Application of plant protection products	2 ha	Two times applied
	Fertilizing	4 ha	Four times applied
	Sowing	1 ha	
	Harvesting	1 ha	
Transportation	Freight, rail	57,72 tkm	
	Lorry, road	9,62 tkm	
Output	Flax straw	6170 kg	100% allocated
	Flax seed	457 kg	0% allocated
Emissions to air	Ammonia	0,971 kg	
	Dinitrogen monoxide	1,14 kg	
	Nitric oxide	0,239 kg	
Emissions to water	Nitrate (groundwater)	40 kg	
	Phosphorus (groundwater)	0,07 kg	
	Cadmium (groundwater)	42,27 mg	
	Chromium (groundwater)	20,87 g	
	Lead (groundwater)	102,7 mg	
	Mercury (groundwater)	0,17 mg	
	Zinc (groundwater)	10,4 g	
	Copper (groundwater)	2,73 g	
	Phosphorus (river)	0,276 kg	
	Cadmium (river)	18,68 mg	
	Chromium (river)	2,18 g	
	Nickel (river)	1,51 g	
	Lead (river)	307,3 mg	
	Mercury (river)	0,44 mg	
	Zinc (river)	1,44 g	
	Copper (river)	1,40 g	

Emissions to soil	Cadmium	2,12 g	
	Chromium	200,9 g	
	Nickel	8,93 g	
	Lead	2,75 g	
	Mercury	1,46 g	
	Zinc	12,29 g	
	Copper	-8,4 g	Copper is taken out of the soil by the plant. This can be transported towards water emissions as well as uptake by the plant itself.

Flax dew retting

Resource category	Name	Value
Input	Flax straw	6170 kg
	Tractor	6,35 kg
	Agricultural machinery	3,27 kg
	Diesel	1049,8 MJ
	Pesticides	7,88 kg
	Land usage	1 ha*a
Transportation	Freight, rail	4,74 tkm
	Lorry, road	0,788 tkm
Output	Flax straw, retted	5121 kg

Flax scutching & hackling

Resource category	Name	Value
Input	Flax straw, retted	5121 kg
	Agricultural machinery	16,1 kg
	Electricity (BE)	4898 MJ
Transportation	Freight, rail	512 tkm
	Lorry, road	256 tkm
Output	Long fibers	1404 kg
	Short fibers	351 kg
	Shives	2561 kg
Final waste flow	Dust	805 kg

Table G-1: Inventory of the production of flax straw, the retting of flax and for the scutching and hackling (for long fibre only) of flax.

References

[1] Van Der Werf Hm, Turunen L. The Environmental Impacts Of The Production Of Hemp And Flax Textile Yarn. Industrial Crops And Products. 2008;27(1):1-10.
[2] Le Duigou A, Davies P, Baley C. Environmental Impact Analysis Of The Production Of Flax Fibres To Be Used As Composite Material Reinforcement. Journal Of Biobased Materials And Bioenergy. 2011;5(1):153-65.
[3] Yelin D. Life Cycle Assessment Of Biobased Fibre-Reinforced Polymer Composites: University Of Leuven; 2014.

Farida Bensadoun, B.ing - M.sc.A

Ijzerenmolenstraat 22 bus 301, 3001 Leuven, Belgium
Tel:. +32 471 35 59 55
Farida.bensadoun@mtm.kuleuven.be, farida.bensadoun@gmail.com
Nationality: Canadian and Algerian
Date of birth: 13-03-1986

Education

February 2012 – …	**Katholieke Universiteit Leuven (KU Leuven), Leuven (Belgium)** **Doctor of Philosophy degree (PhD) in Materials Engineering** Topic: In-Service Behaviour Of Flax Fibre Reinforced Composites For High Performance Applications
May 2009 – May 2011	**Polytechnique Montreal, Montreal (Canada)** **Master of Applied Science (M.sc.A) in Mechanical Engineering** Topic: Composites And Biocomposites Manufacturing Process Development And Characterization Containing Clay Nanoparticles And An Unsaturated Polyester Resin Intended To The Transportation Industry
September 2005 – June 2009	**Polytechnique Montreal, Montreal (Canada)** **Bachelor in Mechanical Engineering (B.ing) with minor in Space Technologies** Bachelor thesis : "Study of the viscoelastic behaviour of fibre reinforcement in compression"

Engineering professional experiences

October 2014 - …	**The European Confederation Of Linen And Hemp (CELC), Belgium/France** Technical Consultant and Member of the European Scientific Committee of the CELC
April 2011 – October 2011	**Chaire sur les Composites à Haute Performance (CCHP), Polytechnique Montreal, Canada** Research Assistant : Composite Manufacturing
June 2008 – August 2008	**Leroy-Somer North-America, Lexington (Tn) USA and Reynosa (Tm) Mexico** R&D Intern – Method and Process Engineering Topic: Process auditing of the LSA40 built in Reynosa
May 2007 – August 2007	**Leroy-Somer, Angoulême, France** Mechanical engineering intern : Research and Development Team Topic: Cost evaluation of the new LSA40 Alternator

Other professional experiences

September 2012-…	**KU Leuven, Leuven (Belgium)** Teaching assistant: Polymers and Composites practical sessions
January 2009 – January 2012	**Polytechnique Montreal, Montreal (Canada)** Laboratory and exam surveillance Teaching assistant : "Éléments de Machine" course
January 2009 – January 2012	**Bureau en Gros (Staples Canada), Laval (Qc) Canada** Copy & Print Associate

March 2006 – June 2008	**BMO Bank of Montreal, Montreal (Qc) Canada** Direct Banking Manager
December 2001 – January 2007	**Harvey's (CARA Corp.), Laval (Qc) Canada** Team Leader

Languages

French	Full professional proficiency
English	Full professional proficiency
Spanish	Intermediate proficiency
Arabic	Mother tongue (functional)

Technical Knowledge

Research Techniques	Polymer rheology, Materials characterization (mechanical testing, impact and fatigue testing, DMA, DSC, TGA, rheology), Composite manufacturing processes, Life Cycle Analysis (LCA)
Software	Microsoft office, Catia V5, Universal Analysis, Wisetex, ESAComp

Honours

2016	Recipient of the *Fonds Wetenschappelijk Onderzoek* (FWO) conference travel grant for the 17th European Conference on Composite Materials (ECCM17)
2015	Recipient of the *Fonds Wetenschappelijk Onderzoek* (FWO) conference travel grant for the 20th International Conference on Composite Materials (ICCM20)
2012 - 2014	Recipient of the Fonds de recherche du Québec – Nature et technologies (FRQNT) 3 years PhD scholarship
2011	Master's thesis selected as one of the best of Polytechnique Montreal in 2011
2006 - 2007	Engineer Ethics Report "The collapse of the De la Concorde Bridge" selected among the best in 2007 edition Second year Mechanical engineering robot competition: Team ranked 1st

Extracurricular activities

2012-…	Open Days at the Materials Engineering department of the KU Leuven Participation at the KU Leuven and CELC booth of the Journée Européennes des Composites (JEC)
2006 - 2011	Active member of the Technical Society "Esteban, the Solar Car" of Polytechnique Montreal • Build a solar car shell in composite, fundraising, 3D design and competition logistics and safety • October 2009: Participation in the World Solar Challenge (WSC) across the Australian desert (Darwin – Adelaide)
2010 - 2011	Columnist for the graduate student newspaper "Le Recherché" of Polytechnique Montreal

Farida Bensadoun - Research Contributions

Journal articles: Articles accepted or submitted in refereed journals

- **Bensadoun, F**., Kchit, N., Billotte, C., Bickerton, S., Trochu, F., Ruiz, E., "A Study of Nanoclay Reinforcement of Bio-Composites made by Liquid Composite Molding", International Journal of Polymer Science, Volume 2011 (2011), Article ID 964193, May 2011.
- **Bensadoun, F.**, Kchit, N., Billotte, C., Trochu, F. Ruiz, E., "A Comparative Study of Dispersion Techniques for Nanocomposite made with Nanoclays and an Unsaturated Polyester Resin", Journal of Nanomaterials, Volume 2011 (2011), Article ID 406087, August 2011.
- U. Pineda, N. Montés ,F. Sánchez, **F. Bensadoun**, E. Ruiz, " Towards a Quality Monitoring to Control the Degree of Cure in the Manufacturing of Composite Parts", Advanced Science Letters,Volume 19, Number 3, pp. 869-872(4), March 2013.
- Pil L., **Bensadoun F**., Pariset J., Verpoest I., Why are designers fascinated by flax and hemp fibre composites?, Composites Part A: Applied Science and Manufacturing, Volume 83, Pages 193-205, April 2016.
- **Bensadoun, F.**, Vallons K.A., Lessard L.B., Verpoest, I., Van Vuure, A.W., Fatigue Behaviour Assessment of Flax-Epoxy Composites, Composites Part A: Applied Science and Manufacturing, Volume 82, Pages 253-266, March 2016.
- **Bensadoun, F.**, Baets, J., Verpoest, I., Van Vuure, A., Designing with Flax Fibre Reinforced Composites-Characterization of Textile Architectures, Composites Part A: Applied Science and Manufacturing, submitted April 2016.
- **Bensadoun, F.**, Depuydt, D., Baets, J., Verpoest, I., Van Vuure, A., Impact Properties of Flax Composites, Composite Structures, submitted April 2016.
- **Bensadoun, F.**, Verpoest, I., Van Vuure, Interlaminar Fracture Toughness of Flax-Epoxy Composites, Journal of Reinforced Plastics and Composites, submitted April 2016.
- **Bensadoun, F.**, Vanderfeesten B., Verpoest, I., Van Vuure, A.W., Van Acker K., Environmental Impact Assessment of End of Life Options for Flax-MAPP Composites, Industrial Crops and Products, submitted April 2016.
- **Bensadoun F.**, Verpoest I., Baets J., Mussig J., Graupner N., Davies P., Gomina M., Kervoelen A., Baley C., Development and validation of an Impregnated Fibre Bundle Test for natural fibres used as reinforcement in composites, Journal of Reinforced Plastics and Composites, submitted June 2016.
- Straumit I., Vanaerschot A., **Bensadoun F**., Verpoest I., van Vuure A.W, Vandepitte D., Wevers M., Lomov S.V, Reconstruction and stochastic modelling of a twill flax/epoxy composite geometry from X-ray computed tomography data, submitted to Composites Part A: Applied Science and Manufacturing, June 2016.

Conferences with review committee

- N. Kchit, **F. Bensadoun**, T. Carrozani, C. Billotte, E. Ruiz, F. Trochu, "A study of nanoclays composite fabricated by liquid composite molding," in the Proceedings of Flow Processing Composite Materials 2010 (FPCM10), Ascona, Swizerland, 2010.
- **F. Bensadoun**, N. Kchit, E. Ruiz, F. Trochu, "Fabrication and Mechanical Properties of Nanocomposites Fabricated by Resin Infusion with Bioresin and Natural Fibers," in Proceedings of the 8th Workshop on Composite Canada-Japan, Ecole de Technologie Supérieure, Montreal, Canada, 2010
- **F. Bensadoun**, C. Billotte, F. Trochu, E. Ruiz, "Development, Characterization and manufacturing of Nanocomposites and Bio-nanocomposites intended for the Transportation

Industry," (Poster) The Second joint American-Canadian International Conference on Composites , Montreal, Canada, September 2011.

- U. Pineda, **F. Bensadoun**, E. Ruiz, N. Montés, F. Sánchez, "Experimental Analysis by Thermography and Conductive Heat Flux Sensors of the Curing Stage of Composite Parts made by Resin Infusion (RI)", ECCM15, Venice, Italy, 2012
- U. Pineda, N. Montés ,F. Sánchez, **F. Bensadoun**, E. Ruiz, " In-situ calibration experimental method for Infrared thermography applied to the heat transfer analysis for composite parts during manufacturing based on Resin Infusion technique", 11th Quantitative InfraRed Thermography, Naples, Italy, 2012.
- Van Vuure, A., Tran, L., Fuentes Rojas, C., Osorio Serna, L., Trujillo De Los Rios, E., Vo Hong, N., Perremans, D., **Bensadoun, F**., Baets, J., Verpoest, I., Natural fibre composites: Recent developments. 5th Eucass - European Conference for Aerospace Sciences. 5th EUCASS - European Conference for Aerospace Sciences. Munich, Germany, 1-4 July 2013. Bensadoun, F.,
- **Bensadoun, F.**, Depuydt, D., Baets, J., Van Vuure, A., Verpoest, I., Influence of fibre architecture on impact and fatigue behaviour of flax fibre-based composites. ICCM19, International Conference on Composite Materials - 7. Montreal, Canada, 29 July - 3 August 2013.
- **Bensadoun, F**., Depuydt, D., Baets, J., Van Vuure, A., Verpoest, I., Impact resistance, damage and absorbed energy behaviour of flax-based composites. Composite week @ Leuven. Leuven, Belgium, 16-21 September 2013.
- **Bensadoun, F.**, Baets, J., Van Vuure, A., Verpoest, I., Fatigue behaviour of flax reinforced composites. . European Conference on Composite Materials. Seville, Spain, 22-26 June 2014 (art.nr. 1151).
- **Bensadoun, F**., Barburski, M., Straumit, I., Le Quan Tran, N., Fuentes Rojas, C., Zenina, J., Shishkina, O., Pyka, G., Verpoest, I., Van Vuure, A., Wevers, M., Lomov, S., Challenges of X-ray tomography technique on natural fibre-based composites. 11th ECNDT, European Conference on Non-Destructive Testing. Prague, Czech Republic, 6-10 October 2014 (art.nr. 235).
- Straumit, I., Lomov, S.V., **Bensadoun, F**., Wevers M., Automatic transformation of 3D micro-CT images into finite element models with anisotropic local properties. ECCM-16, 16th European Conference on Composite Materials. ECCM. Seville, Spain, 22-26 June 2014.
- **Bensadoun, F.**, Vanderfeesten B., Van Acker K., Verpoest, I., Van Vuure, A.W., End Of Life Technologies For Flax-Thermoplastic Composites And Their Effects On The Environment. 2nd International Conference on Natural Fibers (ICNF 2015), Sao Miguel (Azores), Portugal, 27-29 April 2015.
- Straumit, I., **Bensadoun, F**., Lomov S.V., Wevers M., Voxel-based modelling of textile composites from μCT data: problem of matrix-yarns-voids segmentation. 9th European Solid Mechanics Conference (ESMC 2015). Leganés-Madrid, Spain. July 6 - 10, 2015.
- **Bensadoun, F.**, Vallons K.A., Lessard L.B., Verpoest, I., Van Vuure, A.W., Residual Properties And Damage Evolution Of Flax-Epoxy Composites Subjected To Fatigue Loading. 20th International Conference on Composite Materials (ICCM20). Copenhagen, Denmark, 19-24 July 2015.
- Straumit, I., **Bensadoun, F**., Lomov S.V., Wevers M., Effective properties of unidirectional flax/epoxy composites with twisted yarns, 20th International Conference on Composite Materials (ICCM20). Copenhagen, Denmark, 19-24 July 2015.
- **Bensadoun, F.**, Vallons K.A., Lessard L.B., Verpoest, I., Van Vuure, A.W., Comportement Post-Fatigue Des Composites Lin-Epoxy (french abstract), Colloque Fatigue et durabilité des composites biosourcés, 25-27 Mai 2016, accepted for oral presentation.

- **Bensadoun, F.**, Verpoest, I., Van Vuure, A.W., Are Flax-Epoxy Composites Tough?, The seventeenth European Conference on Composite Materials (ECCM17), 26-30 June, accepted for oral presentation.
- **Bensadoun F**., Verpoest I., Baets J., Mussig J., Graupner N., Davies P., Gomina M., Kervoelen A., Baley C., Impregnated Fibre Bundle Test for Natural Fibre Composites: Fibres Properties, The seventeenth European Conference on Composite Materials (ECCM17), 26-30 June, accepted for oral presentation.

Other contributions

- **F. Bensadoun**, N. Kchit, E. Ruiz, F. Trochu, "A Study on Polymer Nanoclay Composites: Processing, Mechanical and Flammability Properties," (Poster) Colloque du Centre de recherche en plasturgie et en composite (CREPEQ), 2009, Montreal, Canada, 2009.
- **F. Bensadoun**, N. Kchit, C. Billotte, E. Ruiz, F. Trochu, "A Study on Bionanocomposites for the Transportation Industry," (Poster) Colloque du Centre de recherche en plasturgie et en composite (CREPEQ) and 26th Research Day, Ecole Polytechnique Montreal, Montreal, Canada, December 2010 and May 2011.
- **F. Bensadoun,** J. Gutierrez, "Étude du comportement viscoélastique d'un renfort fibreux en compression", Technical Report (Bachelor thesis), Ecole Polytechnique de Montreal, 2009.
- **Bensadoun, F**., Baets, J., Van Vuure, A., Verpoest, I. (2013). Fatigue behaviour of Flax composites: Influence of fibre architecture. ECOCOMP 2013, International Conference on Sustainable Materials, Polymers and Composites. Edinburg, UK, 3-4 July 2013.(poster)
- **Bensadoun, F**., Baets, J., Van Vuure, A., Verpoest, I. (2013). Comportement en fatigue et impact des composites à base de lin. Journées Jeunes Chercheurs : Eco-composites et Composites Bio-sourcés. Institut Supérieur de l'Automobile et des Transports (ISAT) – Nevers, 10-11 April 2013. (oral presentation, abstract only)
- **Bensadoun, F.**, Baets, J., Van Vuure, A., Verpoest, I. (2014). The influence of textile architectures on the fatigue behaviour of flax/epoxy composites. International Conference on Mechanics of Composite Materials. Riga, Latvia, 2-6 June 2014. (oral presentation, abstract only)
- **Bensadoun, F**., Baets, J., Depuydt, D., Van Vuure, A., Verpoest, I. (2014). Impact properties characterization of flax fibre-reinforced composites. International Conference on Mechanics of Composite Materials. Riga, Latvia, 2-6 June 2014. (oral presentation, abstract only)
- Pariset J., **Bensadoun F.**, European flax/linen & hemp fibres: advanced natural materials for the composite industry. JEC Green efficiency, European flax/linen & hemp fibres seminar, Houston (Tx), USA. June 4th 2015. (oral presentation, abstract only)

Bachelor and Master Thesis student supervision

2009-2011

- Élizabeth Michaud, *Identification des sources de variabilité dans le protocole d'évaporation du styrène dans la production de pièces composites à base de résine UP et de nanoparticules d'argile,* Internship, Chemical Engineering Department, Polytechnique Montréal, April-August 2009.
- Tommy Carozzani, *Élaboration de nanocomposites- Polyester insaturé avec nanoparticules d'argile*, Internship for Master studies, Mechanical Engineering Department, Polytechnique Montréal, September 2009.
- Thierry-Grégoire Gauthier, *Fabrication d'une pièce à géométrie complexe en bio-composites nano-chargés*, Bachelor Thesis, Mechanical Engineering Department, Polytechnique Montréal, April 2010.
- Émilie Charrette, *Caractérisation des résines polyester insaturées nanochargées : dispersion, fabrication et tests,* Bachelor Thesis, Chemical Engineering Department, Polytechnique Montréal, April 2010.
- Coralie Motillon, *Fabrication et caractérisation de nanocomposites polyester à base de particules d'argile*, Internship for Master studies, Mechanical Engineering Department, Polytechnique Montréal, August 2010.
- Jean-Nicolas Rhéaume Perey, *Fabrication d'un bateau avec des bio-composites de source naturelle*, Bachelor Thesis, Mechanical Engineering Department, Polytechnique Montréal, April 2011.

2012-2015

- Delphine Depuydt, *Characterization of the impact behaviour of flax fibre composites*, Master Thesis, Materials Engineering, KU Leuven, 2013
- Yao Zhao, *Creep behaviour and viscoelastic properties of Flax/Epoxy composites*, Master Thesis, Materials Engineering, KU Leuven, 2014
- Jan Vertommen, Manufacturing of chemically treated thermoplastic flax fibre composites, Master Thesis, Materials Engineering, KU Leuven, 2014.
- Bart Vanderfeesten, *Environmental impact of newly developed composites with thermoplastic matrix for high volume applications,* Master Thesis, Materials Engineering, KU Leuven, 2014.
- Elias Cloots, *Influence of the temperature during the service life of chemically treated flax fiber composites*, Master Thesis, Materials Engineering, KU Leuven (Groep T), 2014.
- Bastien Grillet, *Investigation on the influence of moisture on the mechanical properties of chemically treated flax fiber polyester composites*, Master Thesis, Materials Engineering, KU Leuven, 2015.
- Wouter de Saeger, Effect of chemical treatments on the impact properties of flax fiber composites, Master Thesis, Materials Engineering, KU Leuven (Groep T), 2015.
- Kristof Vanden Bergh, *Development of low-cost, sustainable bio-composite roof panels for developing countries*, Master Thesis, Materials Engineering, KU Leuven, 2015.
- Frederick Puttemans, *Strong and tough natural fibre composites through hybridization*, Master Thesis, Materials Engineering, KU Leuven, 2015.
- Elias De Keyser, *Can Flax Fibres replace E-glass as reinforcement in composites for small-scale wind turbine blades? | A comparative study*, Bachelor Thesis, Materials Engineering, KU Leuven, 2015.